Examining the Contribution of Maternal Circulating Factors on Altered Fetal Growth in Pregnancies Complicated by Gestational Diabetes Mellitus

Manon Dwynwen Owen

Submitted in Accordance with the Requirements for

the Degree of Doctor of Philosophy in Medicine

The University of Leeds

School of Medicine

Leeds Institute of Cardiovascular

and Metabolic Medicine

September 2024

Intellectual Property and Publication Statement

I confirm that the work submitted is my own, except where work which has formed part of jointly authored publications has been included. My contribution and the other authors to this work has been explicitly indicated below. I confirm that appropriate credit has been given within the thesis where reference has been made to the work of others.

Manon D. Owen, Margeurite G. Kennedy, Rachel C. Quilang, Eleanor M. Scott, Karen Forbes; The role of microRNAs in pregnancies complicated by maternal diabetes. Clin Sci. 2024; 138(18):1179–1207.

- This review forms as the general introduction and part of the general discussion of this thesis.
- Information was collated and draft was written by Manon D. Owen. Margeurite G. Kennedy contributed towards sections associated with GDM, fetal outcomes and the placenta, however this content has been changed for this thesis. Rachel C. Quilang was involved in initial planning, discussion and supervision. Scott EM and Forbes K supervised and edited the draft. All co-authors approved the final draft.

Owen MD, Baker BC, Scott EM, Forbes K. Interaction between Metformin, Folate and Vitamin B12 and the Potential Impact on Fetal Growth and Long-Term Metabolic Health in Diabetic Pregnancies. Int J Mol Sci. 2021; 28;22(11):5759.

- Parts of this review are used for the general introduction and metformin results chapter introduction of this thesis.
- Information was collated and draft was written by Owen MD. Baker BC advised on sections relating to the role of folate in pregnancy. Scott EM and Forbes K supervised and edited the draft. All co-authors approved the final draft.

Acknowledgements

Firstly, thank you to my supervisors Dr Karen Forbes and Professor Eleanor Scott for their guidance, mentoring and support throughout my PhD. Their expertise and rigorous approach to designing research methodologies has cultivated my ability to solve problems with creativity while also develop self-confidence in my own ideas. I would also like to thank Dr Rachel Quilang for her invaluable guidance throughout my research project, as well as Dr Abigail Byford for training me in the lab during the initial stages of my PhD. I am also deeply grateful to the other Leeds Pregnancy Research Group members (Georgia Fakonti, Dr Maggie Kennedy, Dr Naima Endesh, Dr Katie Hugh, Dr Rachel Farrelly, Dr Rebecca Spencer, Dr Amanda Leow, Dr Nicole Watt) for their support and encouragement over the last four years. Additionally, I would like to extend thanks to collaborators such as Dr Leander Stewart, Dr Neil Turner, Professor Lee Roberts, Melaine Reay, Simon Futers, Dr Nadira Yuldashev, Professor Niamh Forde, Professor Susan Ozanne and Dr Jayne Charnock for their expertise and guidance, as well as the BHF for funding this research.

Importantly, thank you to the women from the Leeds Teaching Hospitals and the MAGiC and PRiDE clinical studies for donating their placenta and blood samples to this research. Thanks to Professor Ponnusamy Saravanan for providing samples from the PRiDE clinical study. Thank you also to Dr Jane Luk and Dr Amanda MacCannell for their advice and support in the lab, as well as Dr Karen Porter for her support as my postgraduate research tutor. I am also grateful to Ruth Hughes and Sally Boxall from the Bioimaging facility, and to LICAMM SOT for facilitating this project. To the LICAMM BHF programme, thank you for providing me with invaluable opportunities for academic growth throughout the last four years. In particular, thank you Abbie and Katie for your incredible friendship and for inspiring me to persevere through (many!) challenging times.

I Elan, diolch am fod y ffrind gora' erioed dros y ddwy flynedd diwethaf ac am neud Leeds yn le i'w gofio am byth. Rhods, diolch am fod yn gefn i fi drwy bob rhan o'r cyfnod yma ac am fod yn chdi. Yn olaf, byswn i heb allu g'neud hyn heb chi Mam a Dad, diolch am bob dim – ma' hwn i chi. Caru chi.

Abstract

Introduction: Gestational diabetes mellitus (GDM) is associated with suboptimal fetal growth and increased offspring susceptibility to cardiometabolic diseases. In GDM, several components of the maternal environment are altered, including metformin treatment, and extracellular vesicles (EVs) and their micro-RNA (miRNA) cargo. Metformin, EVs and miRNAs have the potential to enter the placenta, a key regulator of fetal growth, but it remains to be established if these factors impact placental and fetal development in GDM.

Methods and Results: Transcriptomic analysis of placental tissue from women with GDM treated with metformin or placebo demonstrated that *in-vivo* exposure to metformin altered transcriptomic pathways associated with vascular development, growth and metabolism. Using a human placental explant model, it was demonstrated that some but not all of the changes observed in the placenta of women treated with metformin were attributed to direct actions of metformin on the placenta. Indirect actions of metformin on the placenta remain to be established but may include changes to EVs or their miRNA cargo. Our group has previously established that EVs and their miRNA cargo, including miR-375-3p, are altered in the circulation of women with GDM that deliver large-for-gestational-age infants. To establish a causative association between maternal EVs or their miRNA cargo and fetal growth in GDM, pregnant C57BL6/J mice were injected via tail vein at E11.5, E13.5 and E15.5 with miR-375-3p or human maternal plasma EVs isolated from uncomplicated and GDM pregnancies with various growth outcomes. At E18.5, dams were culled, and pups and placentae were weighed. Mouse placental and fetal weight were markedly impacted by miR-375-3p and human maternal EVs, where omics analyses demonstrated that EVs/miRNA-375-3p may be impacting fetal growth by altering placental metabolism.

Conclusion: Maternal circulating factors significantly impact placental and fetal development in GDM. *Ex-vivo* models of pregnancy should consider the impact of *in-vivo* circulating factors.

COVID-19 Pandemic Impact Statement

My PhD studies began in October 2020, which coincided with the COVID-19 pandemic national lockdown. At that time, access to the Leeds Institute of Cardiovascular and Metabolic Medicine was extremely restricted to adopt social distancing practices. As such, I was unable to begin laboratory experiments until April 2021. However, my training in the laboratory was still hindered during this period, as institute restrictions continued until late summer 2021 where laboratory access was prioritised to post-doctoral researchers and final-year PhD students. This meant only a limited number of research group members were allowed in the institute at any given time and my hours in the laboratory were restricted. To overcome this, I conducted and published a literature review on the “Interaction between Metformin, Folate and Vitamin B12 and the Potential Impact on Fetal Growth and Long-Term Metabolic Health in Diabetic Pregnancies”. This provided a solid foundation for my understanding of the subject area.

Table of Contents

List of Figures

List of Tables

List of Abbreviations

5-HIAA	5-hydroxyindoleacetic acid
5OP	5-oxoproline
8OHdG	8-hydroxy-2'-deoxyguanosine
AC	Acylcarnitine
AFC	Automatic fraction collector
AGA	Appropriate-for-gestational-age
AMP	Adenosine monophosphate
AMPK	AMP-activated protein kinase
ANOVA	Analysis of variance
ATP	Adenosine triphosphate
AWERB	Animal and welfare ethical review board
BAIBA	β-aminoisobutyric acid
BCL2	B-cell lymphoma 2
BHIBA	β-aminoisobutyric acid
BM	Basal membrane
BMI	Body mass index
BSA	Bovine serum albumin
C14MC	Chromosome 14 miRNA cluster
C19MC	Chromosome 19 miRNA cluster
CALD1	Caldesmon
CD31/PECAM1	Platelet endothelial adhesion molecule
CD47	Cluster of Differentiation 47
cDNA	Complementary DNA
CGM	Continuous glucose monitoring
CI	Confidence interval
DAB	Diaminobenzidine
DAG	Diacylglyerol
DEG	Differentially expressed gene
DEP	Differentially expressed protein
DGCR8	DiGeorge syndrome critical region
DMEM	Dulbecco's modified eagle medium
DNA	Deoxyribonucleic acid

DOHaD	Developmental origins of health and disease
DPX	Dibutylphthalate polystyrene xylene
EDTA	Ethylenediaminetetraacetic acid
EFA	Essential fatty acid
EGFR	Epidermal growth factor receptor
ELISA	Enzyme-linked immunosorbent assay
EMPOWaR	Efficacy of metformin in pregnant obese women: a randomised controlled trial
EMT	Epithelial–mesenchymal transition
ENO1	Enolase 1
EOT2D	Early onset T2DM
ERα	Estrogen receptor α
EV	Extracellular vesicle
EVT	Extravillous trophoblast
FABP4	Fatty acid-binding protein 4
FAT	Fatty acid translocase
FATP	Fatty acid binding protein
FBS	Fetal bovine serum
FC	Fold change
FDR	False discovery rate
FFA	Free fatty acid
GDM	Gestational diabetes mellitus
GLP	Glucagon like peptide
GLP-1	Glucagon-like peptide-1
GLUT	Glucose Transporter
GROW	Gestation-related optimal weight
Hba1C	Haemoglobin A1c
hCG	Human chorionic gonadotropin
HDL	High-density lipoprotein
HPLC	High performance liquid chromatography
HRP	Horseradish peroxidase
HUVEC	Human umbilical vein endothelial cells
IGF	Insulin-like growth factors

IGF2R	Insulin-like growth factor 2 receptor
IHC	Immunohistochemistry
IPA	Ingenuity pathway analysis
ITGB1	Integrin β1
ITGB3	Integrin β3
KPNA3	Importin α3
LA	Linoleic acid
LC	Liquid chromatography
LC3	Light chain 3
LCMS	Liquid chromatography mass spectrometry
LC-PUFA	Long-chain polyunsaturated fatty acids
LDH	Lactate dehydrogenase
LDL	Low-density lipoprotein
LGA	Large-for-gestational-age
LN	Liquid nitrogen
Log_2FC	Log_2FoldChange
MAG	Monoacylglycerol
MAGiC	Maternal glucose in pregnancy study
MGV	Mean grey value
miRNA	Micro RNA
mRNA	Messenger RNA
mTOR	Mammalian target of rapamycin
MVM	Microvillous membrane
NADH	Nicotinamide-adenine dinucleotide
NHS	National Health Service
NICE	National Institute for Health and Care Excellence
NO	Nitric oxide
NRT	No reverse transcriptase
NT miRNA	Negative control miRNA mimic
NTA	Nanoparticle tracking analysis
NTC	No template control
OAA	Oxaloacetate
OCT	Organic cation transporter

OGTT	Oral glucose tolerance test
pAMPK	Phospho AMPK
PBS	Phosphate buffered saline
PCA	Principal component analysis
PCOS	Polycystic ovary syndrome
PCR	Polymerase chain reaction
PG	Prostaglandin
PGDM	Pre-existing maternal diabetes
PINK1	PTEN -induced kinase 1
PPAR	Peroxisome proliferator-activated receptor
PPARG1β	Peroxisome proliferator-activated receptor gamma coactivator 1-β
pre-miRNA	Precursor miRNA
PRiDE	Micronutrients in pregnancy as a risk factor for gestational diabetes and effects on mother and baby study
pri-miRNA	Primary miRNA
PRKAG2	Protein kinase AMP-activated non catalytic subunit gamma 2
PSG	Penicillin, streptomycin and glutamine
PVDF	Polyvinylidene fluoride
QPCR	Quantitative polymerase chain reaction
RIPA	Radioimmunoprecipitation assay
RNA	Ribonucleic acid
ROI	Region of interest
ROS	Reactive oxygen species
ROX	5-carboxy-X-rhodamine
RPM	Revolutions per minute
RT	Room temperature
RT-qPCR	Real-time quantitative reverse transcription PCR
scDNA	Single-cell DNA sequencing
SEC	Size exclusion chromatography
SEM	Standard error of the mean
SGA	Small-for-gestational-age

SLC6A8	Solute carrier family 6 member 8
T1DM	Type-1 diabetes mellitus
T2DM	Type- diabetes mellitus
TAE	Tris-acetate-EDTA
TAG	Triacylglycerides
TBS	Tris-buffered saline
TBST	Tris-buffered saline with Tween20
TCA	Tricarboxylic acid
TEM	Transmission electron microscope
TMT	Tandem mass tag
TSG101	Tumour susceptibility 101 protein
TTC3	Tetratricopeptide repeat domain 3
UTR	Untranslated region
VEGF	Vascular endothelial growth factor

Publications Relating to This Thesis

Published Review Articles:

- **Manon D. Owen**, Margeurite G. Kennedy, Rachel C. Quilang, Eleanor M. Scott, Karen Forbes; The role of microRNAs in pregnancies complicated by maternal diabetes. Clin Sci. 2024; 138(18):1179–1207.
- **Owen MD**, Baker BC, Scott EM, Forbes K. Interaction between Metformin, Folate and Vitamin B12 and the Potential Impact on Fetal Growth and Long-Term Metabolic Health in Diabetic Pregnancies. Int J Mol Sci. 2021; 28;22(11):5759.

Published Abstracts:

- **Manon D Owen**, Rachel Quilang, Abigail Byford, Leander Stewart, Melanie Reay, Naima Endesh, Simon Futers, Neil Turner, Nadira Yuldasheva, Jayne Charnock, Rebecca Spencer, Niamh Forde, Beth Holder, Susan Ozanne, Eleanor M Scott, Karen Forbes. Maternal Extracellular Vesicle Derived miR-375-3p Promotes Fetal Overgrowth in Healthy Pregnant Mice. Plenary Oral Presentation-001. Reproductive Sciences Vol. 31, Supplement 1, March 2024.
- **Manon Owen,** Katie Hugh, Rachel Quilang, Eleanor Scott, Karen Forbes. Metformin Exposure *In-utero* Influences Placental Pathways Associated with Mitochondrial Activity. Endocrine Abstracts. 2022. 86, P269. Poster presentation at the Society for Endocrinology annual conference, Harrogate, UK.

1 General Introduction

1.1 Diabetes in Pregnancy

The global prevalence of diabetes is estimated to surge in the next twenty years, affecting more women of reproductive age (1). With maternal diabetes currently affecting 21.1 million live births worldwide (1), the influence of diabetes and associated hyperglycaemia on maternal health and the developing fetus is of increasing concern. Of the pregnancies affected by maternal hyperglycaemia, 19.7% are attributed to pre-existing maternal diabetes (PGDM), including type-1 diabetes mellitus (T1DM) or type-2 diabetes mellitus (T2DM) (1). T1DM is characterised by pancreatic β-cell destruction, resulting in insulin insufficiency and hyperglycaemia. For most people, this pancreatic destruction is driven by autoimmunity (2). Moreover, T2DM is a heterogenous condition characterised by hyperglycaemia that is driven by insulin resistance and/or impaired pancreatic β-cell insulin secretion. This type of diabetes presents with varying underlying pathophysiology but is strongly associated with adiposity and a background of skeletal muscle, liver and adipose tissue insulin resistance (3).

The remaining 80.3% of pregnancies affected by maternal hyperglycaemia are attributed to gestational diabetes mellitus (GDM) (1). GDM is defined as maternal glucose intolerance that is first identified during pregnancy (4,5). During healthy pregnancy, it is known that there is a certain degree of maternal insulin resistance to establish sufficient carbohydrate reserve to the fetus for optimal growth (6). However, as well as insulin resistance, individuals with GDM manifest pancreatic β-cell dysfunction, which in turn contributes towards maternal hyperglycaemia. Although the aetiology of GDM is still unclear, it is thought that these maternal hallmarks may already be underlying prior to conception, only exacerbated during the maternal metabolic adaptations that occur in pregnancy (7).

1.1.1 Diagnosis and Treatments

T1DM is often diagnosed during childhood or adolescence but it may also manifest later in life. Insulin therapy is the main treatment for T1DM, including contemporary strategies such as continuous glucose monitoring (CGM), insulin pumps and closed-loop systems (2). In contrast, although T2DM is traditionally

diagnosed with advancing age, diagnosis is now becoming more prevalent in children and young adults; this is known as early onset T2DM (EOT2D). This is a concern as it is a more severe condition if diagnosed <40 years-of-age and associated with greater risk of complications. As such, T2DM is now far more common than T1DM in women of child-bearing age (3,8,9). Lifestyle interventions such as exercise, diet changes and weight loss are the main initial treatment strategy for T2DM. However, multiple oral hypoglycaemic agents and injectables such as insulin and glucagon-like peptide-1 (GLP-1) agonists are also commonly required (3).

GDM is typically diagnosed at weeks 24-28 gestation through an oral glucose tolerance test (OGTT) (10,11). The diagnostic criteria for GDM can vary widely, resulting in broad clinical manifestations of GDM (10). However, the current recommendations for GDM diagnosis in the United Kingdom include >5.6 mmol/L fasting plasma glucose or >7.8 mmol/L 2-hour glucose following a 75g 2-hour OGTT (12). Although the pathogenesis of GDM is yet to be established, clinical risk factors such as maternal body mass index (BMI), age, previous GDM pregnancies, family history and ethnicity have been associated with the onset of GDM (10). Lifestyle interventions such as exercise and diet modifications have been adopted as the main treatments for GDM. However, hypoglycaemic agents such as metformin and insulin are also used if maternal glycaemic levels do not improve. Glibenclamide is used rarely (10).

1.1.2 Adverse Maternal Outcomes

Pregnancies complicated by PGDM and GDM are associated with short- and long-term adverse outcomes for the mother. Indeed, people with PGDM and GDM are at increased risk of developing preeclampsia (13,14). Preeclampsia is a condition known as high blood pressure and proteinuria during the third trimester of pregnancy which can lead to reduced placental blood flow, resulting in a lack of nutrient and oxygen exchange at the feto-placental interface. As well as affecting the developing fetus, preeclampsia is associated with increased maternal risk of cardiovascular and cerebrovascular disease onset postpartum (15,16). It is well established that individuals with PGDM and GDM are at

increased risk of developing diabetic comorbidities (4,5,17,18). Moreover, it is known that a diagnosis of GDM increases the risk of post-partum maternal T2DM onset by 7-fold (19). It has also been shown that GDM increases the risk of future maternal cardiovascular diseases by two-fold compared to those who experience healthy, uncomplicated pregnancies (20). A recent study demonstrated that individuals with GDM manifest hemodynamic maladaptation, where myocardial contractility is weakened and left ventricular mass is increased in late pregnancy, leading to impaired maternal myocardial energetics (20).

1.1.3 Adverse Perinatal Outcomes

1.1.3.1 Congenital Abnormalities

PGDM and GDM can both increase the risk of stillbirth and congenital anomalies (21–23). Specifically, PGDM is associated with oral clefts, congenital heart disease and disorders of the central nervous system, digestive system, musculoskeletal system, and genitourinary system (23). GDM is also associated with congenital anomalies but to a lower degree than PGDM (23). Organogenesis occurs early in pregnancy and is a pivotal gestational period for the development of congenital anomalies (24). Previous studies have shown that an intrauterine environment exposed to diabetic stressors such as hyperglycaemia may contribute towards the development of congenital anomalies (25,26). Although it is suggested that individuals who develop GDM manifest underlying β-cell dysfunction prior to pregnancy, insulin resistance is likely to be more prominent during organogenesis in those with PGDM. As such, this may contribute towards the increased cases of congenital anomalies observed with PGDM compared to GDM (23).

1.1.3.2 Altered Fetal Growth

Neonates exposed to maternal diabetes *in-utero* are more likely to be classed as large-for-gestational-age (LGA) (weighing above the 90th percentile for their gestational age) (27–30). LGA births have shown to be associated with neonatal hypoglycaemia, shoulder dystocia and stillbirth (7,21). Fetal overgrowth is also referred to as ‘macrosomia’ in various studies, where neonates are classed as

macrosomic if they weigh above 4000g regardless of gestational age (31). How diabetic pregnancy leads to fetal overgrowth is still not fully understood. The 'Pederson hypothesis' postulates that excess glucose levels in the diabetic maternal circulation is transported into the placenta and thus promotes a hyperglycaemic state in the fetus which triggers hyperinsulinaemia and excess fat storage and adiposity (32–34). In contrast, maternal diabetes is also associated restricted fetal growth, resulting in neonates to be classed as small-for-gestational-age (SGA) (weighing below the 10th percentile for their gestational age) (**Figure *1***) (35,36). Pre-term delivery is currently the only available treatment for SGA and LGA pregnancies, which can lead to further adverse fetal outcomes (37). The current methods of identifying pregnancies at risk of altered fetal growth include fetal ultrasound, clinical assessments and measurements of maternal metabolites, however all of these methods lack sensitivity (38).

It has been demonstrated that altered fetal growth or *in-utero* exposure to maternal diabetes increases the risk of offspring cardiometabolic disease onset throughout life (39–43). As such, this perpetuates a transgenerational cycle of cardiometabolic disease, where these offspring are at increased risk of experiencing pregnancies complicated by maternal diabetes themselves. This transgenerational cycle of disease is elucidated by the developmental origins of health and disease (DOHaD) hypothesis, where it is suggested that suboptimal *in-utero* exposures have capacity to program offspring disease susceptibility later in life (43,44). Indeed, this hypothesis proposes that the maternal diabetic milieu during pregnancy may lead to offspring epigenetic changes, thus programming disease predisposition (43). Continuous glucose monitoring (CGM), insulin pumps, sensor-augmented pump therapy, closed-loop systems and metformin therapy have all been employed as contemporary treatment strategies to regulate maternal glucose levels and health outcomes in pregnancies complicated by maternal diabetes (45–48). However, despite apparently well-managed maternal glucose levels, the prevalence of abnormal fetal growth remains high in pregnancies affected by PGDM and GDM, with LGA occurring in ~10% of treated GDM, ~25% of treated T2DM and >50% of treated T1DM pregnancies (7,21,49–52). This suggests that in addition to glucose, other components of the maternal

circulation, including maternal therapeutics, may play a role in altering fetal development in diabetic pregnancies.

1.1.4 Adverse Perinatal Outcomes with Metformin Therapy

For decades, insulin therapy has been the gold standard treatment for managing diabetes in pregnancy, to reduce excess maternal glucose delivered to the fetus and reduce the likelihood of LGA. Insulin is effective in maintaining glucose homeostasis. However, this therapy is associated with maternal weight gain, hypoglycaemia and increased maternal blood pressure which may contribute towards gestational hypertension development (45,53). With the global diabetes epidemic ever-increasing, the cost, storage and administration requirements of insulin are becoming unfeasible. Accordingly, many countries have assigned metformin as the first-line treatment T2DM pregnancies and GDM pregnancies (45).

Metformin has proven beneficial for long-term health in women with T2DM by reducing inflammation, weight gain, cardiovascular disease severity and atherothrombosis (45,54). Metformin has also been associated with reduced maternal weight gain in GDM pregnancies (55). However, evidence from human and mouse studies suggest metformin exposure *in-utero* may adversely affect long-term offspring health (45,54). Although metformin has demonstrated to reduce LGA prevalence, this therapy is associated with an increased prevalence of SGA births (56). Evidence suggests that SGA offspring exposed to metformin *in-utero* demonstrate ‘catch up growth’ during childhood (**Table *1***) and thus have an increased predisposition of childhood obesity and cardiometabolic disease during adulthood (45). Further understanding of metformin’s mechanism of action on adversely affecting offspring development is essential to manage this transgenerational cycle of cardiometabolic disease.

Table 1 Current literature on the effects of metformin on fetal growth.

Reference	Model	Effects Demonstrated by Metformin
Salomäki et al. 2013 (57)	Pregnant mouse model of GDM treated with metformin from E0.5 - E17.5. Offspring fed high fat diet later in development.	Fetal weight was lower on E18.5 in dams exposed to metformin *in-utero* vs untreated dams. Offspring exposed to metformin were heavier than untreated offspring and showed higher mesenteric fat and liver weight. Gene set enrichment analysis of differentially expressed genes in the metformin vs untreated murine offspring show metformin influences transgenerational effects via fetal programming.
Stolzenbach et al. (2024) (58)	Pregnant mouse model treated with high fat diet or control diet. Dams treated with metformin from E0 to 3 weeks postpartum. Offspring fed standard diet for 8 weeks and high fat diet for the next 4 weeks.	Offspring of dams exposed to metformin demonstrated lower body weight and white adipose tissue mass after eating high fat diet. Epigenetic changes leading to altered genes associated with impaired adipogenesis and lipogenesis.
Hanem et al. 2019 (59)	Offspring follow-up of pregnant women with polycystic ovarian syndrome taking metformin vs placebo.	Offspring exposed to metformin *in-utero* demonstrated elevated BMI at 4 years old vs offspring exposed to placebo.
Ijäs et al. 2015 (60)	Offspring follow-up of women with GDM on metformin vs insulin therapy.	Infants exposed to metformin *in-utero* were heavier at 12- and 18-months old vs offspring exposed to insulin.
	Metformin in Gestational Diabetes: The Offspring Follow-Up (MiG TOFU) Study:	
Rowan et al. 2011 (61)	Women with GDM on metformin vs insulin therapy: offspring follow-up at 2 years old.	Offspring exposed to metformin *in-utero* demonstrated increased subcutaneous adiposity and larger mid upper arm circumferences, bicep and subscapular skinfolds vs insulin exposed offspring.
Rowan et al. 2018 (62)	Women with GDM on metformin vs insulin therapy: offspring follow-up at 9 years old.	Offspring exposed to metformin *in-utero* demonstrated significantly higher body mass index (BMI), arm and waist circumference, triceps skinfold and abdominal fat volume vs insulin exposed offspring.
Feig et al. 2023 (63)	Women with T2DM treated with metformin or placebo: offspring follow-up at 24-months.	No difference in offspring overall BMI and skinfolds at 24 months. BMI trajectory significantly different in males. Offspring treated with metformin demonstrated higher BMI between 6-24 months.

1.2 The Placenta

The human placenta is a transient organ that regulates optimal fetal growth during pregnancy through its endocrine and immunologic actions (64,65). The placenta is a key regulator of fetal development and is core to the developmental origins of health and disease (DOHaD) hypothesis, where it is premised that suboptimal *in-utero* exposures are associated with disease onset later in life (44). Not only does the placenta maintain an optimal *in-utero* environment throughout gestation, but its development invokes direct consequential effects on fetal growth and disease predisposition (66).

1.2.1 Placental Development in Healthy Pregnancy

During embryogenesis, the blastocyst (or the pre-implantation embryo) differentiates into two layers, known as the inner cell mass, and the trophectoderm which forms the outermost layer of the blastocyst (67). The layer of the trophectoderm that is in direct contact with the inner cell mass, known as the polar trophectoderm, subsequently attaches and fuses with the uterine epithelial surface to establish the primary syncytium. This specialised endometrial surface is coined as the decidua. Lacunae filled with fluid are then formed within the syncytium (67,68).

Underlying the syncytium are cytotrophoblast cells. These cells proliferate through the primary syncytium and differentiate into the multinucleated syncytiotrophoblast, giving rise to primary villi and the intervillous space (previously known as the lacunae) (67). These villous structures then begin to branch and expand, with the syncytiotrophoblasts located at the outermost syncytial layer of the chorionic villi. As extraembryonic mesenchymal cells invade the villous core, secondary villi are then established. Around 18 days after fertilisation, tertiary villi are formed as fetal capillaries are established in the villous core (**Figure *1***) (67,68). Vasculogenesis and angiogenesis contribute towards the development of the placental vascular system and although the precise mechanisms responsible for this remain to be established, various growth factors including vascular endothelial growth factor (VEGF) are essential regulators (69). Various other cells such as placental macrophages, also known as Hofbauer

cells, play a role in the vascularisation of the placenta (70). Throughout gestation, the syncytium expands by proliferation, differentiation and fusion of the underlying cytotrophoblasts of the placenta, where material is continuously shed into the maternal circulation (71,72). The most important hormone secreted by the syncytiotrophoblast is human chorionic gonadotropin (hCG) (73). hCG is responsible for progesterone secretion via the corpus luteum, stimulates uterine angiogenesis and syncytiotrophoblast differentiation, halts maternal immune attacks on the placenta, as well as regulating and supporting optimal fetal growth and development during gestation (74).

As the villous tree develops, cytotrophoblast cells also differentiate into extravillous trophoblasts (EVTs) which invade the maternal decidua and remodel uterine spiral arteries to establish feto-placental blood flow (71). To meet the growing metabolic demands of the fetus, placental development is tightly regulated throughout pregnancy. These processes are regulated by growth factors, including insulin-like growth factors (IGFs), intracellular signalling cascades, mitochondrial respiration and microRNAs (miRNAs) (75–79).

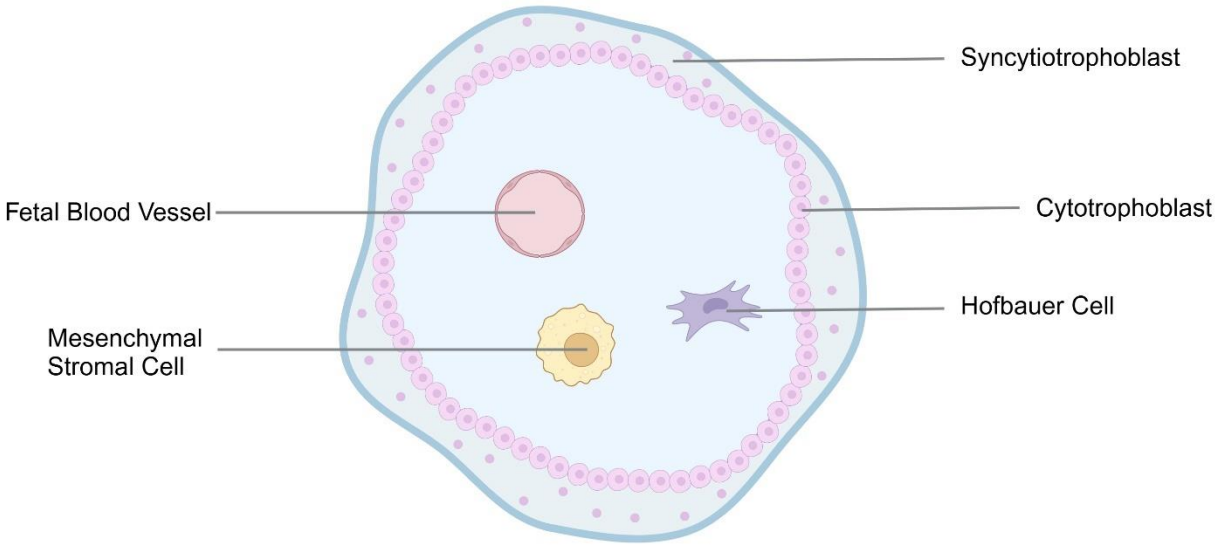

Figure 1 Cross section of the placental chorionic villi.

The key structures of the chorionic villi include fetal blood vessels, mesenchymal stromal cells, Hofbauer cells, cytotrophoblasts and the syncytiotrophoblast. Created using Biorender.com.

1.2.2 Placental Nutrient Transport in Healthy Pregnancy

Being at the interface between maternal and fetal circulations, the placenta also functions to exchange oxygen, carbon dioxide, nutrients and water between both circulations (64). The syncytium is in direct contact with the maternal circulation, where key nutrients are transported through the syncytial microvillous membrane (MVM). Nutrients are then transported through the syncytial basal membrane (BM) into the fetal circulation via the umbilical vein (80–82). Maternal-fetal nutrient transfer capacity of the placenta during gestation has a profound impact on fetal growth, where fetal size is predominantly positively correlated to placental size, function and levels of nutrient transfer (64).

1.2.2.1 Glucose Transport

Glucose is transported through the human placenta by facilitated diffusion via proteins known as GLUT transporters. There are 14 isoforms of the GLUT transporter which are further categorised into three classes; class I (GLUT1-4, GLUT14), class II (GLUT5, 7, 9, 11) and class III (GLUT6, 8, 10, 13). Interestingly, reports show that differently from the other GLUT transporters, GLUT12 is voltage dependent and plays a role in alpha-methyl-D-glucopyranoside transport (83).

GLUT1 is ubiquitously expressed in the placenta but is mostly found in the MVM of the syncytiotrophoblast (83,84). Moreover, gestational age influences the expression of GLUT1 found on the syncytiotrophoblast BM (85,86). GLUT3 is also mainly expressed on the syncytiotrophoblast MVM and similarly to GLUT1, GLUT3 levels are strongly associated with gestational age, where its expression markedly reduces as gestation advances. This suggests that GLUT3 is important to sustain fetal growth during early development when the placenta is maturing (83). GLUT4 is known as an insulin-regulated transporter which is predominantly localised in the syncytiotrophoblast and shows a similar reduction in expression throughout gestation (83). As well as the cytotrophoblast and syncytiotrophoblast, GLUT8 has also been found in extravillous trophoblasts, cultured trophoblasts and the HTR8/SVneo cell line (83). There are two sub-isoforms of GLUT9 (GLUT9a and GLUT9b) which play a key role in placenta uric acid transport but the mechanisms involved remain unknown (87). The localisation and function of

GLUT10 in the human placenta is less established than the other GLUT isoforms, however studies have suggested its involvement in promoter methylation throughout gestation (83). Similarly to GLUT4, GLUT12 is identified as an insulin-regulated transporter and therefore the localisation and expression of this isoform are associated with insulin activity. However, in contrast to GLUT4, studies have shown that GLUT12 glucose transport is ion-coupled, suggesting GLUT12 may influence additional functional outcomes in the placenta compared to GLUT4 (83,88).

1.2.2.2 Fatty Acid Transport

To an extent, saturated fatty acids and monounsaturated fatty acids can be synthesised by the fetus *de novo* via glucose. However, essential fatty acids (EFAs), linoleic acid (LA) and alpha-linolenic acid cannot be synthesised *de novo* and thus must be transported from the maternal circulation to the fetus during pregnancy (89). This is also true for long-chain polyunsaturated fatty acids (LC-PUFAs), as desaturase enzymes are absent in the placenta and insufficient in the developing fetus, thereby restricting the metabolism of EFAs to LC-PUFAs (89).

Although various maternal free fatty acids (FFA) can diffuse through the human placenta, a large proportion of maternal circulating FFAs are bound to lipoproteins and thus must undergo hydrolysis via the placental lipoprotein lipase enzyme for their release (89,90). Transporters then facilitate the uptake of these FFAs; these transporters are known as fatty acid binding proteins (FABPs), fatty acid transport proteins (FATPs) and fatty acid translocase (FAT), also referred to as CD63 (89,90). Reports also show that low-density lipoprotein (LDL) and high-density lipoprotein (HDL) receptors are localised in the placenta, allowing an additional mechanism for FFAs to be transported to the fetus following phospholipase A2 hydrolysis (89).

1.2.2.3 Amino Acid Transport

Placental amino acid uptake is mediated by specific transporters located in the syncytiotrophoblast (82). The uptake of various maternal amino acids is mediated

by accumulative transporters located at the MVM (82,91). However, following uptake, some amino acids may be exchanged for other amino acids via exchanger transporters (82,91,92). Non-exchange efflux transporters are also found in the syncytium to regulate amino acid net transport (82). Sodium-dependent transporters, including System A, ASC, N, $X_{GA,}$ β, $B^{o,+}$ and GLY, are localised in the placental syncytiotrophoblast, where they facilitate small neutral amino acid transport (91,92). Cationic amino acids uptake is mediated via y^+, $b^{o,+}$, y^+L and $B^{o,+}$ transport systems (92). The y^+L and $b^{o,+}$ systems are recognised as glycoprotein-associated transport systems, along with the asc, L, x_c^- and T transporter systems (91,92). The distribution and localisation of all transporter subtypes in the MVM and BM of the human placenta syncytiotrophoblast remain to be established. Moreover, amino acids may also be transported from the fetal circulation to the placenta via the syncytiotrophoblast BM (82,91,92).

1.3 microRNAs

1.3.1 microRNA Biogenesis

miRNAs are essential for most cellular and biological processes, including regulating placental development. miRNAs are temporal noncoding RNAs which modulate gene network expression post-transcriptionally by suppressing mRNA translation via signalling mRNA for degradation or deadenylation (93,94) (**Figure 2**). These single-stranded, 22-23 nucleotide-long miRNAs are highly conserved structures which are produced from a tightly regulated process. First a hairpin loop structure, known as primary(pri)-miRNA is transcribed from genic or intergenic (known as mirtrons) regions in the nucleus. These pri-miRNA are then processed to 60-70 nucleotide-long precursor (pre-) miRNA and then 22-23 nucleotide mature miRNA molecules through a sequence of events involving the endonucleases, Drosha and Dicer. Following the processing of pre-miRNA, it was previously thought that one strand of the miRNA duplex was degraded, leaving only one functionally active mature strand. However, it has now become apparent that both strands of the miRNA duplex are functionally active. As such, this has coined the -3p and -5p nomenclatures used to describe miRNAs, in order to

differentiate the mature miRNAs deriving from the 3’ and 5’ terminals of the pre-miRNA hairpin structure (95). Mature, functionally active miRNA strands then bind the 3’ -untranslated region (UTR), or in some instances, 5-UTR, of target messenger RNA (mRNA) to induce translational repression or mRNA degradation; reviewed in (94,96) (**Figure 2**). miRNAs work in tandem to regulate broad gene networks, resulting in pleiotropic downstream effects in the cell or tissue in which they reside. Interestingly, many miRNAs are temporally synthesised in a tissue-specific manner, including the placenta whereby distinct expression profiles are found at different stages of gestation (97–99), suggesting that miRNAs may play specific roles in the placenta. Indeed, several studies have shown that miRNAs are key regulators of placental development and function (97).

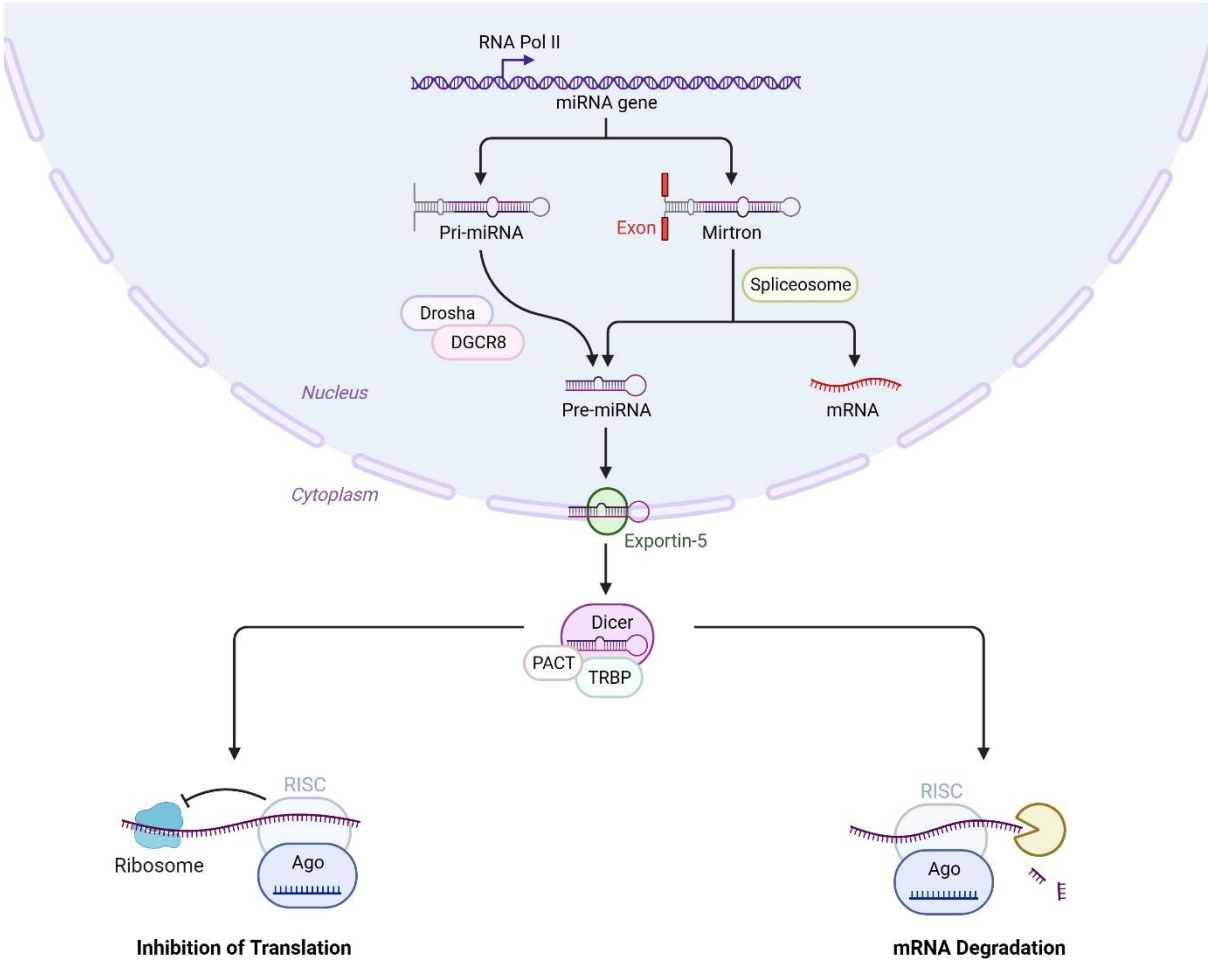

Figure 2 miRNA Biogenesis and Processing.

Primary (pri)-miRNA is synthesised from genic regions, which undergoes further processing by Drosha and DiGeorge syndrome critical region gene 8 (DGCR8) to form precursor (pre)-miRNA in the cell nucleus. Pre-miRNA may also directly derive from intergenic or 'mirtron' regions without Drosha involvement. Exportin-5 then transports pre-miRNA to the cytoplasm to be processed and matured by Dicer (RNAse III endonuclease) and its cofactors transactivation response element RNA binding protein (TRBP) and protein activator of interferon-induced protein kinase (PACT). miRNA is loaded into an RNA induced silencing complex (RISC) which leads to argonaute (Ago) catalytic protein recruitment, resulting in inhibition of translation or mRNA degradation (adapted from Huang, E. (2022). miRNA Processing Mechanisms in the Brain. Biorender.com). Created using Biorender.com.

1.3.2 microRNAs in the Placenta

Some of the most compelling evidence for a role of miRNAs in the placenta is evident from evolutionary studies. Recently, a group of 13 miRNA gene families have been shown to originate early in placental mammal evolution, suggesting a key role in processes specific to placental mammals (100). Whilst these miRNAs are expressed in many cells and tissues, evidence supporting this comes from a recent study showing that within the endometrium, some of these evolutionary conserved miRNAs have an important role in regulating the initial stages of implantation (101). Given their expression in the human placenta, it is likely that these miRNAs also play key roles in the placenta. Other evidence for a strong link between the evolutionary conservation of miRNAs across various placental mammals comes from work demonstrating that some miRNA genes arise from different evolutionary chromosomal clusters and are significantly or exclusively expressed in the placenta of various mammalian species (102).

The chromosome 19 miRNA cluster (C19MC) is a key maternally imprinted, primate specific, cluster found within the human placenta, where 46 genes encode 59 mature, placental-specific miRNAs (97,98,103,104). Indeed, miRNAs originating from C19MC are the predominant miRNAs found in term human trophoblasts and are key in regulating trophoblastic mRNA and protein profiles to maintain cellular homeostasis (103). Placental targets of C19MC miRNAs have also been mapped to functions associated with DNA binding, protein phosphorylation, cytokine response, oxidative stress and regulation of growth and apoptosis (104). It has been demonstrated that C19MC miRNA expression is elevated in villous trophoblasts compared to extravillous trophoblasts, contributing towards their phenotypic differences at various stages of pregnancy. Specifically, it is suggested C19MC miRNA expression during later stages of pregnancy contributes towards a reduction in extravillous trophoblasts invasion, a process which is most abundant during early gestation (105). More recently, C19MC miRNAs have been identified as fundamental for cellular pluripotency during early human development where C19MC miRNAs have been found to be expressed in human embryonic stem cells and as such, key for trophoblast differentiation and proliferation (106,107). The temporal expression pattern of the miR-371-3 cluster, located downstream to C19MC, during pregnancy is still

unclear, however this cluster is primarily expressed in placental tissue and is key for regulating cellular proliferation and apoptosis (108,109). Thus, the marked or exclusive expression of these miRNA clusters within the placenta suggests that they have key functional relevance in this organ.

The eutherian specific, paternally imprinted chromosome 14 miRNA cluster (C14MC) is another key cluster consisting of 52 miRNA genes which encodes 84 mature miRNAs that are mostly exclusively expressed in the placenta (110–113). This cluster is divided into genomic regions known as the miR-127/miR-136 and miR-379/miR-410 clusters (114). With C14MC being conserved with minimal structural changes from its derivative precursor sequence, it is suggested that C14MC miRNAs are vital for placental mammal evolution, playing a key role in embryonic development, RNA metabolism and transcriptional maintenance (109). The role of C14MC miRNAs in pregnancy is yet to be fully established, however the miR-127/miR-136 cluster has been shown to be involved in fetal capillary development and the miR-379/miR-410 cluster has been demonstrated to influence trophoblast proliferation and migration (114,115). Interestingly, C19MC and C14MC have opposing trends in trophoblastic expression during pregnancy, where C14MC expression is significant during early gestation before declining as gestation advances and C19MC expression is at its highest towards late gestation (116,117). This demonstrates the stage-specific roles of various miRNA profiles during gestation to ensure optimal placental growth (97). The factors involved in modulating the temporal miRNA profile in the placenta remain to be fully elucidated, however oxygen tension, epigenetic regulation as well as environmental toxins and signalling molecules are demonstrated to be key regulators (98,118).

Another cluster involved in placental development is miR-17/92. This cluster is not placenta-specific but consists of 6 miRNAs (miR-17, miR-18a, miR-19a, miR-19b, miR-20a, and miR-92a) which mediate key placental growth processes such as angiogenesis, trophoblast proliferation, spiral artery remodelling and cell cycle regulation (119,120). This cluster, alongside its paralog clusters, miR-106a-363, and miR-106b-25, modulate syncytiotrophoblast differentiation and aromatase levels via C-myc signalling, thus regulating cytotrophoblast hCYP19A1 and hGCM1 expression and hCG-β secretion (121). Evidence also points towards

miR-17/92 and miR-106a-363 clusters playing a role in trophoblast differentiation through the regulation of estrogen receptor α (ERα) (121). As such, expression of these cluster miRNAs is elevated during early pregnancy as cytotrophoblast differentiation and proliferation is active, whereas late pregnancy shows low levels of these cluster miRNAs as syncytiotrophoblasts terminally differentiate and placental vascularisation decreases (121).

Whilst there is a clear evolutionarily conserved role for some placental miRNAs, more than 2000 mature miRNAs have been detected in the human placenta and the vast majority of these are highly conserved across different cells and tissues, likely due to their roles in key physiological or homeostatic processes. Indeed, the top four most abundant placental miRNAs (miR-30d-5p, miR-100-5p, miR-143-4p and miR-21-5p) play significant roles in tissues beyond the placenta (78,122–126). miR-30d has been associated with cancer progression and cardiac hypertrophy (127,128). miR-100-5p is known to regulate skeletal muscle myogenesis (129) and miR-143-3p has been demonstrated to regulate vascular smooth muscle differentiation and modify autophagy in endometrial stromal cells (130,131). miR-21 is highly conserved and is almost ubiquitously expressed, where its abundance has been associated with HTR8/SVneo cell proliferation and pregnancies complicated by preeclampsia (132,133). It has also been shown that miR-21 plays a key role in epithelial-mesenchymal transition (134). There are other various regulatory miRNAs which are key for placental development (107), some of which include; let-7a and miR-145, which regulate trophoblast proliferation and vascular development and cell turnover of other tissues (78,122–126); miR-96-5p which regulates proliferation and migration of trophoblasts as well as in vascular smooth muscle cells (135,136); miR-29a which regulates muscle and skeletal function and homeostasis, immune system modulation and haematopoiesis of various tissues (137,138); and miR-125b which regulates trophoblast migration and invasion, as well as playing a role in mitochondrial biogenesis and adipocyte development and function (139,140). Given the abundance of other miRNAs in the placenta and evidence that several are altered in pregnancy complications such as fetal growth restriction, other yet unreported roles for miRNAs is likely. Indeed miR-16, miR-21 and miR-199a are examples of this. These miRNAs are associated with fetal growth and whilst their

functional roles in the placenta remain to be established, these miRNAs regulate insulin sensitivity and glucose metabolism in other cells and tissues (141–146). Exploring these roles in the placenta would further our understanding of the currently unreported roles of various miRNAs in pregnancy.

The placental angioarchitecture potentially leaves placental capillaries susceptible to various environmental stimuli found in the maternal circulation (147). As a result, pregnancies complicated by maternal diabetes manifest distinct placental hallmarks that may affect feto-placental nutrient transfer and fetal growth.

1.3.3 Placental Development in Pregnancies Complicated by Maternal Diabetes

The increasing prevalence of maternal hyperglycaemia during pregnancy has given rise to extensive research on the effects of diabetes on placental development and fetal health. It is already established that altered fetal growth in pregnancies complicated by maternal diabetes is associated with altered placental development (148). Generally, diabetic pregnancies present with alterations in placental villous maturity, angiogenesis and placental weight (148,149). Not only does the placenta adapt histologically and molecularly with PGDM and GDM, but these morphological changes also contribute towards altered uteroplacental blood flow which in turn impact fetal nutrient and oxygen supply. Indeed, uteroplacental flow adaptions have been associated with altered fetal growth, and T1DM, T2DM and GDM pregnancies all demonstrate placental hallmarks which contribute towards feto-placental malperfusion (150–157). To date, most studies reporting the impact of maternal diabetes on the placenta have focussed on GDM. However, even in the limited studies available for T1DM and T2DM pregnancies, it is clear that different types of diabetes exert distinct phenotypic differences on the placenta. As such, it is also important to consider the effect of both GDM and PGDM on placental development.

1.3.3.1 Gestational Diabetes Mellitus

In contrast to uncomplicated pregnancies, GDM manifests with placental histological adaptions such as villous immaturity, villous oedema, decidual vasculopathy, chorangiosis, fibromuscular sclerosis, villous agglutination, retroplacental hemorrhage, altered fibrinoid necrosis, increased volume of intervillous space, terminal villous volume and surface area, as well as increased syncytiotrophoblast turnover and knotting (11,158–161). These changes, along with altered placental amino acid and lipid transport result in aberrant feto-placental nutrient transfer (11). Altered DNA methylation patterns and differentially expressed genes associated with cell death and activation, immune response and organ development have also been characterised in the placentae of those with GDM compared to uncomplicated pregnancies (162–164). Other

hallmarks of GDM placentae altered oxidative stress and autophagy, mitochondrial dysfunction and placental macrophage (Hofbauer cell) accumulation, resulting in increased expression of inflammatory factors (165–171).

1.3.3.2 Type-1 Diabetes Mellitus

Various studies have demonstrated that T1DM pregnancies present with unique placental hallmarks associated with altered vascularisation which have not been reported in the placentae of those with GDM. These alterations include increased vascular leakiness, and increased capillary diameter, branching and capillary wall elongation, resulting in a higher villous volume and surface area (172–174). Accelerated villous maturation is also more prominent in T1DM placentae compared to GDM (175). Interestingly, placental GLUT1 protein expression is also higher in T1DM pregnancies compared to GDM and has been positively correlated to fetal weight (176), suggesting altered glucose transfer. Although placentae of T1DM do not manifest as many lipid modifications as GDM, placental glycosylation and acylation pathways are more pronounced (177). In contrast to GDM, people with T1DM manifest hyperglycaemia prior to conception and during early pregnancy. As such, these findings suggest that glucose and lipid metabolism, as well as glycosylation and acylation pathways in the placenta may be more sensitive to diabetic stimuli during early gestation rather than later in pregnancy. This may also be the case for placental vascularisation and villous maturation, where individuals with GDM do not present with these placental morphologies. Although it is not fully established whether these hallmarks are altered during early pregnancy/first trimester placenta of people with T1DM, it has been demonstrated that hyperglycaemia reduces first-trimester trophoblast turnover in T1DM placentae (178). Further studies are needed to elucidate the broader effects of the T1DM diabetic milieu on the placenta in early pregnancy.

It is thought that the duration of T1DM may be associated with adverse outcomes during early pregnancy. Indeed, impaired placental extracellular matrix remodelling is a feature of T1DM pregnancies which has been shown to be augmented in longer-term T1DM mouse models (179–181). Another feature of

T1DM pregnancies is altered placental cellular stress (182). Markedly reduced placental aerobic respiration activity and upregulated hydrogen peroxide levels are observed in individuals with T1DM compared to BMI-matched normoglycaemic people (183). However, T1DM placentae illustrate protective mechanisms against oxidative stress compared to GDM, where there is increased glutathione peroxidase activity, higher abundance of reduced glutathione and lower levels of oxidised glutathione (184). Perhaps these protective mechanisms in T1DM may be as a consequence of longer-term adaptations to the diabetic milieu from conception, compared to those with GDM who are exposed to a diabetic environment for a shorter duration later in pregnancy and thus have a brief time-frame to develop protective adaptations in the placenta. This interpretation may also explain why placental infarcts were observed to be less abundant in T1DM pregnancies compared to GDM (150). However, T2DM pregnancies also manifest with maternal hyperglycaemia as early as conception and interestingly, more infarcts were observed in the placentae of people with T2DM than T1DM (185). It is possible that this finding may reflect study design, where pregnancy loss was not captured and only surviving pregnancies with fewer abnormalities were included in the study. T1DM is associated with more extreme first-trimester hyperglycaemia, congenital abnormalities and pregnancy loss than T2DM, and therefore perhaps this led to the collection of healthier placental samples of T1DM pregnancies compared to T2DM (185).

Another placental feature of T1DM pregnancies is heightened baseline vascular tone. It is thought that this may be a result of increased nitric oxide (NO) pathway activity in diabetes, unrelated to insulin levels (186). Altered uterine NO-mediated vasodilation has been demonstrated in pregnant mice with GDM, where augmented superoxide levels may promote increased NO scavenging (187,188). Aberrant adenosine-stimulated vasocontractility has also been identified in the feto-placental vasculature of GDM and T1DM pregnancies (189). However, further research is needed to investigate whether altered placental NO activity applies for GDM and T2DM pregnancies or is unique to T1DM. Moreover, systemic endothelial dysfunction has been associated with PGDM and GDM pregnancies (190,191).

Despite intensive strategies to achieve normoglycaemia in pregnant individuals with T1DM, these pregnancies still manifest distinct placental hallmarks contributing towards adverse fetal outcomes compared to GDM and healthy, uncomplicated pregnancies. As such, more studies are needed to explore the mechanisms contributing towards altered placental morphologies in T1DM pregnancies.

1.3.3.3 Type-2 Diabetes Mellitus

T2DM pregnancies are characterised by upregulated placental glucose, amino acid and fatty acid transporter expression compared to BMI-matched normoglycaemic pregnancies (192,193). This highly suggests that feto-placental nutrient transfer and metabolism are altered in T2DM. With T2DM being a heterogenous condition that is predominantly associated with adiposity, it is possible that the altered placental nutrient transfer observed in these individuals may reflect maternal nutrient excess that is associated with T2DM pregnancies. As such, it is reasonable to assume that pathological placental development in individuals with T2DM may be driven by metabolic disturbances of various metabolic tissues rather than pancreatic dysfunction exclusively. Indeed, lipoperoxidation is another placental feature of T2DM pregnancies, as well as placental calcification which is mostly identified in T2DM compared to T1DM and GDM pregnancies (193,194). These placental hallmarks have been associated with maternal adiposity in mice, where increased placental labyrinth lipid peroxidation and calcification have been identified in male offspring of obese dams (195). Moreover, placental calcification has been identified as a predictor of suboptimal uteroplacental flow (196) and this is further evidenced by the increased prevalence of decidual vasculopathy in T2DM compared to GDM pregnancies (150).

Maternal obesity has also been demonstrated to influence placental labyrinth adaptations to cellular stress (195). It is possible that this could be a response to the altered placental aerobic respiratory activity that is observed in people with T2DM (183). Inflammation is another feature mostly associated with T2DM pregnancies compared to T1DM and GDM (194). This hallmark is consistent with

placental features of pregnancies complicated by maternal obesity, where it is suggested that increased inflammation may be a response to exacerbated cellular oxidative stress and altered metabolism (197).

Moreover, similarly to T1DM, accelerated placental villous maturation has also been identified in T2DM pregnancies (175,176). Disorders of villous maturity are associated with fetal death (198) and it has been demonstrated that PGDM increases the risk of stillbirth, where obesity can amplify this risk (22). These findings, along with the altered placental glucose metabolism identified exclusively in PGDM pregnancies (176,192) further suggest that placental glucose transport and villous maturation may be most susceptible to the maternal diabetic milieu at earlier stages of pregnancy. Additional studies on first trimester placental tissue are required to validate the effects of PGDM on adverse fetal outcomes compared to GDM pregnancies.

1.3.3.4 Factors Contributing Towards Placental Pathology in Diabetes

In-utero hyperglycaemia is inherent to GDM, T1DM and T2DM pregnancies. However, each diabetes type demonstrates a distinct set of placental features. This is unsurprising given the variance in clinical manifestations and pathophysiological characteristics belonging to each type and thus suggests that factors other than glucose may contribute towards placental phenotypic adaptations in diabetes. This is further supported by studies showing that individuals with well-managed glucose levels still manifest with pathological placental hallmarks (199–201). These changes in the placenta could potentially be explained by the increasing evidence demonstrating that in addition to glycaemic control, fetal sex, maternal weight, ethnicity and the underlying pathophysiology and duration of the diabetes types, can all contribute towards distinct pathological hallmarks (149,181). Moreover, factors found in the maternal circulation may affect placental development and contribute towards altered fetal growth in pregnancies complicated by maternal diabetes.

1.3.4 microRNAs in Pregnancies Complicated by Maternal Diabetes

1.3.4.1 Placental miRNAs

To date, no studies have investigated the placental miRNA profile in PGDM pregnancies, however, many studies have identified an altered placental miRNA profile in GDM pregnancies compared to healthy pregnancy (Table *2*). Whilst the mechanisms through which a diabetic environment alters placental miRNA levels remain to be elucidated, it is clear that miRNAs have an integral role in feto-placental development and that they may contribute to adverse outcomes in these pregnancies.

Using various models, it has been established that miRNAs that have been identified to be altered by maternal diabetes in placental tissue have many overlapping targets; sharing functional hallmarks associated with placental growth, insulin signalling, glucose metabolism, inflammation and vascular development (127,202–232) (**Table *2***, **Figure *3***). Indeed, among these dysregulated miRNAs is miR-9, which has also demonstrated to regulate human umbilical vein endothelial cell (HUVEC) angiogenesis, proliferation, migration and invasion (233). Additionally, people with GDM not only demonstrate dysregulated miR-222 expression in their placental tissue but also in their adipose tissue (215,234,235). Interestingly, this miRNA is a key regulator of ERα expression in estrogen-induced insulin resistance (235). miR-503 is another dysregulated miRNA found in the placenta of individuals with GDM (230). This miRNA regulates inflammation-mediated angiogenesis, where hyperglycaemia increases its expression in HUVECs (230,236–238). In addition to altered vascular function, various other hallmarks in the GDM placenta are known to be closely associated with altered fetal growth and therefore suggest possible mechanisms linking maternal diabetes to altered fetal growth (239–243).

Table 2 Altered Placental miRNA Regulation and Their Known Targets and Functional Outcomes in Pregnancies Complicated by Maternal Diabetes.

Diabetes Type	miRNA Regulation	Model	Target	Functional Outcome	Ref.
GDM	↓ miR-29b	Human placental tissue and HTR-8/SVneo cells	↑ HIF3A	↑ cell migration and invasion	(203)
GDM	↓ miR-143	Human placental tissue and primary syncytiotrophoblast	↓ PPARγ ↓ PGC1α ↑ hPL ↑ GLUT1 ↑ mTOR	↓ mitochondrial respiration	(204)
GDM	↓ miR-21	Human placental tissue and HTR-8/Svneo cells	↑ PPARα	↓ cell growth and infiltration	(205)
GDM	↑ miR-518d	Human placental tissue and HEK-293T cells	↓ PPARα	Altered fatty acid and glucose metabolism	(206)
GDM	↑ miR-98	Human placental tissue, JEG-3 and HEK-293T cells	↓ MeCP2 ↓ TRPC3	↑ global DNA methylation ↓ insulin-mediated- uptake of glucose	(207)
GDM	↓ miR-138-5p	Human placental tissue and HTR-8/Svneo cells	↑ *TBL1X*	↑ cell proliferation and placental growth	(208)
GDM	↓ miR-9 ↓ miR-22	Human placental tissue, primary syncytiotrophoblast, HEK-293T and HTR-8/Svneo cells	↑ *GLUT1* ↑ *HK2*	↑ glucose uptake, lactate secretion and cell viability ↓ apoptosis	(234)
GDM	↑ miR-140-3p	Human placental tissue and umbilical vein endothelial cells, HEK-293T and HTR-8/Svneo cells	↓ IR-α ↓ IGFR1	Defective insulin receptor signalling	(209)
GDM	↓ miR-132	Human placental tissue and BeWo and HTR-8/Svneo cells	PTEN	↓ cell proliferation	(210)
GDM	↓ miR-6795-5p	Human placental tissue, HEK-293T and HTR-8/Svneo cells	PTPN1	Altered insulin signalling, cell growth and glucose metabolism	(211)
GDM	↑ miR-136	Human placental tissue, BeWo and HTR-8/Svneo cells	↓ E2F1	↓ cell proliferation	(212)
GDM	↓ miR-345-3p	Human placental tissue, HEK-293T and HTR-8/Svneo cells	↑ BAK1	↑ apoptosis ↓ proliferation and migration	(213)
GDM	↑ miR-95 ↑ miR-548am ↓ miR-1246	Human placental tissue	↓ GLUT1 ↓ GLUT3 ↓ GLUT4	Aberrant insulin signalling pathway	(214)

GDM	↓ miR-22 ↓ miR-372	Human placental tissue and HTR-8/Svneo cells	↓ GLUT4	Aberrant insulin signalling pathway	(215)
GDM	↓ miR-30d-5p	Human placental tissue and HTR-8/Svneo cells	↑ RAB8A	↑ cell proliferation, migration, invasion and glucose uptake	(127)
GDM	↑ miR-1323	Human HTR-8/Svneo and BeWo cells	↓ TP53INP1	↓ cell viability	(216)
GDM	↑ miR-657	Human placental mononuclear macrophages and THP-1 cells	↓ FAM46C	↑ cell proliferation, migration and polarisation towards M1 phenotype	(217)
GDM	↑ miR-199a	Human placental tissue and JEG-3 cells	↓ MeCP2 ↓ TRPC3	Altered methylation patterns and glucose metabolism	(218)
GDM	miR-195-5p	Human pulmonary microvascular endothelial cells and mouse placental tissue	↓ VEGFA	↑ endothelial cell dysfunction	(219)
GDM	↓ miR-6869-5p	Human placental mononuclear macrophages and THP-1 cells	↑ PTPRO	↓ cell proliferation, inflammatory response ↑ polarisation towards M2 phenotype	(220)
GDM	↑ miR-101	Human umbilical vein endothelial cells	↓ EZH2	↓ gene transcription	(221)
GDM	↑ miR-134-5p	HTR-8/Svneo and HEK-293T cells	↓ FOXP2	↑ inflammation and apoptosis	(222)
GDM	↑ miR-137	Human umbilical vein endothelial cells, U937 and THP-1 cells	↑ CCL2	↓ cell viability and angiogenesis ↑ inflammatory cytokine secretion, cell activation, monocyte chemotaxis and adhesion	(223)
GDM	↓ miR-9-5p	Human placental tissue and primary syncytiotrophoblast	↑ HK2 ↑ GLUT1 ↑ PFK ↑ LDH	Altered aerobic glycolysis and mitochondrial complex expression	(224)
GDM	↑ miR-195-5p	Human umbilical vein endothelial cells and HEK-293T cells	↓ EZH2	↓ cell proliferation and viability ↑ apoptosis	(225)
GDM	↓ miR-96-5p	Human placental tissue and HTR-8/Svneo cells	-	↓ cell viability	(226)
GDM	↓ miR-193b	HTR-8/Svneo cells	↑ IGFBP5	↑ autophagy and apoptosis	(227)
GDM	↑ miR-34b-3p	Human umbilical vein endothelial cells	↓ PDK1	↓cell viability and migration	(228)

GDM	↑ miR-190b	Human placental tissue, Min6 cells and mouse β-cells	↓ NKX6-1	↓ cell activity, proliferation, islet insulin secretion	(229)
GDM	↑ miR-503	Human placental tissue, INS-1 and HEK-293T cells	↓ mTOR	Pancreatic β--cell dysfunction	(230)
GDM	↑ miR-144 ↓ miR-125b	Human placental tissue	-	Abnormal glucose metabolism	(231)
GDM	↓ miR-96	Human placental tissue, INS-1 and HEK-293T cells	↑ PAK1	↓ insulin secretion and β-cell function	(232)
GDM and T2DM	↓ miR148a-3p ↓ miR29a-3p	Human placental tissue and umbilical vein endothelial cells	AMPKα1 IGFR1 IRS1/2 PPARγ PI3K	Altered insulin signalling and glucose metabolism	(202)
T1DM	*No studies identified.*				
T2DM	*No studies identified.*				

AMPK; Adenosine Monophosphate-Activated Protein Kinase, BAK; BCL-2 Homologous Antagonist Killer, CCL; C-C Motif Chemokine Ligand , E2F1; E2F Transcription Factor 1, EZH2; Enhancer of Zeste 2 Polycomb Repressive Complex 2 Subunit, FAM46C; Family with Sequence Similarity 46, Member C, FOXP; Forkhead Box Protein P, GALNT; Polypeptide N-Acetylgalactoaminyltransferase, GLUT; Glucose Transporter, HIF; Hypoxia-Inducible Factor, HK; Hexokinase, hPL; Human Placental Lactogen, IGFBP; Insulin-Like Growth Factor-Binding Protein, IGFR; Insulin-Like Growth Factor, IR; Insulin Receptor, IRS; Insulin Receptor Substrate, LDH; Lactate Dehydrogenase, MeCP; Methyl CpG Binding Protein, mTOR; Mammalian Target of Rapamycin, NKX6-1; NK6 Homeobox 1, PAK; p21-Activated Kinase, PDK; Pyruvate Dehydrogenase Kinase, PFK; Phosphofructokinase, PGC; Peroxisome Proliferator-Activated Receptor-γ Coactivator, PI3K; Phosphoinositide 3-Kinase, PPAR; Peroxisome Proliferator-Activated Receptor, PTEN; Phosphatase and Tensin Homolog, PTPN; Protein Tyrosine Phosphatases, Non-Receptor Type, PTPRO; Protein Tyrosine Phosphatase Receptor Type O, RAB8A; Ras-Related Protein Rab-8A, TBL1X; Transducin β Like 1 X-Linked, TP53INP; Tumour Protein p53-Inducible Nuclear Protein, TRPC; Transient Receptor Potential Channel, VEGF; Vascular Endothelial Growth Factor.

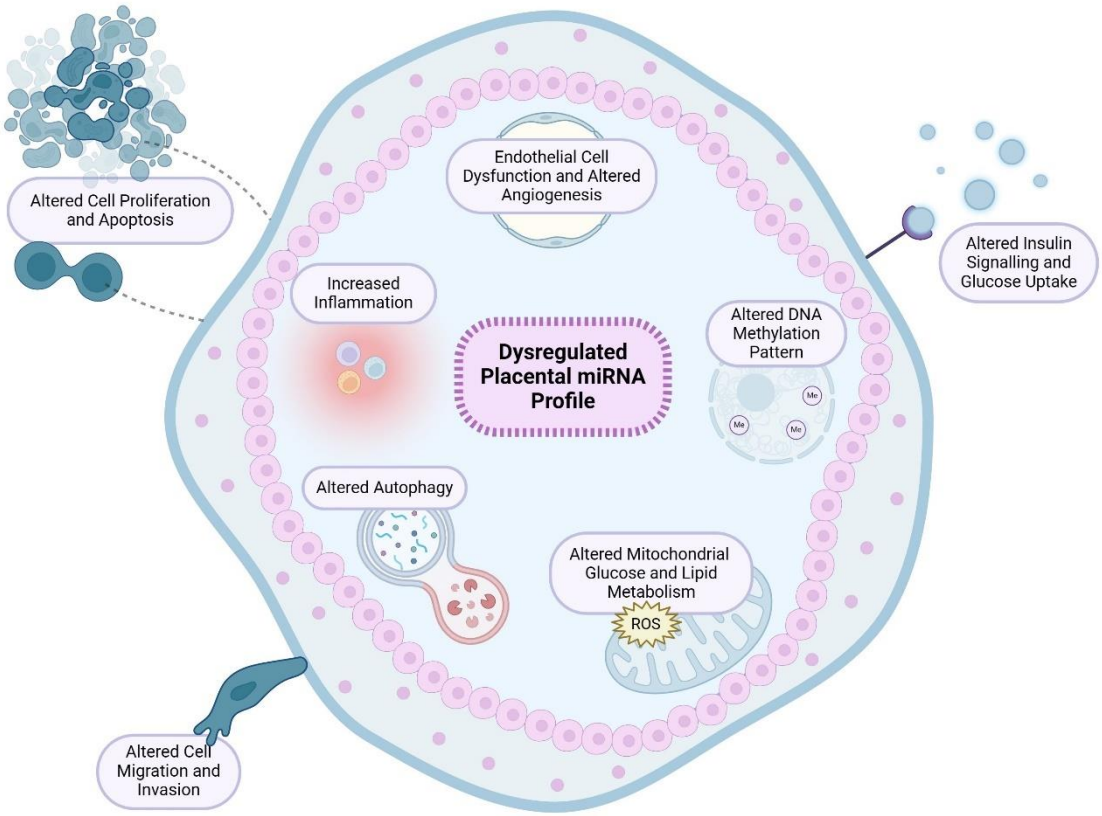

Figure 3 Effect of Maternal Diabetes on Placental miRNA Profile and Functional Outcomes.

Pregnancies complicated by maternal diabetes are associated with a dysregulated placental miRNA and proteomic profile. As a result, studies have identified maternal diabetes leads to alterations in placental growth, insulin signalling and glucose uptake, epigenetic regulation, cell migration and invasion, vascular development, inflammation, autophagy and mitochondrial metabolism (244). Created using Biorender.com.

1.3.4.2 Aetiology of Altered miRNA Profiles in the Placenta

The aetiology of altered placental miRNA expression in maternal diabetes remains unclear. One possible mechanism is that maternal diabetes may be characterised by aberrant miRNA biogenesis. Previous research shows placental Dicer dysregulation leads to changes in trophoblast proliferation, suggesting Dicer-dependent miRNAs are involved in regulating placental development (245). Similar findings have been observed in the placentae of people with GDM, where Dicer, Drosha and DGCR8 expression are found to be altered, leading to changes in miRNA biogenesis (246). Nonetheless, given that the majority of miRNAs are Dicer, Drosha and DGCR8-dependent miRNAs, this is unlikely to explain why only specific miRNAs are altered in the placenta of individuals with maternal diabetes. An alternative hypothesis is that high glucose levels, or other components of the diabetic environment, may be directly altering miRNA expression in the placenta and various maternal tissues. In turn, miRNAs may be important mediators between glucose fluctuations and downstream functional effects in the placenta. Of interest, many of the miRNAs with key roles in feto-placental growth and regulation are known to be glucose sensitive, which is an important consideration in pregnancies complicated by maternal diabetes (136,138,140,142,143,247–250). Not all studies report the status of maternal glucose control, however, variation in the placental hallmarks observed in T1DM, T2DM and GDM pregnancies suggests factors other than glucose may be involved. This is further evidenced by a previous report demonstrating that people with T1DM who have a well-controlled glycaemic profile manifest similar placental pathologies to those with sub-optimal glycaemic control (251). With T2DM being associated with maternal adiposity and thus increased influence of lipids and adipokines (3), this further exemplifies the differences in the diabetic milieu across the various diabetic subtypes. Indeed, other maternal macro- and micronutrients that are altered in maternal diabetes, such as folate and vitamin B12 levels, have capacity to alter placental development and miRNA expression (252–254). In addition, maternal ethnicity, diet, exercise, medication, infection, age, socioeconomic status and gestational age have all been identified as factors which influence placental miRNA regulation (255).

1.4 Extracellular Vesicles

In addition to considering the role of miRNAs that are detected in the placenta, the role of miRNAs in the circulation should also be considered. Whilst miRNAs are transcribed and functionally active in their tissue of origin, they can be released into circulation encapsulated in extracellular vesicles (EVs). EVs are produced from all cells and tissues and can be subcategorised according to size, biogenesis, density, molecular composition or cellular origin into the following classes; small EVs (typically <200 nm in diameter) and large EVs (typically >200 nm in diameter) (256–258). EVs contain DNA, miRNAs, mRNAs, proteins and lipids, with their cargo reflecting phenotypic hallmarks of their cell of origin (**Figure *4***) (259,260). As such, EVs and their cargo demonstrate potential as biomarkers for different pathological conditions. However, other 'hormonal-like' roles for EVs are also emerging. When released from cells, EVs can be transported into local and distal cells via a range of mechanisms, such as clathrin-dependent and clathrin-independent endocytosis, lipid raft-mediated internalisation, phagocytosis and macropinocytosis (261) and thus can influence the transcriptome of target cells. This change in transcriptome may be mediated via the miRNA cargo of EVs. As such, EV-mediated transport in the human circulation allows systemic bidirectional interorgan crosstalk via miRNA regulation (259).

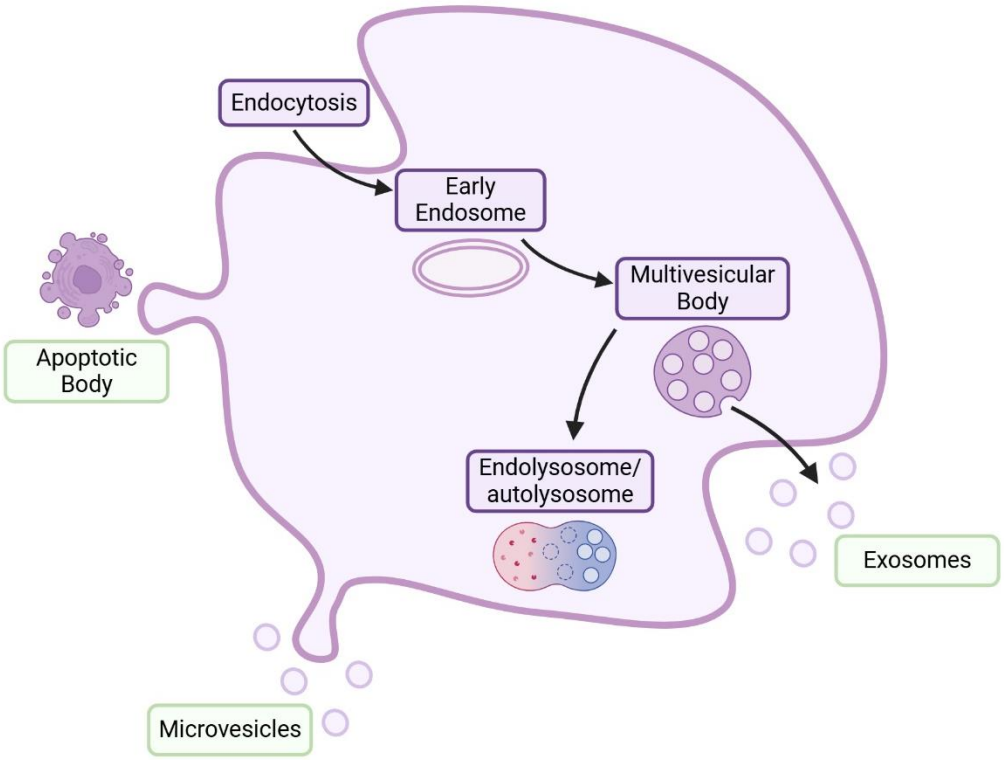

Figure 4 Extracellular Vesicle Biogenesis.

Extracellular vesicles are characterised according to their biogenesis. Exosomes (30-150nm) are derived from the budding of the endosome following endocytosis, to form multivesicular bodies (MVBs) which contain intraluminal vesicles which then fuse with the plasma membrane to be released as extracellular vesicles. Microvesicles (100-1000nm) are synthesised through budding of the plasma membrane. Apoptotic bodies (50-5000nm) are released during apoptosis. Depending on their size, extracellular vesicles are classed as 'small' (<200 nm) or 'large' (>200 nm) (260). Created using Biorender.com.

1.4.1 Extracellular Vesicles and the Placenta

It has been reported that the concentration of EVs in the maternal circulation is increased in pregnancy, and that placental-derived EVs play a key role in regulating maternal glucose homeostasis (262–264). Interestingly, EV-labelling techniques in *in-vivo* murine models have shown that placental EVs can interact with various maternal cells and tissues, including endothelial and immune cells, lung, kidney and liver (262). This suggests that placenta-derived EVs may also have other important roles in regulating maternal homeostasis during pregnancy. Moreover, EV size may affect the distribution pattern of placental EVs to various maternal organs (262). As such, the overall functional effect of placental miRNAs on wider maternal or fetal metabolic organs remains to be elucidated.

Whilst the specific EV cargo involved in these interactions have not been fully elucidated, several studies suggest that they are likely attributed to miRNAs. Indeed, the presence of trophoblast-specific C19MC and non-C19MC miRNAs in the maternal circulation during pregnancy has been reported (115,265,266) and placenta-derived EV miRNA profiles have been shown to be altered with gestational age (267,268). Functional roles for placental derived EV miRNAs have also been reported. Indeed, EV-encompassed C19MC and miR-17-92 cluster miRNAs have been shown to play immunomodulatory roles during pregnancy by influencing events in maternal immune cells (103,269–271).

While the concept of feto-maternal signalling via EVs and their miRNA cargo is well regarded in the literature, evidence is also emerging for a role of EVs and their cargo in maternal-placental communication. Indeed, EV labelling techniques have demonstrated bidirectional EV interorgan crosstalk between placental and maternal tissues (272). The functional consequence of maternal-placental EV communication has also been established, where maternal macrophage EVs have shown to regulate placental cytokine levels (272). It has also been demonstrated that placental glucose metabolism is impacted by maternal adipose tissue EVs (259). Whilst the EV cargo responsible for exerting these maternal-placental effects of EVs has yet to be established, there are reports that miRNAs released from maternal organs can traffic into placental and fetal tissues to influence feto-placental development (259,265,273). Recent work within our group also supports this hypothesis (274–276). It is therefore possible that whilst

many miRNAs are produced by the placenta, others mature miRNAs present in the placenta are a consequence of being transported to the placenta from maternal (or fetal) circulations, and that these may be altered in pathological conditions.

1.4.2 Extracellular Vesicles in Pregnancies Complicated by Maternal Diabetes

Although no studies have investigated the expression of EV-encompassed miRNAs in PGDM pregnancies, several EV-encompassed miRNAs have been shown to be altered in the maternal circulation in pregnancies complicated by GDM (268,277). Whilst the tissue source of the majority of miRNAs in maternal circulation in GDM is unknown, it is likely that they originate from both maternal and placental tissue.

Indeed, this is supported by the observation that whilst individuals with GDM have lower circulating levels of placenta-derived small EVs compared to pregnant individuals without diabetes, the overall level of EVs in maternal circulation is higher in GDM compared to those without diabetes (278). This could suggest that the diabetic environment may be altering the release of various maternal organ EVs and their miRNA cargo into the circulation. Indeed, it has been shown that the hyperglycaemic component of the diabetic environment can modulate EV secretion and their miRNA cargo (263). Some studies suggest that these changes in EV-miRNA cargo are protective adaptations against a hyperglycaemic environment (277). However, it has also been postulated that EV-miRNAs may be involved in the pathogenesis of GDM where changes to EV-miRNA profiles have been detected in early pregnancy, prior to the diagnosis of GDM (268). It remains to be established whether miRNAs that circulate to the placenta via EVs contribute towards altered placental development in pregnancies complicated by maternal diabetes, and if so, whether they originate from specific maternal organs. Considering the tissue-of-origin of circulating miRNAs may help to delineate this.

Moreover, the proportional reduction in placenta-derived small EVs in the maternal circulation of individuals with GDM could also suggest that the diabetic

environment reduces placental tissue EV release and biogenesis. Studies have shown that placenta-EV miRNA profile is altered in pregnant people with maternal diabetes. The functional effects of these miRNAs have been associated with cell proliferation, migration, angiogenesis, inflammation and glucose metabolism (**Table *3***) (267,268,279–282). It remains to be established whether the effects of these placenta-derived EV-miRNAs in pregnancies complicated by maternal diabetes are limited to maternal organs or if they extend to fetal tissues. However, with placenta-derived EVs being able to interact with various maternal metabolic tissues and regulate maternal glucose homeostasis (262–264), it is possible that the altered placental EV release and miRNA content stimulated by the diabetic milieu may lead to changes in maternal metabolism and contribute towards GDM. Recent evidence shows that placenta-derived EVs from GDM pregnancies manifest an altered miRNA profile which is associated with aberrant insulin signalling and altered primary skeletal muscle cell insulin-stimulated migration and glucose uptake (267,268,282) (**Table *3***). As such, these findings suggest that placenta-derived EV-miRNAs likely play a role in influencing maternal metabolism in GDM.

Not only is the secretion and miRNA cargo of placenta-EVs affected by maternal diabetes, but evidence also suggests that EV production by maternal metabolic organs may be affected, which can in turn influence placental metabolism and maternal health in GDM (260). Indeed, Nair et al. have demonstrated that continuous infusion of human maternal EVs from GDM pregnancies into healthy non-pregnant mice reduces pancreatic islet glucose-stimulated insulin secretion and promotes glucose intolerance, where skeletal muscle miRNA expression and glucose sensitivity are altered (282). EVs derived from the adipose tissue of pregnant individuals with GDM have demonstrated to impact glucose metabolism in placental cells, causing alterations in glycolytic, gluconeogenic and glycogen storage processes (260). While this study does not ascribe the effects of these adipose tissue-EVs to miRNA activity, glucose-sensitive miRNAs have been reported in adipose tissue which may impact insulin sensitivity (283). In people with GDM, adipose tissue miRNA profile is altered; miR-222 was found to be upregulated and suggested to be a key regulator of insulin resistance (235). Placenta-derived EVs from individuals with GDM also showed altered expression

levels of this miRNA (267). Another recent study suggested that maternal visceral fat thickness may predict the risk of developing GDM via adipose tissue derived EV-miR-148 family signalling (284). Interestingly, it has been previously reported that miR-148 is altered in placental tissue of those with GDM and T2DM, with its targets associated with insulin signalling and glucose metabolism (202). As such, maternal diabetes has a significant influence on maternal organ EV-miRNA cargo which could contribute towards altered feto-placental development.

Table 3 Altered Maternal and Placental EV miRNAs and Their Known Targets and Functional Outcomes in Pregnancies Complicated by Maternal Diabetes.

Diabetes Type	miRNA Regulation	Source	Target	Functional Outcome	Ref.
GDM	↑ miR-135a-5p	Maternal plasma EVs (including characterisation of placenta-derived EVs based on PLAP expression)	↑ SIRT1	↑ trophoblast proliferation, invasion and migration	(279)
GDM	↑ miR-130b-3p	Secreted EVs from cultured placental MSCs	↓ ICAM-1	↑ HUVEC proliferation, migration and angiogenesis	(280)
GDM	↓ miR-140-3p ↓ miR-574-3p	Secreted EVs from cultured placental villous explants	↓ VEGF	↑ cell proliferation, migration and tube formation	(281)
GDM	↑ miR-125a-3p ↑ miR-224-5p ↑ miR-584-5p ↑ miR-186-5p ↑ miR-22-3p ↑ miR-99b-5p ↑ miR-433-3p ↑ miR-197-3p ↑ miR423-3p ↓ miR-208a-3p ↓ miR-335-5p ↓ miR-451a ↓ miR-145-3p ↓ miR-369-3p ↓ miR-483-3p ↓ miR-203a-3b ↓ miR-574-3p ↓ miR-144-3p ↓ miR-6795-5p ↓ miR-550a-3-3p ↓ miR-411-5p ↓ miR-550a-3-3p ↓ miR-140-3p	Secreted EVs from cultured placental villous explants	-	↓ primary skeletal muscle cell insulin-stimulated migration and glucose uptake	(282)
GDM	↓ miR-516-5p ↓ miR-517-3p ↓ miR-518-5p ↓ miR-222-3p ↓ miR-16-5p	Maternal urine EVs (including characterisation of placenta-derived EVs based on PLAP expression)	IRS4 GALNT RECK ALG3 AKT3 TIMP3 KIT L2HGDH KI2FC RAP1 HOXC8 PD-L1	Altered insulin signalling, metabolic homeostasis and inflammatory response	(267)

GDM	↑ miR-520h ↑ miR-1323 ↑ miR-136-5p ↑ miR-342-3p	Maternal serum EVs (including characterisation of placenta-derived EVs based on PLAP expression)	↓ AMPK ↓ GLUT2	Altered β-cell insulin secretion, β--oxidation and glucose transport	(268)
T1DM	*No studies identified.*				
T2DM	*No studies identified.*				

AKT; RAC-Gamma Serine/Threonine-Protein Kinase, ALG3; Asparagine-Linked Glycosylation Protein 3 Homolog, AMPK; Adenosine Monophosphate-Activated Protein Kinase, GALNT; Polypeptide N-Acetylgalactoaminyltransferase, GLUT; Glucose Transporter, HOX; Homeobox, HUVEC; Human Umbilical Vein Endothelial Cells, ICAM; Intracellular Adhesion Molecule, IRS; Insulin Receptor Substrate, KI2FC; Kinesin Family Member 2C, KIT; KIT Proto-Oncogene, Receptor Tyrosine Kinase, L2HGDH; L-2-Hydroxyglutarate Dehydrogenase, MSC; Mesenchymal Stem Cell, PD-L; Programmed Death-Ligand, PLAP; Placental Alkaline Phosphatase, RAP; Ras-Related Protein, RECK; Reversion Inducing Cysteine Rich Protein with Kazal Motifs, SIRT; Sirtuin, TIMP3; Tissue Inhibitor of Metalloproteinase-3, VEGF; Vascular Endothelial Growth Factor.

1.5 Maternal Extracellular Vesicles and their microRNA Cargo in Pregnancies Complicated by Maternal Diabetes

1.5.1 Altered Fetal Growth

The miRNAome at the maternal-fetal interface has a direct influence on fetal growth and development (285–287). Maternal diabetes impacts the maternal-fetal miRNAome by influencing placental miRNA expression and EV-mediated interorgan communication, which in turn has been linked to altered fetal growth (259,282,288). Although lacking, a few studies have determined associations between fetal growth and miRNA expression levels in the maternal circulation and in placental tissue in pregnancies complicated by maternal diabetes (**Table *4***). The epidermal growth factor receptor (EGFR) pathway has been identified as a functional target of various miRNAs which are altered in the placenta of GDM pregnancies resulting in fetal overgrowth (289). It is known that this signalling pathway plays a key role in placental and fetal development. As such, it is possible that the miRNAs identified to be associated with altered fetal growth in pregnancies complicated by maternal diabetes are key for regulating optimal fetal development (**Table *4***).

Table 4 miRNAs Associated with Altered Fetal Growth in Pregnancies Complicated by Maternal Diabetes.

Model	Source	miRNA Regulation	Functional Outcome/Target	Fetal Growth Outcome	Ref.
GDM	Human placental tissue	↑ miR-508-3p ↓ miR-27a ↓ miR-9 ↓ miR-137 ↓ miR-92a ↓ miR-33a ↓ miR-30d ↓ miR-362-5p ↓ miR-502-5p	EGFR signalling	Macrosomia	(289)
(259,260)	Human maternal serum and placental tissue	↑ miR-16 / ↓ miR-16	CUL4A SMAD1 EGFR ACTB RRP12 DAB2	Macrosomia / SGA	(292,293)
GDM	Human maternal plasma and placental tissue	↓ miR-517a	↑ IGF-1 and trophoblast proliferation	Macrosomia	(294)
GDM and T2DM	Human placental tissue	↓ miR-126-3p	IRS1 PI3K	Lower birth weight	(202)

ACTB; β-actin, CUL4A; Cullin 4A, DAB2; Disabled-2, EGFR; Epidermal Growth Factor Receptor, IGF-1; Insulin-Like Growth Factor 1, IRS1; Insulin Receptor Substrate 1, PI3K; Phosphatidylinositol 3-Kinase, RRP12; Ribosomal RNA Processing 12 Homolog, SMAD1; Small Body Size and Mothers Against Decapentaplegic Family 1

1.5.2 Altered Fetal Development and Health

Maternal diabetes is associated with adverse offspring health outcomes, including an increased risk of developing cardiometabolic complications throughout life compared to offspring from uncomplicated pregnancies (295–297). Increasing evidence suggests that maternal circulating factors may play a role in the development of these adverse adaptations. For example, it has been shown that injection of maternal EVs from diabetic mice into healthy pregnant mice contributes towards fetal cardiac developmental deficiency (298). Similar findings have been demonstrated with fluorescently-labelled maternal EVs in a diabetic mouse model, where the maternal EVs were able to cross the placenta and increase the risk of congenital heart defects in the offspring (299). Although not specific to maternal diabetes, a recent investigation found that visceral adipose tissue EVs from obese mice contributed towards reduced fetal cardiac function in healthy lean pregnant mice by altering events in the placenta (300). Although these studies do not investigate the role of EV-miRNA cargo contributing towards these adverse effects, increasing evidence supports the role of miRNAs in epigenetic programming and cardiovascular disease (301). Indeed, studies have shown that offspring of pregnancies affected by maternal diabetes demonstrate altered fatty acid oxidation and glucose metabolism as a result of altered miRNA regulation (302,303). Specifically, a recent pilot study has characterised a set of miRNAs associated with diabetes and cardiovascular disease to be dysregulated in the circulation of children exposed to GDM *in-utero* (304). Interestingly, many of these miRNAs have demonstrated to be altered in the maternal circulation and placental tissue of GDM pregnancies previously discussed in this chapter. Other animal studies have shown that baboon offspring exposed to GDM *in-utero* also demonstrate altered cardiac miRNA expression, thereby increasing the risk of cardiac hypertrophy, myocardial infarction and cardiomyopathy (305). Another study showed that fetal cardiac tissue from pregnant diabetic-induced mouse models demonstrated let-7e-5p, miR-139-5p, and miR-195-5p upregulation and increased cardiac wall thickness (306).

Suboptimal maternal nutrition during pregnancy can programme offspring lipid metabolism and insulin resistance, thus contributing towards the development of T2DM (307). Indeed, GDM has been demonstrated to alter fetal lipid metabolism

in a sex-dependent manner via miRNA activity, whereby the liver of male rat fetuses demonstrated downregulated miR-130 expression, resulting in peroxisome proliferator-activated receptor (PPAR)-γ upregulation. Conversely, female rat fetal liver exclusively demonstrated miR-9 downregulation and PPARδ upregulation in response to GDM (308). The sex-specific influence of GDM on fetal hepatocyte miRNA regulation is becoming increasingly apparent, therefore our understanding of the contribution of miRNAs to the development of metabolic disorders, adipogenesis, obesity and fatty liver disease onset in offspring of GDM pregnancies is continuously progressing (309). However, further research is needed to elucidate whether the sex-dependent effects on miRNA expression in male and female offspring of pregnancies complicated by maternal diabetes are due to increased vulnerability or advanced environmental adaptation to hyperglycaemia (310).

Evidence also suggests that miRNAs modulate fetal cerebrovascular development. It is theorised that dysregulation of miRNAs contributes to the increased risk of neurodevelopmental disorders in diabetic pregnancies (304,311,312). To date, most studies investigating the effects of maternal diabetes on offsprings' long-term health have only focused on GDM. In recent years, it has become apparent that postpartum circulating EV-miRNA profile is altered in lactating individuals with T1DM, where dysregulated miRNAs have been associated with disease progression and inflammation, thus increasing offspring risk of immune-mediated diseases (313). However, the long-term impact of maternal PGDM on offspring health and development requires further research.

1.5.3 Maternal Cardiometabolic Health

GDM is known to increase the risk of adverse maternal outcomes, both during pregnancy and postpartum (314). Preeclampsia is associated with increased maternal risk of cardiovascular and cerebrovascular disease onset postpartum (15,16). miRNAs may play a role in the pathophysiology of preeclampsia. Indeed, a dysregulated miRNA profile has been identified in preeclamptic placentae, where miR-106a~363 cluster expression is altered compared to healthy

uncomplicated pregnancy (315). C19MC miRNAs are also implicated in preeclampsia, where placental miR-516-5p, miR-517*, miR-520a*, miR-525 and miR-526 expression are upregulated (316). More recently, there is a call to further identify a robust miRNA biomarker profile that is uniquely altered in people with preeclampsia and determine whether their expression is resolved post-recovery (317).

Individuals with GDM are also at higher risk of developing T2DM postpartum (19). It has been demonstrated that postpartum levels of several circulating miRNAs, including miR-16-5p, miR-17-5p, miR-29a-3p, miR-195-5p and miR-369-3p, are associated with postpartum diabetes onset in people with GDM (318,319). In a 15-year follow-up study, circulating miR-24-3p expression, along with maternal weight and BMI, has also been associated with the future progression of dysglycaemia in individuals with GDM postpartum (320). Interestingly, a mediterranean diet has demonstrated to improve insulin sensitivity and inflammation in people with GDM post-partum through the regulation of miR-222 and miR-103 (321). Whilst the mechanism and relationship between miRNAs and postpartum diabetes status remains to be established, the altered levels of miRNAs in circulation could potentially contribute towards reduced insulin sensitivity by influencing maternal organs, for example downregulation of miR-369 has previously been reported in the pancreas in T2DM (322). miR-24 expression levels have also been shown to both inversely correlate with Hemoglobin A1c (Hba1C) levels and to influence endothelial cell function in T2DM (323). This corroborates with the observation that people with GDM have increased postpartum endothelial dysfunction (324), and various endothelial cell models demonstrating miRNA dysregulation under GDM conditions (**Table *2***).

In addition to increased rates of T2DM following a GDM pregnancy, the risk of future cardiovascular diseases is increased by two-fold for individuals diagnosed with GDM compared to those who experience healthy, uncomplicated pregnancies. This includes risk of stroke, ischemic heart disease and heart failure (20). The mechanisms linking GDM to post-partum cardiac health remain to be established but 11 maternal circulating miRNAs (miR-13p, miR-20a-5p, miR-20b-5p, miR-23a-3p, miR-100-5p, miR-125b-5p, miR-126-3p, miR-181a-5p, miR-195-5p, miR-499a-5p and miR-574-3p) associated with cardiovascular

disease have been found to be increased in the first trimester of GDM pregnancies compared to healthy uncomplicated pregnancy (325). These findings therefore suggest that EVs and their miRNA cargo may play a role in postpartum adverse maternal cardiometabolic health observed in GDM pregnancies, however further studies are needed to establish the aetiology behind these associations.

1.6 Summary

Regulated placental development is essential to maintain an optimal *in-utero* environment for fetal growth during pregnancy. However, pregnancies complicated by GDM are often associated with altered fetal growth. Suboptimal fetal growth can increase offspring susceptibility to adverse short- and long-term health outcomes, including the onset of cardiometabolic diseases throughout life. Factors found in the maternal circulation play a key role in the development of the placenta. Pregnancies complicated by GDM manifest distinct changes in the maternal circulating milieu which can alter the development of the placenta and impact fetal growth. Indeed, despite demonstrating beneficial effects for maternal health, metformin therapy is associated with altered fetal growth but the mechanisms responsible and its effects on the placenta are yet to be established. Maternal circulating EVs play a key role in mediating bidirectional interorgan cross-talk at the feto-placental interface during pregnancy and studies have shown that components of the maternal diabetic milieu can alter the biogenesis and activity of EVs which may impact placental development. The role of maternal EVs in regulating fetal growth in GDM pregnancies remains unknown. However, it has been demonstrated that maternal EV miRNA profile is altered in GDM which can contribute towards altered fetal growth. miRNAs serve as potential biomarkers for maternal and fetal health during pregnancy. As such, understanding the mechanisms through which factors within the maternal diabetic circulation contribute towards altered fetal growth in GDM may lead to improved short- and long-term maternal and fetal health outcomes.

1.7 Hypothesis

Maternal circulating factors, including EVs, contribute towards altered fetal growth in pregnancies complicated by GDM by impacting on placental development and function.

1.8 Aims

1. To establish the impact of metformin exposure on the human placenta in pregnancies complicated by GDM.
2. To determine if maternal EVs and their miRNA cargo contribute towards altered fetal growth in pregnancies complicated by GDM.
3. To determine if maternal EVs and their miRNA cargo impact placental development and function in pregnancies complicated by GDM.

2 Materials and Methods

2.1 Transcriptomic Analysis of *In-vivo* Metformin Exposure on the Human Placental Transcriptome

2.1.1 Microarray Data Source and Processing

Previous work in the Forbes' group processed publicly available microarray data from the 'Effect of metformin on maternal and fetal outcomes in obese pregnant women' (EMPOWaR) study (EudraCT number 2009-017134-47; 10/MRE00/12), to establish the impact of *in-vivo* metformin exposure on placental gene expression (326,327). Included in the study were pregnant women over 16-years old with normal glucose tolerance and a BMI over 30 kg/m^2. For analysis, participants were stratified to only include women who developed GDM (diagnosed via OGTT at 28-36 weeks' gestation) and received either metformin (500-2500mg) or matched placebo from 12-16 weeks' gestation until delivery. Confounding factors such as birthweight and fetal sex were taken into account, resulting in female AGA offspring placental transcriptomic data being analysed (metformin n=10, placebo n=6). Placental RNA sequencing data (E-MTAB-6418) was exported from ArrayExpress database (EMBL-EBI) (326,328) and data was normalised to background signal and adjusted via Benjamini Hochberg method using GenomeStudio v2.0 (329,330). To detect subtle differences in gene expression, differentially expressed genes (DEGs) included in functional enrichment analyses were significantly detected against background signal ($p \leq 0.01$) and statistically ($p \leq 0.01$) and biologically ($-0.58 \leq Log2FoldChange\ (Log_2FC) \geq 0.58$) significant based on previously reported methods (331–333) (**Figure *5***).

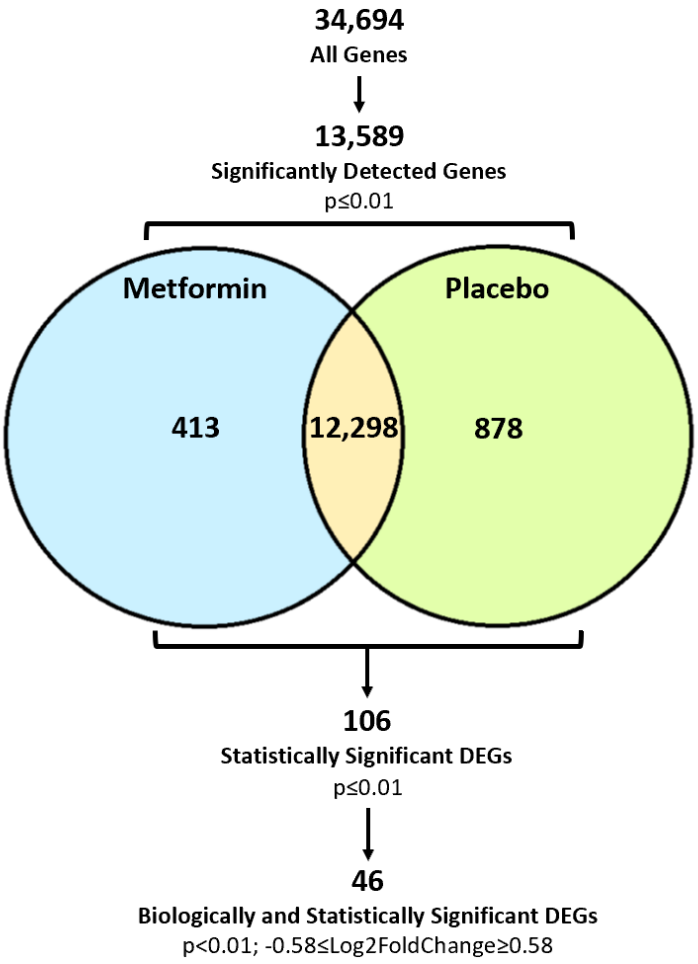

Figure 5 Flow diagram based on previous work from the Forbes group of differentially expressed genes included in functional enrichment analysis of *in-vivo* metformin exposure on the human placental transcriptome.

A total of 34,694 genes were detected before 21,105 were excluded due to insignificant detection against background signal. Of the remaining 13,589 genes, 106 were identified as statistically significant ($p \leq 0.01$), with 46 of these genes also defined as biologically significant ($-0.58 \leq Log_2FC \geq 0.58$). Adapted from Katie Hugh, MRes dissertation.

2.1.2 Functional Enrichment Analysis of *In-vivo* Metformin Exposure on the Human Placental Transcriptome.

2.1.2.1 Ingenuity Pathway Analysis

Ingenuity pathway analysis (IPA) was used to determine predicted canonical pathways, upstream regulators, associated diseases and functions, and molecular networks of DEGs in placental tissue of obese women with GDM taking metformin compared to placebo. IPA provides statistical significance and directionality of DEGs, where activation z-score demonstrates predicted activation state (negative z-score infers inhibition, positive z-score infers activation, z-score of 0 infers no definitive direction of change in terms of inhibition or activation) (334). Ensembl ID and Log_2FC were imported and threshold was set at $p<0.05$ or -log (p value) > 1.3 for associated upstream regulators and diseases and function analysis. Where annotated genes or terms was extensive, the top 20-25 annotated were plotted.

2.2 Assessing the Direct Impact of Metformin on the Human Placenta Using Human Placental Explants

2.2.1 Placental Tissue Collection and Processing

Human term placentae were collected from Leeds Teaching Hospital NHS trust within 30 minutes of elective caesarean section (REC reference: 18/LO/0067; IRAS project ID: 234385). Placentae were from healthy, uncomplicated term pregnancies and singleton term deliveries (38-41 weeks' gestation). Informed consent was obtained before elective caesarean section. Maternal demographic information and fetal birth weight were recorded (**Table *5***). Birthweight centiles were calculated using Gestation-Related Optimal Weight (GROW) software (version 6.7.5.1_14, UK), where < 10^{th} centile was referred to as small for gestational age (SGA); birthweight > 90^{th} centile was referred to as large for gestational age (LGA) and birthweight between 10-90^{th} centile was referred to as appropriate for gestational age (AGA). Following birth, placentae were processed. Umbilical cord and fetal membranes were discarded before recording placental weight. For whole organ representation, ~5cm^3 thickness sections were taken from the edge, middle and centre of the placenta before being repeatedly

washed with sterile phosphate buffered saline (PBS) to remove maternal blood. Chorionic and basal plates were removed (~-0.5cm^3 thickness).

Placental villous explants of ~2mm^3 sections were dissected from the edge, middle and centre of the placenta to represent whole placental tissue, before being submerged in sterile PBS. One explant from each of the edge, middle and centre sections was placed in a Netwell^{TM} (3477; Costar, UK) which were placed in each well of a 12-well plate containing 2mL media. Media comprised of Dulbecco's modified eagle medium (DMEM)-F12 without L-glutamine, HEPES and glucose (L0091-500; Biowest), supplemented with 10% fetal bovine serum (FBS, A2720803; Thermo Fisher), 1% penicillin-streptomycin-glutamine (PSG, 15140122; Thermo Fisher Scientific) and 5.5mM D-glucose solution (G8644; Sigma-Aldrich). Samples were kept incubated at 37°C in a humidified chamber with a 5% CO_2 / 95% air gas mixture (**Figure *6***). To allow for syncytiotrophoblast shedding and regeneration that occurs in human placental explants (335), placental villous explants were cultured for 4 days with media replenished every 24 hours. On day 4 of culture, media was replaced with explant media containing 40μM, 100μM or 1mM metformin (D150959; SigmaAldrich) and FBS substitute 10% exosome-free FBS (A2720803; Thermo- Fisher Scientific). As FBS contains EVs, exosome-free FBS was used in the culture media so that the direct effects of metformin on the human placenta could be studied. Explants were cultured for up to 72 hours and media collected at 24-hour intervals throughout the culture period. For protein analysis, explants were stored at -80°C and for histology purposes, explants were immersed in 10% neutral buffered formalin solution (HT501128, Merck Life) for 24 hours before being transferred to 70% ethanol and stored at 4°C. For RNA analysis, explants were placed in RNA*later* (R0901, Sigma) for 24 hours at 4°C and snap frozen in liquid nitrogen (LN) and stored at -80°C. Media was stored at -80°C (**Figure *6***).

Demographics	Samples (n=7)
Maternal Age (Years)	33.286±2.784
Maternal BMI Prior to Delivery (kg/m^2)	32.909±2.251
Maternal Ethnicity (%)	White British (86%) Greek (14%)
Parity	1.429±0.202
Gestational Age (Days)	275.429±0.869
Fetal Sex (%)	Male (71%) Female (29%)
Birthweight (g)	3486.429±129.388
BWC (%)	AGA (100%)
Placenta (g)	507.571±53.481

Table 5 Demographic details of patient placental tissue used for explant culture.

BMI; body mass index, BWC; birthweight centile, AGA; appropriate for gestational age. Data presented as mean±SEM.

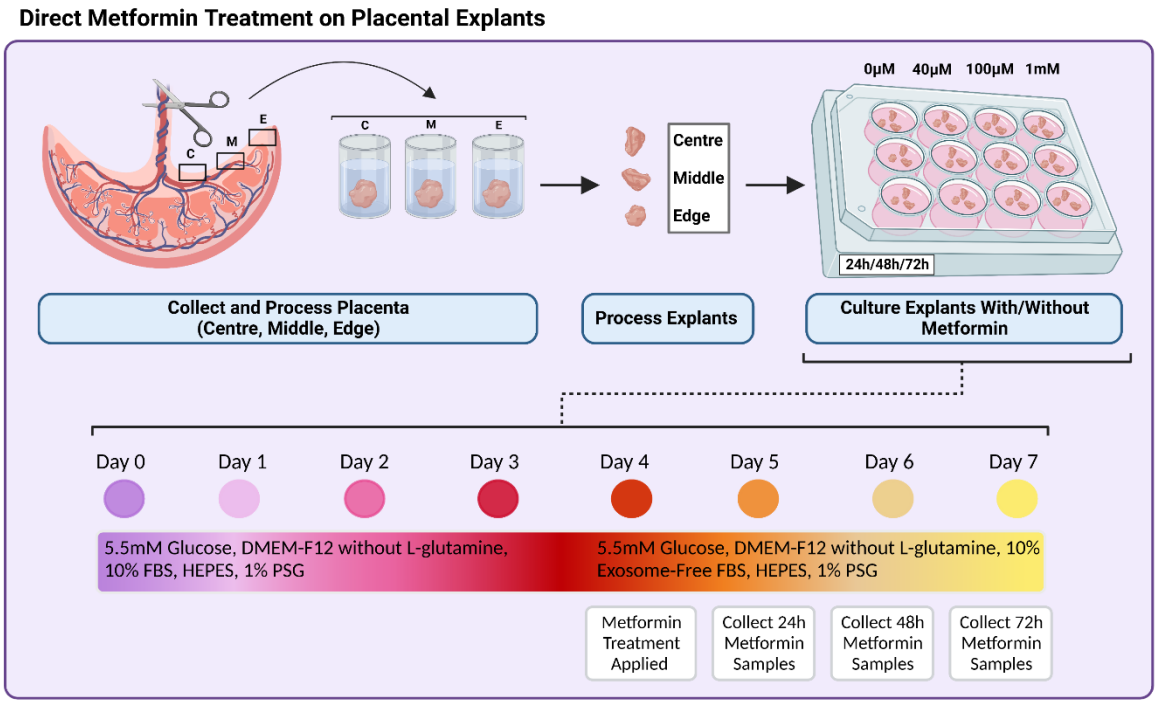

Figure 6 Placental villous explants cultured with metformin.

Centre, middle and edge placental sections were removed of fetal membranes, chorionic and basal plates before being washed in PBS and cut into ~2mm^3 explants sections. Centre, middle and edge placental explants were placed in a netwell in 2ml culture media comprising of DMEM-F12 without L-glutamine, supplemented with 10% fetal bovine serum, HEPES and glucose, 1% penicillin-streptomycin-glutamine (PSG) and 5.5mM D-glucose solution. On day 4, explants were cultured with 0, 40μM, 100μM or 1mM metformin, supplemented with DMEM-F12, 10% exosome-free FBS, 1% PSG, and 5.5.mM D-glucose solution for 24, 48 or 72 hours respectively. Created using Biorender.com.

2.3 Human Placenta Explant Culture Media Assays

2.3.1 Glucose Monitoring

To determine the effect of metformin on placental glucose uptake, media stored from placental villous explants cultured with metformin was probed for glucose using GlucCell® Glucose Monitoring System (CLS-1322-02, GPE Scientific, UK). In triplicate, 3 µl of culture media was placed on a GlucCell® test strip (CLS-1324-01, GPE Scientific) and glucose measurements were recorded in mM.

2.3.2 Lactate Dehydrogenase Enzyme Linked Immunosorbent Assay

To determine tissue necrosis, lactate dehydrogenase (LDH) concentration was measured in placental explant culture media in duplicate, using Cytotoxicity Detection Kit (11644793001, Roche Diagnostics, Switzerland) as per manufacturer instructions. Rabbit muscle LDH (10127876001, Roche Diagnostics) was diluted in reagent grade water to 1U/mL and standards were made via 1:2 serial dilution; 0.5 - 0.0078125 U/mL. Enzymatic activity was stopped by adding 50 µL of 1M HCl (35328, Honeywell, Fluka) to each well before absorbance at 492nm and 690nm was measured with the PowerWave HT Microplate Spectrophotometer (Agilent Technologies) using Gen5 Microplate Reader software. Concentration was calculated as 690nm-492nm absorbance values, normalised to explant weigh (mg).

2.3.3 β-Human Chorionic Gonadotropin Enzyme Linked Immunosorbent Assay

β-hCG release from placental explants was assessed using enzyme-linked immunosorbent assay (ELISA), as a measure of hormonal secretion capacity of the tissue. Placental explant media samples were firstly concentrated using Amicon Ultra-0.5 3K Centrifugal Filter Devices (UFC500396; Merck), as per manufacturer instructions, where final samples had a concentration volume of 80µl and concentration factor of x6. β-hCG ELISA kits (EIA-1911, DRG ® Diagnostics, Germany) were used to measure sample absorbance at 450nm and 620nm, in duplicate, as per manufacturer instructions. Final concentrations were

calculated using a four-parameter logistic curve generated by a Multiskan GO Microplate Spectrophotometer (51119300, Thermo Scientific) via SkanIt Software 4.1 and normalised to explant weight.

2.4 Human Placenta Histology

2.4.1 Tissue Processing and Paraffin-Wax Embedding

Formalin-fixed placental explants were placed in CellSafe Biopsy Cassettes (EBG-0304-12A, CellPath, ProMarc) and submerged in 70% ethanol before being dehydrated and embedded in paraffin-wax on a 14-hour programme in a Tissue Processor (TP1020, Leica). The programme ran as follows; 3.5 hours in 70% ethanol, 3.5 hours in 90% ethanol, 45 minutes in 100% ethanol (repeated 5 times), 30 minutes in xylene (repeated 3 times) and 1 hour in paraffin wax (repeated twice). From hot paraffin wax, tissues were transferred from cassettes and optimally placed in disposal base molds (15x15x5mm, Generon) filled with hot paraffin wax. Lid of cassette was then placed on top of the mold before being left to set at 4°C. Molds were disposed and excess wax trimmed prior to sectioning.

2.4.2 Haematoxylin and Eosin Staining of Formalin Fixed Paraffin-Embedded Tissue

Paraffin embedded tissue was sectioned at 5 µm using a microtome (RM2125RTF, Leica) and placed on pre-coated Poly-L-Lysine adhesion slides (VWR, Avantor, 631-0107) in a 37°C-heated water bath before being left to dry at room temperature. Slides were then placed in an oven at 55°C for 20 minutes, or until wax melted. Paraffin was cleared from the tissue by immersing slides in Histo-Clear (HS-200, National Diagnostics) three times for 5 minutes each, and tissue was rehydrated by immersing slides twice in 100% ethanol, twice in 95% ethanol and once in 70% ethanol for 1 minutes each. Slides were then placed in distilled water before being immersed in filtered haematoxylin (HHS16, Sigma-Aldrich) for 1 minute and transferred into cold water for nuclear staining. To remove cytoplasmic staining, slides were placed in acid:alcohol (0.25% HCl in ethanol) for 3 seconds and transferred again into cold water. Sections were then

blued by being immersed in hot water for 2 minutes. Slides were further placed in eosin for 1 minute before being transferred into cold water. To dehydrate sections, slides were placed in 70% ethanol and twice in 95% ethanol for 10-15 seconds each, before being immersed twice in 100% ethanol for 5 minutes and once in Histo-Clear for 10 minutes. Dibutylphthalate polystyrene xylene (DPX; LAMB/DPX, ThermoFisher Scientific) was used to mount tissue slides on 22x50 coverslips before being left to dry.

2.4.3 Immunohistochemistry of Formalin-Fixed Paraffin-Embedded Tissue

Paraffin embedded tissue was sectioned and de-waxed as described in section 2.4.2. To rehydrate tissues, slides were immersed in HistoClear (HS-200, National Diagnostics) three times for 10 minutes each, twice in 100% ethanol, once 70% ethanol for 3 minutes before being placed in cold tap water for 3-5 minutes. For antigen retrieval, slides were immersed in 1X sodium citrate buffer (0.01M, pH 6.0) before being boiled in the microwave for 10 minutes and left to cool for 20 minutes. Slides were then placed in cold tap water to further cool before being dried and placed in a humidity chamber. ImmEdge Pen (H-4000, 2B Scientific) was used to circle around each tissue section before adding 100µl 3% hydrogen peroxide (31642, Sigma-Aldrich) to each tissue section for 15 minutes at room temperature (RT) to block endogenous peroxidase activity. Sections were washed with 1X tris-buffered saline (TBS) (0.2 M Tris base, 1.5 M NaCl, pH 7.4) for 5 minutes and repeated three times before applying a protein block (5% BSA;BSAV-RO, Sigma-Aldrich) diluted in 1X TBS for 1 hour at RT. Protein block was removed and 50-100 µl diluted primary antibody in 1X TBS was applied to each section overnight at 4°C (**Table *6***).Rabbit or mouse IgG isotype antibody was used as a negative control at the same concentration as the primary antibody of interest. As a secondary antibody negative control, 1X TBS was also applied on a few tissue sections overnight. Following overnight exposure, excess liquid was removed from each tissue section, where they were washed in 1X TBS for 5 minutes, three times, before applying a diluted biotinylated secondary antibody for 1 hour at RT (**Table *6***).

Avidin peroxidase (A3151, Merck) was then diluted to give a final concentration of 5µg/ml in 1X high salt TBS (0.05 M Tris base, 3M NaCl, pH 7.6) and was added to each section for 30 minutes before a further three washes with 1X TBS. For colour development, diaminobenzidine (DAB) (ImmPACT DAB EqV, SK41-3, Vector Laboratories) was prepared following manufacturer instructions and 50 µl was added to each tissue section before promptly timing the appearance of brown staining under the microscope. Once optimal development had occurred, tissue sections were washed with distilled water. Nuclei in tissue sections were counterstained using filtered haematoxylin for a few seconds before being placed in cold tap water. Cytoplasmic staining was removed with acid:alcohol (0.25% HCl in 70% ethanol) before slides were transferred again to cold tap water and then hot tap water for 2 minutes. Slides were transferred back into cold tap water before being dehydrated in 70%, 95% and 100% ethanol for 3 minutes each, respectively. Slides were then placed in HistoClear for 10 minutes, twice, before being mounted on 22x50 coverslips with DPX (LAMB/DPX, ThermoFisher Scientific) and left to dry (**Figure 7**).

.

Table 6 Antibodies used for Immunohistochemistry.

Antibody	Species	Company	Concentration	Dilution
Primary Antibodies				
Monoclonal Anti-Human M30 CytoDEATH (12140322001)	Mouse	Roche	0.0066 mg/mL	1:100
Monoclonal Anti-Human Ki-67 Antigen Clone MIB-1 (M7240)	Mouse	Dako	0.046 mg/mL	1:200
Monoclonal Anti-Human CD31, Endothelial Cell Clone JC70A (M0823)	Mouse	Dako	0.201 mg/mL	1:200
Monoclonal Anti-Cytokeratin-7 (M7018)	Mouse	Dako	0.196 mg/mL	1:500
Monoclonal Anti-8-Hydroxy-2'-Deoxyguanosine [N45-1] (ab48508)	Mouse	Abcam	1.2 mg/mL	1:4000
Polyclonal Anti-Phospho-AMPK Alpha-1,2 (Thr183, Thr172) (44-1150G)	Rabbit	ThermoFisher	0.8 mg/mL	1:20
Polyclonal Anti-AMPK Alpha-1 (PA586105)	Rabbit	Fisher Scientific	1 mg/mL	1:100
IgG Control Antibody (I-2000-1)	Mouse	Vector Laboratories	0.5 mg/mL	Matched to M30 antibody
IgG Control Antibody (I-2000-1)	Mouse	Vector Laboratories	2 mg/mL	Matched to each antibody
IgG Control Antibody (I-1000-5)	Rabbit	Vector Laboratories	5 mg/mL	Matched to each antibody
Biotinylated Secondary Antibodies				
Biotinylated Anti-Mouse IgG (H+L) (16729)	Goat	AAT BioQuest	1 mg/mL	1:200
Biotinylated Anti-Rabbit IgG (E0353)	Swine	Dako	0.5 mg/mL	1:200

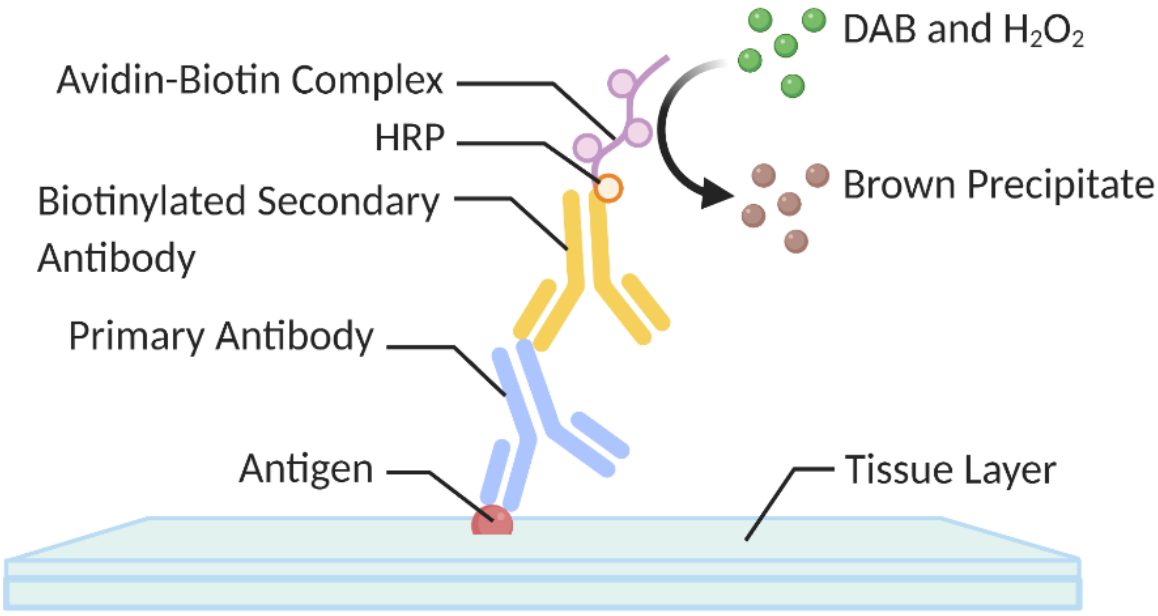

Figure 7 Schematic diagram of immunohistochemistry performed on placental tissue.

Primary antibody is incubated overnight to bind to antigen of interest before tissue is incubated with biotinylated secondary antibody. Further incubation with avidin peroxidase produces an avidin-biotin complex which allows antigen colour development with diaminobenzidine (DAB). HRP; Horseradish peroxidase. Created using Biorender.com.

2.4.4 Histology Analysis

Histological slides were imaged at x20 on the Slide Scanner at the Bioimaging Facility (Faculty of Biological Sciences, University of Leeds). QuPath (version 0.3.2) was used to analyse DAB-stained images. Tissue detection was performed by drawing a polygon around the whole tissue section, excluding any artefacts, and designing a pixel classifier threshold for annotation. DAB-positive cells were detected via the software's 'positive cells detection' method and thresholds were modified for each antigen. A published script was used to analyse CD31 stained tissue (336), followed by normalisation to total tissue area. Representative images for figure panels were captured using Zeiss Zen 3.7.

2.5 Human Placenta Western Blotting

2.5.1 Protein Extraction

Placental explants were weighed to be ~20-30mg and placed in tissue lyser tubes filled with 500µl 1X radioimmunoprecipitation assay (RIPA) buffer (0.5M Tris-HCl, pH 7.4, 1.5M NaCl, 2.5% deoxycholic acid, 10% NP-40, 10mM ethylenediaminetetraacetic acid (EDTA); 20-188, Merck) containing cOmplete™ mini protease inhibitor cocktail pill (4693124001; Roche) and 1% cocktails of tyrosine and serinethreonine phosphatase inhibitors (Cocktail 2 (P57261ML) & 3 (P00441ML); SigmaAldrich). One clean stainless steel 5mm bead (69989; Qiagen) was added and samples were placed in a TissueLyserII (Qiagen) at 27/s for 30 seconds, four times. When samples looked foamy and sufficiently lysed, steel beads were removed and samples were kept on ice for 30 minutes, while vortexing occasionally. Samples were centrifuged at 15,700 x *g* for 10 minutes at 4°C to pellet cell debris. Supernatant was placed in fresh tubes and cell pellet was discarded. Samples were stored at -80°C.

Protein samples were purified and concentrated using Amicon Ultra-0.5 3K Centrifugal Filter Devices (UFC500396; Merck), as per manufacturer instructions. Final protein sample had a concentration volume of 80µl and concentration factor of x6.

2.5.2 BioRad Protein Assay

To calculate protein concentration, protein standards were made from a serial dilution of 1mg/ml Bovine serum albumin (BSA; BSAV-RO, SigmaAldrich) to give a colorimetric protein standard curve (0.000µg/µl-1.000µg/µl). Placental samples were diluted 1:10. In triplicate, 10µl of each sample was plated on a 96-well microplate and 100µl Quick Start Bradford 1X dye reagent (5000205; BioRad Laboratories) was added to each well. The plate was left to incubate at RT for 10 minutes. Absorbance of samples was analysed on PowerWave HT Microplate Spectrophotometer (Agilent Technologies) at 550nm. A standard curve was created and used to calculate protein concentration of samples.

2.5.3 SDS-PAGE and Western Blotting

The impact of metformin on AMPK activation (AMPK phosphorylation) was determined to assess if physiologically relevant concentrations of metformin possibly impact the placenta (45). As such, AMPK and phosphorylated AMPK were proteins of interest for western blotting. Firstly, 5µl of 90% NuPAGE™ LDS Sample Buffer (4X, NP0007; Thermo Fisher) and 10% NuPAGE™ Sample Reducing Agent (10X, NP0009; Thermo Fisher) was added to 30µg of protein samples and heated to 95°C for 5 minutes. Nonphosphorylated AMPK cell extracts (total cell extracts from C2C12 cells prepared with CIP/λ phosphatase) were used as a negative control and phosphorylated AMPK cell extracts (total cell extracts from C2C12 cells prepared by serum starvation) were used as a positive control (9158; Cell Signaling Technology). Samples were loaded on to 10% Mini-PROTEAN® TGX™ Precast Protein Gels (15-well; 4561036, BioRad), alongside 5µl of PageRuler™ Prestained Protein Ladder (10 to 180 kDa, 26616; Thermo Fisher) and 10µl of AMPK Control Cell Extracts. Gels were immersed in 1X running buffer (0.25M Trizma base, 1.92M glycine and 0.03M SDS) and proteins were separated by electrophoresis at 50V for 5 minutes followed by 100V for 90 minutes. Proteins were transferred from gels on to activated ImmoblionP PVDF Membrane with 0.45µl pore size (IPVH20200; Merck) using 1X transfer buffer (0.25M Trizma base and 1.92M glycine, 20% methanol (V/V)) and a constant voltage of 100V for 60 minutes. Membranes were incubated in 3% BSA

in 1X Tris-Buffered Saline with Tween-20 (TBST; 3M NaCl, 396mM Trizma base, 0.03% tween-20) at RT for 60 minutes to prevent non-specific binding of antibodies, before being incubated overnight with a primary antibody for the protein of interest (diluted in 1X TBST as shown in **Table 7** at 4°C). The membrane was then washed in 1X TBST (8 times for 5 mintues at 175/s on agitator at RT) before being incubated in diluted secondary antibody in 1X TBST (**Table 7**) for 60 minutes at RT on the same agitator settings. Membranes were then washed again 8 times for 5 minutes in 1X TBST. Blots were imaged using G:Box (Syngene, Bangalore, India) after adding SuperSignal West Femto Maximum Sensitivity Substrate (1:1 volume) (10391544; Thermo Fisher Scientific). For reprobing, the membrane was immersed in strip buffer (0.1M glycine, pH 2.5 with HCl) with agitation (175/s) at RT. The membrane was rinsed with three times 1X TBST and then blocked in 3% BSA in 1X TBST at RT for 30 minutes before applying another primary antibody for a protein of interest and continuing steps as previously described above.

Semi-quantitative analysis of western blot bands was performed by densitometry using FIJI Image J software. Imaged blots were converted to greyscale and inverted before a mean grey value (MGV) measurement was taken from a defined region of interest (ROI) of each band. Background MGV measurement was taken beneath each band along the gel using the same predefined ROI, before being subtracted from the gel band measurement to calculate relative protein density values.

Table 7 Antibodies used for western blotting.

Antibody	Dilution	Company	Blocking	Membrane
Primary Antibodies				
Phospho-AMPKα (Thr172) (40H9) Rabbit mAb #2535	1:1000	Cell Signalling	3% BSA	PVDF
AMPKα (D5A2) Rabbit mAb #5831	1:1000	Cell Signalling	3% BSA	PVDF
Secondary Antibodies				
Anti-rabbit IgG, HRP-linked Antibody #7074	1:1250	Cell Signalling	3% BSA	PVDF

2.6 Human Placenta mRNA Expression

2.6.1 Total RNA Extraction

Placental explants were weighed to be ~20-40mg and total RNA was extracted using miRVANA total RNA isolation kit (10547465; Invitrogen), as per manufacturer instructions. Eluate containing RNA was collected and stored at 80°C. NanoDrop ND-1000 Spectrophotometer (LabTech International, Heathfield, UK) was used to measure RNA concentration and purity. Molecular grade water was used as a blank measurement before 1µl of total RNA sample was analysed. Average RNA concentration (ng/µL), A260/280 and A260/230 values were recorded.

2.6.2 Reverse Transcription Real-Time Polymerase Chain Reaction (RT-qPCR)

To measure the impact of metformin on placental vascular development, *ITGB3* gene expression was assessed in cultured human placental explants (337). Key genes involved in placental mitophagy, *PINK1, BCL2, PARK2* and *MAP1LC3B,* were also assessed in response to metformin (338,339). Gene expression of *PPARGC1B* was also determined to measure the impact of metformin on mitochondrial metabolism (340,341).

Stratagene AffinityScript QPCR cDNA Synthesis Kit (200436; Agilent Technologies) was used as per manufacturer instructions, to convert 100 ng of human placental reference RNA (740000-1, Agilent) or RNA samples (in a total reaction volume of 12.5µl) into cDNA. No reverse transcriptase (NRT) control was used, where reverse transcriptase was substituted with DNAse/RNAse free water. No template control (NTC) was also used, where RNA was substituted with DNAse/RNAse free water. Samples were placed in the Venti 96-well Thermal Cycler (Thermofisher) for a programme set at the following incubations; 25°C for 10 minutes, 42°C for 60 minutes, 70°C for 15 minutes and 4°C indefinite hold. Samples were stored at -20°C.

mRNA PCR Brilliant III SYBR kit (600882; Agilent) was used to quantify cDNA as per manufacturer instructions. cDNA samples were diluted 1:10 in DNAse/RNAse free water. Diluted reference cDNA was further serially diluted 1:2 (10 ng/ml, 5 ng/ml, 2.5 ng/ml, 1.25 ng/ml, 0.625 ng/ml, 0.3125 ng/ml, 0.15625 ng/ml, 0.078125 ng/ml) to gain a standard curve. 5-carboxy-X-rhodamine (ROX) reference dye was diluted 1:500 in DNAse/RNAse free water and added to the SYBR green master mix, alongside 0.36 µM of specific primers for genes of interest (**Table *8***). Master mix and diluted cDNA samples were loaded on a 96-well PCR plate and centrifuged at full speed for 30 seconds before being placed in a 96-well LightCycler (Roche, Basal, Switzerland) at the following programmes; 1 incubation cycle at 95°C for 3 minutes, 40 amplification cycles of 95°C for 20 seconds and primer specific annealing temperature for 20 seconds (Table 8), 95°C for 1 minute, 55°C for 30 seconds and a temperature increase of 0.2°C/cycle up to 95°C to collect continuous fluorescence data of melt curve analysis (**Figure *8***). LightCycler 96 1.1 software (Roche, Basal, Switzerland) was used to analyse results. Data was normalised to the mean of three reference genes: YWHAZ, 18S and β-actin and the 2-ΔΔCt method was used to express gene expression relative to control.

Table 8 Primer sequences for qPCR in human placental explants.

Gene	Primer Direction	5' to 3' Sequence	Annealing Temp (°C)	GC content (%)	NCBI Ref
YWHAZ	Forward	ACTTTTGGTACATTGTGGCTTCAA	55	37.5	NM_001135702
	Reverse	CCGCCAGGACAAACCAGTAT		55.0	
β-ACTIN	Forward	CATGTACGTTGCTATCCAGGC	50	52.4	NM_001101
	Reverse	CTCCTTAATGTCACGCACGAT		47.6	
18S rRNA	Forward	GCTGGAATTACCGCGGCT	52	61.1	X03205.1
	Reverse	CGGCTACCACATCCAAGGA		57.9	
PINK1	Forward	GCCTCATCGAGGAAAAACAGG	60	52.4	NM_032409
	Reverse	GTCTCGTGTCCAACGGGTC		63.2	
MAP1LC3B	Forward	AAACGGGCTGTGTGAGAAAAC	60	47.62	NC_000016.10
	Reverse	TGAGGACTTTGGGTGTGGTTC		52.38	
PARK2	Forward	GTGTTTGTCAGGTTCAACTCCA	60	45.45	NC_000006.12
	Reverse	GAAAATCACACGCAACTGGTC		47.62	
ITGB3	Forward	GTGACCTGAAGGAGAATCTGC	60	52.4	NM_000212
	Reverse	CCGGAGTGCAATCCTCTGG		63.2	
PPARGC1B	Forward	GATGCCAGCGACTTTGACTC	60	55.0	NM_001172698
	Reverse	ACCCACGTCATCTTCAGGGA		57.9	
BCL2	Forward	CGACGACTTCTCCCGCCGCTACCGC	70	72.0	NC_000018.10
	Reverse	CCGCATGCTGGGGCCGTACAGTTCC		68.0	

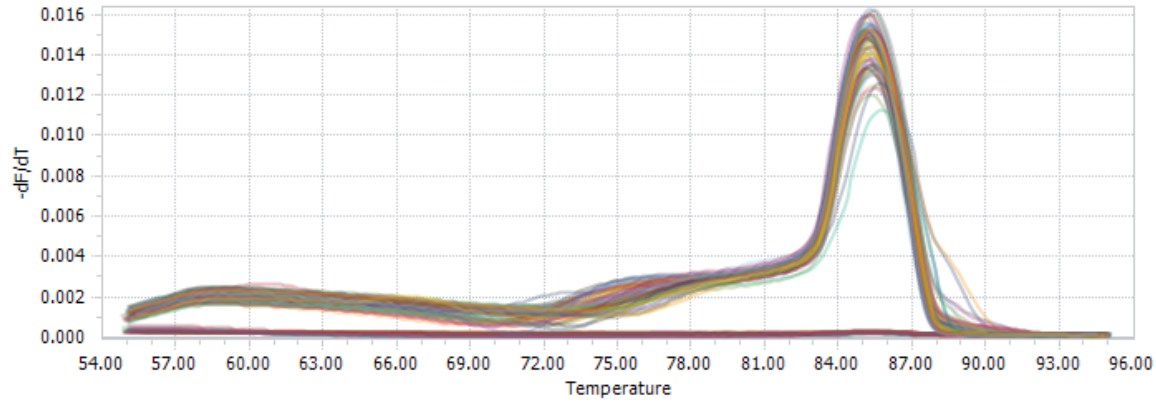

Figure 8 Example of primer melt curve to analyse specificity.

LightCycler 96 (Roche, Basal, Switzerland) was set at the following programmes; 1 incubation cycle at 95°C for 3 minutes, 40 amplification cycles of 95°C for 20 seconds and primer specific annealing temperature for 20 seconds, 95°C for 1 minute, 55°C for 30 seconds and a temperature increase of 0.2°C/cycle up to 95°C to collect continuous fluorescence data of melt curve analysis. LightCycler 96 1.1 software (Roche, Basal, Switzerland) was used to analyse results.

2.7 Human Placenta Mitochondrial Function

2.7.1 Citrate Synthase Activity Assay

Citrate synthase activity was measured in protein lysates (using RIPA lysis buffer; 20-188, Merck) of metformin-treated placental explants, as a marker of intact mitochondrial inner membrane, using Citrate Synthase Assay Kit (CS0720; Sigma-Aldrich) as per manufacturer instructions. Working master mix was prepared; 100 mM Tris-HCl, pH 8.0, 0.2 mM acetyl CoA, 0.1 mM 5,5'-Dithio-Bis-(2-Nitrobenzoic Acid) (DTNB) and 0.2mM acetyl-CoA. Master mix was loaded onto a 96-well microplate before 1 µL of sample homogenate was added in triplicate to make a total reaction volume up to 200 µL, whilst also allocating wells for blank controls. Sample absorbance was measured at 412nm at 37°C using PowerWave HT Microplate Spectrophotometer (Agilent Technologies), set with a delay of 5 minutes to allow temperature equilibration. Following initial absorbance reads, 10 µL of oxaloacetate (OAA) (freshly prepared to 10mM by dissolving OAA in 90% ddH2O and 10% 1M TrisHCl- buffer, pH 8.1) was added to all experimental wells to start the reaction. Kinetic absorbance was promptly read for 5 minutes or until signal plateau, using Gen5 Microplate Reader software. Temperature equilibration, OAA addition and absorbance reading steps were performed with only 3 rows of the plate at a time. Citrate synthase activity was measured by calculating mean sample absorbance/min and normalising to explant weight using the following equation, as per kit manufacturer instructions:

$$\boldsymbol{units}\ (\mu\boldsymbol{mole/ml/min}) = \frac{\frac{\Delta \boldsymbol{A}412}{\boldsymbol{min}} \times \boldsymbol{V(ml)} \times \boldsymbol{dil}}{\boldsymbol{\varepsilon^{mM}} \times \boldsymbol{L(cm)} \times \mathrm{Venz}(\boldsymbol{ml})}$$

2.8 Metabolomics Analysis of Human Placental Tissue

To evaluate the impact of metformin on mitochondrial function and metabolism, metabolomics analysis was performed on cultured human placental explant tissue.

2.8.1 Metabolite Extraction

Human placental explant tissue (12 mg) was lysed with 600 µL 2:1 methanol:chloroform (15624740, Fisher Scientific; 366927, Merck Life Science) and a clean stainless steel 5mm bead (69989; Qiagen) at 25Hz for 2min in a TissueLyserII (Qiagen). Once the samples were fully lysed, 200 µL of chloroform and 200 µL HPLC grade minimum water (83645.4, VWR International) were added. Samples were vortexed for 1 minute and centrifuged at 13,600 x *g* for 20 minutes to extract biphasic metabolites. The top aqueous fraction was separated from the lower organic fraction and placed in an evacuated, heated centrifuge (Savant SpeedVac® SPD11/V; Thermo Scientific) at 40°C for 6 hours, with small holes punched in the Eppendorf lids. Once dry, aqueous fractions were stored at -80°C.

2.8.2 Detection and Analysis of Metabolites by Liquid Chromatography-Mass Spectrometry

Aqueous metabolite fractions were reconstituted in 100 µL high performance liquid chromatography (HPLC) grade minimum water (83645.4, VWR International) and 100 µL of internal standard spiking solution (ISSS; 10 µM palmitoyl-L-carnitine-(N-methyl-d3) (Sigma), 10 µM palmitic acid-d31 (Sigma), and 10 µM deoxycholic acid-d6 (Sigma)). After samples were sonicated for 30 minutes and placed in liquid chromatography (LC) vials, LC-mass spectrometry (LCMS) was performed. Equipment used and parameters for bile acid and acyl carnitine detection are found in a previously published paper (342). Detection of tricarboxylic acid (TCA) cycle metabolites was carried out based on previously reported parameters (343). Tryptophan metabolite detection was also performed based on a previously published method (344). Peaks for all metabolites were processed and integrated using Water TargetLynx (Waters Corporation) and individual peaks were normalised to explant weight.

2.9 miRabel Analysis of Proteomic Changes in miR-375-3p Overexpressed Human Placental Explants

The impact of miR-375-3p overexpression on placental proteomic targets was investigated in human term placental explants. Term human placental explants from healthy AGA pregnancies were previously processed by the Forbes group as described in section 2.2.1. For the first 72 hours of culture, explants were cultured in serum-containing media before being transferred to serum-free culture media containing 200nM *mir*Vana® miRNA mimics for 72 hours; *mir*Vana® miRNA mimic was specific for hsa-miR-375-3p (target sequence: UUUGUUCGUUCGGCUCGCGUGA) and mirVana™ miRNA Mimic, Negative Control #1 (200nM; Thermofisher) was also used. Explants were kept incubated at 37°C in a humidified chamber with a 5% CO_2 / 95% air gas mixture before being processed for downstream analysis.

Protein lysates were prepared in RIPA buffer as previously described in section 2.5.1. Protein lysates (50ug) from human placental villous explants that had been cultured with miR-375-3p mimics were analysed by Tandem Mass Tag (TMT) labelling as a service conducted at the University of Bristol Proteomics Facility. Initial fractions were generated via TMT labelling and high pH reversed-phase chromatography Nano-LCMS was performed to produce spectra from further fractioning. Proteome Discoverer software v2.1 (Thermo Scientific) was used to quantify data. UniProt human (150,786 sequences) and 'Common Contaminants' (~200 records) databases using SEQUEST algorithm were used to compare our dataset (54-56). Total peptide amount was quantified for the normalisation of samples, where they were also categorised to a 'pool of common peptides' and a 5% false discovery rate (FDR). To detect subtle differences, biologically and statistically significant differentially expressed proteins (DEPs) were defined as $p \leq 0.05$ (adjusted), $-0.41 \geq Log_2FC \geq 0.58$.

miRabel online prediction tool (345) was then used to identify the predicted targets of miR-375-3p. Of the mapped targets, it was determined which of these overlapped and demonstrated the same directional change as the miR-375-3p proteomic targets identified in the human placental explants. This analysis informed downstream QPCR validation experiments when establishing homology between miR-375-3p targets in human and mouse placentae.

2.10 Human Maternal Plasma Extracellular Vesicles

A general workflow of the collection, isolation, pooling and characterisation of human maternal extracellular vesicles is outlined below (**Figure 9**).

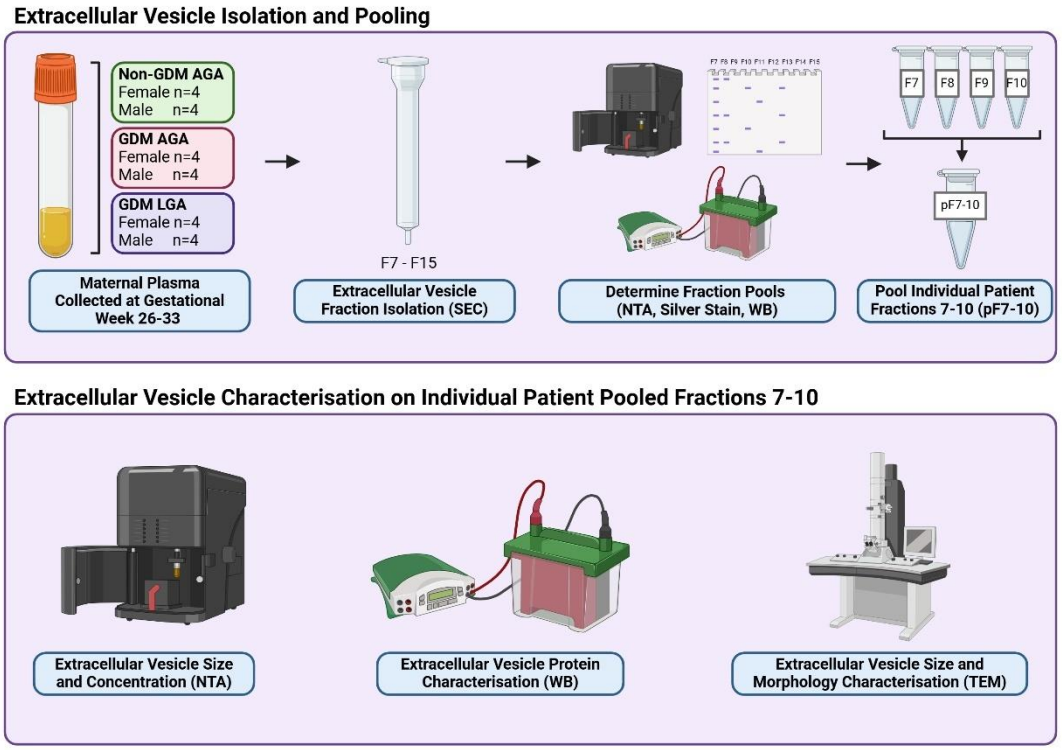

Figure 9 Workflow of plasma extracellular vesicle isolation, pooling and characterisation.

Maternal plasma was collected at 26-33 weeks of gestation, isolated via size exclusion chromatography (SEC) and fraction purity was determined via nanoparticle tracking analysis (NTA), silver staining and western blotting (WB). Fractions 7-10 were then pooled (pF7-10) for each patient and EV characterisation was determined via NTA to determine EV size and concentration, WB to identify EV-enriched markers and transmission electron microscopy (TEM) to identify EV morphology and artefacts. Created using Biorender.com.

2.10.1 Human Maternal Plasma Collection

Maternal plasma samples were acquired from the 'Efficacy of metformin in pregnant obese women: a randomised controlled trial' (PRiDE; NCT03008824, REC: 12/WM/0010) study, 'Maternal Glucose in Pregnancy' (MAGiC; IRAS ID: 271768, REC: 0/YH/0011) study and 'Understanding the placental structure, function and pathophysiology underlying the development of adverse pregnancy outcomes such as pre-eclampsia, intrauterine growth restriction, gestational diabetes, and preterm birth' (REC: 13/YH/0344 IRAS: 130157) study (**Appendix *24***). An OGTT was performed to determine GDM diagnosis, where fasting glucose levels <5.6mmol/litre and/or postprandial glucose levels of <7.8mmol/litre were defined as GDM in agreement with NICE guidelines (18). Maternal medical history, demographic information and fetal birth weight were recorded. Birthweight centiles were calculated using GROW software (version 6.7.5.1_14, UK), where < 10th centile was referred to as SGA; birthweight > 90th centile was referred to as LGA and birthweight between 10-90th centile was referred to as AGA. Samples were categorised according to GDM diagnosis and fetal weight (AGA or LGA). For every category, an equal number of male and female pregnancies was selected per group, and overall mean maternal BMI was matched as much as possible given the availability of samples. Maternal and fetal demographics of the samples used are outlined below (**Table *9***).

Table 9 Demographic details of human maternal plasma samples.

Demographics	Non-GDM AGA (n=8)	GDM AGA (n=8)	GDM LGA (n=8)	Significance
Maternal Age (Years)	32.09±1.46	33.11±1.36	28.50±1.73	ns
Maternal BMI Prior to Delivery (kg/m^2)	31.91±0.98	32.55±2.23	32.80±1.03	ns
Maternal Ethnicity (%)	White European (87.5%) Pakistani (12.5%)	White European (75%) Black African (12.5%) South Asian (12.5%)	White European (87.5%) South Asian (12.5%)	ns
Parity	1.5±2.0	1.125±2.0	1.125±3.0	ns
Gestational Age at Collection (Days)	186.0±14.0	193.0±53.0	196.0±8.0	ns
Fetal Sex (%)	Male (50%) Female (50%)	Male (50%) Female (50%)	Male (50%) Female (50%)	ns
Fetal Birthweight (g)	3494±131.5	3418±84.03	4226±122.8	Non-GDM AGA vs GDM AGA (ns) Non-GDM AGA vs GDM LGA (p=0.0005) GDM AGA vs GDM LGA (p=0.0002)

Maternal age, BMI and fetal birthweight data were analysed using ordinary one-way ANOVA followed by Tukey's multiple comparisons test, presented as mean±SEM. Maternal ethnicity and fetal sex data presented as %, where maternal ethnicity data was analysed using Chi-squared test. Parity and gestational age data were analysed using Kruskal-Wallis test followed by Dunn's multiple comparisons test and presented as median±range. Body mass index (BMI), birthweight centile (BWC), appropriate for gestational age (AGA).

2.10.2 Human Maternal Plasma Processing

Maternal blood samples were collected from pregnant women at 28 weeks gestation into EDTA blood collection tubes (Becton Dickinson, New Jersey, US). Within 4 hours of collection, blood samples were centrifuged in a horizontal rotor for 20 minutes at 1200 x *g*, RT to separate the plasma layer from the buffy coat and red blood cells. Plasma was then stored at -80 °C in 200 µL aliquots.

2.10.3 Human Maternal Plasma Extracellular Vesicle Isolation

EVs were isolated from plasma samples by size exclusion chromatography (SEC) using an automatic fraction collector (AFC) (IZON Science, New Zealand) and qEVoriginal/35nm columns with legacy resin (SP5, IZON Science, New Zealand). Plasma samples of 200µL were diluted in sterile-filtered PBS (Sigma-Aldrich, USA) to bring volume up to 500 µL before being centrifuged at 1500 x *g* for 10 minutes. Columns were flushed with 15 mL PBS and centrifuged plasma volume was loaded. Following screen prompts on AFC, fractions 1-6 were collected as void volume before fractions 7-15 were collected for EV analysis. Each EV fraction was 500µL and was stored at 80°C.

2.10.4 Human Maternal Plasma Extracellular Vesicle Characterisation

2.10.4.1 Preparing Extracellular Vesicles for Silver Staining and Western Blotting

EV fractions 7-15 from individual patients were lysed in 1X radioimmunoprecipitation assay lysis buffer (RIPA; 20-188, EMD Millipore Corp., MA, USA) cocktail, containing a protease inhibitor (Roche, ref: 04693124001), 1% cocktail 2 (Ref: P5726-1ML, Sigma-Aldrich) and 1% cocktail 3 (Ref: P0044-1ML, Sigma-Aldrich) diluted in distilled water (1:6 of EV:1X RIPA). Samples were left to lyse on ice for 20 minutes. For reduced conditions, 4X Laemmli buffer, pH 6.8 (1610747; BioRad Laboratories) with 10% β-mercaptoethanol (1610710; BioRad Laboratories) was added at 1X to make a total sample volume of 30 µL. For non-reduced conditions, similar steps were performed in the absence of β-

mercaptoethanol. Samples were then placed in a hot block at 70°C for 10 minutes before being stored at 80°C.

2.10.4.2 Silver Staining

Silver staining was performed on maternal plasma EV fractions 7-15 to determine which fractions yielded minimal protein contamination. In 12% MP TGX Stain-Free Precast Protein Gels (4568043; BioRad Laboratories), 30 µL of EV protein lysate was loaded alongside 5µl of PageRuler™ Pre-stained Protein Ladder (10 to 180 kDa, 26616; Thermo Fisher Scientific) in 1X running buffer (0.25M Trizma base, 1.92M glycine and 0.03M SDS). Electrophoresis was set at 50V for 5 minutes before increasing to 100V for 90 minutes. Gels were washed in ultrapure water for 10 minutes, fixed in 30% ethanol:10% acetic acid solution for 30 minutes, washed in 10% ethanol for 10 minutes before washing again in ultrapure water for 10 minutes. Pierce Silver Stain Kit (10096113; Thermo Fisher Scientific) was used as per manufacturer instructions to prepare stain working solution and gels was left to develop for 90 minutes. Gels were washed again with ultrapure water before being immersed in developer working solution for 2 minutes and then transferred into 5% acetic acid for 10 minutes to stop the staining reaction. Gels were imaged using the G:Box (Syngene, Bangalore, India).

2.10.4.3 Protein Quantification of Extracellular Vesicles

Micro BCA Protein Assay kit (23235, Thermo Scientific) was used for EV protein quantification, as per manufacturer instructions. In duplicate, 20 µL of each standard and sample was plated into a 96-well microplate, with 1:4 dilution of EVs:PBS. Working solution was added to bring total volume to 40 µL before incubating at 60°C for 60 minutes in a thermal cycler (T100™ Thermal Cycler; BioRad). Samples were incubated for 5 minutes at RT before reading absorbance values on the NanoDrop 2000 Spectrophometer (ThermoScientific) at 562 nm in triplicate. Average blank absorbance reading was subtracted from individual sample readings and a standard curve was plotted to determine EV protein concentration.

2.10.4.4 Western Blotting

EVs, either in reduced or non-reduced conditions (depending on the protein marker of interest, Table 10) were loaded to 4-15% Mini-PROTEAN® TGX™ Precast Protein Gels (BioRad) at 50µg, to make a total volume of 20µL/well alongside 5µl of PageRuler™ Prestained Protein Ladder (10 to 180 kDa, 26616; ThermoFisher). Gels were immersed in 1X running buffer (0.25M Trizma base, 1.92M glycine and 0.03M SDS) and proteins were separated by electrophoresis at 50V for 5 minutes followed by 120V for 60 minutes. Proteins were transferred from gels on to activated Immobilon PVDF Membrane with 0.45µl pore size (IPVH20200; Merck) using 1X transfer buffer (0.25M Trizma base and 1.92M glycine, 20% methanol (V/V)) and a constant voltage of 100V for 40 minutes. Membranes were incubated in 3% BSA in 1X TBST (3M NaCl, 396mM Trizma base, 0.03% tween-20) at RT for 60 minutes to prevent non-specific binding of antibodies, before being incubated overnight with specific primary antibodies for the protein of interest (**Table *10***) at 4°C. The membrane was then washed in 1X TBST (6 times for 5 minutes at 175/s on agitator at RT) before being incubated in diluted secondary antibody in 1X TBST (**Table *10***) for 60 minutes at RT on the same agitator settings. Membranes were then washed again 6 times for 5 minutes in 1X TBST. Blots were imaged using G:Box (Syngene, Bangalore, India) after adding SuperSignal West Femto Maximum Sensitivity Substrate (1:1 volume) (10391544; ThermoFisher). For reprobing, the membrane was immersed in strip buffer (0.1M glycine, pH 2.5 with HCl) with agitation (175/s) at RT. The membrane was rinsed three times with 1X TBST and then blocked in 3% BSA in 1X TBST at RT for 30 minutes before applying another primary antibody for a protein of interest and continuing steps as previously described above.

Table 10 Antibodies used for western blotting of EV-enriched proteins.

Target	Dilution	Company	Conditions	In EV-enriched fractions?
Primary Antibody				
CD63 (MX-49.129.5), Mouse monoclonal IgG1 (sc -5275)	1:100 dilution with 3% BSA/TBSt	Santa Cruz Biotechnology	No RIPA Non-reduced	Yes
TSG101 (C-2), Mouse monoclonal (sc-7964)	1:100 dilution with 3% BSA/TBSt	Santa Cruz Biotechnology	RIPA Reduced	Yes
Calnexin, Rabbit polyclonal (A303-695A-M)	1:500 dilution with 3% BSA/TBSt	Bethyl	RIPA Reduced	No
Secondary Antibody				
Goat anti-mouse HRP, polyclonal (P044701-2)	1:1250 dilution with 3% BSA/TBSt	Dako		
Goat anti-rabbit HRP, polyclonal (P044801-2)	1:1250 dilution with 3% BSA/TBSt	Dako		

Non-reduced = 4X Laemmli buffer (diluted to 1X) incubated for 10 minutes at 70°C. Reduced = 4X Laemmli buffer (diluted to 1X) + 10% β-mercaptoethanol, incubated for 10 minutes at 70°C.

2.10.4.5 Nanoparticle Tracking Analysis

Concentration (particles/mL) and diameter (nm) of maternal plasma EVs were analysed under Brownian motion via nanoparticle tracking analysis (NTA) using the NanoSight NS300 (Malvern Panalytical Ltd, UK). Plasma samples were diluted 1:250 and three 60 second captures were taken at 37°C with a camera level set at 14 and a detection threshold of 5.0. At least 20-100 particles were captured per frame (**Figure *10***).

2.10.4.6 Pooling Individual EV Fractions

After performing silver staining, western blotting and nanoparticle tracking analysis on maternal plasma EV fractions 7-15, equal volumes of fractions 7-10 (p7-10) were pooled from each individual patient and stored at -80°C. Pooled plasma EVs (p7-10) were further subjected to western blotting and nanoparticle tracking analysis, as well as electron microscopy.

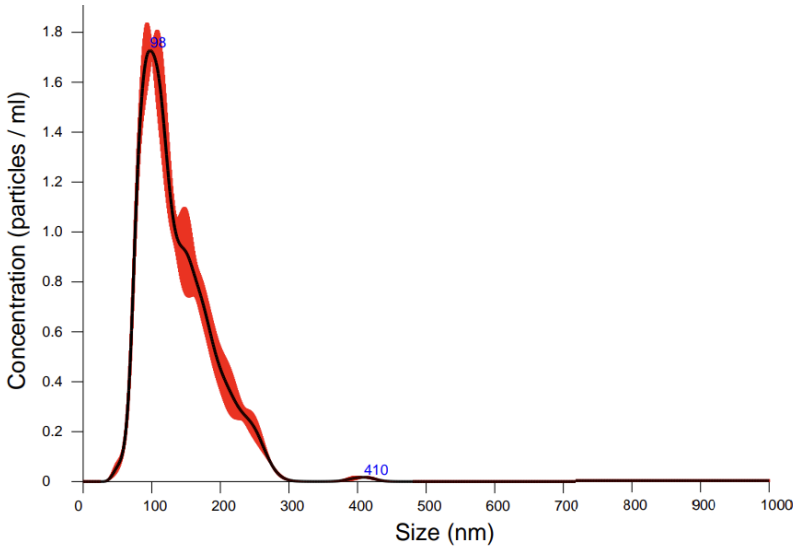

Figure 10 Example of nanoparticle tracking trace measuring EV size and concentration.

Size (nm) and concentration (particles/mL) of EVs are determined via nanoparticle tracking analysis under Brownian motion using NanoSight NS300. Size distribution is determined via the Stokes-Einstein equation.

2.10.4.7 Electron Microscopy

Previously performed by the Forbes group, pooled plasma EVs (p7-10) (5µL) were applied on a carbon-coated grid surface and were adhered for 60 seconds (Astbury Centre, University of Leeds, UK). Filter paper was used to discard excess liquid, before 5µL ultrapure water was rapidly applied and removed. Uranyl acetate (1%, 5µL) was applied, rapidly removed before being applied again for 10 seconds. Once dry, grids were viewed at x10K, x20K and x40K using JEM-1400 transmission electron microscope (TEM; JEOL, Massachusetts). Grids were stored at room temperature.

2.10.5 Generating Extracellular Vesicle Samples for *In-vivo* Analyses in Mice

2.10.5.1 Pooling Extracellular Vesicle Treatment Groups

Pooled maternal EV fractions 7-10 (pF7-10) from various patients (**Table *11***, **Table *12***, **Table *13***) were further pooled to produce injection treatment groups. To minimise sex-dependent effects, the average EV concentration coming from male and female pregnancies was matched in all treatment groups as much as possible. These pools were stored at -80°C and NTA was performed, as in 2.X, to determine final concentration for standardising injections (**Figure *11***).

Table 11 Pooled Extracellular Vesicles for Non-GDM AGA Treatment Group.

Sample (p7-10)	Concentration (Particles/mL)	Volume of Pooled F7-10 (mL)
Males		
Patient 1	1.11E+11	0.35
Patient 2	1.26E+11	0.3
Patient 3	1.66E+11	0.3
Patient 4	1.24E+11	0.3
TOTAL	**1.65E+11**	**1.25**
Females		
Patient 5	4.92E+10	0.43
Patient 6	6.90E+10	0.4
Patient 7	1.62E+11	0.3
Patient 8	1.82E+11	0.3
TOTAL	**1.65E+11**	**1.43**

Table 12 Pooled Extracellular Vesicles for GDM AGA Treatment Group.

Sample (p7-10)	Concentration (Particles/mL)	Volume of Pooled F7-10 (mL)
Males		
Patient 9	4.80E+10	0.22
Patient 10	8.45E+10	0.3
Patient 11	6.03E+10	0.3
Patient 12	8.05E+10	1.6
TOTAL	**1.65E+11**	**2.42**
Females		
Patient 13	6.95E+10	0.92
Patient 14	6.23E+10	0.53
Patient 15	4.69E+10	0.85
Patient 16	5.93E+10	0.45
TOTAL	**1.64E+11**	**2.75**

Table 13 Pooled Extracellular Vesicles for GDM LGA Treatment Group

Sample (p7-10)	Concentration (Particles/mL)	Volume of Pooled F7-10 (mL)
Males		
Patient 17	6.67E+10	0.365
Patient 18	6.62E+10	0.335
Patient 19	7.31E+10	0.72
Patient 20	9.96E+10	0.75
TOTAL	**1.66E+11**	**2.17**
Females		
Patient 21	9.52E+10	0.4
Patient 22	1.18E+11	0.4
Patient 23	1.28E+11	0.4
Patient 24	7.37E+10	0.4
TOTAL	**1.66E+11**	**1.6**

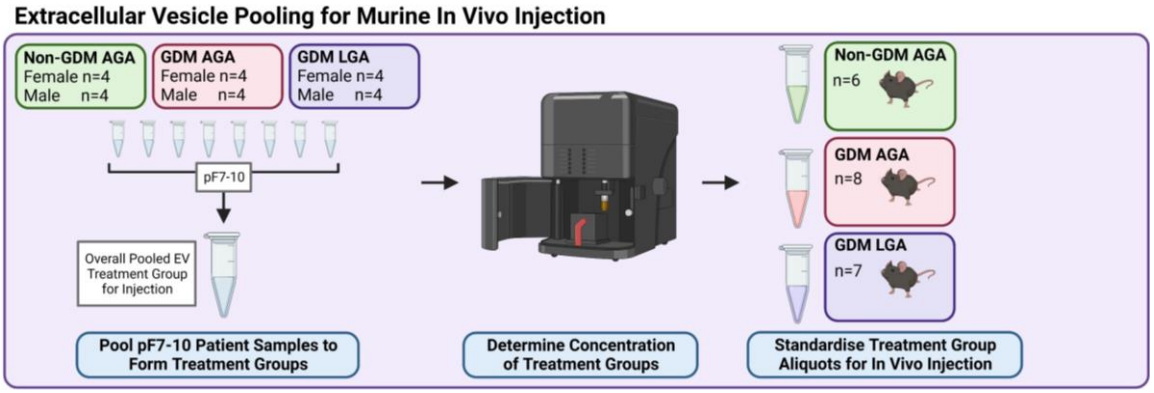

Figure 11 Pooling plasma extracellular vesicles to develop mouse injection treatment groups.

pF7-10 maternal plasma EVs from various patients were further pooled to generate treatment groups for mouse injections. NTA was performed to determine concentrations used for injections, leaving enough sample for 3 injections per mouse. Created using Biorender.com.

2.11 *In-vivo* Injection of Human Maternal Plasma Extracellular Vesicles and hsa-miR-375-3p into Healthy Pregnant Mice

2.11.1 Animal Model

All experimental procedures were aligned with the Home Office Animals (Scientific Procedures) Act 1986 Amendment Regulations 2012 and approved by University of Leeds Animal and Welfare Ethical Review Board (AWERB) (project license (PL); PP2103311). Healthy C57BL6/J mice (6-20 weeks) were purchased from Charles River Laboratories and were fed a standard chow diet *ad libitum*. Females were weighed before being mated with 6–20 week-old males. Plugging was confirmed the following day (E0) and pregnancy was confirmed by weighing mice at E11.5 and confirming a weight gain of at least 3g (19). Pregnant mice were weighed again at days E13.5, E15.5 and E18.5. Maternal hysterectomised weight was also assessed at E18.5. Experimental procedures on pregnant mice were carried out under PL protocol 12.

2.11.2 Delivery of Human Maternal Plasma Extracellular Vesicles and hsa-miR-375-3p Mimics to Healthy Pregnant Mice

To achieve a final *in-vivo* concentration of 1.5E+9 particles/mL, pregnant C57BL6/J mice were injected via tail vein with 150 µL of human plasma EVs isolated and pooled as described in section 2.10, diluted in PBS, from either non-GDM-AGA, GDM-AGA or GDM-LGA pregnancies. As a vehicle control, 150 µL of PBS was used. In a total volume of 150 µL and diluted in PBS, mirVana™ hsa-miR-375 miRNA mimic (4464070; Invitrogen) was injected at 1 mg/kg based on E11.5 weight and mirVana™ miRNA mimic negative control (4464061; Invitrogen) was also injected at 1 mg/kg based on E11.5 weight. Injections were blinded and administered on days E11.5, E13.5 and E15.5 by Naima Endesh or Melanie Reay (University of Leeds) (**Figure *12***).

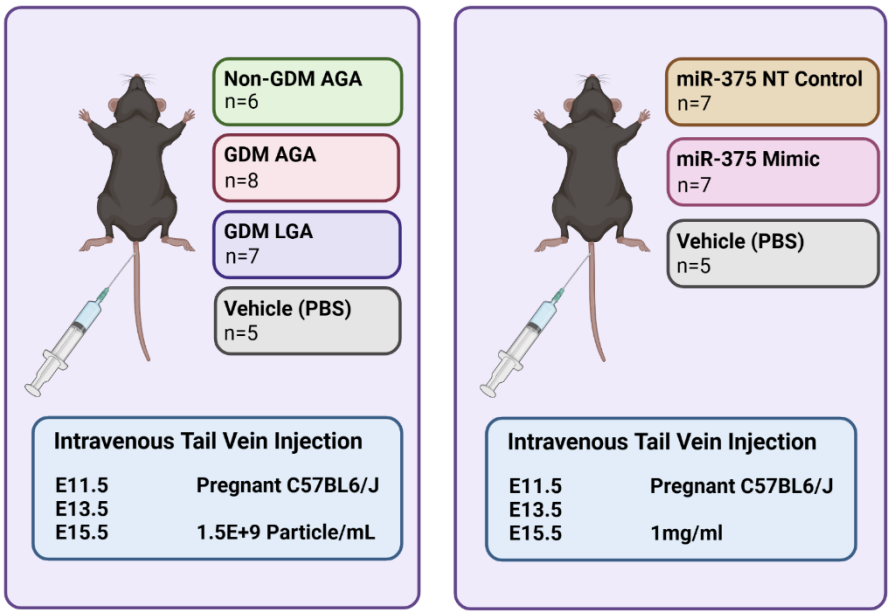

Figure 12 Experimental design of the *in-vivo* mouse project.

Healthy pregnant C57BL6/J mice were injected via tail vein with maternal plasma extracellular vesicles (from Non-GDM AGA, GDM AGA or GDM LGA pregnancies), miRNA mimics or vehicle control (PBS) treatments at days E11.5, 13.5 and 15.5. Created using Biorender.com.

2.12 Mouse Harvesting

Animals were sacrificed via terminal anaesthesia with 100% w/w isofane (988-3245; HenrySchein) at E18.5 under Schedule 1 practice.

2.12.1 Mouse Placenta and Fetus Processing

Mouse uterine tract was harvested under protocol 1 of PL, placed in cold PBS and number of resorptions were identified. Fetuses were excised from the amniotic sac, necks were snipped and umbilical cord was trimmed before weight of placenta and fetus were recorded. Each placenta was processed carefully and dissected in half using a razor blade (20). Half of the sample was processed for histology, by immersing in 10% neutral buffered formalin solution; HT501128, Merck Life. The other half of the placenta was further divided in two sections; one section was snap frozen whilst the other was immersed in RNA*later* (R0901, Sigma) (**Figure *13***). Snap frozen placentae were stored at 80°C. Fixed placentae were stored at 4°C and transferred into 70% ethanol after 24 hours. RNA*later* was removed after 24 hours and placentae were stored at 80°C. Fetuses were weighed and fixed in 10% neutral buffered formalin solution (HT501128; Merck Life) at 4°C before being transferred into 70% ethanol after 48 hours. Fetal crown-rump length, abdominal traverse diameter, head length and biparietal diameter were measured. Fetal tail tips were snap frozen and from each litter, two fetal hearts were harvested and weighed before being snap frozen and stored at 80°C (**Figure *13***).

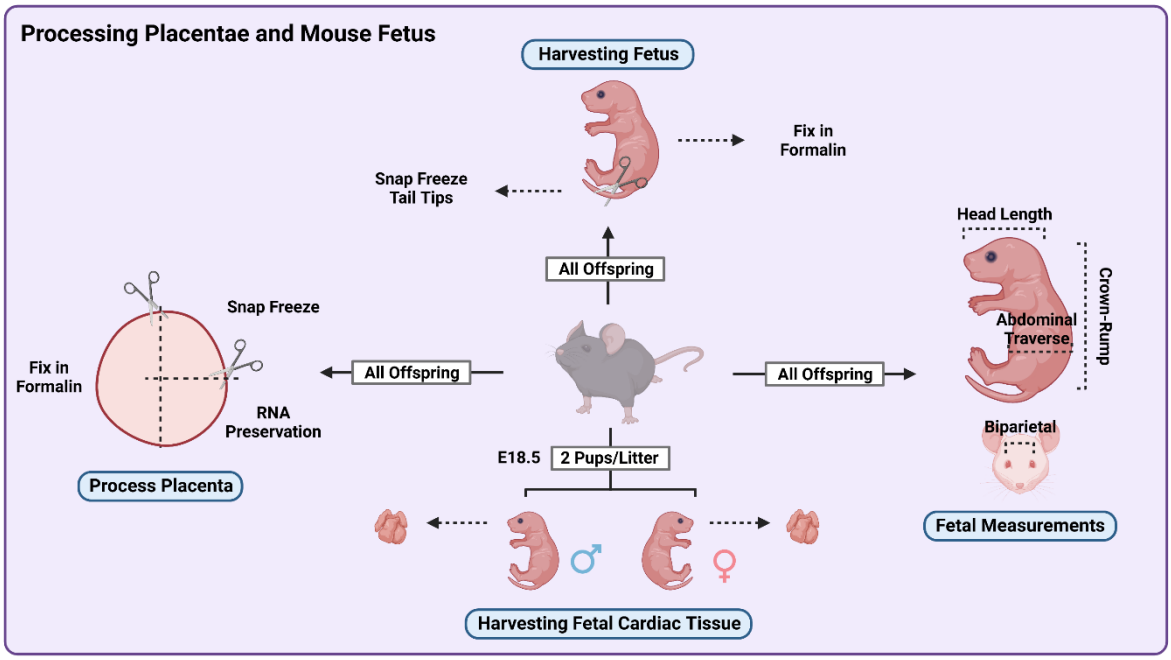

Figure 13 Flow diagram of mouse offspring and placenta processing.

Placenta from each fetus was weighed and processed for snap freezing, fixing in formalin and RNA preservation in RNA *Later*. Each fetus was weighed, fixed in formalin and tails were snipped for genotyping. Fetal measurements were taken of head length, crown-rump length, abdominal traverse diameter and biparietal diameter. From each litter, one male and one female were processed (visually sexed by identifying a dark spot underneath the tail, indicative of male) for fetal heart harvesting. Fetal heart was weighed and stored at -80°C. Created using Biorender.com.

2.12.2 Processing of Tissue for Mouse Maternal Cardiac and Hypertrophy-Associated Analyses

Maternal cardiac tissue was harvested and placed in PBS whilst still contracting for ‘self-washing’. Connective tissue was trimmed and cardiac tissue was weighed before cardiac apex was collected for gene expression analysis. Remaining heart tissue was coated upright in O.C.T. compound (411243; VWR International) and submerged in LN-cooled isopentane (277258; SigmaAldrich). Maternal tibia length was measured using a calliper (DRAPER Expert). Cardiac apex, remaining O.C.T. compound-coated whole heart, ear and tibia were all snap frozen before being stored at 80°C (**Figure *14***).

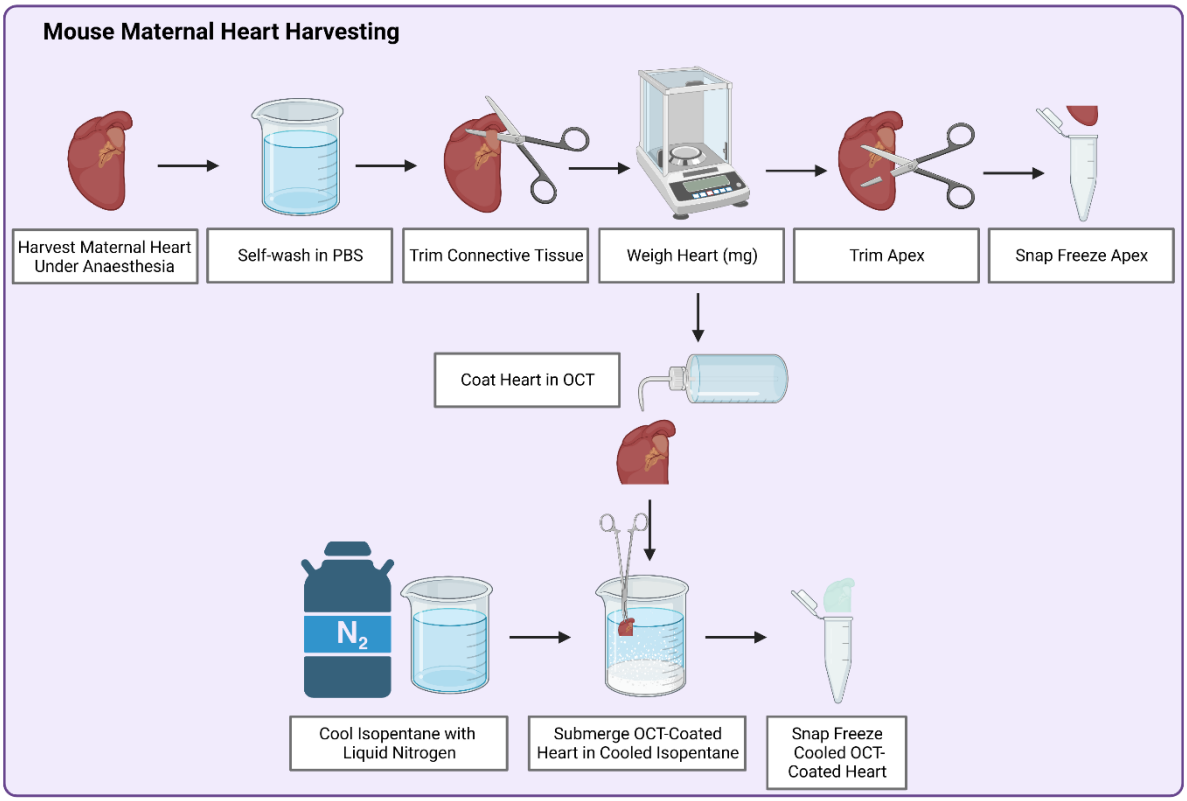

Figure 14 Flow diagram of mouse maternal cardiac tissue processing.

Maternal cardiac apex was trimmed and snap frozen. Remainder of whole heart was coated in OCT before being submerged in cooled isopentane and snap frozen. Created using Biorender.com.

2.12.3 Processing of Maternal Metabolic Organs

Maternal adipose tissue, pancreas, skeletal muscle and liver were harvested, weighed and either snap frozen or fixed in 10% neutral buffered formalin solution (HT501128, Merck Life) for 24 hours before being stored in 70% ethanol for future analyses.

2.12.4 Processing of Maternal Plasma from Mice

Maternal blood was collected from the inferior vena cava using a 0.3 mL syringe with 30Gx8mm needle (1203346, Becton Dickinson) and dispensed into a Microvette® 500 500µL (20.1341, Sarstedt Ltd). Immediately following harvest, the plasma layer was separated from the buffy coat and red blood cells using a centrifuge with a horizontal rotor for 20 minutes at 1200 x *g*. Plasma samples were then stored at -80 °C.

2.13 Mouse Fetal Sex Determination

Mouse offspring were initially sexed visually by identifying a dark spot underneath the tail (indicative of a male). To confirm observations, DNA gel electrophoresis was performed for genotyping. For DNA extraction, mouse fetal tail tips were lysed in 150 µl Direct PCR (Tail) Lysis Reagent (102-T; Viagen Biotech) and 1 µL proteinase K (20 mg/mL; EO0492, Thermo Scientific) and left to incubate overnight at 55°C. Proteinase K was inactivated by incubating samples at 85°C for 45 minutes before samples were diluted with 1 mL milliQ water and centrifuged at 8000 RPM for 1 minute. Samples were stored at -20°C before performing PCR.

To perform DNA gel electrophoresis, primers for gender determination genes were designed based on a previously published method (**Table *14***) (346). Sex-determining Region Y Protein (*Sry*) gene was used as a marker for the *Y* chromosome, and the Nuclear Receptor Binding SET Domain Protein 3 (*DXNds3)* gene was used as an internal control for the *X*-chromosome. A master-mix was made up for each PCR reaction (**Table *15***) which was performed in a 0.2 mL Eppendorf and 4 µL of DNA was added to make a total reaction volume

of 50 µL. In a Venti 96-well Thermal Cycler (Thermofisher), samples were run at 94 °C for 5 minutes then 94 °C, an annealing temperature of 55 °C and 72 °C for 1 minute each for 35 cycles, before finishing at 72 °C for 10 minutes.

PCR products were run on a 2% agarose gel (R0491; Thermo Scientific) made with 1X Tris-acetate-EDTA (TAE) buffer (40 mM Tris (pH 7.6), 20 mM acetic acid, 1 mM EDTA). SYBR Safe DNA gel stain (S33102; Invitrogen) was added to the gel mixture at 1:10,000 before loading 20 µL of the PCR products and 5 µL of GeneRuler 100 bp DNA Ladder (SM0323; Thermo Scientific). Gel was immersed in 1X TAE buffer and run at 100V for 60 minutes before being imaged on the G:Box (Syngene, Bangalore, India) (**Figure *15***).

Table 14 Primers Used for Genotyping Mouse Fetal Tail Tips

Gene	Primer Direction	5' to 3' Sequence	Annealing Temp (°C)	GC content (%)	Reference
Sry	Forward	TCTTAAACTCTGAAGAAGAGAC	55	36	(13)
	Reverse	GTCTTGCCTGTATGTGATGG		50	
DXNds3	Forward	GAGTGCCTCATCTATACTTACAG	55	43	(13)
	Reverse	TCTAGTTCATTGTTGATTAGTTGC		33	

Table 15 PCR Master Mix for Genotyping Mouse Fetal Tail Tips

Mastermix	x1 PCR reaction
MyTaq™ Red Mix (BIO-25044; Meridian Bioscience)	25 µl
PCR H_2O (Sigma-Aldrich)	5 µl
SRY2 primer (5 µM, final conc 500nM)	4 µl
SRY4 primer (5 µM, final conc 500nM)	4 µl
NDS3 primer (5 µM, final conc 500nM)	4 µl
NDS4 primer (5 µM, final conc 500nM)	4 µl
PCR DNA Product	4 µl
Total	50 µl

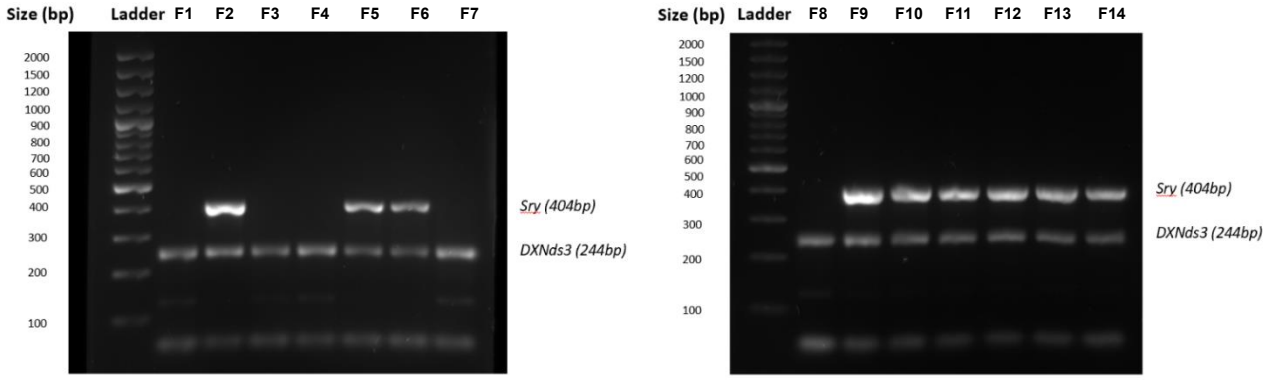

Figure 15 Example of Genotyping Mouse Fetal Tail Tips via DNA Gel Electrophoresis.

Primers for *Sry* (a marker for the *Y* chromosome; 404 bp) and *DXNds3* (a marker for the *X* chromosome; 244 bp) genes were designed to genotype mouse fetal tail tips. F2,5,6,9-14 were identified as male and F1,3,4,7,8 were identified as female. PCR DNA product was run on a 2% agarose gel in 1XTAE buffer. Abbreviations: F-fetus.

2.14 Total RNA Extraction from Mouse Placenta

Total RNA from mouse placental tissue was isolated using miRNeasy Tissue/Cells Advanced Mini Kit (217604; Qiagen) according to manufacturer instructions. Mouse placental tissue was weighed ~20mg and lysed in buffer RLT with a clean stainless steel 5mm bead (69989; Qiagen) at 27Hz for 2min in a TissueLyserII (Qiagen). Eluate containing RNA was collected and stored at 80°C. NanoDrop ND-1000 Spectrophotometer (LabTech International, Heathfield, UK) was used to measure RNA concentration and purity. Molecular grade water was used as a blank measurement before 1µL of total RNA sample was analysed from each sample. Average ng/µL, A260/280 and A260/230 values were recorded.

2.15 Analysis of miRNA Expression in Mouse Placenta

Total RNA from mouse placenta was processed using miRCURY LNA RT kit (339340; Qiagen) following manufacturer instructions by starting with 5ng/µL RNA diluted in DNAse/RNAse-free water and using NRT and NTC controls, to generate cDNA. Samples were incubated in a Venti 96well Thermal Cycler (Thermofisher) as per kit instructions. cDNA was stored at -20°C prior to performing QPCR using miRCURY LNA SYBR® Green PCR kit (339345; Qiagen) and individual PCR primer assays (**Table *16***) were used to detect individual mature miRNA. cDNA samples were diluted 1:30 in DNAse/RNAse-free water and a master mix was prepared as per manufacturer instructions (no ROX reference dye was used). PCR plates were placed in a 96-well Lightcycler (Roche, Basal, Switzerland) (**Table *17***) and relative gene expression was normalised to UniSp6 expression via the $2^{-\Delta\Delta Ct}$ method.

2.16 RNA Extraction and miRNA Expression in Human Maternal Plasma Extracellular Vesicles

Human maternal plasma EV pools from Non-GDM AGA, GDM AGA and GDM LGA pregnancies (**Table *11***, **Table *12***, **Table *13***) were concentrated using Satorius Vivacon500, 2000 MWCO (VN01H92). Collection tubes were firstly pre-rinsed with PBS before samples were added and set to centrifuge at 18°C at 14,000 x *g*

for 30 minutes. Samples were then reverse filtered by centrifuge at 2500 x *g* for 2 minutes. miRNeasy Serum/Plasma Kit (217184, Qiagen) was then used to extract RNA, where 5 volumes of QIAzol lysis reagent (79306, Qiagen) was added to each EV sample and left to incubate at RT for 5 minutes. UniSp2, UniSp4, UniSp5 Spike-in at a volume of 1µL was added to each sample and chloroform (15624740, Fisher Scientific; 366927, Merck Life Science) was added in equal volume to the starting volume of each sample and then shaken for 15 seconds. After being left to incubate at RT for 2-3 minutes, samples were centrifuged for 15 minutes at 12,000 x *g* at 4°C. The aqueous phase of each sample was then transferred to a new collection tube and 1.5 volumes of 100% ethanol was added to the aqueous phase and mixed via pipetting. Into a RNeasy spin column in a 2ml collection tube, 700µL of sample was added and centrifuged at 8000 x *g* for 15 seconds at RT. Flow-through was discarded and this step was repeated until all of the sample had passed through the spin column. Buffer RWT (700µL), Buffer RPE (500µL and 80% ethanol (500µL) were added to the spin column in succession, where the sample was centrifuged at 8000 x *g* for 15 seconds at RT after each addition and the flow-through discarded. The spin column was then placed in a new 2ml collection tube, where the lid was open and the sample was centrifuged at full speed for 5 minutes to dry the membrane. The flow-through was discarded. In a new collection tube, the spin column was placed and 14µL of RNAse-free water was added directly to the spin column membrane, where the sample was centrifuged for 1 minute at full speed to elute the RNA. RNA was stored at -80°C.

For EV miRNA analysis, miRCURY LNA RT kit (339340; Qiagen), miRCURY LNA SYBR® Green PCR kit (339345; Qiagen) and individual PCR primer assays (**Table *16***) were used, where samples were prepared as per section 2.15.

Table 16 Primers Used for miRCURY LNA PCR

miRNA	Primer ID	Target Sequence
UniSp6	EXIQON_LNA_Control Primer Set (203401-03)	5'CUAGUCCGAUCUAAGUCUUCGA
hsa-miR-375-3p	EXIQON_miCURY LNA UniRT PCR Primer (MfgID: 107928424)	5'UUUGUUCGUUCGGCUCGCGUGA
hsa-miR-1-3p	miRCURY LNA miRNA PCR Assay (YP00204344)	5'UGGAAUGUAAAGAAGUAUGUAU
hsa-miR-133a-3p	miRCURY LNA miRNA PCR Assay (YP00204788)	5'UUUGGUCCCCUUCAACCAGCUG
hsa-miR-145-5p	miRCURY LNA miRNA PCR Assay (YP00204483)	5'GUCCAGUUUUCCCAGGAAUCCCU
hsa-miR-499-5p	miRCURY LNA miRNA PCR Assay (YP00205935)	5'UUAAGACUUGCAGUGAUGUUU
hsa-miR-200c-3p	miRCURY LNA miRNA PCR Assay (YP00204482)	5'UAAUACUGCCGGGUAAUGAUGGA

Table 17 Lightcycler Programme Used for miRCURY LNA SYBR® Green PCR

Step	No. Cycles	Temperature (°C)	Time (s)	Acquisition
Preincubation	1	95	120	N/a
2-Step Amplification	45	95	10	None
		56	60	Single
Melting	1	95	60	None
		60	30	None
		95	1	Continuous
Cooling	1	37	30	None

2.17 Assessment of mRNA Expression in Mouse Placenta

Stratagene AffinityScript QPCR cDNA Synthesis Kit (200436; Agilent Technologies) and mRNA PCR Brilliant III SYBR kit (600882; Agilent) were used to convert 100 ng of mouse placenta RNA into cDNA, and thus cDNA into DNA as per section 2.6.2. Primers for specific genes were used in the QPCR reaction (**Table *18***). Data was normalised to the mean of housekeeping gene β-actin and relative gene expression was quantified using the 2-ΔΔCt method.

Table 18 Primer sequences for qPCR on Mouse Placenta

Gene	Primer Direction	5' to 3' Sequence	Annealing Temp (°C)	GC content (%)	Ref	NCBI Ref
β-actin	Forward	GGCTGTATTCCCCTCCATCG	56	60	(347)	NM_007393.5
	Reverse	CCAGTTGGTAACAATGCCATGT		45		
CD47	Forward	GGTGGGAAACTACACTTGCGAAG	57	52	*Sequence available on OriGene*	NM_001368415.1
	Reverse	CTCCTCGTAAGAACAGGCTGATC		52		
PECAM1	Forward	CCAAAGCCAGTAGCATCATGGTC	57	52	*Sequence available on OriGene*	NM_008816.3
	Reverse	GGATGGTGAAGTTGGCTACAGG		55		
ENO1	Forward	TACCGCCACATTGCTGACTTGG	57	55	*Sequence available on OriGene*	NM_001379127.2
	Reverse	GCTTGTTGCCAGCATGAGAACC		55		
SLC6A8	Forward	ATCCTGGCACTCATCAACAGCG	57	55	*Sequence available on OriGene*	NM_133987.2
	Reverse	GGTAGGCAATGAAGGCTAGACC		55		
FABP4	Forward	TGAAATCACCGCAGACGACAGG	57	55	*Sequence available on OriGene*	NM_024406.4
	Reverse	GCTTGTCACCATCTCGTTTTCTC		48		
IGF2R	Forward	CTTCTCCACCAGGATCGTGTTC	57	55	*Sequence available on OriGene*	NM_010515.2
	Reverse	GTCCTTCACCTGGCAGTTGTCT		55		
CALD1	Forward	CTGTCAGAGGACAAGAAGCCGT	57	55	*Sequence available on OriGene*	NM_001347100.1
	Reverse	GGAGACTACTGCTGCTTGGTGA		55		
ITGB1	Forward	CTCCAGAAGGTGGCTTTGATGC	57	55	*Sequence available on OriGene*	NM_010578.2
	Reverse	GTGAAACCCAGCATCCGTGGAA		55		
TTC3	Forward	GATCTGGAGCTGCATCAGTAGC	57	55	*Sequence available on OriGene*	NM_009441.2
	Reverse	CACATCTTGCCGAAGGTGGTCA		55		
PRKAG2	Forward	CTCCTCATCCAAAGAGTCTTCGC	57	52	*Sequence available on OriGene*	NM_145401.2
	Reverse	TGGGTGTTGACGGAGAAGAGGA		55		
KPNA3	Forward	GGTGGTTCTCAACTGTGATGTCC	57	52	*Sequence available on OriGene*	NM_008466.5
	Reverse	GAACTTGCTGCTGATTGCCTGC		55		

2.18 Assessment of Metabolites in Mouse Maternal Plasma

Blood glucose was measured using SD Code-Free blood glucose test strips from SD Biosensor Inc (01GS11C) using a SD Code-Free blood glucose meter. Other maternal plasma metabolites were processed at Core Biochemical Assay Laboratory (CBAL), Cambridge University Hospitals NHS Foundation Trust; free fatty acids were analysed using free fatty acid half-micro kit (Roche Diagnostics, UK), total triglycerides and cholesterol were analysed using Dimension EXL analyzer (Siemens Healthineers, UK), insulin and leptin were analysed using the MesoScale Discovery (Rockville, MD, USA) electrochemiluminescence immunoassay mouse Metabolic assay.

2.19 Mouse Placenta Metabolomics

Metabolite extraction from mouse placental tissue (13 mg) was performed the same as in human placental explants (section 2.8.1). Aqueous metabolite fractions were processed and analysed the same as human placental explants (section 2.8.2).

Organic metabolite fractions were reconstituted in 200µL of isopropyl alcohol (IPA) before being sonicated in a water bath for 10 minutes and placed in liquid chromatography (LC) vials for LCMS. Equipment used and parameters used for positive mode and negative mode metabolites are found in a previously published paper (342). Peaks for all metabolites were processed and integrated using Water TargetLynx (Waters Corporation) and individual peaks were normalised to explant weight. Lipoprotein(a), lysophosphatidylinositols, phosphatidic acids, phosphatidylcholines, phosphatidylethanolamines, phosphatidylinositols, phosphatidylserines, ceramides, hexosylceramides, lysophosphatidylcholines, lysophosphatidylethanolamines, lysophosphatidylglycerols, phosphatidylcholines, sphingomyelins and sphingosines were undetected or mass spectrometry peaks were inconsistently truncated.

MetaboAnalyst.ca was used for one factor analysis, where data was autoscaled and a permutation test was performed to confirm the use of a volcano plot univariate analysis. To detect subtle differences, biologically and significantly altered metabolites were defined as $[Log2FC] \geq 0.26$, $p < 0.05$.

2.20 Mouse Placenta Histology

Fixed mouse placental tissue (processing details in section 2.12.1) were transferred to cassettes (HIS0034; Scientific Laboratory Supplies) and processed in a Tissue Processor (TP1020, Leica) before being positioned in paraffin wax as outlined in (348). Placental sections of 5μM thickness were transferred to pre-coated Poly-L-Lysine adhesion slides (VWR, Avantor, 631-0107). To measure labyrinth structure, double-label immunohistochemistry for lectin and cytokeratin staining was performed, using the protocol and reagents outlined in (349). QuPath (version 0.3.2) was used to analyse DAB-stained images. Surface area was measured by drawing a polygon around the desired tissue area.

2.21 Statistical Analysis

GraphPad Prism 9.3.1 (GraphPad Software Inc., USA) was used for statistical analysis. Shapiro-Wilk test ($p>0.05$) was used to determine normality of data. Where the data was not normally distributed, non-parametric tests such as Mann-Whitney U test for comparison between two groups or Kruskall-Wallis followed by Dunn's multiple comparisons test for comparison between three or more groups were conducted, and the data was presented as the median with 95% CI. For normally distributed data, various parametric tests were used and presented as mean±SEM; t-tests were used to compare two groups, one-way analysis of variance (ANOVA) followed by Holm-Šídák multiple comparisons test was used to compare one factor between three or more groups and two-way ANOVA followed by Tukey's multiple comparisons test was used to compare two factors between three or more groups. Statistically significant differences in fold change were determined with Wilcoxon Signed-Rank test and data was presented as the median. For clustered data, an adjusted mixed-effects linear regression model was performed using StataMP 18 (64-bit) and data was presented as mean±SEM. Differences between categorical data was assessed using Chi-Squared test. 'n' was defined as 'number of samples'.

3 Investigating the Effect of *In-vivo* and *Ex-vivo* Metformin Exposure on Placental Development

3.1 Introduction

Offspring exposed to metformin *in-utero* in pregnancies complicated by GDM have an increased risk of being born SGA and developing childhood adiposity (45). This increases the predisposition of cardiometabolic complications during adulthood and provokes a transgenerational cycle of preventable disease, however the mechanisms responsible are currently unknown (45,54,56).

Metformin is a synthetic guanidine analogue and increases cellular insulin sensitivity by inhibiting mitochondrial complex I (nicotinamide-adenine dinucleotide (NADH):ubiquinone oxidoreductase). This increases NADH levels, elevates reactive oxygen species (ROS) synthesis and in turn, decreases adenosine triphosphate (ATP) production. This leads to an increase in AMP:ATP ratio which activates AMP activated protein kinase (AMPK) heterotrimer. AMPK activation involves AMP binding to the ɣ subunit of AMPK and subsequent Thr172 phosphorylation in the activation loop of its α-subunit (45,350,351). This leads to suppression of gluconeogenesis and the nutrient sensor, mammalian target of rapamycin (mTOR). mTOR inhibition enhances activity of insulin receptor tyrosine kinase and glucose transporter GLUT4, increases glycogenesis, but suppresses lipolysis and hepatic glucose-6-phosphatase activity. GLP-1 activity is also amplified by metformin which increases cellular insulin release. Both AMP deaminase and mitochondrial glycerol-3-phosphate dehydrogenase (G3PDH) are also targets of metformin inhibition, which further contribute towards reduced gluconeogenesis and improved glycaemic control (**Figure *16***) (45,351).

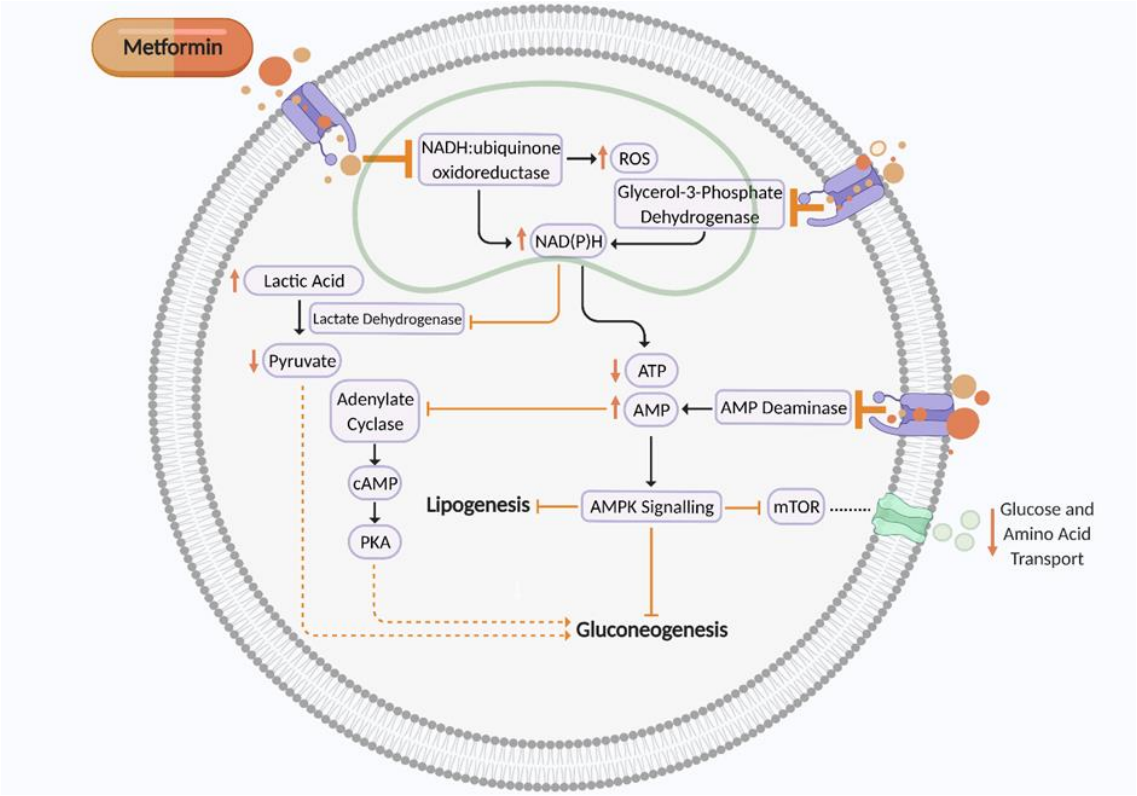

Figure 16 Putative mechanism of action of metformin on cellular metabolism and mitochondrial aerobic respiration to suppress gluconeogenesis

Metformin inhibits mitochondrial complex I, AMP deaminase and mitochondrial glycerol 3 phosphate dehydrogenase (G3PDH). This inhibition regulates glucose levels by suppressing gluconeogenesis. Reactive oxygen species (ROS), Nicotinamide adenine dinucleotide phosphate (NAD(P)H), Adenosine triphosphate (ATP), Adenosine monophosphate (AMP), Cyclic AMP (cAMP), Protein kinase A (PKA), mammalian target of rapamycin (mTOR) (45). Created using Biorender.com.

Unlike insulin, metformin has capacity to reach placental and fetal tissues as studies have shown metformin levels in serum samples from placental, umbilical cord and fetal tissues to be equal or greater than maternal concentrations (352–354). Interestingly, pregnancy is believed to increase metformin bioavailability, volume of distribution and clearance (355,356). Although not fully established, at present it is thought organic cation transporter 3 (OCT3) is the main transporter involved in placental metformin uptake (357). This transporter is found at the placental-fetal interface on the fetal capillaries and syncytiotrophoblast basal membrane. Norepinephrine transporter (NET), serotonin transporter (SERT) and OCT-novel type 2 are also transporters found on the placental maternal interface which have demonstrated a role in metformin placental uptake (45,358,359).

Various animal and human models have identified metformin to influence essential placental developmental processes such as growth, mitochondrial function and metabolism (**Table *19***). However, controversy remains as to whether metformin may be inducing protective or adverse epigenetic modifications in the placenta. Discrepancies in the functional outcomes of metformin on the placenta may be due to the wide range of models used amongst studies, where some studies examine the effect of metformin in specific placental cell lines, and others in explant or *in-vivo* models (**Table *19***). The effects of metformin *in-vivo* may be complicated by maternal metabolism and so it is unclear if any impact on the placenta may be a direct or indirect consequence of metformin. Understanding the mechanisms of metformin on the placenta may help to prevent adverse effects of metformin on placental and offspring development, while also allowing its beneficial effects on maternal health. It is well established that metformin has pleiotropic effects on the development, function and metabolism of various tissues and organs, including adipose tissue, skeletal muscle, liver, kidney and gastrointestinal tract (351,360–362). As such, metformin has demonstrated to impact EV profile and cargo in the circulation of non-pregnant individuals (363–369). It has previously been shown that maternal EVs may be internalised into human placental tissue (272). It therefore remains to be understood whether the effects of *in-vivo* metformin exposure on placental development are mediated through its direct actions on the placenta or through its indirect actions, possibly mediated via EVs.

In-vitro models reporting the effects of metformin use supraphysiological concentrations which may not accurately reflect *in-vivo* conditions (370–374). In this study, the impact of metformin on placental development will be investigated using an *in-vivo* model and it will be determined, using physiological concentrations, if the effects of metformin *in-vivo* are a consequence of its direct actions on the placenta or likely attributed to indirect actions. This may help elucidate the mechanisms through with metformin alters fetal growth in pregnancies complicated by GDM.

Table 19 Contrasting literature on the impact of metformin on placental development

Reference	Model	Effects Demonstrated by Metformin	Significance
Hosni et al. 2021 (375)	Fat-sucrose diet/streptozotocin (FSD/STZ) rat model of GDM treated with metformin *(in-vivo)*	- ↓ fetal blood glucose - ↓ fetal weight - ↑ placental insufficiency - ↑ placental oxidative stress - ↑ angiogenesis related genes	Metformin-mediated reduction in placental weight in pregnancies complicated by GDM may be a consequence of placental insufficiency.
Jiang et al. 2020 (376)	Human GDM and T2DM placental explants cultured and treated with metformin *(ex-vivo)* Mouse placental explants treated with maternal metformin and high fat diet *(in-vivo)*	Male human placental explants: - AMPK activation - ↑ H3K27 acetylation - ↓ DNMT1 protein abundance - ↓ PGC1α promoter methylation and ↑ PGC1α mRNA expression Improved male murine placental efficiency: - ↓ PGC1α promoter methylation and ↑ PGC1α expression - ↑ TFAM expression Improved glucose homeostasis in male offspring	Effects of metformin may be fetal sex-dependent. Metformin may improve placental efficiency by facilitating placental mitochondrial biogenesis. Metformin may be protective to the offspring by suppressing epigenetic changes evoked by maternal diabetes.

Brownfoot et al. 2020 (372) Cluver et al. 2019 (377) Kaitu'u-Lino 2018 (378) Brownfoot et al. 2016 (371)	Human primary tissues exposed to metformin; placental explants, endothelial cells and placental villous explants, whole maternal vessels, maternal omental vessel explants *(in vitro and ex-vivo)*	- ↓ sFlt-1 and sEng secretion from primary endothelial cells, preterm preeclamptic placental villous explants and villous cytotrophoblast cells - ↓ VCAM-1 mRNA expression in endothelial cells - ↑ whole maternal blood vessel angiogenesis - ↓ sFlt mRNA expression - ↓ TNFα-mediated endothelial cell dysfunction	Metformin enhances placental angiogenesis and reduces endothelial dysfunction by decreasing endothelial and trophoblastic antiangiogenic factor secretion via mitochondrial electron transport chain inhibition. Metformin is being trialled as a medication for preeclampsia (PACTR201608001752102).
Wang et al. 2019 (379)	Pregnant mice fed an isocaloric diet (control), high-fat diet or high-fat diet plus metformin *(in-vivo)*	- ↓ placental weight compared to control - partially rescued high-fat diet induced ↓ in placental and fetal weight - ↑ VEGF and MMP-2 protein expression	Metformin improves high fat-diet induced reduction in placental and fetal growth, potentially by modulating placental vasculature.
Szukiewicz et al. 2018 (380)	Human placental lobules perfused with metformin under normoglycemic or hyperglycaemic conditions *(ex-vivo)*	- ↓ CX3CL1 and TNFα secretion - ↑ placental CX3CR1 protein expression - ↓ placental NFκB p65 protein	Metformin has anti-inflammatory effects in the placenta.
Correia-Branco et al. 2018 (381)	HTR-8/SVneo extravillous trophoblast cell line exposed to metformin *(in vitro)*	- ↓ proliferation - ↑ apoptosis - inhibited folic acid uptake - inhibited glucose uptake - effects of metformin were prevented by inhibition of mTOR, JNK and PI3K pathways	Metformin impairs placental development and nutrient transport via PI3K, mTOR, JNK and PI3K pathways.
Arshad et al. 2016 (382)	Human placental explants; from healthy pregnancy, non-treated diet-controlled GDM pregnancy and metformin-treated GDM pregnancy *(ex-vivo)*	- ↓ similar morphology in metformin-treated GDM placenta and non-treated healthy placenta, except for increased cord width - ↓ placental width in metformin-treated GDM placenta compared to non-treated GDM placenta - ↓ chorangiosis, placental thickness and syncytial knots in metformin-treated placenta compared to non-treated GDM placenta	Metformin may improve placental morphology by restoring diabetic placental hallmarks to characteristics similar to healthy placenta.

Han et al. 2015 (383)	Human first trimester trophoblasts treated with or without metformin *(in vitro)*	- ↓ trophoblast cytokine and chemokine release in normal and high glucose culture concentrations - no antiangiogenic or antimigratory effects	Metformin may potentially decrease placental glucose-induced inflammatory response.
Alzamendi et al. 2012 (384)	Pregnant rats fed a normal or high-fructose diet, treated with metformin *(in-vivo)*	- ↓ fetal weight - ⇔ on placental weight or blood vessel area - improved fructose-diet induced ↓ blood vessel area	Metformin reduces fetal weight in mice fed a normal diet. Metformin prevents high-fructose diet induced placental dysfunction.
Jamal et al. 2012 (385)	Pregnant women with PCOS treated with metformin *(in-vivo)*	- ⇔ on birthweight - ↓ uterine artery pulsatility index	Metformin adversely affected uteroplacental circulation.
Tarry-Adkins et al. (2022) (386)	Isolated cytotrophoblasts from term placenta of non-diabetic donors, cultured with metformin *(in-vitro)*	- Reduced basal mitochondrial respiration and ATP production - Reduced markers of oxidative stress	Metformin alters placental energy production.

AMP-activated protein kinase (AMPK); adenosine triphosphate (ATP); DNA methyltransferase (DNMT); peroxisome proliferator-activated receptor-gamma coactivator (PGC)-1α; mitochondrial transcription factor A (TFAM); soluble fms-like tyrosine kinase-1 (sFlt-1); soluble endoglin (sEng); vascular cell adhesion molecule 1 (VCAM-1); tumour necrosis factor alpha (TNFα); vascular endothelial growth factor (VEGF); matrix metalloproteinase-2 (MMP-2); nuclear factor kappa B (NF-κB); mammalian target of rapamycin (mTOR); c-Jun N-Terminal Kinase (JNK); hosphatidylinositol-3-kinase (PI3K) (45).

3.2 Hypothesis

Metformin alters placental development and function via direct and indirect mechanisms.

3.3 Aims

1) Establish the impact of *in-vivo* metformin exposure on the placental transcriptome in pregnancies complicated by GDM.

2) Establish the direct impact of metformin exposure on placental development and function.

- **a.** Determine metformin activation in *ex-vivo* placental villous explants.
- **b.** Determine the effect of metformin on vascular development
- **c.** Determine the effect of metformin on placental growth and function.
- **d.** Determine the effect of metformin on placental metabolism.

3.4 Results

3.4.1 Transcriptomic Analysis of Indirect Metformin Exposure *(In-vivo)* on the Placental Transcriptome

3.4.1.1 Differentially Expressed Genes in the Placental Transcriptome of Obese Women with GDM Receiving Metformin Compared to Placebo

To examine the effect of *in-vivo* metformin exposure on the placenta, transcriptomic datasets from the 'Effect of metformin on maternal and fetal outcomes in obese pregnant women' (EMPOWaR) study (EudraCT number 2009-017134-47; 10/MRE00/12) were assessed. Women with GDM were included in this study and so this dataset was utilised to examine the impact of metformin on the placenta in GDM. Data from the study was previously processed by the Forbes group (Katie Hugh MRes dissertation), where differentially expressed genes (DEGs) were identified in the placental transcriptome of obese women with GDM treated with metformin compared to placebo (387). In the EMPOWaR study, 108 patients were recruited where 30 were diagnosed with GDM. Of those diagnosed with GDM, 12 were treated with metformin and 18 were treated with placebo. In the metformin-treated group, 10 pregnancies resulted in female AGA infants, 1 pregnancy resulted in a male AGA infant and another pregnancy resulted in a male LGA infant. Therefore, as most pregnancies exposed to metformin resulted in female AGA outcomes, only female AGA pregnancies were included in the transcriptomic analyses for both metformin (n=10) and placebo (n=6) treatments (**Table *20***, **Table *21***). Following stratification, 46 DEGs, defined as $-0.58 \leq Log_2FC \geq 0.58$, ($p<0.01$) to identify subtle differences in gene expression, were detected (**Figure *17***). However, 8 of these annotated genes were uncharacterised, therefore a total of 38 genes were included in functional analysis, where 9 genes were upregulated, and 29 genes were downregulated by metformin compared to placebo (**Table *22***).

Table 20 Pregnancy outcomes of women diagnosed with GDM treated with metformin or placebo in the EMPOWaR study

Treatment group	Fetal size	Number of patients	Fetal sex	
			Male	Female
Placebo	AGA	12	6	**6***
	LGA	5	4	1
	SGA	1	1	0
Metformin	AGA	11	1	**10***
	LGA	1	1	0
	SGA	0	0	0

Birthweight was classified in accordance with WHO Growth Charts (115). Analysis included placental transcriptomic data from women diagnosed with GDM with female AGA pregnancy outcomes (n = 16). * = included in transcriptomic analysis. *Katie Hugh MRes dissertation.*

Table 21 Demographic details of women diagnosed with GDM treated with metformin or placebo in the EMPOWaR study, included in placental transcriptomic analysis

	Metformin (n=10)	Placebo (n=6)	Significance
	Median	Median	
Maternal Characteristics			
Maternal Age (Years)	29 (19 – 35)	31.5 (23 – 41)	0.98
Smoking Status	Non-smoker (100%)	Non-smoker (83.3%) Active (16.7%)	0.38
GDM Diagnosis (Weeks)	36 (28 – 36)	36 (28 – 36)	>0.99
Delivery Method	Caesarean (90%) Vaginal (10%)	Caesarean (66.7%) Vaginal (33.3%)	0.52
Offspring Characteristics			
Fetal sex	Female (100%)	Female (100%)	>0.99
Gestational Age (Days)	275.5 (267-283)	272.5 (261 - 283)	0.82
Birthweight (g)	3235 (2884-3920)	3345 (3058 – 3495)	>0.99
Weight Categorisation	34 (10-88)	44 (20 – 58)	>0.99

Demographic details of participants included in placental transcriptomic analysis from the EMPOWaR study. Significant differences were found between treatment groups (Mann-Whitney U Test, Fisher's Exact Test). *Adapted from Katie Hugh, MRes dissertation.*

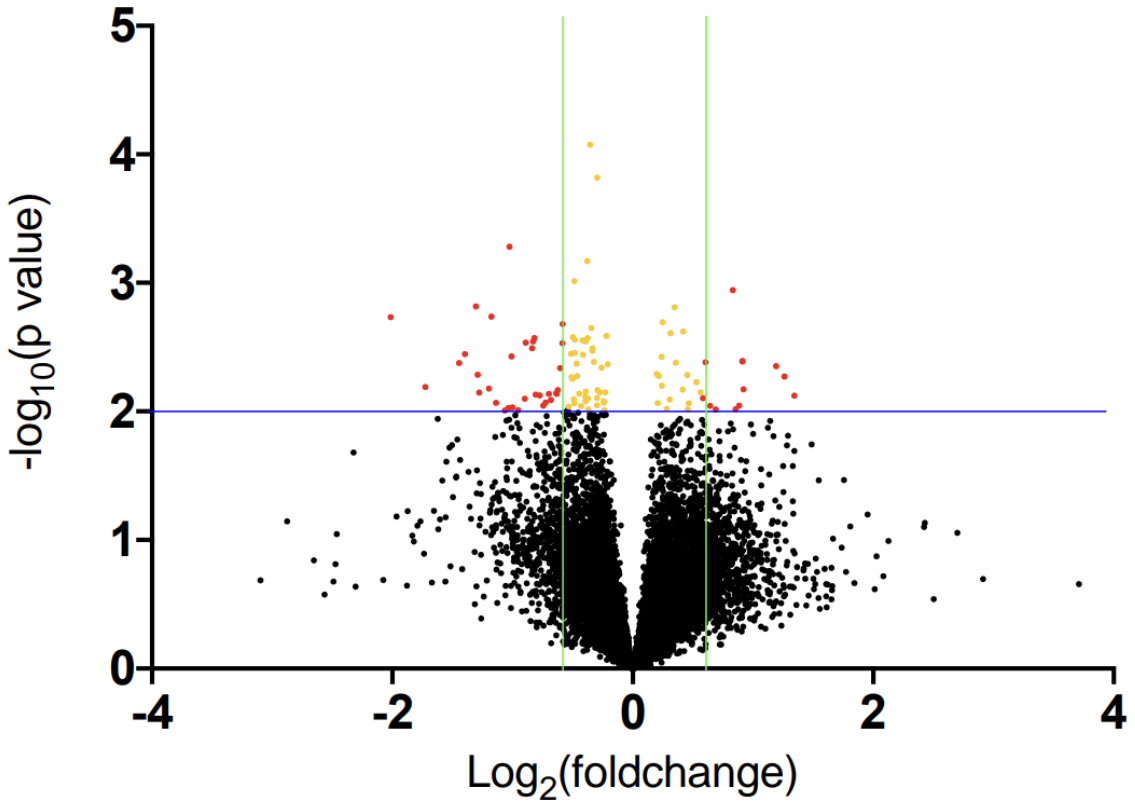

Figure 17 Volcano plot of differentially expressed genes (DEGs) included in functional enrichment analyses of the placental transcriptome of women with GDM taking metformin compared to placebo.

Placental transcriptomic data from the EMPOWaR study was compared between women diagnosed with GDM with female AGA pregnancy outcomes treated with metformin (n=10) or placebo (n=6). Genes detected as statistically significant (yellow; $p \leq 0.01$) and biologically significant (red; $-0.58 \leq Log_2FC \geq 0.58$) were defined as differentially expressed genes (DEGs) and were included in functional enrichment analyses. Key: blue, p=0.01; green, $-0.58 \leq Log_2FC \geq 0.58$; black, ns. *Katie Hugh MRes dissertation.*

Table 22 List of differentially expressed genes (DEGs) in women with GDM taking metformin compared to placebo

Gene Name	Gene Stable ID	P Value	Fold Change	Log_2Fold Change
SHLD1	ENSG00000171984	0.008	2.538	1.344
MIRLET7BHG	ENSG00000197182	0.005	2.398	1.262
PPARGC1B	ENSG00000155846	0.004	2.285	1.192
MAP3K7CL	ENSG00000156265	0.004	1.882	0.912
EIF4E3	ENSG00000163412	0.004	1.882	0.912
MT2A	ENSG00000125148	0.009	1.845	0.883
FAM24B	ENSG00000213185	0.010	1.808	0.854
NEFH	ENSG00000100285	0.009	1.563	0.644
GPSM2	ENSG00000121957	0.008	1.499	0.584
JHY	ENSG00000109944	0.002	0.667	-0.585
KDELR1	ENSG00000105438	0.003	0.666	-0.586
YIPF2	ENSG00000130733	0.005	0.657	-0.606
HYAL4	ENSG00000106302	0.007	0.649	-0.624
PINK1	ENSG00000158828	0.007	0.645	-0.633
KCTD17	ENSG00000100379	0.007	0.643	-0.637
LINC00997	ENSG00000281332	0.008	0.623	-0.682
ZNF568	ENSG00000198453	0.007	0.617	-0.698
ANKDD1A	ENSG00000166839	0.009	0.605	-0.726
GPATCH1	ENSG00000076650	0.009	0.597	-0.744
PHF21B	ENSG00000056487	0.007	0.585	-0.774
OSCP1	ENSG00000116885	0.003	0.567	-0.819
TIAM1	ENSG00000156299	0.003	0.563	-0.829
PRSS8	ENSG00000052344	0.003	0.560	-0.837

MFAP2	ENSG00000117122	0.008	0.536	-0.899
MAPRE3	ENSG00000084764	0.010	0.516	-0.955
PGAP3	ENSG00000161395	0.009	0.500	-1.001
KIF17	ENSG00000117245	0.004	0.497	-1.010
HOXB2	ENSG00000173917	0.009	0.488	-1.034
TMEM164	ENSG00000157600	0.010	0.478	-1.064
ALOXE3	ENSG00000179148	0.009	0.454	-1.138
MGAT5	ENSG00000152127	0.002	0.443	-1.176
LINC01881	ENSG00000220804	0.007	0.413	-1.277
CCDC113	ENSG00000103021	0.005	0.409	-1.291
ARHGEF34P	ENSG00000204959	0.002	0.404	-1.306
LINC01119	ENSG00000239332	0.004	0.380	-1.396
ITGB3	ENSG00000259207	0.004	0.367	-1.444
TMPRSS6	ENSG00000187045	0.006	0.302	-1.726
ERICH5	ENSG00000177459	0.002	0.247	-2.015

Placental transcriptomic data from the EMPOWaR study was compared between women diagnosed with GDM with female AGA pregnancy outcomes treated with metformin (n=10) or placebo (n=6). Differentially expressed genes (DEGs) defined as $-0.58 \leq Log_2FC \geq 0.58$, ($p<0.01$). Upregulated genes are shaded in green and downregulated genes are shaded in red.

3.4.1.2 Functional Enrichment Analysis of the Placental Transcriptome of Obese Women with GDM Receiving Metformin Compared to Placebo

3.4.1.2.1 Ingenuity Pathway Analysis

IPA was conducted to predict the functional consequence of DEGs that were altered in placental tissue obtained from obese women with GDM taking metformin compared to obese women with GDM taking placebo. IPA considers statistical significance and directionality of DEGs which increases the robustness of data interpretation (334). DEGs were mapped to 75 disease and function terms and 6 IPA canonical pathways over the determined statistical significance threshold of -log(p-value)>1.3=p-value<0.05 (**Figure *18***). The top 25 mapped disease and function terms included terms that are known to be relevant for placental development and function such as 'Cellular Development', 'Embryonic Development', 'Cellular Function and Maintenance' and 'Cellular Growth and Proliferation', 'Cell Death and Survival', 'Cardiovascular Disease' and 'Metabolic Disease' (**Figure *18***A). All top 25 mapped disease and function terms generated a z-score of 0, indicating no definitive direction of change in terms of activation or inhibition. Canonical Pathways attributed to DEGs included 'Actin Cytoskeleton Signalling', 'Fatty Acid α-oxidation', 'RAC signalling', 'Tumour Microenvironment Pathway' and pathways enriched in Metazoa, including 'Chondroitin Sulfate Degradation (Metazoa)' and 'Dermatan Sulfate Degradation (Metazoa)' (**Figure *18***B).

3.4.1.2.2 Upstream Regulators

Several upstream molecules which could be responsible for the DEGs in obese women with GDM taking metformin compared to placebo were identified (**Figure *19***). Mapped upstream regulators were above the determined statistical significance threshold of -log(p-value)>1.3=p-value<0.05. All upstream regulators demonstrated a z-score of 0, indicating no definitive direction of change in terms of activation or inhibition, except WW Domain Binding Protein 2 (WBP2) which demonstrated a positive z-score of 1, indicating mild activation. WBP2 demonstrated the highest statistical significance, with this transcription regulator

being mapped to 4 placental DEGs (ALOXE3, ITGB3, MAPRE3, OSCP1). Interestingly WBP2 is an oncogene, that similar to metformin, induces phosphorylation of AMPK to activate the AMPK pathway, affecting lipid metabolism and contributing to high-fat diet-induced fatty liver and insulin resistance (388). miR-449 was another predicted upstream regulator with high statistical significance; this was mapped to the regulation of CCDC113 and JHY. Huntingtin encoding gene, HTT, was also mapped to the regulation of 5 of the placental DEGs (HOXB2, KCTD17, NEFH, PPARGC1B, TIAM1). HTT has previously been characterised in early placental development, where metformin has demonstrated protective effects from mutant HTT toxicity by regulating mitochondrial dynamics (389,390). Interestingly, peroxisome proliferator-activated receptor gamma coactivator 1-β (PPARG1β) was also identified as an upstream regulator for two placental DEGs known as PGAP3 and PPARG1β, a transcription regulator associated with diabetes and a master regulator of mitochondrial biogenesis and fatty acid β-oxidation (391).

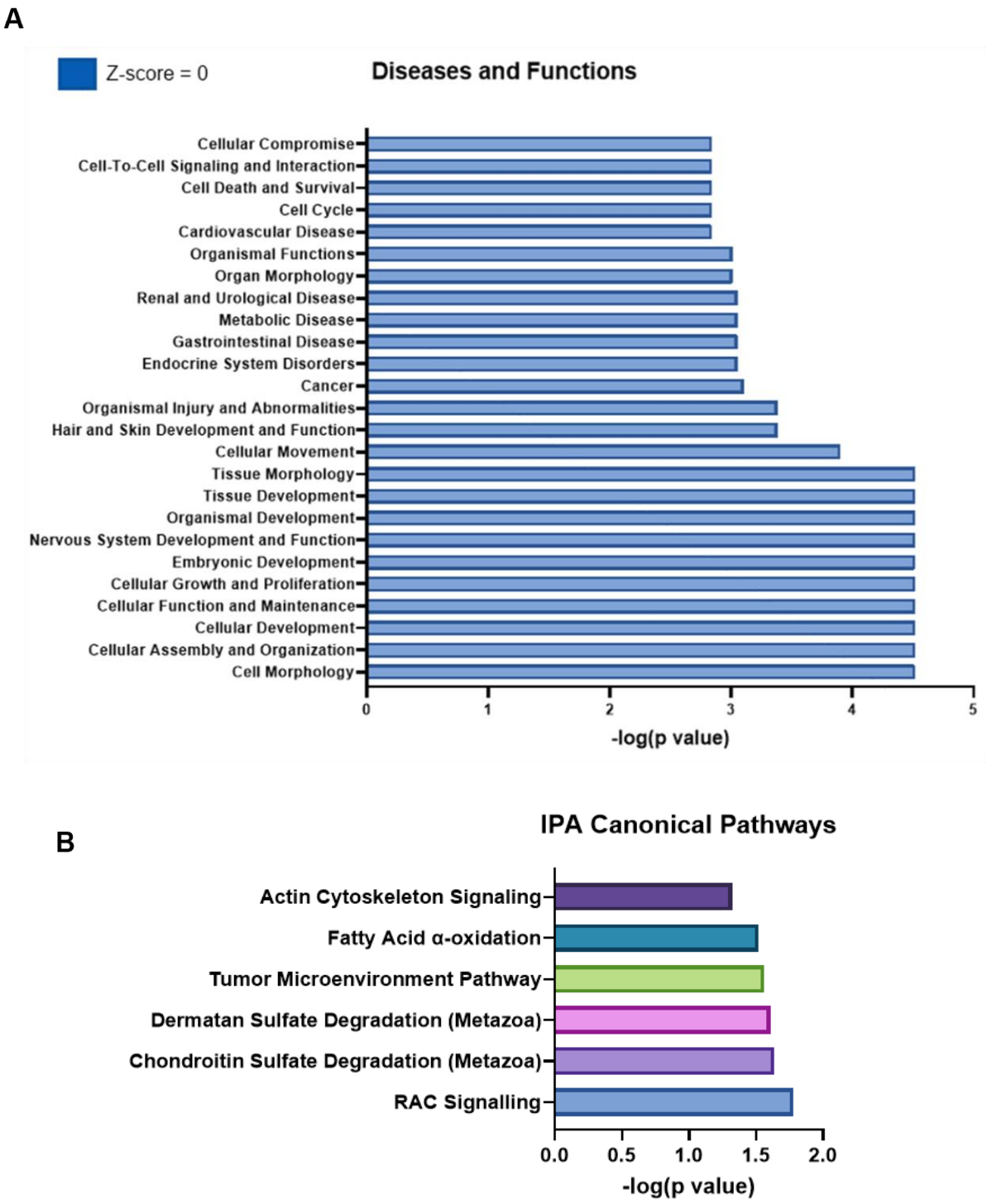

Figure 18 Predicted diseases, functions and canonical pathways of DEGs in obese women with GDM taking metformin compared to placebo.

DEGs were analysed by Ingenuity Pathway Analysis (IPA). (A) Diseases and functions mapped to placental DEGs (-log(p-value)>1.3=p-value<0.05). Key: blue, z-score=0, indicating no direction of change in terms of activation or inhibition. (B) Significant canonical pathways mapped to DEGs (-log(p-value)>1.3=p-value<0.05).

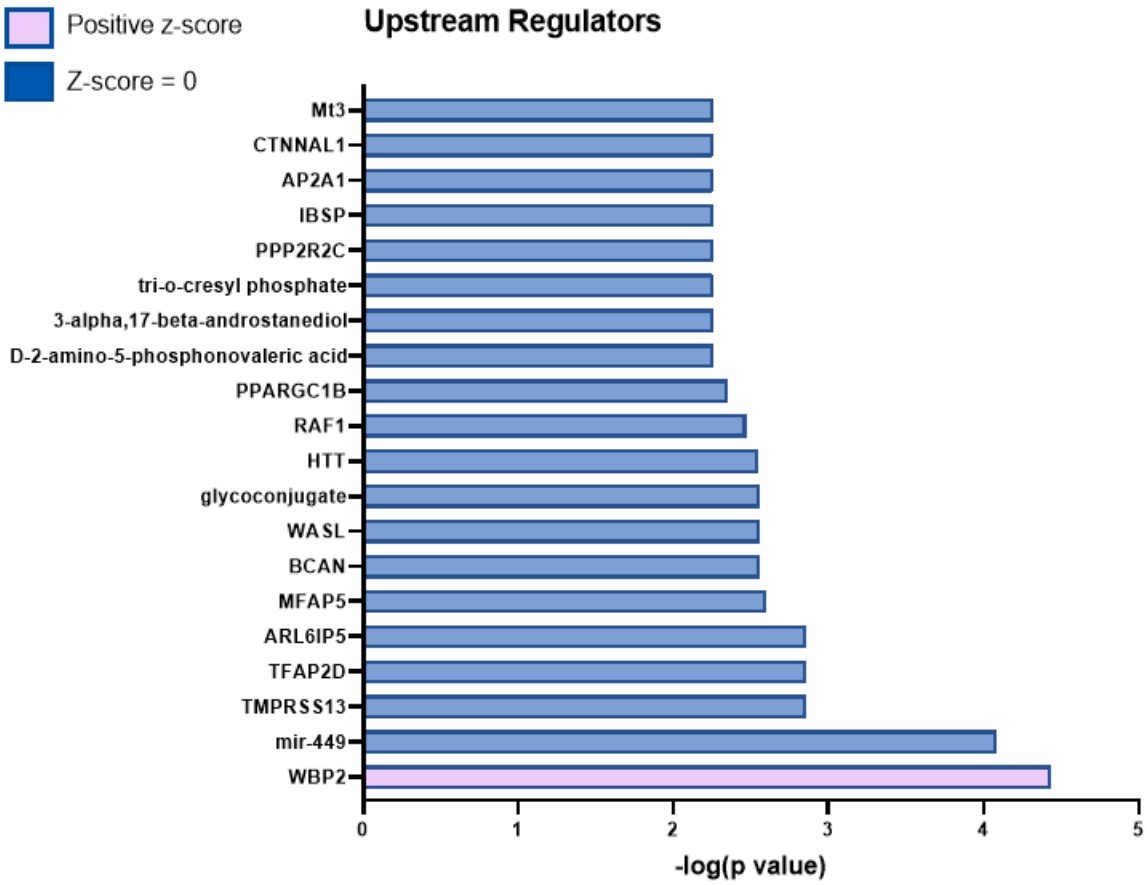

Figure 19 Upstream regulators of DEGs in the placental transcriptome of obese women with GDM taking metformin compared to placebo.

Upstream regulators mapped to placental DEGs (-log(p-value)>1.3=p-value<0.05). Key: pink, positive z-score indicating activation; blue, z-score=0 indicating no direction of change in terms of activation or inhibition.

3.4.1.2.3 Biological Networks

Further analyses were performed in IPA to establish interactions between DEGs. Three biological networks were generated: A network for cell-to-cell signalling and interaction/hematological system development and function/immune cell trafficking (**Figure *20***A), cellular/embryonic/organismal development (**Figure *20***B) and lipid metabolism/connective tissue disorders/organismal injury and abnormalities (**Figure *20***C). Networks demonstrated interactions between DEGs (red indicating upregulation, green indicating downregulation) and predictive interactions between other genes not included in the imported dataset (orange predicting activation, blue predicting inhibition). Although association between some DEGs in the biological networks could not be predicted, these results demonstrate that *in-vivo* metformin exposure may impact placental processes such as vascular development, cellular development and metabolism, which may have a functional effect on fetal development and metabolic health.

A Cell-to-cell signalling and interaction/hematological system development and function/immune cell trafficking

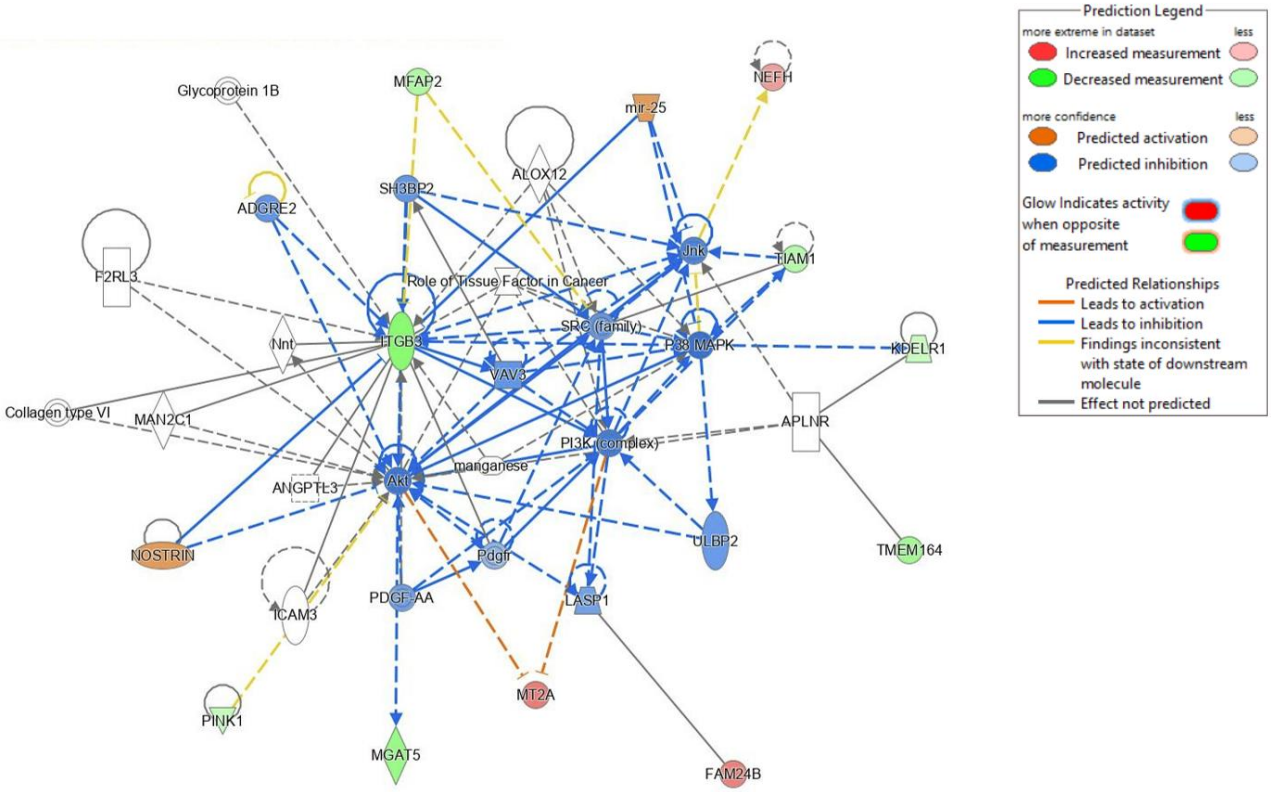

B Cellular/embryonic/organismal development

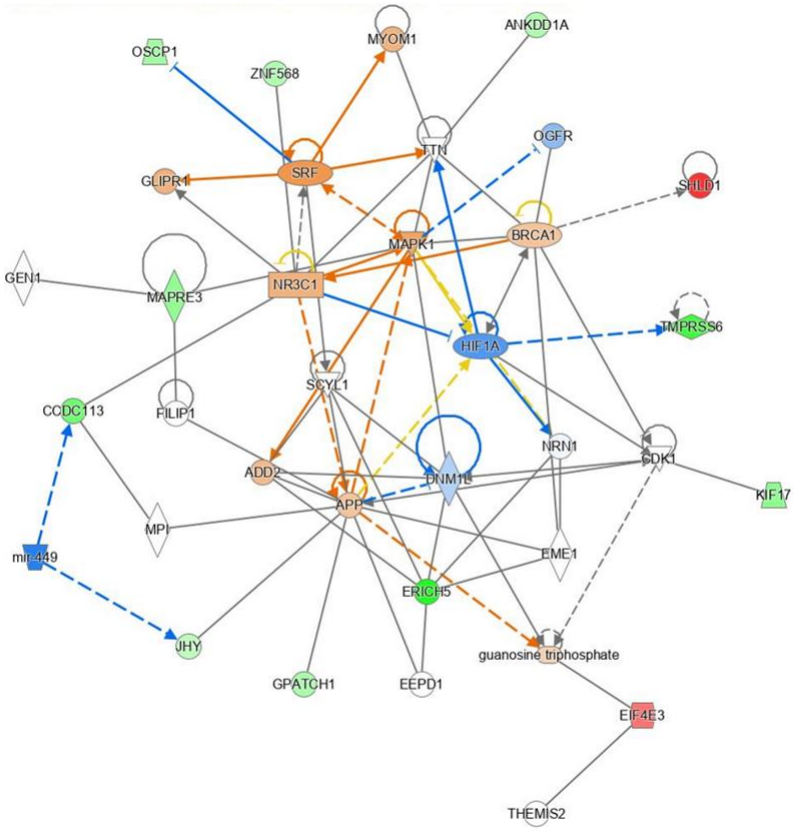

C Lipid metabolism/connective tissue disorders/organismal injury and abnormalities

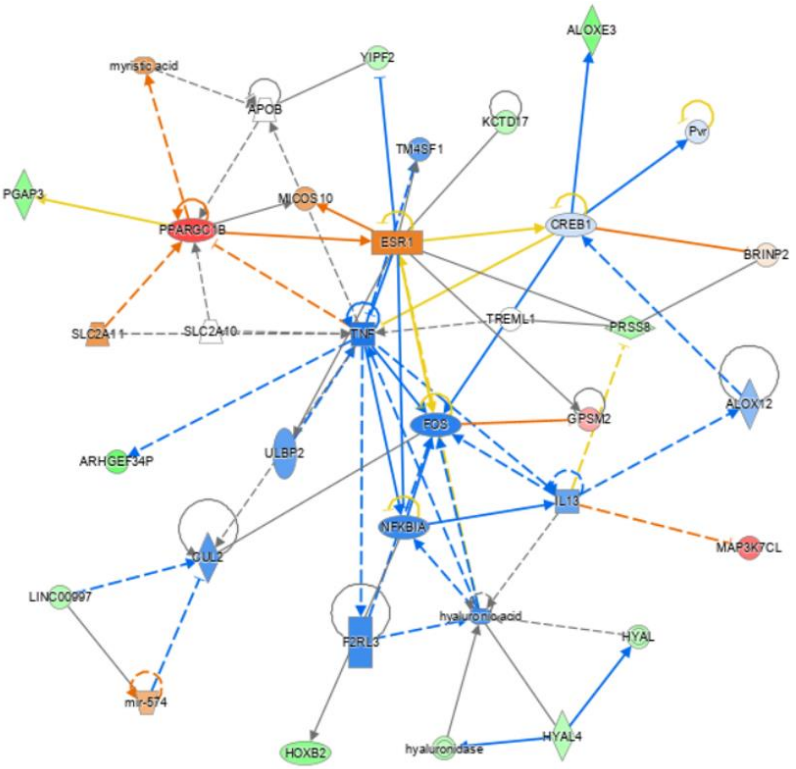

Figure 20 Biological networks associated with DEGs in placental tissue obtained from obese women with GDM taking metformin compared to placebo.

A) Cell-to-cell signalling and interaction/hematological system development and function/immune cell trafficking **(B)** Cellular/embryonic/organismal development **(C)** Lipid metabolism/connective tissue disorders/organismal injury. Networks demonstrate interactions between DEGs (red indicating upregulation, green indicating downregulation) and predictive interactions between other genes not included in the imported dataset (orange predicting activation, blue predicting inhibition). Placental DEGs were defined as -log(p-value)>1.3=p-value<0.05.

3.4.2 Impact of Direct Metformin Exposure on the Placental Transcriptome

Adaptations to placental transcriptomic pathways in response to *in-vivo* metformin exposure may play a role in the pathophysiology of adverse fetal outcomes that are associated with metformin therapy. However, while an *in-vivo* model is essential to further our understanding of the physiological role of metformin, this model does not determine if the effects exerted on the placenta are a direct consequence of metformin or an indirect consequence via other actions of metformin on maternal metabolism.

Previous studies have utilised isolated cell models to ascertain the impact of supraphysiological concentrations of metformin on the placenta (370,371). In contrast to an in-vitro model, all cell types are present in an explant model of the human placenta. Given that the transcriptomic analysis demonstrated *in-vivo* exposure of metformin influenced complex biological networks in the placenta, the impact of physiological concentrations of metformin on a human placental explant model was assessed. This was to determine if the effects of metformin *in-vivo* are a consequence of its direct actions on the placenta or are likely attributed to indirect actions.

3.4.2.1 Metformin Activation in the Placenta

Recent studies have demonstrated that *in-vivo*, maternal metformin levels are in the region of 100nM-10μM, which corresponds to placental metformin concentrations in the region of 0.01-0.25nMol/mg (386). Furthermore, it was established that culture of healthy isolated placental trophoblast cells in 100μM metformin resulted in cellular metformin levels of 0.05nMol/mg (386). To model *in-vivo* concentrations of metformin in the placenta, we therefore used concentrations in the range of 0-1mM.

Metformin exerts its action by activation of AMPK (45,351). To determine if these physiologically relevant concentrations of metformin have the potential to affect the placenta, the impact of metformin on AMPK activation was established. Immunohistochemistry (IHC) revealed that AMPK was localised to placental syncytiotrophoblast, cytotrophoblast and villous stroma (**Figure *21***). Western

blotting revealed activation (phosphorylation) of AMPK was minimal under basal conditions (**Figure *22***) but increased in a dose-dependent manner following exposure of placental explants to metformin for 24 hours, with significant difference in activation observed with 100 μM (from 0.891 ± 0.167 A.U. to 1.994 ± 0.326 A.U., p=0.043, n=4) and 1mM metformin (from 0.891 ± 0.167 A.U. to 2.210 ± 0.223 A.U., p=0.015, n=4) compared to control conditions. IHC revealed that p-AMPK was detected within cytotrophoblasts and in the villous stroma (**Figure *21***). This demonstrates that physiologically relevant concentrations of metformin can exert direct actions on the placenta and validifies the use of the placental villous explant model to study the direct actions of metformin in the placenta

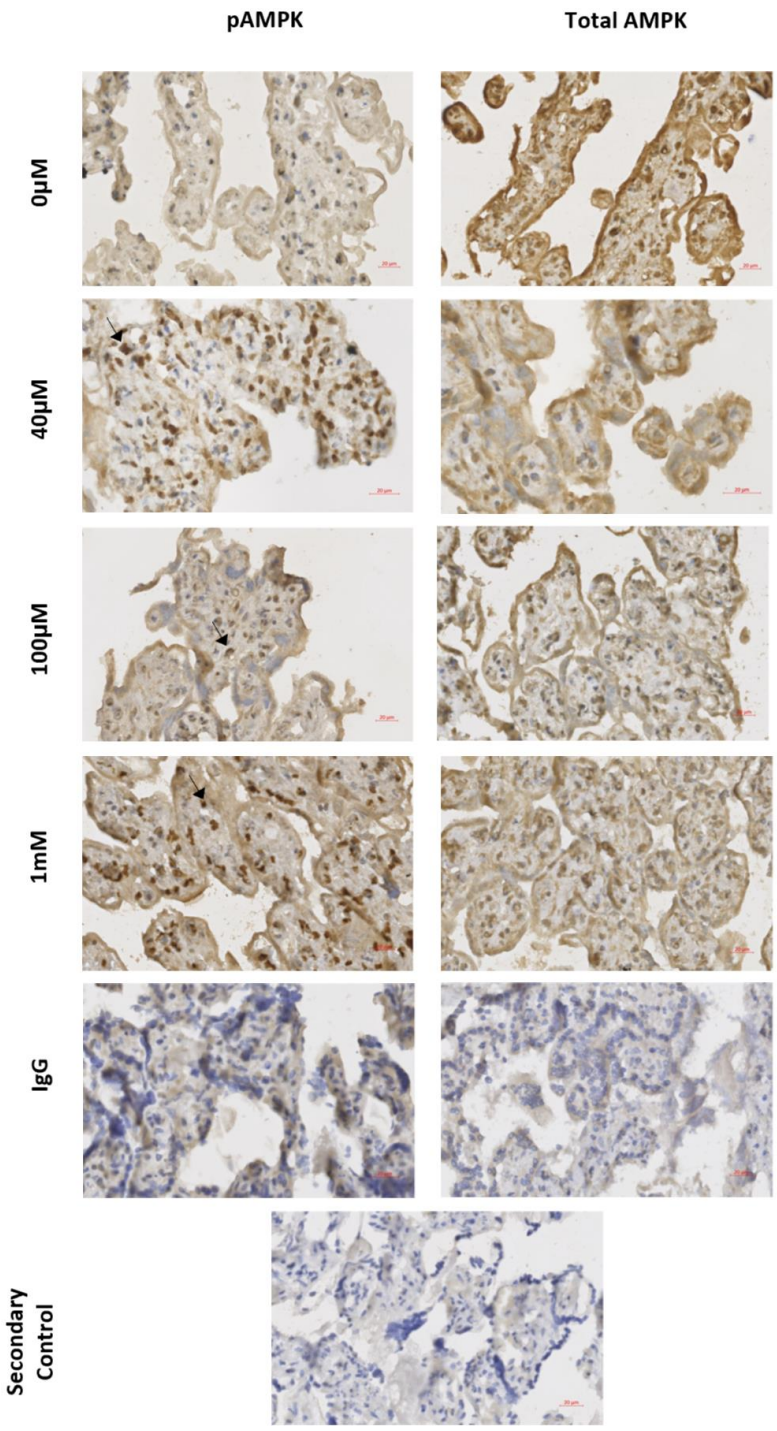

Figure 21 Localisation of total- and phospho-AMPK in placental villous explants following metformin treatment.

Placental villous explants were cultured for 4 days, then treated with metformin at 0, 40µM, 100µM or 1mM for 24 hours. Placental samples were formalin fixed paraffin embedded (FFPE) and immunohistochemistry was conducted using total AMPK alpha1 antibody (rabbit polyclonal, 1:100) or anti-phospho-AMPK alpha-1,2 (Thr183, Thr172; rabbit polyclonal 1:20) in 1X TBS overnight at 4°C before being incubated with a biotinylated secondary IgG (rabbit, 1:200) in 1X TBS for 1 hour at RT. Non-immune rabbit IgG control and secondary IgG control were used. Histological slides imaged at x20. Arrows indicate phospho-AMPK staining. Scale bar: 20µm.

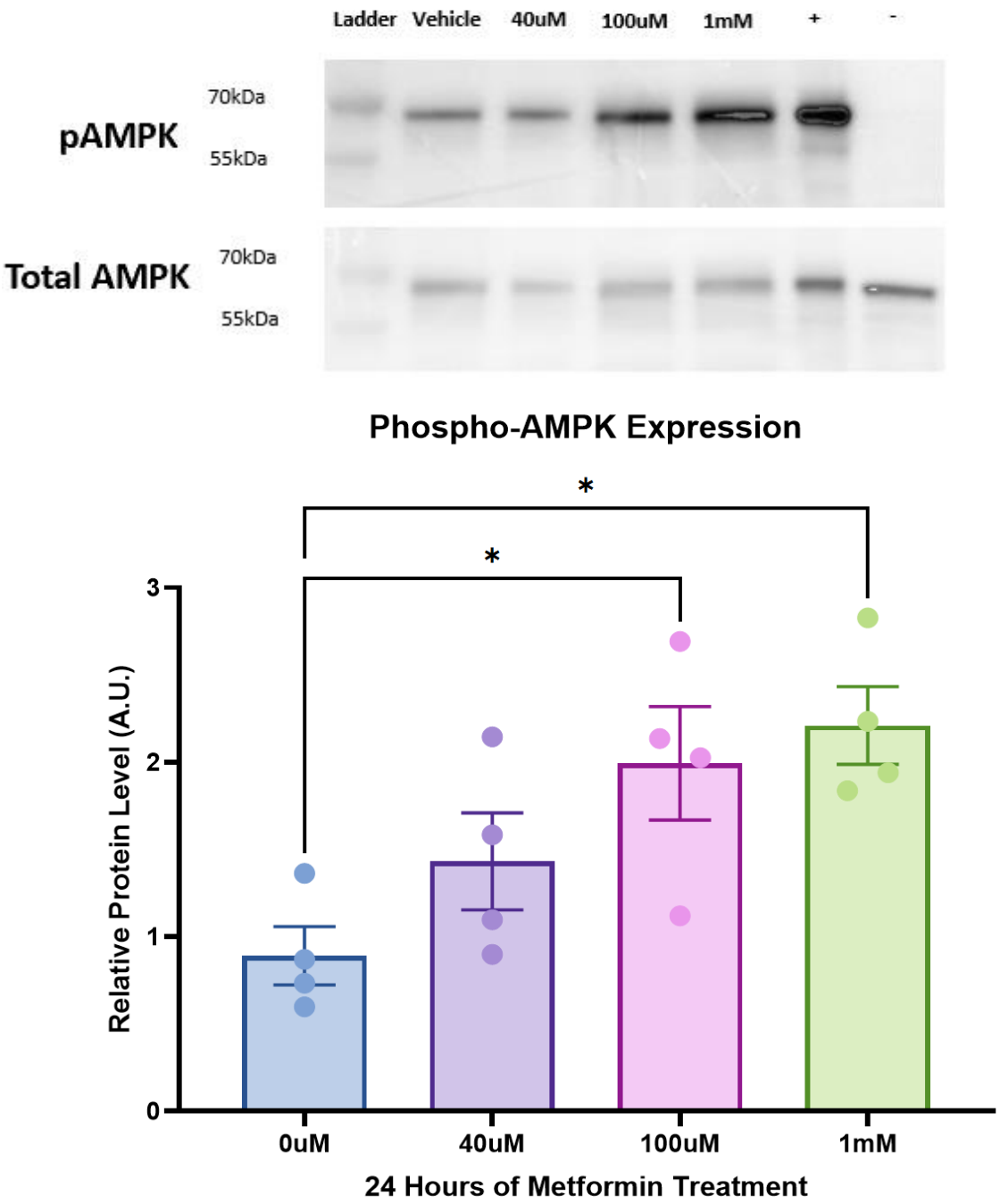

Figure 22 AMPK activation in placental villous explants treated with metformin after 24 hours.

Placental villous explants were cultured for 4 days, then treated with metformin at 0, 40μM, 100μM or 1mM for 24 hours. Samples were subjected to western blotting and probed for pAMPKα (Thr172) (rabbit monoclonal, 1:1000) and AMPKα (rabbit monoclonal, 1:1000). Relative densitometry was calculated using ImageJ. One-way ANOVA (with Tukey's post-hoc test) was performed to measure significant differences between groups. Data is presented as mean ±SEM (n=4), *=$p \leq 0.05$. Arbitrary Units (A.U.).

3.4.2.2 Direct Impact of Metformin on Vascular Development in the Placenta.

As metformin had activated the AMPK pathway after 24 hours of culture, markers of placental development were assessed after 72 hours of metformin exposure in placental villous explants, where longer-term impacts on gene and protein expression could be assessed.

ITGB3 was identified as a key regulator in the 'cell-to-cell signalling and interaction/hematological system development and function/immune cell trafficking' biological network detected in the transcriptomic analysis and was downregulated with *in-vivo* metformin exposure (**Figure *20***A, **Table *22***). Direct exposure of physiological concentrations of metformin also downregulated *ITGB3* expression in human placental explants. The most significant decrease was observed with 100μM metformin (median FC=0.58, p=0.016, n=7), followed by 1mM metformin (median FC=0.71, p=0.031, n=7), compared to control (**Figure *23***).

Protein expression of CD31 was analysed in the human placental explants to investigate the direct impact of metformin on placental vascular differentiation. IHC demonstrated CD31 to be localised to endothelium of blood vessel lumens (**Figure *24***). Although a significant reduction in CD31 expression was observed with 40μM metformin compared to control (median FC=0.58, p=0.047, n=7), no significant changes in expression were observed at higher metformin concentrations (**Figure *24***).

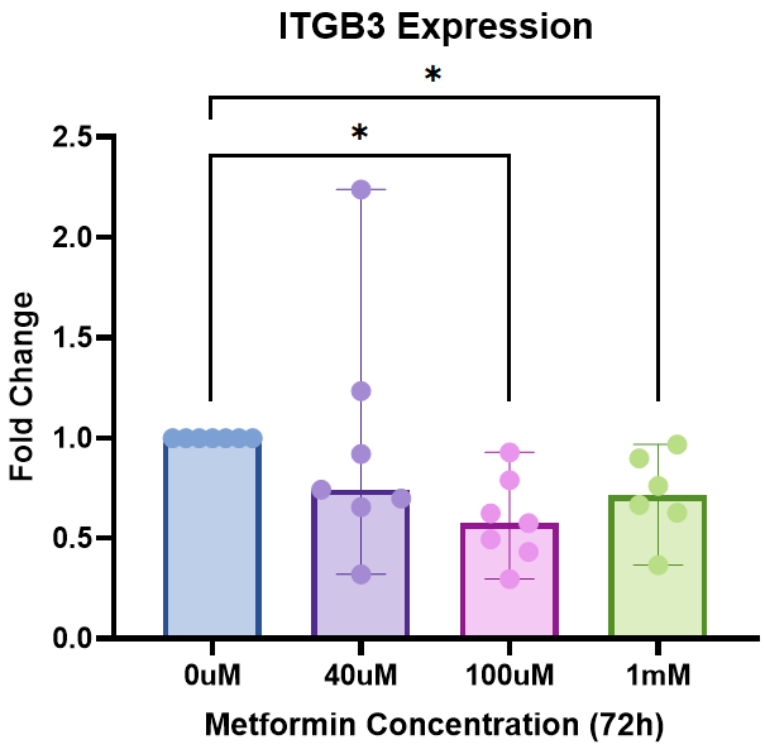

Figure 23 ITGB3 mRNA expression in placental villous explants at 72 hours of metformin treatment.

Placental villous explants were treated with metformin (40µM-1mM) and total RNA was extracted. Gene expression was analysed using RT-qPCR before being normalised to mean expression of *YWHAZ, β-ACTIN* and *18S*; (2^(-Ct)*10^(2). Wilcoxon Signed-Rank test was performed. Data presented as median fold change (compared to control 0µM) with range (95% CI) (n=7); *=p ≤ 0.05.

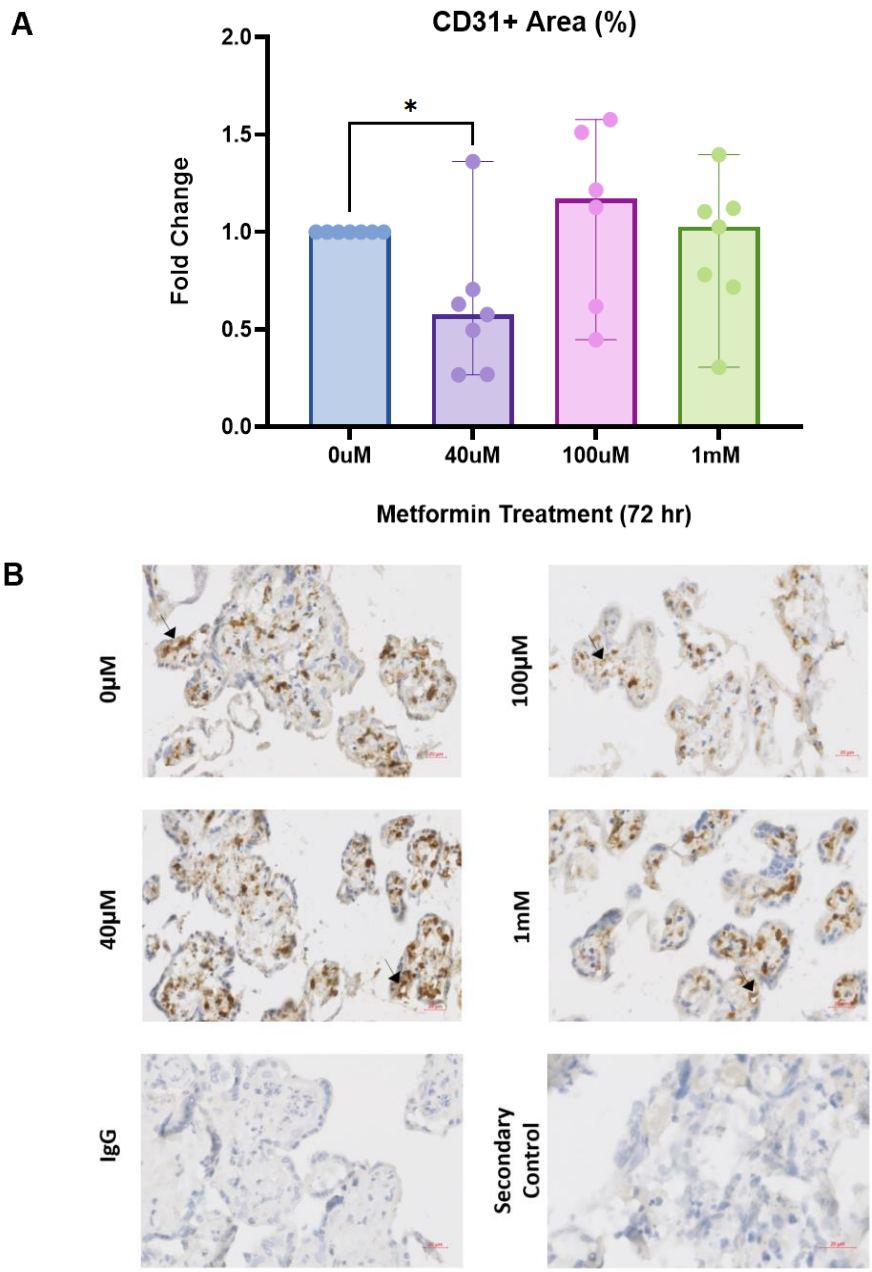

Figure 24 Immunostaining of vascular marker CD31 in placental villous explants at 72 hours of metformin treatment.

Placental villous explants were cultured for 4 days, then treated with metformin at 0, 40µM, 100µM or 1mM for 72 hours. Placental samples were formalin fixed paraffin embedded (FFPE) and immunohistochemistry was conducted using anti-human CD31, endothelial cell clone JC70A antibody (mouse, 1:200) in 1X TBS overnight at 4°C before being incubated with a biotinylated secondary mouse IgG control (mouse, 1:200) in 1X TBS for 1 hour at RT. Non-immune mouse IgG control and secondary IgG control were used. (A) Positive cell detection was quantified using QuPath. Wilcoxon Signed-Rank test was performed. Data presented as median fold change (compared to control 0µM) with range (95% CI) (n=7); *=$p \leq 0.05$. (B) Histological slides imaged at x20. Arrows indicate CD31 staining localised to endothelium of blood vessel lumens. Scale bar: 20µm.

3.4.2.3 Direct Impact of Metformin on Cellular Development in the Placenta.

3.4.2.3.1 Cellular Growth and Proliferation

To determine the functional impact of direct metformin exposure on placental development and growth, human placental explants were stained for proliferative nuclear protein marker Ki67. A reduction in Ki67 expression was observed with 40μM metformin (median FC=0.45, n=7, p=0.578), however this was not statistically significant compared to control. No change in expression was identified with 100μM metformin (median FC=1.10, n=7, p=0.469). Moreover, although not significant, an increase in Ki67 expression was observed with 1mM metformin compared to control (median FC=1.75, n=7, p=0.297) (**Figure *25***).

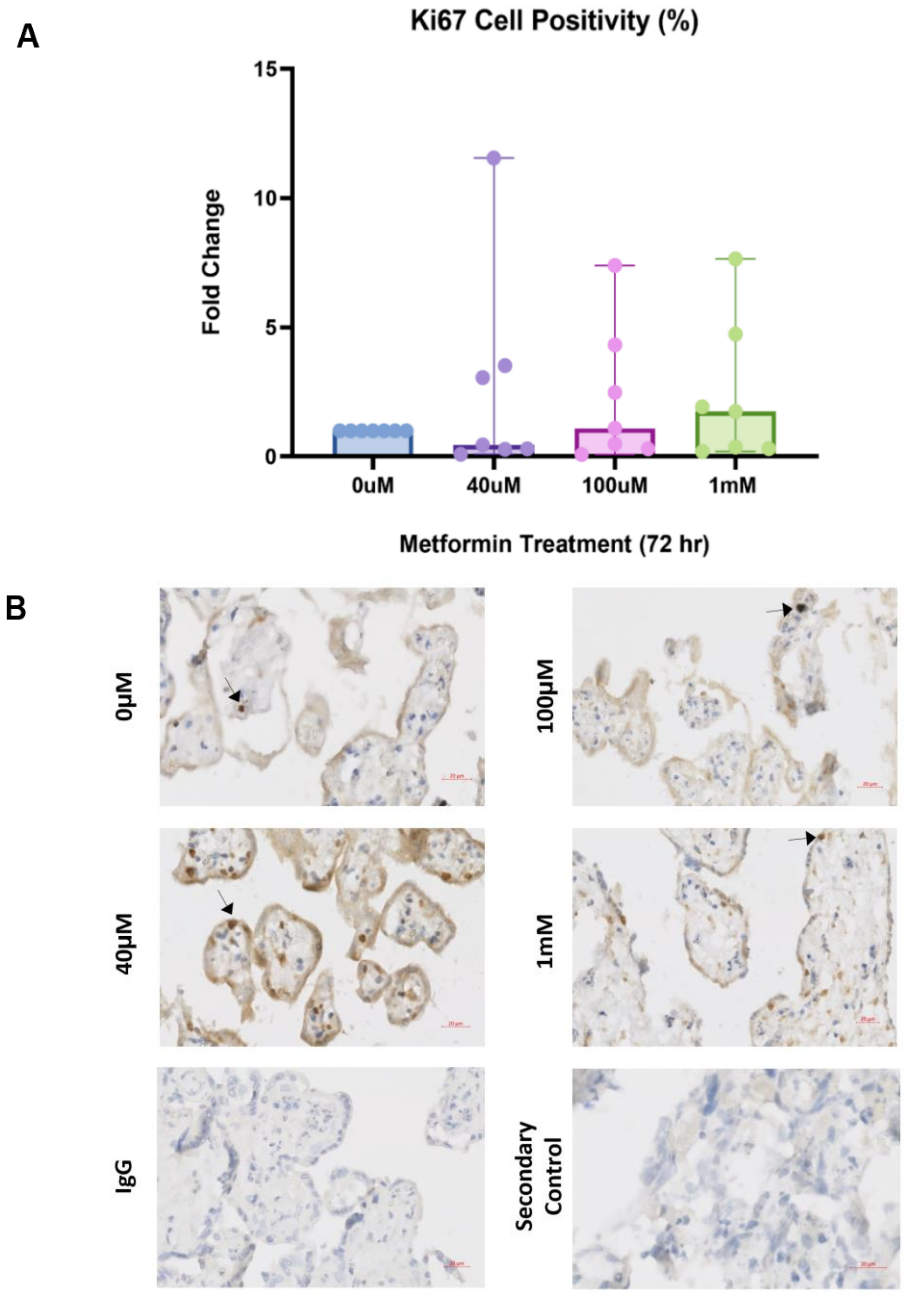

Figure 25 Immunostaining of proliferative marker Ki67 in placental villous explants at 72 hours of metformin treatment.

Placental villous explants were cultured for 4 days, then treated with metformin at 0, 40µM, 100µM or 1mM for 72 hours. Placental samples were formalin fixed paraffin embedded (FFPE) and immunohistochemistry was conducted using anti-human Ki-67 antigen clone MIB-1 antibody (mouse, 1:200) in 1X TBS overnight at 4°C before being incubated with a biotinylated secondary mouse IgG control (mouse, 1:200) in 1X TBS for 1 hour at RT. Non-immune mouse IgG control and secondary IgG control were used. (A) Positive cell detection was quantified using QuPath. Wilcoxon Signed-Rank test was performed. Data presented as median fold change (compared to control 0µM) with range (95% CI) (n=7); *=p ≤ 0.05. (B) Histological slides were imaged at x20. Arrows indicate Ki-67 staining. Scale bar: 20µm.

3.4.2.3.2 Cellular Death and Toxicity

Controversy remains in the literature as to whether metformin impacts lactate turnover (392,393). The expression of lactate dehydrogenase (LDH) is also a common marker of tissue necrosis (394). Therefore, to confirm the direct effect of physiological metformin concentrations on placental villous explant lactate turnover, LDH levels were measured in the culture media over 72 hours (**Figure *26***). Media from day 1 of culture demonstrated the highest levels of LDH (0.023 ± 0.010 [U/ml]mg, n=4), likely due to it being only 24 hours since processing the explants. No differences in culture media LDH levels were observed over 72 hours, however a non-significant decrease was observed by day 2 (0.011 ± 0.004 [U/ml]mg, n=6, p=0.829) and remained relatively stable until day 5, where a further non-significant decrease was observed compared to day 1 (0.007 ± 0.002 [U/ml]mg, n=7, 0.324). Relative to day 1, LDH levels remained low at day 6 (0.010 ± 0.006 [U/ml]mg, n=7, p=0.451) and day 7 (0.008 ± 0.004 [U/ml]mg, n=7, p=0.558). This demonstrates that the human placental explant models were viable at days 5-7 when metformin treatment was exerted (**Figure *26***A).

No significant changes in culture media LDH levels were observed with direct metformin exposure over 72 hours of culture. After 24 hours of direct metformin exposure, 1mM metformin (0.003 ± 0.001 [U/ml]mg) demonstrated a non-significant reduction in culture media LDH concentration compared to control (0.007 ± 0.002 [U/ml]mg), p=0.452, n=6). At 48 hours, addition of 100μM metformin (0.011 ± 0.005 [U/ml]mg, p=0.993, n=5) and 1mM metformin (0.011 ± 0.004 [U/ml]mg, p=0.993, n=5) demonstrated a non-significant increase in culture media LDH concentration compared to control (0.010 ± 0.006 [U/ml]mg). A non-significant reduction in LDH concentration was observed with 40μM metformin (0.007 ± 0.002 [U/ml]mg, p=0.879, n=5) at 48 hours compared to control. By 72 hours, culture media LDH concentration was at its lowest with 100μM metformin treatment (0.005 ± 0.002 [U/ml]mg, n=7, p=0.691) compared to control. No change was observed with other concentrations of metformin at 72 hours. The effect of time was also examined on LDH concentration in response to direct metformin exposure in human placental explants, however no differences were observed. This suggests metformin had no direct effect on placental explant lactate turnover (**Figure *26***B).

To further investigate the cytotoxic effect of direct metformin exposure after 72 hours, human placental explants were stained for apoptotic M30 marker. No differences were observed, however a non-significant reduction in M30 expression was observed with 40µM metformin (median FC=0.71, n=7, p=0.219) and 100µM metformin (median FC= 0.64, n=7, p>0.999) compared to control. This downward trend was lost with 1mM metformin (median FC=1.02, n=7, p=0.688) (**Figure *27***).

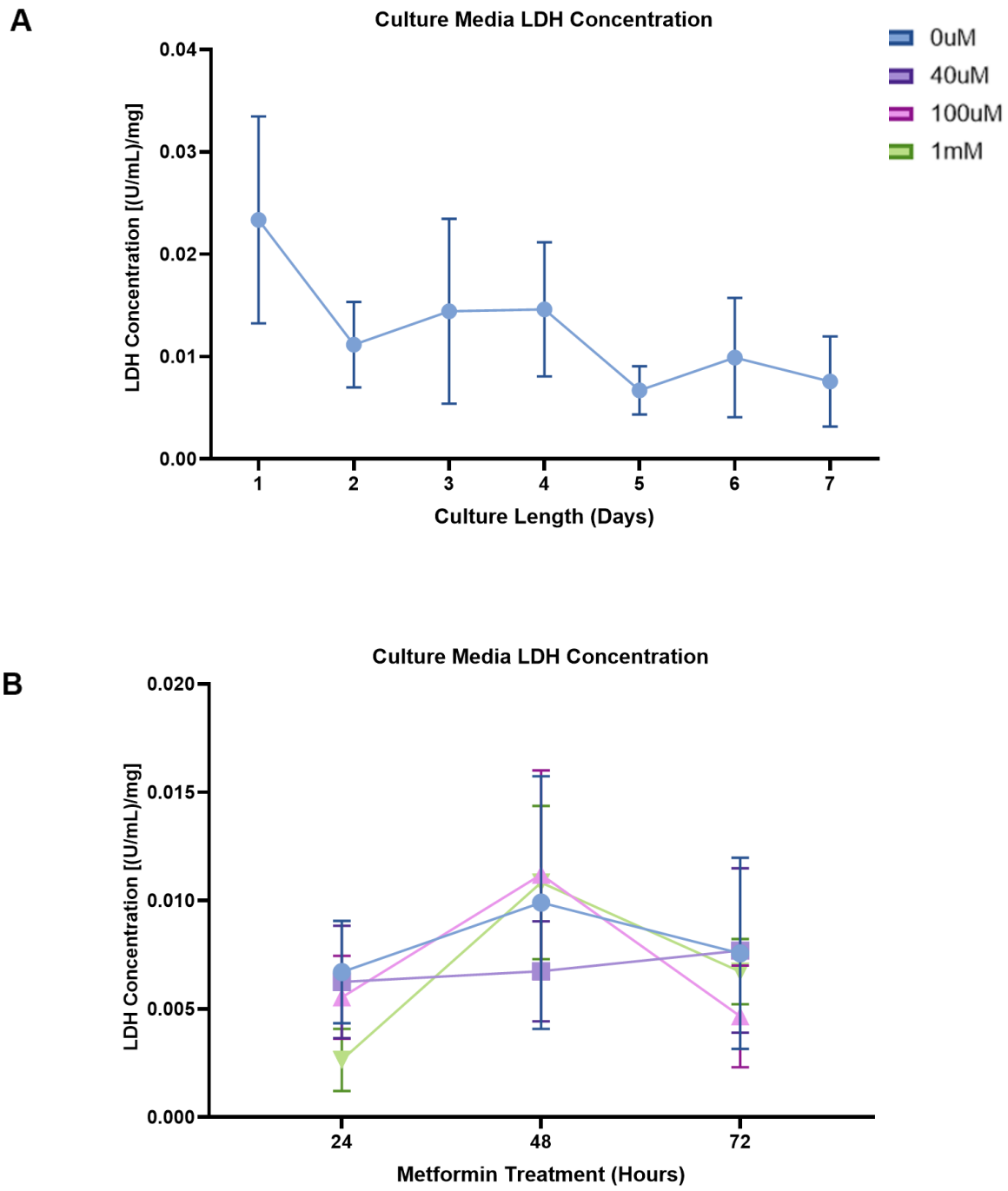

Figure 26 Culture media lactose dehydrogenase concentration in placental villous explants treated with metformin (24-72 hours).

Lactose dehydrogenase concentration was measured in placental explant culture media. Media comprised of 5.5mM glucose before metformin treatment (0μM, 40μM, 100μM, 1mM for 24, 48, 72 hours respectively) was induced on day 5 of culture. (A) Two-way ANOVA mixed-effects model, followed by Tukey's multiple comparisons test was performed; data presented as mean ±SEM (n=7). (B) Two-way ANOVA mixed-effects model with Geisser-Greenhouse correction, followed by Tukey's multiple comparisons test was performed; data presented as mean ±SEM (n=7).

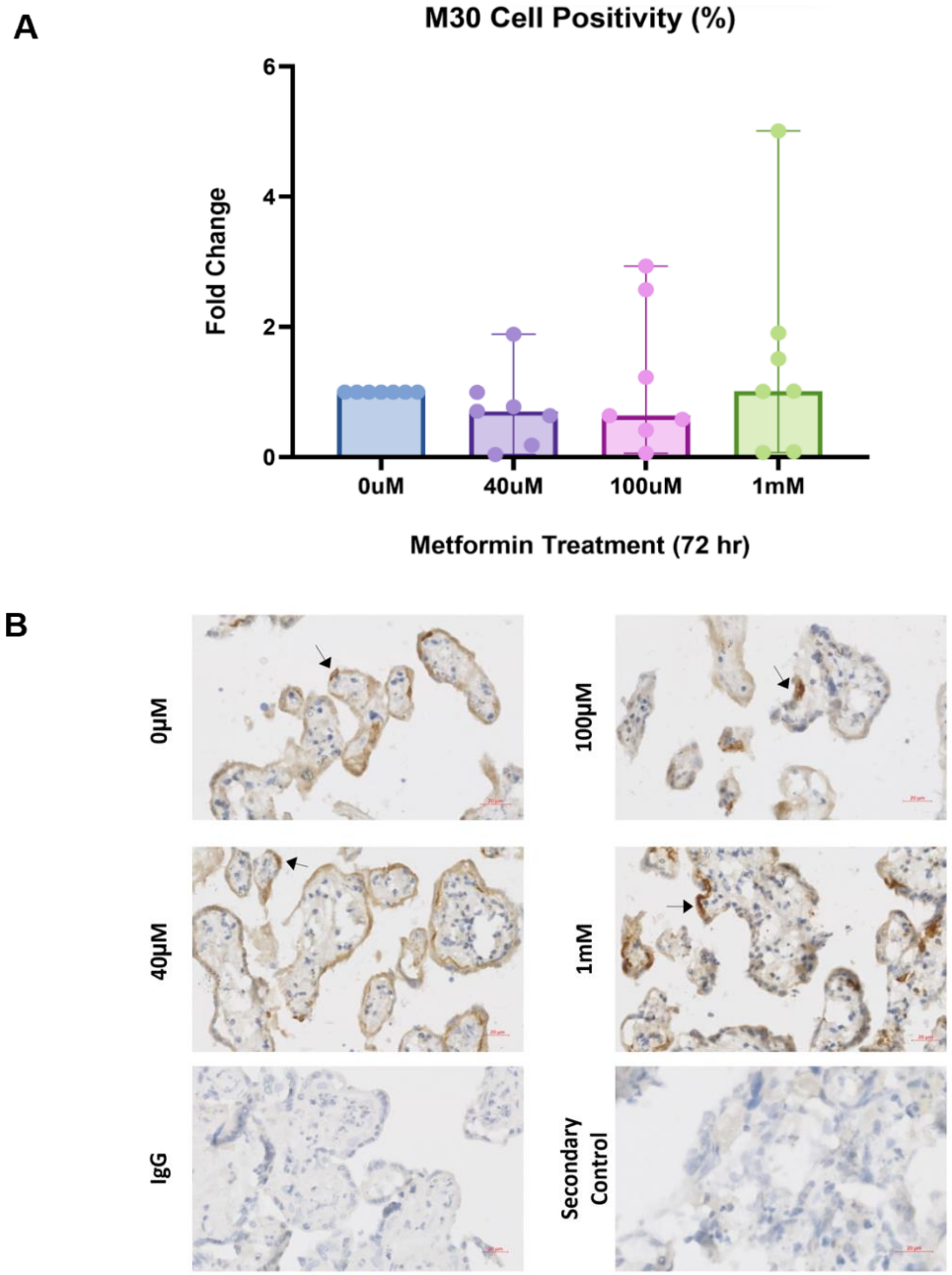

Figure 27 Immunostaining of apoptotic marker M30 in placental villous explants at 72 hours of metformin treatment.

Placental villous explants were cultured for 4 days, then treated with metformin at 0, 40μM, 100μM or 1mM for 72 hours. Placental samples were formalin fixed paraffin embedded (FFPE) and immunohistochemistry was conducted using Anti Human M30 CytoDEATH antibody (mouse, 1:100) in 1X TBS overnight at 4°C before being incubated with a biotinylated secondary mouse IgG control (mouse, 1:200) in 1X TBS for 1 hour at RT. Non-immune mouse IgG control and secondary IgG control were used. (A) Positive cell detection was quantified using QuPath. Wilcoxon Signed-Rank test was performed. Data presented as median fold change (compared to control 0μM) with range (95% CI) (n=7); *=p ≤ 0.05. (B) Histological slides were imaged at x20. Arrows indicate apoptotic M30 marker staining. Scale bar: 20μm.

3.4.2.3.3 Trophoblast Endocrine Function

Levels of culture media β-hCG, a hormone secreted by placental syncytium (74), was assessed to determine the endocrine function and thus viability of our placental explant villous model (**Figure *28***). Secretion of β-hCG into explant media was at its highest at day 1 of culture (17.24 ± 9.794 (mIU/ml)mg, n=4) before a non-significant decrease in concentration was observed at day 2 (6.562 ± 3.425 (mIU/ml)mg, n=6, p=0.381). Compared to day 1, a further non-significant decrease was shown at day 3 (1.504 ± 0.454 (mIU/ml)mg, n=6, p=0.090). This reduction was sustained until day 6 of culture (2.204 ± 0.563 (mIU/ml)mg, n=5). By day 7, βHCG concentration started to rise (9.030 ± 7.297 (mIU/ml)mg, n=7) (**Figure *28***A). Consistent with other studies in placenta, this suggests that syncytial degradation occurs during the early days of placental explant culture, but by day 7, the syncytiotrophoblast layer is regenerated (335). This was further observed histologically through haematoxylin and eosin staining, and performing IHC for epithelial marker Cytokeratin-7, which in the placenta, is expressed in trophoblast cells (**Figure *29***).

Direct exposure of metformin had no significant effect on placental β-hCG secretion after 24 hours. At 48 hours, a non-significant increase in culture media β-hCG concentration was observed with 1mM metformin compared to control (from 2.204 ± 0.563 (mIU/ml)mg to 3.912 ± 1.446 (mIU/ml)mg, n=5, p=0.704). After 72 hours of metformin culture, a downward dose-dependent trend was observed in β-hCG secretion, where 1mM metformin (2.530 ± 1.157 (mIU/ml)mg) demonstrated the biggest decrease compared to control (9.030 ± 7.297 (mIU/ml)mg) (n=7, p=0.815), however this finding was not statistically significant (**Figure *28***B).

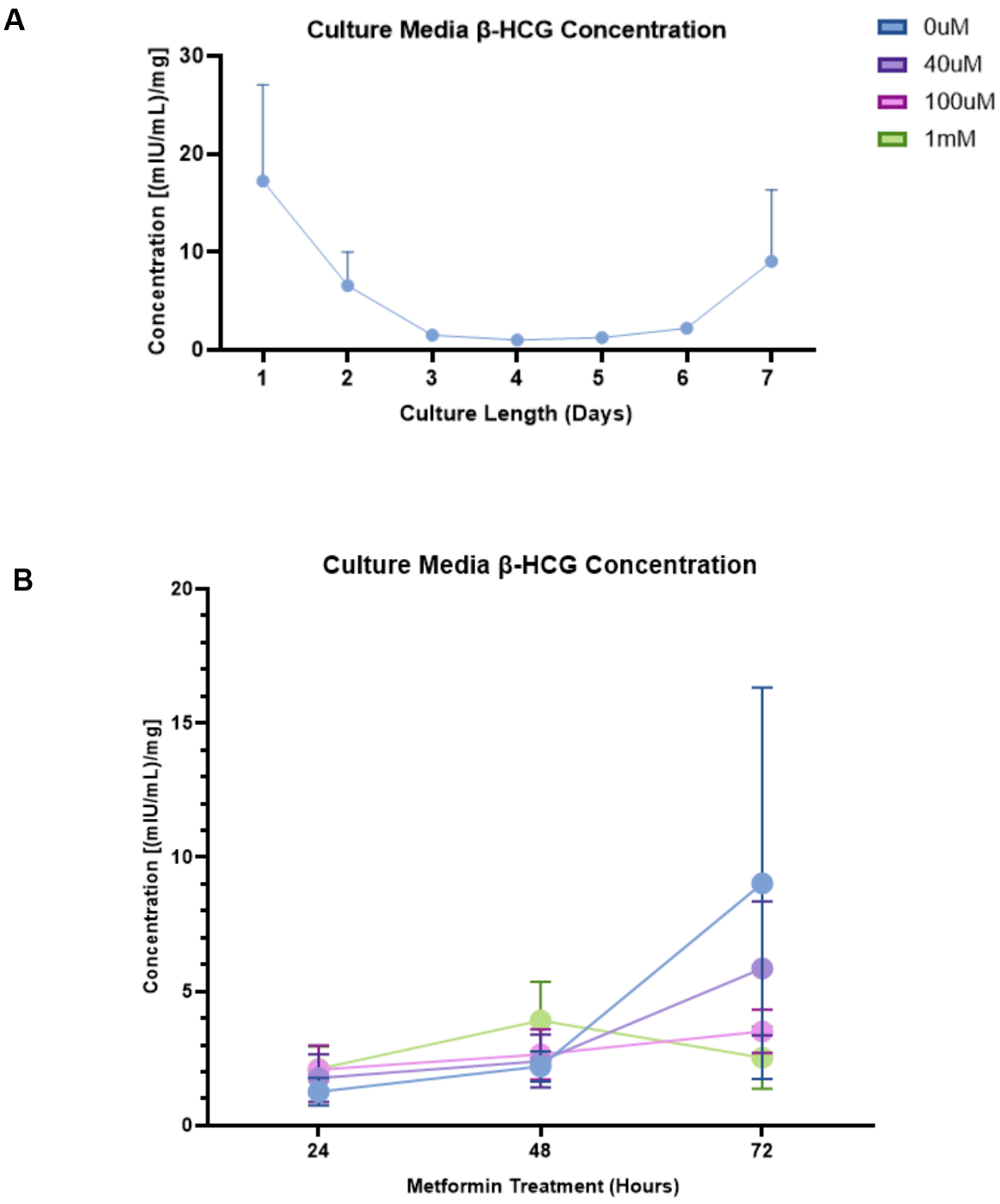

Figure 28 Culture media β-hCG concentration in placental villous explants treated with metformin (24-72 hours).

Lactose dehydrogenase concentration was measured in placental explant culture media. Media comprised of 5.5mM glucose before metformin treatment (0μM, 40μM, 100μM, 1mM for 24, 48, 72 hours respectively) was induced on day 5 of culture. (A) Data presented as mean ±SEM (n=7). (B) Two-way ANOVA mixed-effects model with Geisser-Greenhouse correction, followed by Tukey's multiple comparisons test was performed; data presented as mean ±SEM (n=7).

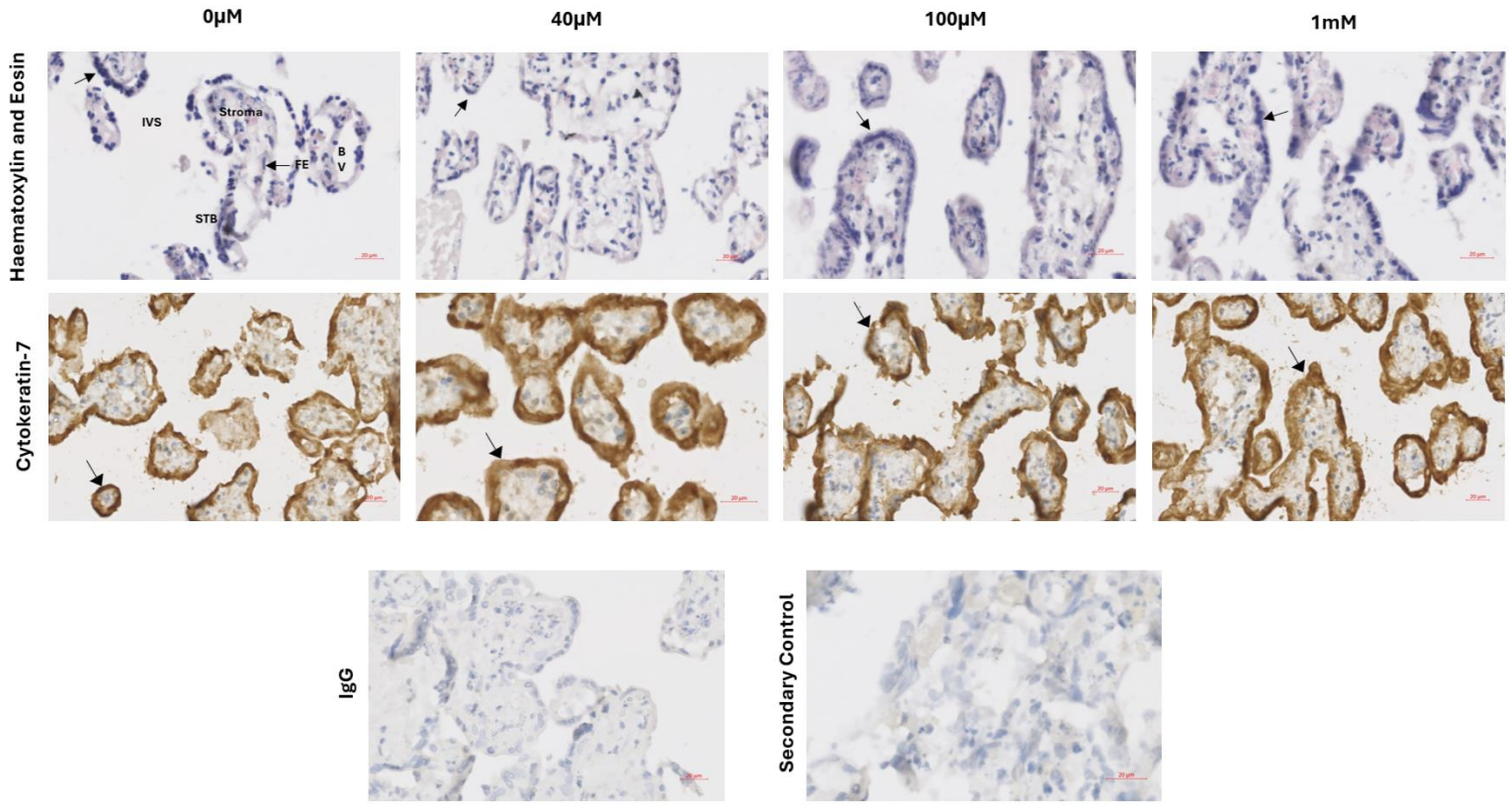

Figure 29 Representative images of haematoxylin and eosin, and cytokeratin-7 staining in placental villous explants at 72 hours of metformin treatment.

Placental villous explants were cultured for 4 days, then treated with metformin at 0, 40µM, 100µM or 1mM for 72 hours. Placental samples were formalin fixed paraffin embedded (FFPE) and subjected to haematoxylin and eosin staining or immunostaining of cytokeratin-7. Haematoxylin and eosin staining confirmed syncytiotrophoblast regeneration and model viability. Distinct dark blue staining surrounding the trophoblast layer indicates syncytial presence. Immunohistochemistry was conducted using Anti-Cytokeratin-7 antibody (mouse, 1:500) in 1X TBS overnight at 4°C before being incubated with a biotinylated secondary mouse IgG control (mouse, 1:200) in 1X TBS for 1 hour at RT. Non-immune mouse IgG control and secondary IgG control were used. Histological slides were imaged at x20. Unlabelled arrows indicate syncytiotrophoblast. Scale bar: 20µm. Key: STB - syncytiotrophoblast; IVS – intervillous space; BV – blood vessel, FE – fetal endothelium.

3.4.2.4 Direct Impact of Metformin on Placental Metabolism

3.4.2.4.1 Glucose Uptake

Metformin has previously been shown to alter glucose uptake in various tissues (395). *In-vivo*, women with GDM that have been treated with metformin have blood glucose levels of 5.5mM (396). Human placental explants were therefore cultured in 5.5mM glucose to mimic this *in-vivo* concentration. To establish the effects of metformin on glucose utilisation during culture, GlucCell® Monitoring System was used to record medium glucose concentration (mM) throughout the placental villous explant culture period (**Figure *30***). No significant differences were observed in placental explant culture media glucose levels over 72 hours. A non-significant decrease in glucose levels was observed from day 1 to day 2 of culture (0.175 ± 0.033 mM/mg to 0.126 ± 0.027 mM/mg, p=0.985, n=4/6) and an upward trend to 0.171 ± 0.043 mM/mg was observed on day 5 (n=6). However, a non-significant decrease to 0.102 ± 0.023 mM/mg was observed on day 7 of culture (n=6, p=0.136) compared to day 5. Culture media glucose levels were at their lowest on day 7 of culture (**Figure *30***A).

Metformin had no impact on placental explant culture media glucose levels. No change in media glucose levels was observed at 24 hours. At 48 hours, a non-significant reduction in culture media glucose levels was observed with 40μM metformin compared to control, from 0.153 ± 0.047 mM/mg to 0.088 ± 0.028 mM/mg (n=5, p=0.353), although this was not seen with other concentrations of metformin. By 72 hours, 40μM metformin demonstrated a non-significant increase in culture media glucose levels (0.135 ± 0.073 mM/mg, n=5, p=0.974) compared to control (0.102 ± 0.023 mM/mg, n=6), while a non-significant decrease in culture media glucose levels was observed with 100μM metformin (0.085 ± 0.015 mM/mg, p=0.926, n=7) and 1mM metformin (0.058 ± 0.008 mM/mg, p=0.543, n=5) compared to control (**Figure *30***B).

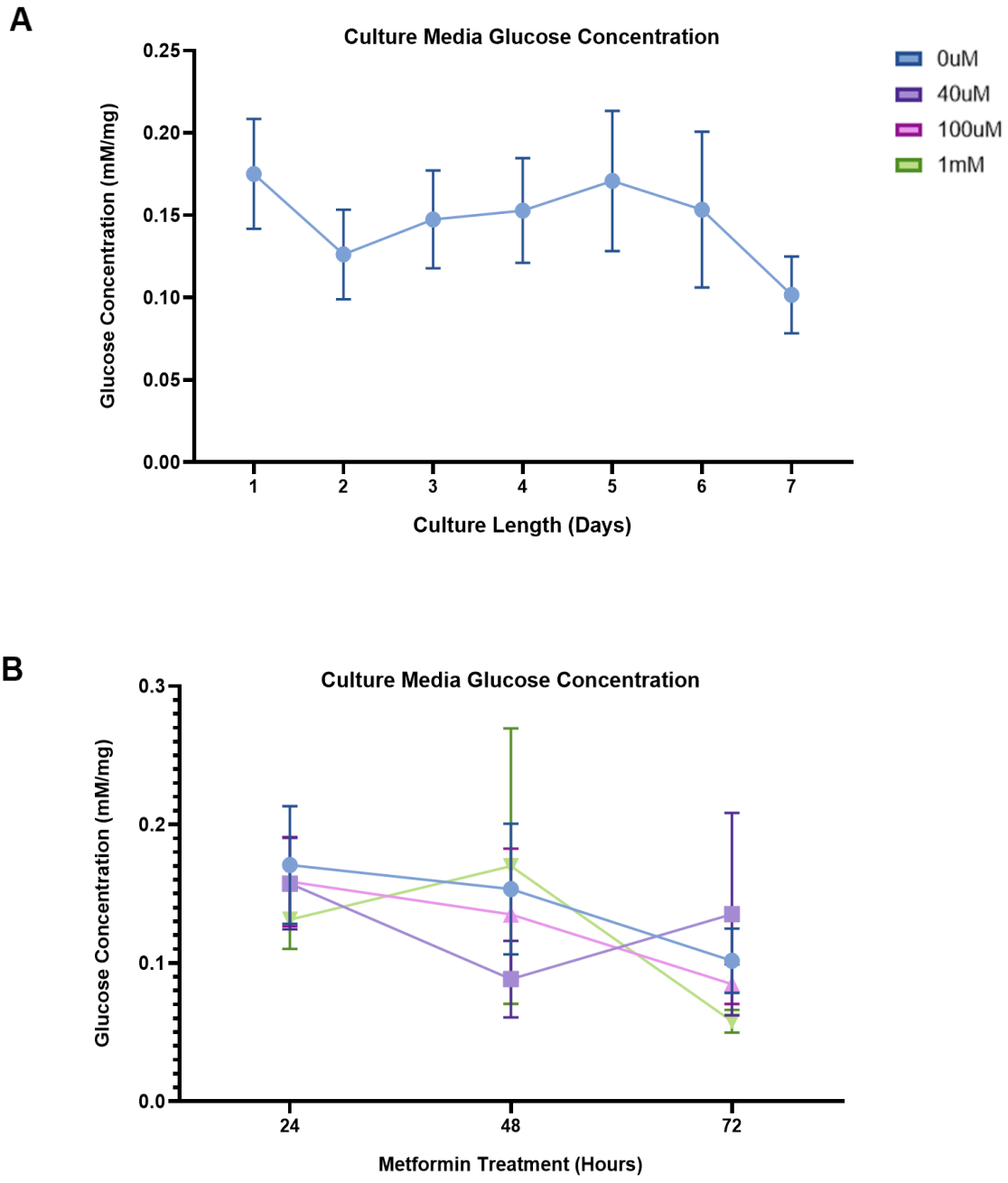

Figure 30 Culture media glucose concentration in placental villous explants treated with metformin (24-72 hours).

Glucose concentration of placental explant culture media was recorded using GlucCell® Monitoring System. Media comprised of 5.5mM glucose before metformin treatment (0μM, 40μM, 100μM, 1mM for 24, 48, 72 hours respectively) was induced on day 5 of culture. (A) Data presented as mean ±SEM (n=7). (B) Two-way ANOVA mixed-effects model with Geisser Greenhouse correction, followed by Tukey's multiple comparisons test was performed; data presented as mean ±SEM (n=7).

3.4.2.4.2 Mitochondrial Metabolism

Altered placental mitophagy, a process whereby damaged mitochondria are marked for lysosomal degradation, is a hallmark of restricted fetal growth (74). To determine the effect of direct metformin exposure on placental mitophagy, expression of key genes involved in placental mitophagy (*PINK1, PARKIN, LC3, BCL2*) (338,339) was assessed in *ex-vivo* placental explants in response to metformin treatment.

PINK1 was found to be downregulated in the placenta of obese women with GDM with *in-vivo* metformin exposure (**Table *22***). In contrast, direct metformin exposure had no impact on *PINK1* expression in human placental explants compared to control (**Figure *31***A). Metformin had no impact on *PARKIN* and *LC3* expression (**Figure *31***B,C), however 100μM metformin demonstrated a non-significant decrease in *LC3* expression compared to control (median FC= 0.60, n=7, p=0.078). Interestingly, a dose-dependent decrease was observed in placental *BCL2* expression with direct metformin exposure, with 100μM metformin (median FC=0.49, n=7, p=0.016) and 1mM metformin (median FC= 0.32, n=7, p=0.016) demonstrating a significant decrease in fold change compared to control (**Figure *31***D).

Oxidative damage may occur when excessive levels of reactive oxygen species (ROS) are generated due to mitochondrial dysfunction (397). Therefore, to further investigate the functional impact of direct metformin exposure on mitochondrial efficiency, human placental explants were stained for 8-hydroxy-2'-deoxyguanosine (8OHdG) as a marker of oxidative damage to DNA (397). IHC showed some 8OHdG positivity in trophoblasts under basal conditions (**Figure *32***). This appeared to increase with metformin treatment both in trophoblasts and the villous stroma. Quantification of IHC confirmed that there was an increase in 8OHdG expression with 40μM metformin compared to control (median FC=1.23, n=7, p=0.047). However, no significant effects were observed with higher concentrations of metformin (100μM - median FC=1.19, n=7, p=0.375; 1mM - median FC=1.06, n=7, p>0.999) (**Figure *32***).

It has previously been reported that metformin impacts mitochondrial activity after prolonged exposure (398–400). As such, citrate synthase activity, a marker of

intact mitochondrial inner membrane (401), was assessed in human placental explants treated with metformin between 24-72 hours (**Figure *33***). Metformin demonstrated no significant impact on citrate synthase activity over 72 hours of culture. After 24 hours of metformin exposure, it was demonstrated that citrate synthase activity was at its highest with 100μM metformin compared to basal levels (0.031 ± 0.013 to 0.047 ± 0.017 absorbance/min/mg, p=0.863, n=5),. By 48 hours, citrate synthase activity in human placental explants exposed to metformin remained similar to basal levels. However, after 72 hours of culture, a non-significant dose-dependent decrease in citrate synthase activity was observed with metformin, with the lowest activity levels demonstrated by 1mM metformin compared to control (0.023 ± 0.010 compared to 0.041 ± 0.006 absorbance/min/mg, respectively, p=0.484, n=5) (**Figure *33***).

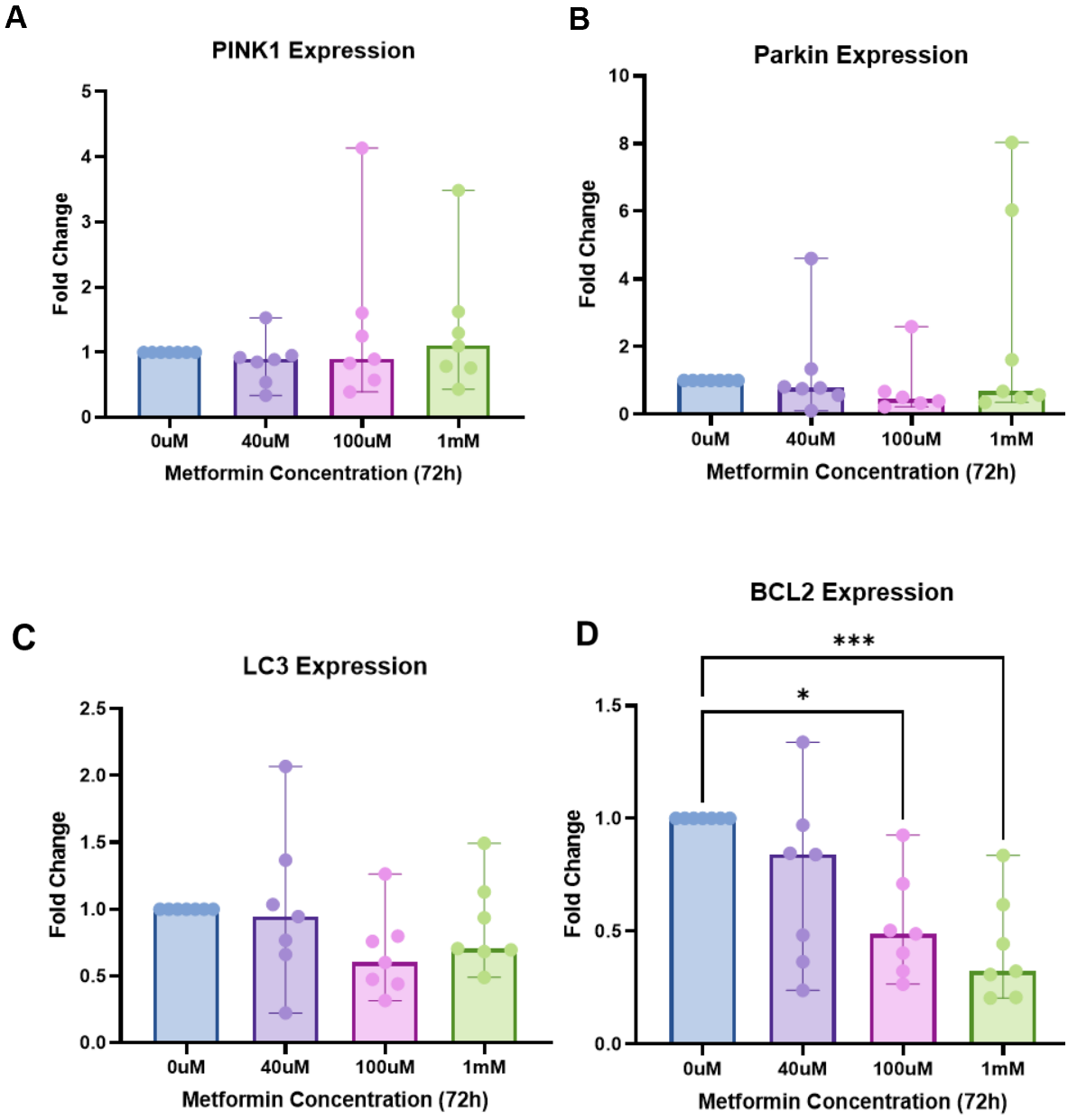

Figure 31 mRNA expression of genes involved in placental mitophagy in placental villous explants at 72 hours of metformin treatment.

Placental villous explants were treated with metformin (40μM-1mM) and total RNA was extracted. Gene expression was analysed using RT-qPCR before being normalised to mean expression of *YWHAZ*, *β-ACTIN* and *18S*; (2^(-Ct)*10^(2). Wilcoxon Signed-Rank test was performed. Data presented as median fold change (compared to control 0μM) with range (95% CI) (n=7); *=p ≤ 0.05.

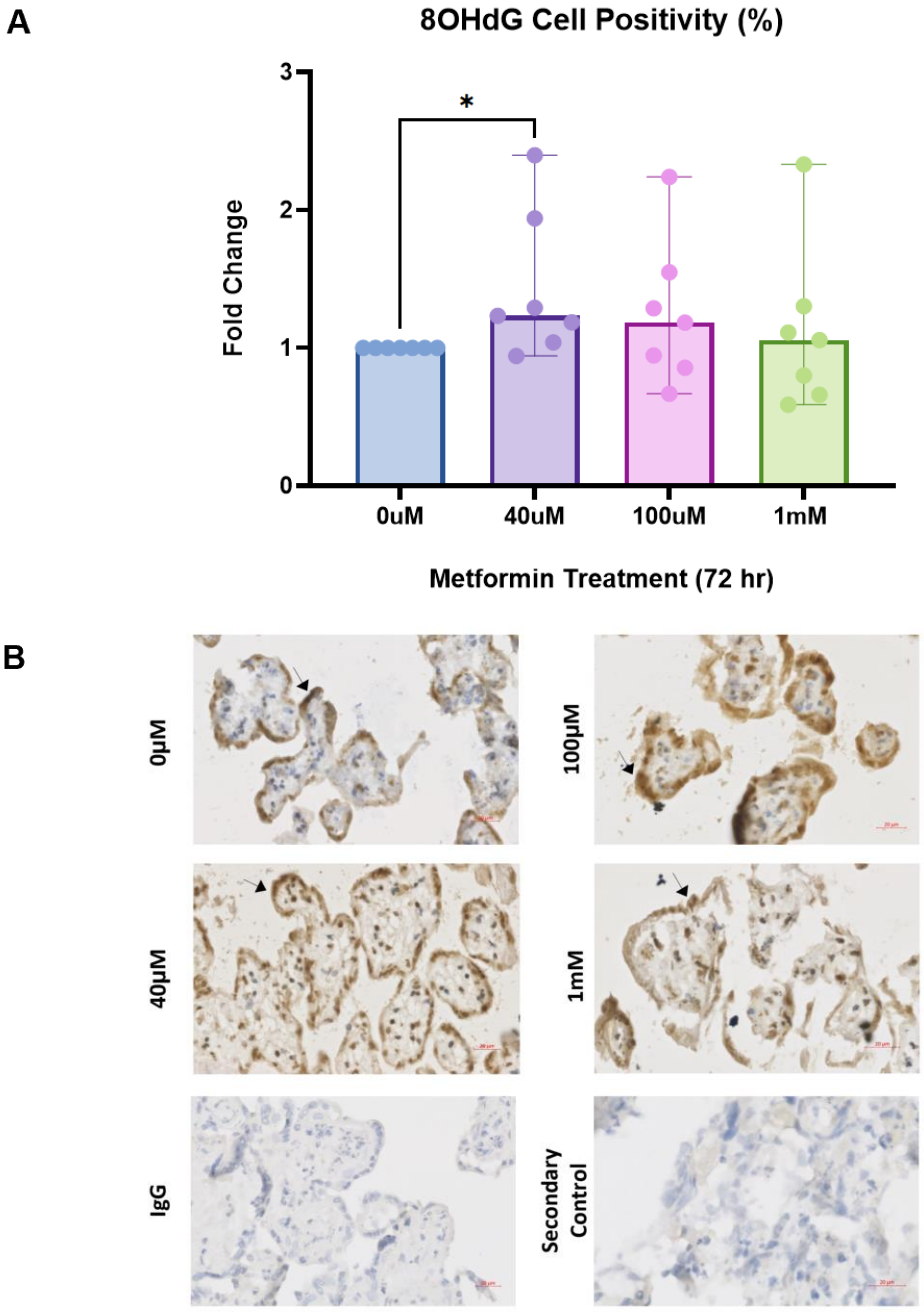

Figure 32 Immunostaining of oxidative stress marker 8OHdG in placental villous explants at 72 hours of metformin treatment.

Placental villous explants were cultured for 4 days, then treated with metformin at 0, 40μM, 100μM or 1mM for 72 hours. Placental samples were formalin fixed paraffin embedded (FFPE) and immunohistochemistry was conducted using Anti-8-Hydroxy-2'-Deoxyguanosine [N45-1] antibody (mouse, 1:4000) in 1X TBS overnight at 4°C before being incubated with a biotinylated secondary mouse IgG control (mouse, 1:200) in 1X TBS for 1 hour at RT. Non-immune mouse IgG control and secondary IgG control were used. (A) Positive cell detection was quantified using QuPath. Wilcoxon Signed-Rank test was performed. Data presented as median fold change (compared to control 0μM) with range (95% CI) (n=7); *=p ≤ 0.05. (B) Histological slides were imaged at x20. Arrows indicate 8OHdG marker staining. Scale bar: 20μm.

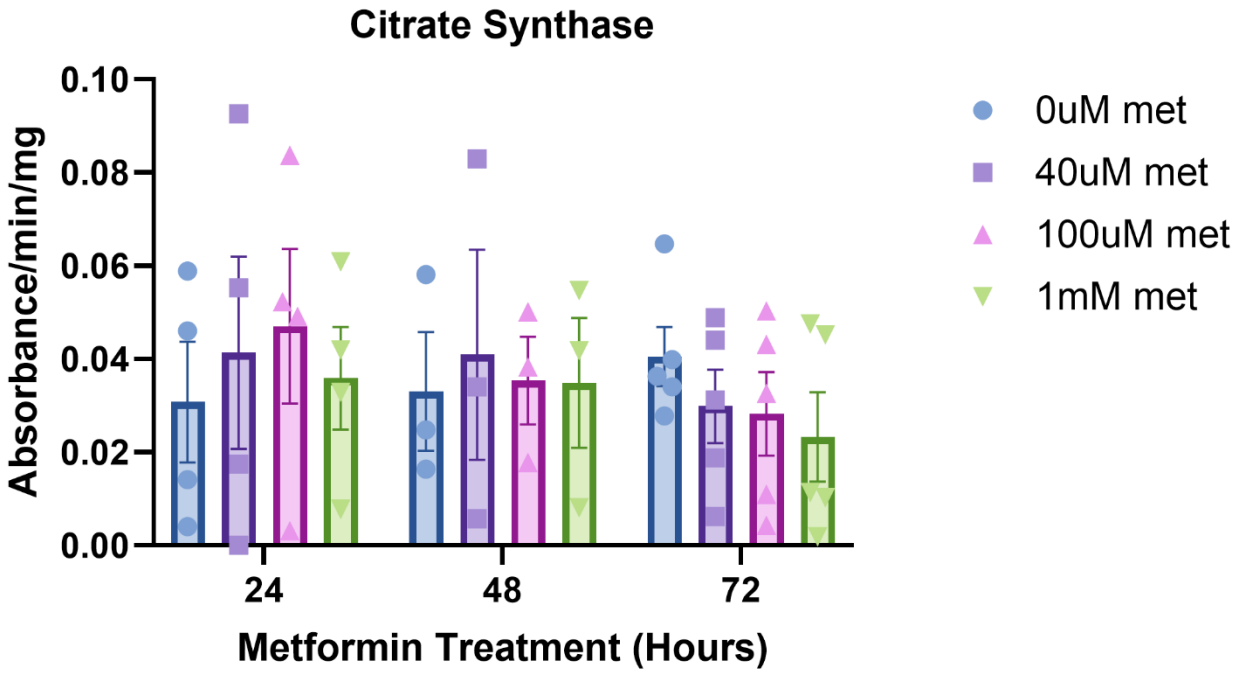

Figure 33 Citrate synthase activity in placental villous explants exposed to metformin treatment for 24-72 hours.

Protein lysate from placental villous explant tissue treated with metformin (40μM-1mM) was processed to measure citrate synthase activity as a marker of intact mitochondrial inner membrane. Kinetic absorbance was measured at 412nm at 37°C. Activity was determined by calculating mean sample absorbance/min normalised to explant weight (mg). Two-way ANOVA mixed-effects model with Geisser-Greenhouse correction, followed by Tukey's multiple comparisons test was performed. Data presented as mean ±SEM (n=5).

3.4.2.4.3 TCA Cycle Metabolites

To further investigate the impact of metformin on placental mitochondrial function and metabolism, various metabolites (Appendix 1, Appendix 2) and components of the TCA cycle were assessed in human placental explants directly exposed to metformin between 24-72 hours (**Figure *34***). No change was observed in succinate, fumarate and cis-aconitate levels (**Figure *34***B,G,H). While there was a time-dependent reduction in malic acid levels under control conditions (from 5583 ± 585.4 to 3589 ± 253.9 absorbance/mg between 48-72 hours culture, p=0.042, n=6), there was no additional effect in explants treated with metformin (**Figure *34***A).

Metformin did not exert significant changes in TCA cycle metabolites at individual time points, however metformin did exert time-dependent changes in some metabolites. Between 24-48 hours, no difference was observed in isocitrate levels under control conditions. However, 40μM metformin increased isocitrate levels by 102% between 24-48 hours (from 193.5 ± 82.14 to 390.9 ± 72.85 absorbance/mg, n=6, p=0.017, log2FC=1.015) (**Figure *34***E, **Table *23***). Lactic acid levels were increased by 35% by 100μM metformin between 24-48 hours (from 29418 ± 3344 to 39677 ± 3658 absorbance/mg, n=6, p=0.045, log2FC=0.432) (**Figure *34***C, **Table *23***). This was a 13% increase compared to control conditions (log2FC=0.291) (**Table *23***).

Between 48-72 hours, while statistically insignificant under control conditions (log2FC=-1.702), 100μM metformin reduced isocitrate levels by 41% (from 396.9 ± 83.80 to 232.8 ± 63.38 absorbance/mg, n=6, p=0.0120, log2FC=-0.770) (**Figure *34***E, **Table *23***). Citrate levels were also reduced by 32% by 100μM metformin between 48-72 hours (from 794.3 ± 157.7 to 539.2 ± 102.2 absorbance/mg, n=6/7, p=0.003, log2FC=-0.559) (**Figure *34***F, **Table *23***). This was a non-significant 69% reduction under control conditions (log2FC=-1.347) (**Table *23***). At this time point, 1mM metformin reduced lactic acid levels by 27% (from 44025 ± 3002 to 33031 ± 2741 absorbance/mg, n=6/7, p=0.011, log2FC=-0.448) (**Figure *34***C, **Table *23***). This was a non-significant 19% reduction under control conditions (log2FC=-0.302) (**Table *23***).

Between 24-72 hours, a significant 60% reduction in pyruvate levels was observed with 1mM metformin, where levels were reduced from 121.6 ± 25.78 to 48.21 ± 14.74 absorbance/mg (n=7, p=0.0321, log2FC=-1.335). This was similar to control conditions, where a non-significant 64% reduction was observed (log2FC=-1.420) (**Figure *34***D) (**Table *23***).

3.4.2.4.4 Fatty Acid Oxidation

Transcriptomic analysis identified fatty acid β-oxidation as a canonical pathway of DEGs in obese women with GDM treated with metformin compared to placebo. Acylcarnitines (ACs) are involved in fatty acid transport in the mitochondria (402) and thus were measured as biomarkers of fatty acid β-oxidation in human placental explants directly exposed to metformin.

No effect was observed under control conditions between 24-48 hours. Between 48-72 hours, AC12:0 (from 322.0 ± 78.25 to 228.4 ± 46.86 absorbance/mg, n=6, p=0.042), AC10:0 (from 161.1 ± 34.75 to 107.2 ± 26.74 absorbance/mg, n=6, p=0.048) and AC10:1 (from 66.79 ± 16.52 to 48.20 ± 11.49 absorbance/mg, n=6, p=0.042) levels were significantly reduced under control conditions (**Figure *35***H,J,K). There was no additional effect on these metabolites in explants treated with metformin at this time point.

Similarly to TCA cycle metabolites, metformin did not exert significant changes in acylcarnitine metabolites at individual time points, however metformin did exert time-dependent changes in some metabolites. Between 48-72 hours, long-chain AC18:0 levels were reduced by 27% by 100μM metformin (from 882.8 ± 330.6 to 643.0 ± 245.2 absorbance/mg, n=6/5, p=0.028, log2FC= -0.457) (**Figure *35***A, **Table *24***). This was unchanged under control conditions (log2FC=0.041) (**Figure *35***A , **Table *24***). AC14:1 (from 102.4 ± 22.81 to 61.78 ± 26.30 absorbance/mg, n=4/5, p=0.038, log2FC=-0.729) and AC2:0 (from 61737 ± 15077 to 64225 ± 14818 absorbance/mg, n=6/5, p=0.012, log2FC=0.057) levels were also altered by 100μM metformin at this time point (**Figure *35***F, **Table *24***). These metabolites were not significantly altered under control conditions at this time point (log2FC=-0.093, log2FC=0.098, respectively) (**Figure *35***F, **Table *24***). Short-chain AC6:0 (from 1331 ± 178.4 to 886.4 ± 105.5 absorbance/mg, n=6/7, p=0.024, log2FC=-0.587)

and AC5:0 (from 4253 ± 629.7 to 2538 ± 236.6 absorbance/mg, n=6/7, p=0.047, logFC=-0.124) levels were reduced by 1mM metformin between 48-72 hours (**Figure *35***N,O, **Table *24***). At this time point, these metabolites were not significantly altered under control conditions (log2FC=-0.547 and log2FC=-1.561, respectively) (**Figure *35***N,O, **Table *24***).

Between 24 hours and 72 hours, 1mM metformin increased levels of medium-chain AC12:1 (from 55.47 ± 6.620 to 95.95 ± 17.31 absorbance/mg, n=7, p=0.037, log2FC=0.791), AC10:0 (from 63.78 ± 13.52 to 169.0 ± 38.41 absorbance/mg, n=7, p=0.028, log2FC=1.406) and AC10:1 (from 21.05 ± 5.026 to 56.67 ± 12.67 absorbance/mg, n=7, p=0.037, log2FC=1.429) (**Figure *35***I,J,K, **Table *24***). At this time point, these metabolites were not significantly altered under control conditions (log2FC=0.320, log2FC=0.068 and log2FC=0.062, respectively) (**Figure *35***I,J,K, **Table *24***).

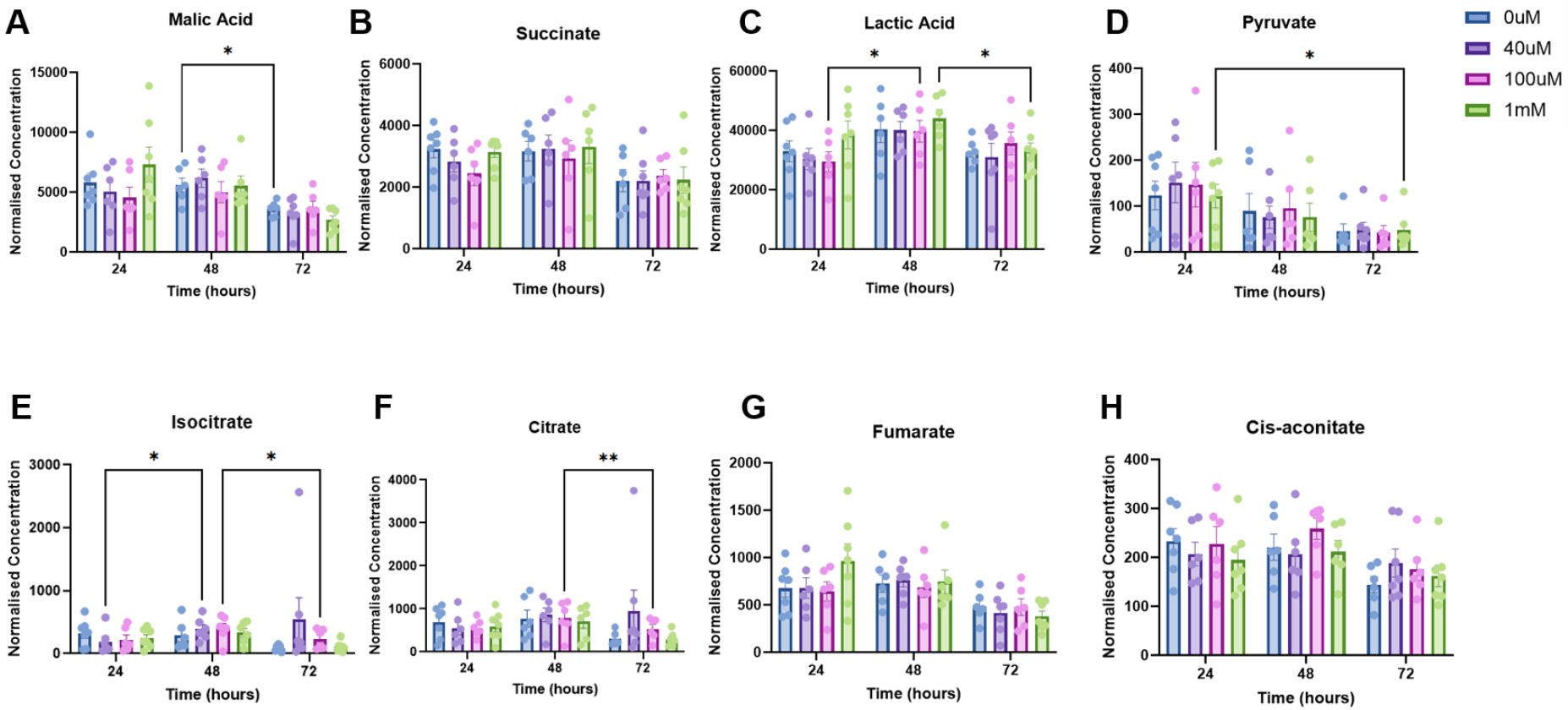

Figure 34 TCA cycle intermediates in placental villous explants treated with metformin (40μM-1mM), for 24-72 hours.

Liquid chromatography-mass spectrometry was performed on aqueous placental explant fractions to detect TCA cycle metabolites. Data was analysed via a two-way mixed effects ANOVA, followed by a Geisser-Greenhouse correction and Tukey's multiple comparisons test and presented as mean ±SEM. (n=7); *=$p \leq 0.05$.

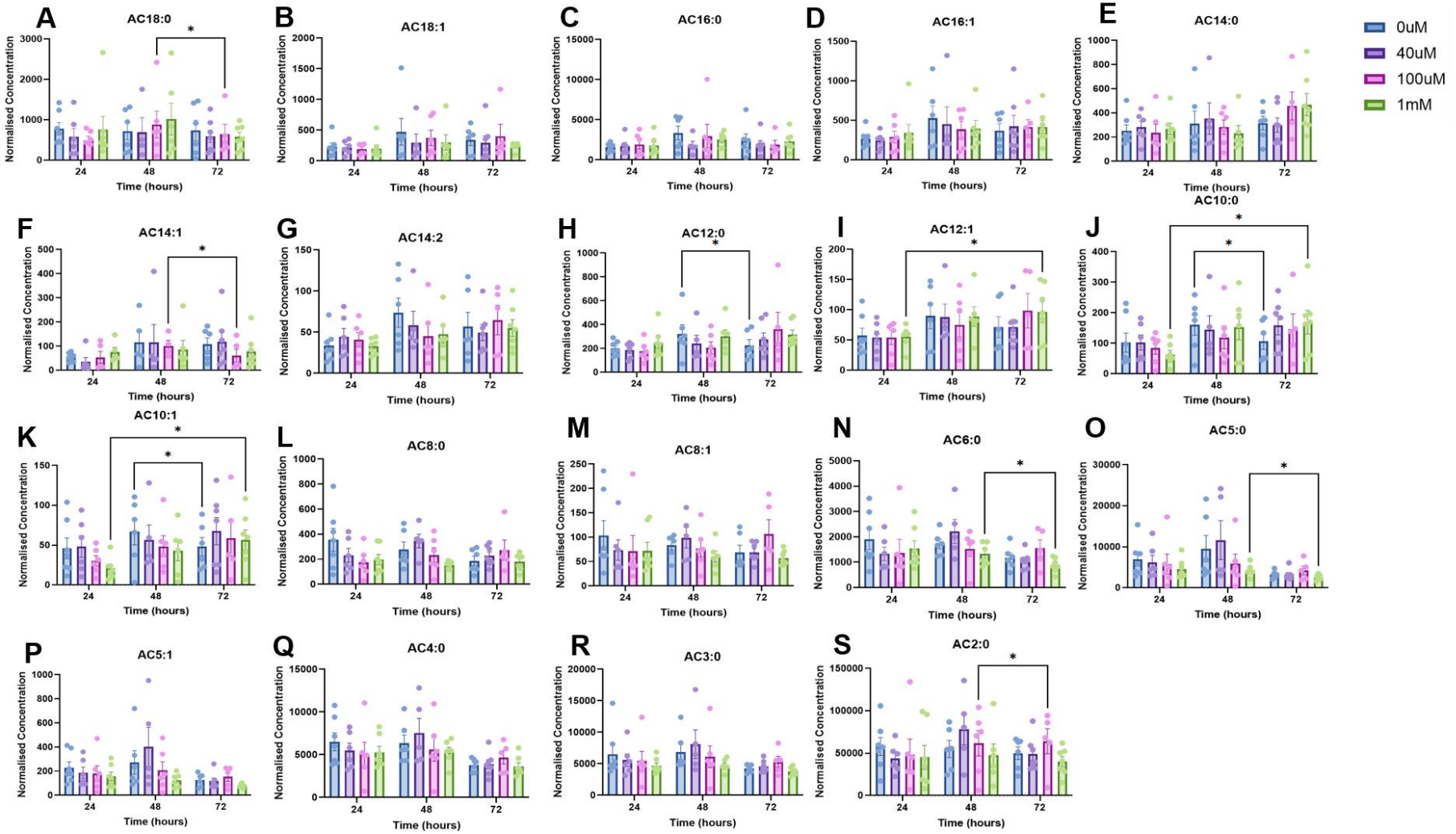

Figure 35 Acylcarnitine metabolites in placental villous explants treated with metformin (40μM-1mM), for 24-72 hours.

Liquid chromatography-mass spectrometry was performed on aqueous placental explant fractions to detect acylcarnitine metabolites. Data was analysed via a two-way mixed effects ANOVA, followed by a Geisser-Greenhouse correction and Tukey's multiple comparisons test and presented as mean ±SEM. (n=7); *=$p \leq 0.05$.

Table 23 Log2FC of significantly altered TCA cycle metabolites in human placental explants exposed to metformin.

Metformin	Significantly Altered Metabolites in Response to Metformin Treatment Log2FC TCA Cycle			
	Lactic Acid	Pyruvate	Isocitrate	Citrate
24 vs 48 Hours				
Control (0μM)	0.291		-0.175	
40μM			1.014	
100μM	0.432			
1mM				
48 vs 72 Hours				
Control (0μM)	-0.302		-1.702	-1.347
40μM				
100μM			-0.770	-0.559
1mM	-0.448			
24 vs 72 Hours				
Control (0μM)		-1.420		
40μM				
100μM				
1mM		-1.335		

Table 24 Log2FC of significantly altered acylcarnitine metabolites in human placental explants exposed to metformin.

Metformin	Significantly Altered Metabolites in Response to Metformin Treatment Log2FC Acylcarnitines							
	AC18:0	AC14:1	AC12:1	AC10:0	AC10:1	AC6:0	AC5:0	AC2:0
24 vs 48 Hours								
Control (0μM)								
40μM								
100μM								
1mM								
48 vs 72 Hours								
Control (0μM)	0.041	-0.093				-0.547	-1.561	0.098
40μM								
100μM	-0.457	-0.729						0.057
1mM						-0.586	-0.124	
24 vs 72 Hours								
Control (0μM)			0.320	0.067	0.062			
40μM								
100μM								
1mM			0.791	1.406	1.429			

3.4.2.4.5 Analysis of Upstream Metabolic Regulator

Metabolomics data suggests that metformin may be directly influencing mitochondrial function and fatty acid oxidation in placental explants (**Figure *18***). PPARGC1β is a master regulator of mitochondrial metabolism (391) and transcriptomic analysis of *in-vivo* metformin exposure demonstrated this gene to be upregulated in the placenta of obese women with GDM taking metformin (**Table *22***). To determine if the direct actions of metformin on placental metabolism were mediated via PPARGC1β*,* qPCR analysis was performed. In contrast to the increase in PPARGC1β levels observed *in-vivo*, there was a dose-dependent decrease in PPARGC1β expression in human placental explants directly exposed to metformin, where higher concentrations demonstrated statistically significant effects (100 μM – median FC=0.63, n=7, p=0.031; 1mM – median FC=0.45, n=7, p=0.016) compared to control (**Figure *36***).

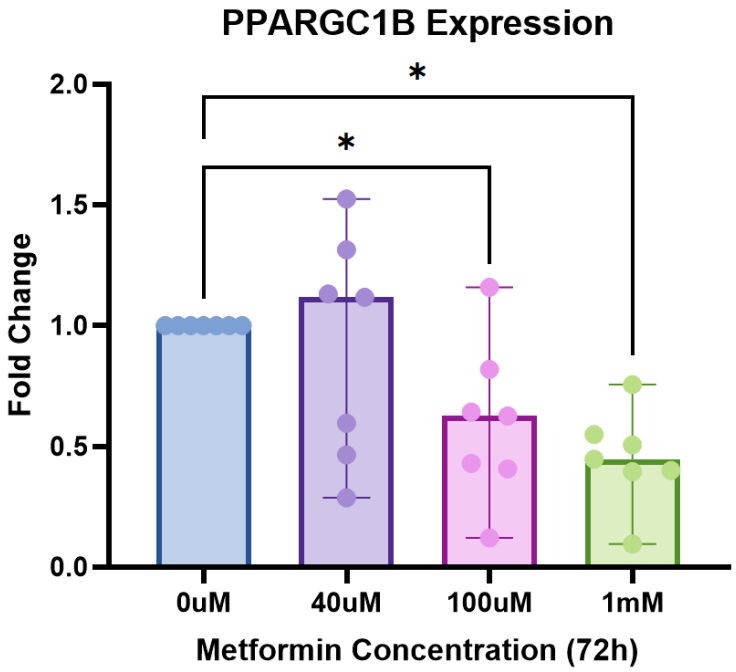

Figure 36 PPARGC1B mRNA expression in placental villous explants at 72 hours of metformin treatment.

Placental villous explants were treated with metformin (40µM-1mM) and total RNA was extracted. Gene expression was analysed using RT-qPCR before being normalised to mean expression of *YWHAZ*, *β-ACTIN* and *18S*; 2^(-Ct)*10^(2). Wilcoxon Signed-Rank test was performed. Data presented as median fold change (compared to control 0µM) with range (95% CI) (n=7); *=p ≤ 0.05

3.5 Discussion

Metformin is associated with adverse neonatal outcomes, such as altered fetal growth and increased offspring predisposition to cardiometabolic complications throughout life, but the mechanisms are unclear (45,54,56). In this study, it has been demonstrated that metformin impacts genes involved in biological networks associated with vascular development, cellular development and metabolism. Using an *ex-vivo* placental model, it has been demonstrated that some, but not all, of these changes are likely attributed to the direct actions of metformin on the placenta. This suggests that *in-vivo*, metformin is likely to have off-target or indirect actions on the placenta.

3.5.1 The Effect of Metformin on Placental Vascular Development

Transcriptomic analysis identified vascular development as a biological network that was affected by *in-vivo* exposure to metformin in the placenta of obese women with GDM. It was demonstrated that both *in-vivo* and *ex-vivo* metformin exposure induced ITGB3 downregulation in the placenta, where higher concentrations of metformin demonstrated the most significant downregulation in human placental explants. Integrins are key for successful placental development (403), where dysregulated integrin interaction in placental endothelial cells has been associated with fetal growth restriction (404). Indeed, altered placental ITGB3 gene expression has previously been associated with fetal growth restriction (405) and trophectoderm ITGB3 knockdown in sheep has resulted in reduced embryo growth and altered vascular development in the placental allantoic membrane (337). These findings suggest that ITGB3 is a key developmental gene in the placenta, which is directly impacted by metformin and may play a role in influencing pathological fetal growth in pregnancies complicated by GDM. Moreover, metformin has also demonstrated to regulate ITGB3 in other tissues (406,407), suggesting that metformin may also have indirect actions on placental vasculature.

In response to metformin, the activated state of AMPK (pAMPK) was identified in the villous stroma of human placental explants and levels of vascular marker,

CD31, was significantly reduced with 40μM metformin after 72 hours of culture, however no marked effect was observed with higher concentrations. A limitation to this assay may be that a 72-hour culture period is insufficient to identify changes in vasculature. The literature shows that placentae from pregnancies complicated by GDM have elevated VEGF and CD31 expression (408). Other studies have found that metformin markedly reduces anti-angiogenic factors in placental explants and is known to regulate other vascular beds (409,410), as well as improve hyperglycaemic endothelial dysfunction (411). In contrast to the findings of this chapter, a recent study reported that only supratherapeutic doses of metformin altered angiogenesis during pregnancy (412).

Moreover, placental explants were cultured in 5.5mM glucose to mimic *in-vivo* concentrations of women with GDM treated with metformin. However, by 72 hours of metformin treatment, it was demonstrated that culture media glucose levels were lower and therefore did not represent *in-vivo* conditions of pregnancies complicated by GDM. As such, this may have influenced placental protein expression after 72 hours of metformin culture. Confirming the concentration of metformin in the placental explant tissue after culture would further confirm if this model closely represented *in-vivo* conditions.

3.5.2 The Effect of Metformin on Placental Cellular Development and Function

Cellular development was another biological network that was identified to be affected by *in-vivo* exposure to metformin in the placenta of obese women with GDM. As such, markers of placental turnover were measured in human placental explants in response to direct metformin exposure after 72 hours. The activated state of AMPK (pAMPK) was identified in cytotrophoblasts, suggesting metformin may have a role in the development of these cells. However, metformin demonstrated no significant impact on the expression levels of proliferation and apoptosis protein markers, or culture media LDH levels in human placental explants. These findings suggest that metformin had no marked cytotoxic effect on the human placental explants, aligning with a previous study showing that metformin exposure exerted no cytotoxic effects on placental explants (413).

However, it has previously been reported that therapeutic doses of metformin improve trophoblast cell survival and apoptosis in response to insulin (414). Moreover, another group found metformin to negatively affect proliferation rate and culture growth of extravillous trophoblast HTR-8/SVneo cells, as cellular apoptotic index was elevated (381). Indeed, a concentration as low as 0.01mM of metformin, and in combination with hyperglycaemia (20mM), evoked a decrease in cell growth, suggesting metformin may have significant impact on placentation during the first trimester of pregnancy. This could suggest that metformin has greater impact on placental cell turnover in hyperglycaemic conditions. However, this could also suggest that perhaps metformin has greater impact on placental growth and development during early pregnancy and thus the mature term placental villous explant model may not reflect the true effects of metformin on growth and proliferation. Interestingly, a recent publication has found that initiating metformin treatment during early pregnancy is associated with increased preterm births (415), however it has been shown to be protective against fetal growth restriction in women with polycystic ovary syndrome (PCOS) (416). The effect of metformin on placental development may therefore differ depending on villous maturity and the gestational period of treatment initiation.

The direct effect of metformin on human placental explants does not reflect the predicted impact of metformin on placental development identified in the *in-vivo* transcriptome data. This also contrasts with previous literature showing that metformin improves placental development and structure in GDM pregnancies to be comparable to healthy placentae from uncomplicated pregnancies (382). In future, it would be interesting to assess placental development and growth in explant tissue obtained from women with GDM treated with metformin during pregnancy, to determine if the predicted impact of metformin on placental development is observed. This would further establish if metformin may be impacting placental development and growth via direct or indirect mechanisms. However, it was also observed that during the tissue fixation process in this study, some placental explants did not manifest intact villi and thus the tissue may have been disrupted. Probing for placental growth markers via western blotting may further confirm these observations.

In this study, metformin demonstrated no significant effect on explant culture media β-hCG levels. However, a non-significant dose-dependent reduction in explant culture media β-hCG levels was observed after 72 hours. As such, further research would benefit from repeating this assay with a larger sample size and longer culture period to determine if metformin may be impacting placental endocrine function via the syncytium. β-hCG levels in the late first trimester of pregnancy has been associated with fetal growth (417). As such, this suggests that the impact of metformin on placental endocrine function may contribute towards adverse fetal outcomes. Moreover, another in-vitro study has demonstrated that trophoblast hCG production was not impacted by 200 μM metformin after 72 hours (370). However, an effect was observed at a supraphysiological concentration of 2mM metformin; a concentration that is x50 higher than the observed *in-vivo* concentration in the placenta (352–354,370). This supraphysiological concentration of metformin was shown to impair trophoblast differentiation and metabolism, observations which were absent with therapeutic concentrations of metformin, suggesting that clinical use of metformin may not affect trophoblast viability and endocrine function. Furthermore, a recent study has demonstrated that metformin treatment *in-vivo*, combined with insulin treatment, reduces β-hCG secretion in GDM patients to a higher degree than insulin alone (418). This suggests that metformin may influence placental endocrine function via β-hCG production.

3.5.3 Effect of Metformin on Placental Metabolism

3.5.3.1 Glucose Metabolism

Placental villous explants in this study were cultured in 5.5mM glucose to mimic *in-vivo* glucose levels of women with GDM treated with metformin (56,396,419). As expected, there was a reduction in media glucose levels over time in culture under control conditions, demonstrating glucose uptake/metabolism by the placental explants. However, levels of glucose in the culture media reduced to a greater extent in explants treated with metformin (100μM-1mM) than under control conditions, suggesting that metformin may stimulate tissue uptake of glucose. A previously reported perfused human single-cotyledon model has

demonstrated that 1µg/mL metformin had no effect on placental glucose uptake or transport (420). However, this concentration is markedly lower than the concentrations of metformin used in this chapter. The human single-cotyledon model was also only perfused with metformin for 3 hours and glucose was not added to the perfused solution. Although not in placenta, a previous report has demonstrated that metformin significantly stimulated glucose uptake in human skeletal muscle cultured in 5mM glucose, in a concentration and time-dependent manner, where maximal uptake was observed after 8 hours of 50 µM metformin treatment (421). This study also showed that metformin has higher efficiency for glucose uptake in hyperglycaemic culture environments (25mM glucose) (421). As such, this suggests that metformin may have greater capacity in stimulating placental uptake of glucose during hyperglycaemic states in women with GDM. Repeating this assay and investigating glucose uptake in placental villous explants cultured in mild hyperglycaemia (7mM glucose) may further our understanding of this.

Moreover, it is also possible that the actions of metformin on placental glucose metabolism relies on *in-vivo* metabolites which are absent in an *ex-vivo* model. Indeed, transcriptomic analysis from this study demonstrated that SLC2A10 and SLC2A11 genes, encoding GLUT10 and GLUT10/11, were mapped to the lipid metabolism biological network associated with DEGs in placental tissue obtained from obese women with GDM taking metformin compared to placebo. It has also been shown that *in-vivo* exposure to metformin in a high-fat diet rat model increases placental glucose transporter 1 (GLUT1), GLUT3 and GLUT4 expression via AMPK stimulation (422). It is known that GDM is associated with overexpressed GLUT1 and hexokinase 2 (HK2) protein levels (234). However, a recent study has demonstrated that miR-9 and miR-22 are downregulated in placentae complicated by GDM and are negatively associated with GLUT1 and HK2 protein levels (234). Interestingly, it has been shown that metformin may downregulate miR-9 expression *in-vivo* and may play a role in influencing miR-22 regulation (423,424). As such, measuring glucose transporter expression in placental explant models directly exposed to metformin would provide further insight into the direct and indirect effects of metformin on placental glucose metabolism.

3.5.3.2 Mitochondrial Metabolism

Regulated mitochondrial activity and mitophagy are essential to maintain cellular homeostasis and oxidative stress levels (425). Mitochondrial dysfunction, including altered mitophagy and ROS accumulation, have been associated with restricted fetal growth and GDM (426–428). Metformin has previously been identified to influence mitophagy in T2DM patients (429). In this chapter, transcriptomic analysis demonstrated that *in-vivo* metformin exposure in obese women with GDM was associated with altered mitochondrial development and function, where PINK1 expression was identified to be downregulated. In placental explants, no direct effect of metformin was observed in the expression of this gene which could suggest that metformin indirectly alters PINK1 expression *in-vivo*. However, when western blotting was performed to further examine PINK1 levels in human placental explants (data not shown), no bands were visible, suggesting that there may be low levels of PINK1 in isolated human placental explants. In addition to PINK1, mitochondrial metabolism is regulated by several other mitophagy-related genes, including PARKIN, LC3 and BCL2. A downward non-significant trend in PARKIN and LC3 expression and a dose-dependent decrease in BCL2 expression was observed. This is in contrast to a recent study demonstrating that metformin upregulated placental BCL2 expression, however it should be noted that this study was conducted in a preeclamptic rat model (430).

A non-significant dose-dependent decrease in citrate synthase activity, a marker of intact mitochondrial inner membrane (401), was demonstrated after 72 hours of direct metformin exposure in human placental explants. The current literature also demonstrates that metformin reduced syncytiotrophoblast mitochondrial content in obese women and male offspring of lean women (431). However, in GDM, metformin only impacted syncytiotrophoblast mitochondrial function at supraphysiological doses, where this effect was demonstrated to be sex-specific. Interestingly, Hebert and Myatt also showed that metformin did not affect superoxide generation in male offspring, however a dose-dependent reduction was observed in female offspring from obese and lean mothers (431). In contrast, Tarry-Adkins et al. have reported that physiological concentrations of metformin reduced trophoblast markers of oxidative stress (386). No change in oxidative

damage marker, 8OHdG, was observed in human placental explants with higher concentrations of metformin in this chapter. Placental tissue was collected from male and female offspring in our study, where maternal demographics was heterogenous. It is therefore possible that these confounding factors hindered our observations on the direct effects of metformin on mitochondrial function and oxidative stress in the placenta.

Exposure to metformin *in-utero* has been associated with altered fatty acid metabolism in fetal tissues and trophoblasts (432,433). Transcriptomic analysis identified fatty acid oxidation as a canonical pathway impacted by *in-vivo* metformin exposure in obese women with GDM treated with metformin compared to placebo. Fatty acid oxidation is integral for the generation of TCA cycle metabolites to regulate mitochondrial energetics (434). It has been reported that metformin exposure in fetal tissues may decrease TCA cycle intermediates, namely citrate, thus promoting restricted fetal growth as a result of reduced lipogenesis and biomass (435,436). A previous study has showed that 200μM metformin directly induced no changes in trophoblast TCA cycle intermediates, but a significant increase was observed in lactate, α-ketoglutarate, succinate, and malate levels with a supraphysiological concentration of 2mM metformin (370). However, mitochondrial-dependent ATP production and basal respiration has been shown to be directly affected by metformin at physiological concentrations (0.01-0.1mM) in trophoblasts (386). Although a time-dependent effect was observed in our human placental explant model, this was more pronounced with physiological and supraphysiological concentrations of metformin. Indeed, direct metformin exposure demonstrated to mainly affect the metabolites at the initial stages of the TCA cycle; namely, lactic acid, pyruvate, citrate and isocitrate. Changes in the expression of these metabolites were mainly observed at higher concentrations of metformin (100μM and 1mM) and across all culture time points. Moreover, it is possible that the reduction in culture media glucose levels at 72 hours may have minimised the direct effect of metformin on TCA cycle activity at this time point, where it has previously been discussed that metformin demonstrates increased glucose metabolism in high glucose environments (421).

Acylcarnitines are integral for fatty acid oxidation as they facilitate fatty acid transfer to the mitochondria (437). Similarly to the TCA cycle metabolites, a time-

dependent effect on acylcarnitine expression was observed in our human placental explant model, however this was more pronounced with physiological and supraphysiological concentrations of metformin. It was apparent that metformin had a significant impact on long-chain, medium-chain and short-chain acylcarnitines. Interestingly, medium-chain acylcarnitine upregulation has been associated with GDM, T2DM onset and β-cell dysfunction (402). Moreover, it is known that glucose availability impacts fatty acid oxidation (438,439). Given that the reduction in culture media glucose levels was more pronounced with metformin after 72 hours, this may explain the pronounced increase in acylcarnitine expression in response to metformin after 72 hours of culture. Interestingly, it has previously been demonstrated that maternal tissue acylcarnitine levels are unaffected by *in-utero* metformin and changes are only observed in fetal tissues (432). Another group has found that short-, medium-, and some long-chain acylcarnitines are altered in the circulation of infants exposed to metformin *in-utero* in pregnancies complicated by hyperglycaemia (440). Interestingly, circulating medium- and long-chain acylcarnitine expression has been associated with birthweight in breastfed full-term infants (441). As such, it is possible that metformin may have more of an impact on fetal fatty acid metabolism rather than maternal fatty acid metabolism, thus contributing towards altered fetal growth. However, it has recently been reported that trophoblast lipid metabolism is impacted by physiological concentrations of metformin, thereby potentially altering nutrient availability to the developing fetus (433). Future research should investigate this effect in human placental explants, to better mimic placental physiology.

PPARGC1β has been strongly associated with T2DM and tissue metabolic activity (442). PPARGC1β was identified as an upstream regulator of placental DEGs in obese women with GDM treated with metformin compared to placebo. Transcriptomic analysis also demonstrated PPARGC1β to be associated with altered placental metabolism in obese women with GDM treated with metformin, where its expression was upregulated. This gene encodes PGC-1 protein, a master regulator of mitochondrial biogenesis through the mediation of oxidative phosphorylation and fatty acid oxidation (434). In contrast to *in-vivo* exposure, a dose-dependent reduction in PPARGC1β expression was observed in response

to direct metformin exposure in human placental explants after 72 hours of culture. A reduction in PGC-1 is associated with decreased mitochondrial biogenesis (434). The impact of metformin on this master regulator in the placenta may therefore drive suboptimal placental development and fetal growth in pregnancies complicated by GDM. However, further research is needed to elucidate the role of other *in-vivo* factors contributing towards adverse fetal outcomes in GDM pregnancies exposed to metformin.

3.5.4 *In-vivo* and *Ex-vivo* Metformin Exposure on the Placenta and Future Considerations

Findings from this chapter demonstrate that in-vivo metformin exposure differentially impacted the expression of various placental genes compared to direct exposure of metformin in an ex-vivo placenta model. It is important to note that placental drug transport may vary depending on numerous factors, including transporter expression, gestational age, blood flow and enzyme availability (443), which may explain discrepancies in the in-vivo and ex-vivo models. However, an alternative explanation could be that other indirect actions of metformin, including changes to extracellular vesicles, may impact placental development in-vivo. Indeed, it has been demonstrated that ITGB3, which was impacted by in-vivo and ex-vivo exposure of metformin in this study, plays a role in EV uptake, where the literature also shows integrins to play a key role in placental EV trafficking (444,445). These findings therefore suggest that the influence of in-vivo circulating factors, such as EVs and their miRNA cargo, could indirectly regulate the action of metformin in the placenta; factors which are absent in an ex-vivo model of the human placenta. Various studies have demonstrated metformin to impact EV and miRNA profile within the circulation of people with diabetes (**Table 25**, **Table 26**). This suggests that indirectly modulating maternal circulating factors may be a fundamental mechanistic activity of metformin that should be considered when investigating the influence of metformin on placental and fetal development in GDM. This warrants further studies to analyse maternal EVs and their miRNA cargo from GDM pregnancies treated with or without metformin. Exposing human placental explants to these EVs would also provide further

insight into the indirect effects of metformin on placental vasculature, development and metabolism in-vivo. Unfortunately, blood samples from women with GDM treated with metformin were not available at the time of this PhD project. Instead, an alternative approach was taken, where the next two chapters focus on the impact of EVs and their miRNA cargo on fetal growth and placental development in GDM pregnancies.

Table 25 Metformin-sensitive miRNAs in *in-vivo* models.

Reference	Model	Metformin Dose	Effect of Metformin
(363)	T2DM male and female patients	No dose stated, 3-month treatment	Downregulation of plasma miRNAs: hsa-let-7e-5p, hsa-let-7f-5p, hsa-miR-21-5p, hsa-miR-24-3p, hsa-miR-26b-5p, hsa-miR-126-5p, hsa-miR-129-5p, hsa-miR-130b-3p, hsa-miR-146a-5p, hsa-miR-148a-3p, hsa-miR-152-3p, hsa-miR-194-5p, hsa-miR-99a-5p
(364)	T2DM male and female patients	Initial dose of 425 mg before progressively increasing to 1700mg/day during the first week, for 3 months	Downregulation of plasma hsa-miR-140-5p and hsa-miR-222 Upregulation of plasma hsa-miR-142-3p and hsa-miR-192
(365)	T2DM male and female patients	No details stated	78 miRNAs altered in EV-depleted plasma

Table 26 Impact of metformin on extracellular vesicles.

Reference	Model	Metformin Dose	Effect of Metformin
(365)	T2DM male and female patients	No details stated	Downregulation of 42 EV-encapsulated miRNAs
(366)	Human mesenchymal stem cells	0.2-5mM metformin for 24 hours	Promoted EV release via autophagy-related pathway and altered EV protein profile (increase of cell growth proteins)
(367)	Male and female hypertensive diabetic db/db mice on high salt diet	60mg/kg once a day, 4 days	Altered protein content in EVs (reduced cathepsin B)
(368)	U87MG human glioblastoma cells	5-40mmol for 48 hours	Increased exosome biogenesis and secretion
(369)	T2DM male and female patients	Median dosage of 2500mg	Reduced total, platelet- and endothelial-derived EV concentration

3.6 Summary

Impact of *In-vivo* and *Ex-vivo* Metformin Exposure on Placental Development	
In-vivo	
Transcriptomic analysis	Metformin associated with biological networks of vascular development, cellular development and metabolism
Ex-vivo	
AMPK Activation	Physiologically relevant concentrations of metformin (100μM-1mM) activate the AMPK pathway at 24 hours
Vascular Development	• Downregulated *ITGB3* expression with higher metformin concentrations (100μM-1mM) at 72 hours • CD31 protein expression not affected by higher metformin concentrations at 72 hours
Cellular Development	**Cellular Growth and Proliferation** • No effect on Ki67 protein expression after 72 hours of metformin culture **Cellular Death and Toxicity**

	• No effect on M30 protein expression after 72 hours of metformin culture • No effect on culture media LDH concentration **Trophoblast Endocrine Function** • Non-significant dose-dependent decreasing trend in β-HCG concentration after 72 hours of metformin culture
Metabolism	**Glucose Metabolism** • Non-significant reduction in culture media glucose levels with higher doses of metformin after 72 hours **Mitochondrial Metabolism** • Dose-dependent decrease in *BCL2* expression after 72 hours of metformin culture • 8OHdG protein expression not affected by higher metformin concentrations at 72 hours • Non-significant dose-dependent decreasing trend in citrate synthase activity after 72 hours of metformin culture • Time-dependent changes in the levels of TCA cycle and acylcarnitine metabolites in metformin-treated explants • Dose-dependent decrease in *PPARGC1B* expression after 72 hours of metformin culture
Summary	*In-vivo* metformin exposure in obese women with GDM altered placental genes associated with vascular development, cellular development and metabolism. Physiologically relevant concentrations of metformin directly activated the AMPK pathway in human placental explants, where genes involved in vascular development, mitophagy and mitochondrial biogenesis were altered after 72 hours of culture. Mitochondrial metabolism was also impacted in metformin-treated human placental explants over 72 hours of culture. However, not all changes observed with *in-vivo* metformin exposure were observed with direct *ex-vivo* metformin exposure on the placenta. This suggests that *in-vivo*, some effects of metformin on placental development are likely attributed to indirect actions on the placenta.

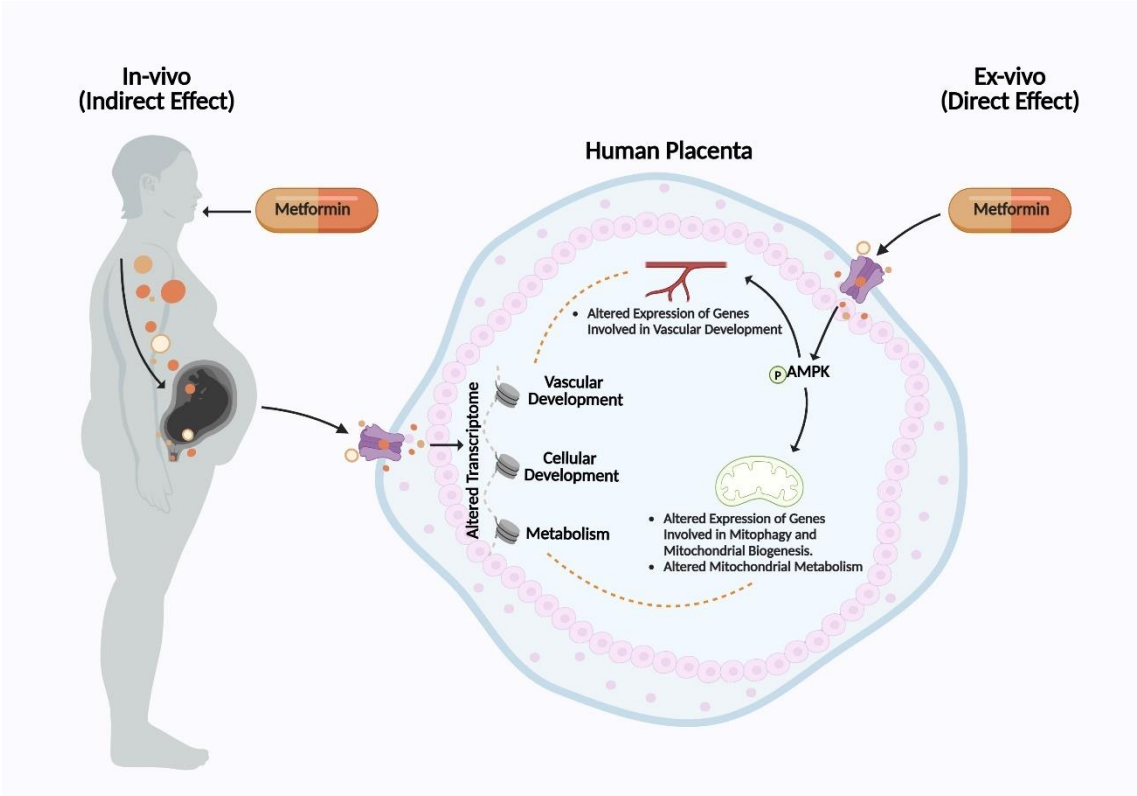

Figure 37 Graphical summary of the effects of *in-vivo* and *ex-vivo* metformin exposure on human placenta.

In-vivo exposure of metformin alters placental transcriptomic pathways associated with vascular development, cellular development and metabolism. Direct metformin exposure in human placental explants leads to activation of the AMPK pathway which impacts genes involved in vascular development, mitophagy and mitochondrial biogenesis *ex-vivo.* Direct metformin exposure in human placental explants also influences mitochondrial metabolism over time *ex-vivo*. Some, but not all placental genes, were impacted by direct metformin exposure in the same way as *in-vivo*. These findings suggest that metformin may influence placental development via direct and indirect effects *in-vivo*. Orange line represents similar effects observed with *in-vivo* and *ex-vivo* metformin exposure. Created using Biorender.com.

4 Investigating the Effect of miR-375-3p in Altered Fetal Growth

4.1 Introduction

4.1.1 Circulating miRNAs in GDM Pregnancies

The maternal environment is altered in several ways in pregnancies complicated by maternal diabetes, where hyperglycaemia, glucose-lowering therapies and altered maternal metabolism can impact various fetal growth-regulating factors (244). Maternal circulating EV-miRNAs are key regulators of feto-placental development, where previous literature demonstrates that maternal EV-miRNA expression profile is altered in GDM pregnancies compared to healthy, uncomplicated pregnancies (**Table *3***). The Forbes group have previously shown that at the time of GDM diagnosis, EV-miRNA profile is altered in maternal serum prior to the onset of LGA compared to those giving birth to AGA neonates (**Figure *38***A). Indeed, it was demonstrated that miR-145-5p was downregulated and miR10a-5p, miR-1-3p, miR-19b-3p, miR-200c-3p, miR-27a-3p, miR-16-5p, miR-374-5p, miR-375 and miR-196-5p were upregulated in maternal serum of LGA compared to AGA pregnancies (**Figure *38***A). Four of these altered miRNAs were also upregulated in placental tissue; miR-1-3p, miR-133a-3p, miR-200c-3p and miR-375-3p (**Figure *38***B). Interestingly, the primary transcript for these miRNAs were present in human placental tissue, except for miR-375-3p, where only its mature functionally active form was expressed (**Figure *38***C). As previous research has showed that EVs are able to circulate and internalise into placental tissue (272), these findings suggest that miR-375-3p may be circulating to the placenta via the maternal circulation. While detecting the source of origin of miRNAs is difficult, we have previously shown that miR-375-3p is pancreas-specific, where miR-375-3p release from pancreas-derived EVs is increased under mild hyperglycaemic conditions that reflect glucose levels of women with GDM that deliver AGA or LGA infants (**Figure *39***A-D). Fluorescently labelling these EVs further showed that they can internalise into human placental tissue, resulting in increased placental levels of miR-375-3p (**Figure *39***E).

By overexpressing miR-375-3p mimic in healthy human term placental explants (100nM, 72 hours) and performing TMT mass spectrometry, the Forbes group

demonstrated 376 DEPs (190 downregulated, 186 upregulated) in explants treated with miR-375-3p compared to control miRNA mimic (**Figure *40***). Using, protein-protein interaction cluster analysis alongside Ingenuity Pathway Analysis and overrepresentation analyses, it was demonstrated that these DEPs were enriched in pathways involved in vascular development, mitochondrial function, glucose metabolism and growth (**Figure *40***).

Taken together, these data suggest that in pregnancies complicated by GDM, a hyperglycaemic environment promotes the release of EV-miR-375-3p from the maternal pancreas, where these EVs/miRNAs traffic to the placenta to influence placental development and function to likely contribute to increased fetal growth. However, while we can postulate this, we do not have direct evidence that miR-375-3p is causative of LGA in GDM pregnancies, as only a correlation can be established in a human model. As such, this current study aimed to determine if there is a direct causation between maternal circulating miR-375-3p and fetal overgrowth using a pregnant mouse model.

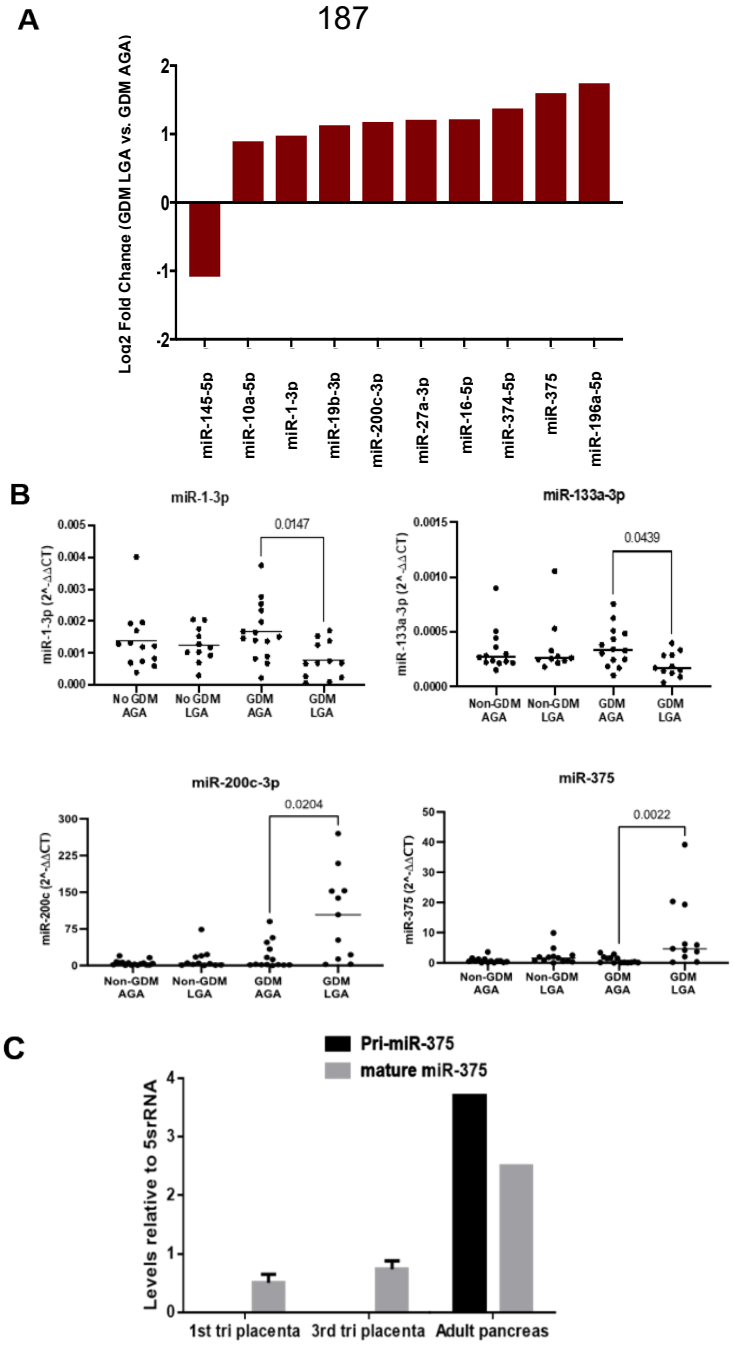

Figure 38 miR-375-3p is upregulated in maternal circulation and term placental tissue of GDM-LGA pregnancies and is pancreas-specific.

Previous unpublished work from the Forbes lab showing (A) that at the time of GDM diagnosis (24-28 weeks), EV-miRNA profile is altered in maternal serum of LGA outcome pregnancies compared to AGA outcome pregnancies (downregulated - miR-145-5p; upregulated - miR10a-5p, miR-1-3p, miR-19b-3p, miR-200c-3p, miR-27a-3p, miR-16-5p, miR-374-5p, miR-375, miR-196-5p). (B) miR-1-3p, miR-133a-3p, miR-200c-3p and miR-375 are altered in human term placental tissue of GDM-LGA pregnancies compared to GDM-AGA pregnancies. (C) The primary transcript for miR-375 is present in human adult pancreas tissue but absent in first and third trimester human placental tissue. Mature miR-375 transcript is present in human adult pancreas tissue, as well as first and third trimester human placental tissue.

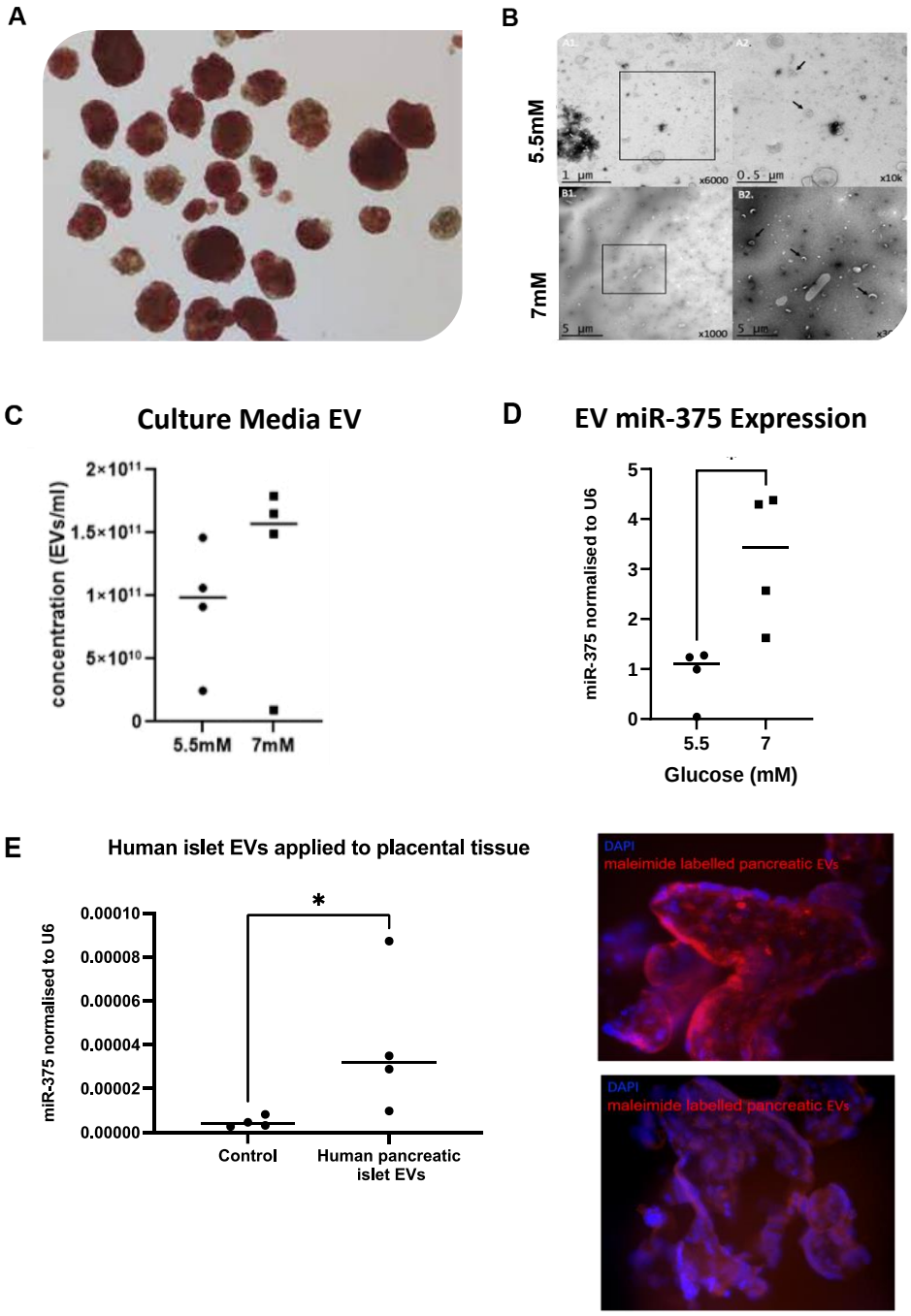

Figure 39 miR-375-3p is released in EVs from pancreatic islets and is internalised into human placenta.

Previous unpublished work from the Forbes lab showing (A) Human pancreatic islets were obtained by the International Islet Distribution Programme and (B) cultured under 5.5mM and 7mM glucose conditions for 3 days before EVs were isolated from conditions media (n=4). (C) A higher concentration of pancreatic-EVs was secreted into the conditioned media under mild hyperglycaemic conditions, (D) where these EVs expressed higher levels of miR-375 (n=4). (E) EVs were maleimide-488-labelled and applied to term placental explants for 24 hours (n=4). Tissue was embedded in OCT and EV uptake was visualised by fluorescent microscopy. Human pancreatic islet EVs resulted in increased human placental expression levels of miR-375.

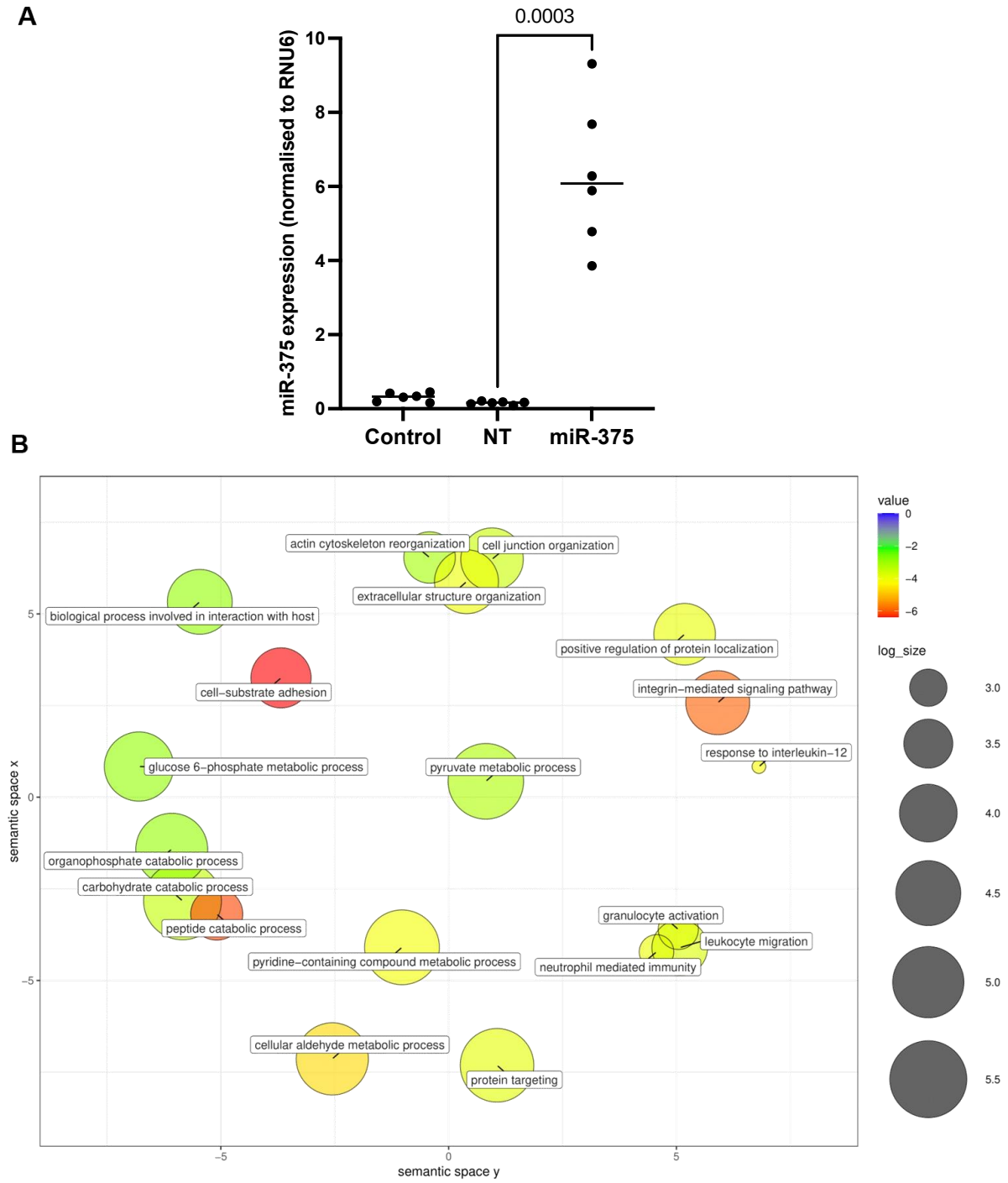

Figure 40 Overexpression of miR-375-3p alters the protein expression and pathways associated with vascular development, mitochondrial function, glucose metabolism and growth in term human placenta explants.

Previous unpublished work from the Forbes lab showing (A) QPCR confirmed human term placental explants were overexpressed with miR-375-3p following delivery of miR-375-3p mimic (100nm, 72 hours, n=6) and (B) proteomics were performed via TMT mass spectrometry analysis. Functional enrichment analysis was performed and web-based REVIGO tool was used to visualise non-redundant gene ontology terms of differently expressed proteins.

4.1.2 The Mouse as a Model of Human Pregnancy

Mouse studies have immensely enhanced our understanding of human pregnancy, with both species demonstrating haemochorial placentae, where trophoblast cells are surrounded by the maternal circulation (446,447). In mice, the placenta is structured into distinct layers, known as the labyrinth zone (containing chorion-derived epithelial cells and allantois-derived vascular cells), the junctional zone (containing parietal giant cells, glycogen trophoblasts and spongiotrophoblasts) and the maternal decidua (containing maternal vasculature, uterine decidual cells, glycogen trophoblast and spiral artery-associated trophoblast giant cells) (**Figure *41***) (448). Maternal-fetal nutrient, waste and gas exchange occurs in the labyrinth zone of the mouse placenta, where exchange efficiency is affected by the surface area of this zone (349). Within this zone, three layers of trophoblast cells are located between maternal blood spaces and fetal endothelial cells (448). The junctional zone is the endocrine zone of the mouse placenta, where growth factors and energy are also synthesised for the development of the fetus and placenta (448). Interestingly, it has been reported that impaired development of the junctional zone is associated with altered fetal growth (448). The mouse placenta structure is established by gestational days 10-11, where it is fully mature by day 15 (448).

Although this placental structure differs from human, mice share various homologous placental cell types with humans, including proliferative and invasive trophoblasts, giving rise to the mouse syncytium (446). However, relative to human pregnancy, mice do not demonstrate an intervillous space and trophoblast invasion occurs later in gestation compared to humans (446). In human pregnancy, trophoblasts invade into the inner third of the myometrium to allow maternal-fetal nutrient exchange, whereas this invasion is confined to the decidua basalis in mice (447). As such, this reflects potential differences in feto-placental nutrient transfer in mice compared to human pregnancy. While absent in humans, mice manifest an inverted yolk sac placenta which plays a key role in rodent embryogenesis (447). With the C19MC encoding placenta-specific miRNAs exclusively found in primates (97,98,447), this also denotes differences in mouse and human placental development. Indeed, decidualisation occurs later in pregnancy in mice; this process is observed prior to conception in humans but

post embryo implantation in mice (446). This later developmental timeline similarly applies to placental maturity in mice compared to humans, where the conclusive structure of the human placenta is observed around 3 weeks into gestation compared to mid-gestation in mice (446).

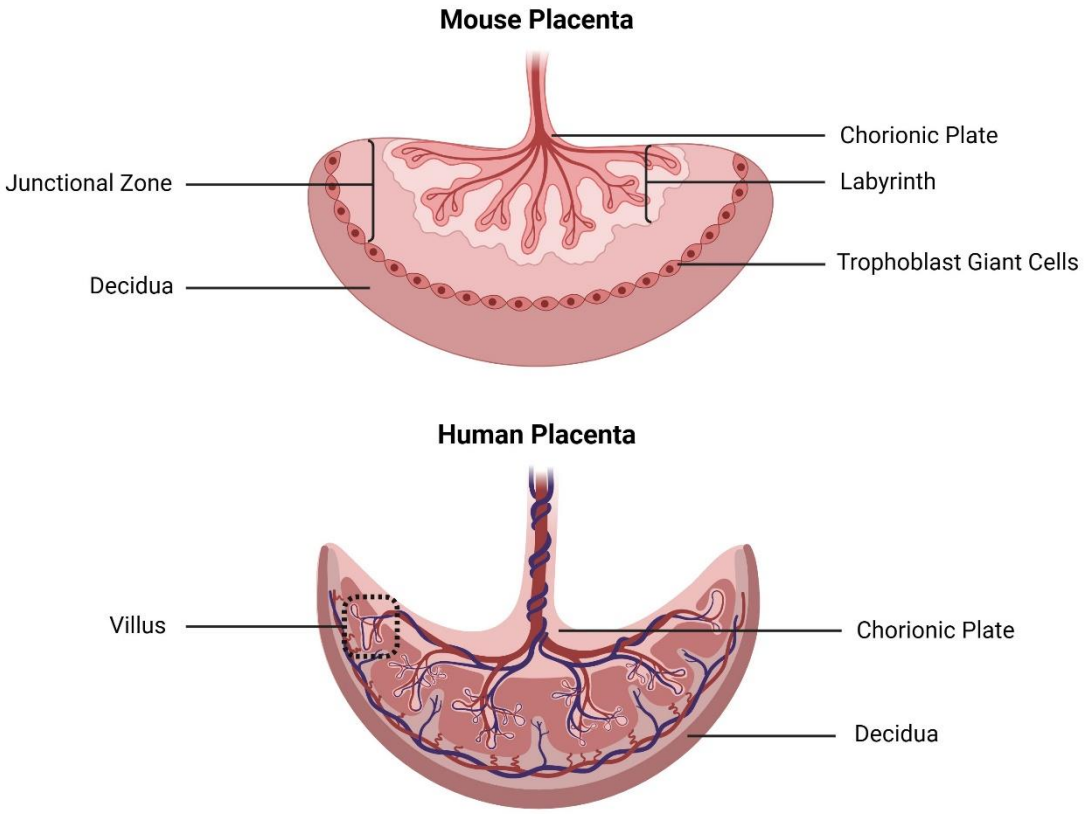

Figure 41 Mouse and Human Placental Structure.

Mouse and human placentae demonstrate a haemochorial structure, where trophoblast cells are in direct contact with the maternal circulation. Both human and mice demonstrate a decidua and chorionic plate in their placental structures. However, human placentae manifest an intervillous space within their villous structure, unlike mouse placentae. Mouse placentae are divided into three main zones, known as the labyrinth zone, junctional zone and decidual zone. Created using Biorender.com.

Despite these differences in placental structure and development, mice demonstrate short gestation periods (449) and sizeable litter sizes, allowing offspring follow-up studies to be performed that would otherwise be considerably time-consuming in humans. Mice also manifest a similar immune system to humans and demonstrate defined genetics (449), enabling less biological variability in humans and therefore increased experimental reproducibility. Using a mouse model to evaluate the effects of pregnancy on fetal growth and development offers opportunities for causation studies that would otherwise be unsafe in humans.

Therefore, a mouse model of pregnancy will be utilised to establish if there is a direct causation between enhanced levels of miR-375-3p in circulation and LGA. This will not only further our understanding of the role of EV-miRNAs in feto-placental development, but also strengthen the evidence for maternal miR-375-3p to be used as a biomarker for LGA in GDM pregnancies.

4.2 Hypothesis

In-vivo delivery of miR-375-3p into the maternal circulation alters fetal growth and placental development in healthy pregnant mice.

4.3 Aims

1) Deliver miR-375-3p to the maternal circulation of healthy pregnant mice and assess pregnancy outcomes.
2) Establish the impact of miR-375-3p on mouse fetal growth.
3) Establish the mechanism of which miR-375-3p impacts fetal growth by assessing maternal metabolism and placental development and function.

4.4 Results

4.4.1 Pregnancy outcomes after delivery of miR-375-3p to the maternal circulation of healthy pregnant mice.

4.4.1.1 miR-375-3p does not impact litter size, pregnancy resorptions, fetal sex or maternal survival in healthy pregnant mice.

Healthy pregnant mice were injected with miR-375-3p mimic or NT miRNA mimic at E11.5, E13.5 and E15.5 at a concentration of 1 mg/kg, based on previous work (123). PBS was used as a vehicle control. At E18.5, mice were culled and pregnancy outcomes were investigated (**Figure *42***). All dams from each treatment group survived pregnancy, therefore there were no safety concerns in terms of maternal mortality (data not shown). Dams treated with PBS and NT miRNA demonstrated similar litter sizes of 8 offspring (**Figure *43***A). Although a median of 6 offspring per litter was demonstrated in dams treated with miR-375-3p, this reduction in litter size was not of statistical significance compared to PBS and NT miRNA (**Figure *43***A). In mice treated with vehicle, there was a low level of resorptions (median=0) and this was not affected by NT miRNA or miR-375-3p (**Figure *43***B). In vehicle treated mice, 58.23% (± 0.084%, n=6) of pups were male. This was not affected by NT miRNA (44.29 ± 0.096%, n=5) or miR-375-3p (56.90 ± 0.087%, n=7) (**Figure *43***C).

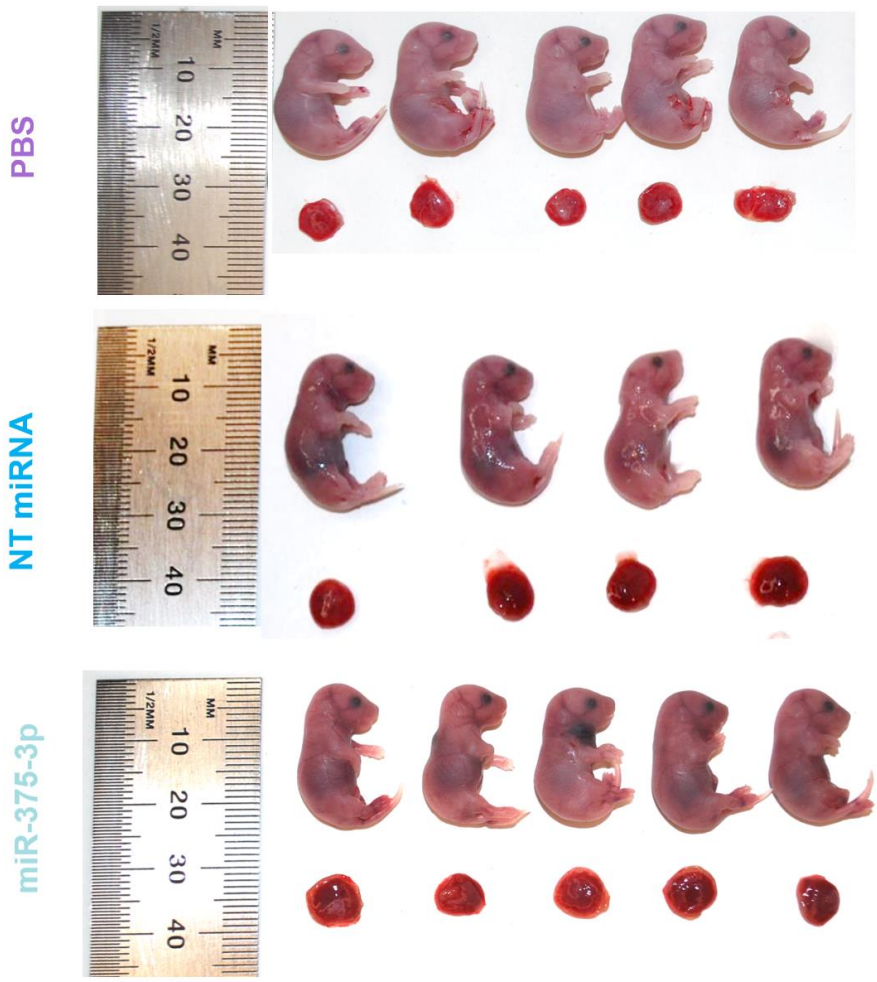

Figure 42 Representative images of E18.5 mouse fetuses and their respective placentae exposed to PBS and miR-375-3p mimic during gestation.

Healthy pregnant C57BL6/J female mice were injected with miR-375-3p (n=7) or NT miRNA mimics (n=7) at E11.5, E13.5 and E15.5 at 1mg/kg (based on E11.5 weight). PBS (n=5) was used as a vehicle control. Mice were sacrificed at E18.5 and pups were weighed. Ruler shows measurements in mm.

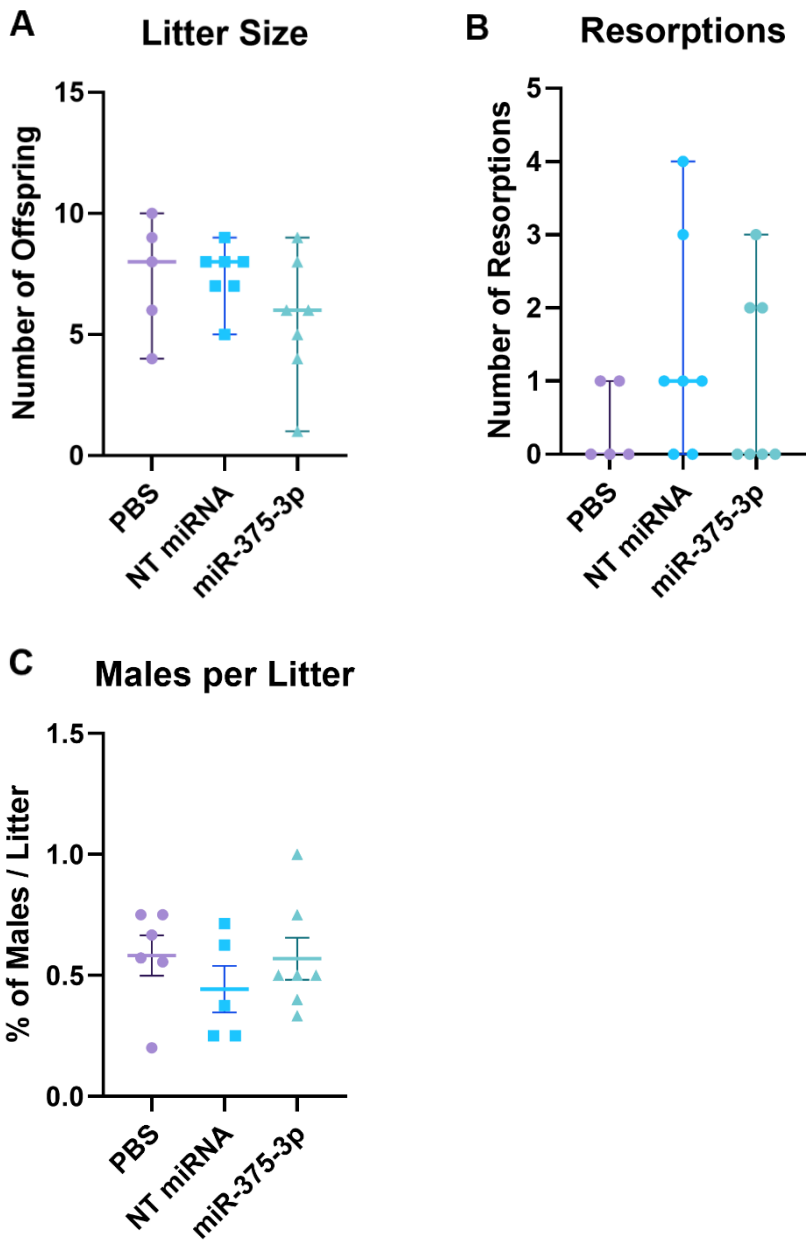

Figure 43 Litter outcomes of mice exposed to PBS, NT miRNA and miR-375-3p mimics during gestation.

Healthy pregnant C57BL6/J female mice were injected with miR-375-3p (n=7) or NT miRNA mimics (n=7) at E11.5, E13.5 and E15.5 at 1mg/kg (based on E11.5 weight). PBS (n=5) was used as a vehicle control. Mice were sacrificed at E18.5 and pups were weighed. (A) Litter size and (B) Resorptions were measured in response to treatments. Kruskal-Wallis nonparametric test was performed followed by Dunn's multiple comparisons test to determine statistical significance. Data presented as median with 95% with CI. The number of (C) Males per litter was measured in response to treatments and an ordinary one-way ANOVA was performed, followed by Tukey's multiple comparisons test. Data presented as mean±SEM.

4.4.2 The impact of maternal circulating miR-375-3p on fetal growth in healthy pregnant mice.

4.4.2.1 Delivery of miR-375-3p to the mouse maternal circulation increases fetal growth.

To determine the effect of maternal circulating miR-375-3p on fetal growth, pups were culled at E18.5 and weighed (**Figure *44***). PBS treated mice demonstrated mean fetal weight of 1.981g (±0.018g, n=37 clustered to 5 dams). No difference in fetal weight was observed with NT miRNA mimic compared to PBS (p=0.330; n=52 clustered to 7 dams/n=37 clustered to 5 dams, respectively; adjusted for fetal sex and litter size). As such, the effect of miR-375-3p on fetal growth was compared to NT miRNA mimic. Although statistically non-significant, an increase in fetal weight was observed following delivery of miR-375-3p to pregnant dams (from 1.212 ± 0.016g to 1.306 ± 0.021g; p=0.183; n=39 clustered to 7 dams; adjusted for fetal sex and litter size). As such, pups exposed to miR-375-3p were 0.094g heavier than pups exposed to NT miRNA mimic. This equalled to a total body weight increase of 8% (**Figure *44***, **Appendix *3***, **Appendix *4***).

LGA is defined as a neonate weighing above the 90th percentile for their gestational age (450). Fetal growth curves were generated by plotting a non-linear fit of a histogram, and birth centiles were determined based on fetal weights from dams treated with NT miRNA (90th centile - 1.38g; n=52 clustered to 7 dams) (**Figure *45***). A higher proportion of pups exposed to maternal miR-375-3p during gestation were over the 90th centile for birthweight compared to NT miRNA (n=13 and n=5, respectively) (**Figure *45***).

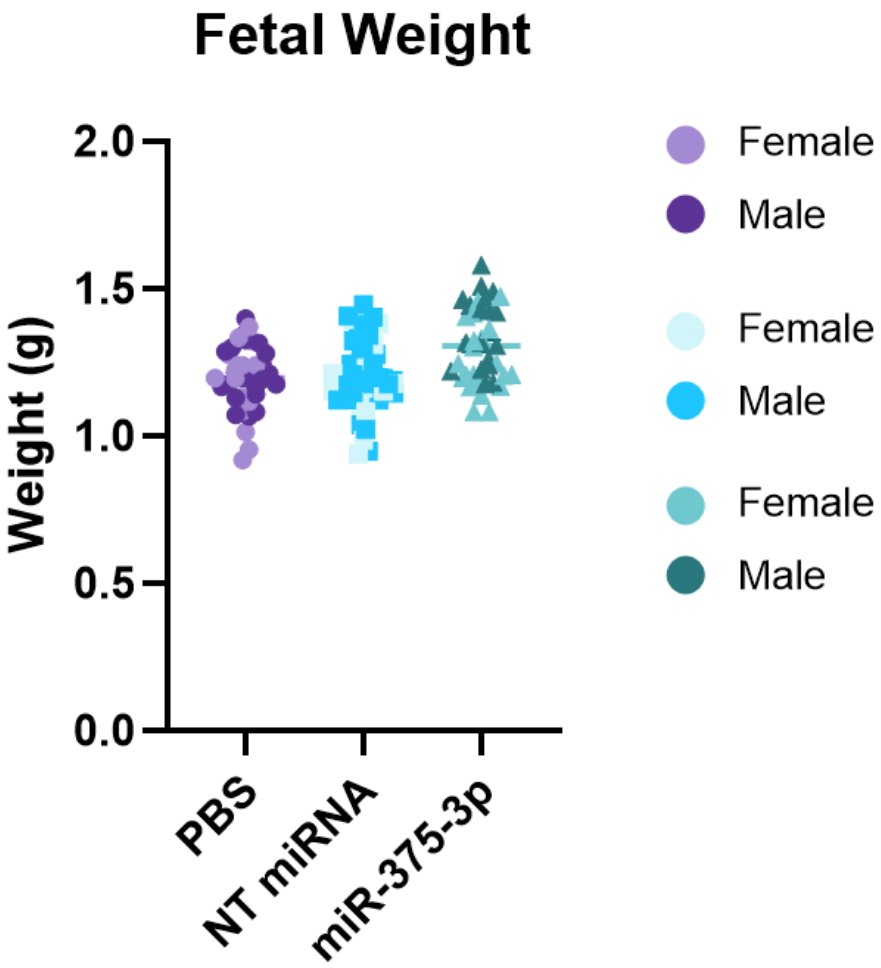

Figure 44 Fetal weight of mice exposed to PBS, NT miRNA and miR-375-3p mimics during gestation at E18.5.

Fetal weight in mice treated with miR-375-3p, NT miRNA and PBS throughout gestation at E18.5. Healthy pregnant C57BL6/J female mice were injected with miR-375-3p or NT miRNA mimics at E11.5, E13.5 and E15.5 at 1mg/kg (based on E11.5 weight). PBS was used as a vehicle control. Mice were sacrificed at E18.5 and pups were weighed. Mixed-effects non-linear regression model was performed using Stata, where each litter was clustered and adjustments were made for fetal sex and litter size. Data presented as mean±SEM; *=p ≤ 0.05. Light data points; female, dark data points; male.

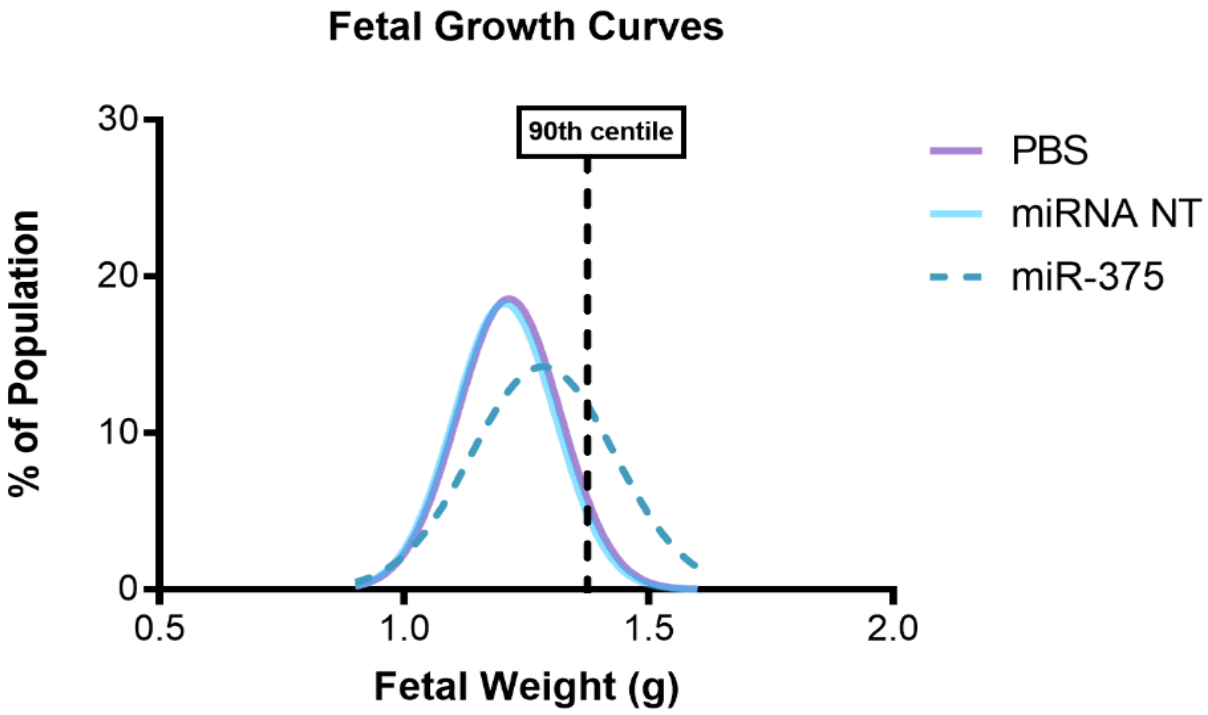

Figure 45 Fetal growth curves of mice exposed to PBS, NT mRNA or miR-375-3p mimics during gestation at E18.5.

Fetal growth curves of mice treated with miR-375-3p, NT miRNA and PBS throughout gestation at E18.5. Healthy pregnant C57BL6/J female mice were injected with miR-375-3p (n=7) or NT miRNA (n=7) mimics at E11.5, E13.5 and E15.5 at 1mg/kg (based on E11.5 weight). PBS (n=5) was used as a vehicle control. Mice were sacrificed at E18.5 and pups were weighed. Non-linear fit of a histogram was generated to determine distribution of fetal weight and birthweight centiles were measured based on NT miRNA treatment.

4.4.3 The impact of maternal circulating miR-375-3p on feto-placental development in healthy pregnant mice.

4.4.3.1 Delivery of miR-375-3p to the mouse maternal circulation increases placental growth.

Mouse placentae were harvested at E18.5 to further understand the mechanism through which delivery of miR-375-3p to the maternal circulation increased mouse fetal weight. Pregnancies exposed to PBS demonstrated mean placental weight of 0.09056g (± 0.003 g; n=37 clustered to 5 dams) (**Figure *46***). Placental weight was similar for pregnancies exposed to NT miRNA mimic (0.094 ± 0.002 g, n=43 clustered to 7 dams) compared to PBS (p=0.569, adjusted for fetal sex and litter size). As such, the effect of miR-375-3p on placental growth was compared to NT miRNA mimic. miR-375-3p significantly increased placental weight (0.115 ± 0.003 g; n=39 clustered to 7 dams) compared to NT miRNA mimic when adjusted for fetal sex and litter size (p=0.00007). This 0.021 g increase was equal to a 22.2% increase in weight (**Figure *46***, **Appendix *5***, **Appendix *6***).

Placental growth curves were generated by plotting a non-linear fit of a histogram. Weight centiles were determined based on NT miRNA treatment (90^{th} centile - 0.115 g, n=43 clustered to 7 dams) (**Figure *47***). A higher proportion of placentae from the miR-375-3p treatment group were over the 90^{th} centile for weight compared to NT miRNA controls (n=22 and n=4, respectively) (**Figure *47***).

Fetal:placental weight ratio was also calculated to determine if maternal delivery of miR-375-3p impacted overall feto-placental development in healthy pregnant mice (**Figure *48***). Fetal:placental weight ratio was unchanged between mice exposed to PBS and NT miRNA mimic (p=0.692, adjusted for fetal sex and litter size). When compared to NT miRNA and adjusted for fetal sex and litter size, miR-375-3p significantly reduced fetal:placental weight ratio (from 12.88 ± 0.302 to 11.59 ± 0.294; p=0.004; n=43 clustered to 7 dams/n=39 clustered to 7 dams, respectively) (**Figure *48***, **Appendix *7***).

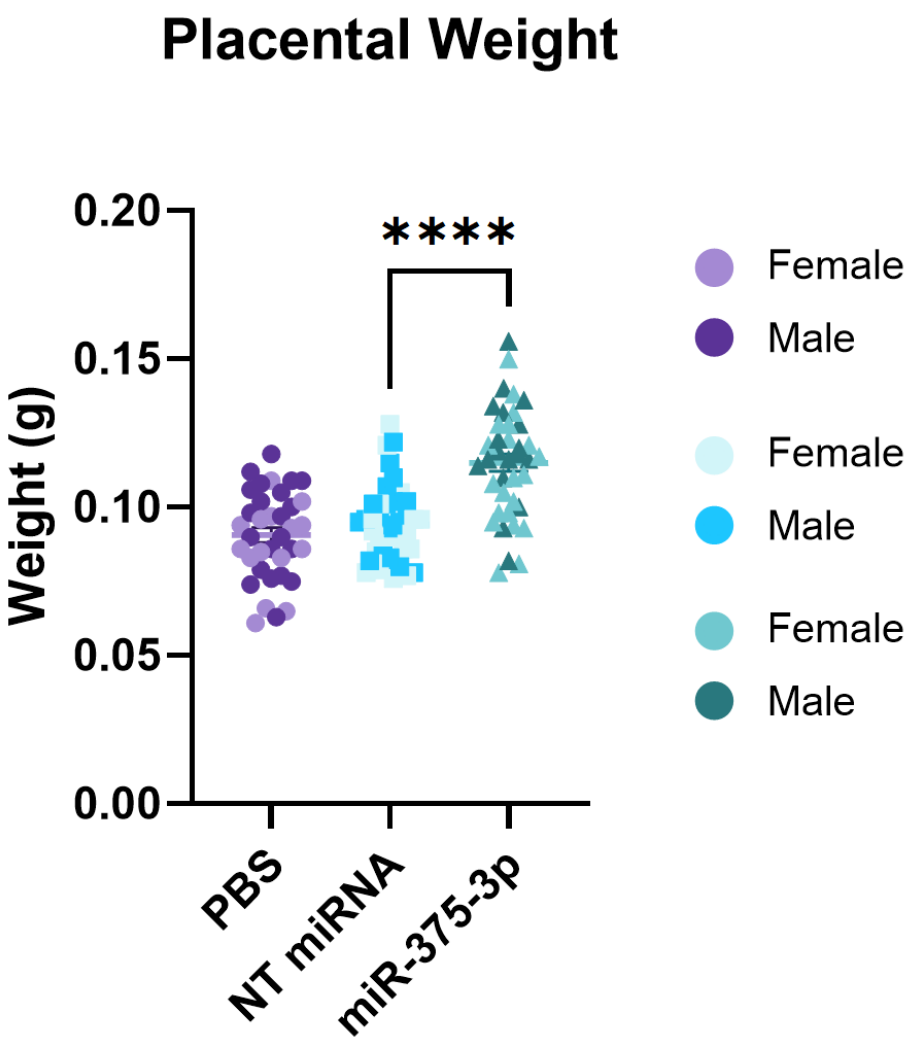

Figure 46 Placental weight of mice exposed to PBS, NT miRNA or miR-375-3p mimics during gestation at E18.5.

Healthy pregnant C57BL6/J female mice were injected with NT miRNA (n=7) or miR-375-3p (n=7) mimic at E11.5, E13.5 and E15.5 before being sacrificed at E18.5. PBS (n=5) was used as a vehicle control. Pups and placentae were sacrificed and weighed. Mixed-effects non-linear regression model was performed using Stata, where each litter was clustered and adjustments were made for fetal sex and litter size. Data presented as mean±SEM; ****=p ≤ 0.0001. Light data points; female, dark data points; male.

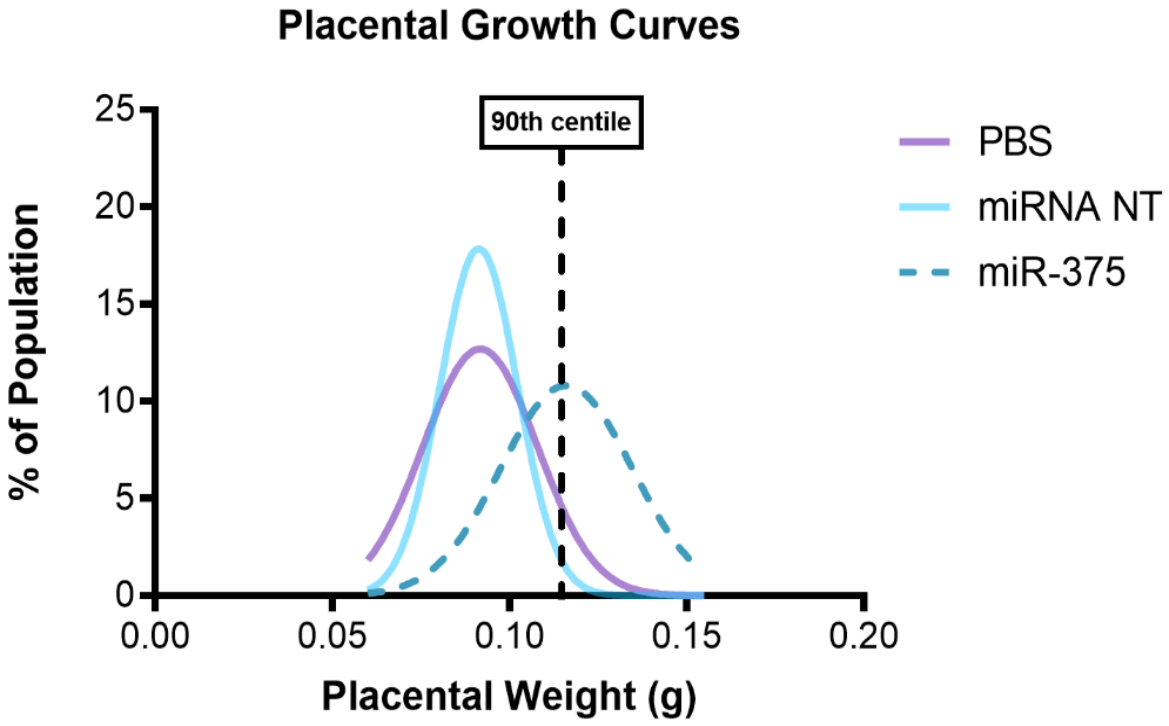

Figure 47 Placental growth curves of mice exposed to PBS, NT miRNA or miR-375-3p mimics during gestation at E18.5.

Healthy pregnant C57BL6/J female mice were injected with NT miRNA (n=7) or miR-375-3p (n=7) mimic at E11.5, E13.5 and E15.5 before being sacrificed at E18.5. PBS (n=5) was used as a vehicle control. Placentae were harvested and weighed. Non-linear fit of a histogram was generated to determine distribution of placental weight and centiles were measured based on NT miRNA treatment.

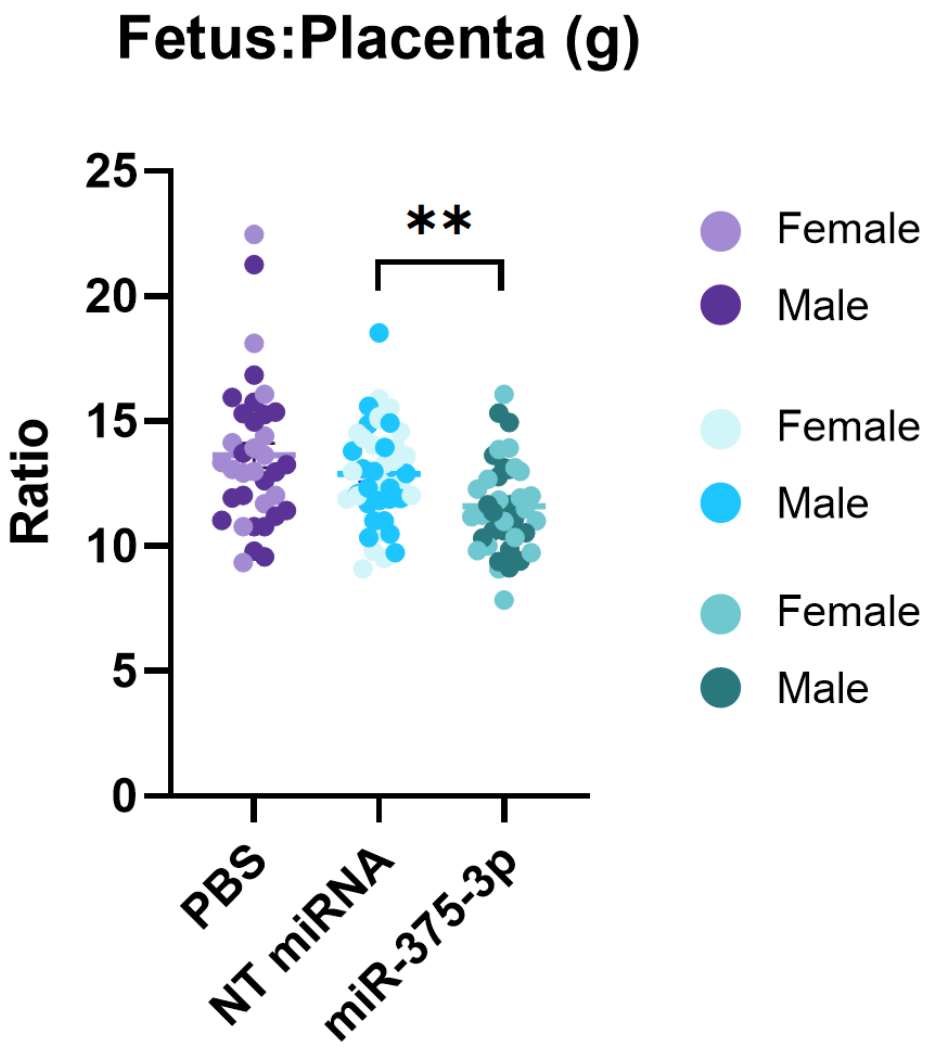

Figure 48 Fetal:placental weight ratio of mice exposed to PBS, NT miRNA or miR-375-3p mimics during gestation at E18.5.

Healthy pregnant C57BL6/J female mice were injected with NT miRNA (n=7) or miR-375-3p (n=7) mimic at E11.5, E13.5 and E15.5 before being sacrificed at E18.5. PBS (n=5) was used as a vehicle control. Pups and placentae were harvested and weighed. Mixed-effects non-linear regression model was performed using Stata, where pups were clustered to each mother and adjustments were made for fetal sex and litter size. Data presented as mean±SEM; **=p ≤ 0.01, ***=p ≤ 0.001. Light data points; female, dark data points; male.

4.4.4 The impact of maternal circulating miR-375-3p on maternal metabolism in healthy pregnant mice.

4.4.4.1 Delivery of miR-375-3p to the mouse maternal circulation may impact maternal metabolism.

To assess whether mouse pregnancy outcomes in response to maternal delivery of miR-375-3p were dependent on maternal health, maternal metabolic health was evaluated. Maternal weight was recorded throughout gestation and weight gain was calculated. Dams treated with PBS (n=5) and NT miRNA mimic (n=7) demonstrated a similar increase in weight throughout gestation (**Figure *49***A). Although not statistically significant, miR-375-3p dams (n=7) were lighter at every recorded time-point than dams treated with PBS and NT miRNA mimic. As a result, dams treated with miR-375-3p gained weight at a slower rate than those treated with PBS and NT miRNA, however this was statistically insignificant (**Figure *49***B). When compared to NT miRNA mimic, dams treated with miR-375-3p demonstrated a non-significant decrease in weight (from 31.67 ± 0.757g to 28.86 ± 0.663g; p=0.061; n=5/7, respectively) (**Figure *49***A). No difference in weight was detected by E18.5 (**Figure *50***A), where assessment of maternal hysterectomised weight showed that miR-375-3p had no marked effect on maternal weight gain (**Figure *50***B). By calculating overall maternal pregnancy weight gain (E18.5 hysterectomised weight – pre-pregnancy weight), this also demonstrated no significance in maternal weight between treatment groups (**Figure *50***C).

Absolute weight of maternal organs at E18.5 and organ weight as % of hysterectomised weight were established. No change was observed in total maternal liver weight between control dams and dams treated with miR-375-3p (**Figure *51***A). When normalised for maternal hysterectomised weight, dams treated with NT miRNA and miR-375-3p demonstrated a non-significant increase in maternal liver weight compared to PBS (**Figure *51***A). A non-significant increase in maternal pancreas weight was observed in dams treated with NT miRNA and miR-375-3p compared to those treated with PBS (**Figure *51***B), however this effect was lost following correction for maternal hysterectomised weight. No difference in total or normalised maternal skeletal muscle weight was observed in control dams and dams treated with miR-375-3p (**Figure *51***C).

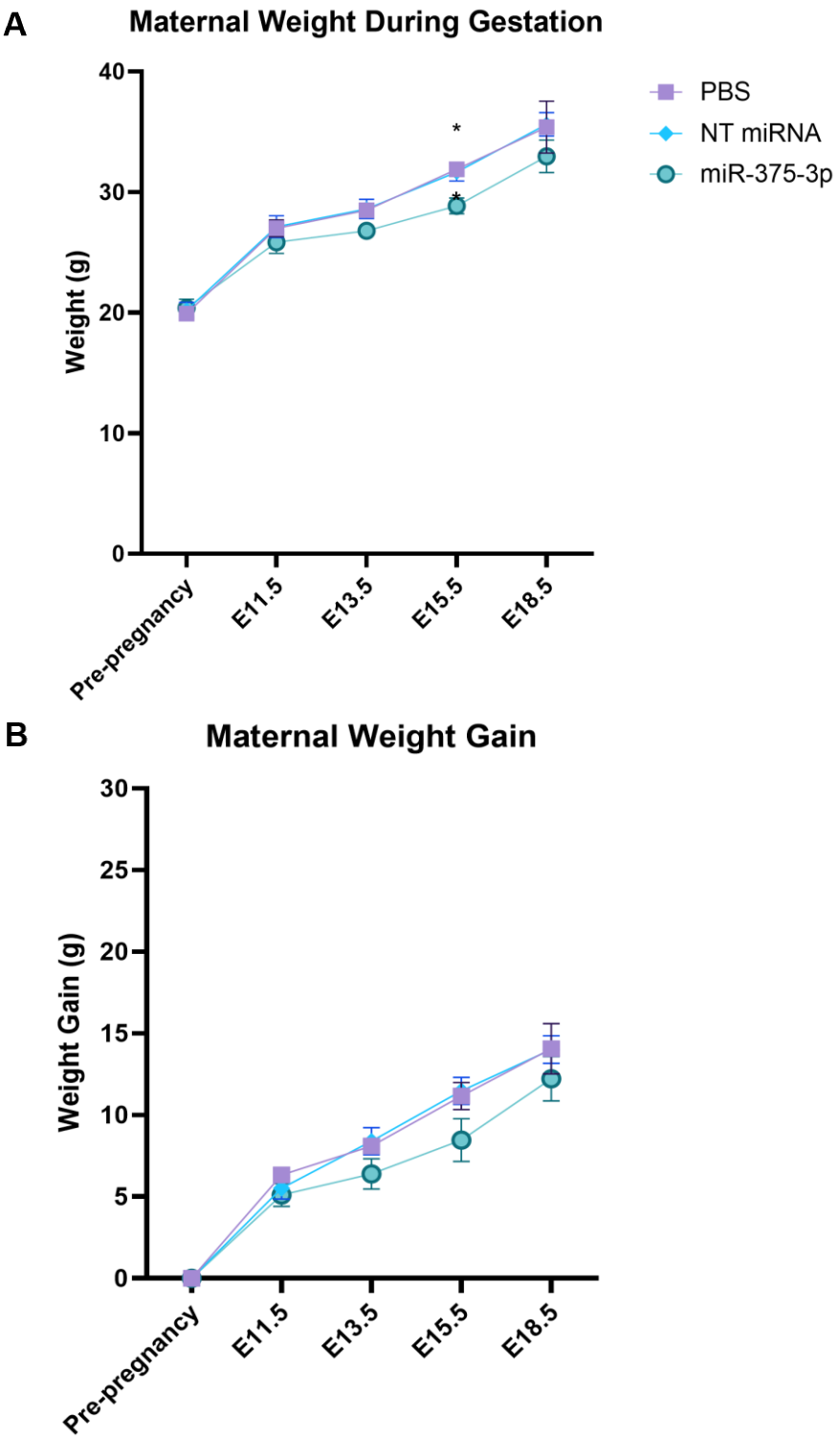

Figure 49 Maternal weight and weight gain during gestation in mice exposed to PBS, NT miRNA or miR-375-3p mimics during gestation at E18.5.

Healthy pregnant C57BL6/J female mice were injected with NT miRNA (n=7) or miR-375-3p (n=7) mimic at E11.5, E13.5 and E15.5 before being sacrificed at E18.5. PBS (n=5) was used as a vehicle control. Pre-pregnancy weights were recorded and maternal weight measured at each injection time-point and before birth. Two-way ANOVA (with Geisser-Greenhouse correction) followed by a Tukey's multiple comparisons test were performed. Data presented as mean±SEM; *=$p<0.05$.

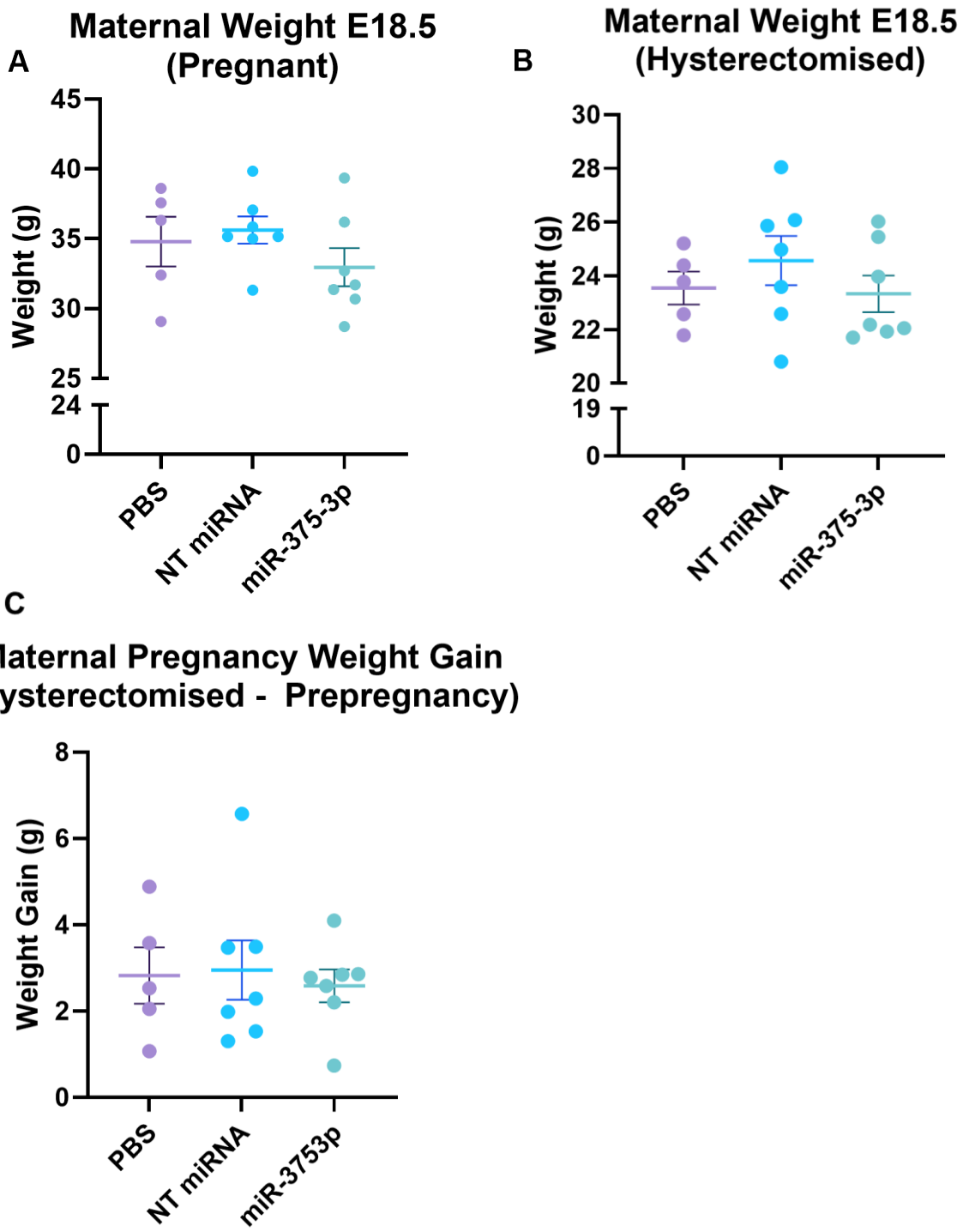

Figure 50 Maternal pregnancy weight, hysterectomised weight and overall pregnancy weight gain of mice exposed to PBS, NT miRNA or miR-375-3p mimics during gestation at E18.5.

Healthy pregnant C57BL6/J female mice were injected with NT miRNA (n=7) or miR-375-3p (n=7) at E11.5, E13.5 and E15.5 before being sacrificed at E18.5. PBS (n=5) was used as a vehicle control. Pre-pregnancy weights were recorded and maternal pregnancy and hysterectomised weights at E18.5 were measured. Ordinary one-way ANOVA was performed. Data presented as mean±SEM.

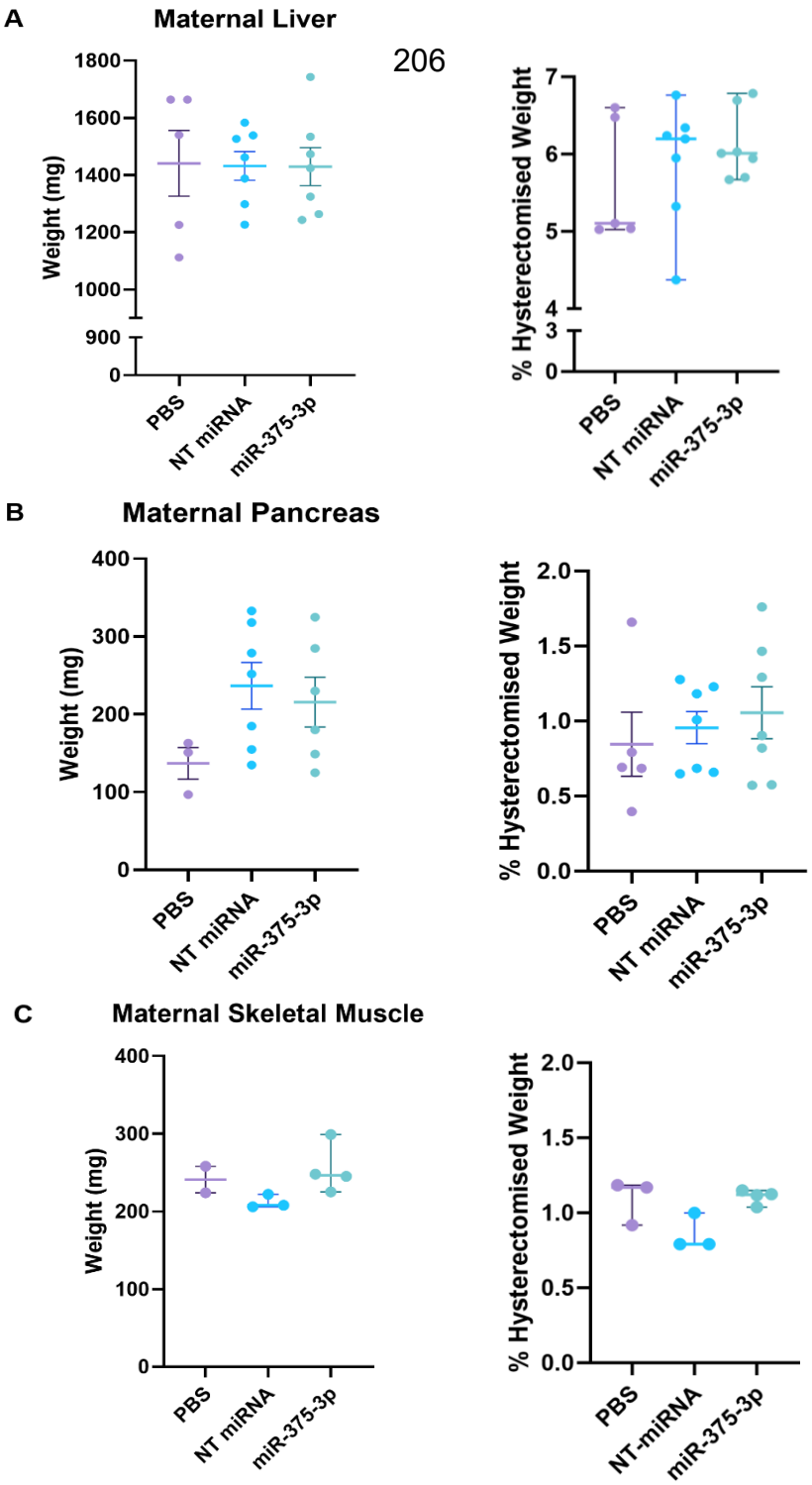

Figure 51 Maternal metabolic organ weights in pregnant mice exposed to PBS, NT miRNA or miR-375-3p mimics during gestation at E18.5.

Healthy pregnant C57BL6/J female mice were injected with NT miRNA (n=7) or miR-375-3p (n=7) mimic at E11.5, E13.5 and E15.5 before being sacrificed at E18.5. PBS (n=5) was used as a vehicle control. Maternal pancreas, liver and skeletal muscle weights were recorded alongside maternal hysterectomised weights. Normally distributed data was analysed using an Ordinary one-way ANOVA test followed by Tukey's multiple comparisons test and presented as mean±SEM. Data that was not normally distributed was analysed using a nonparametric Kruskal-Wallis test followed by Dunn's multiple comparisons test and data presented as median with 95% CI.

Dams treated with miR-375-3p demonstrated similar maternal heart weight to those treated with PBS and NT miRNA mimic (**Figure *52***A,B). Maternal heart:tibia length was assessed as a marker of hypertrophy (451), however this was also unchanged between treatment groups (**Figure *52***C,D).

Maternal plasma metabolites were measured, where a non-significant increase in plasma glucose levels was observed in dams treated with miR-375-3p (16.22 ± 1.124mmol/L; n=5) compared to PBS (11.37 ± 3.159mmol/L; n=3) (p=0.1466) and NT miRNA mimic (13.35 ± 1.010 mmol/L; n=6) (p=0.346) (**Figure *53***A). Plasma leptin levels were lowest in dams treated with PBS (1713pg/mL; n=2). Dams treated with NT miRNA demonstrated a non-significant increase in leptin levels (2394pg/mL; n=6) compared to PBS (p=0.471). However, those treated with miR-375-3p showed the highest levels (2684pg/mL; n=5) but this was not statistically significant compared to PBS (p=0.160) and NT miRNA mimic (p>0.999) (**Figure *53***B). In contrast, PBS treatment demonstrated the highest plasma levels of triacylglycerol precursors known as free fatty acids (FFAs) (452), (915.8umol/L; n=2) compared to NT miRNA mimic (585.2umol/L; p=0.958; n=6) and miR-375-3p (508.9umol/L; p=0.128; n=5), however this finding was not statistically significant (**Figure *53***C). Plasma cholesterol levels were at their lowest in dams treated with PBS (0.848mmol/L; n=2) but were similar between dams treated with NT miRNA and miR-375-3p mimics (1.080mmol/L and 1.024mmol/L, respectively; p>0.999; n=6/5, respectively) (**Figure *53***D). Compared to treatment with NT miRNA mimic, a non-significant increase in insulin levels was observed in dams treated with miR-375-3p (from 0.098 µg/L to 0.1512µg/L; p=0.100; n=3) (**Figure *53***E). Plasma triglyceride levels were similar in all treatment groups (**Figure *53***F). While none of these findings were statistically significant at present, it is possible that by increasing sample sizes, miR-375-3p may be impacting fetal growth indirectly via maternal metabolic factors such glucose and insulin. Alternatively, it is possible that miR-375-3p may be influencing fetal growth via directly impacting the placenta.

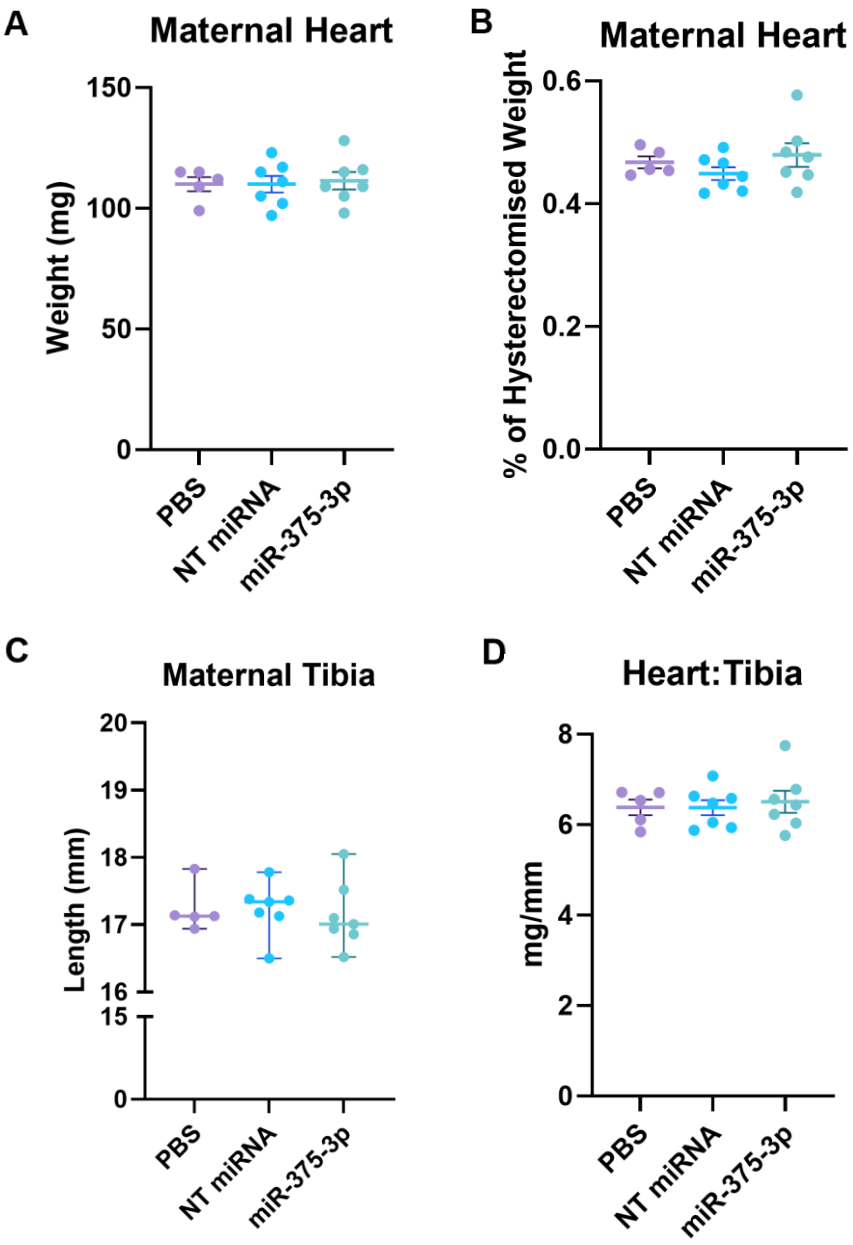

Figure 52 Maternal cardiac tissue weight and cardiac hypertrophy indicators in in pregnant mice exposed to PBS, NT miRNA or miR-375-3p mimics during gestation at E18.5.

Healthy pregnant C57BL6/J female mice were injected with NT miRNA (n=7) or miR-375-3p (n=7) mimic at E11.5, E13.5 and E15.5 before being sacrificed at E18.5. PBS (n=5) was used as a vehicle control. (A) Maternal absolute cardiac tissue weight and (B) maternal cardiac tissue weight relative to maternal hysterectomised weight were recorded. (C) Maternal tibia length was measured and (D) maternal cardiac tissue weight relative to maternal tibia length was also recorded, as a marker of maternal cardiac hypertrophy. Normally distributed data was analysed using an Ordinary one-way ANOVA test followed by Tukey's multiple comparisons test and presented as mean±SEM. Data that was not normally distributed was analysed using a nonparametric Kruskal-Wallis test followed by Dunn's multiple comparisons test and data presented as median with 95% CI.

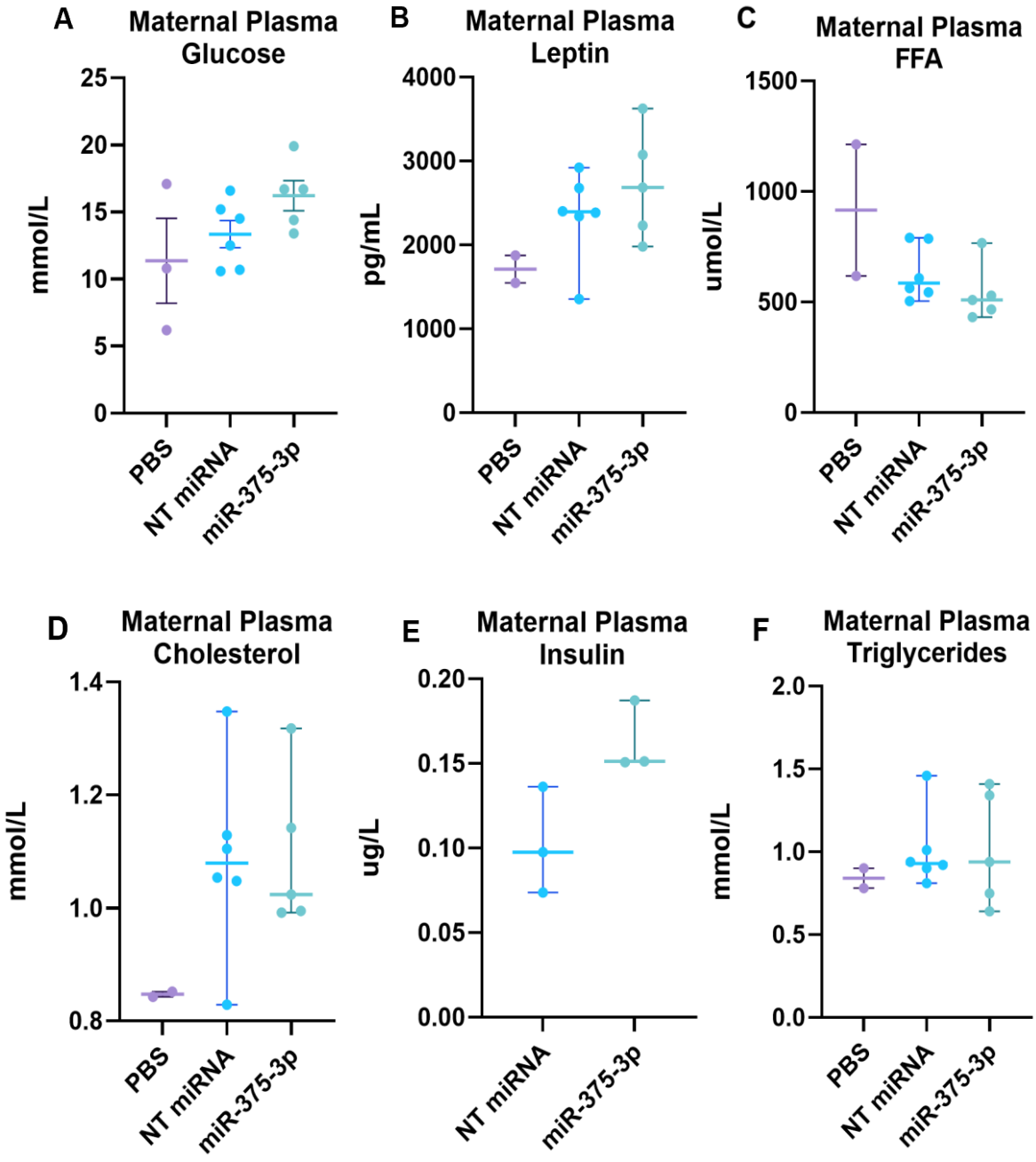

Figure 53 Maternal plasma glucose, leptin, FFA, cholesterol, insulin and triglyceride levels in pregnant mice exposed to PBS, NT miRNA or miR 375 3p mimics during gestation at E18.5.

Healthy pregnant C57BL6/J female mice were injected with NT miRNA (n=7) or miR-375-3p (n=7) mimic at E11.5, E13.5 and E15.5 before being sacrificed at E18.5. PBS (n=5) was used as a vehicle control. Maternal blood was processed for plasma extraction. Plasma metabolites were analysed at Core Biochemical Assay Laboratory (CBAL), Cambridge. (A) Ordinary one-way ANOVA was performed. Data presented as mean±SEM. (B-D,F) Kruskal-Wallis nonparametric test was performed followed by Dunn's multiple comparisons test. Data presented as median with 95% CI. (E) Mann-Whitney nonparametric test was performed to determine statistical significance. Data presented as median with 95% CI.

4.4.5 The impact of maternal circulating miR-375-3p on placental development and function in healthy pregnant mice.

4.4.5.1 Downregulated placental miR-375-3p targets are homologous in human and mouse, affecting pathways associated with placental metabolism, growth and vascular development.

In humans, the Forbes group have previously demonstrated that placenta levels of miR-375-3p are increased in GDM-LGA pregnancies and evidence suggests that this is attributed to trafficking of miR-375-3p from the maternal circulation. To determine if miR-375-3p from the maternal circulation also traffics to the placenta in mice, levels of miR-375-3p were assessed in placentae from dams treated with miR-375-3p or NT miRNA mimics, as PBS and NT miRNA control treatments demonstrated similar effects on fetal and placental growth and maternal metabolism. QPCR analysis revealed a non-significance increase of placental miR-375-3p following injection of miR-375-3p mimic into the maternal circulation compared to mice treated with NT miRNA mimic ($p=0.052$) (**Figure *54***). This suggests that miR-375-3p is trafficked to the placenta and has potential to directly influence events in the placenta.

In healthy human term placental explants, miR-375-3p overexpression has demonstrated to directly impact actions in the placenta. Specifically, the placental proteome (376 significant proteins, $p<0.05$) is altered, where analysis showed that these altered proteins were associated with placental metabolism, growth and vascular development (**Figure *40***B). To ascertain if miR-375-3p has the potential to directly impact mouse placenta in a similar manner, it was investigated if there were homologous changes between human placental explants with miR-375-3p overexpression and mouse placentae following miR-375-3p treatment. Of the proteins altered in human placenta, the 190 downregulated proteins were compared with 7383 predicted targets of ‘hsa-mir-375’ identified from miRabel (345). This revealed that 59 of the downregulated proteins in our human placental explants were also predicted targets of miR-375-3p (**Figure *55***) and many of these have known roles in placental and fetal growth.

Next, it was assessed if levels of these molecules were altered in placentae (E18.5) from pregnant dams treated with miR-375-3p mimics compared to NT

miRNA control treatments. No change was observed with *Prkag2* gene expression (**Figure *56***F) however, half of the assessed genes were downregulated in the mouse placenta, as identified in human. *Kpna3* (p=0.001), *Itgb1* (p=0.002), *Igf2r* (p=0.042) and *Slc6a8* (p=0.002) expression were significantly downregulated with maternal miR-375-3p overexpression compared to NT miRNA control (**Figure *56***A,B,D,H). There was also a non-significant reduction in *Pecam1, Cd47* and *Ttc3* expression (**Figure *56***C,E,G). While any direct targets of miR-375-3p in the placenta would likely be reduced, for completeness, levels of various proteins that were increased in human placental explants following miR-375-3p overexpression were also assessed in mouse placenta. No change was identified in *Fabp4* expression (p=0.124) (**Figure *57***A). While *Eno1* (p=0.040) and *Cald1* (p=0.001) expression levels were altered in the mouse placenta following miR-375-3p treatment compared to NT miRNA mimic (**Figure *57***B,C), the directionality of change contrasted with the human placenta, where these targets were downregulated in the mouse placenta at E18.5.

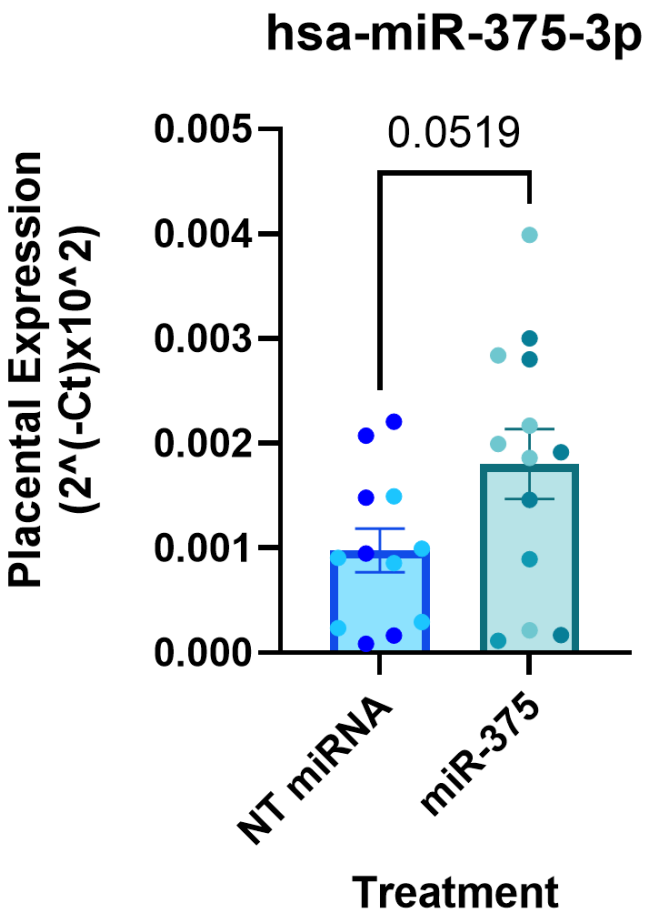

Figure 54 hsa miR-375-3p expression in placentae of mice exposed to miR-375-3p or NT miRNA during gestation at E18.5.

Healthy pregnant C57BL6/J female mice were injected with NT miRNA (n=7) or miR-375-3p (n=7) mimic at E11.5, E13.5 and E15.5 before being sacrificed at E18.5. Placental mature miRNA was isolated and reverse transcribed (n=1 male, n=1 female from each litter) before miRNA expression was analysed using qPCR and normalised to *UniSp6* expression; 2^(-Ct)*10^(2). Unpaired two-tailed parametric t-test was performed to measure significant differences. Data presented as mean±SEM. Light data points; female, dark data points; male.

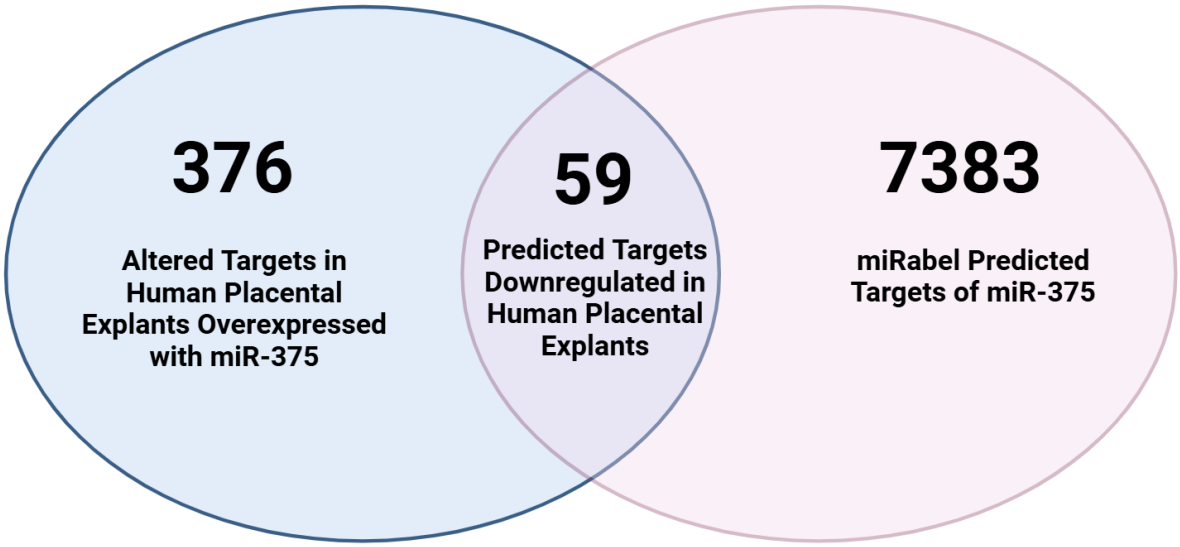

Figure 55 Overlapping downregulated targets of miR-375-3p in human placental explants and miRabel prediction database.

Previous work from the Forbes group demonstrates that 376 proteomic targets are altered in the human placenta in response to miR-375-3p overexpression. miRabel was used as online tool to identify 7383 predicted targets of miR-375-3p. From these predicted targets, 59 were identified to be altered downregulated in the human placental explants overexpressed with miR-375-3p. *Figure created using Biorender.com.*

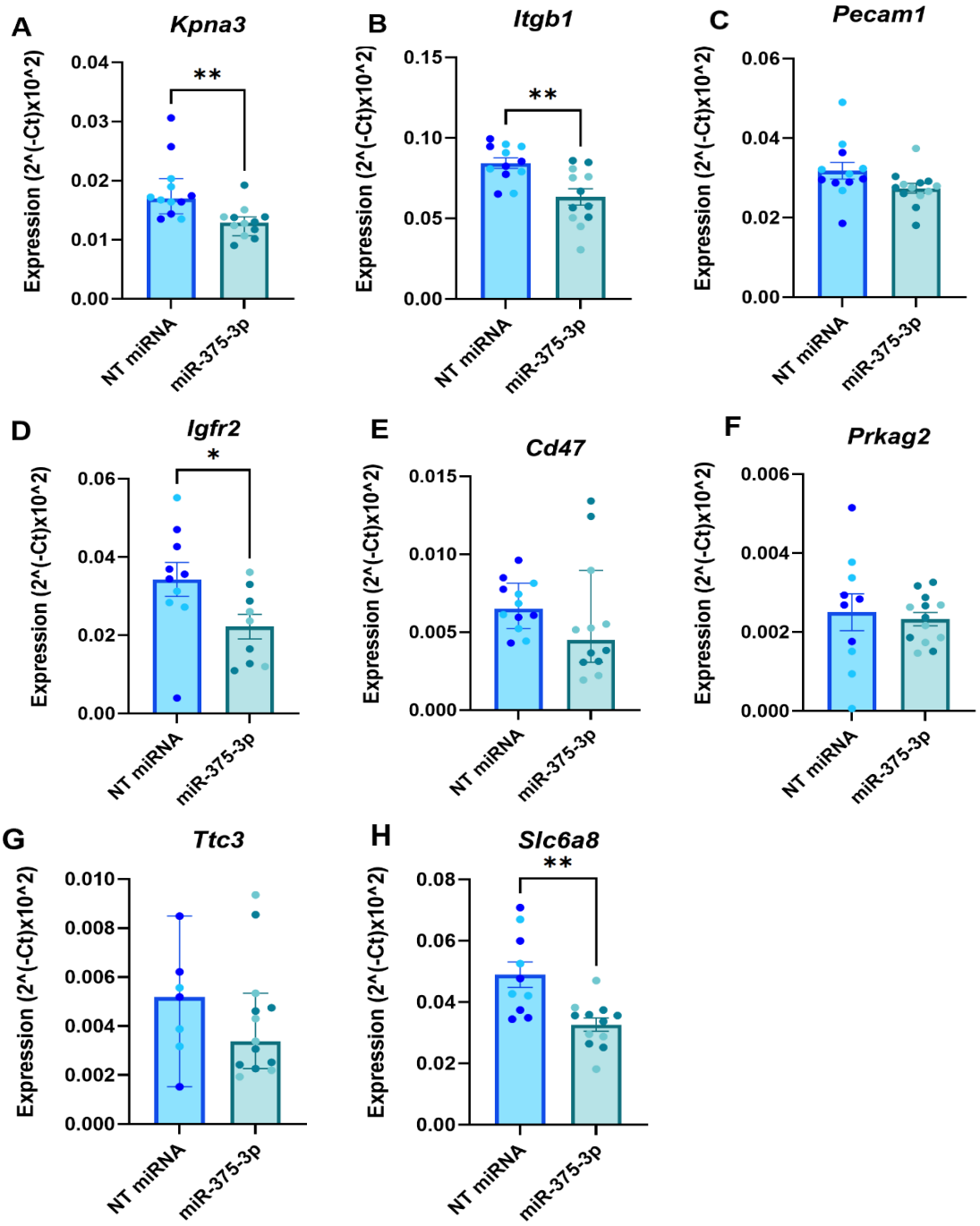

Figure 56 Mouse placenta mRNA expression of miR-375-3p targets identified in human placenta.

Healthy pregnant C57BL6/J female mice were injected with NT miRNA (n=7) or miR-375-3p (n=7) mimic at E11.5, E13.5 and E15.5 before being sacrificed at E18.5. Placental mature miRNA was isolated and reverse transcribed (n=1 male, n=1 female from each litter) before miRNA expression was analysed using qPCR and normalised to β-actin; (2^(-Ct)*10^(2). Unpaired two-tailed parametric t-test was performed for normally distributed data (presented as mean±SEM). Unpaired two-tailed Mann-Whitney non-parametric t-test was performed for data that was not normally distributed (presented as median with 95% CI). *=p ≤ 0.05, **=p ≤ 0.01. Light data points; female, dark data points; male.

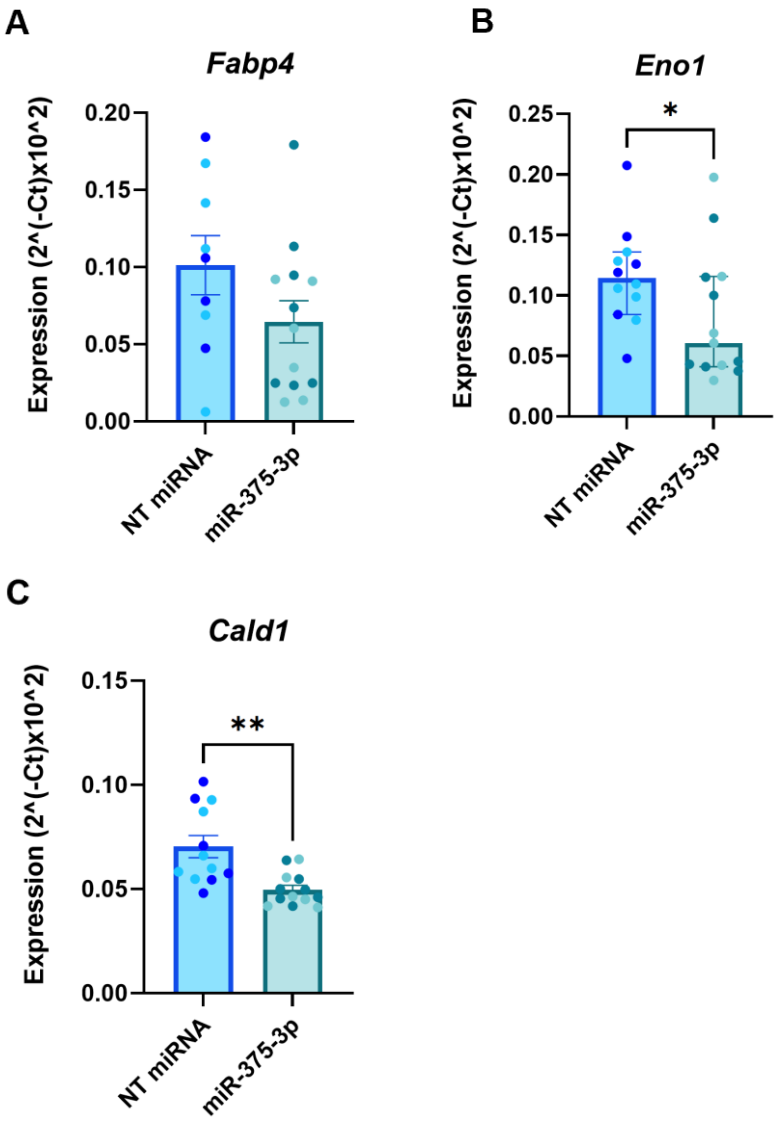

Figure 57 Mouse placenta mRNA expression of miR-375-3p targets identified in human placenta.

Healthy pregnant C57BL6/J female mice were injected with NT miRNA (n=7) or miR-375-3p (n=7) mimic at E11.5, E13.5 and E15.5 before being sacrificed at E18.5. Placental mature miRNA was isolated and reverse transcribed (n=1 male, n=1 female from each litter) before miRNA expression was analysed using qPCR and normalised to β-actin; (2^(-Ct)*10^(2). Unpaired two-tailed parametric t-test was performed for normally distributed data (presented as mean±SEM). Unpaired two-tailed Mann-Whitney non-parametric t-test was performed for data that was not normally distributed (presented as median with 95% CI). *=p ≤ 0.05, **=p ≤ 0.01. Light data points; female, dark data points; male.

4.4.5.2 Delivery of miR-375-3p to the mouse maternal circulation impacts placental metabolism.

Many of the genes altered by miR-375-3p in the mouse placenta are involved in metabolic processes (453–463). Previous proteomic data from the Forbes group also shows that miR-375-3p impacts targets associated with metabolism in human placenta (**Figure *40***B). Based on the predicted function of the altered proteins in the human placenta, aqueous metabolite fractions were extracted from mouse placenta at E18.5, where TCA cycle metabolites, putative adipokines, tryptophan metabolites and acylcarnitine metabolites were measured in mouse placenta at E18.5. To detect subtle differences in placental metabolites in response to miR-375-3p and NT miRNA, metabolites were considered statistically and biologically significant if $[Log_2FC] \geq 0.26$, $p < 0.05$.

Principal component analysis (PCA) showed that both treatments demonstrated distinct and differential metabolite profiles in the mouse placenta (**Figure *58***). As a permutation test on this dataset yielded a significance value of $p=0.179$, univariate analysis was performed to measure the effect of miR-375-3p on the mouse placenta metabolome. A volcano plot demonstrated that β-aminoisobutyric acid (BAIBA), 5-oxoproline (5OP), acetyl-5-hydroxy-tryptamine and short-chain acylcarnitine (AC)-6:0 were significantly downregulated and melatonin was significantly upregulated in response to miR-375-3p compared to control (**Figure *59***).

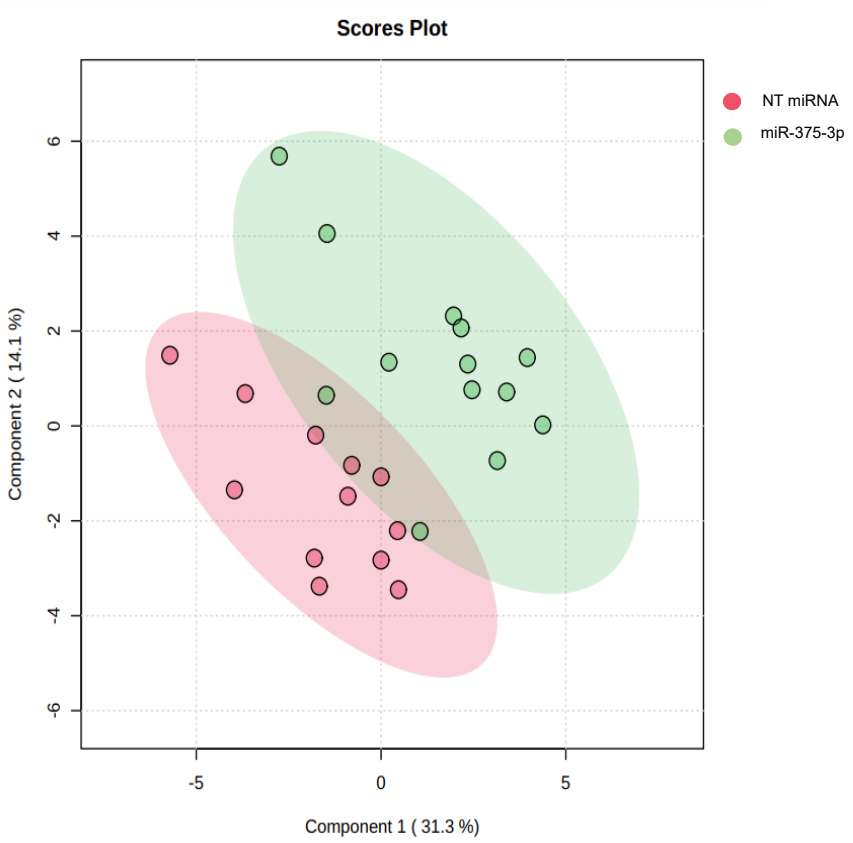

Figure 58 PCA of altered placental metabolites in healthy pregnant mice exposed to NT miRNA and miR-375-3p mimics.

Healthy pregnant C57BL6/J female mice were injected with NT miRNA (n=6) or miR-375-3p (n=7) mimics at E11.5, E13.5 and E15.5 before being sacrificed at E18.5. Placental tissue was harvested and processed for metabolite extraction. LCMS was performed on aqueous metabolite fractions, where peaks were normalised to placental tissue weight and analysed using MetaboAnalyst.ca. A one factor statistical analysis was performed, where data was auto scaled. PCA (2D score) plot was generated to measure placental metabolite profiles.

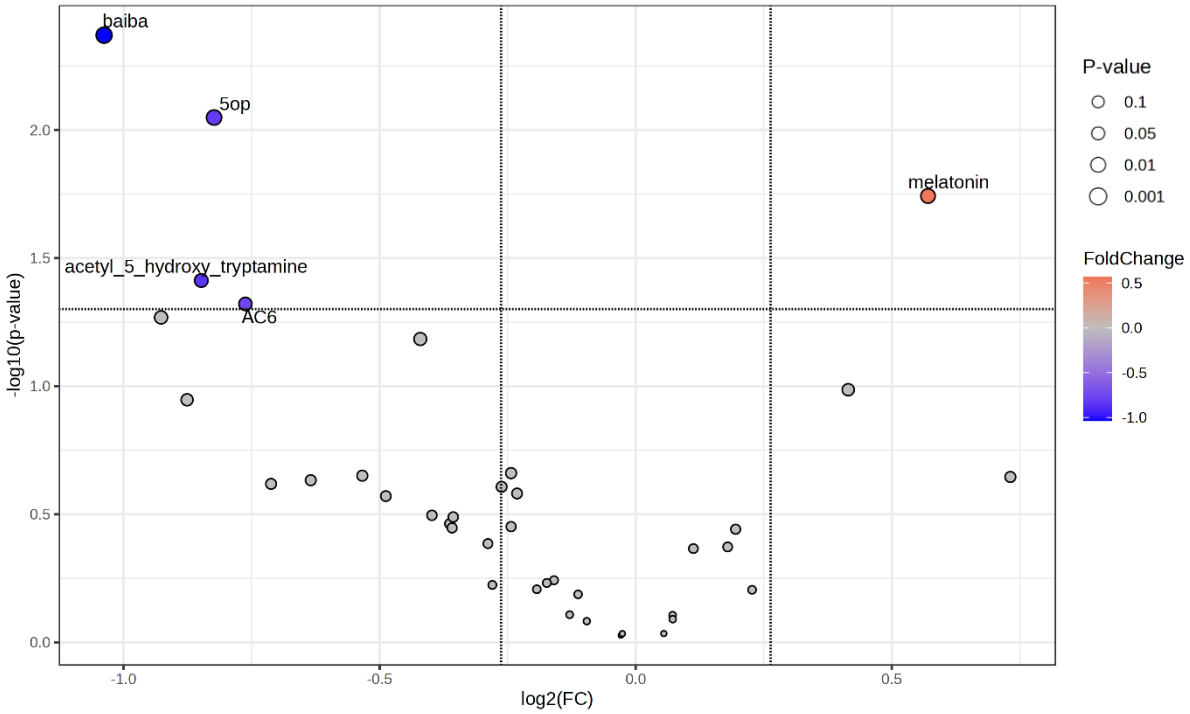

	FC	Log2(FC)	Raw P Value	Log10(p)
BAIBA	0.487	-1.038	0.004	2.370
5OP	0.565	-0.823	0.009	2.049
Melatonin	1.485	0.571	0.018	1.742
Acetyl 5 Hydroxy Tryptamine	0.556	-0.848	0.039	1.413
AC6	0.590	-0.762	0.048	1.321

Figure 59 Volcano plot and statistical scores of significantly altered placental metabolites in healthy pregnant mice exposed to NT miRNA and miR-375-3p mimics.

Healthy pregnant C57BL6/J female mice were injected with NT miRNA (n=6) or miR-375-3p (n=7) mimics at E11.5, E13.5 and E15.5 before being sacrificed at E18.5. Placental tissue was harvested and processed for metabolite extraction. LCMS was performed on aqueous metabolite fractions, where peaks were normalised to placental tissue weight and analysed using MetaboAnalyst.ca. A one factor statistical analysis was performed, where data was auto scaled. Direction of comparison: miR-375-3p/NT miRNA, [Log2FC]≥0.26, $p<0.05$. β-aminoisobutyric acid (BAIBA), 5-oxoproline (5OP), Acylcarnitine 6 (AC6:0).

4.4.5.3 Delivery of miR-375-3p to the mouse maternal circulation impacts placental lipid profile.

Lipids are essential regulators of placental metabolism (90,464). To understand the effect of miR-375-3p on the placental lipidome, organic metabolite fractions were extracted from mouse placenta at E18.5, where lipids in negative and positive ion modes were measured. Lipoprotein(a), lysophosphatidylinositols, phosphatidic acids, phosphatidylcholines, phosphatidylethanolamines, phosphatidylinositols, phosphatidylserines, ceramides, hexosylceramides, lysophosphatidylcholines, lysophosphatidylethanolamines, lysophosphatidylglycerols, phosphatidylcholines, sphingomyelins and sphingosines were undetected or mass spectrometry peaks were inconsistently truncated. To detect subtle differences in the placental lipidome in response to miR-375-3p and NT miRNA, lipid species were considered statistically and biologically significant if $[Log_2FC] \geq 0.26$, $p < 0.05$.

Principal component analysis (PCA) identified that mice treated with miR-375-3p and NT miRNA had some distinction in their placental lipid profiles (**Figure *60***). As a permutation test on this dataset yielded a significance value of p=0.645, univariate analysis was performed to measure the effect of miR-375-3p on the mouse placenta lipidome (**Figure *61***). A volcano plot demonstrated that the expression of various triacylglycerides (TAGs) were significantly lower in placentae treated with miR-375-3p compared to control, specifically TAG 48:0, 52:4, 50:1, 52:3, 54:6, 52:2 and 54:5. Monoacylglycerols (MAGs) 16:0, 18:0 and free fatty acid (FFA) 22:3 expression was also significantly higher in with miR-375-3p treatment compared to control (**Figure *61***).

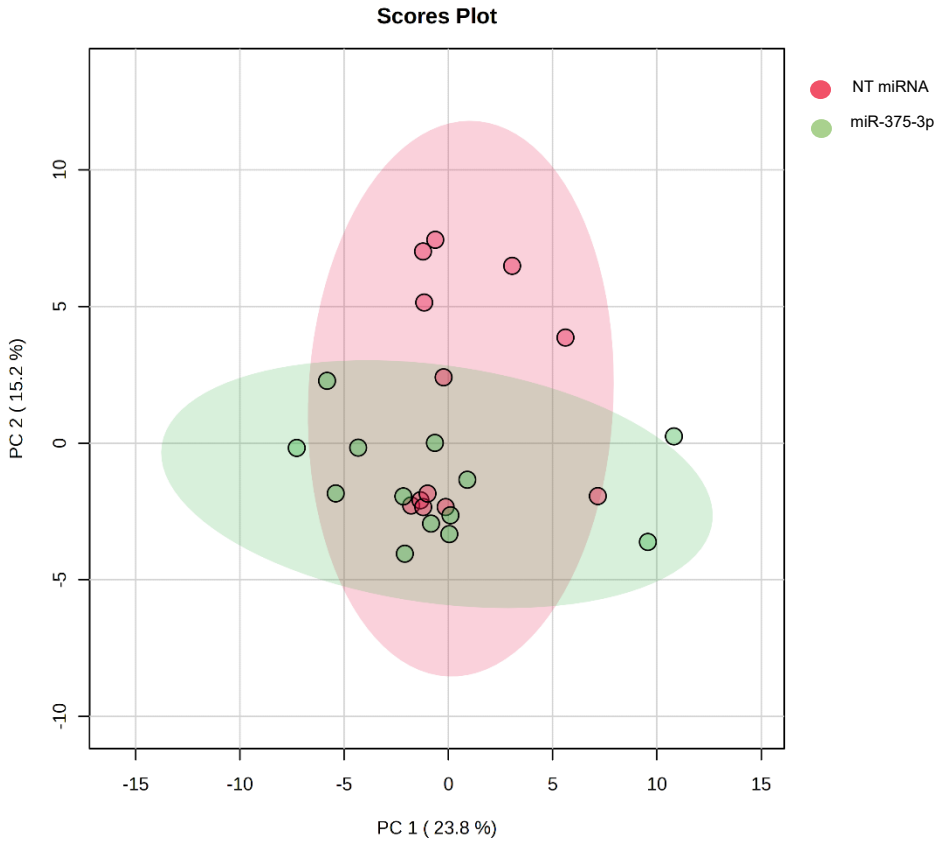

Figure 60 PCA of altered placental lipids in healthy pregnant mice exposed to NT miRNA and miR-375-3p mimics.

Healthy pregnant C57BL6/J female mice were injected with NT miRNA (n=6) or miR-375-3p (n=7) mimics at E11.5, E13.5 and E15.5 before being sacrificed at E18.5. Placental tissue was harvested and processed for metabolite extraction. LCMS was performed on organic metabolite fractions, where peaks were normalised to placental tissue weight and analysed using MetaboAnalyst.ca. A one factor statistical analysis was performed, where data was auto scaled. PCA (2D score) plot was generated to measure placental lipid profiles.

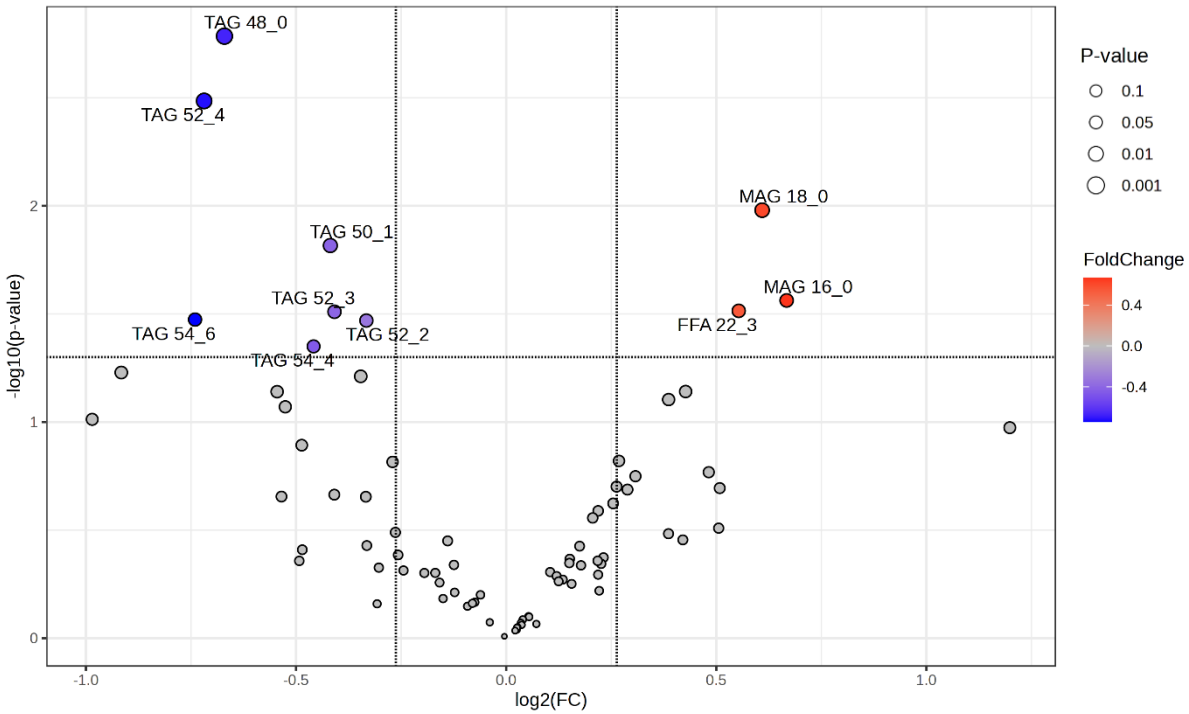

	FC	Log2(FC)	Raw P Value	Log10(p)
TAG 48:0	0.628	-0.671	0.002	2.785
TAG 52:4	0.608	-0.719	0.003	2.485
MAG 18:0	1.525	0.609	0.010	1.980
TAG 50:1	0.748	-0.419	0.015	1.817
MAG 16:0	1.588	0.667	0.027	1.563
FFA 22:3	1.468	0.553	0.031	1.514
TAG 52:3	0.753	-0.409	0.031	1.510
TAG 54:6	0.599	-0.740	0.034	1.474
TAG 52:2	0.794	-0.333	0.034	1.470
TAG 54:4	0.728	-0.458	0.045	1.350

Figure 61 Volcano plot and statistical scores of significantly altered placental lipids in healthy pregnant mice exposed to NT miRNA and miR-375-3p mimics.

Healthy pregnant C57BL6/J female mice were injected with NT miRNA (n=6) or miR-375-3p (n=7) mimics at E11.5, E13.5 and E15.5 before being sacrificed at E18.5. Placental tissue was harvested and processed for lipid extraction. LCMS was performed on organic metabolite fractions, where peaks were normalised to placental tissue weight and analysed using MetaboAnalyst.ca. A one factor statistical analysis was performed, where data was auto scaled. Direction of comparison: miR-375-3p/ NT miRNA, [Log2FC]≥0.26, $p<0.05$. Triacylglyceride (TAG), monoacylglycerol (MAG), free fatty acid (FFA).

4.4.6 Sex-dependent effects of maternal circulating miR-375-3p on mouse fetal and placental development.

4.4.6.1 Fetal and placental growth in male and female offspring.

After establishing a direct causation between enhanced levels of miR-375-3p in maternal circulation and LGA, it was next explored if miR-375-3p similarly impacted male and female pregnancy outcomes. When exclusively investigating male fetal growth, it was demonstrated that miR-375-3p significantly increased fetal weight (1.361 ± 0.029g) compared to NT miRNA mimic (1.206 ± 0.028g) (p=0.005) (**Figure *44***, **Appendix *3***). However, although there was an increase in female fetal weight with miR-375-3p (1.255 ± 0.026g) compared to NT miRNA mimic (1.181 ± 0.027g), this upward trend in weight did not reach statistical significance (p=0.166) (**Figure *44***, **Appendix *3***). This suggests that fetal growth of males is more affected by the actions of maternal circulating miR-375-3p in pregnancy than females. Moreover, compared to NT miRNA mimic, both male and female placental weight were significantly increased with miR-375-3p (from 0.091 ± 0.002g to 0.120 ± 0.004g, p=4.31E-07 and from 0.088 ± 0.002g to 0.111 ± 0.004, p=0.004, respectively) (**Figure *46***, **Appendix *5***). As a result, compared to NT miRNA mimic, there was a non-significant downward trend in fetal:placental weight for both males (p=0.055) and females (p=0.064) in response to miR-375-3p (**Figure *48***, **Appendix *7***).

4.4.6.2 Placental miR-375-3p targets in male and female offspring.

When exclusively assessing female placentae, miR-375-3p was significantly upregulated after exposure to miR-375-3p mimic compared to NT miRNA (p=0.029, n=6), however this upward trend was not statistically significant for males p=0.598, n=7/6) (**Figure *54***). Compared to control, male placentae demonstrated a non-significant decrease in *Itgb1* expression in response to miR-375-3p mimic (p=0.058, n=6), however a significant decrease was observed in females (p=0.027, n=6) (**Figure *56***). Compared to control, a similar trend in placental expression levels was also identified in response to miR-375-3p mimic for *Igfr2* (males – p=0.281, n=6/5; females – p=0.029, n=4), *Slc6a8* (males – p=0.079, n=6/7; females – p=0.041, n=4/5), *Cald1* (males – p=0.038, n=6/7; females – p=0.020, n=6) and *Kpna3* (males – p=0.043, n=6/7; females – p=0.008,

n=6/5) (**Figure *56***, **Figure *57***). No statistical significance was observed in placental expression levels for the following genes in either sex; *Pecam1* (males – p=0.375, n=7/6; females – p=0.093, n=6), *Cd47* (males – p=0.394, n=6; females – p=0.231, n=6), *Fabp4* (males – p=0.471, n=7/4; females – p=0.145, n=6/5), *Ttc3* (males – p=0.527, n=7/4; females – p=0.905, n=6/3), *Eno1* (males – p=0.153, n=7/6; females – p=0.393, n=6), *Prkag2* (males – p=0.347, n=7/5; females – p=0.821, n=6/5) (**Figure *56***, **Figure *57***).

4.4.6.3 The placental metabolome and lipidome in male and female offspring.

As miR-375-3p impacted male and female growth to varying degrees, the placental metabolome and lipidome was compared between male and female offspring. Male and female offspring demonstrated distinct placental metabolome and lipidome profiles at E18.5 (Appendix 8). miR-375-3p altered the placental metabolome to a greater extent for males than females when compared to NT miRNA mimic, where acetyl-5-hydroxy-tryptamine, BAIBA, 5OP, AC2:0 and AC14:0 were all significantly downregulated and melatonin was upregulated in male placentae (**Figure *62***A). In female placentae, miR-375-3p only significantly upregulated 5-HIAA expression (**Figure *62***A). Moreover, miR-375-3p had a greater effect on the female placental lipidome, where TAG 48:0 and 52:4, and MAG 16:1 were significantly downregulated compared to treatment with NT miRNA mimic. Only FFA 16:2 was downregulated in the placentae of males in response to miR-375-3p (**Figure *62***B).

A

Placental Metabolome

Females

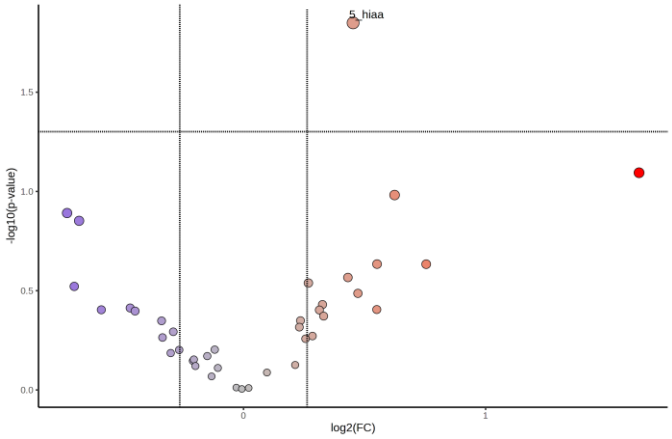

Males

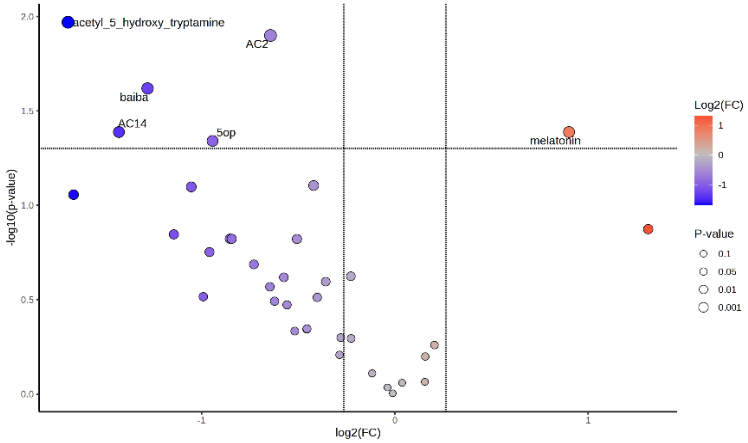

	FC	Log2(FC)	Raw P Value	Log10(p)
Females				
5-HIAA	1.369	0.453	0.014	1.849
Males				
Acetyl-5-hydroxytryptamine	0.310	-1.691	0.011	1.970
AC2:0	0.640	-0.643	0.013	1.900
BAIBA	0.412	-1.279	0.024	1.619
AC14:0	0.372	-1.427	0.041	1.388
Melatonin	1.867	0.901	0.041	1.388
5OP	0.520	-0.943	0.046	1.341

B

Placental Lipidome

Females

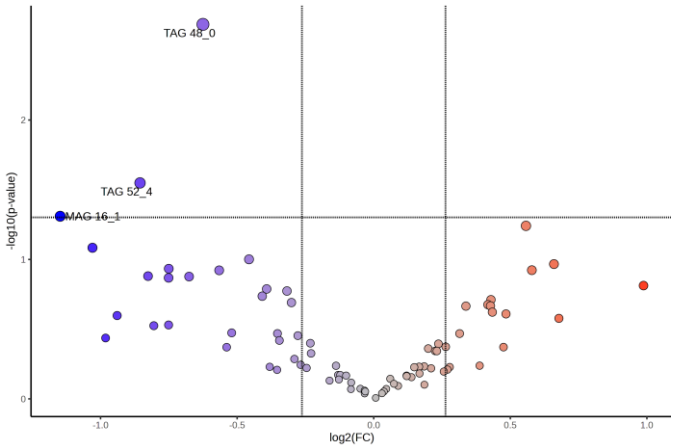

Males

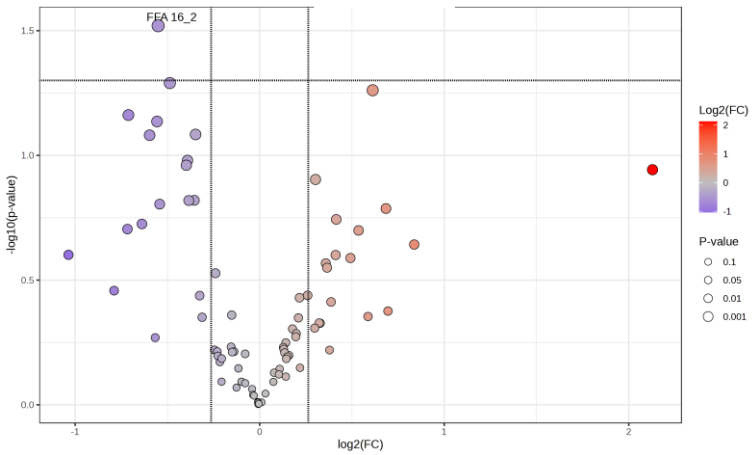

	FC	Log2(FC)	Raw P Value	Log10(p)
Females				
TAG 48:0	0.648	-0.625	0.002	2.686
TAG 52:4	0.553	-0.855	0.028	1.549
MAG 16:1	0.451	-1.148	0.049	1.310
Males				
FFA 16:2	0.683	-0.550	0.030	1.520

Figure 62 Altered placental metabolites and lipids in male and female mouse offspring exposed to NT miRNA and miR-375-3p mimics during gestation.

Healthy pregnant C57BL6/J female mice were injected with NT miRNA (n=6) or miR-375-3p (n=7) mimics at E11.5, E13.5 and E15.5 before being sacrificed at E18.5. Placental tissue was harvested from male (n=7) and female (n=6) pups and processed for metabolite extraction. LCMS was performed on aqueous and organic metabolite fractions, where peaks were normalised to placental tissue weight and analysed using MetaboAnalyst.ca. Data was separated for fetal sex. A one factor statistical analysis was performed. Volcano plot; direction of comparison: miR-375-3p/NT miRNA control, [Log2FC]≥0.26, $p<0.05$. Acylcarnitine (AC), β-Aminoisobutyric acid (BAIBA), free fatty acid (FFA), monoacylglycerol (MAG), triacylglyceride (TAG), 5-Hydroxyindoleacetic acid (5-HIAA), 5-oxoproline (5OP).

4.4.6.4 Delivery of miR-375-3p to the mouse maternal circulation differentially impacts male and female placental structure.

Mouse placentae were processed for histological staining and double-labelled to identify placental zones; labyrinth zone, junctional zone and decidua zone (**Figure *63***). Tissue processing and fixation artefacts were detected in various placental samples, many of which demonstrated damaged decidua. This could be observed in the representative images in **Figure *63***. The total placental surface area was firstly measured. Female surface area remained similar between those treated with NT miRNA and miR-375-3p (**Figure *64***A), however with an n=1 for the miR-375-3p treatment group, this may not truly reflect the impact of miR-375-3p on the female placenta. When compared to NT miRNA mimic, males demonstrated a non-significant increase in placental total surface area with miR-375-3p treatment (from 22983425 ± 3549697 μm^2 to 33162532 ± 935108 μm^2; p=0.050; n=3) (**Figure *64***F). Placental zones were then calculated relative to the total placental surface area (**Figure *64***). The relative surface area of the labyrinth and junctional zones was similar for both female and male offspring treated with miR-375-3p and NT miRNA (**Figure *64***B,C,G,H). To account for many samples demonstrating damaged decidua, the surface area of the junction zone relative to the labyrinth zone was calculated. No difference in junctional/labyrinth zone surface area was identified with miR-375-3p treatment compared to NT miRNA mimic in males and females (**Figure *64***D,I). No difference was observed in the relative surface area of the decidua zone between treatments (**Figure *64***E,J).

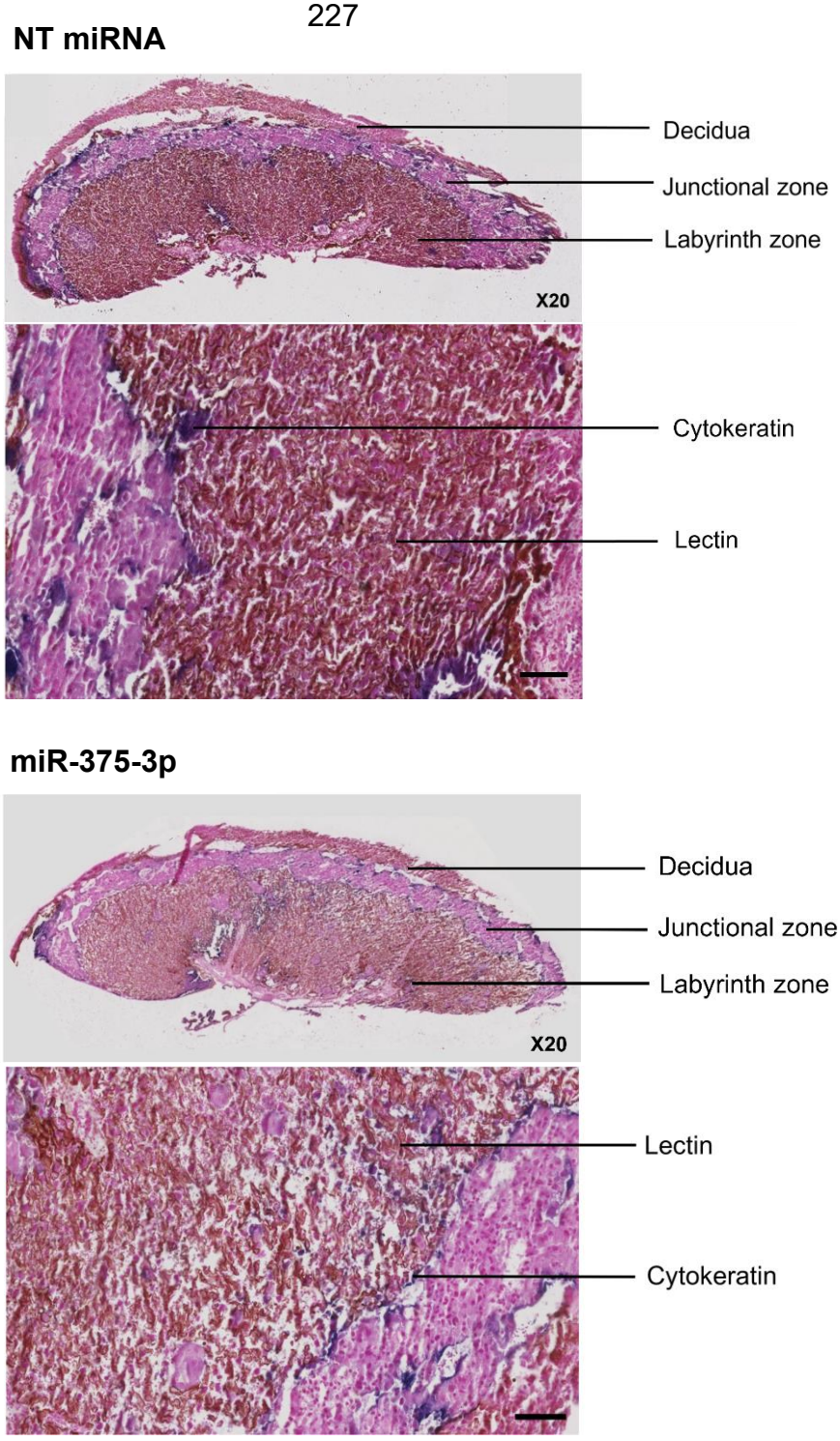

Figure 63 Representative immunohistochemistry images of E18.5 mouse placentae exposed to NT miRNA or miR-375-3p mimics throughout gestation.

Healthy pregnant C57BL6/J female mice were injected with NT miRNA or miR-375-3p mimics at E11.5, E13.5 and E15.5 before being sacrificed at E18.5. Placental tissue was harvested, fixed in 10% formalin before being transferred into 70% ethanol after 24 hours. Placentae were then processed as outlined in (348) and orientated in paraffin wax. Sections of 5μM thickness were sliced and placental zones were double-labelled for lectin and cytokeratin as per (349). Histological slides were imaged at x20. Scale bar: 100μM.

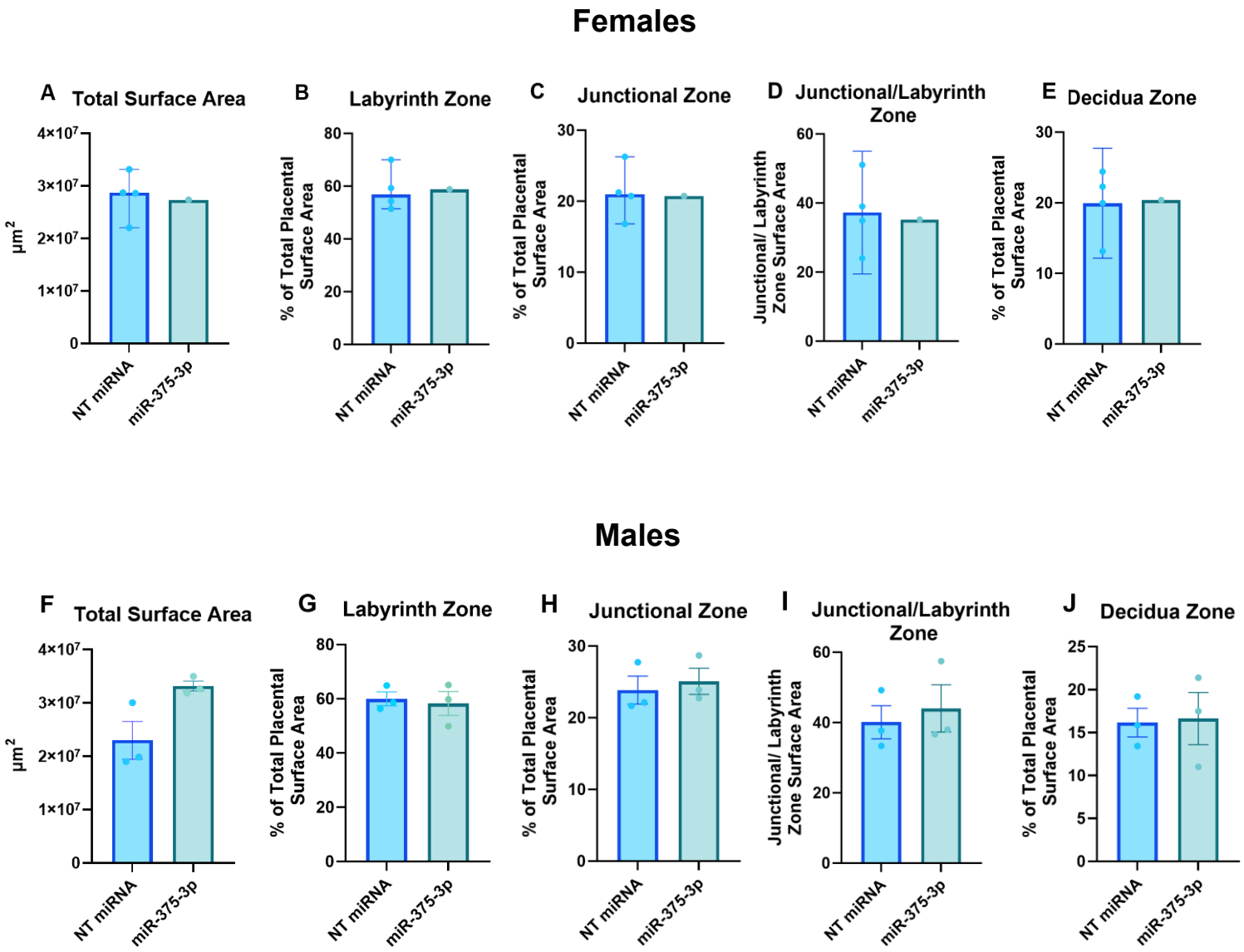

Figure 64 Female and male mouse placental zones at E18.5 after exposure to NT miRNA or miR-375-3p mimics throughout gestation.

Healthy pregnant C57BL6/J female mice were injected with NT miRNA or miR-375-3p mimics at E11.5, E13.5 and E15.5 before being sacrificed at E18.5. Placental tissue was harvested from male and female offspring, fixed in 10% formalin before being transferred into 70% ethanol after 24 hours. Placentae were then processed as outlined in (348) and orientated in paraffin wax. Sections of 5µM thickness were sliced and placental zones were double-labelled for lectin and cytokeratin as per (349). Histological slides were imaged at x20. Scale bar: 100µM). Surface area of placental zones was detected using QuPath software. Unpaired two-tailed parametric t-test was performed for normally distributed data (presented as mean±SEM). Data that was not normally distributed (presented as median with 95% CI).

4.5 Discussion

The findings of this chapter demonstrate that *in-vivo* delivery of miR-375-3p into the maternal circulation of healthy pregnant mice influences fetal and placental growth, where male fetal growth was increased and male and female placental growth was increased. Results indicate that this effect is independent of maternal health and that miR-375-3p alters fetal growth by impacting placental development. Mouse placenta miR-375-3p targets are homologous to human, affecting pathways associated with placental metabolism, growth and vascular development. Functional metabolomic and lipidomic analyses show that miR-375-3p impacts placental nutrient metabolism, where effects may be different for male and female offspring. These findings suggest that maternal miR-375-3p can circulate into and alter events in placental tissue which in turn influences fetal growth. This model mimics the *in-vivo* maternal environment in GDM pregnancies with LGA outcomes.

4.5.1 Administration of miR-375-3p to the maternal circulation of healthy pregnant mice and pregnancy outcomes

Results showed that *in-vivo* delivery of miR-375-3p into the maternal circulation of healthy pregnant mice via tail vein injection at a concentration of 1 mg/kg on E11.5, E13.5 and E15.5 was not embryonic lethal, where there were no resorptions, and did not affect maternal survival. This demonstrates that the dose used was safe. As intraperitoneal administration is associated with inflammation and inconsistencies in substance absorption and distribution (465), miRNA mimics were administered via tail vein injections in this study to allow direct delivery to the maternal circulation and hence mimic the *in-vivo* environment in women with GDM who deliver LGA infants. Other studies have delivered miRNA mimics to mice at this dose via tail vein injection, where no safety concerns were reported and predicted effects were observed (466,467). In this study, we performed periodical injections to deliver miR-375-3p mimics to the circulation. While ideally a continuous infusion of miRNA treatments to the mice which more closely mimics the interaction between the maternal circulating milieu and feto-

placental development in human pregnancies complicated by GDM would have been preferential in the study design, we were unable to do this due to ethical regulations. This may be a limitation for this study. However, Beards et al. have also previously reported targeted delivery of miRNA inhibitors at a concentration of 1mg/kg via tail vein injection to healthy pregnant mice at three periodical gestational time points; E12.5, E14.5 and E16.5 (123). This study did not report safety concerns associated with this dose pattern and predicted effects were observed, where *in-vivo* delivery of miRNA inhibitors increased mouse placental and fetal weights. Moreover, as the mouse placenta is distinctly formed by E11 and is fully developed by E15 (448), the injection time points E11.5, E13.5 and E15.5 were used for this study. This was to ensure that the effect of miRNA treatments on placental development and growth could be investigated. Additionally, mouse embryo organogenesis is initiated around E8.5, where there is altered expression of key genes associated with organ formation (468). As early organogenesis is considered from this time point up until E13.5 (469), the injection time points used in this study also ensured that embryos were exposed to miR-375-3p early in organogenesis. This was to mimic the maternal circulating milieu in human pregnancies complicated by GDM, where the Forbes group have previously demonstrated that miR-375-3p is associated with hyperglycaemia and its expression is upregulated in the maternal serum of women with GDM prior to altered fetal growth (**Figure *38***,**Figure *39***).

No significant differences were observed in litter size and ratio of male-female pups with miR-375-3p. There are no current studies reporting the involvement of miR-375-3p in sex determination signalling pathways. Although dams and offspring did not demonstrate any visible toxic effects, further research is needed to investigate the effect and toxicity of miR-375-3p on maternal and fetal organs on a molecular level which may impact study observations. Follow-up studies are also necessary to assess the longer-term impact of the diabetic environment on organ development.

4.5.2 The impact of maternal circulating miR-375-3p on uncorrelated increased feto-placental growth in healthy pregnant mice.

This study demonstrated that *in-vivo* delivery of miR-375-3p significantly increased fetal growth in healthy pregnant mice, where a higher proportion of pups were above the 90th centile for birthweight compared to those treated with control treatments. Interestingly, it was demonstrated that fetal growth of males was more significantly affected by the over-expression of miR-375-3p in the maternal circulation compared to females. However, placental growth was similarly affected by miR-375-3p for both male and female offspring, where placental and fetal growth were positively correlated. As previous human studies conducted by the Forbes group examining the association between miR-375-3p and LGA in GDM pregnancies have not been separated for sex, it is possible that this may also manifest in human pregnancies.

Although controversy remains (470), it has previously been reported that male pregnancies complicated by suboptimal maternal glucose tolerance are more at risk of macrosomia than similarly affected female pregnancies (471). It has also previously been demonstrated that sex differences may be observed in feto-placental development as early as conception (472). Findings from this study align with previous literature showing that male offspring demonstrate accelerated fetal growth compared to females, where energy resources are more channelled towards the development of the fetus than the placenta (472). It is therefore possible that males were more susceptible to the growth-stimulating effects of miR-375-3p and thus have higher susceptibility to adverse stimuli during pregnancy. miR-375-3p demonstrated to reduce fetal:placental weight, indicating that fetal and placental growth were uncorrelated in response to miR-375-3p. However, interestingly, results showed that females exposed to miR-375-3p demonstrated a more prominent reduction in fetal:placental weight than males when compared with PBS. This suggests that energy resources were directed more towards placental growth than fetal growth for female offspring, where they manifested placental tissue that was proportionally bigger relative to the fetus. In turn, this indicates that males directed more energy to the growing fetus than the placenta, consistent with previous literature (472). However, it has previously been reported that lower fetal:placental weight ratio is associated with

placental pathologies and adverse neonatal outcomes, where the risk of offspring overweight at 1 years old in association with GDM pregnancies is only observed in female infants (473,474). A reduction in fetal:placental weight may also indicate placental insufficiency, where placental nutrient transfer capacity is suboptimal relative to fetal demands and thus the placenta demonstrates compensatory overgrowth that is uncorrelated to the fetus (475). However, it has also been reported that female offspring are more adaptable to a suboptimal *in-utero* environment than males (476). Therefore, overall, these findings suggest that females either manifest placental insufficiency and are therefore more susceptible to programming later in life due to suboptimal *in-utero* development in response to miR-375-3p, or are somehow able to compensate their growth and avoid beccoming LGA despite the changes in their placental development.

Indeed, it has been reported that compensatory growth mechanisms may occur during organogenesis if fetal growth trajectory is altered and that placental nutrient capacity can be adapted in large placentae to regulate fetal nutrient transfer (468,477). Moreover, it has previously been demonstrated that placental growth becomes restricted at mid-gestation whereas fetal growth is accelerated during later stages of gestation, where following birth, offspring demonstrate ‘catch-up’ growth (478). Given these findings, it is reasonable to suggest that perhaps the impact of miR-375-3p on the placenta may occur before its effects on the fetus. Indeed, this phenomenon has been demonstrated when examining the influence of IGF2 signalling on mammalian fetal growth (478). This is an important consideration when investigating the relationship between fetal and placental growth, as current literature suggests that placental growth responds to fetal endocrine signals that stimulate nutrient availability to meet growth demands (479). Therefore, as this study had an end point of E18.5 and did not monitor offspring growth trajectories postpartum, it is possible that the full extent of the effects of miR-375-3p on offspring development and growth may have been missed.

Over-expression of miR-375-3p in placenta following miR-375-3o delivery to the maternal circulation suggests that the miR-375-3p mimic had circulated and internalised into placental tissue, where its expression was lower in placental tissue of control mice. However, it is possible that miR-375-3p was not distributed

to fetal tissue to the same extent as placental tissue during the gestational time points of treatment administration. It has previously been shown that miRNAs can internalise into placental tissue (123), however fluorescent labelling techniques would provide further indication of the biodistribution of miRNA mimics in mice during pregnancy.

4.5.3 The mechanism by which circulating miR-375-3p alters feto-placental growth in healthy pregnant mice.

4.5.3.1 The effect of miR-375-3p on maternal metabolism.

Evidence shows that maternal constraints influence fetal development and that placental growth is impacted by maternal pregnancy conditions (479). As such, this study investigated whether the changes to fetal and placental growth in healthy pregnant mice in response to miR-375-3p was dependent on maternal metabolism. Dams treated with miR-375-3p were lighter than control dams throughout gestation and consequently gained weight at a slower rate during pregnancy, suggestive of a systemic effect of miR-375-3p, however this effect was non-significant. By calculating maternal hysterectomised weight, no difference was observed in the overall maternal pregnancy weight gained since pre-pregnancy between dams treated with miR-375-3p and control treatments. This finding differs from clinical evidence showing that women who develop maternal diabetes during pregnancy demonstrate increased weight gain throughout gestation (480). Moreover, it has been reported that maternal weight gain is not a significant risk factor for the development of maternal diabetes in pregnancy for people with healthy BMI (480). As this study involved mice with healthy BMI pre-conception, this suggests that observations on maternal weight gain may not be the best indicator of the effect of miR-375-3p on maternal metabolism. This is strengthened by evidence demonstrating that the relationship between maternal weight gain, feto-placental growth and the periconceptional environment differs depending on the number of offspring in the pregnancy (481). Given the considerable difference in the number of offspring between human and mouse pregnancies, this further demonstrates that measuring maternal weight gain as an indicator of feto-placental growth in mice may not be a relevant to human pregnancies.

No significant change in maternal pancreas weight was observed with miR-375-3p in our study. This differs from previous reports showing that miR-375-3p alters β and α-cell mass by regulating cell growth and proliferation (482). However, as these cells are miniature relative to whole organ weight, it is possible that changes to β and α-cell mass may not be reflected in overall liver weight measurements in our study. miR-375-3p is known to be a key regulator of β-cell glucose-regulated insulin secretion (482). Indeed, previous studies demonstrate that miR-375-3p acts on targets such as myotrophin, resulting in reduced β-cell glucose-regulated insulin secretion (483). Another identified miR-375-3p target is PDK1, where miR-375-3p reduces its protein expression which in turn reduces the action of glucose on insulin DNA synthesis and expression (484). Results from our study do not align with these findings in the literature, where an upward trend in insulin levels were observed in response to *in-vivo* delivery of miR-375-3p into healthy pregnant mice. Given that the literature findings were based on *in-vitro* and *ex-vivo* models and that miRNAs synchronously regulate gene networks, it is possible that the *in-vivo* model in this study provides a more accurate representation of physiological interactions and conditions.

As glucose disposal is mainly mediated by skeletal muscle, this organ undergoes many metabolic adaptations during pregnancy and may be significantly impacted by insulin resistance (485). Results from our study demonstrated that maternal skeletal muscle weight was largely unaffected by miR-375-3p, however a non-significant upward trend in maternal plasma glucose levels was observed compared to control. It has previously been reported that glucose stimulates the cAMP-PKA pathway to increase insulin secretion (483). This could therefore suggest that miR-375-3p increases maternal glucose levels and activates the cAMP-PKA pathway in our mouse models, which in turn stimulates insulin secretion. This is interesting given that GDM is associated with altered insulin regulation and high plasma glucose levels, alongside previous findings from the Forbes group showing that miR-375-3p expression and secretion from pancreas-derived EVs is stimulated by mild hyperglycaemia. Collectively, these findings suggest that miR-375-3p may be impairing maternal glucose uptake, thereby leading to increased insulin secretion which may contribute towards

insulin resistance. Follow-up studies and longer-term exposure to miR-375-3p would provide further insight into the effects of miR-375-3p on maternal glucose and insulin sensitivity.

Leptin, a hormone derived from adipose-tissue that maintains energy homeostasis (486), was demonstrated to be increased with *in-vivo* delivery of miR-375-3p into healthy pregnant mice in our study. Although this finding was not statistically significant, this result corroborates findings from a previous study reporting that miR-375 inhibition is associated with reduced leptin expression (487). Interestingly, leptin is known as a key regulator of T2DM and cardiovascular disease development (487). This suggests that miR-375-3p may play a role in the long-term health of women with GDM postpartum, as it is known that GDM increases the risk of maternal T2DM onset postpartum (19). As a key metabolic organ, maternal liver weight demonstrated to be largely unaffected by miR-375-3p overexpression in our study compared to control treatments. Moreover, miR-375-3p downregulation has previously been associated with inflammatory cytokine inhibition in non-alcoholic fatty liver disease by regulating adipokine expression (487). This indicates that although maternal liver weight was unchanged, it is possible that miR-375-3p may be altering liver metabolism and function on a molecular level which was unexplored in this study.

Our study further demonstrated that miR-375-3p had no distinct effect on maternal plasma cholesterol levels and that triglyceride levels were clearly unchanged compared to control animals. However, a non-significant downward trend in FFA levels was observed with miR-375-3p treatment compared to control. It is known that FFAs increase gluconeogenesis and insulin secretion and regulate endogenous glucose production (488). Insulin resistant phenotypes are typically associated with elevated FFA levels which inhibits muscle insulin-stimulated uptake of glucose (488). This differs from observations made in our study which demonstrate that miR-375-3p reduces FFA levels but increases glucose and insulin levels. It is possible that our study was not sufficiently powered to clearly identify statistically significant changes to maternal plasma metabolites in response to miR-375-3p. However, our results suggest that miR-375-3p may not directly be inducing an insulin resistant phenotype in our mouse models.

It is known that GDM increases the risk of T2DM onset by 7-fold postpartum (19). Pregnancies complicated by GDM have also been associated with altered maternal cardiac energetics and postpartum maternal cardiac remodelling (20,489). miR-375-3p has been identified as a key regulator of cardiovascular development (459). However, results from our study demonstrated that miR-375-3p had no effect on maternal cardiac hypertrophy indicators, suggesting that this miRNA may not play a role in the adverse postpartum maternal cardiovascular outcomes in pregnancies complicated by GDM. As a consequence, this further indicates that miR-375-3p did not directly induce a maternal diabetic phenotype in our mouse model. However, it is possible that miR-375-3p may have induced histological changes that were not explored in this study. Given that the risk of T2DM onset for women with GDM occurs around 5-10 years postpartum (45), it may be useful to conduct a follow-up study on pregnant dams treated with miR-375-3p to explore the effect of this miRNA on maternal cardiac function postpartum.

As sex differences were identified in offspring development, it is likely that either the effects of miR-375-3p are not exclusively dependent on maternal metabolism and that miR-375-3p predominantly effects fetal growth by impacting events in the placenta, or that the influence of miR-375-3p on maternal metabolism indirectly impacts placental development, where females are more adaptable to these stimuli than males. Blocking the actions of miR-375-3p on the placenta via a specific miR-375-3p inhibitor after delivery to the maternal circulation would further our understanding of these putative mechanisms.

4.5.3.2 Placental miR-375-3p targets in human and mouse.

Previous findings from the Forbes group demonstrated that in human placenta, miR-375-3p overexpression altered targets associated with placental vascular development, mitochondrial function, glucose metabolism and growth. To determine if altered fetal growth observed in our mouse model was driven by the altered placental targets identified in the human placenta model in response to miR-375-3p, we aimed to identify whether miR-375-3p placental targets are homologous in human and mouse. Using miRabel database, 7383 predicted

targets of miR-375-3p were identified; 59 of which were downregulated and overlapped with downregulated targets identified in human placenta explants. The gene expression of several of these downregulated overlapping targets from various functional classes were measured in term mouse placenta. Results confirmed that placental miR-375-3p expression was higher in mice treated with miR-375-3p compared to control, demonstrating that this miRNA mimic had circulated and was overexpressed in mouse placental tissue. However, when separating the data for fetal sex, it was demonstrated that this effect was mainly observed in females rather than males. This could therefore explain why placental gene levels were more significantly affected in females than males, where perhaps the female placental transcriptome is more susceptible to the actions of miR-375-3p.

It was evident from our findings that miR-375-3p downregulated nearly all examined mouse placental genes that were also downregulated in human placenta, thus highly suggesting homology between miR-375-3p placental targets in human and mouse. However, a few miR-375-3p targets that were identified to be upregulated in human placenta were downregulated in mouse placenta. These targets included *Eno1* which plays a role in trophoblast growth and invasion (462), *Cald1* which contributes towards cytoskeletal remodelling (461), and *Fabp4* which has been identified to play a role in preeclampsia pathogenesis (460). Moreover, this discrepancy in the direction of miR-375-3p placental target regulation may be due to interspecies differences or *in-vivo* effects in our mouse compared to the *ex-vivo* human placental model. As such, this suggests that downregulated miR-375-3p targets are homologous in mouse and human but upregulated human placenta miR-375-3p targets may not be homologous in mouse. Moreover, sex differences could also play a role in this discrepancy, as the human model did not account for fetal sex. Indeed, in the mouse model, it was demonstrated that the downregulation of *Cald1* and *Fabp4* was more prominent in females than males, and the reverse was observed for the downregulation of *Eno1*.

Although not statistically significant, *Pecam-1* was downregulated in mouse placenta in response to miR-375-3p overexpression. *Pecam-1* has previously been reported to contribute towards spiral artery transformation (463), but more

recent data suggests this marker does not contribute towards pregnancies complicated by altered fetal growth that are hallmarked by aberrant trophoblast invasion (490). *Cd47* and *Ttc3* placental gene expression were also downregulated in our mouse model; *Cd47* is a known key regulator of maternal-fetal immunity (491) and recent evidence supports the role of *Ttc3* in epithelial-mesenchymal transition processes (454). Moreover, significant downregulation was observed in *Kpna3* expression in mouse placental tissue in rseponse to miR-375-3p overexpression, where this decrease was more notable in females than males. Although not in placental tissue, it has previously been shown that *Kpna3* is involved in activating epithelial-mesenchymal transition (EMT) (453). This is interesting given that EMT has been associated with the pathogenesis of altered fetal growth (492,493). miR-375-3p also signficantly downregulated *Itgb1* expression in mouse placental tissue, where this decrease was more prominent in females than males. Using a porcine model, it has previously been demonstrated that although not in placental tissue, endometrial *Itgb1* expression is associated with fetal size. Moreover, it was also found that porcine placental I *Itgb1* expression was negatively correlated with the percentage of males per litter (494). *Itgb1* is involved in regulating trophoblast infiltration, where its downregulation has demonstrtated to inhibit this process (458). A HTR-8/SVneo cell model has demonstrated that *Itgb1* regulates trophoblast proliferation, migration and apoptosis by stimulating PI3K/Akt pathway (457). Another placental target significantly downregulated by miR-375-3p was *Slc6a8,* where females demonstrated a more significant reduction in expression compared to males. *Slc6a8* is a sodium and chloride dependent transporter that has specificity for creatine, a metabolite that is key for ATP regeneration to stimulate cell proliferation and migration (456). *Slc6a8* is found in placental tissue as well as on trophoblasts encompassing fetal villi – this is a key site for maternal-fetal glucose, fatty acid and amino acid transfer (456,495). Interestingly, these metabolites were demonstrated to be altered in the mouse placenta in response to miR-375-3p. The effect of *Slc6a8* expression on metabolite active transport between maternal and fetal circulations remains unknown, however current literature suggests a possible association between impaired creatine metabolism and placental insufficiency (495). Similar to our findings, it has been previously reported that reduced chorionic villous *Slc6a8*

expression is associated with heavier birthweight (496). However, given that females demonstrated a more prominent reduction in placental *Slc6a8* expression but males demonstrated a more prominent increase in fetal growth in response to miR-375-3p, this suggests that there may not be a direct correlation between *Slc6a8* expression levels and birthweight. *Igfr2* was another placental target that was downregulated in our mouse model in response to miR-375-3p overexpression. This placental target was mainly affected in females than males in response to miR-375-3p. The IGF2-IGF2R signalling axis is key for pairing placental and fetal growth during pregnancy by regulating fetoplacental microvascular development, trophoblast morphogenesis and feto-placental nutrient exchange (455). This signalling axis has also been previously associated with altered fetal growth, where its expression in the placenta has been identified to regulate cellular signalling pathways which influence trophoblast apoptosis (497–499). It is thought that elevated IGF2R levels in late pregnancy is a compensatory mechanism to inhibit additional growth signals (500). Aberrant IGF axis signalling has been demonstrated in pregnancies complicated by diabetes (501). This may therefore explain the uncorrelated fetus:placental weight observed in our mouse model in response to miR-375-3p, where nutrient transfer may be dysregulated via IGF2R signalling, contributing towards altered fetal growth.

4.5.3.3 miR-375-3p and placental metabolism.

As findings from our mouse model suggested miR-375-3p may alter fetal growth by impacting placental efficiency, the effect of miR-375-3p overexpression on the mouse placenta metabolome was explored. Metabolites of putative adipokines, tryptophan, acylcarnitines and the TCA cycle were examined. Of all metabolites measured, it was evident that miR-375-3p significantly affected placental amino acid metabolism. This is an interesting finding given that the expression profile of various maternal amino acids has previously been associated with pathological fetal growth (502). When separating the data for fetal sex, it was evident that miR-375-3p mainly affected male placental amino acid metabolism. Placental BAIBA expression was significantly downregulated by miR-375-3p. BAIBA is a non-protein amino acid that is a key regulator of lipid and carbohydrate

metabolism and thus is strongly associated with metabolic syndrome (503). It has been shown that BAIBA plays a role in regulating mitochondrial biogenesis and oxidative stress by mediating AMPK and PI3K/Akt signalling pathways (504,505). Although its role in diabetes pathogenesis is unclear, evidence strongly shows BAIBA to induce protective metabolic effects by inducing anti-inflammatory effects while also increasing insulin sensitivity and altering lipid metabolism, demonstrating favourable effects in diabetic environments (503,506). Indeed, elevated BAIBA expression has shown to be inversely correlated with cardiometabolic risk factors (507,508). These findings suggest that miR-375-3p may play a role lipid and carbohydrate metabolism by mediating placental amino acid profile, thereby inducing hallmarks and outcomes of metabolic disease in pregnancy.

Placental 5-OP was also significantly downregulated by miR-375-3p, however this was not demonstrated in female placentae. Accumulation of this metabolite is elevated in pregnancy and is associated with glutathione synthesis deficiency as consequence of low glycine levels and increased *γ*-glutamyl cysteine metabolism (509). Glutathione is a key mediator of cellular oxidative stress, where low levels of this metabolite have previously been linked to developmental diseases associated with premature birth (509). These findings therefore indicate that miR-375-3p altered male placental glutathione metabolism in our mouse model. An association between 5-OP levels and fetal growth has previously been explored, where its concentration has been negatively correlated with early fetal growth (510,511). This metabolite has been linked to myocardial dysfunction, and maternal ethnicity may influence its expression levels during pregnancy (512,513).

Acetyl-5-hydroxytryptamine, also known as acetyl-serotonin, is another amino acid which is a precursor for melatonin, that was found to be downregulated in mouse placental tissue with miR-375-3p overexpression. This effect was not observed in female placentae. The role of melatonin, which was found to be upregulated in male mouse placenta in response to miR-375-3p, has been well characterised in pregnancy (514). Melatonin is essential for circadian rhythm (515,516). It is synthesised from the pineal gland as well as villous cytotrophoblasts and syncytiotrophoblasts and is known for its anti-apoptotic

effects to regulate syncytiotrophoblast turnover (515). Reduced expression of melatonin receptors has been identified in placental tissue of pregnancies complicated by placental insufficiency and pathological fetal growth (517). Oxidative stress has been linked to altered fetal growth and it has been demonstrated that melatonin stimulates placental antioxidative enzymes to improve placental efficiency and alter fetal weight (515,518). Indeed, its protective effects against mitochondrial damage have shown to improve optimal fetal growth (519). Its actions have also shown to improve placental endocrine function, hemodynamics and placental-uterine nutrient transfer (516,520–522). As such, this suggests that miR-375-3p may be stimulating melatonin biosynthesis as a compensatory mechanism of placental insufficiency.

GDM has also been associated with altered expression of long-chain fatty acylcarnitines in the placenta which is an indication of mitochondrial dysfunction (523). Short-chain acylcarnitine, hexanoylcarnitine or AC6:0, was found to be impacted by miR-375-3p. Previous work has suggested AC6:0 may be synthesised from cytoplasmic granules found within fetal stem vessel endothelia and may play an important role in maternal-fetal immunological regulation during pregnancy (524). However, more recent evidence demonstrates AC6:0 may be secreted by trophoblasts (525). Placental AC6:0 expression is shown to be increased in females compared to males, indicating improved placental mitochondrial activity in female pregnancies (526). Moreover, when separating the data for fetal sex, no impact on AC6:0 expression was observed in either male or female placentae response to miR-375-3p. AC2:0 and AC14:0 expression were downregulated in male placentae by miR-375-3p. Elevated postnatal circulating AC2:0 expression in LGA neonates has been associated with obesity and metabolic syndrome features (527). Interestingly, when exclusively examining female placentae, no acylcarnitines were impacted by miR-375-3p, where 5-HIAA was the only significantly altered metabolite. This metabolite has previously been associated with reduced fetal growth (528). Overall, these findings suggest the male placental metabolome may be more susceptible to the effects of miR-375-3p.

GDM has already been associated with altered ceramide and sphingolipid expression (523). In the placental tissue of our mouse model, it was found that

these lipid species were undetected, or mass spectrometry peaks were excessively truncated and therefore no meaningful measurements could be analysed. This was also the case for phosphatidylcholine, phosphatidylethanolamine, phosphatidylinositol, phosphatidylserine, lysophosphatidylcholine, lysophosphatidylethanolamine, lysophosphatidylglycerol and phosphatidylcholine species. Lipid screening revealed miR-375-3p significantly altered the mouse placental lipidome in this study. The species predominantly affected were triacylglycerides (TAGs). TAGs are a major source of lipids for the developing fetus, where evidence shows trophoblast cells have a 10-fold preference in the uptake of TAG derivatives compared to free fatty acids (529). Recent evidence suggests TAGs may be useful biomarkers to identify altered fetal growth during pregnancy (530). Placenta TAG expression has also been shown to be regulated by glucose levels, where TAG accumulation has been associated with GDM and a reduction in fatty acid oxidation (531). Indeed, it has been shown that dysregulated placental TAG metabolism may lead to impaired fatty acid oxidation and maternal-fetal lipid transfer, resulting in fetal overgrowth in pregnancies complicated by maternal diabetes (532–534). Free fatty acids are precursors of TAGs and their transfer across the maternal-fetal interface has been associated with offspring adiposity (452). FFA species were also upregulated with miR-375-3p overexpression in our mouse model. Altered placental expression of long-chain polyunsaturated fatty acids has previously been associated with GDM (531,535,536). Moreover, monoacylglycerol (MAG) species were also found to be altered in mouse placental tissue of this study following exposure to miR-375-3p. MAGs are derived from the breakdown of TAGs and have been previously associated with altered fetal growth (537,538). These findings therefore indicate that miR-375-3p increases placental lipolysis and nutrient availability, thus contributing towards placental dysfunction and altered fetal growth. By labelling free fatty acids, it has been shown that maternal obesity reduces placental lipid storage capacity and increases maternal-fetal lipid transfer (539). This therefore suggests that miR-375-3p may stimulate fetal overgrowth by increasing maternal-fetal lipid transfer and impairing placental capacity of fatty acid storage. Moreover, it is important to note that when separating the data for fetal sex, miR-375-3p altered these lipid species in a sex-dependent manner, where TAG and MAG expression

was altered in female but not male placentae, and FFA expression was altered in male but not female placentae. As such, these sex-specific effects should be considered when evaluating the effect of miR-375-3p in human pregnancies.

As the mouse labyrinth zone is key for nutrient exchange and is associated with fetal weight gain (455), the impact of miR-375-3p on the relative size of each placental zone in the mouse was measured as an indicator of altered placental metabolism and efficiency. Indeed, smaller junctional and labyrinth zones have been identified in a mouse model of diabetes in pregnancy (540). Interestingly, altered IGF axis signalling has been associated with the development of the junctional zone of the placenta (455); this was a placental target of miR-375-3p that was identified in our study. Although male total placental surface area was increased with miR-375-3p compared to control, no difference was observed in females, however this may be due to low n numbers. No differences in the relative surface area of each mouse placental zone were identified in response to miR-375-3p. It is possible that this lack of difference may be due to low statistical power, in that many placentae were damaged during histological processing and therefore could not be included in analysis as the placental zones were not distinctive. Further analysis on trophoblast cell turnover, fetal capillary volume and maternal intervillous volume would be useful to explore the effect miR-375-3p on placental functional development. However, our placental samples were overstained and therefore identifying these markers was not possible. Further work is needed to optimise the lectin and cytokeratin staining protocol for these samples.

4.5.4 The impact of maternal circulating miR-375-3p on fetal growth in pregnancies complicated by GDM.

The Forbes group have previously characterised miR-375-3p to be upregulated at 24-28 weeks gestation in the circulation of pregnant women with GDM who had LGA compared to AGA outcomes. miR-375-3p was also found to be upregulated in term placental tissue of women with GDM who delivered LGA neonates compared to AGA neonates. As the primary transcript for this miRNA was undetectable in human term placental tissue, this was suggestive of mature

miR-375-3p being transported to the placenta via the maternal circulation. The Forbes group previously demonstrated that this miRNA was pancreas specific, where EV miR-375-3p secretion and expression was increased in mild hyperglycaemic conditions, resulting in increased human placenta uptake of miR-375-3p. It was demonstrated that miR-375-3p overexpression altered placental proteomic pathways associated with placental growth, metabolism and vascular development. As we identified mouse placental miR-375-3p targets were homologous to human, findings from this mouse *in-vivo* study demonstrate that miR-375-3p may be causative of LGA through altering events in the placenta. However, given that there was no strong evidence of miR-375-3p influencing mouse maternal metabolism, this suggests that miR-375-3p may not be causative of GDM. As mild hyperglycaemia demonstrated to increase pancreatic islet EV secretion and levels of miR-375-3p, this indicates that the hyperglycaemic environment of the diabetic milieu may be driving miR-375-3p biogenesis and secretion. β-cell dysfunction has been associated with increased circulating levels of miR-375-3p (541). It is therefore reasonable to suggest that women who develop GDM and deliver LGA babies may manifest underlying β-cell dysfunction which is then exacerbated with pregnancy. Consequently, it is possible that the maternal risk factors associated with GDM may be linked to underlying pancreatic function and maternal miR-375-3p profile.

The Forbes group have previously identified changes in maternal circulating levels of miR-375-3p at the time of GDM diagnosis. It is possible that the pancreas may need to be exposed to hyperglycaemia or the diabetic milieu for a prolonged period of gestation before any changes in circulating miR-375-3p expression can be observed. Investigating maternal circulating levels of miR-375-3p in the first trimester of GDM and T1DM pregnancies could enhance our understanding of this, where changes in pancreas miR-375-3p biogenesis and secretion may be seen earlier in pregnancy due to diabetic and hyperglycaemic stimuli being present from early conception. Placental expression of miR-375-3p have been examined at term in our human and mouse models. It would therefore be interesting to examine if these changes in placental miR-375-3p can also be observed at the time of GDM diagnosis. Identifying altered maternal circulating miR-375-3p expression earlier in pregnancy would

improve the monitoring and clinical management of pregnancies complicated by altered fetal growth.

Glucose has demonstrated to alter the regulation of β-cell-derived EVs on glucagon secretion and pancreatic function (542,543). However, maternal pancreatic EVs may not be the only source of elevated miR-375-3p levels in the circulation. Human fetal pancreatic slices from diabetic pregnancies demonstrate a more pronounced increase in β-cell mass with gestational age compared to those from nondiabetic pregnancies (544). As such it is possible that increased fetal glucose exposure in GDM may be influencing fetal pancreatic development and EV miR-375-3p cargo released by the fetus itself. As such, maternal hyperglycaemia may be the main driver of fetal overgrowth in GDM. However, this does not explain why some GDM pregnancies still result in AGA infants regardless of improved glucose control and a difference in EV miRNA profile is observed in women with GDM who deliver AGA infants compared to LGA infants. This suggests factors other than glucose, or indirect metabolic consequences of hyperglycaemia, may contribute towards LGA in GDM, where fetal sex may also influence pregnancy outcomes.

Possible mechanisms to explore is that pancreatic EV release may be increased in GDM pregnancies affected by LGA, resulting in a higher proportion of serum EVs of pancreatic origin, containing miR-375-3p, compared to those with AGA outcomes. Determining the proportion of all EV sources in the human circulation would provide better understanding of the broader metabolic implications of GDM on maternal health and the changes occurring in LGA pregnancies. Recent methodologies have been developed whereby EV enriched proteins have been characterised in the human circulation of T1DM, and HLA-DRB1 and DQB1 were found to be associated with pancreatic size (545). However, glucose may be altering EV secretion or biogenesis of other metabolic tissues which may then indirectly impact the pancreatic transcriptome via interorgan EV mediated crosstalk (546,547). It has previously been shown that placental factors in GDM can impact maternal metabolism (548). As such, it would be interesting to examine whether miR-375-3p alters the release of placental EVs and if this in turn impacts on maternal metabolism.

Another possible mechanism is that GDM may be associated with increased placental internalisation of pancreatic EVs. Indeed, *in-vitro* culture of pancreatic cancer cells demonstrated that hypoglycaemic conditions altered EV size and fatty acid composition, leading to a change in membrane fluidity and uptake of EVs into recipient cells (549). Pancreatic EV biogenesis and composition may therefore be altered in GDM, resulting in increased EV internalisation into placental cells in LGA pregnancies.

Other studies have already explored the effects of miR-375-3p on fetal cardiometabolic health beyond the uterine environment. Indeed, miR-375-3p has been identified as a key regulator of fetal pancreatic development, whereby maternal nutrition *in-utero* can influence fetal pancreatic miR-375-3p expression and β-cell mass and function *ex-utero* (550,551). Its involvement in cardiovascular development has also been established, where aberrant miR-375-3p expression has been associated with congenital heart disease (552,553). Both fetal pancreatic and cardiac development are shown to be affected by GDM (554), suggesting that altered maternal miR-375-3p expression in GDM pregnancies with LGA outcomes identified in our study may have a long-term influence on fetal cardiometabolic health.

Altogether, these findings suggest that inhibiting or minimising the action of miR-375-3p on the placenta may be a promising therapeutic strategy for women with GDM at risk of delivering LGA infants. Proof-of-concept studies have already demonstrated targeted delivery of miRNA inhibitors to the placenta in pregnant mice, resulting in altered feto-placental development (123). However, as miR-375-3p is involved in regulating glucose metabolism (555), complete inhibition may have deleterious effects for maternal metabolic homeostasis and fetal demands during pregnancy. With the placenta being a source of EVs in maternal serum during pregnancy and thus involved in EV mediated cross-talk between metabolic tissues, inhibition of placental miR-375-3p expression may present wider systemic effects. Balancing maternal outcomes with fetal demands is therefore a vital consideration when approaching potential therapeutic interventions for GDM pregnancies affected by LGA. As sex differences were observed in our mouse model, fetal sex should also be considered when

investigating the role of miR-375-3p in regulating feto-placental growth in human pregnancies complicated by GDM.

4.6 Summary

Effect of *in-vivo* delivery of miR-375-3p to the maternal circulation on fetal growth in healthy pregnant mice	
Pregnancy Outcomes	No effect on litter size, pregnancy resorptions, fetal sex and maternal survival
Fetal Growth	Increase in weight - Non-significant increase in female pregnancies - Significant increase in male pregnancies
Placental Growth	Increase in weight - Significant increase in male and female pregnancies
Fetal-Placental Growth	Reduction in fetal:placental weight - Significant decrease in male and female pregnancies
Maternal Metabolism	No significant impact
Placental Targets	- miR-375-3p circulated and internalised into placental tissue o Significant increase in placental miR-375-3p levels in female pregnancies o Non-significant increase in placental miR-375-3p levels in male pregnancies - Placental miR-375-3p targets are homologous in mouse and human o Targets associated with placental metabolism, growth and vascular development o Changes in many targets were more pronounced in females
Placental Metabolism	- **Altered amino acid metabolism** o Downregulation of BAIBA, 5-OP, acetyl-5-hydroxytryptamine o Upregulation of melatonin - **Altered lipid metabolism and fatty acid β-oxidation**

	○ Downregulation of TAGs – 48:0, 52:4, 50:1, 52:3, 54:6, 52:2 and 54:5 ○ Upregulation of MAGs – 16:0 and 18:0 ○ Upregulation of FFA 22:3 and 18:0 ○ Downregulation of AC6:0 - Sex-dependent effects demonstrated in the placental metabolome and lipidome
Placental Zones	No effect on labyrinth, junctional and decidual zone size.
Summary	miR-357-3p influences fetal growth by impacting events in the placenta. Placental development and function are affected, where pathways associated with growth, vascularisation and metabolism are altered by miR-357-3p. Pregnant mice exposed to miR-357-3p demonstrate placental hallmarks of mitochondrial dysfunction and altered nutrient bioavailability to the developing fetus. These effects may be independent of maternal metabolism. Fetal sex may influence the impact of maternal circulating miR-375-3p on pregnancy outcomes in GDM.

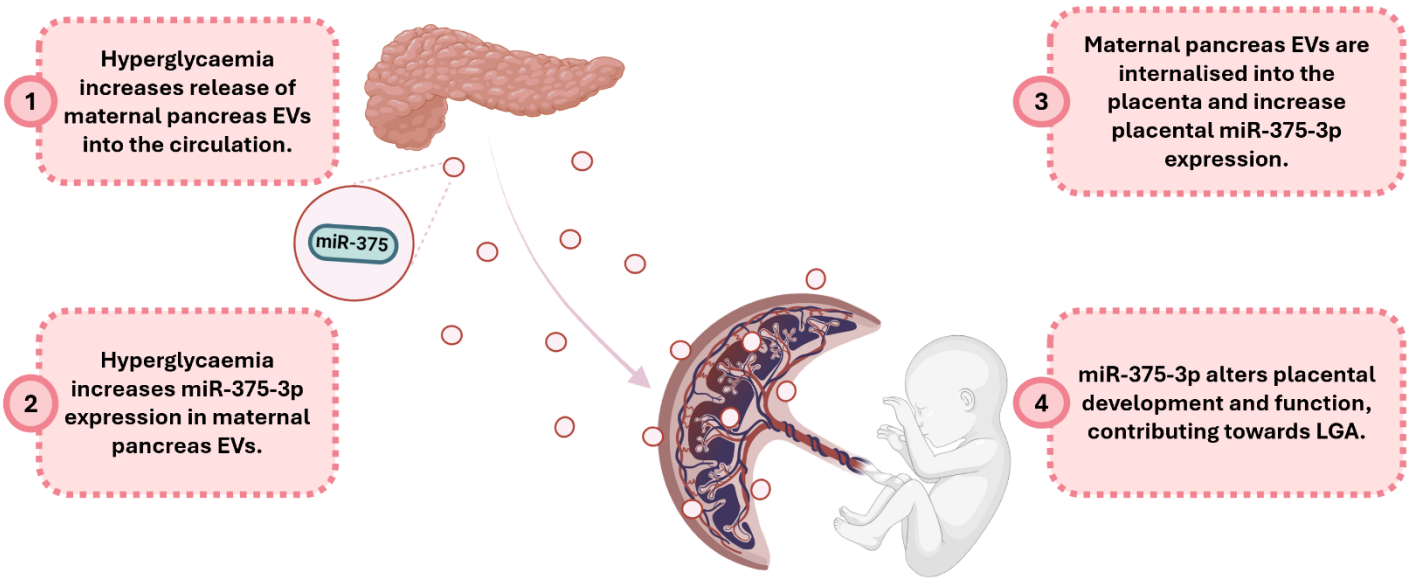

Figure 65 Graphical summary of the putative mechanism of miR-375-3p contributing towards altered fetal growth in pregnancies complicated by GDM.

Maternal EV profile is altered in women with GDM who deliver LGA compared to AGA neonates, where miR-375-3p expression is elevated. GDM-LGA pregnancies also demonstrate increased miR-375-3p expression in term placenta compared to GDM-AGA pregnancies. miR-375-3p is pancreas-specific, suggesting that miR-375-3p circulates to the placenta via EVs in the circulation. Data from the Forbes lab suggests that hyperglycaemia increases pancreas EV release, where EV-miR-375-3p expression is also elevated. Findings show that pancreas EVs can internalise into placental tissue and increase placental miR-375-3p expression. By utilising a pregnant mouse model and omics analyses, findings suggest that miR-375-3p alters placental development and function, thus contributing towards LGA outcomes. Created using Biorender.com.

5 Determining the Role of Maternally-Derived Extracellular Vesicles in Altered Fetal Growth in GDM

5.1 Introduction

Various factors in the maternal circulation may influence fetal development during pregnancy. Findings from the previous chapter suggest that miR-375-3p influences fetal growth by altering events in the placenta. In the maternal circulation, miRNAs are encapsulated in EVs (244,256). It has been suggested that EVs play a role in the maintenance of healthy pregnancy as well as GDM aetiology (244,548), where infusion of small EVs from women with GDM into healthy pregnant mice has shown to induce maternal glucose intolerance and altered skeletal muscle miRNA profile and insulin signalling (556). Women with GDM also manifest higher levels of circulating EVs yet a lower proportion of placenta-derived small EVs compared to those who experience healthy uncomplicated pregnancies (278). This suggests that the diabetic environment may be altering the biogenesis and release of various maternal organ EVs, as well as their miRNA cargo (263,278). Indeed, circulating EV-miRNA profile is altered in women with GDM compared to healthy, uncomplicated pregnancies, where changes have been detected prior to the diagnosis of GDM (268,277). Less is known about the effect of maternal circulating EVs on fetal growth and placental development in GDM pregnancies. However, evidence demonstrates a bidirectional crosstalk between maternal organs and the placenta through the medium of EVs (260,267,268,282). Therefore, with maternal diabetes being associated with altered placenta miRNA profile (**Table *2***), it is possible that maternal EVs play a role in altering placental development in GDM pregnancies (**Table *3***) and contribute towards altered fetal growth. The Forbes group have previously demonstrated that prior to the onset of LGA, maternal EV concentration and miRNA signature is altered in GDM (**Figure *38***). In this chapter, we aimed to establish the effect of maternal circulating EVs from GDM pregnancies on fetal growth by utilising an *in-vivo* model whereby EVs from women with uncomplicated pregnancies or pregnancies complicated by GDM were delivered to healthy pregnant mice and pregnancy outcomes assessed.

5.2 Hypothesis

Maternally-derived EVs contribute towards altered fetal growth in GDM.

5.3 Aims

4) Deliver human maternally-derived EVs to the maternal circulation of mice and assess pregnancy outcomes and maternal health.
5) Establish the impact of human maternally-derived EVs from GDM pregnancies on mouse fetal growth.
6) Establish the mechanism of which human maternally-derived EVs from GDM pregnancies impact fetal growth by assessing maternal metabolism and placental development and function.

5.4 Results

5.4.1 Isolating and Characterising Human Maternal Plasma EVs From Healthy and GDM Pregnancies

Maternal blood was collected from women with healthy uncomplicated pregnancies or GDM pregnancies with AGA or LGA outcomes at 26-33 weeks' gestation. EVs were isolated from plasma via size exclusion chromatography (SEC), which yielded 15 fractions. NTA (**Figure *66***A-C) and silver staining (**Figure *66***D) were then performed on fractions 7-15 to determine which fractions had the most EVs with the least protein contamination, where it was deduced that fractions 7-10 yielded the purest EV content (**Figure *66***D,E). As such, fractions 7-10 were pooled (F7-10) for every patient and characterised for EVs. Electron microscopy demonstrated that the pooled fractions demonstrated the characteristic smooth, circular shape of EVs (**Figure *67***A). Through western blotting, it was also identified that the pooled fractions expressed CD63 transmembrane protein and tumour susceptibility 101 (TSG101) cytosolic protein (**Figure *67***B). Cellular protein contamination marker, Calnexin, was absent in the pooled samples (**Figure *67***B). As such, these pooled EV fractions were used in subsequent experiments.

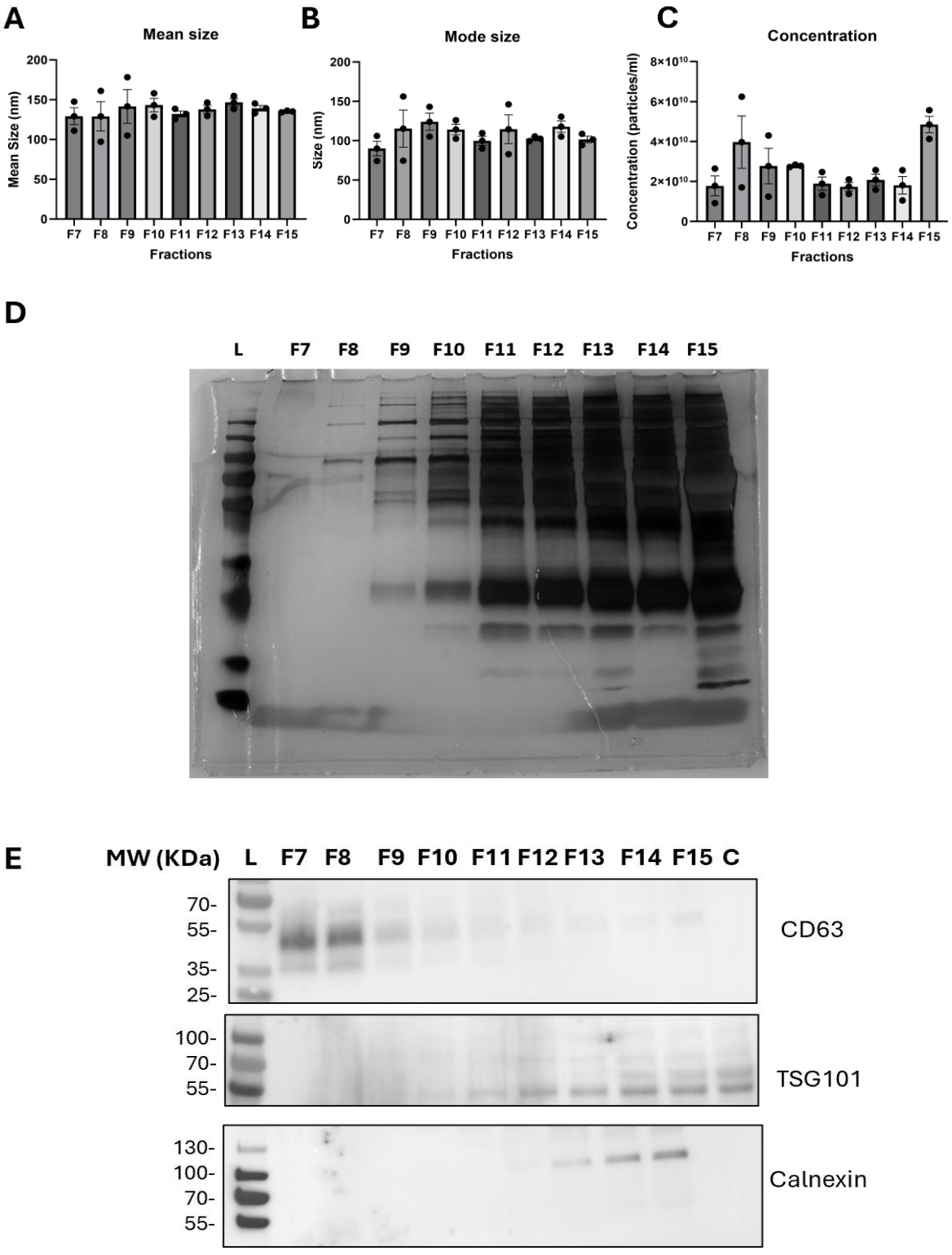

Figure 66 Characterisation of EV fractions 7-15.

EVs were isolated from human maternal plasma using size exclusion chromatography. Fractions 7-15 were characterised via (A-C) nanoparticle tracking analysis (NTA) for EV size and concentration. Data presented as mean±SEM. (D) Silver staining was also performed on fractions 7-15 to determine protein concentration. (E) Western blotting was performed to determine the expression of CD63 and TSG101 proteins in the EV fraction 7-15 samples. Calnexin was used as a negative marker, where whole serum was used as a positive control. Representative data taken from exemplar datasets. Produced by Dr Rachel Quilang.

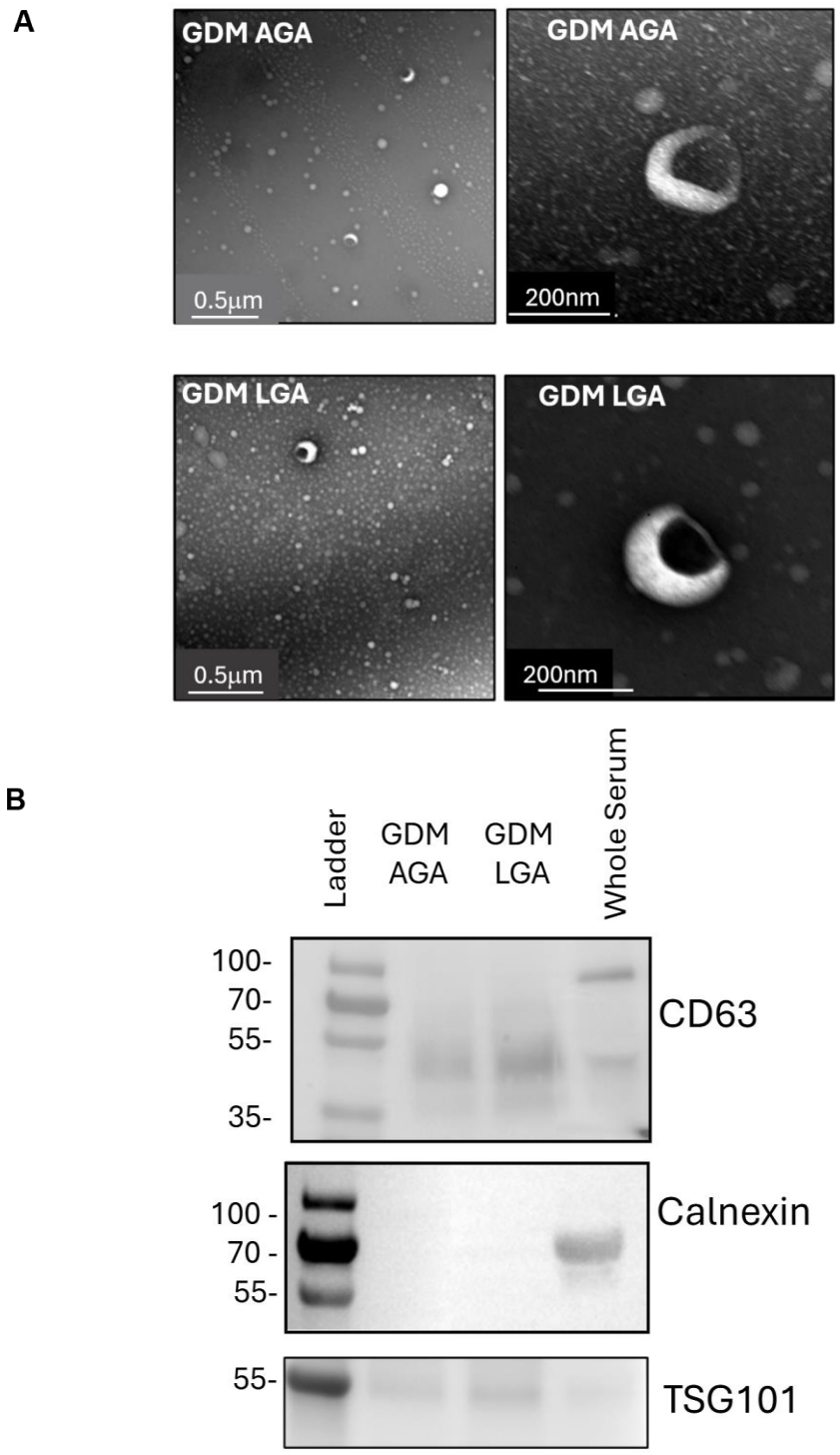

Figure 67 Characterisation of maternal p7-10 plasma EVs from GDM AGA and GDM LGA pregnancies.

EVs were isolated from human maternal plasma using size exclusion chromatography and silver staining was performed to determine protein contamination of fractions and the further pooling of fractions 7-10 from each patient sample. EVs were imaged via electron microscopy, where representative images at X10K and x40K magnification are shown. Western blotting detected the expression of CD63 and TSG101 proteins in the EV samples. Calnexin was used as a negative marker, where whole serum was used as a positive control. Data produced by Dr Rachel Quilang.

EV size in the pooled fractions was determined via NTA, confirming the appropriate diameter associated with and identified to be EVs, rather than alternative artefacts (258) (**Figure *68***).

The EV mean diameter of pooled EV fractions from healthy uncomplicated (non-GDM AGA) pregnancies was 108.3 ± 5.028nm (n=8) (**Figure *68***A). Interestingly, this was increased in GDM AGA pregnancies (125.0 ± 3.745nm; p=0.022; n=8) and GDM LGA pregnancies (137.0 ± 3.270nm; p=0.0002; n=8). An increase in EV mean diameter was also observed with increased birthweight when comparing both GDM pregnancies (p=0.120), suggesting that birthweight has an affect on EV mean diameter (**Figure *68***A). Moreover, these findings demonstrated that the EVs in the pooled fractions were classed as small EVs (**Figure *4***). When subcategorising the pooled small EVs according to fetal sex, a male-specific effect was observed, where a significant increase in mean diameter was demonstrated between heathy uncomplicated pregnancies and GDM LGA pregnancies (from 102.0 ± 8.150nm to 136.9 ± 6.980nm; p=0.006; n=4) (**Figure *68***B). No statistically significant differences were observed in mean EV diameter with female offspring and pregnancy outcomes (**Figure *68***B).

EV mode diameter of pooled small EVs from non-GDM AGA pregnancies was 76.81 ± 3.429nm (n=8) (**Figure *68***C). This was increased in GDM AGA pregnancies (84.28 ± 2.404nm; p=0.146; n=8) and GDM LGA pregnancies (93.45 ± 2.022nm; p=0.0007; n=8). Increased birthweight had a marked impact on EV mode diameter in GDM pregnancies (p=0.062) (**Figure *68***C). When subcategorised for fetal sex, as with mean diameter, only a male-specific effect was observed in EV mode diameter, where GDM LGA male pregnancies demonstrated an increase in EV mode diameter (92.03 ± 3.519nm) compared to non-GDM AGA male pregnancies (69.93 ± 3.911nm) (p=0.001; n=4) (**Figure *68***D).

The concentration of pooled small EVs was also measured and it was identified that the concentration was reduced in maternal plasma of GDM AGA pregnancies compared to non-GDM AGA pregnancies (from 1.2365e11 ± 1.6564e10 particle/ml to 6.3913e10 ± 4.8362e9 particle/ml; p=0.003; n=8) (**Figure *68***E). A reduction was also observed in maternal plasma EV concentration in GDM LGA pregnancies (9.0063e10 ± 8.4598e9 particle/ml) compared to non-GDM AGA

pregnancies (1.2365e11 ± 1.6564e10 particle/ml), although this did not reach statistical significance (p=0.106; n=8). There was no difference in plasma EV concentration between GDM LGA and GDM AGA pregnancies (**Figure *68***E). When subcategorising based on fetal sex, no sex-specific differences in EV concentration were observed (**Figure *68***F).

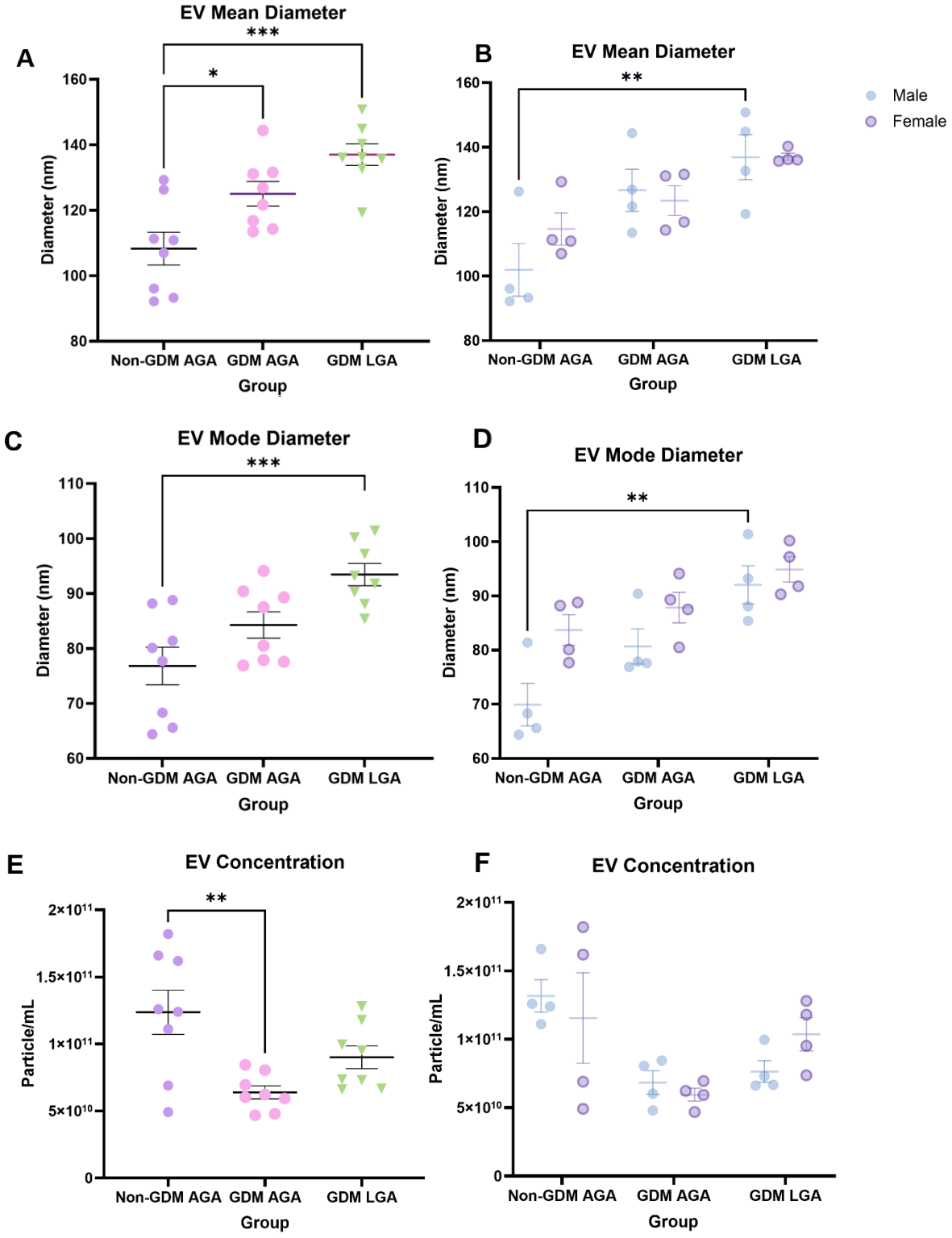

Figure 68 Diameter and concentration of human maternal plasma EVs from healthy uncomplicated, GDM AGA or GDM LGA pregnancies.

Pooled fractions 7-10 of human plasma EVs were characterised under Brownian motion via nanoparticle tracking analysis (NTA). Ordinary one-way ANOVA followed by Tukey's multiple comparisons test was performed. Differences in sex were measured via ordinary two-way ANOVA followed by Tukey's multiple comparisons test. Data presented as mean±SEM. *=p ≤ 0.05, **=p ≤ 0.01, ***=p ≤ 0.001.

5.4.2 Developing Injection Treatment Groups of Human Maternal Plasma EVs

Pooled small EVs from 8 individual patients were further pooled to create one single pooled sample from each patient group that could be utilised for delivery into pregnant mice. It was ensured that the concentration of plasma small EVs originating from female and male pregnancies was equal in each treatment group and overall maternal BMI was as closely matched as possible given the patient samples that were available (**Table *9***, **Table *11***, **Table *12***, **Table *13***). EV concentration of the pooled injection treatment groups was established to determine to the concentration of small EVs to be injected into mice, reserving 3 injections for each mouse. Particle concentration was determined (non-GDM AGA - 6.22E+10 particle/mL; GDM AGA - 6.39E+10 particle/mL; GDM LGA - 5.81E+10 particle/mL) (**Figure *69***A). Mode diameter of small EVs in the non-GDM AGA group and GDM AGA group were similar (77.9nm, 74.5nm respectively), whereas small EVs in the GDM LGA treatment group demonstrated a higher mode diameter (96.5nm) (**Figure *69***B).

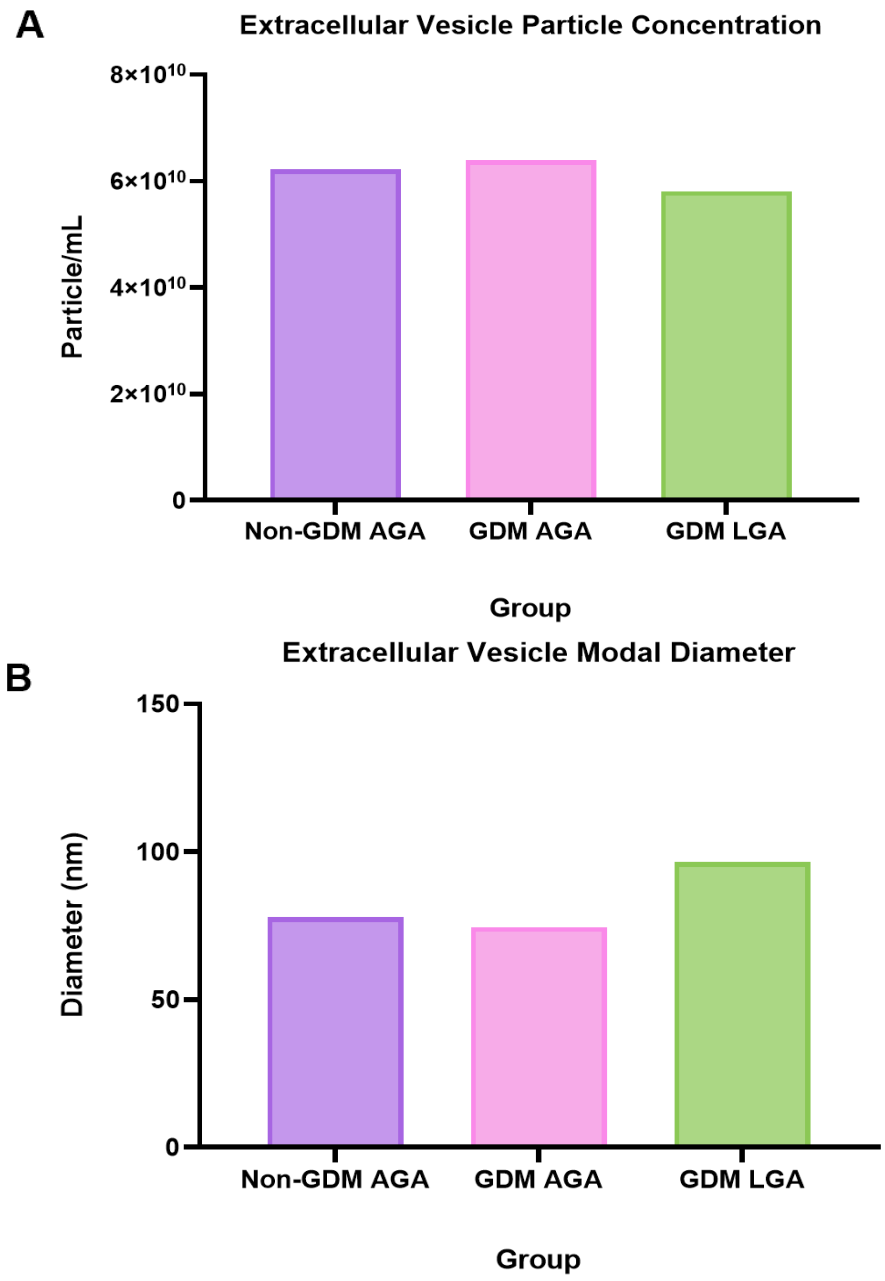

Figure 69 Concentration and modal diameter of human maternal plasma EVs from non-GDM AGA, GDM AGA or GDM LGA pregnancies.

Plasma EV fractions 7-10 from various patients (**Table *9***, **Table *11***,**Table *12***, **Table *13***). (A) EV particle concentration and (B) modal diameter of injection treatments were determined via nanoparticle tracking analysis (NTA).

5.4.3 Establishing the Safety and Litter Outcomes of Human Maternally-Derived EVs Injected into Healthy Pregnant Mice

5.4.3.1 Human maternal pregnancy EVs do not impact litter size, pregnancy resorptions, fetal sex or maternal survival in mice.

The mouse placenta is distinctly formed by E11 and is fully developed by E15 (448), where early embryo organogenesis is initiated around E8.5 until E13.5 (468,469). As such, to examine the impact of maternal pregnancy EVs on pregnancy outcomes, human maternal plasma small EVs from non-GDM AGA pregnancies were injected into healthy pregnant mice at E11.5, E13.5 and E15.5 at an *in-vivo* concentration of 1.5E+9 particles/mL. PBS was used as a vehicle control. No differences in litter sizes (**Figure *70***A) or fetal sex ratios (**Figure *70***B) were observed with pregnancy EVs compared to PBS. There was a tendency towards increased resorptions in EV treated dams (median of 1) compared to PBS treated dams (median of 0), however this did not reach significance (**Figure *70***C). Pregnancy EVs also had no effect on maternal survival, where all dams survived throughout pregnancy (data not shown).

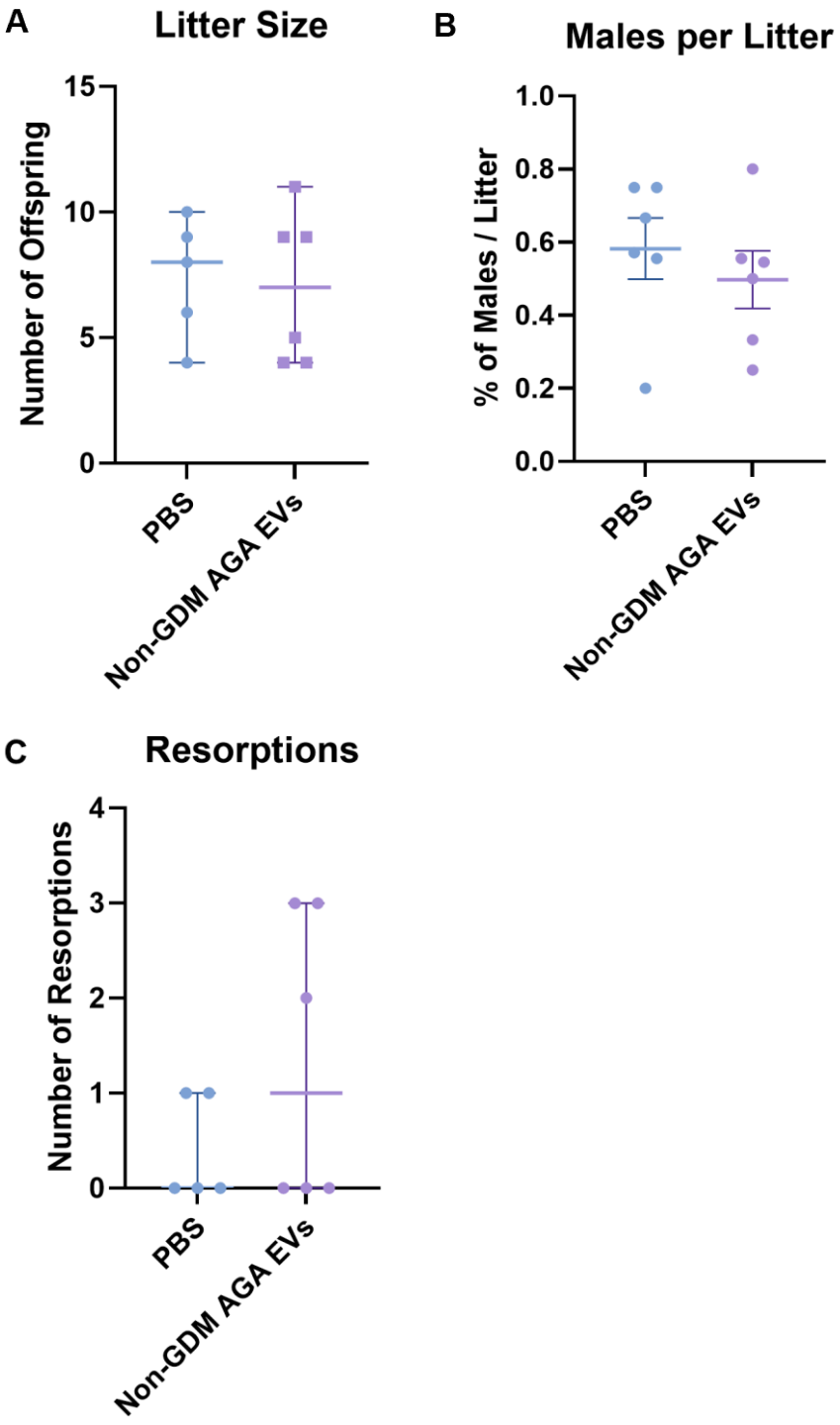

Figure 70 Litter outcomes of mice exposed to PBS or human maternal plasma small EVs from non-GDM AGA pregnancies during gestation.

Litter size, males per litter and resorptions were measured in response to treatments. Mann-Whitney test was performed to determine statistical significance of nonparametric data, where data was presented as median with 95% CI. Unpaired t-test was performed for parametric data and presented as mean±SEM.

5.4.4 Establishing the Impact of Human Maternal Pregnancy EVs on Mouse Fetal-Placental Growth and Maternal Outcomes

5.4.4.1 Human maternal pregnancy EVs impact fetal growth.

To determine if human maternal pregnancy EVs impact fetal growth in mice, human maternal plasma small EVs from non-GDM AGA pregnancies were injected into healthy pregnant mice at E11.5, E13.5 and E15.5. PBS was used as a vehicle control. Pups were then culled, weighed and processed at E18.5. It was demonstrated that human maternal pregnancy small EVs significantly increased fetal weight compared to control (from 1.198 ± 0.018 g to 1.271 ± 0.023 g; p=0.035, adjusted for fetal sex and litter size; n=37 clustered to 5 dams/n=42 clustered to 6 dams) (**Figure *71***). When exclusively investigating male fetal growth, it was demonstrated that small EVs from non-GDM AGA pregnancies increased fetal growth by 8% compared to control (from 1.214 ± 0.019 g to 1.317 ± 0.036 g; p=0.049) (**Figure *71***, **Appendix *9***, **Appendix *10***). Although small EVs from non-GDM AGA pregnancies demonstrated to increase female fetal weight compared to control (from 1.183 ± 0.039 g to 1.252 ± 0.035 g), this did not reach statistical significance (p=0.248) (**Figure *71***, **Appendix *9***, **Appendix *10***).

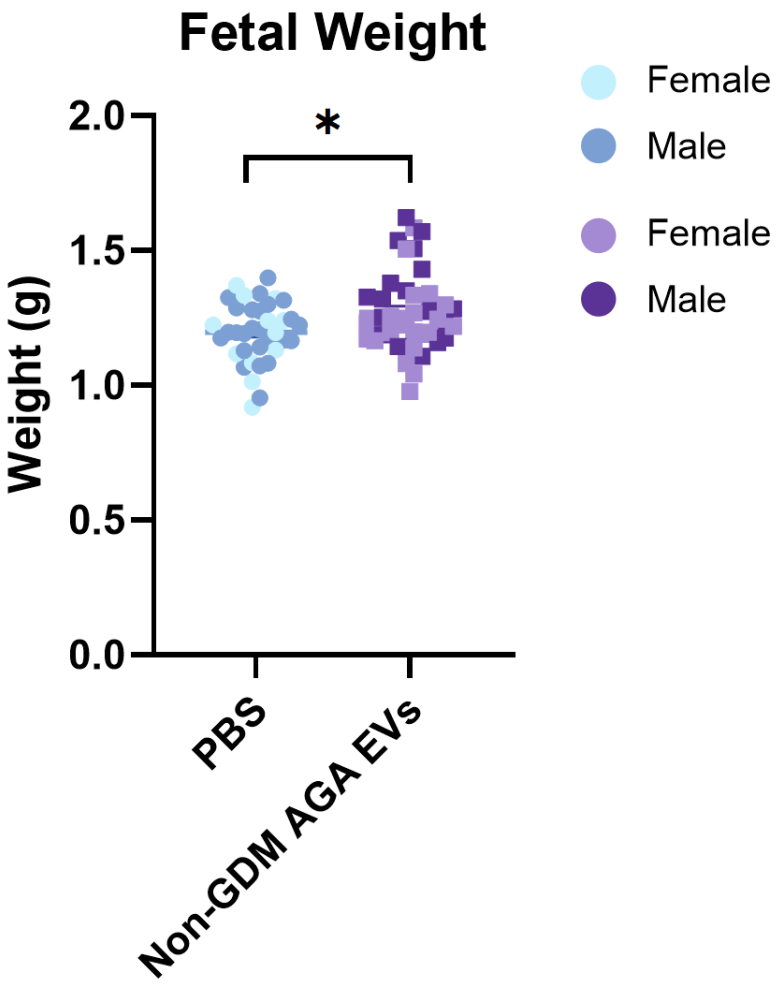

Figure 71 Fetal weight of mice exposed to PBS or human maternal plasma EVs from non-GDM AGA pregnancies during gestation at E18.5.

Healthy pregnant C57BL6/J female mice were injected human maternal EVs from healthy uncomplicated (non-GDM AGA) pregnancies at E11.5, E13.5 and E15.5 at a final *in-vivo* concentration of 1.5E+9 particles/mL. PBS was used as a vehicle control. Mice were sacrificed at E18.5 and pups were weighed. Mixed-effects nonlinear regression model was performed using Stata, where each litter was clustered and adjustments were made for fetal sex and litter size. Data presented as mean±SEM; *=p ≤ 0.05. Light data points; female, dark data points; male.

5.4.4.2 Human maternal pregnancy EVs impact placental growth.

To establish if human maternal pregnancy EVs impact placental growth in mice, mouse placentae from dams that had been injected with maternal plasma small EVs from non-GDM AGA pregnancies were harvested and weighed at E18.5. Maternal small EVs from non-GDM AGA pregnancies significantly increased placental weight compared to control (from to 0.091 ± 0.003 g to 0.100 ± 0.002 g; p=0.012, adjusted for fetal sex and litter size; n=36 clustered to 5 dams/n=36 clustered to 5 dams) (**Figure *72***). When exclusively investigating males, it was demonstrated that small EVs from non-GDM AGA pregnancies increased placental growth by 10% compared to control (from 0.093 ± 0.003 g to 0.103 ± 0.003 g; p=0.050) (**Figure *72***, **Appendix *11***, **Appendix *12***). Although small EVs from non-GDM AGA pregnancies demonstrated to increase female placental weight compared to control (from 0.084 ± 0.004 g to 0.097 ± 0.004 g), this did not reach statistical significance (p=0.295) (**Figure *72***, **Appendix *11***, **Appendix *12***). To determine if maternal pregnancy EVs proportionally impact fetal and placental growth, fetal:placental weight ratio was measured, however no effect was observed (**Figure *73***, **Appendix *13***).

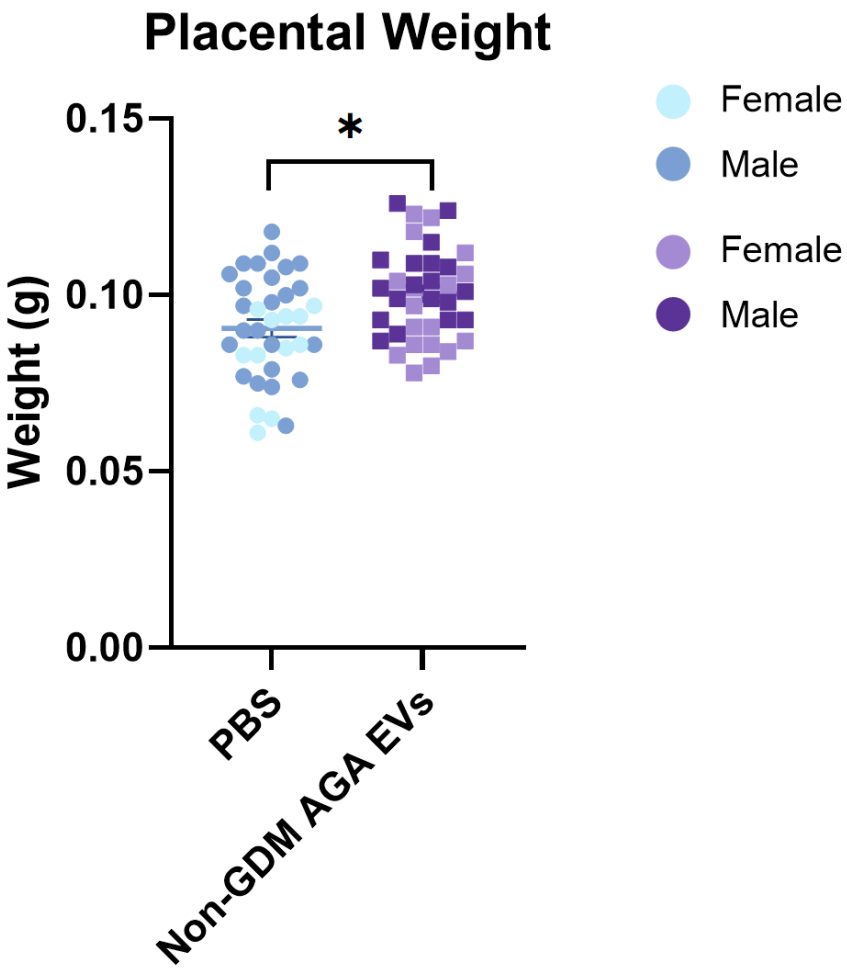

Figure 72 Placental weight of mice exposed to PBS or human maternal plasma EVs from non-GDM AGA pregnancies during gestation at E18.5.

Healthy pregnant C57BL6/J female mice were injected human maternal EVs from healthy uncomplicated (non-GDM AGA) pregnancies at E11.5, E13.5 and E15.5 at a final *in-vivo* concentration of 1.5E+9 particles/mL. PBS was used as a vehicle control. Mice were sacrificed at E18.5, where placentae and pups were weighed. Mixed-effects nonlinear regression model was performed using Stata, where each litter was clustered and adjustments were made for fetal sex and litter size. Data presented as mean±SEM; *=p ≤ 0.05. Light data points; female, dark data points; male.

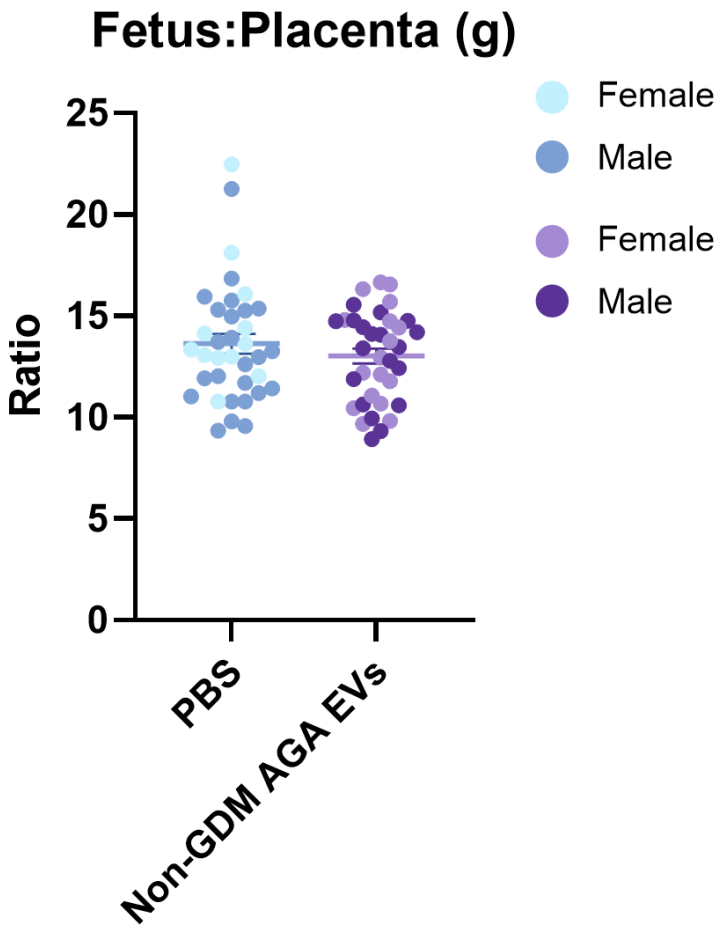

Figure 73 Fetal placental weight ratio of mice exposed to PBS or human maternal plasma EVs from Non-GDM AGA pregnancies during gestation at E18.5.

Healthy pregnant C57BL6/J female mice were injected human maternal EVs from healthy uncomplicated (non-GDM AGA) pregnancies at E11.5, E13.5 and E15.5 at a final *in-vivo* concentration of 1.5E+9 particles/mL. PBS was used as a vehicle control. Mice were sacrificed at E18.5, where placentae and pups were weighed. Mixed-effects non-linear regression model was performed using Stata, where each litter was clustered and adjustments were made for fetal sex and litter size. Data presented as mean±SEM. Light data points; female, dark data points; male.

5.4.4.3 Human maternal pregnancy EVs do not impact maternal cardiometabolic health.

To understand if the effect of human maternal pregnancy EVs on fetal growth is independent of maternal health, indicators of maternal cardiometabolic health were assessed. Maternal weight was recorded at different time-points throughout gestation. Although dams treated with human maternal pregnancy EVs (n=5) weighed marginally lighter than control dams (n=5) throughout pregnancy, there were no marked differences in maternal weight (**Figure *74***A). Maternal weight gain during gestation was also similar between both treatment groups (**Figure *74***B). At E18.5, absolute pregnancy weight was also similar in dams treated with vehicle control and maternal plasma small EVs (**Figure *75***A). Hysterectomised dams treated with maternal plasma small EVs from non-GDM AGA pregnancies were marginally lighter than control dams, however this was not statistically significant (from 23.55 ± 0.615 g to 23.18 ± 0.641 g; p=0.693; n=5/6, respectively) (**Figure *75***B). No differences were found in maternal pregnancy weight gain (E18.5 hysterectomised weight – pre-pregnancy weight) (**Figure *75***C).

Maternal cardiometabolic organs were harvested and weighed at E18.5 and calculated as % of maternal hysterectomised body weight. Maternal plasma small EVs from non-GDM AGA pregnancies had no effect on maternal skeletal muscle or pancreas weight when expressed either as absolute weight or as % of maternal hysterectomised body weight (**Figure *76***A,B). There was no effect of maternal small EVs on absolute weight of maternal liver compared to control dams, however, there was an increase in liver weight when expressed as % of maternal hysterectomised body weight (from median weight of 5.104g to 5.716g; p= 0.4286; n=5/6, respectively) but this was not statistically significant (**Figure *76***C).

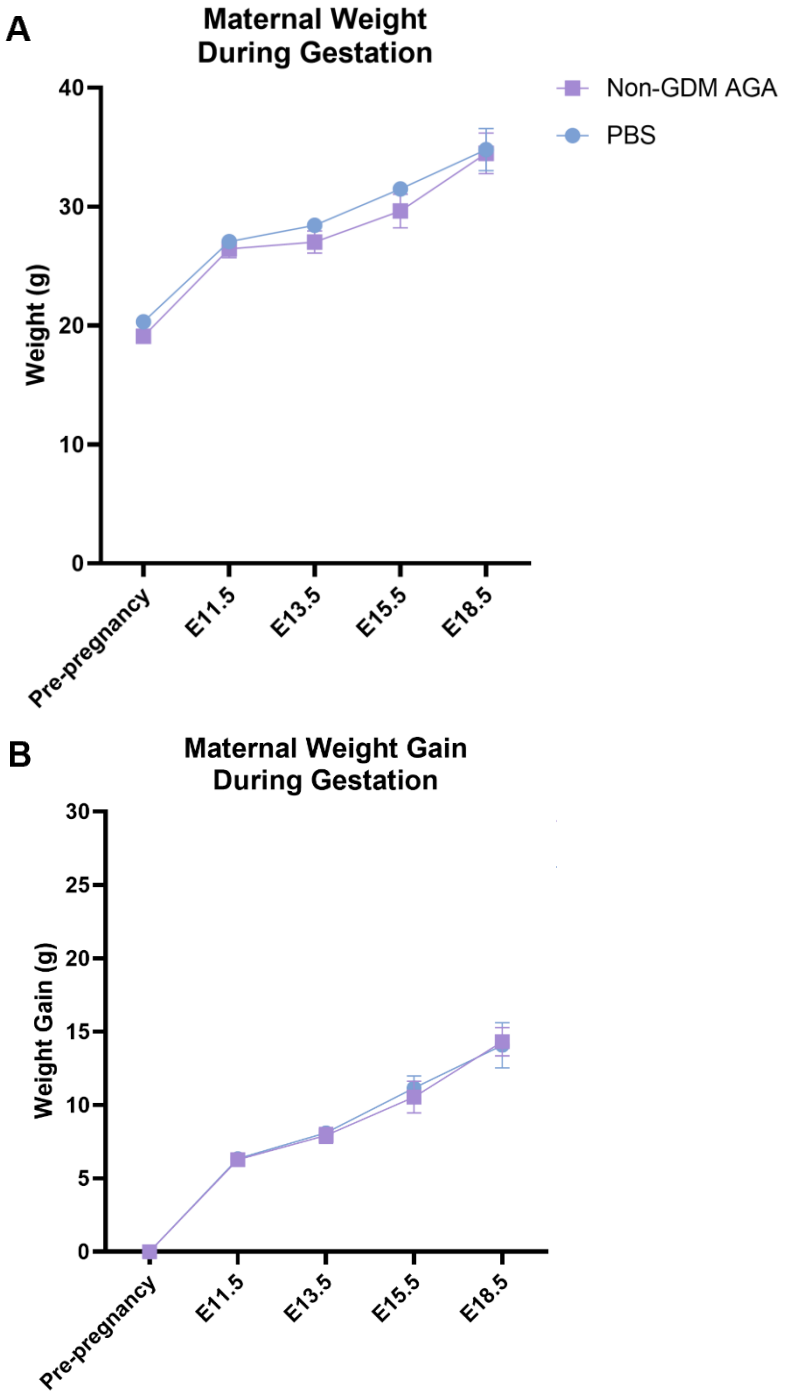

Figure 74 Maternal weight and weight gain during gestation in mice treated with PBS or human maternal plasma EVs from non-GDM AGA pregnancies.

Healthy pregnant C57BL6/J female mice were injected with PBS or human maternal EVs from healthy uncomplicated (non-GDM AGA) pregnancies at E11.5, E13.5 and E15.5 before being sacrificed at E18.5. Pre-pregnancy weights were recorded and maternal weight measured at each injection timepoint and before birth. Two-way ANOVA (with Geisser-Greenhouse correction) was performed. Data presented as mean±SEM.

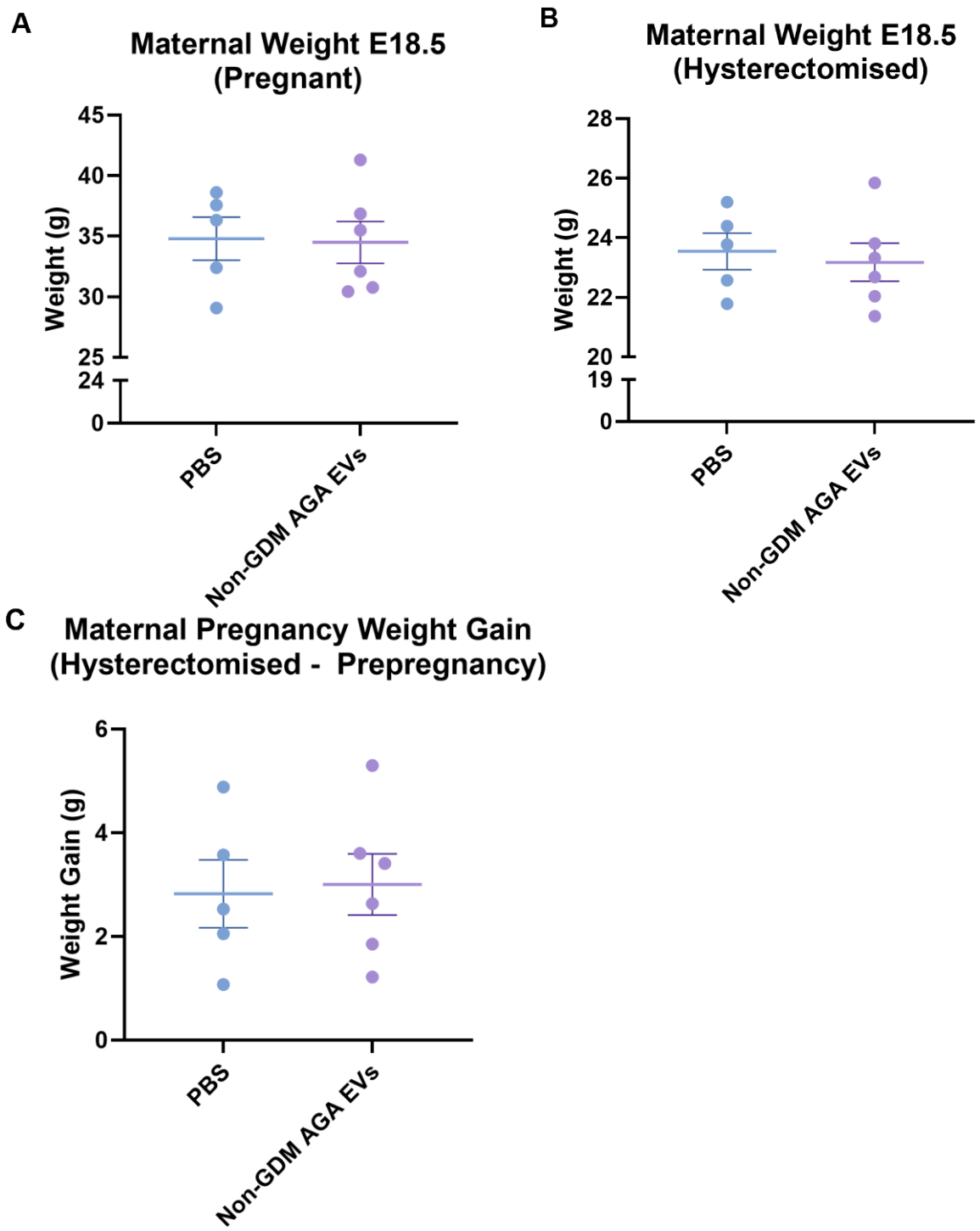

Figure 75 Maternal pregnancy weight, hysterectomised weight and overall pregnancy weight gain of mice treated with PBS or human maternal plasma EVs from non-GDM AGA pregnancies during gestation.

Healthy pregnant C57BL6/J female mice were injected with PBS or human plasma EVs from healthy uncomplicated (non-GDM AGA) pregnancies at E11.5, E13.5 and E15.5 before being sacrificed at E18.5. Pre-pregnancy weights were recorded and maternal pregnancy and hysterectomised weights at E18.5 were measured. Unpaired t-test was performed. Data presented as mean±SEM.

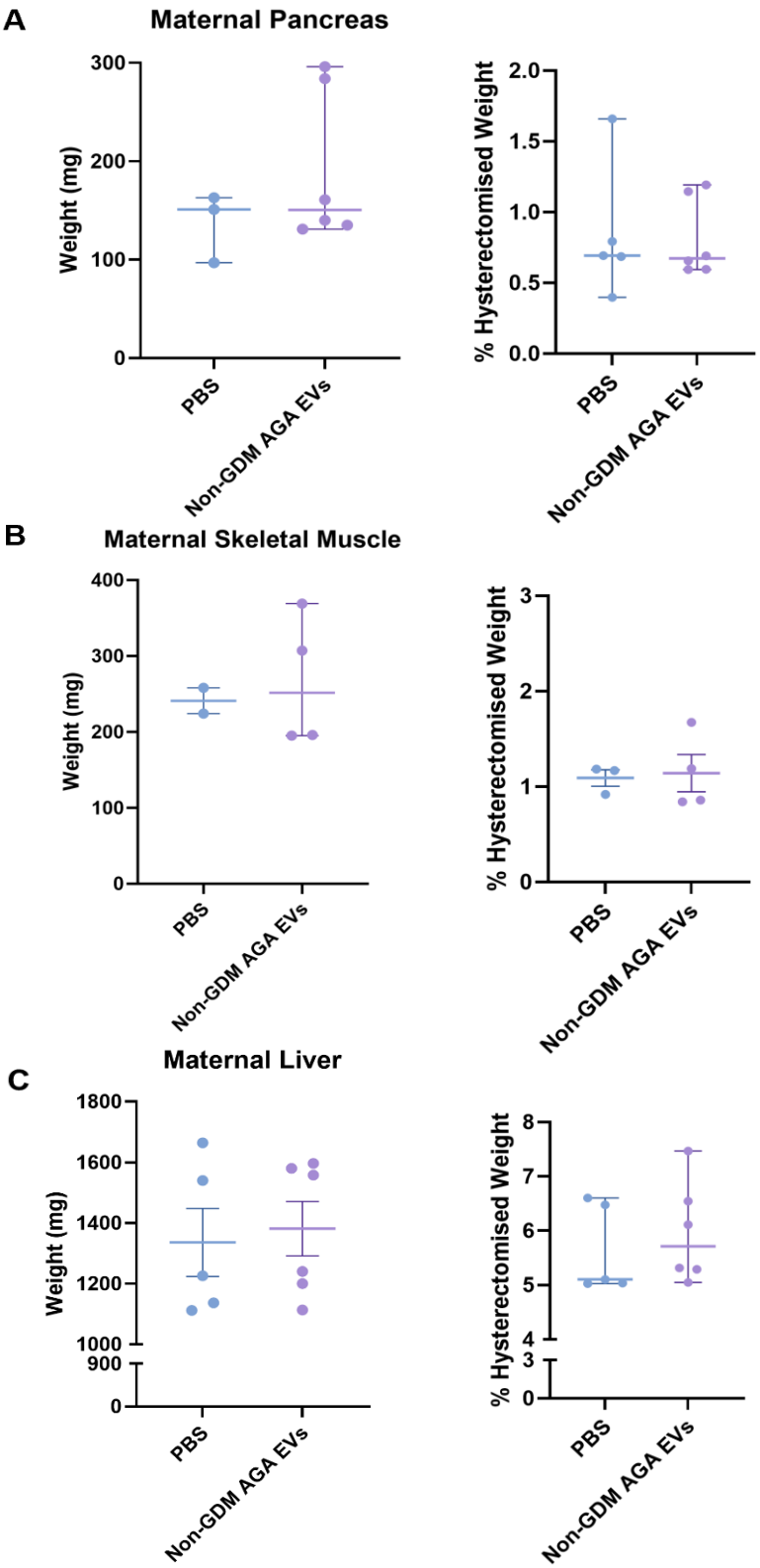

Figure 76 Maternal metabolic organ weights in mice treated with PBS or human maternal plasma EVs from Non-GDM AGA pregnancies during gestation.

Healthy pregnant C57BL6/J female mice were injected with PBS or human maternal plasma EVs from healthy uncomplicated (non-GDM AGA) pregnancies at E11.5, E13.5 and E15.5. Mothers were sacrificed at E18.5 and absolute pancreatic, liver and skeletal muscle weights were recorded alongside maternal hysterectomised weights. Normally distributed data was analysed using an unpaired t-test and presented as mean±SEM. Data that was not normally distributed was analysed using nonparametric Mann-Whitney test and data presented as median with 95% CI.

Indicators of cardiac hypertrophy were also measured to assess maternal cardiovascular health (451). However, no difference in maternal cardiac tissue, tibia length or heart weight: tibea length was observed following treatment with human maternal pregnancy EVs compared to control dams (**Figure *77***).

Maternal plasma metabolites were measured as indicators of metabolic health status. Glucose, leptin, cholesterol and triglyceride levels were higher in dams treated with maternal pregnancy EVs compared to control dams, however these increases did not reach statistical significance. No changes were observed in FFA levels (**Figure *78***).

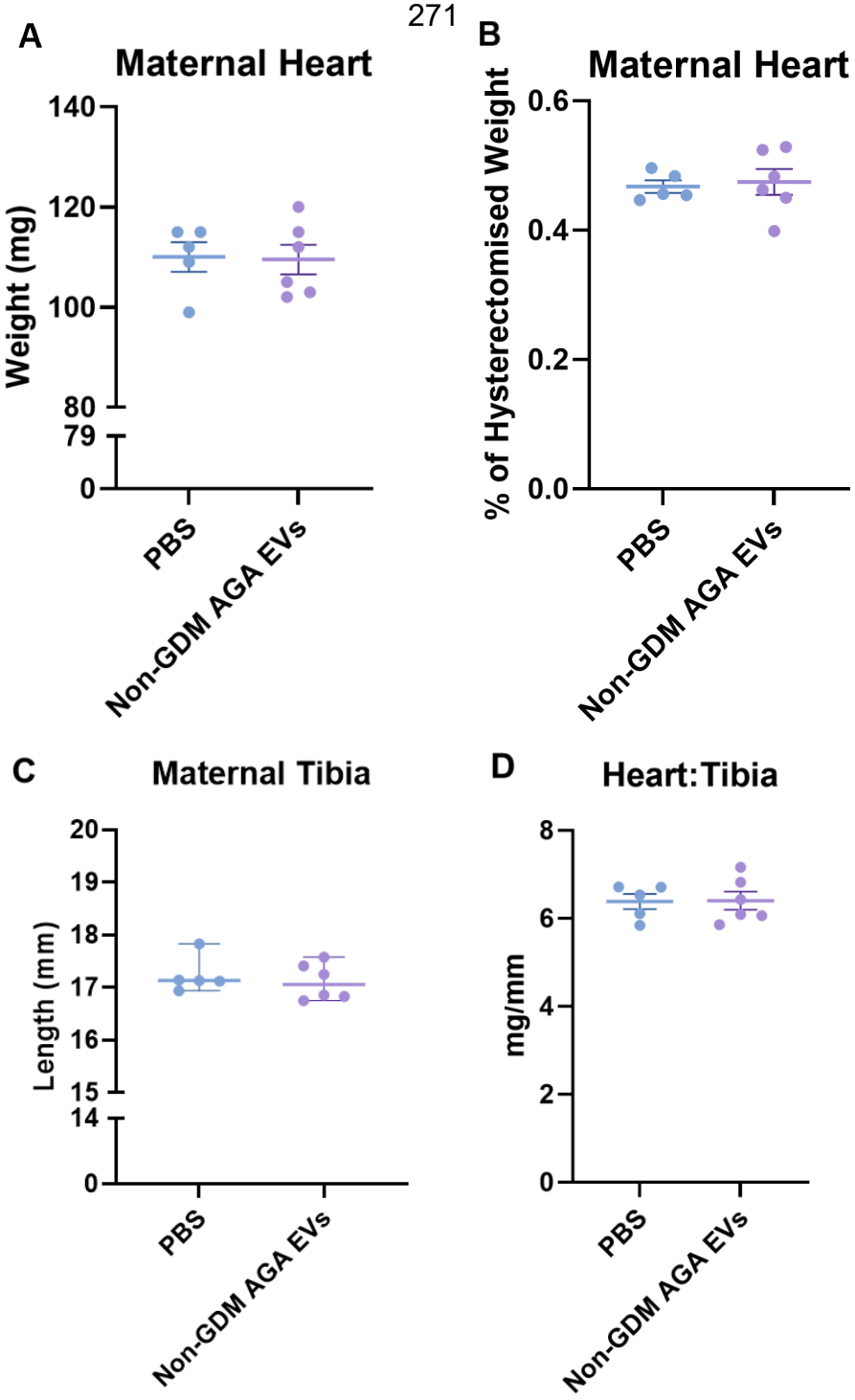

Figure 77 Maternal cardiac tissue weight and cardiac hypertrophy indicators in mice treated with PBS or human maternal plasma EVs from healthy uncomplicated (Non-GDM AGA) pregnancies during gestation.

Healthy pregnant C57BL6/J female mice were injected with PBS or human maternal plasma EVs from healthy uncomplicated (non-GDM AGA) pregnancies at E11.5, E13.5 and E15.5. Mothers were sacrificed at E18.5 and cardiac tissue weight, hysterectomised weight and tibia length were recorded. Normally distributed data was analysed using an unpaired t-test and presented as mean±SEM. Data that was not normally distributed was analysed using nonparametric Mann-Whitney test and data presented as median with 95% CI.

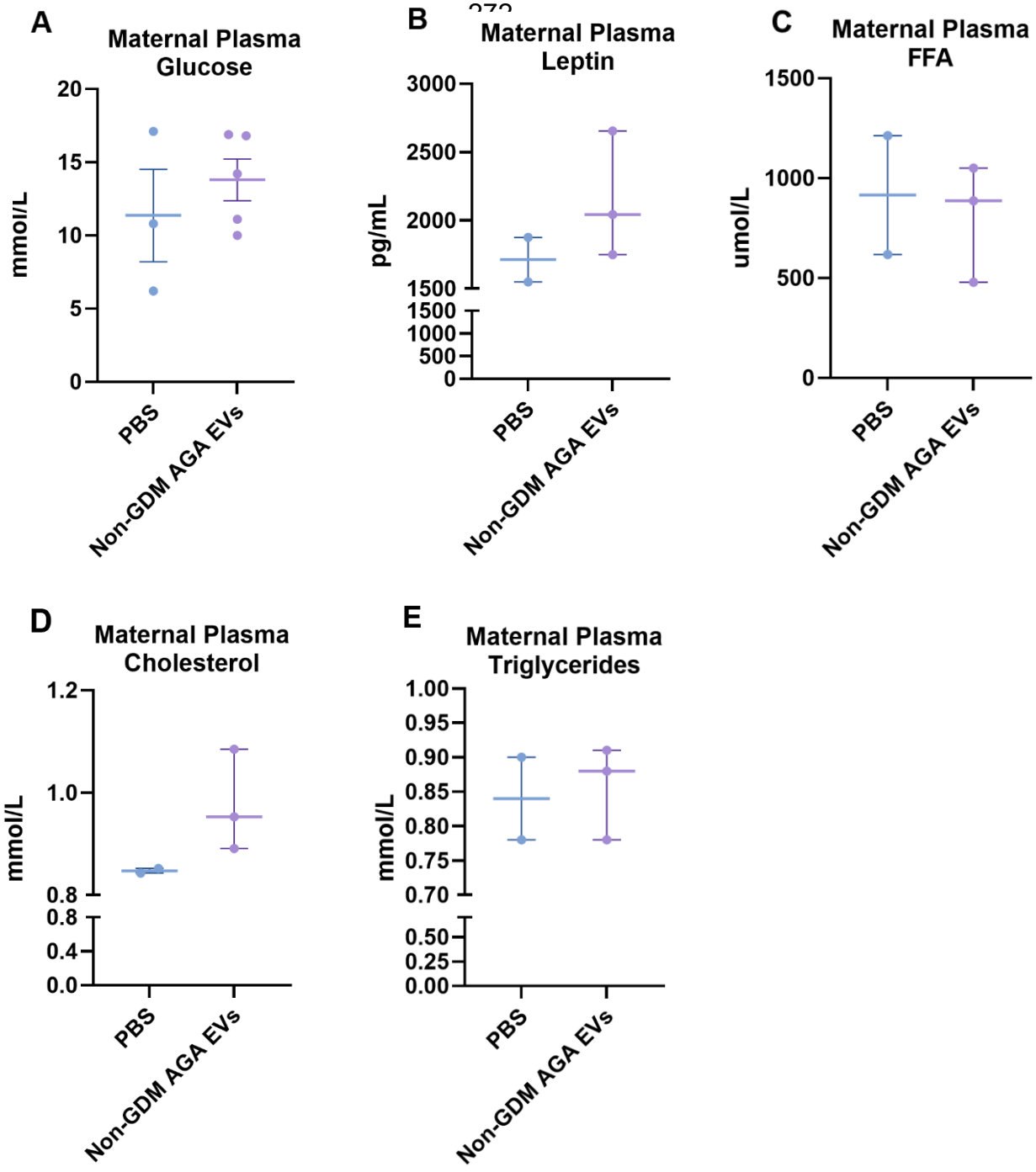

Figure 78 Maternal plasma glucose, leptin, FFA, cholesterol and triglyceride levels in mice treated with PBS or human maternal plasma EVs from non-GDM AGA pregnancies during gestation.

Healthy pregnant C57BL6/J female mice were injected with PBS or human plasma EVs from healthy uncomplicated (non-GDM AGA) pregnancies at E11.5, E13.5 and E15.5. Mothers were sacrificed at E18.5 and maternal blood was processed for plasma extraction. Plasma metabolites were analysed at Core Biochemical Assay Laboratory (CBAL), Cambridge. Normally distributed data was analysed using an unpaired t-test and presented as mean±SEM. Data that was not normally distributed was analysed using nonparametric Mann-Whitney test and data presented as median with 95% CI.

5.4.5 Establishing the Impact of Maternal Pregnancy EVs from Human GDM Pregnancies on Fetal-Placental Growth and Maternal Health in Mice

5.4.5.1 Maternal GDM pregnancy EVs do not impact mouse pregnancy litter size, resorptions, maternal survival and fetal sex.

Using human maternal plasma small EVs from uncomplicated (non-GDM AGA) pregnancies, it was demonstrated that delivery of human pregnancy EVs to mice influenced fetal and placental growth but no effect was observed on maternal health. Moreover, GDM is known to be associated with adverse fetal and maternal pregnancy outcomes (10,15,19,304,442), where it has previously been demonstrated that EVs may play a role in the severity and outcomes of pregnancies complicated by GDM (259,263,277,278,282,301,548,556). To determine the impact of maternal EVs from GDM pregnancies on both mother and fetus, human maternal plasma small EVs from GDM AGA pregnancies were injected into healthy pregnant mice at E11.5, E13.5 and E15.5 at an *in-vivo* concentration of 1.5E+9 particles/mL. Pups were then culled, weighed and processed at E18.5. Pregnancy outcomes of these mice were compared to those treated with human maternal plasma small EVs from non-GDM AGA pregnancies.

EVs from GDM AGA pregnancies had no significant impact on litter size, where dams treated with non-GDM AGA small EVs demonstrated a median litter size of 7 compared to 5.5 from those treated with GDM AGA small EVs (p=0.658; n=6/8, respectively) (**Figure 79**A). The number of resorptions and male offspring per litter was similar for both treatment groups (**Figure 79**B,C). Maternal survival was unaffected, where all dams survived throughout pregnancy (data not shown).

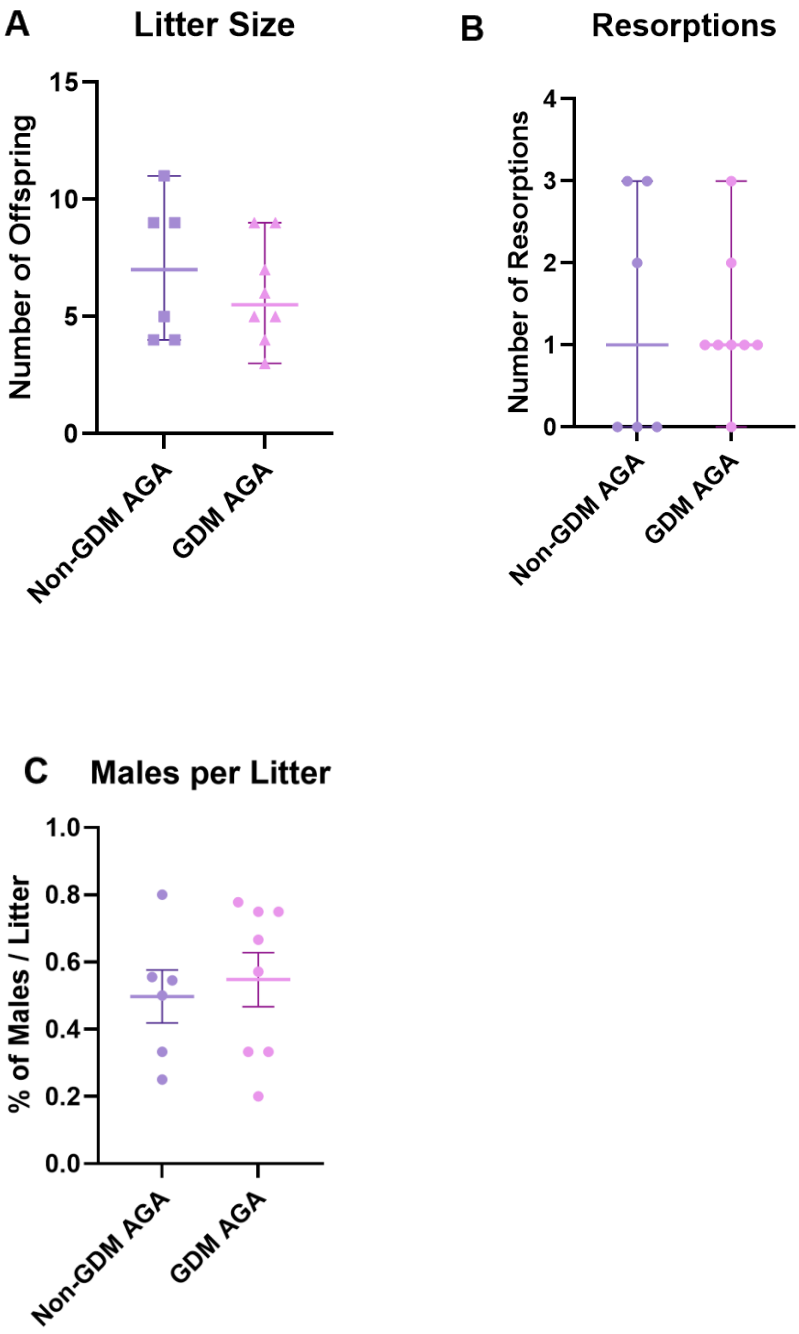

Figure 79 Litter outcomes of mice exposed to human maternal plasma EVs from healthy uncomplicated (non-GDM AGA) pregnancies or GDM AGA pregnancies during gestation.

Litter size, resorptions and males per litter were measured in response to treatments. Mann-Whitney test was performed to determine statistical significance of non-parametric data, presented as median with 95% CI. Unpaired t-test was performed to measure statistical significance of parametric data, presented as mean±SEM.

5.4.5.2 Human maternal EVs from GDM pregnancies impact fetal growth.

Human maternal plasma small EVs from GDM AGA pregnancies significantly decreased fetal growth compared to small EVs from non-GDM AGA pregnancies (from 1.271 ± 0.023 g to 1.242 ± 0.019 g; p=0.009, adjusted for fetal sex and litter size; n=42 clustered to 6 dams/n=48 clustered to 8 dams) (**Figure *80***). When separating the data based on fetal sex, the effect was similar for males and females, where there was a trend towards a reduction in birthweight for both males (from 1.317 ± 0.036 g to 1.268 ± 0.022 g; p=0.292) and females (from 1.252 ± 0.035 g to 1.201 ± 0.028 g; p=0.322) (**Figure *80***, **Appendix *14***, **Appendix *15***).

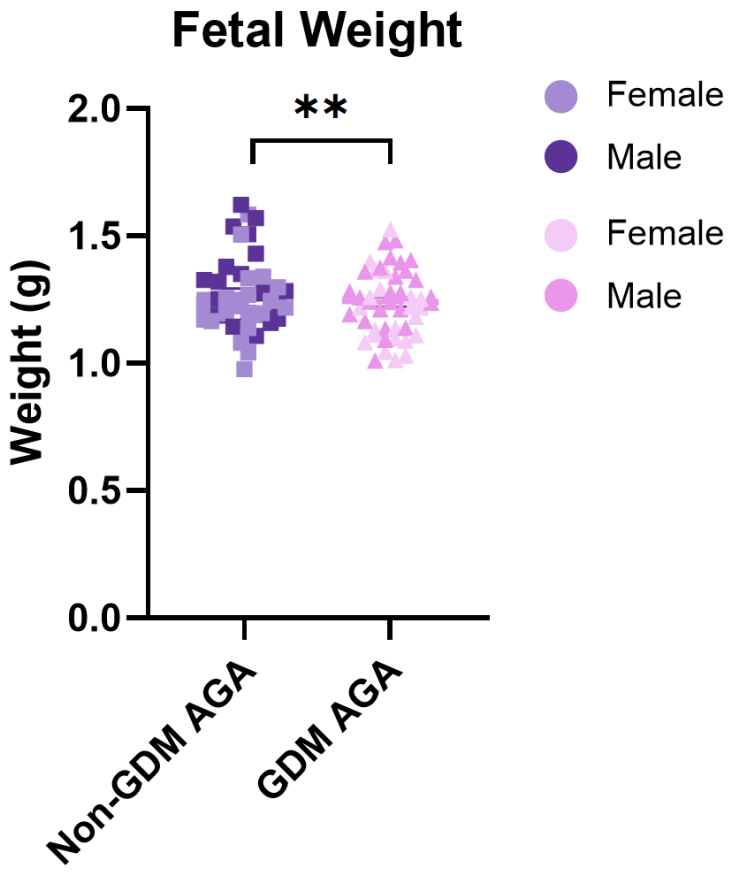

Figure 80 Fetal weight of mice exposed to human maternal plasma EVs from healthy uncomplicated pregnancies (Non-GDM AGA) or GDM pregnancies (with AGA outcomes) during gestation at E18.5.

Healthy pregnant C57BL6/J female mice were injected human maternal EVs from healthy uncomplicated (non-GDM AGA) pregnancies or GDM AGA pregnancies at E11.5, E13.5 and E15.5 at a final *in-vivo* concentration of 1.5E+9 particles/mL. Mice were sacrificed at E18.5 and pups were weighed. Mixed-effects non-linear regression model was performed using Stata, where each litter was clustered and adjustments were made for fetal sex and litter size. Data presented as mean±SEM; *=p ≤ 0.01. Light data points; female, dark data points; male.

5.4.5.3 Human maternal EVs from GDM pregnancies do not impact placental growth and have no effect on fetal-placental weight ratio.

Although a reduction in placental weight was observed, human maternal plasma small EVs from GDM AGA pregnancies had no significant effect on mouse placental weight compared to small EVs from non-GDM AGA pregnancies (from 0.100 ± 0.002 g to 0.095 ± 0.002 g; p=0.536, adjusted for fetal sex and litter size; n=36 clustered to 5 dams/n=39 clustered to 7 dams) (**Figure *81***). When separating the data based on for fetal sex, it was demonstrated that plasma small EVs from GDM AGA pregnancies reduced male placental weight (from 0.103 ± 0.003 g to 0.095 ± 0.003 g; p=0.077) to a greater extent than females (from 0.097 ± 0.004 g to 0.096 ± 0.002 g; p=0.926) when compared to the impact of small EVs from non-GDM AGA pregnancies (**Figure *81***, **Appendix *16***, **Appendix *17***). There was no difference in the fetal:placental weight ratio between both treatment groups. This was also the case when the data was separated based on fetal sex (**Figure *82***, **Appendix *18***).

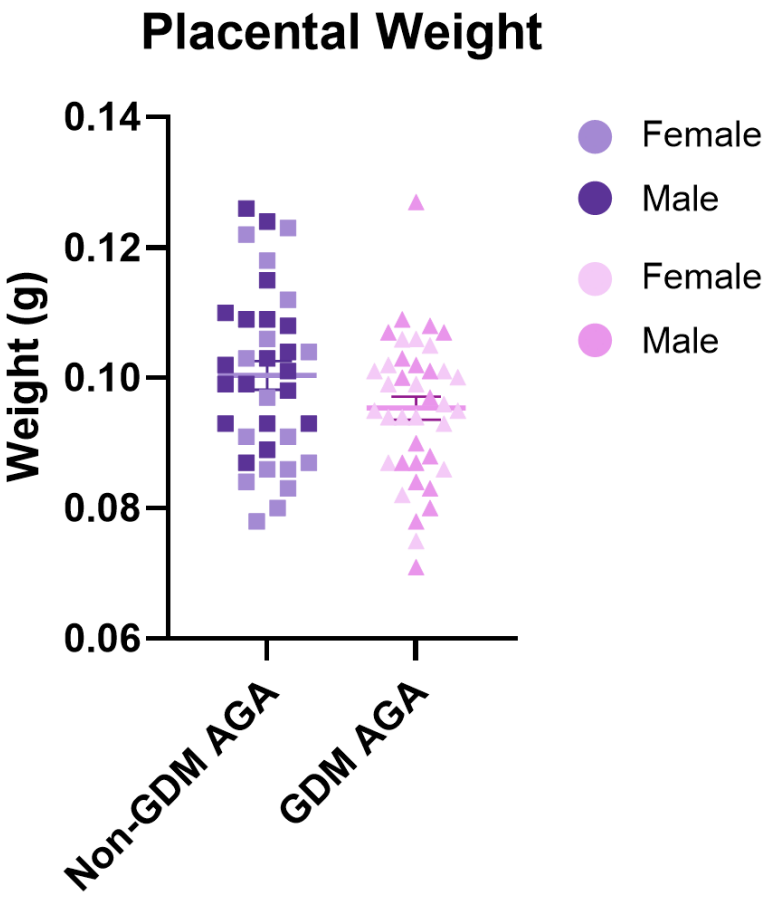

Figure 81 Placental weight of mice exposed to human maternal plasma EVs from healthy uncomplicated (non-GDM AGA) or GDM pregnancies (with AGA outcomes) during gestation at E18.5.

Healthy pregnant C57BL6/J female mice were injected human maternal EVs from healthy uncomplicated (non-GDM AGA) and GDM pregnancies at E11.5, E13.5 and E15.5 at a final *in-vivo* concentration of 1.5E+9 particles/mL. Mice were sacrificed at E18.5, where placentae and pups were weighed. Mixed-effects non-linear regression model was performed using Stata, where each litter was clustered and adjustments were made for fetal sex and litter size. Data presented as mean±SEM. Light data points; female, dark data points; male.

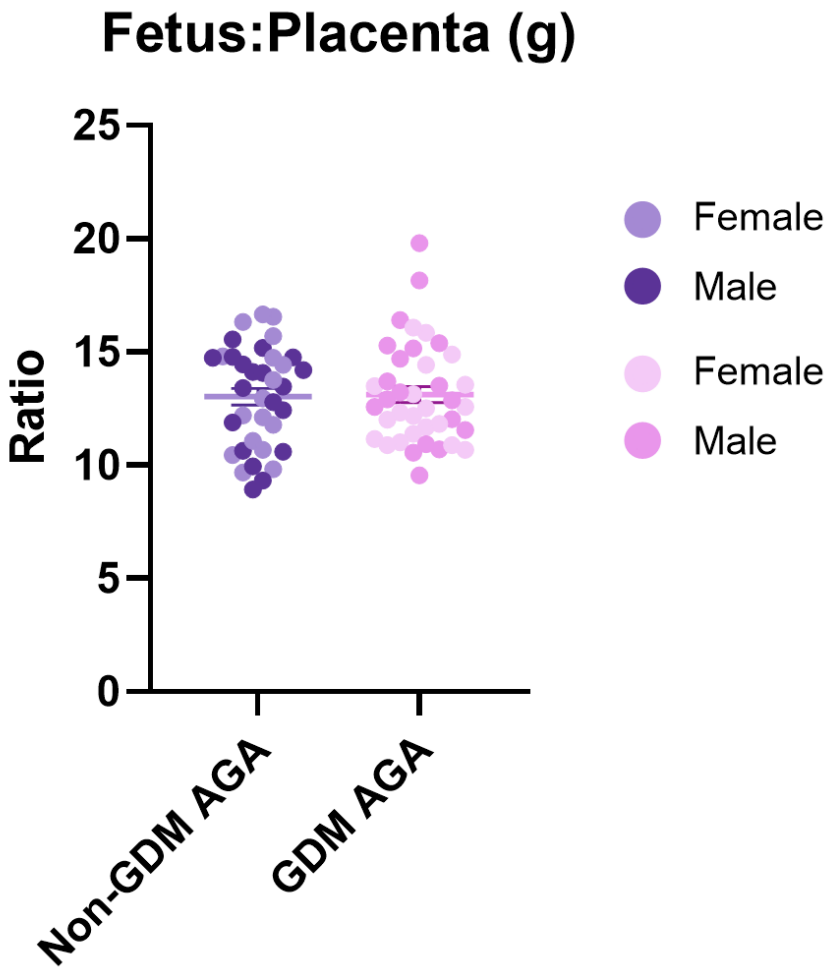

Figure 82 Fetal:placental weight of mice exposed to human maternal plasma EVs from healthy uncomplicated pregnancies (Non-GDM AGA) or GDM pregnancies (with AGA outcomes) during gestation at E18.5.

Healthy pregnant C57BL6/J female mice were injected human maternal EVs from healthy uncomplicated (non-GDM AGA) pregnancies or GDM AGA pregnancies at E11.5, E13.5 and E15.5 at a final *in-vivo* concentration of 1.5E+9 particles/mL. Mice were sacrificed at E18.5 and pups and placentae were weighed. Mixed-effects non-linear regression model was performed using Stata, where each litter was clustered and adjustments were made for fetal sex and litter size. Data presented as mean±SEM. Light data points; female, dark data points; male.

5.4.5.4 Human maternal EVs from GDM pregnancies do not impact maternal cardiometabolic health.

Maternal weight before pregnancy was similar for dams treated with human maternal small EVs from non-GDM AGA and GDM AGA pregnancies (**Figure *83***A). At E11.5, dams treated with non-GDM AGA small EVs demonstrated a heavier weight than dams treated with GDM AGA small EVs, however maternal weight was similar on E13.5 and E15.5 between both treatment groups (**Figure *83***A). When calculating maternal weight gain throughout pregnancy, it was demonstrated that dams treated with GDM AGA EVs gained less weight than those treated with non-GDM AGA small EVs. In particular, at E11.5, dams treated with GDM AGA EVs were significantly lighter (5.171 ± 0.294 g; n=8) than those treated with healthy uncomplicated EVs (6.275 ± 0.377 g; n=6) (p=0.043) (**Figure *83***B). By E18.5, dams treated with GDM AGA small EVs were lighter than dams treated with non-GDM AGA small EVs (from 34.49 ± 1.722 g to 32.21 ± 0.866 g; p=0.224) (**Figure *84***A). Moreover, maternal hysterectomised weight was similar between both treatment groups at E18.5, suggesting that any differences in maternal weight gain were likely attributed to litter size and fetal weights (**Figure *84***B). However, it was demonstrated that dams treated with GDM AGA small EVs gained marginally less pregnancy weight than dams treated with non-GDM AGA small EVs compared to their pre-pregnancy weight, although this finding was not significant (p=0.672) (**Figure *84***C).

No change was observed in maternal pancreas weight (**Figure *85***A), and although a reduction was observed in maternal liver and skeletal muscle weight in dams treated with GDM AGA small EVs (**Figure *85***B,C), this was not significant. Cardiac hypertrophy indicators were also measured and although a decrease was observed in absolute maternal cardiac tissue weight in response to GDM AGA small EVs compared to non-GDM AGA EVs (from 109.5 ± 2.975 g to 103.6 ± 1.861 g; p=0.104; n=6/8, respectively), this was not significant (**Figure *86***A). When normalised for maternal hysterectomised weight and tibia length, no change was observed (**Figure *86***B,C,D). Maternal plasma metabolites were also assessed, however there were no statistically significant differences in any of the parameters measured (**Figure *87***).

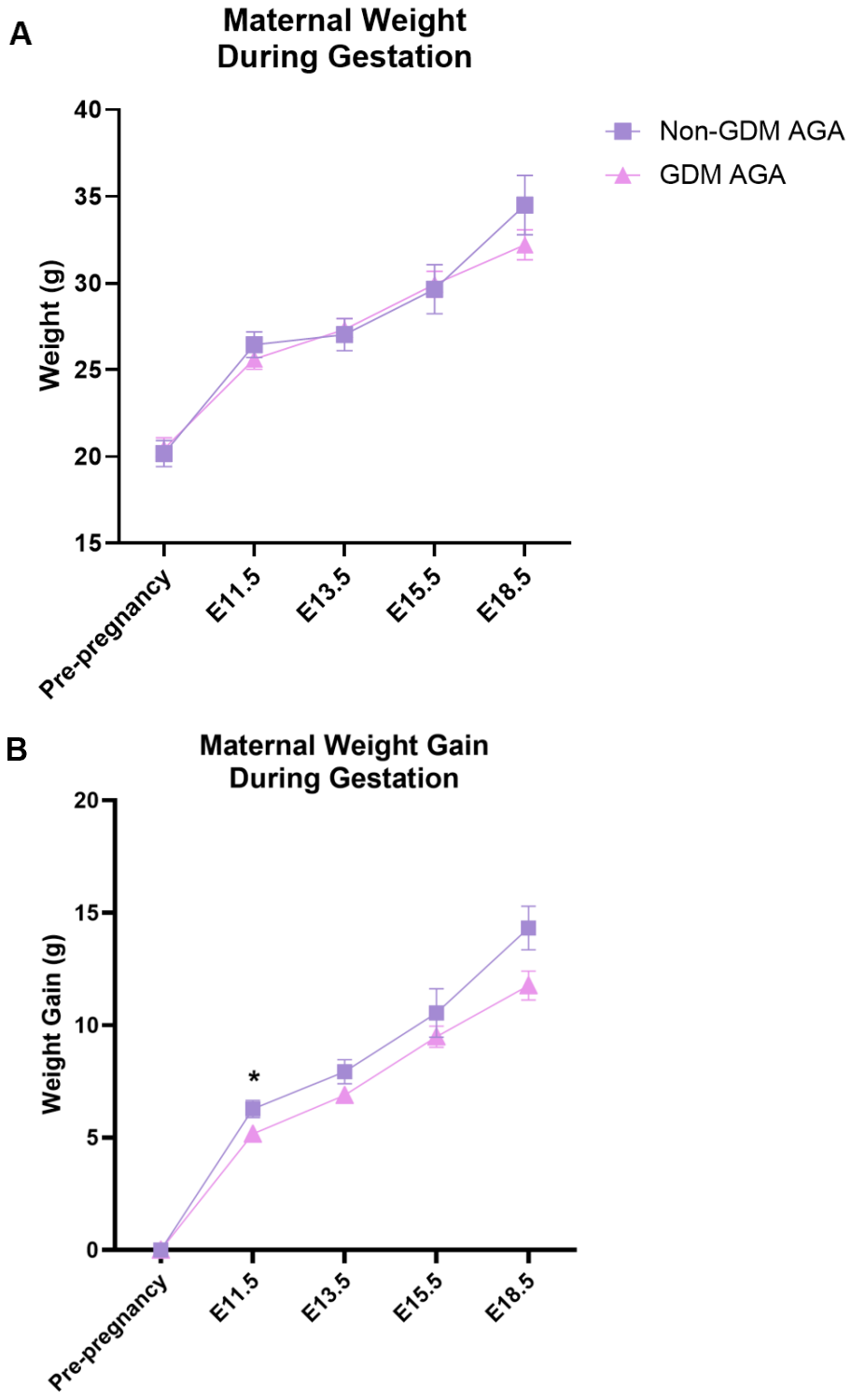

Figure 83 Maternal weight and weight gain during gestation in mice treated with human maternal plasma EVs from healthy uncomplicated (Non-GDM-AGA) or GDM (with AGA outcomes) pregnancies.

Healthy pregnant C57BL6/J female mice were injected with human maternal EVs from healthy uncomplicated (non-GDM AGA) or GDM (with AGA outcomes) pregnancies at E11.5, E13.5 and E15.5 before being sacrificed at E18.5. Pre-pregnancy weights were recorded and maternal weight measured at each injection time-point and before birth. Two-way ANOVA (with Geisser-Greenhouse correction) followed by a Tukey's multiple comparisons test were performed. Data presented as mean±SEM; *=$p<0.05$.

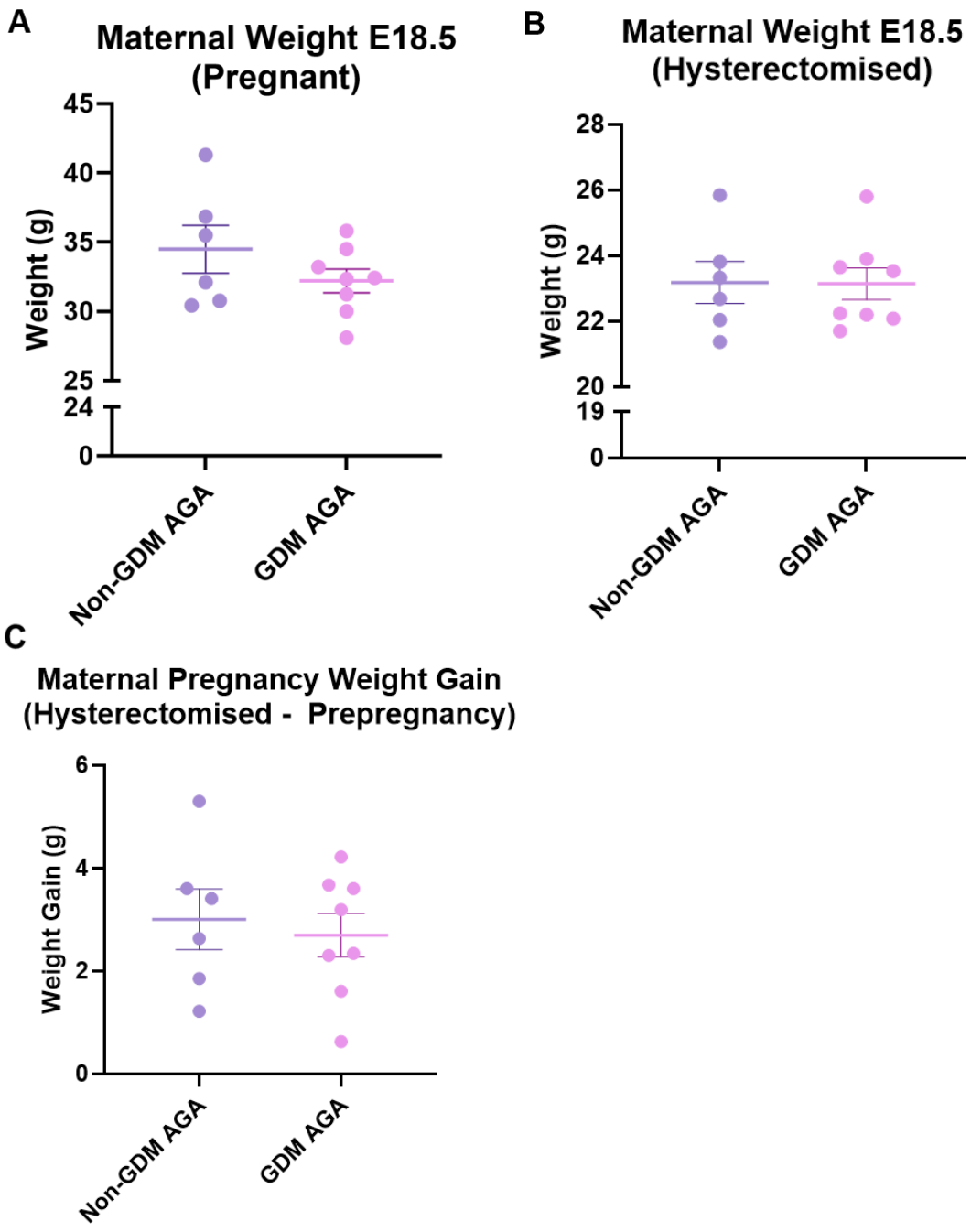

Figure 84 Maternal pregnancy weight, hysterectomised weight and overall pregnancy weight gain of mice treated with human maternal plasma EVs from healthy uncomplicated (non-GDM AGA) or GDM (with AGA outcomes) pregnancies during gestation.

Healthy pregnant C57BL6/J female mice were injected with human plasma EVs from healthy uncomplicated (Non-GDM AGA) or GDM (with AGA outcomes) pregnancies at E11.5, E13.5 and E15.5 before being sacrificed at E18.5. Pre-pregnancy weights were recorded and maternal pregnancy and hysterectomised weights at E18.5 were measured. Unpaired t-test was performed. Data presented as mean±SEM.

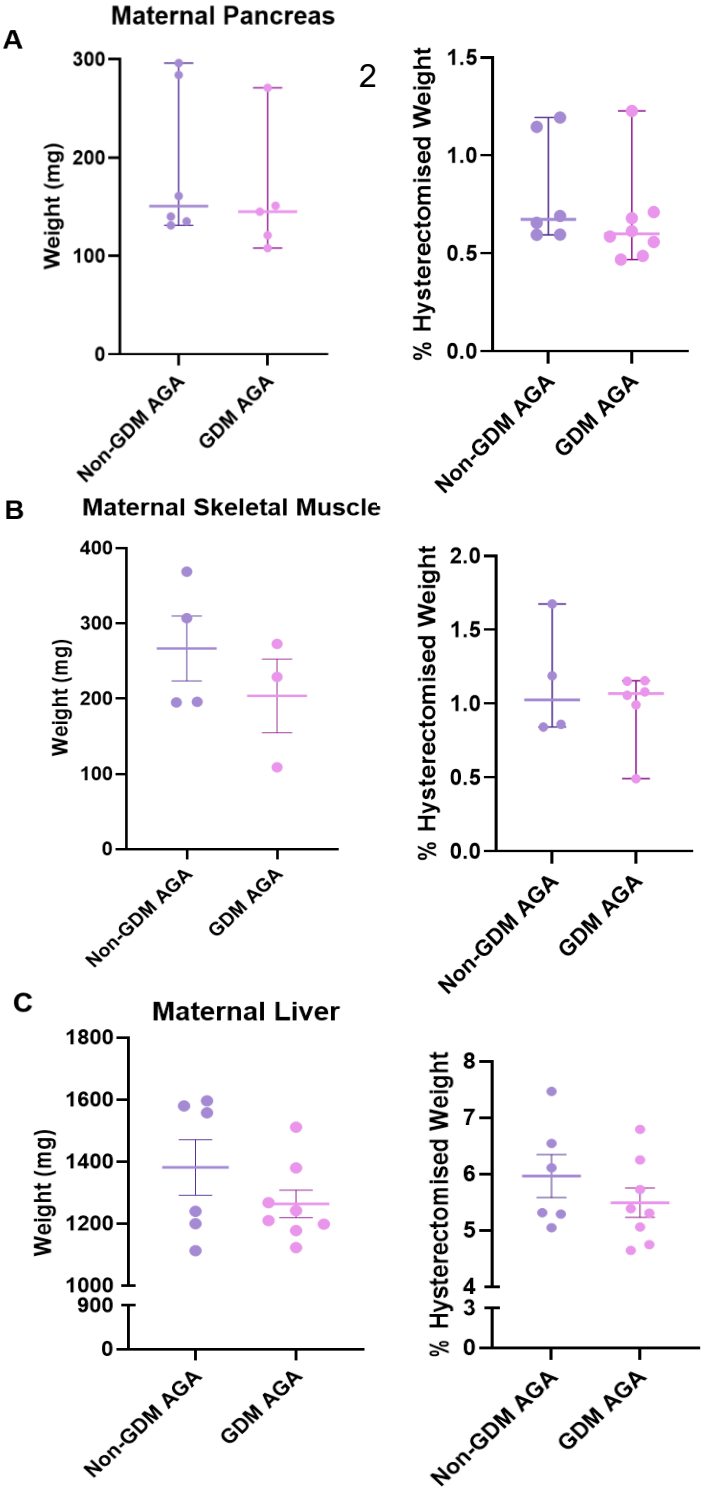

Figure 85 Maternal metabolic organ weights in mice treated with human maternal plasma EVs from healthy uncomplicated (Non-GDM-AGA) and GDM (with AGA outcomes) pregnancies during gestation.

Healthy pregnant C57BL6/J female mice were injected with human maternal plasma EVs from healthy uncomplicated (Non-GDM AGA) and GDM (with AGA outcomes) pregnancies at E11.5, E13.5 and E15.5. Mothers were sacrificed at E18.5 and absolute pancreatic, liver and skeletal muscle weights were recorded alongside maternal hysterectomised weights. Normally distributed data was analysed using an unpaired t-test and presented as mean±SEM. Data that was not normally distributed was analysed using nonparametric Mann-Whitney test and data presented as median with 95% CI.

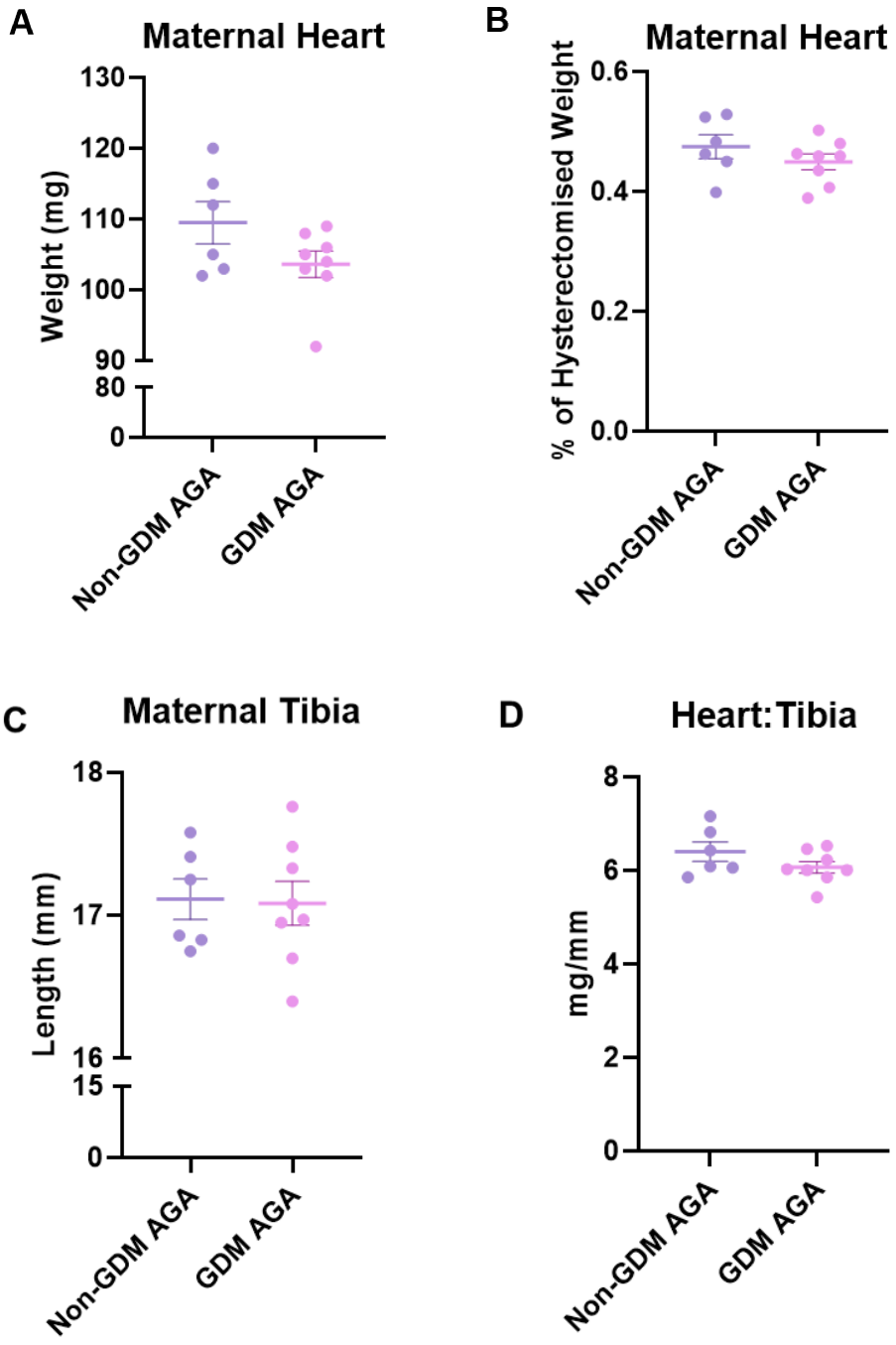

Figure 86 Maternal cardiac tissue weight and cardiac hypertrophy indicators in mice treated with human maternal plasma EVs from healthy uncomplicated (non-GDM AGA) and GDM (with AGA outcomes) pregnancies during gestation.

Healthy pregnant C57BL6/J female mice were injected with human maternal plasma EVs from healthy uncomplicated (Non-GDM AGA) or GDM (with AGA outcomes) pregnancies at E11.5, E13.5 and E15.5. Mothers were sacrificed at E18.5 and cardiac tissue weight, hysterectomised weight and tibia length were recorded. Data was analysed using an unpaired t-test and presented as mean±SEM.

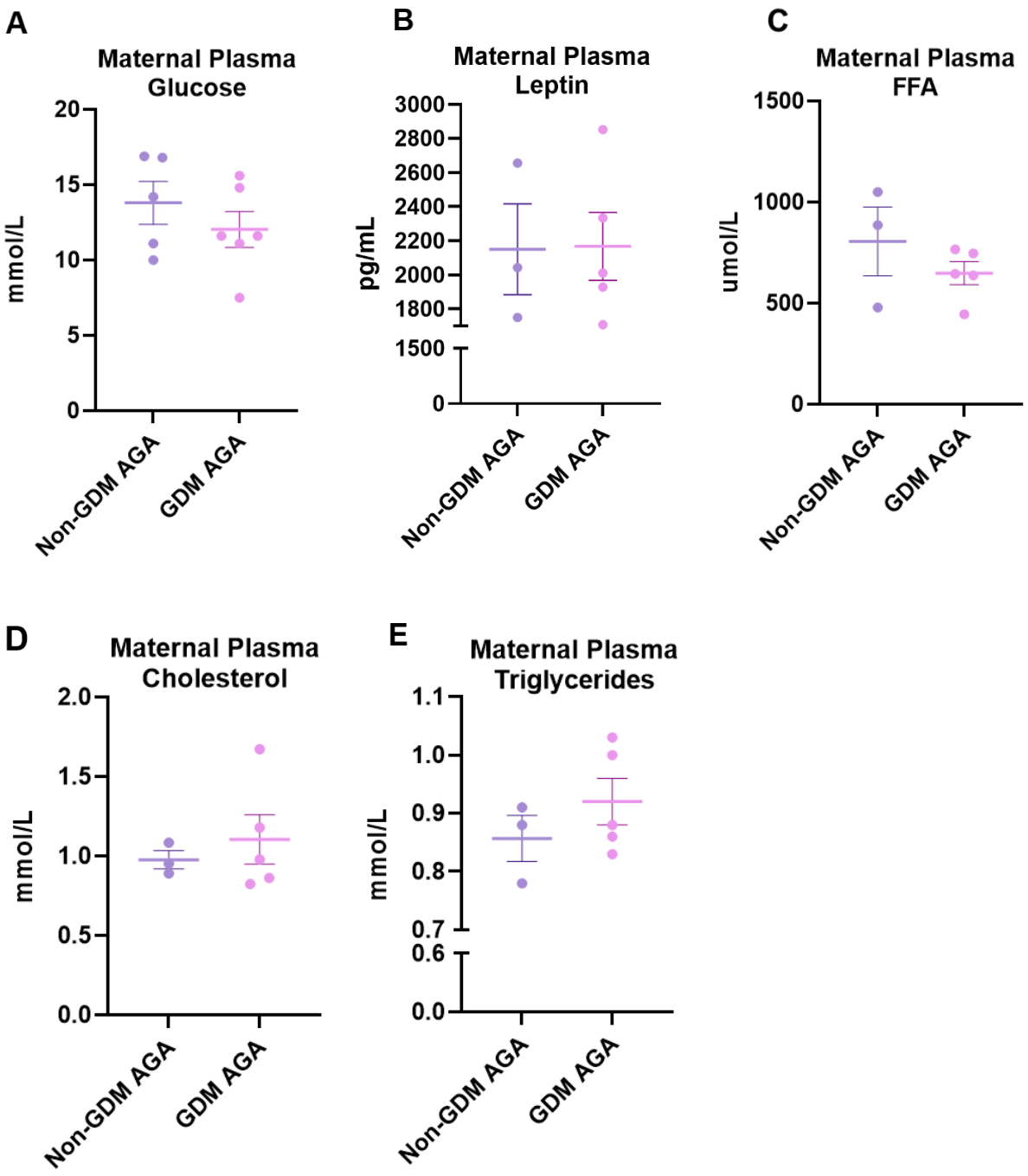

Figure 87 Maternal plasma glucose, leptin, FFA, cholesterol and triglyceride levels in mice treated with human maternal plasma EVs from healthy uncomplicated (Non-GDM AGA) or GDM (with AGA outcomes) pregnancies during gestation.

Healthy pregnant C57BL6/J female mice were injected with human plasma EVs from healthy uncomplicated (Non-GDM AGA) or GDM (with AGA outcomes) pregnancies at E11.5, E13.5 and E15.5. Mothers were sacrificed at E18.5 and maternal blood was processed for plasma extraction. Plasma metabolites were analysed at Core Biochemical Assay Laboratory (CBAL), Cambridge. Data was analysed using an unpaired t-test and presented as mean±SEM.

5.4.6 Establishing the Impact of Human Maternal EVs from GDM LGA Pregnancies on Mouse Litter Outcomes, Feto-Placental Growth and Maternal Outcomes

5.4.6.1 Human maternal EVs from GDM-LGA pregnancies do not impact mouse pregnancy litter size, resorptions, maternal survival and fetal sex.

GDM is associated with LGA outcomes, where offspring are at increased risk of cardiometabolic complications throughout life (33,40,396). To determine the impact of human maternal EVs from GDM-LGA pregnancies on both mother and fetus, healthy pregnant mice were injected with human maternal small EVs from GDM-AGA and GDM-LGA pregnancies at E11.5, E13.5 and E15.5 at an *in-vivo* concentration of 1.5E+9 particles/mL, before pups and placentae were weighed and processed at E18.5. Mouse offspring litter size was increased with human maternal small EVs from GDM LGA pregnancies compared to GDM-AGA pregnancies (median size of 7 and 5.5, respectively), however this change was statistically insignificant (p=0.218; n=7/8, respectively) (**Figure *88***A). The number of resorptions and male offspring per litter was similar for both treatment groups (**Figure *88***B,C). Maternal survival was unaffected, where all dams survived throughout pregnancy (data not shown).

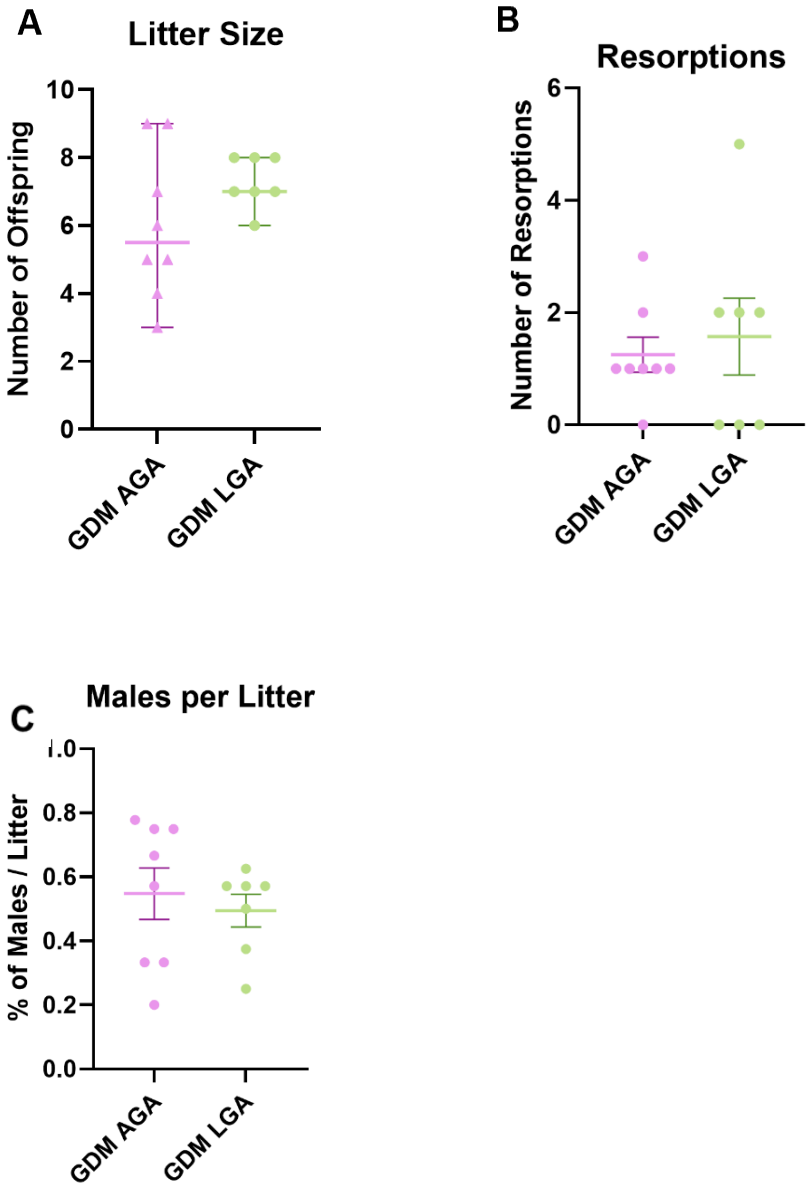

Figure 88 Litter outcomes of mice exposed to human maternal plasma EVs from GDM-AGA or GDM-LGA pregnancies during gestation.

Litter size, resorptions and offspring sex were measured in response to treatments. Mann-Whitney test was performed to determine statistical significance of nonparametric data, presented as median with 95% CI. Unpaired t-test was performed to determine statistical significance of parametric data, presented as mean±SEM.

5.4.6.2 Human maternal EVs from GDM-LGA pregnancies increase fetal growth but mainly impact male offspring.

At E18.5, it was demonstrated that GDM-LGA small EVs increased fetal weight by 9% compared to GDM-AGA small EVs (from 1.242 ± 0.019 g to 1.355 ± 0.020 g; p=0.024, adjusted for fetal sex and litter size; n=48 clustered to 8 dams/n=51 clustered to 7 dams) (**Figure *89***). When assessing both fetal sexes independently, it was demonstrated that the impact of maternal small EVs from GDM-LGA pregnancies on fetal growth was more significant for male offspring (from 1.268 ± 0.022 g to 1.367 ± 0.029 g; p=0.036) than female offspring (from 1.201 ± 0.028 g to 1.335 ± 0.033 g; p=0.052) when compared to GDM-AGA EVs (**Figure *89***, **Appendix *19***, **Appendix *20***).

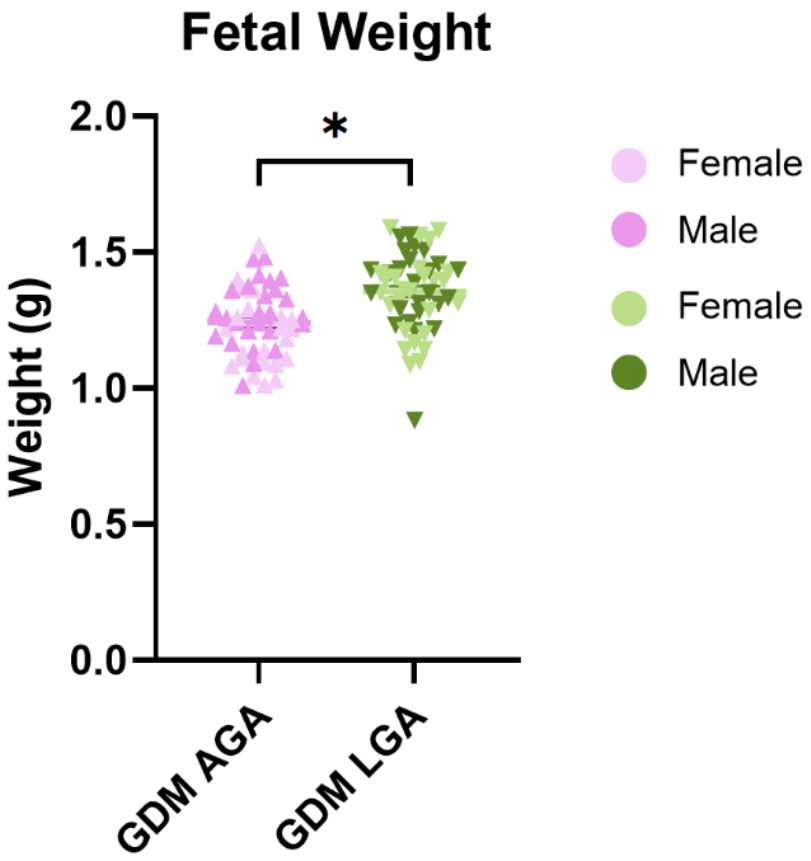

Figure 89 Fetal weight of mice exposed to human maternal plasma EVs from GDM pregnancies with AGA or LGA outcomes during gestation at E18.5.

Healthy pregnant C57BL6/J female mice were injected with human maternal EVs from GDM-AGA or GDM-LGA pregnancies at E11.5, E13.5 and E15.5 at a final *in-vivo* concentration of 1.5E+9 particles/mL. Mice were sacrificed at E18.5 and pups were weighed. Mixed-effects non-linear regression model was performed using Stata, where each litter was clustered and adjustments were made for fetal sex and litter size. Data presented as mean±SEM; *=p ≤ 0.05. Light data points; female, dark data points; male.

5.4.6.3 Human maternal EVs from GDM-LGA pregnancies do not impact placental growth and have no effect on fetal-placental weight ratio.

Although there was a trend towards increased placental weight for mice exposed to GDM-LGA small EVs compared to GDM-AGA small EVs (from 0.095 ± 0.002 g to 0.099 ± 0.002 g; n=39 clustered to 7 dams/n=36 clustered to 6 dams), this did not reach significance (p=0.829, adjusted for fetal sex and litter size) (**Figure *90***, **Appendix *21***, **Appendix *22***). No change was observed in fetus:placenta weight ratio (p=0.383) (**Figure *91***, **Appendix *23***).

When assessing both fetal sexes independently, no change was observed in either sex. However, a non-significant 7% increase in placental weight was observed for males (from 0.095 ± 0.003 g to 0.102 ± 0.003 g; p=0.144) in response to GDM LGA small EVs, whereas a non-significant 3% decrease in placental weight was observed for females (from 0.096 ± 0.002 g to 0.093 ± 0.003 g; p=0.554) (**Figure *90***, **Appendix *21***, **Appendix *22***). A non-significant increase in fetus: placental weight ratio was observed for female offspring (p=0.118) which was not observed in males in response to GDM LGA small EVs (**Figure *90***, **Figure *91***, **Appendix *21***, **Appendix *22***, **Appendix *23***). This suggests that pups grew proportionally to their placentae in each treatment group.

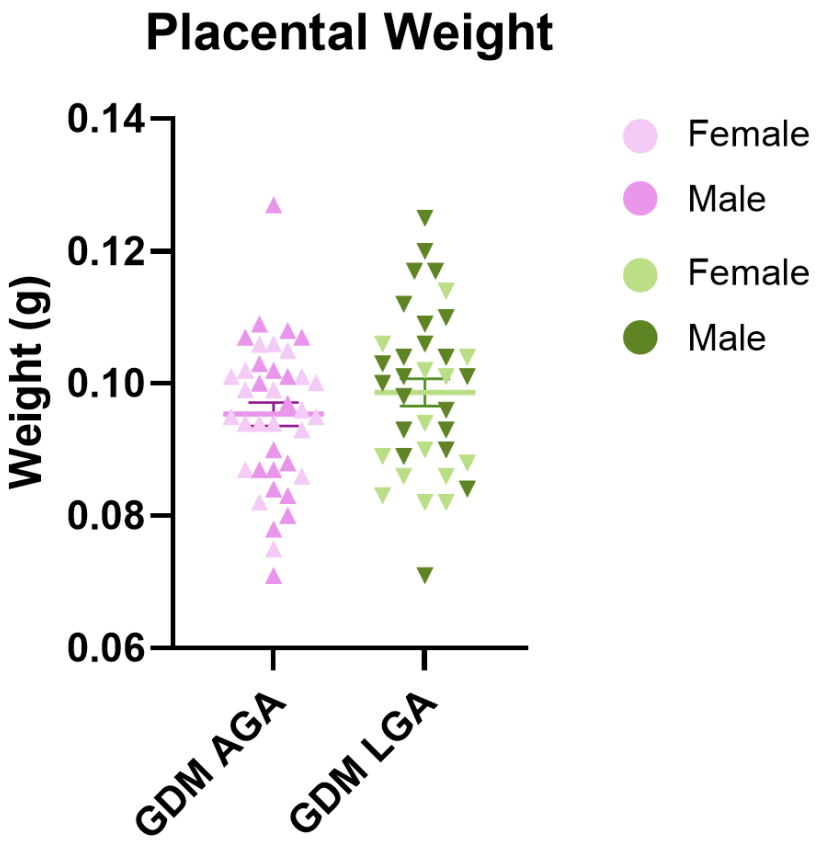

Figure 90 Placental weight of mice exposed to human maternal plasma EVs from GDM pregnancies with AGA of LGA outcomes during gestation at E18.5.

Healthy pregnant C57BL6/J female mice were injected human maternal EVs from GDM pregnancies with AGA or LGA outcomes at E11.5, E13.5 and E15.5 at a final *in-vivo* concentration of 1.5E+9 particles/mL. Mice were sacrificed at E18.5, where placentae and pups were weighed. Mixed-effects non-linear regression model was performed using Stata, where each litter was clustered and adjustments were made for fetal sex and litter size. Data presented as mean±SEM. Light data points; female, dark data points; male.

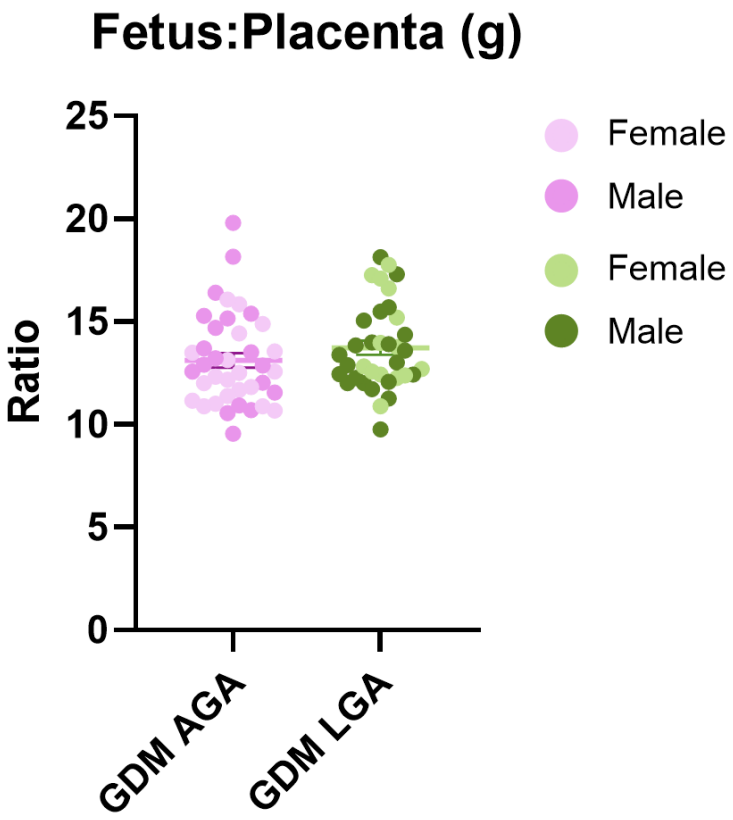

Figure 91 Fetal:placental weight of mice exposed to human maternal plasma EVs from GDM pregnancies with AGA or LGA outcomes during gestation at E18.5.

Healthy pregnant C57BL6/J female mice were injected human maternal EVs from GDM pregnancies with AGA or LGA outcomes at E11.5, E13.5 and E15.5 at a final *in-vivo* concentration of 1.5E+9 particles/mL. Mice were sacrificed at E18.5 and pups and placentae were weighed. Mixed-effects non-linear regression model was performed using Stata, where each litter was clustered and adjustments were made for fetal sex and litter size. Data presented as mean±SEM. Light data points; female, dark data points; male.

5.4.6.4 Human maternal EVs from GDM-LGA pregnancies impact maternal cardiometabolic health.

Throughout gestation, maternal absolute weight appeared to be increased in dams treated with GDM-LGA small EVs compared to GDM-AGA small EVs, however no statistical differences were observed (**Figure *92***A). Moreover, maternal weight gain was significantly increased for dams treated with GDM-LGA small EVs compared to GDM-AGA small EVs at E11.5 (from 5.171 ± 0.294 g to 5.991 ± 0.222 g; p=0.045; n=8/7, respectively) and E13.5 (from 6.883 ± 0.294 g to 7.867 ± 0.194 g; p=0.016; n=8/7, respectively) (**Figure *92***B). However, by E15.5 and E18.5, no differences in maternal weight gain were observed between both treatment groups (**Figure *92***B). At E18.5, no difference was observed in maternal absolute pregnancy weight, hysterectomised weight or pregnancy weight gain (when comparing maternal hysterectomised weight with pre-pregnancy weight) (**Figure *93***). This suggests that changes observed in maternal weight gain throughout pregnancy were likely attributed to the increased mass of the fetal and placental units.

No change was observed in maternal pancreas weight (**Figure *94***A) and although a change was observed in maternal liver and skeletal muscle weight in dams treated with GDM LGA small EVs (**Figure *94***B,C), these findings were not significant. Additionally, no significant differences were observed in maternal plasma metabolites between both treatment groups (**Figure *95***).

Maternal cardiac tissue weight was heavier in dams treated with GDM-LGA small EVs compared to dams treated with GDM-AGA small EVs (median weight of 104.5mg compared to 110.0mg; p=0.00439; n=8/7, respectively) (**Figure *96***A), While this effect was not observed when cardiac tissue weight was calculated as a % of maternal hysterectomised weight (**Figure *96***B), when expressed as maternal heart weight:tibia length ratio, a marker of cardiac hypertrophy (451), an increase was observed for dams treated with GDM-LGA small EVs compared to dams treated with GDM-AGA small EVs (from 6.069 ± 0.12437 g to 6.545 ± 0.14659 g; p=0.0263; n=8/7, respectively) (**Figure *96***D). This was not attributed to differences in maternal tibia length (**Figure *96***C), suggesting that GDM-LGA small EVs were inducing cardiac hypertrophy in pregnant dams.

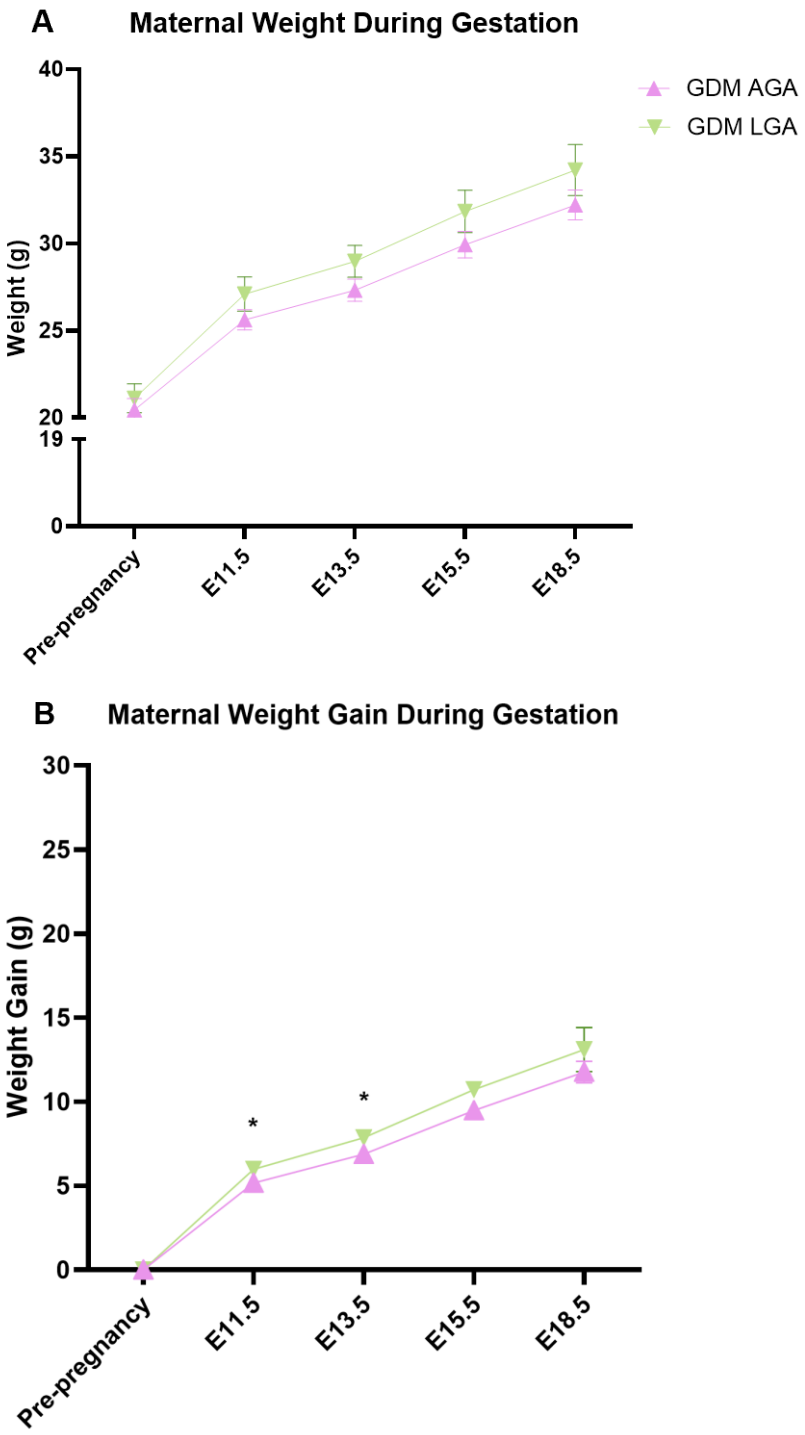

Figure 92 Maternal weight and weight gain during gestation in mice treated with human maternal plasma EVs from GDM pregnancies with AGA or LGA outcomes.

Healthy pregnant C57BL6/J female mice were injected with human maternal plasma EVs from GDM pregnancies with AGA or LGA outcomes at E11.5, E13.5 and E15.5, before being sacrificed at E18.5. Pre-pregnancy weights were recorded and maternal weight measured at each injection time-point and before birth. Two-way ANOVA (with Geisser-Greenhouse correction) followed by a Tukey's multiple comparisons test were performed. Data presented as mean±SEM; *=$p<0.05$.

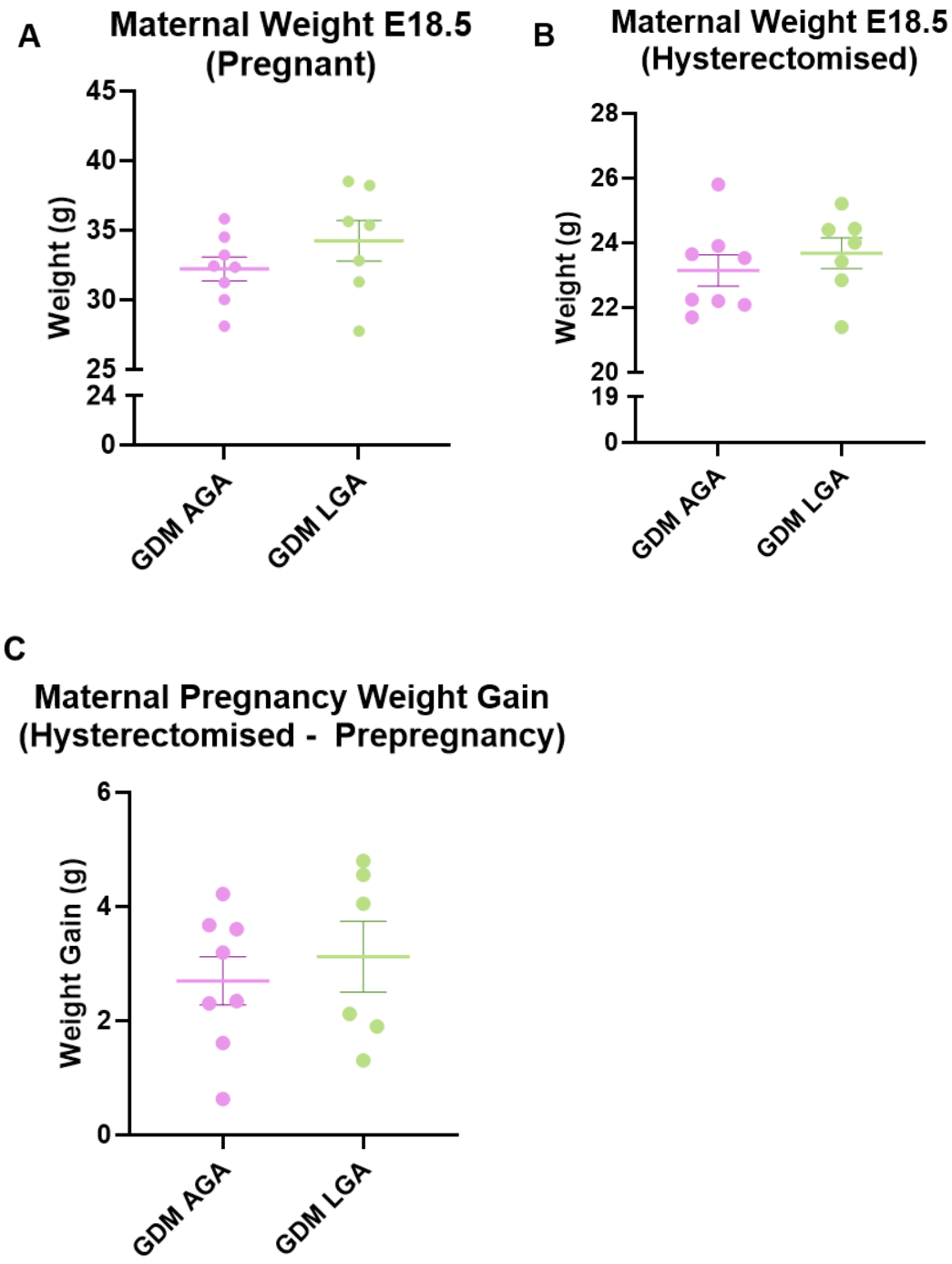

Figure 93 Maternal pregnancy weight, hysterectomised weight and overall pregnancy weight gain of mice treated with human maternal plasma EVs from GDM pregnancies with AGA or LGA outcomes during gestation.

Healthy pregnant C57BL6/J female mice were injected with human plasma EVs from GDM pregnancies with AGA or LGA outcomes at E11.5, E13.5 and E15.5 before being sacrificed at E18.5. Pre-pregnancy weights were recorded and maternal pregnancy and hysterectomised weights at E18.5 were measured. Unpaired t-test was performed. Data presented as mean±SEM.

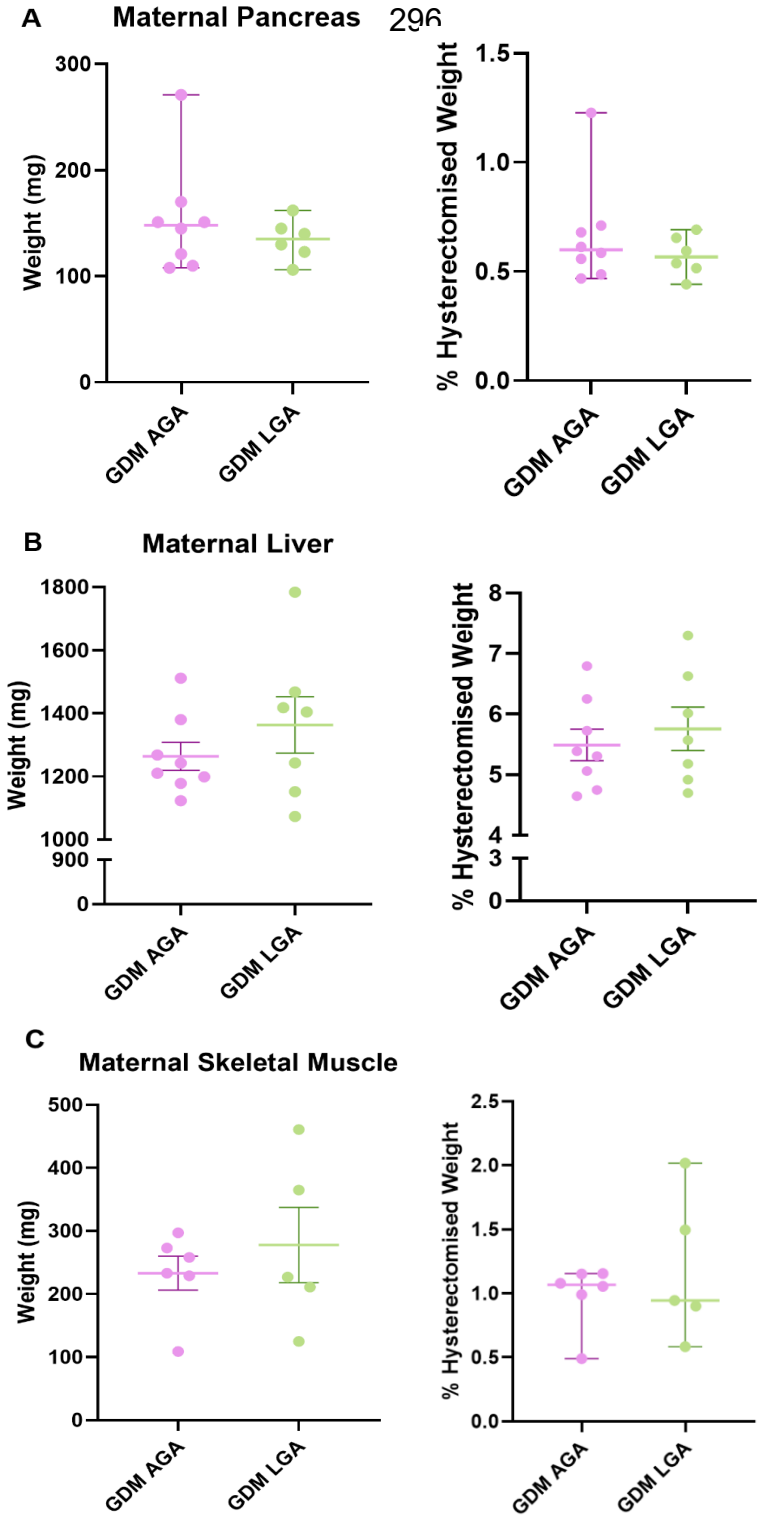

Figure 94 Maternal metabolic organ weights in mice treated with human maternal plasma EVs from GDM pregnancies with AGA or LGA outcomes during gestation.

Healthy pregnant C57BL6/J female mice were injected with human maternal plasma EVs from healthy GDM pregnancies with AGA or LGA outcomes at E11.5, E13.5 and E15.5. Maternal pancreas, liver and skeletal muscle weights were recorded alongside maternal hysterectomised weights. Normally distributed data was analysed using an unpaired t-test and presented as mean±SEM. Data that was not normally distributed was analysed using a nonparametric Mann-Whitney test and data presented as median with 95% CI.

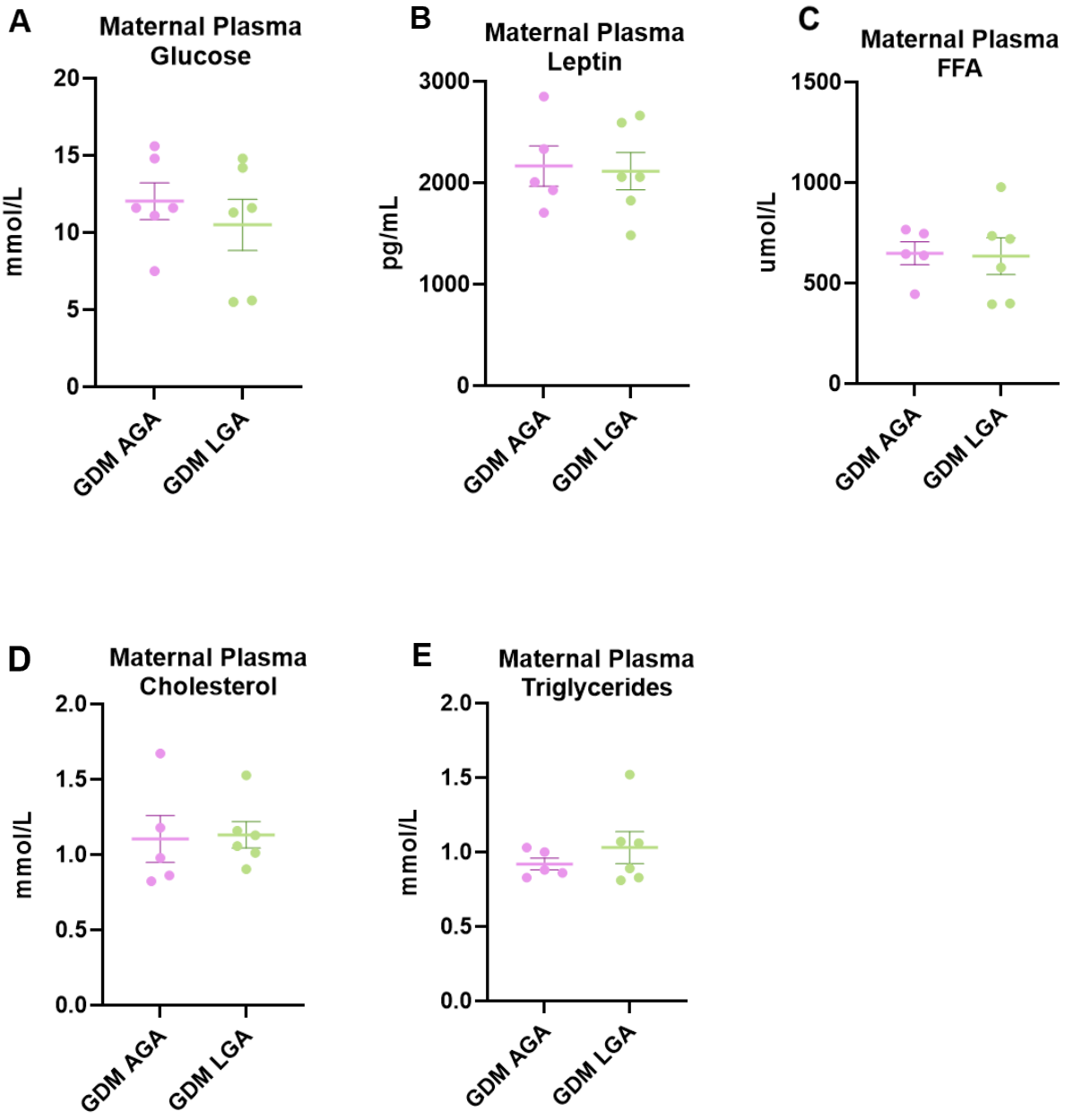

Figure 95 Maternal plasma glucose, leptin, FFA, cholesterol and triglyceride levels in mice treated with human maternal plasma EVs from GDM pregnancies with AGA or LGA outcomes during gestation.

Healthy pregnant C57BL6/J female mice were injected with human plasma EVs from GDM pregnancies with AGA or LGA outcomes at E11.5, E13.5 and E15.5. Mothers were sacrificed at E18.5 and maternal blood was processed for plasma extraction. Plasma metabolites were analysed at Core Biochemical Assay Laboratory (CBAL), Cambridge. Data was analysed using an unpaired t-test and presented as mean±SEM.

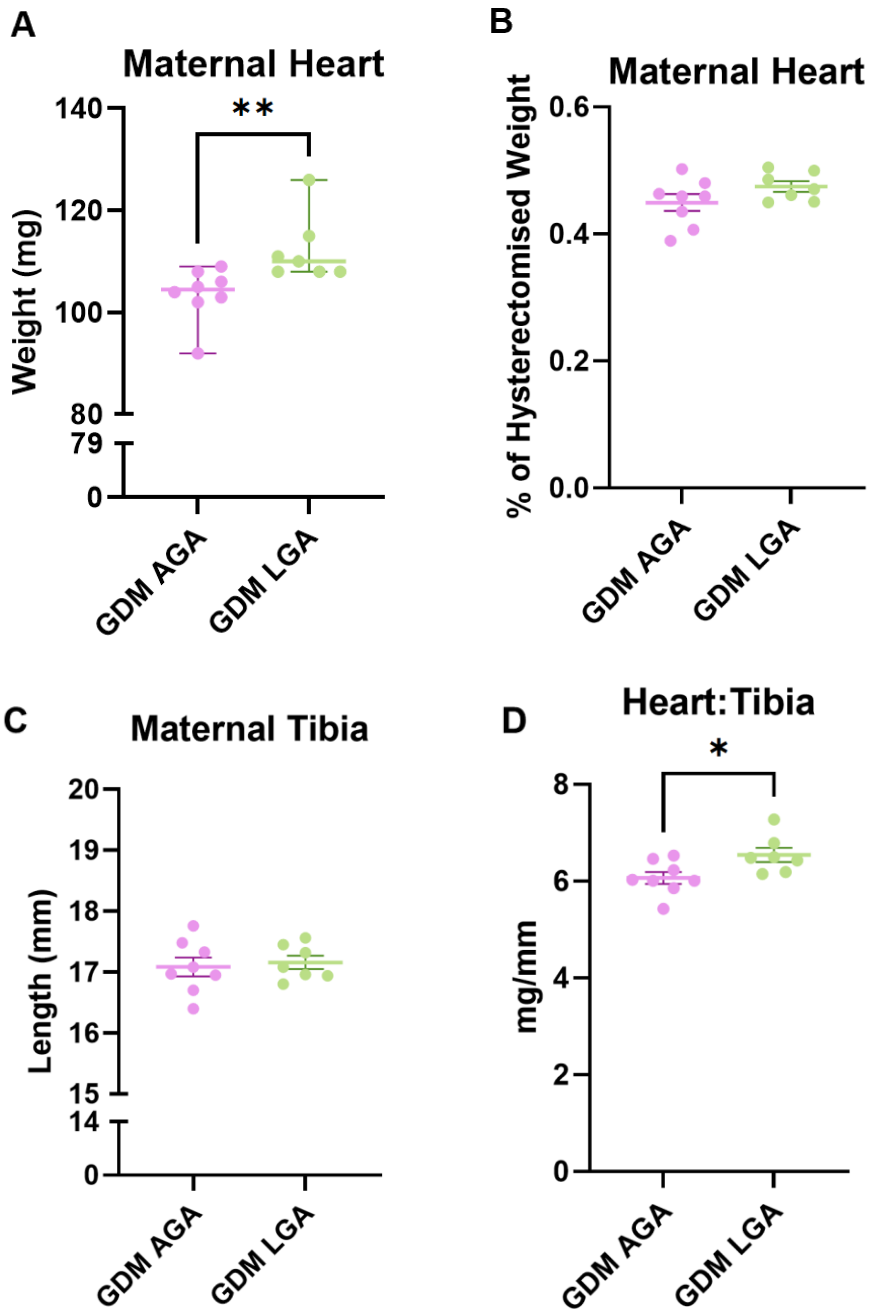

Figure 96 Maternal cardiac tissue weight and cardiac hypertrophy indicators in mice treated with human maternal plasma EVs from and GDM pregnancies with AGA or LGA outcomes during gestation.

Healthy pregnant C57BL6/J female mice were injected with human maternal plasma EVs from GDM pregnancies with AGA or LGA outcomes at E11.5, E13.5 and E15.5. Mothers were sacrificed at E18.5 and cardiac tissue weight, hysterectomised weight and tibia length were recorded. Data that was not normally distributed was analysed using a nonparametric Mann-Whitney test and presented as median with 95% CI. Data that was normally distributed was analysed using an unpaired t-test and presented as mean±SEM; *=p<0.05, **=p<0.01.

5.4.7 Determining the mechanisms in which maternal EVs contribute towards altered fetal growth in healthy pregnant mice by examining the placenta.

5.4.7.1 An omics approach to determine the impact of maternal EVs on placenta metabolism.

It is known that fetal growth is associated with placental metabolism during pregnancy (83,195,496,528,530,534). As such, an omics approach was taken to determine the impact of maternal small EVs on mouse placenta metabolism and whether this may contribute towards different fetal growth outcomes. To detect subtle differences in the placental metabolome, metabolites were considered statistically and biologically significant if $[Log_2FC] \geq 0.26$, $p < 0.05$.

5.4.7.1.1 Healthy Pregnancy EVs

PCA demonstrated that mouse placentae treated with human maternal small EVs from healthy, uncomplicated (Non-GDM AGA) pregnancies had distinct metabolite profiles (**Figure *97***A). Acylcarnitines were most impacted by healthy pregnancy small EVs, where AC6:0, AC16:1, AC16:0, AC18:1 and AC18:0 were significantly upregulated in the placenta compared to mice treated with PBS control (**Figure *97***B). Tryptophan metabolites, acetyl-5-hydroxytryptamine and serotonin, were also significantly upregulated after exposure to healthy pregnancy small EVs compared to control (**Figure *97***B). When separating for fetal sex, it was demonstrated that placental acylcarnitine expression was mostly altered in males than females, where AC6:0, AC12:0 and AC16:1 were significantly upregulated in males but only AC16:0 was significantly upregulated in females (**Figure *98***A,B). Putative adipokine, β-aminoisobutyric acid (BHIBA), was also identified to be upregulated in male placentae and acetyl-5-hydroxytryptamine was upregulated in female placentae after exposure to healthy pregnancy small EVs compared to control (**Figure *98***A,B).

5.4.7.1.2 GDM EVs

When assessing the impact of human maternal small EVs from GDM pregnancies (GDM-AGA) on the mouse placental metabolome, PCA demonstrated a distinct

metabolite profile for placentae treated with healthy pregnancy small EVs and GDM small EVs (**Figure *99***A). It was demonstrated that tryptophan metabolites were mainly impacted, where serotonin, 5-hydroxyindoleacetic acid (5-HIAA) and acetyl-5-hydroxy-tryptamine were significantly downregulated in placentae exposed to GDM small EVs compared to healthy pregnancy small EVs (**Figure *99***B). Moreover, when separating the data for fetal sex, it was evident that the female placental metabolome was more affected by GDM small EVs than the male placental metabolome, as no metabolites were significantly altered in males whereas serotonin and acetyl-5-hydroxytryptamine were significantly downregulated in females (**Figure *100***A,B).

5.4.7.1.3 GDM-LGA EVs

From the PCA plot, it was demonstrated that the placenta metabolite profile of mice exposed to GDM-AGA small EVs and GDM-LGA small EVs were more similar to each other, where a greater overlap in the metabolite profiles was observed (**Figure *101***A). No significant changes in the expression of placental metabolites were identified in mice exposed to GDM-LGA small EVs compared to GDM-AGA small EVs (**Figure *101***B). Interestingly, when separating for fetal sex, it was demonstrated that several TCA cycle metabolites were significantly downregulated in the male placentae of mice exposed to GDM-LGA small EVs compared to GDM-AGA small EVs (**Figure *102***A). These included malic acid, fumarate, lactic acid, isocitrate and citrate. AC4:0 and kynurenine were also significantly downregulated. However, when assessing the female placenta, only AC2:0 was identified to be significantly altered in mice exposed to GDM-LGA small EVs compared to GDM-AGA small EVs (**Figure *102***B). This suggests that the placental metabolome of males is more impacted by GDM-LGA small EVs than females.

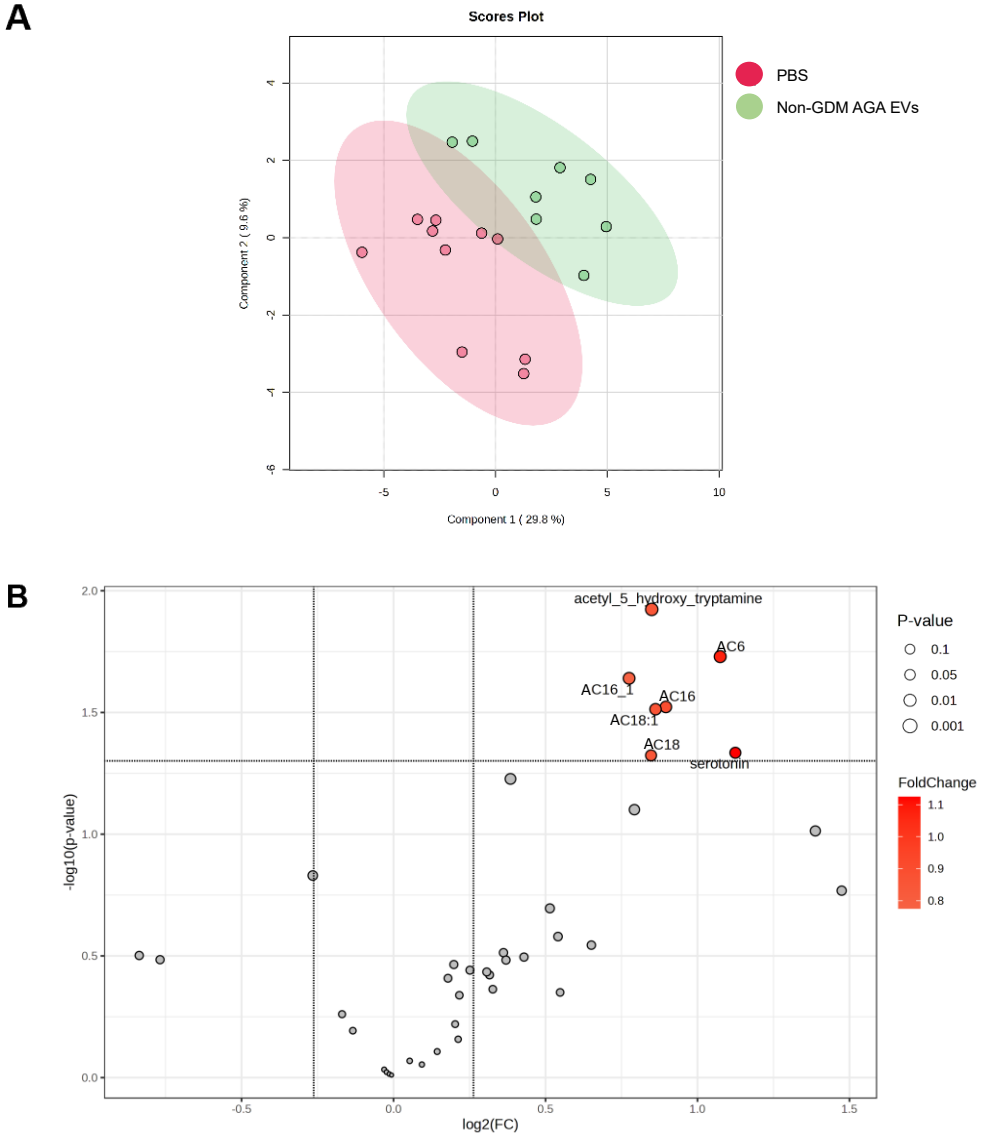

	FC	Log2(FC)	Raw P Value	Log10(p)
Acetyl-5-hydroxytryptamine	1.802	0.850	0.012	1.923
AC6:0	2.106	1.075	0.019	1.730
AC16:1	1.711	0.775	0.023	1.640
AC16:0	1.861	0.896	0.030	1.523
AC18:1	1.818	0.862	0.031	1.513
Serotonin	2.181	1.125	0.046	1.335
AC18:0	1.799	0.847	0.047	1.324

Figure 97 Altered placental metabolites in healthy pregnant mice exposed to PBS and human maternal EVs from healthy pregnancies.

Placental tissue was harvested at E18.5 and processed for metabolite extraction. LCMS was performed on aqueous metabolite fractions, where peaks were normalised to placental tissue weight and analysed using MetaboAnalyst.ca. A one factor statistical analysis was performed, where data was auto scaled. (A) PCA (2D score) plot was generated to measure placental metabolite profiles. (B) Direction of comparison: Non-GDM AGA EVs/PBS, [Log2FC]≥0.26, $p<0.05$.

Placental Metabolome

A **Males**

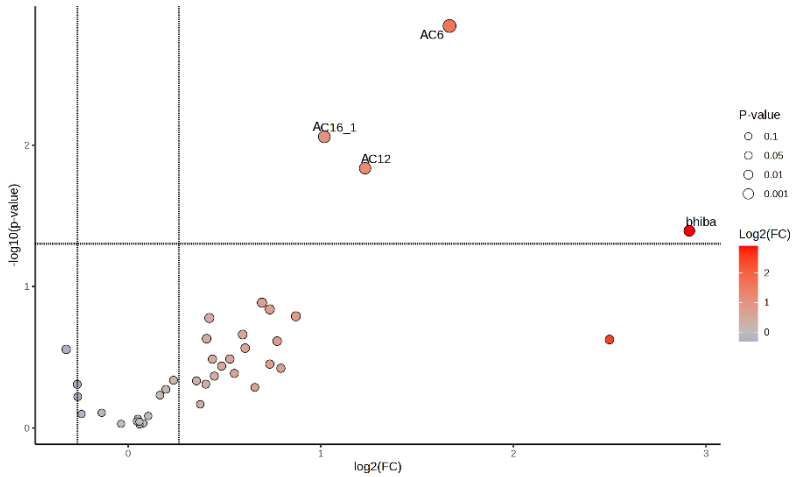

	FC	Log2(FC)	Raw P Value	Log10(p)
AC6:0	3.178	1.668	0.001	2.842
AC16:1	2.026	1.018	0.009	2.059
AC12:0	2.346	1.230	0.015	1.836
BHIBA	7.532	2.913	0.040	1.394

B **Females**

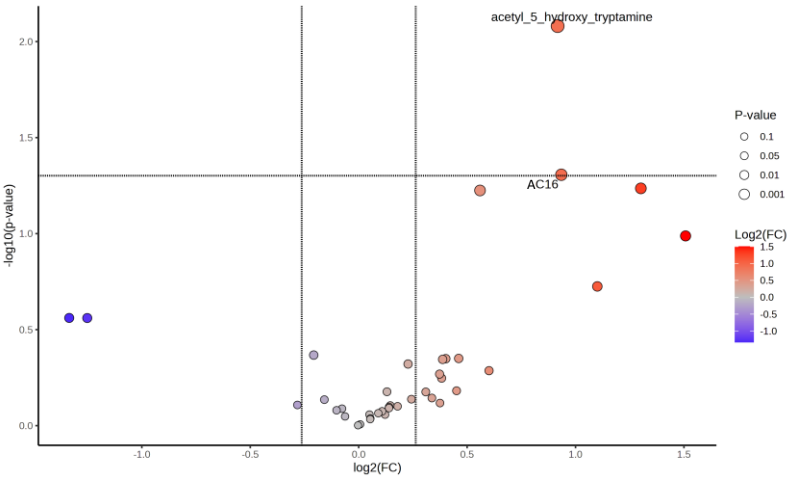

	FC	Log2(FC)	Raw P Value	Log10(p)
Acetyl-5-hydroxytryptamine	1.889	0.917	0.008	2.081
AC16:0	1.911	0.934	0.049	1.307

Figure 98 Altered male and female placental metabolites in healthy pregnant mice exposed to PBS and human maternal EVs from healthy pregnancies.

Placental tissue was harvested at E18.5 and processed for metabolite extraction. LCMS was performed on aqueous metabolite fractions, where peaks were normalised to placental tissue weight and analysed using MetaboAnalyst.ca. Data was separated for fetal sex. A one factor statistical analysis was performed, where data was auto scaled. (A) PCA (2D score) plot was generated to measure placental metabolite profiles. (B) Direction of comparison: Non-GDM AGA EVs/PBS, [Log2FC]≥0.26, $p<0.05$. β-aminoisobutyric acid (BHIBA).

A

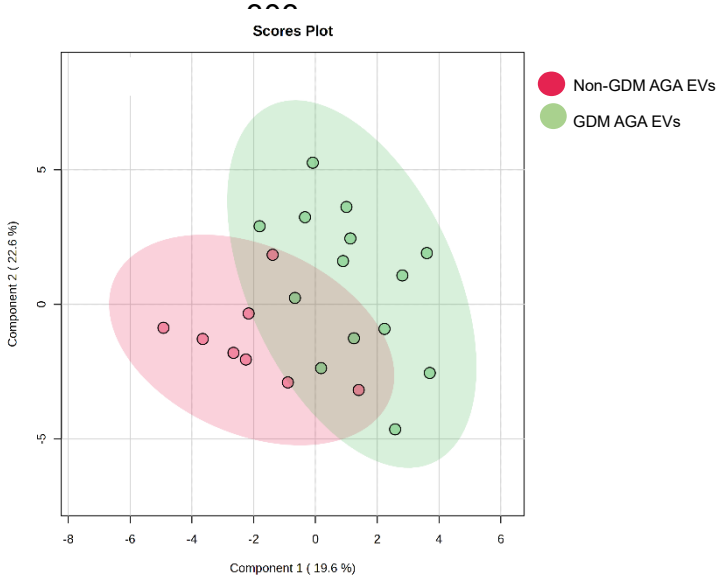

B

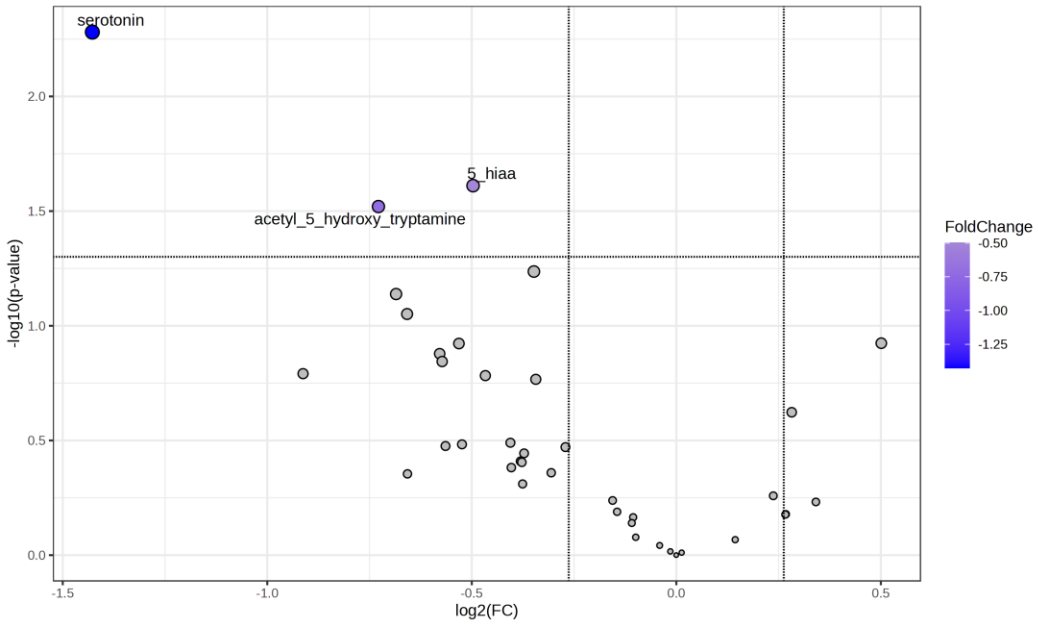

	FC	Log2(FC)	Raw P Value	Log10(p)
Serotonin	0.372	-1.428	0.005	2.280
5-Hydroxyindoleacetic acid (5-HIAA)	0.709	-0.497	0.024	1.611
Acetyl-5-hydroxytryptamine	0.604	-0.728	0.030	1.520

Figure 99 Altered placental metabolites in healthy pregnant mice exposed human maternal EVs from healthy pregnancies and GDM-AGA pregnancies.

Placental tissue was harvested at E18.5 and processed for metabolite extraction. LCMS was performed on aqueous metabolite fractions, where peaks were normalised to placental tissue weight and analysed using MetaboAnalyst.ca. A one factor statistical analysis was performed, where data was auto scaled. (A) PCA (2D score) plot was generated to measure placental metabolite profiles. (B) Direction of comparison: GDM-AGA EVs/Non-GDM AGA EVs, [Log2FC]≥0.26, $p<0.05$. 5-hydroxyindoleacetic acid (5-HIAA).

Placental Metabolome

A **Males**

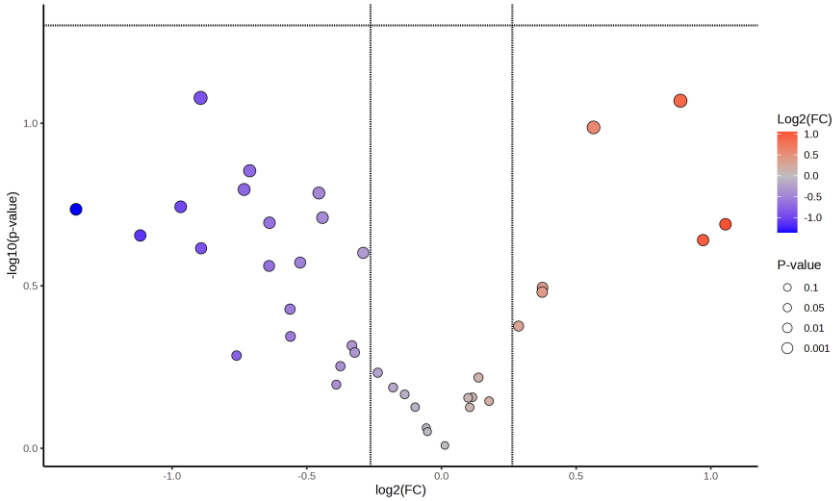

B **Females**

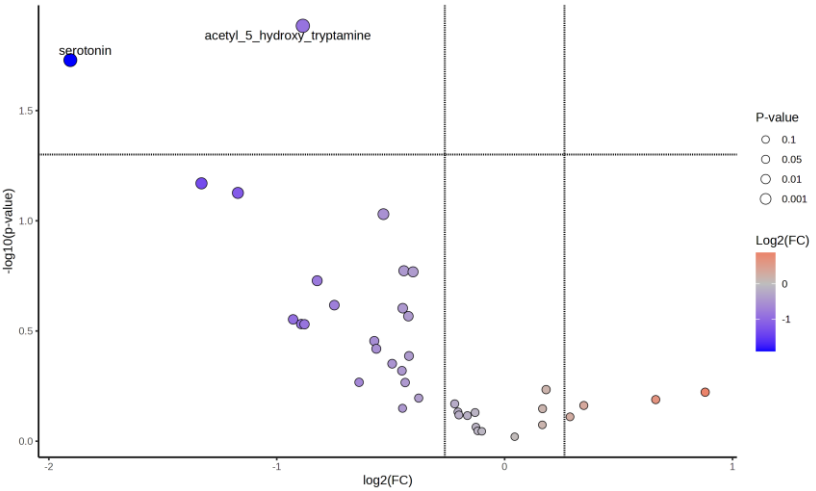

	FC	Log2(FC)	Raw P Value	Log10(p)
Acetyl-5-hydroxytryptamine	0.541	-0.886	0.013	1.885
Serotonin	0.267	-1.906	0.019	1.729

Figure 100 Altered male and female placental metabolites in healthy pregnant mice exposed human maternal EVs from healthy pregnancies and GDM-AGA pregnancies

Placental tissue was harvested at E18.5 and processed for metabolite extraction. LCMS was performed on aqueous metabolite fractions, where peaks were normalised to placental tissue weight and analysed using MetaboAnalyst.ca. Data was separated for fetal sex. A one factor statistical analysis was performed, where data was auto scaled. (A) PCA (2D score) plot was generated to measure placental metabolite profiles. (B) Direction of comparison: GDM-AGA EVs/ Non-GDM AGA EVs, [Log2FC]≥0.26, $p<0.05$.

A

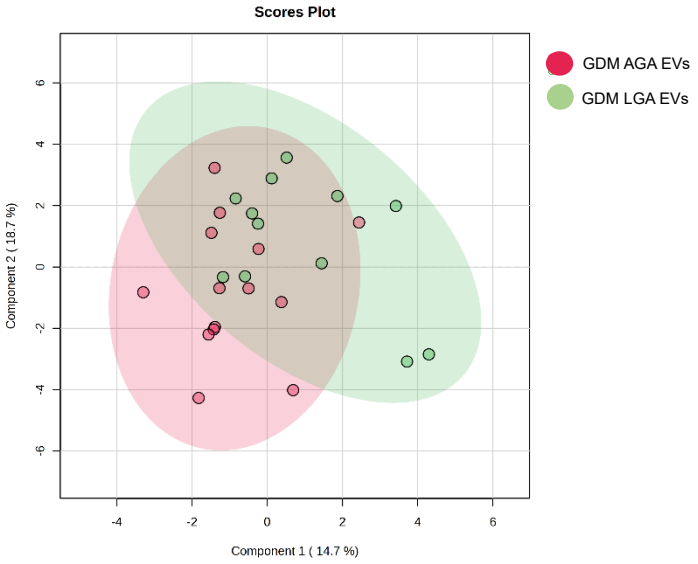

B

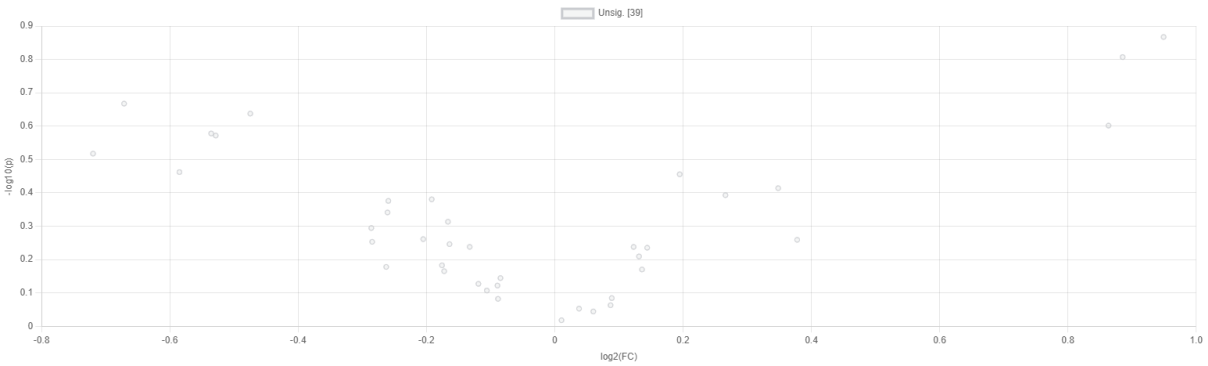

Figure 101 Altered placental metabolites in healthy pregnant mice exposed to human maternal EVs from GDM pregnancies with AGA or LGA outcomes.

Placental tissue was harvested at E18.5 and processed for metabolite extraction. LCMS was performed on aqueous metabolite fractions, where peaks were normalised to placental tissue weight and analysed using MetaboAnalyst.ca. A one factor statistical analysis was performed, where data was auto scaled. (A) PCA (2D score) plot was generated to measure placental metabolite profiles. (B) Direction of comparison: GDM-LGA EVs/GDM-AGA EVs, [Log2FC]≥0.26, $p<0.05$.

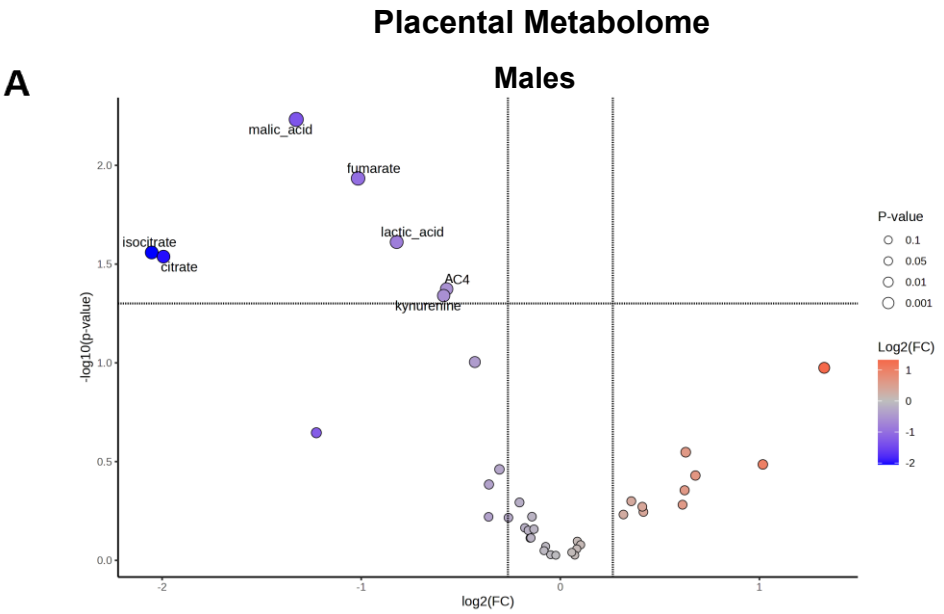

	FC	Log2(FC)	Raw P Value	Log10(p)
Malic acid	0.399	-1.326	0.006	2.232
Fumarate	0.495	-1.016	0.012	1.934
Lactic acid	0.566	-0.822	0.024	1.612
Isocitrate	0.241	-2.052	0.028	1.559
Citrate	0.251	-1.993	0.029	1.538
AC4:0	0.673	-0.571	0.042	1.374
Kynurenine	0.666	-0.586	0.046	1.340

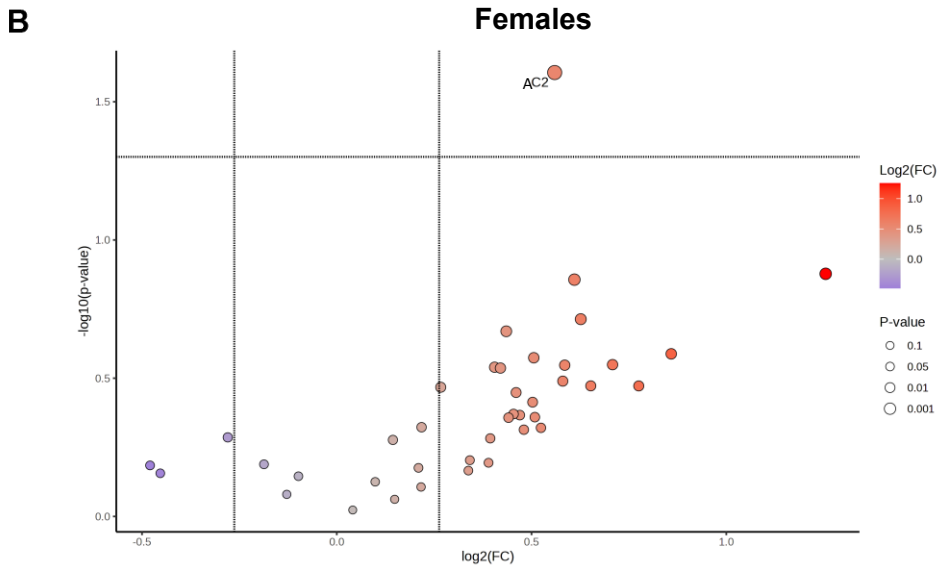

	FC	Log2(FC)	Raw P Value	Log10(p)
AC2:0	1.474	0.559	0.025	1.606

Figure 102 Altered male and female placental metabolites in healthy pregnant mice exposed to human maternal EVs from GDM pregnancies with AGA or LGA outcomes.

Placental tissue was harvested at E18.5 and processed for metabolite extraction. LCMS was performed on aqueous metabolite fractions, where peaks were normalised to placental tissue weight and analysed using MetaboAnalyst.ca. Data was separated for fetal sex. A one factor statistical analysis was performed, where data was auto scaled. (A) PCA (2D score) plot was generated to measure placental metabolite profiles. (B) Direction of comparison: GDM-LGA EVs/GDM-AGA EVs, [Log2FC]≥0.26, $p<0.05$.

5.4.7.2 An omics approach to determine the impact of maternal EVs on placental lipid profile.

Placental lipid profile may influence fetal growth (195,464,530,534), therefore it was assessed if maternal small EVs impact the placental lipidome and if this may contribute towards different fetal growth outcomes. To detect subtle differences in the placental lipidome, lipid species were considered statistically and biologically significant if [Log_2FC]≥0.26, $p<0.05$.

5.4.7.2.1 Healthy Pregnancy EVs

Mouse placentae exposed to human maternal small EVs from healthy, uncomplicated pregnancies (non-GDM AGA) had a similar lipid profile to those exposed to PBS (**Figure *103***A), however the expression of some lipid species was altered between both groups. Indeed, FFA 17:0, FFA 20:0 and PG 16:0-20:3 were significantly downregulated in the EV-treated placentae compared to PBS control (**Figure *103***B). When separating for fetal sex, it was demonstrated that male placentae were not significantly impacted by pregnancy small EVs but female placentae demonstrated reduced expression of FFA 17:0, FFA 22:1, PG 16:0-20:3 and DAG 18:1-18:1 compared to control (**Figure *104***A,B).

5.4.7.2.2 GDM EVs

Next, it was assessed if human maternal EVs from GDM pregnancies (GDM AGA) altered the mouse placental lipidome compared to maternal small EVs from healthy pregnancies. PCA demonstrated some distinction between lipid profiles, however the placental lipidome of both treatment groups mostly overlapped (**Figure *105***A). From the volcano plot, it was also demonstrated that most lipid species were upregulated in mice treated with small EVs from GDM pregnancies compared to healthy pregnancies, where FFA 20:0 and FFA 16:1 levels were significantly elevated (**Figure *105***B). When separating for sex, it was evident that GDM small EVs mostly impacted the male lipidome, where FFA 22:2 and PG 16:0-18:2 were upregulated compared to treatment with healthy pregnancy small EVs (**Figure *106***A). Female placentae demonstrated no significantly altered lipid species in response to GDM small EVs (**Figure *106***B).

5.4.7.2.3 GDM-LGA EVs

Lastly, the placenta lipid profile was assessed in mice treated with human maternal small EVs from GDM-AGA and GDM-LGA pregnancies. PCA showed both treatment groups had similar placental lipid profiles, however some distinction was also observed (**Figure *107***A). FFAs and DAGs were significantly downregulated in the placentae of mice treated with GDM LGA small EVs compared to GDM AGA small EVs (**Figure *107***B). These species included; FFA 14:0, FFA 16:0, FFA 22:2, FFA 17:1, FFA 22:3, FFA 22:4, FFA 22:1 and DAG 16:1-18:0, DAG 18:1-18:1, DAG 16:0-18:0, DAG 18:1-18:3. Distinction in the placental lipidome was observed when the data was separated based on fetal sex (**Figure *108***). In males, it was demonstrated that FFA 22:3 was downregulated and TAG 52:5 and TAG 50:3 were upregulated (**Figure *108***A). Moreover, the female placental lipidome was most affected by GDM LGA small EVs compared to GDM AGA small EVs, where FFA 14:0, FFA 17:1, FFA 20:0, FFA 22:1 and DAG 16:1-18:0 were all identified to be significantly downregulated (**Figure *108***B).

A

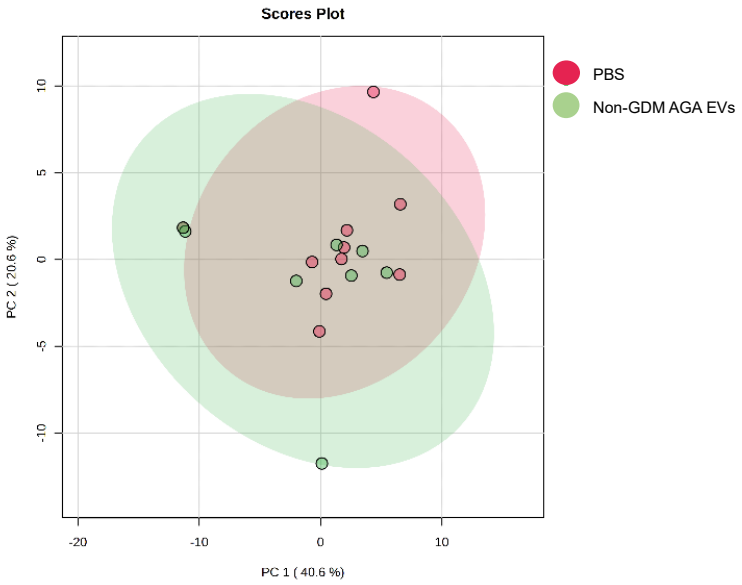

B

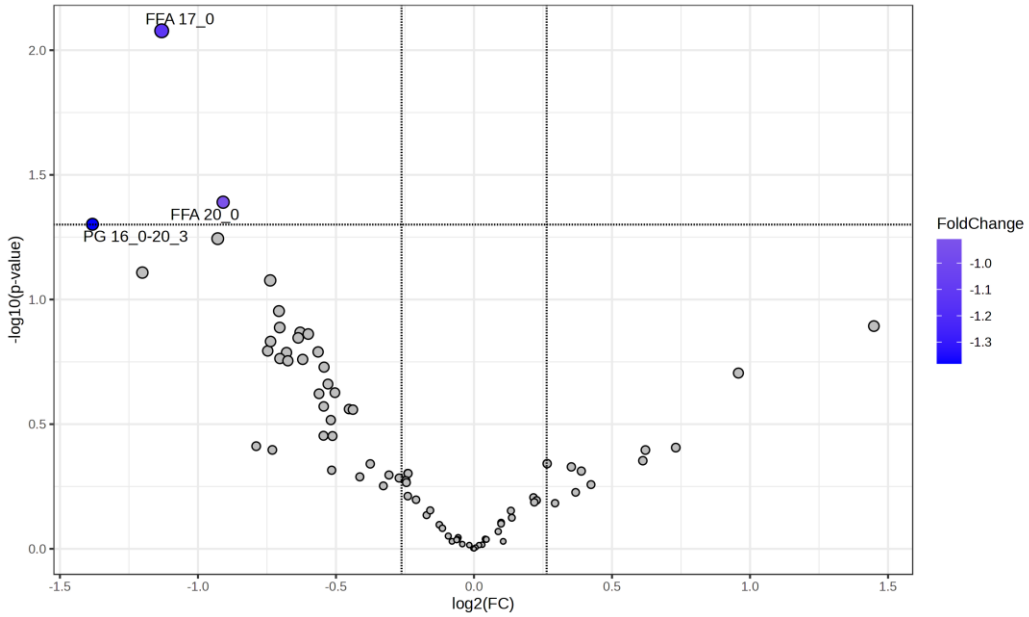

	FC	Log2(FC)	Raw P Value	Log10(p)
FFA 17:0	0.456	-1.131	0.008	2.078
FFA 20:0	0.533	-0.909	0.041	1.390
PG 16:0-20:3	0.384	-1.382	0.050	1.302

Figure 103 Altered placental lipids in healthy pregnant mice exposed to PBS and human maternal EVs from healthy pregnancies.

Placental tissue was harvested at E18.5 and processed for lipid extraction. LCMS was performed on organic metabolite fractions, where peaks were normalised to placental tissue weight and analysed using MetaboAnalyst.ca. A one factor statistical analysis was performed, where data was auto scaled. (A) PCA (2D score) plot was generated to measure placental lipid profiles. (B) Direction of comparison: Non-GDM AGA EVs/PBS, [Log2FC]≥0.26, $p<0.05$.

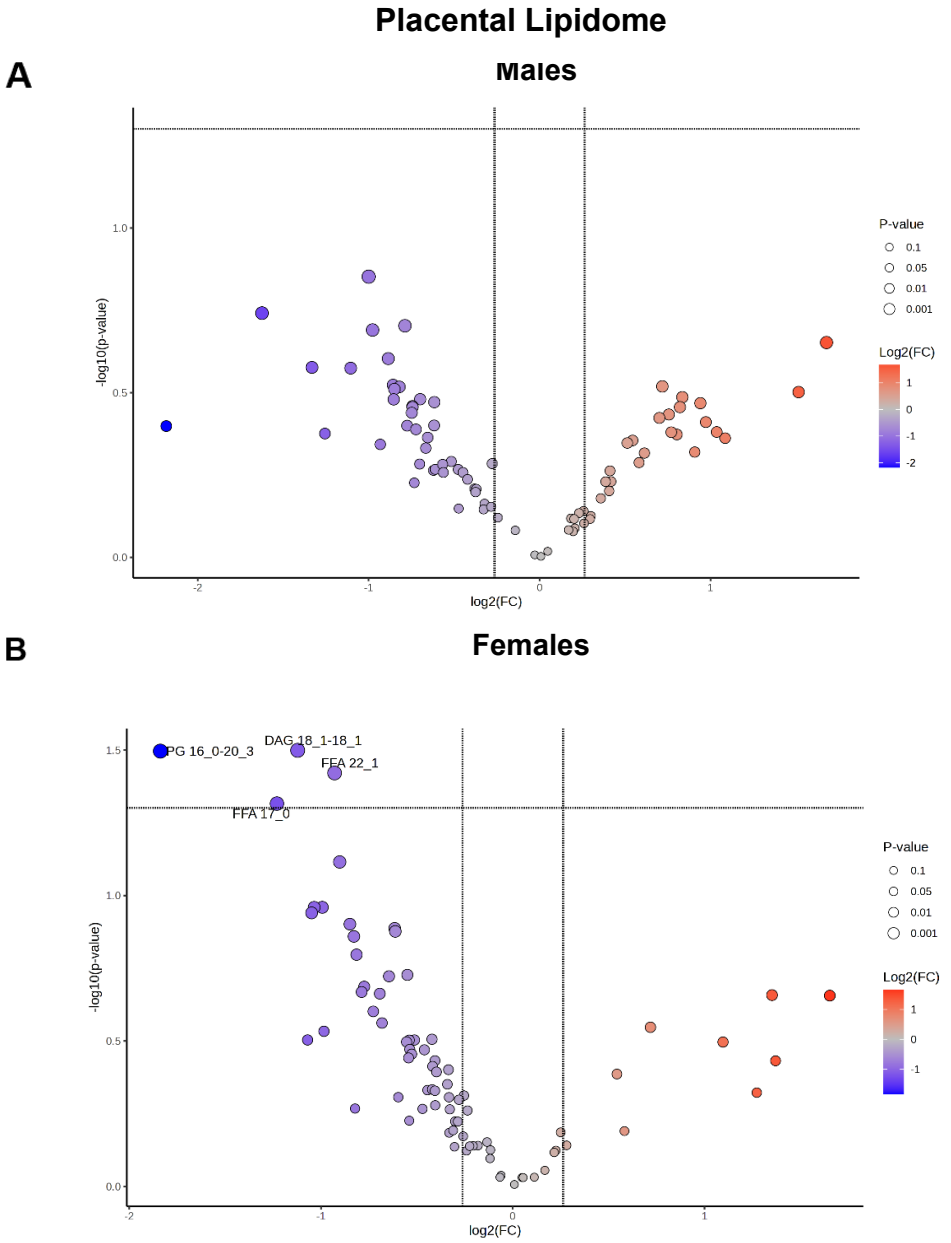

	FC	Log2(FC)	Raw P Value	Log10(p)
DAG 18:1-18:1	0.460	-1.122	0.032	1.499
PG 16:0-20:3	0.280	-1.838	0.032	1.496
FFA 22:1	0.525	-0.929	0.038	1.421
FFA 17:0	0.426	-1.230	0.048	1.316

Figure 104 Altered male and female placental lipids in healthy pregnant mice exposed to PBS and human maternal EVs from healthy pregnancies.

Placental tissue was harvested at E18.5 and processed for lipid extraction. LCMS was performed on organic metabolite fractions, where peaks were normalised to placental tissue weight and analysed using MetaboAnalyst.ca. Data was separated based on fetal sex. A one factor statistical analysis was performed, where data was auto scaled. (A) PCA (2D score) plot was generated to measure placental lipid profiles. (B) Direction of comparison: Non-GDM AGA EVs/PBS, [Log2FC]≥0.26, $p<0.05$. Diacylglyerol (DAG), free fatty acid (FFA), prostaglandin (PG).

A

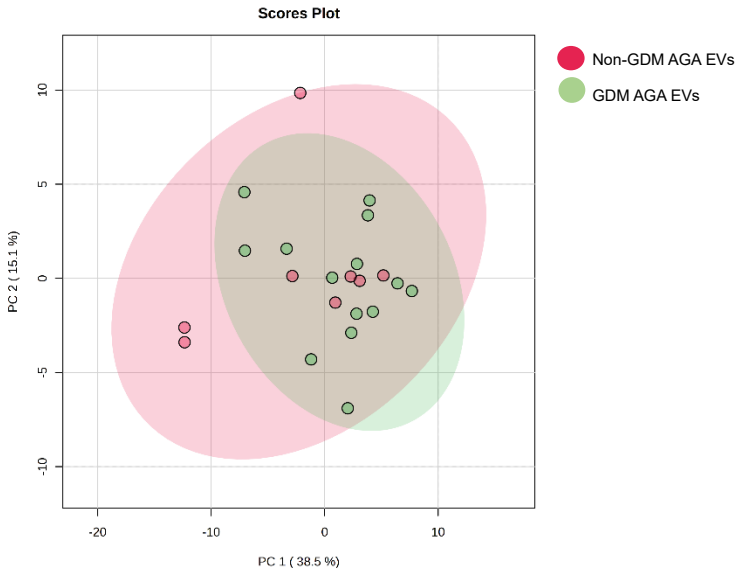

B

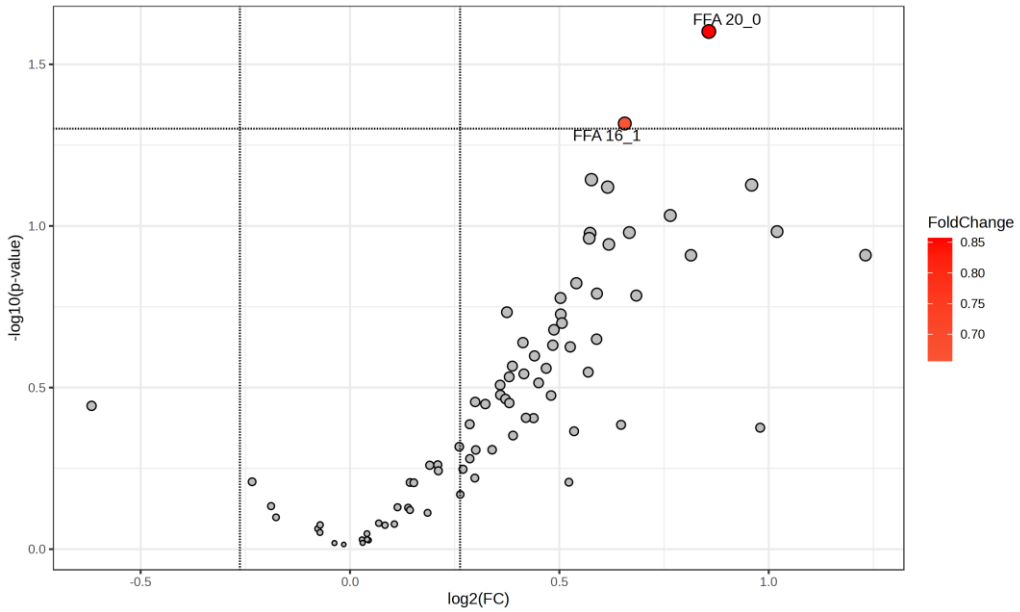

	FC	Log2(FC)	Raw P Value	Log10(p)
FFA 20:0	1.811	0.857	0.025	1.602
FFA 16:1	1.576	0.656	0.048	1.317

Figure 105 Altered placental lipids in healthy pregnant mice exposed human maternal EVs from healthy pregnancies and GDM-AGA pregnancies.

Placental tissue was harvested at E18.5 and processed for lipid extraction. LCMS was performed on organic metabolite fractions, where peaks were normalised to placental tissue weight and analysed using MetaboAnalyst.ca. A one factor statistical analysis was performed, where data was auto scaled. (A) PCA (2D score) plot was generated to measure placental lipid profiles. (B) Direction of comparison: GDM-AGA EVs/ Non-GDM AGA EVs, [Log2FC]≥0.26, $p<0.05$. Free fatty acid (FFA).

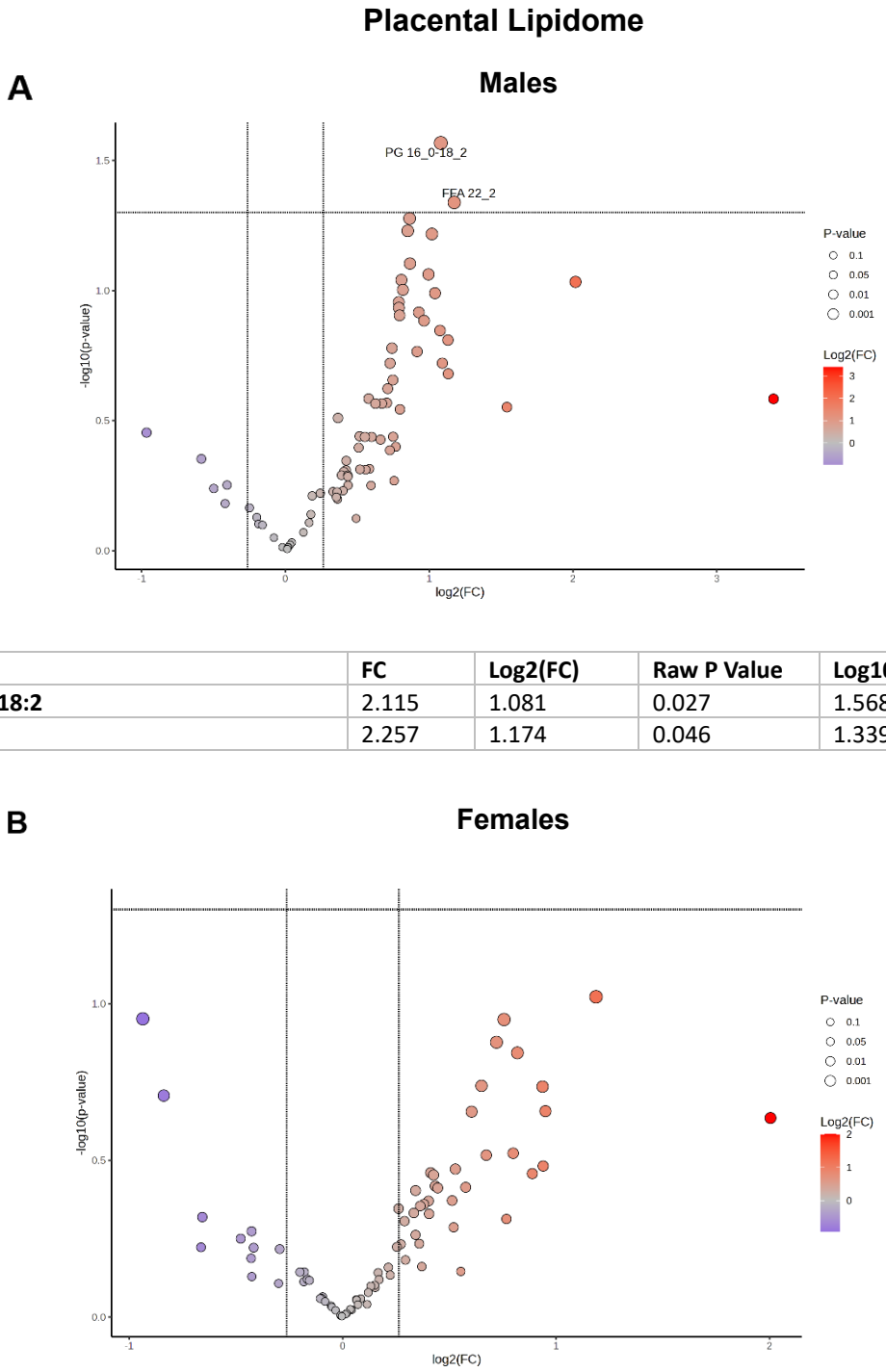

	FC	Log2(FC)	Raw P Value	Log10(p)
PG 16:0-18:2	2.115	1.081	0.027	1.568
FFA 22:2	2.257	1.174	0.046	1.339

Figure 106 Altered male and female placental lipids in healthy pregnant mice exposed to human maternal EVs from healthy pregnancies and GDM-AGA pregnancies.

Placental tissue was harvested at E18.5 and processed for lipid extraction. LCMS was performed on organic metabolite fractions, where peaks were normalised to placental tissue weight and analysed using MetaboAnalyst.ca. Data was separated based on fetal sex. A one factor statistical analysis was performed, where data was auto scaled. (A) PCA (2D score) plot was generated to measure placental lipid profiles. (B) Direction of comparison: GDM-AGA EVs/ Non-GDM AGA EVs, [Log2FC]≥0.26, $p<0.05$. Free fatty acid (FFA), prostaglandin (PG).

A

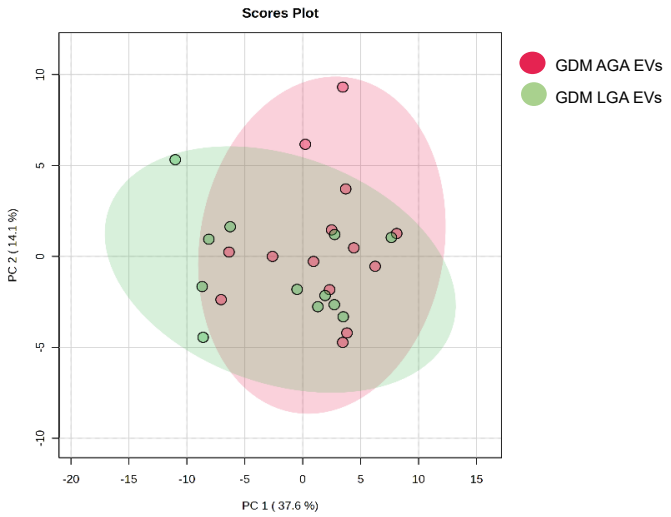

B

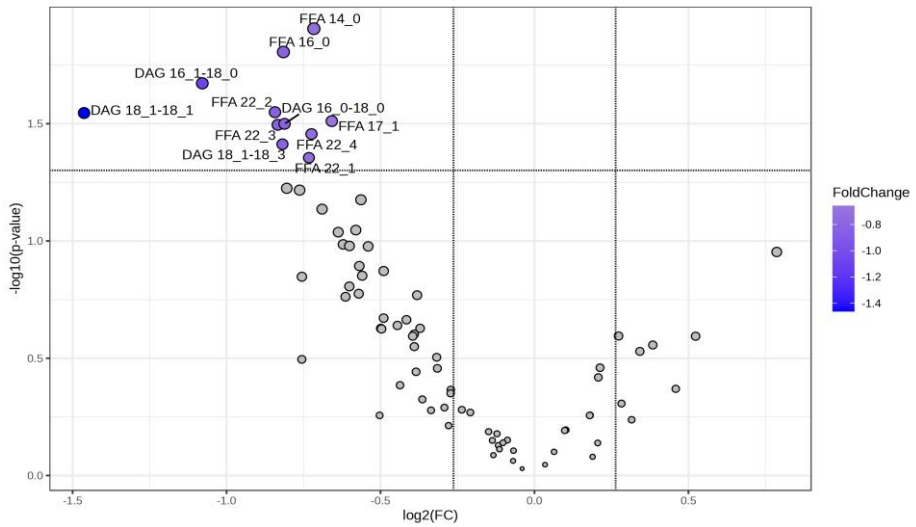

	FC	Log2(FC)	Raw P Value	Log10(p)
FFA 14:0	0.609	-0.717	0.012	1.905
FFA 16:0	0.568	-0.815	0.016	1.806
DAG 16:1-18:0	0.473	-1.079	0.021	1.672
FFA 22:2	0.558	-0.843	0.028	1.549
DAG 18:1-18:1	0.363	-1.463	0.028	1.546
FFA 17:1	0.634	-0.658	0.031	1.511
DAG 16:0-18:0	0.570	-0.812	0.032	1.500
FFA 22:3	0.561	-0.834	0.032	1.495
FFA 22:4	0.605	-0.724	0.035	1.456
DAG 18:1-18:3	0.567	-0.819	0.039	1.412
FFA 22:1	0.602	-0.733	0.044	1.355

Figure 107 Altered placental lipids in healthy pregnant mice exposed to human maternal EVs from GDM pregnancies with AGA or LGA outcomes.

Placental tissue was harvested at E18.5 and processed for lipid extraction. LCMS was performed on organic metabolite fractions, where peaks were normalised to placental tissue weight and analysed using MetaboAnalyst.ca. A one factor statistical analysis was performed, where data was auto scaled. (A) PCA (2D score) plot was generated to measure placental lipid profiles. (B) Direction of comparison: GDM-LGA EVs/ GDM-AGA EVs, [Log2FC]≥0.26, $p<0.05$. Diacylglyerol (DAG), free fatty acid (FFA).

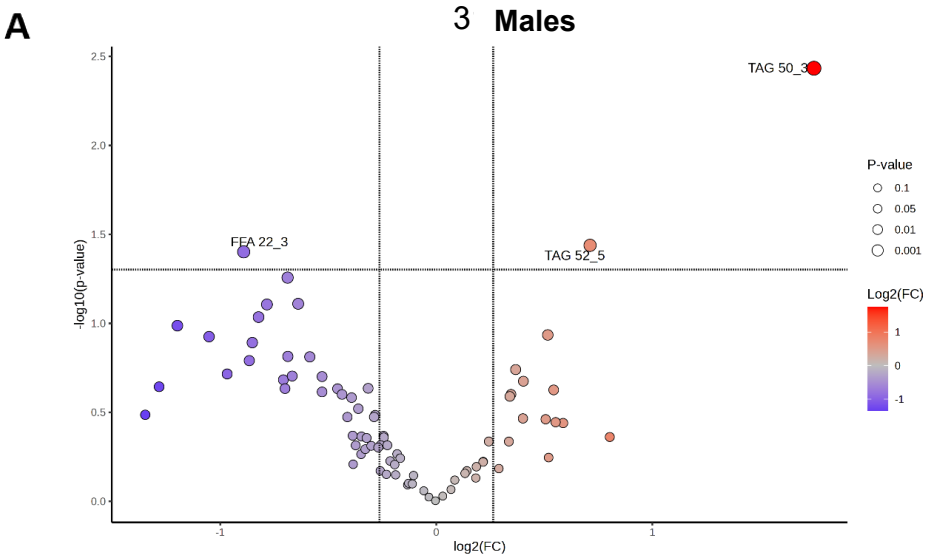

	FC	Log2(FC)	Raw P Value	Log10(p)
TAG 50:3	3.359	1.748	0.004	2.434
TAG 52:5	1.638	0.712	0.036	1.439
FFA 22:3	0.539	-0.891	0.040	1.402

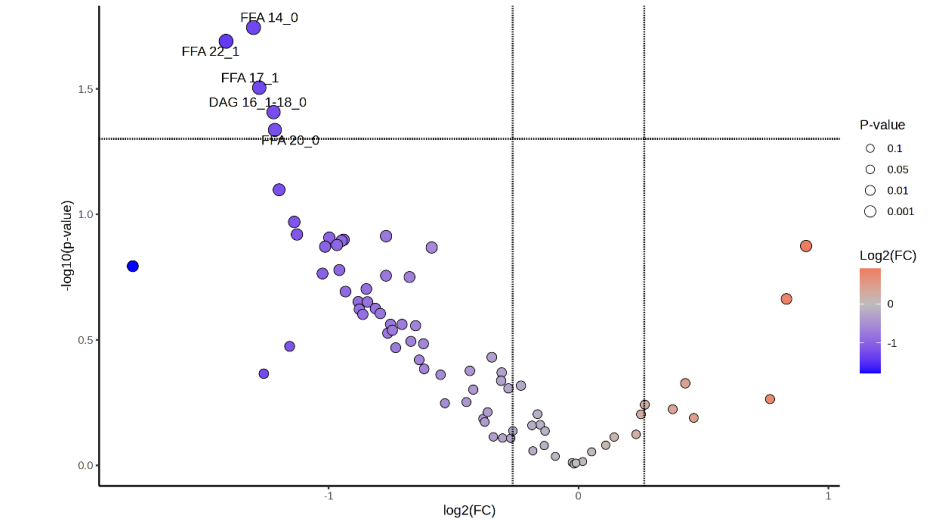

	FC	Log2(FC)	Raw P Value	Log10(p)
FFA 14:0	0.406	-1.301	0.018	1.745
FFA 22:1	0.376	-1.411	0.020	1.690
FFA 17:1	0.412	-1.278	0.031	1.505
DAG 16:1-18:0	0.429	-1.221	0.039	1.407
FFA 20:0	0.431	-1.215	0.046	1.337

Figure 108 Altered male and female placental lipids in healthy pregnant mice exposed to human maternal EVs from GDM pregnancies with AGA or LGA outcomes.

Placental tissue was harvested at E18.5 and processed for lipid extraction. LCMS was performed on organic metabolite fractions, where peaks were normalised to placental tissue weight and analysed using MetaboAnalyst.ca. Data was separated based on fetal sex. A one factor statistical analysis was performed, where data was auto scaled. (A) PCA (2D score) plot was generated to measure placental lipid profiles. (B) Direction of comparison: GDM-LGA EVs/GDM-AGA EVs, [Log2FC]≥0.26, $p<0.05$. Diacylglyerol (DAG), free fatty acid (FFA).

5.4.7.3 A histological approach to determine the impact of human maternal EVs on mouse placenta development.

The impact of human maternal small EVs on placental development was further explored by processing and double-labelling mouse placentae to identify placental zones (**Figure *109***). The surface area of each zone was measured and calculated relative to the total placental surface area. Many placental samples demonstrated tissue processing and fixation issues, as observed in the representative images in **Figure *109***. To account for many samples demonstrating intact decidua, the surface area of the junction zone relative to the labyrinth zone was calculated.

5.4.7.3.1 Healthy Pregnancy EVs

Placentae exposed to small EVs from healthy pregnancies (non-GDM AGA) and PBS control demonstrated similar total placental surface area as well as the surface area of the junctional, labyrinth and decidua zones (all $p>0.999$; n=3/2, respectively) (**Figure *110***). The same observations were also identified when separating the data for fetal sex, however this finding may be due to low n numbers.

5.4.7.3.2 GDM EVs

Small EVs from GDM pregnancies (GDM-AGA) demonstrated no impact on total placental surface area, junctional and labyrinth zone surface area or junctional/labyrinth zone surface area when compared to the impact of healthy pregnancy EVs ($p>0.999$; n=4/3, respectively) (**Figure *110***A-D). No change was observed in decidua surface area with GDM small EVs compared to healthy pregnancy EVs ($p=0.182$; n=4/3, respectively) (**Figure *110***E). When compared to PBS control, this finding was significant ($p=0.043$). No significant findings were observed when separating the data for sex.

5.4.7.3.3 GDM-LGA EVs

No significant findings were observed when examining the impact of GDM-LGA small EVs on the placental total surface area and zones (**Figure *110***). The same was also observed when separating the data based on fetal sex.

A PBS

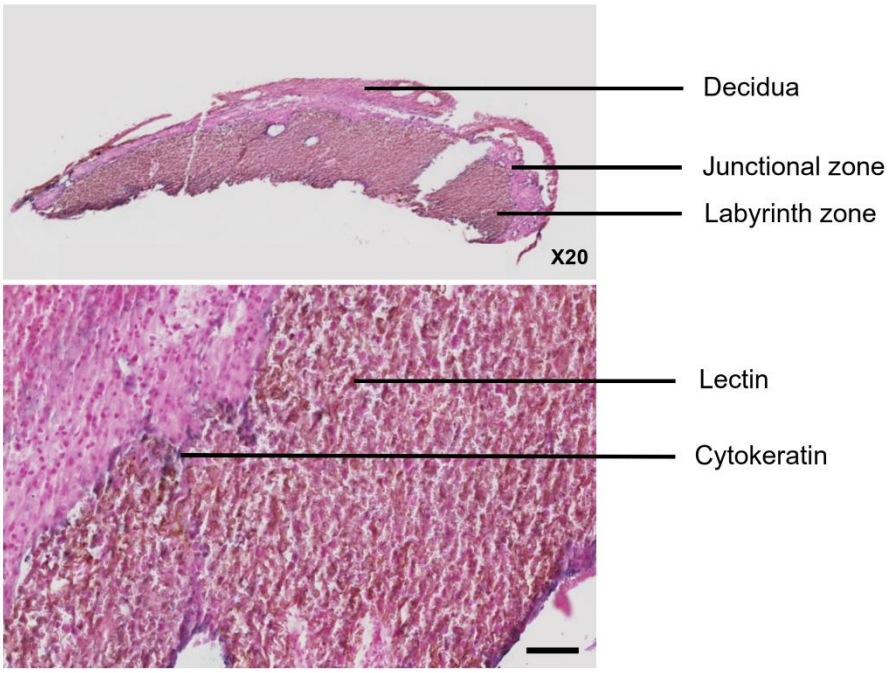

B Non-GDM AGA EVs

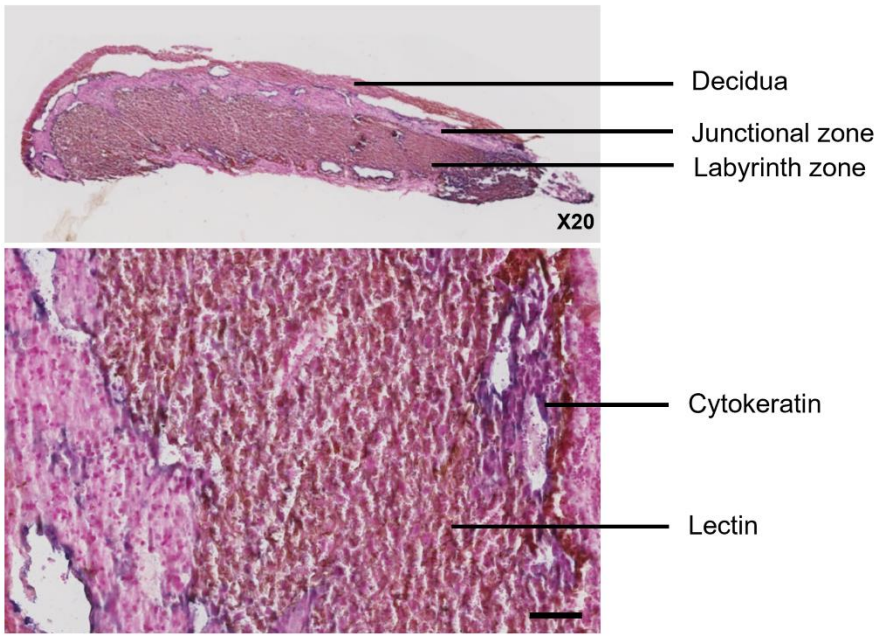

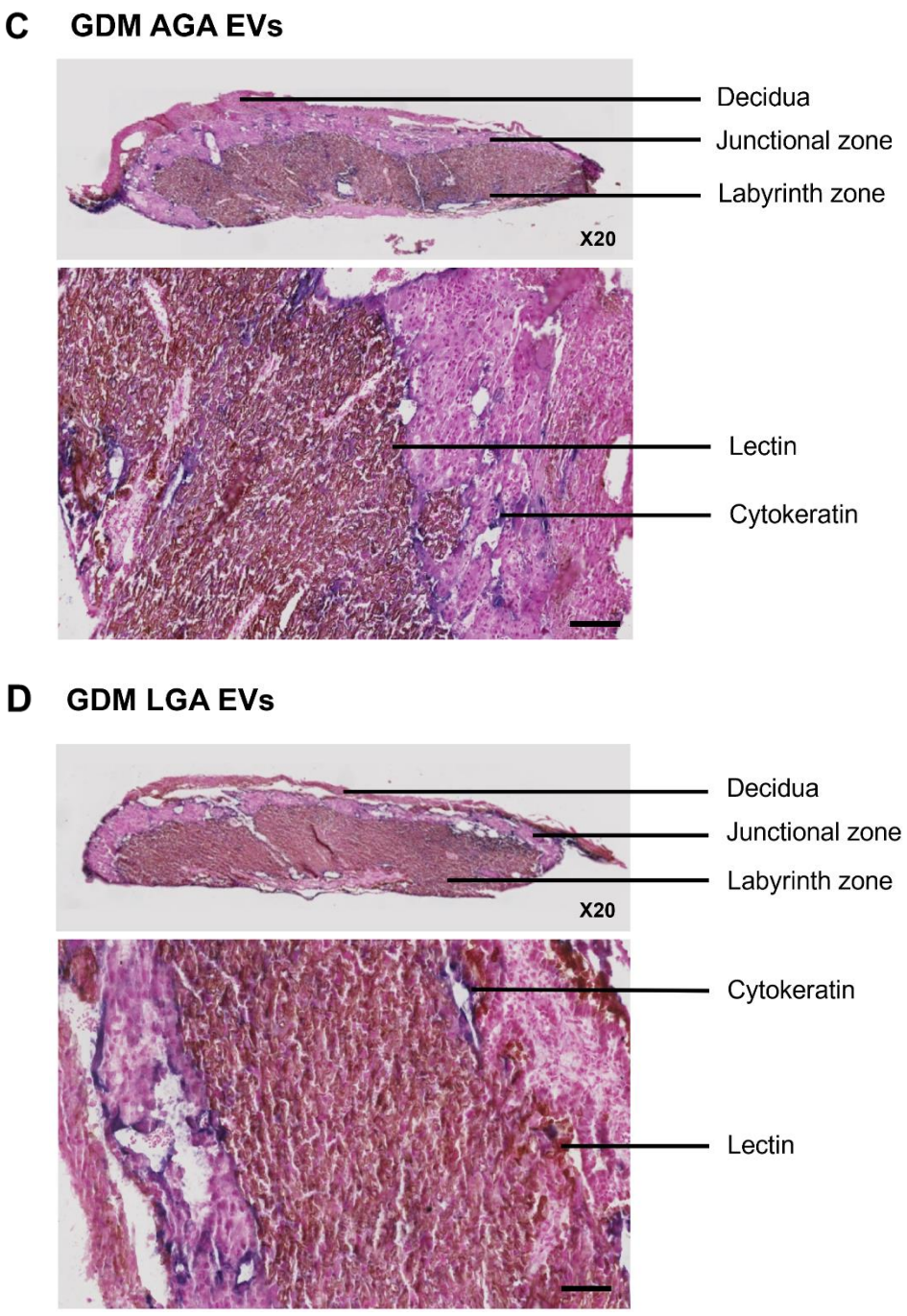

Figure 109 Representative immunohistochemistry images of E18.5 mouse placentae exposed to PBS and maternal EVs from healthy uncomplicated pregnancies, GDM AGA or GDM LGA pregnancies during gestation.

Healthy pregnant C57BL6/J female mice were injected with PBS or human plasma EVs from healthy uncomplicated pregnancies, GDM AGA or GDM LGA pregnancies at E11.5, E13.5 and E15.5 before being sacrificed at E18.5. Placental tissue was harvested, fixed in 10% formalin before being transferred into 70% ethanol after 24 hours. Placentae were then processed as outlined in (348) and orientated in paraffin wax. Sections of 5μM thickness were sliced and placental zones were double-labelled for lectin and cytokeratin as per (349). Histological slides were imaged at x20. Scale bar: 100μM.

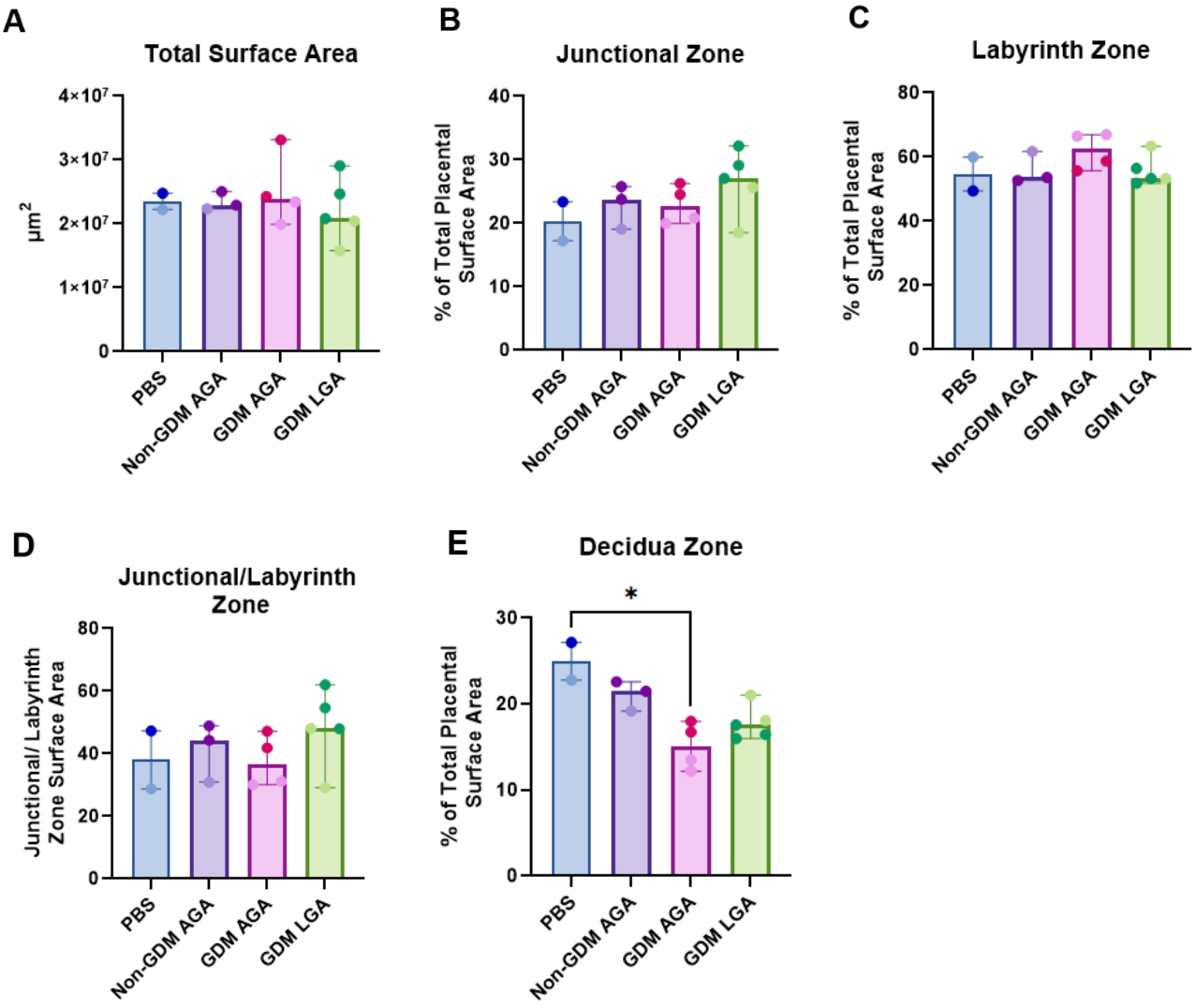

Figure 110 Mouse placental zones at E18.5 after exposure to PBS and maternal EVs from healthy uncomplicated pregnancies, GDM AGA or GDM LGA pregnancies during gestation.

Healthy pregnant C57BL6/J female mice were injected with PBS or human plasma EVs from healthy uncomplicated pregnancies, GDM AGA or GDM LGA pregnancies at E11.5, E13.5 and E15.5 before being sacrificed at E18.5. Placental tissue was harvested, fixed in 10% formalin before being transferred into 70% ethanol after 24 hours. Placentae were then processed as outlined in (348) and orientated in paraffin wax. Sections of 5μM thickness were sliced and placental zones were double-labelled for lectin and cytokeratin as per (349). Surface area of placental zones was detected using QuPath software. Histological slides were imaged at x20. Scale bar: 100μM. Light data points; female, dark data points; male. Kruskal-Wallis test was performed and data presented as median with 95% CI; *=p<0.05.

5.4.8 Determining the aetiology of maternal EVs on altering feto-placental development in healthy pregnant mice by examining miRNA expression.

Previous work from the Forbes group shows that the expression of some miRNAs is altered in maternal small EVs of women with GDM prior to the onset of altered growth (**Figure *38***A). Previous data also demonstrates that of these altered miRNAs, miR-1-3p, miR-133a-3p, miR-200c-3p and miR-375-3p are upregulated in term placental tissue of GDM pregnancies with LGA outcomes (**Figure *38***B). Findings from chapter 4 further demonstrate that miR-375-3p may contribute towards altered fetal growth by impacting events in the placenta (**Figure *65***). Therefore, to determine whether the impact of maternal EVs on mouse feto-placental growth may be attributed to EV trafficking of miRNAs to the placenta, miRNA levels were assessed in the human maternal small EVs delivered to the healthy pregnant mice and in mouse placental tissue.

miR-1-3p, miR-133a-3p and miR-200c-3p expression levels were undetected in all human maternal small EV treatment groups (data not shown). However, miR-375-3p expression was non-significantly higher in the GDM-LGA small EVs compared to healthy pregnancy small EVs (non-GDM AGA) and GDM-AGA small EVs. Healthy pregnancy small EVs demonstrated non-significantly higher levels of miR-375-3p compared to GDM AGA small EVs (**Figure *111***).

No significant changes in miR-375-3p expression was detected in mouse placental tissue in response to human maternal small EVs (**Figure *112***A). Placental miR-133a-3p levels were lower in mice exposed to maternal GDM small EVs with AGA and LGA outcomes compared to healthy pregnancy small EVs and PBS control, however this finding was statistically insignificant (**Figure *112***B). Although statistically insignificant, miR-133a-3p expression levels were highest in mouse placentae exposed to healthy pregnancy small EVs (**Figure *112***B). In contrast, placentae exposed to PBS control and healthy pregnancy small EVs demonstrated lower levels of miR-1-3p than small EVs from GDM-AGA and GDM-LGA pregnancies, where placentae exposed to GDM-LGA small EVs showed the highest levels of miR-1-3p, however these findings were not statistically significant (**Figure *112***C). A non-significant reduction in miR-200c-3p expression was observed in mouse placental tissue exposed to human maternal

small EVs compared to PBS control (**Figure *112***D). No significant findings were identified when separating the data for fetal sex.

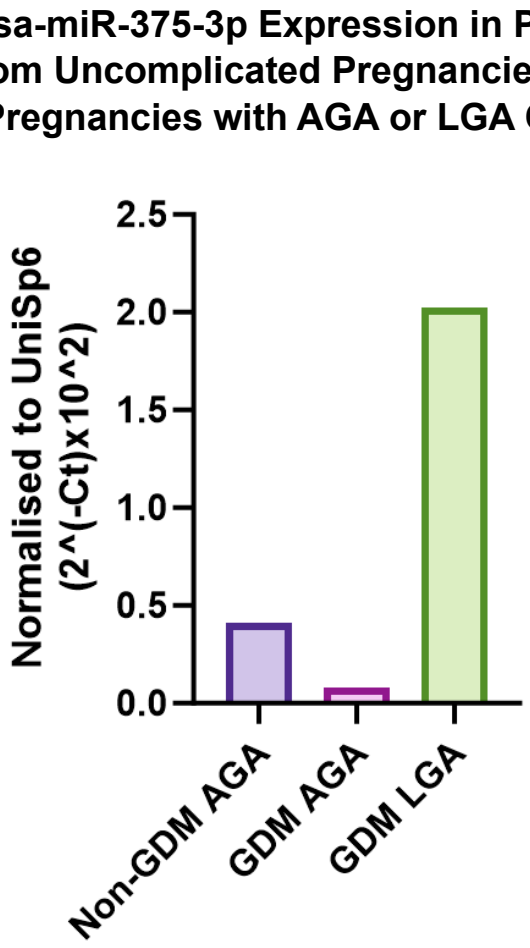

Figure 111 hsa-miR-375-3p expression in pooled human maternal plasma EVs (pF7-10) from uncomplicated, GDM-AGA and GDM-LGA pregnancies that were injected into healthy pregnant mice.

Plasma EV fractions 7-10 from healthy uncomplicated pregnancies and GDM pregnancies with AGA or LGA outcomes were pooled to generate EV treatment groups for mouse injections in chapter 4. RNA was extracted from EVs before qPCR was performed. hsa-miR-375-3p expression was normalised to *UniSp6* expression; (2^(-Ct)*10^(2).

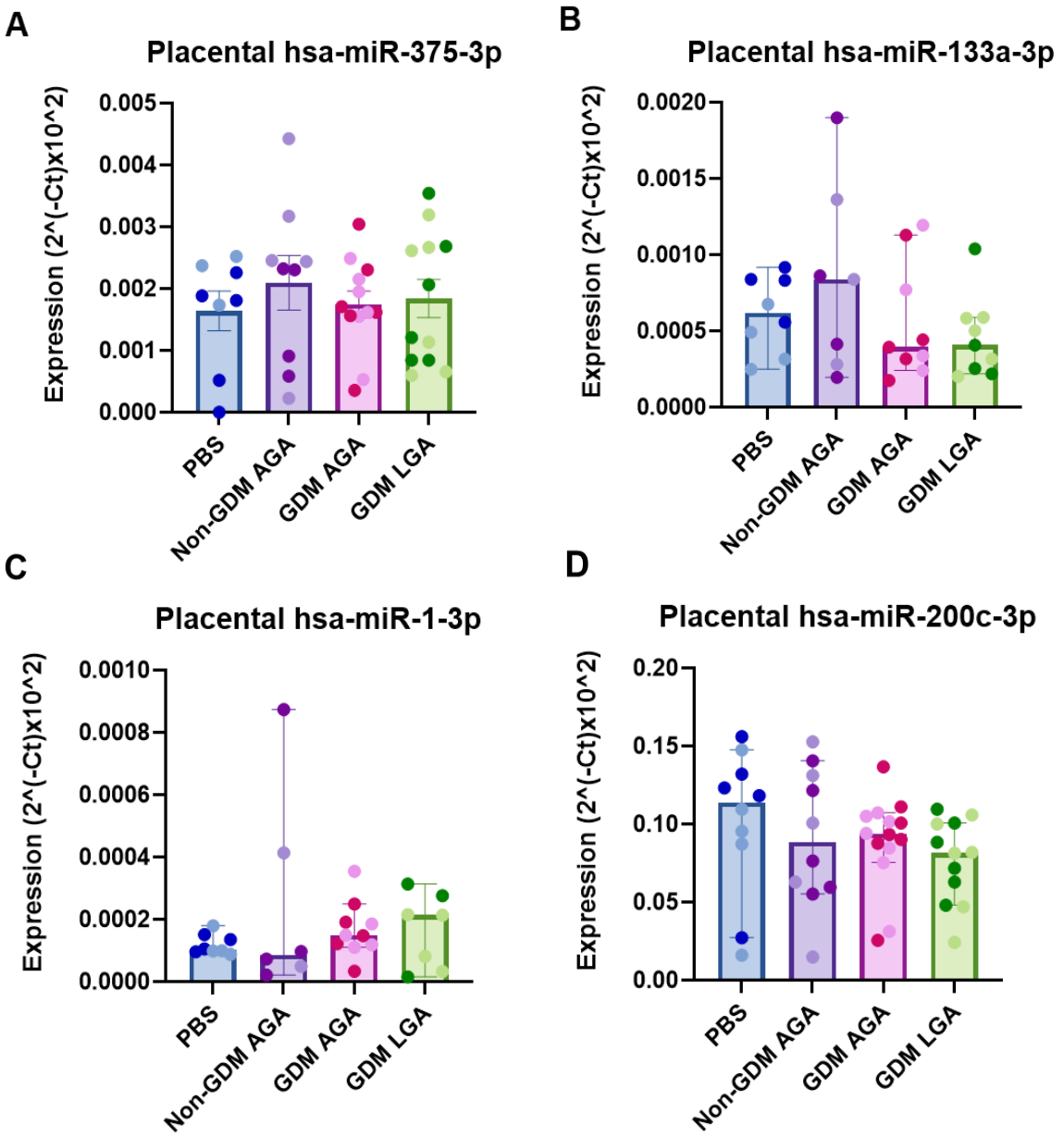

Figure 112 Placental hsa-miR-375-3p, hsa-miR-133a-3p, hsa-miR-1-3p and hsa-miR-200c-3p expression in mice exposed to PBS or human maternal plasma EVs from healthy uncomplicated pregnancies, GDM-AGA or GDM-LGA pregnancies during gestation at E18.5.

Healthy pregnant C57BL6/J female mice were injected with PBS or human plasma EVs from healthy uncomplicated pregnancies, GDM-AGA or GDM-LGA pregnancies at E11.5, E13.5 and E15.5 before being sacrificed at E18.5. Placental mature miRNA was isolated and reverse transcribed before miRNA expression was analysed using qPCR and normalised to *UniSp6* expression; (2^(-Ct)*10^(2). Ordinary one-way ANOVA followed by Tukey's multiple comparisons test was performed for normally distributed data and presented as mean±SEM. Kruskall-Wallis followed by Dunn's multiple comparisons test was performed for nonparametric data and presented as median with 95% CI. Light data points; female, dark data points; male.

As identified in chapter 4 (**Figure *55***, **Figure *56***, **Figure *57***), the expression of key placental regulatory genes was assessed in mouse placenta. *Itgb1, Igf2r, Cd47, Ttc3* and *Cald1* (**Figure *113***B,D,E,G,K) all demonstrated a similar downward trend in expression levels, where placentae exposed to healthy pregnancy small EVs demonstrated the highest expression levels. A significant increase in expression was observed in response to healthy pregnancy small EVs compared to PBS control treatment for *Itgb1* (p=0.001; n=9) and *Igf2r* (p=0.034; n=9/7 respectively) (**Figure *113***B,D). *Itgb1* (p=0.003; n=9/13, respectively) and *Cd47* (p=0.029; n=9/12, respectively) expression levels were also significantly decreased between placentae treated with small EVs from healthy pregnancies and GDM-AGA pregnancies (**Figure *113***B,E). Comparing healthy pregnancy small EVs and GDM-LGA small EVs treatment, *Itgb1* (p<0.0001; n=9/8, respectively), *Igfr2* (p=0.019; n=9/11, respectively), *Cd47* (p=0.003; n=9/11, respectively), *Ttc3* (p=0.007; n=9/11, respectively), and *Cald1* (p=0.010; n=9/11, respectively) were significantly downregulated in mouse placental tissue (**Figure *113***B,D,E,G,K). *Prkag2* expression levels were highest in placentae treated with small EVs from healthy pregnancies, where placentae exposed to small EVs from GDM-AGA and GDM-LGA pregnancies demonstrated lower and similar expression levels, however these findings were statistically not significant (**Figure *113***F).

Fabp4 expression levels were highest in placentae exposed to PBS compared to maternal small EVs. This observation was statistically significant when comparing PBS control treatment with the GDM-AGA small EVs (p=0.036; n=8/13, respectively) and GDM-LGA small EVs (p=0.006; n=8/10, respectively) treatment groups (**Figure *113***I). No statistically significant findings were observed for *Kpna3* and *Pecam1* expression (**Figure *113***A,C). *Slc6a8* and *Eno1* expression levels were similar for all treatment groups (**Figure *113***H,J).

When separating the data based on fetal sex, it was demonstrated that *Itgb1* expression was significantly increased in male placentae exposed to healthy pregnancy small EVs compared to PBS (p=0.044; n=4). *Fabp4* expression was also significantly reduced in male placentae exposed to GDM-LGA small EVs compared to PBS (p=0.031; n=6/4, respectively). Male placental *Itgb1* and *Prkag2* was significantly reduced in response to GDM-AGA small EVs compared to healthy pregnancy small EVs (p=0.016 and p=0.015, respectively). *Itgb1* levels

was also significantly reduced in males exposed to GDM-LGA small EVs compared to healthy pregnancy small EVs (p=0.002) (**Figure *113***B,F,I).

Cald1, Ttc3 and *Itgb1* placental expression were significantly reduced in females exposed to GDM-LGA small EVs compared to healthy pregnancy small EVs (p=0.014; p=0.048 and p=0.015, respectively) (**Figure *113***B,G,K).

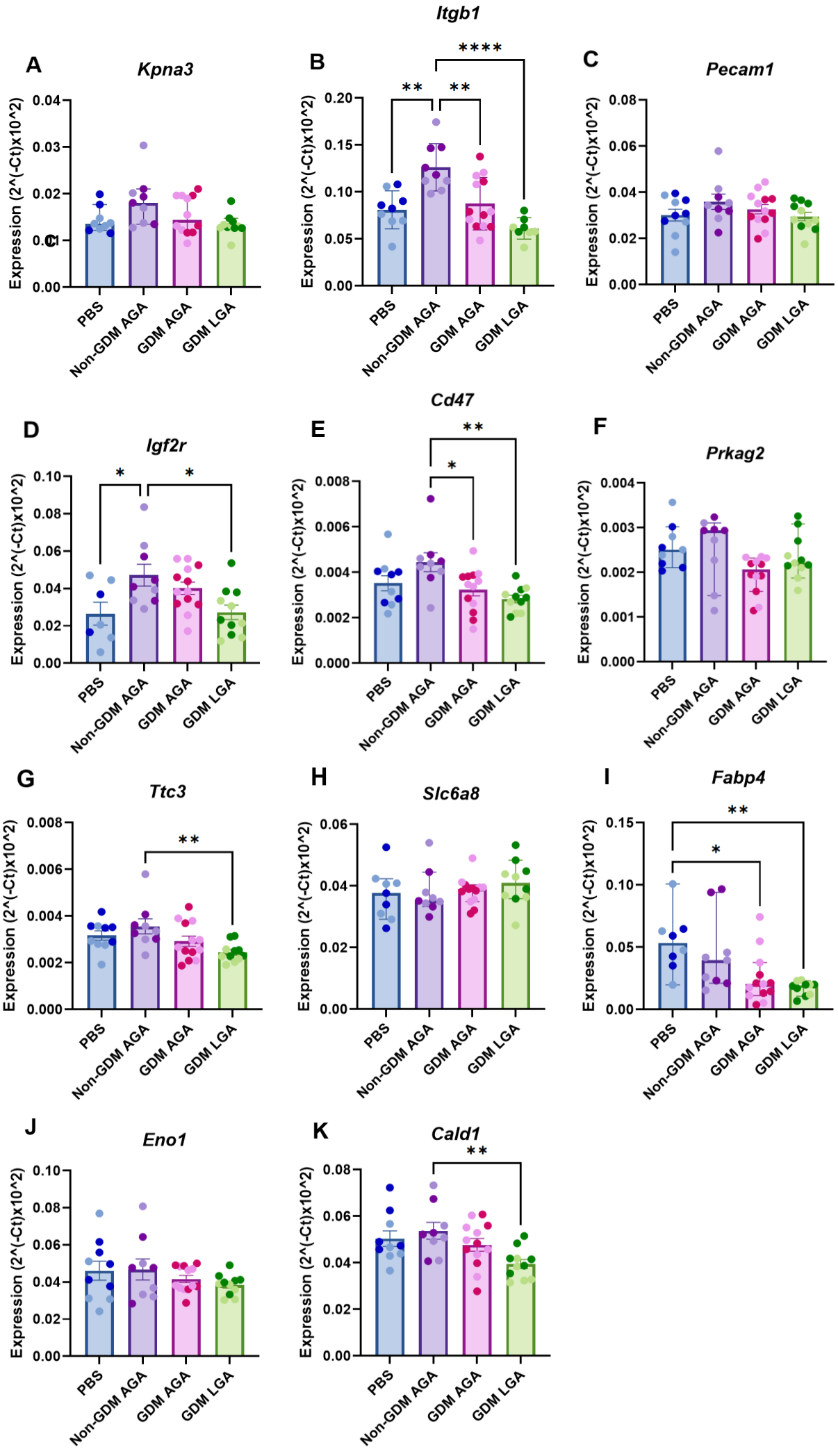
A
Kpna3
B
Itgb1
C
Pecam1
D
Igf2r
E
Cd47
F
Prkag2
G
Ttc3
H
Slc6a8
I
Fabp4
J
Eno1
K
Cald1
Expression (2^(-Ct)x10^2)
PBS
Non-GDM AGA
GDM AGA
GDM LGA

Figure 113 Mouse placenta mRNA expression of key placental regulatory genes.

Healthy pregnant C57BL6/J female mice were injected with PBS or human plasma EVs from healthy uncomplicated pregnancies, GDM-AGA or GDM-LGA pregnancies at E11.5, E13.5 and E15.5 before being sacrificed at E18.5. Placental mature miRNA was isolated and reverse transcribed (n=1 male, n=1 female from each litter) before miRNA expression was analysed using qPCR and normalised to β-actin; (2^(-Ct)*10^(2)). Ordinary one-way ANOVA followed by Tukey's multiple comparisons test was performed for normally distributed data and presented as mean with SEM. Kruskall-Wallis followed by Dunn's multiple comparisons test was performed for nonparametric data and presented as median with 95% CI. Light data points; female, dark data points; male.

5.5 Discussion

Findings of this chapter demonstrate that *in-vivo* delivery of human maternal plasma small EVs into the maternal circulation of healthy pregnancy mice impacts placental and fetal growth, where they may contribute towards various adverse pregnancy outcomes associated with GDM. Results suggest that healthy pregnancy maternal small EVs influence the placental metabolome, lipidome and transcriptome, thereby suggesting they play a key role in maintaining optimal nutrient bioavailability to the fetus. However, it was demonstrated that in GDM pregnancies, maternal small EVs differentially impact fetal and placental development, where LGA may also contribute towards adverse maternal cardiometabolic adaptations and suboptimal placental nutrient bioavailability to the fetus.

5.5.1 Administration of human maternal plasma small EVs to the maternal circulation of healthy pregnancy mice and pregnancy outcomes

To mimic the *in-vivo* environment of pregnancy, tail vein injections were performed in this study to facilitate direct delivery of human maternal plasma small EVs into the maternal circulation of healthy pregnant mice. As discussed in chapter 4, although a continuous infusion of small EVs would best mimic the *in-vivo* environment of pregnancy, three periodical injections were performed due to ethical regulations. These periodical injections at E11.5, E13.5 and E15.5 gestational timepoints coincided with the formation and development of the placenta as well as early organogenesis (448,468,469). Previous studies have examined the impact of pregnancy-related EVs using animal models, however there is considerable variability in the concentration administered across studies, ranging from 1.1E+10/mL to 9.16E+10/mL (557). Other studies have reported the administration of 40µg to 100µg total EV protein into pregnant mice (557). Due to EV sample availability, human maternal plasma small EVs were injected at an *in-vivo* concentration of 1.5E+9 particles/mL. When measured for protein content, the pooled human maternal plasma small EVs contained over 200µg total EV

protein (data not shown) and thus it was established that the concentration used was sufficient to observe any effects in pregnant mice.

Moreover, it is known that maternal circulating EV concentration is increased in pregnancy, where it has been demonstrated that maternal circulating EV concentration significantly increases with gestational age due to increased EV production by the placenta (264,558). However, it has been established that GDM is characterised by a further increase in maternal circulating EV concentration, where the proportion of placenta-derived small EVs in the circulation is altered (278). This study did not account for the difference in maternal circulating EV concentration between healthy pregnancies and GDM pregnancies as it would be complex to decipher whether any effects observed would be due to the difference in concentration or the treatment itself. However, future research may benefit from gradually increasing the dose of human maternal plasma small EVs injected into healthy pregnant mice across various gestational time points to better mimic the *in-vivo* environment of pregnancy.

No visible toxic effects were observed with the human maternal plasma small EV treatments, however further research is warranted to examine the toxicity of human maternal plasma small EV treatments on pregnant mice and their offspring on a molecular level.

5.5.2 Impact of Healthy Pregnancy Maternal Small EVs on Fetal and Maternal Pregnancy Outcomes

In-vivo delivery of human maternal plasma small EVs from healthy pregnancies into healthy pregnant mice demonstrated to increase fetal and placental growth compared to control treatment, suggesting that maternal circulating EVs have a profound role in offspring development. In particular, growth of the male fetus and placenta was more significantly impacted than that of females. This finding aligns with current clinical data, where it has been demonstrated that the birthweight of males is significantly higher than females in healthy pregnancy (559). Interestingly, it has been reported that male offspring are at increased risk of adverse immediate birth outcomes compared to females, thereby warranting the

need to investigate sex-specific changes which occur in the intrauterine environment during pregnancy (559).

It has been shown that compensatory growth mechanisms may occur during organogenesis if fetal growth trajectory is altered during pregnancy, where male offspring are more susceptible to changes in the intrauterine environment than females (195,560,561). It is therefore possible that female offspring are more able to adapt to the impact of maternal pregnancy small EVs on feto-placental development, wheres males are more sensitive to the growth stimulating effects of maternal pregnancy small EVs.

Although it is known that maternal EVs are key regulators of maternal metabolism (262–264), human maternal plasma small EVs from healthy pregnancies demonstrated no significant impact on mouse maternal cardiometabolic health. However, maternal small EVs demonstrated to alter the placental metabolome, lipidome and transcriptome. As such, this suggests that during healthy pregnancy, maternal small EVs regulate feto-placental growth by directly impacting the placenta. In particular, it was demonstrated that in healthy pregnancy, maternal small EVs predominantly upregulated the expression of placental acylcarnitines (AC6:0, AC16:0, AC16:1, AC18:0, AC18:1) and downregulated the expression of various free fatty acids (FFA 17:0, FFA 20:0). Although not statistically significant, other downregulated lipid species included FFAs 16:1, 18:4, 16:0 and 20:1. As such, these findings suggest that maternal small EVs stimulate placental fatty acid metabolism in healthy pregnancy, where increased acylcarnitine expression and reduced FFA expression indicates increased FFA shuttling to the mitochondria to produce ATP energy via β-oxidation (402,562). This may be a key mechanism whereby maternal EVs regulate the growing metabolic demands of the fetus throughout pregnancy, in that placental energy production is increased. LC-PUFA are not synthesised *de-novo*, therefore the fetus is dependent on placental transfer of LC-PUFA, particularly at later stages of pregnancy when fetal uptake exceeds maternal intake in order to maintain accelerated growth of major fetal organs such as the brain (562). Evidence shows that dysregulated placental lipid metabolism may promote oxidative stress and lead to altered lipid transfer to the fetus, thereby contributing towards adverse pregnancy outcomes (562). This further demonstrates the key role of maternal

pregnancy small EVs in maintaining optimal fetal growth during pregnancy through regulating placental lipid metabolism.

Maternal small EVs from healthy pregnancies also upregulated placental expression of tryptophan metabolites, serotonin and acetyl-5-hydroxytryptamine (also known as acetyl-serotonin). When separated based on fetal sex, it was demonstrated that acetyl-serotonin was significantly altered in female placentae but not male placentae. Acetyl-serotonin is a precursor for melatonin, which is essential for placental antioxidative enzymes to regulate placental efficiency and fetal growth (515,517,518). The role of placental serotonin is also well characterised in pregnancy, where this neurotransmitter is key for fetal brain development (563). The placenta is the only source of serotonin for the fetus, where altered expression of this neurotransmitter in the placenta may be associated with altered fetal growth and neurodevelopmental disorders (563). As such, findings from this study suggest that the activity of maternal pregnancy small EVs on placental metabolism is vital to maintain optimal fetal growth and organ development during pregnancy.

When examining sex differences, it was demonstrated that the impact of maternal plasma small EVs on placental acylcarnitine expression was mainly observed in males, whereas the impact of maternal plasma small EVs on the expression of placental lipid species was mainly altered in females. This finding aligns with current literature demonstrating sex-specific distinctions in placental lipid metabolism, where it was found that females manifest increased placental lipid oxidation to maintain metabolic demands during pregnancy, resulting in increased placental antioxidant expression to sustain redox homeostasis throughout pregnancy (526).

Interestingly, findings from this chapter demonstrated that human maternal plasma small EV mean and mode diameter was lower in male pregnancies than female pregnancies, however this finding was statistically insignificant. It has previously been reported that placental EVs of various sizes manifest distinct proteomic profiles, suggesting that EV-mediated interaction within the feto-placental interface may be influenced by EV size (564). There is currently a lack of studies examining sex-specific distinctions in pregnancy-related EV profiles. In

a recent study, it has been identified that lipid composition of placenta small EVs is similar between male and female noncomplicated pregnancies, suggesting that placenta EV interaction and function is similar for males and females (565). However, another study has demonstrated that male and female pregnancies manifest distinct maternal EV-miRNA profiles at various gestational timepoints (566), suggesting miRNA cargo released from EVs originating from the placental and/or other maternal organs may be altered between male and female pregnancies. Moreover, sex-specific changes in pregnancy may also indicate that EVs originating from the fetus itself may be contributing towards altered feto-placental development. Indeed, it has been shown that EV transfer is bidirectional between the placenta and the fetus, where evidence also demonstrates that the placenta may respond to fetal endocrine signals to promote nutrient transfer (479,557).

No differences were observed in the placental zone structures between male and female pregnancies of mice treated with human maternal plasma small EVs from healthy pregnancies and PBS control, however this may have been due to low statistical power. Placental *Igf2r* and *Itgb1* expression were increased following exposure to maternal pregnancy small EVs. Current evidence shows that IGF2-IGF2R signalling is increased during late gestation to inhibit additional fetal growth (500). It is also known that *Itgb1* is a key regulator of trophoblast infiltration and turnover (457,458). These results therefore further exemplify the key role of maternal pregnancy EVs in regulating feto-placental development during healthy pregnancy. Although not in females, maternal pregnancy small EVs demonstrated to significantly increase *Itgb1* expression in male placentae compared to PBS control. As such, this suggests that male pregnancies may manifest increased trophoblast turnover and nutrient transfer to the developing fetus, resulting in greater fetal and placental growth than females.

Findings demonstrated that maternal pregnancy small EVs have no effect on placental miR-375-3p, miR-1-3p, miR-200c-3p and miR-133a-3p expression. However, these miRNAs were identified to be altered in the maternal circulation of GDM-LGA pregnancies and not healthy pregnancies. Future research would therefore benefit from investigating if placental expression of other miRNAs may be impacted by maternal small EVs in healthy pregnancy. This may provide

further insight into the aetiology of maternal small EVs in regulating feto-placental development during pregnancy.

5.5.3 Impact of Maternal Small EVs from GDM Pregnancies on Fetal and Maternal Pregnancy Outcomes

Human maternal plasma small EVs from GDM pregnancies with AGA outcomes demonstrated to reduce fetal growth compared to such EVs from healthy pregnancies. This finding aligns with clinical data demonstrating that treated GDM pregnancies are characterised by reduced birthweight compared to healthy normoglycaemic pregnancies (567). However, clinical data also shows that despite reducing birthweight, treating GDM does not alter offspring adiposity 1 year after birth (567). Future research should aim to assess the long-term impact of maternal pregnancy small EVs from GDM-AGA pregnancies on offspring adiposity. This would determine whether the effect of maternal pregnancy EVs align with long-term clinical outcomes related to GDM pregnancies with AGA outcomes. Although not statistically significant, placental growth was also reduced in pups exposed to maternal pregnancy EVs from GDM-AGA pregnancies, however this effect was more prominent in males than females. This is also found in the literature, where evidence demonstrates that males have smaller placentae than females, suggesting that males manifest reduced placental reserve capacity during suboptimal *in-utero* conditions (568). *Itgb1* was significantly reduced in the placenta of mice exposed to GDM-AGA small EVs compared to healthy pregnancy EVs, and when stratifying for fetal sex, it was identified that this phenomenon was only observed in males, suggesting that placental trophoblast infiltration and turnover may be impaired in males (457,458). Interestingly, it has been reported that male GDM pregnancies manifest altered placental O-GlcNAc transferase expression which may affect trophoblast endocrine function (569). Under *in-vitro* conditions, altered placental O-GlcNAc transferase expression demonstrated no significant impact in females, indicating that sex-specific effects in GDM may be partly attributed to altered placental endocrine function via O-GlcNAc transferase regulation in males.

Maternal small EVs from GDM pregnancies with AGA outcomes demonstrated no impact on maternal metabolic parameters compared to healthy pregnancies. This contradicts current literature demonstrating that EVs are key regulators of maternal glucose metabolism throughout gestation, where their cargo may play a role in the pathogenesis of GDM (264,268). However, although not characterised in this thesis, it is possible that the maternal plasma EV samples injected into mice in this study were collected from well-controlled GDM pregnancies. Moreover, evidence demonstrates that fetal sex may impact maternal metabolism, whereby a male fetus has been associated with weaker maternal β-cell function, leading to increased risk of GDM onset in pregnancy (570). Maternal plasma EV samples injected into mice in this study originated from equally numbered male and female pregnancies, and given that murine pregnancies are characterised by mixed-sex litters, sex-specific effects on maternal metabolism may have been missed in this study.

GDM pregnancies demonstrated a reduction in maternal plasma small EV concentration compared to healthy pregnancy, where no sex-specific differences were observed. This is contradictory to the current literature demonstrating that maternal circulating EV concentration is elevated in GDM compared to healthy pregnancy (278). Maternal obesity, ethnicity and age are known to influence maternal EV production and cargo (571,572). It is therefore possible that this discrepancy in maternal EV concentration may be due to the maternal demographics of the GDM samples, where although the overall pooled groups were matched as closely as possible, interpatient heterogeneity was still observed. Indeed, other studies have demonstrated no change or lower maternal circulating EV concentration in GDM pregnancies compared to healthy pregnancies (573). As maternal EV size was lower in GDM-AGA pregnancies compared to healthy pregnancies, this suggests that GDM may be altering EV cargo and thus changing EV-mediated interaction within the feto- and maternal-placental interface during pregnancy (564). Indeed, it has been evidenced that GDM is characterised by altered placenta EV-miRNA profile which in turn may influence maternal organ function, contributing towards the pathogenesis of GDM (574). Indeed, although not significant, placental expression of miR-133a-3p was downregulated in mouse placentae exposed to GDM small EVs compared to

healthy pregnancy EVs in this study. miR-133a-3p has previously been identified to be altered in maternal circulating EVs of GDM pregnancies complicated by altered fetal growth (575). Evidence shows that miR-133a-3p is involved in vascular development (575), suggesting that maternal small EVs may impair placental vascularisation and thus influence fetal development in GDM pregnancies.

Maternal plasma small EVs demonstrated no significant impact on the placental lipidome in the context of GDM compared to healthy pregnancy, where only FFA 16:1 and FFA 20:0 were upregulated. When separating for fetal sex, no impact was observed on the female placental lipidome but PG 16:0-18:2 and FFA 22:2 were upregulated in male placentae. In contrast, previous literature demonstrates that even well-controlled GDM is characterised by altered placental lipid expression, particularly unsaturated FFA expression (576). Moreover, a non-significant reduction in *Fabp4* levels was observed in the placenta of mice exposed to GDM-AGA small EVs compared to healthy pregnancy EVs, where this finding was statistically significant when compared to PBS control mice. However, this contrasts with a previous study showing that placental FABP4 expression is unchanged with GDM, although it was found that maternal weight increased its expression (535). It is therefore possible that maternal BMI heterogeneity within the pooled EV treatment groups may have influenced these results (571,572). Furthermore, it has been shown that placental FABP4 is dispensable for fetal growth and placental lipid metabolism during pregnancy (577).

Maternal plasma small EVs from GDM pregnancies with AGA outcomes had a profound effect on placental tryptophan metabolite expression, where serotonin, 5-HIAA and acetyl-5-hydroxytryptamine (acetyl-serotonin) were all downregulated compared to control animals. Tryptophan is only acquired via dietary intake and is key for fetal protein synthesis during pregnancy (578). As such, acetyl-serotonin and serotonin are key regulators of optimal fetal development, where the placenta is the sole source of serotonin for the developing fetus (515,517,518,563). As such, impaired placental serotonin metabolism has been associated with fetal growth restriction and placental insufficiency, however it is still uncertain if impaired placental serotonin

metabolism is involved in fetal growth restriction pathogenesis (578). When stratifying the data for fetal sex, it was identified that acetyl-serotonin and serotonin were significantly downregulated in female placentae but not male placentae. This suggests that maternal small EVs may be more likely to promote placental insufficiency in female pregnancies than male pregnancies. However, as placental growth was more reduced in male placentae than female placentae, it is possible that females are better able to elicit compensatory mechanisms to regulate fetal growth trajectory during pregnancy. Indeed, it has been shown that females are not as susceptible to changes in the intrauterine environment as males (195,560,561). Interestingly, it has been demonstrated that serotonin is essential for β-cell proliferation and maternal glycaemic control in pregnancy, where reduced serotonin levels has been associated with lower β-cell population, insulin secretion dysregulation and glucose intolerance in pregnant mice (579). An association between gestational vitamin B6 deficiency, reduced pancreatic islet serotonin levels, impaired β-cell turnover, glucose intolerance and insulin resistance has also been established (579).

A marginal increase in labyrinth zone surface area was observed in response to GDM-AGA small EVs compared to healthy pregnancies, resulting in a slight reduction in junctional/labyrinth zone surface area, however these findings were insignificant. Previous literature has also shown that placental labyrinth and junctional zone surface areas are not significantly altered in rat models of diabetes (580). Moreover, a non-significant reduction in placental decidua zone surface area was observed in mice exposed to GDM-AGA small EVs compared to healthy pregnancy small EVs, where this reduction was statistically significant when compared to PBS control animals. This aligns with current literature demonstrating that decidua mean surface area of diabetic rats is decreased compared to control rats (580). Previous work also demonstrates that E18 placenta of diabetes-induced rats manifest thinner decidua basalis than control rats, which is characterised by lymphocyte accumulation (581). Further research should therefore aim to elucidate whether these changes associated with immunity are also observed in the placenta in response to maternal plasma EVs from GDM pregnancies with AGA outcomes. Indeed, GDM is known to impair immunoendocrine regulation and interestingly, it was demonstrated that

maternal-fetal immunity regulator, *Cd47,* was downregulated in the placentae of mice exposed to GDM-AGA small EVs compared to healthy pregnancy EVs (491,582).

5.5.4 Impact of Maternal Small EVs from GDM Pregnancies with LGA outcomes on Fetal and Maternal Pregnancy Outcomes

Fetal growth was increased in mice treated with human maternal small EVs from GDM pregnancies with LGA compared to AGA outcomes, thereby reflecting clinical outcomes associated with GDM (396). Placental growth was unchanged with GDM-LGA small EVs exposure, however the surface area of the placental junctional zone and junctional/labyrinth zone was non-significantly increased compared to the effect of GDM-AGA small EVs. The junctional zone is essential for placental endocrine function and energy production for the fetus and placenta (583). This finding also aligns with current literature demonstrating that altered development of the placental junctional zone is associated with altered fetal growth (448). By investigating the placental lipidome, it was demonstrated that several lipid species were altered in response to GDM small EVs from pregnancies with LGA compared to AGA outcomes. As such, this suggests that GDM pregnancies resulting in LGA compared to AGA are characterised by altered placental lipid metabolism. Several FFA species were reduced in the placenta of mice exposed to GDM-LGA small EVs, suggestive of increased FFA shuttling to the developing fetus, resulting in increased fetal lipid supply. However, as no change in placental TAG expression was demonstrated, it is also possible that GDM-LGA small EVs may promote rapid removal or suppress importation of TAGs in placental tissue, which in turn may increase lipid transfer to the developing fetus and thus contribute towards LGA. Indeed, it has previously been reported that altered lipid metabolism may play a role in fetal overgrowth in GDM pregnancies (534,584). These placental changes in GDM pregnancies complicated by altered fetal growth may be attributed to maternal EV composition, where it has previously been reported that circulating placental EV lipid profile is altered with birthweight (565). As such, future research should aim to assess lipid content of maternal circulating EVs GDM pregnancies with various fetal growth outcomes.

When stratifying for fetal sex, it was demonstrated that fetal growth was increased to a greater significance in males than females in response to GDM-LGA small EVs. This sex difference may be attributed to the sex-specific effects of GDM-LGA small EVs on the placental metabolome, where no significant effect was observed for females but TCA cycle metabolites were significantly downregulated in male placentae, namely citrate, isocitrate, fumarate and malic acid. A reduction in placental lactic acid levels was also observed in males, suggesting that GDM-LGA small EVs may impair placental glucose metabolism in male placentae. Interestingly, although not observed in females, male placentae also demonstrated upregulated TAG 50:3 and TAG 52:5 expression in response to GDM small EVs from LGA compared to AGA pregnancies. These findings therefore suggest that GDM-LGA small EVs may promote a metabolic shift towards lipid metabolism for energy production in male placentae, rather than carbohydrate metabolism. Indeed, excess lipid transfer to the developing fetus is known to induce fetal hyperinsulinaemia, resulting in fetal fat development and overgrowth (585). However, results showed that FFA expression was reduced in male placentae exposed to GDM-LGA small EVs, where FFA 22:3 expression was significantly downregulated. A non-significant reduction in FFA 16:0, FFA 22:2 and FFA 22:4 levels was also observed, suggesting that placental lipolysis may be impaired. Furthermore, as metabolites of the TCA cycle were downregulated, these findings suggest that GDM-LGA small EVs may be suppressing FFA β-oxidation for energy production in the male placentae. As a consequence, GDM-LGA small EVs may be driving mitochondrial dysfunction in the male placentae, leading to altered feto-placental nutrient transfer. Indeed, it has previously been demonstrated that GDM is characterised by placental mitochondrial dysfunction which may be a contributor towards altered fetal growth in pregnancies (171,586). Another study has shown that maternal hyperglycaemia may impact placental β-oxidation, where altered placental lipid metabolism may enhance feto-placental lipid transport and contribute towards increased fetal growth in pregnancies complicated by maternal diabetes (532). As such, findings from this chapter align with the current literature where interestingly, a previous study has also reported that male pregnancies may be more susceptible to placental mitochondrial dysfunction through reduced β-oxidation than females (54). Accordingly, this hallmark may contribute to the

increased prevalence of LGA in male offspring than female offspring in GDM pregnancies (587).

The placental transcriptome was also impacted by GDM small EVs from LGA compared to AGA pregnancies in a sex-dependent manner. Specifically, *Itgb1* and *Fabp4* gene expression were significantly altered in male placentae exposed to GDM-LGA small EVs compared to healthy pregnancy small EVs and PBS control, respectively. Moreover, *Cald1, Ttc3* and *Itgb1* placental expression were significantly altered in females exposed to GDM-LGA small EVs compared to healthy pregnancy small EVs. Interestingly, results demonstrated that maternal EV mean and mode diameter were non-significantly increased in human GDM male pregnancies with LGA outcomes compared to AGA outcomes, with this increase being statistically significant when compared to healthy male pregnancies. As various EV sizes are associated with distinct proteomic profiles (564), it is possible that EV-mediated interaction within the feto-placental interface may be altered in male pregnancies complicated by GDM and LGA. Therefore, although aetiology of sex-dependent changes in the placenta in GDM pregnancies complicated by LGA remains to be elucidated, future research should aim to characterise maternal EV cargo and composition of both male and female GDM pregnancies with various fetal growth outcomes.

Itgb1, Igf2r, Cd47, Ttc3, Fabp4 and *Cald1* were all downregulated in placentae exposed to GDM-LGA small EVs compared to other maternal small EV treatments, where these findings were significant when compared to PBS control animals. As demonstrated in chapter 4, these genes are targets of miR-375-3p and were also identified to be downregulated in mouse placentae exposed to miR-375-3p overexpression. Previous work from the Forbes group demonstrates that miR-375-3p is upregulated in the maternal circulation of GDM pregnancies resulting in LGA outcomes compared to AGA outcomes. Interestingly, results from this chapter show that miR-375-3p expression was increased in the GDM-LGA small EVs treatment group compared to maternal plasma GDM AGA small EVs and healthy pregnancy small EVs, thereby further strengthening previous findings that miR-375-3p may be associated with LGA in GDM pregnancies. However, although genes were similarly altered in placentae exposed to miR-375-3p overexpression (Chapter 4) and GDM-LGA small EVs from human pregnancies,

the placental lipidome and metabolome were differentially altered in response to both treatments and placental miR-375-3p expression was unchanged in mice exposed to GDM-LGA small EVs. This therefore suggests that maternal EVs may promote LGA outcomes in GDM pregnancies through additional mechanisms on the placenta, potentially by indirectly impacting maternal metabolism.

Indeed, hallmarks of maternal cardiac hypertrophy were observed in mice exposed to maternal small EVs from GDM pregnancies with LGA compared to AGA outcomes. This is an interesting finding, given that GDM is associated with long-term adverse maternal cardiovascular health postpartum compared to healthy pregnancy (20). Unlike other miRNAs previously identified to be significantly altered in term placental tissue of human GDM pregnancies with LGA outcomes compared to AGA outcomes (**Figure *38***), a non-significant upward trend in placental miR-1-3p expression was observed in mice exposed to maternal small EVs from GDM-LGA pregnancies compared to GDM-AGA and healthy pregnancy small EVs. miR-1-3p is a cardiac-associated miRNA, known to regulate vascular smooth muscle cell differentiation (575,588,589). Interestingly, miR-1-3p was undetected in the pooled small EVs from human maternal GDM-LGA pregnancies. As such, this strongly suggests that maternal EVs may influence the maternal heart in GDM pregnancies complicated by LGA, resulting in increased miR-1-3p release into the maternal circulation which may then be trafficked to the placenta. Further research should therefore aim to investigate the impact of maternal EVs on maternal cardiac tissue and whether birthweight influences maternal long-term cardiovascular health in GDM pregnancies.

5.6 Summary

Effect of human maternal plasma EVs on pregnancy outcomes in healthy pregnant mice			
	Non-GDM AGA EVs vs PBS	**GDM AGA vs Non-GDM AGA EVs**	**GDM LGA vs GDM AGA EVs**
Fetal Growth	Increased • Significant increase in male pregnancies • Non-significant increase in female pregnancies	Decreased • Non-significant decrease in male pregnancies • Non-significant decrease in female pregnancies	Increased • Significant increase in male pregnancies • Non-significant increase in female pregnancies
Placental Growth	Increased • Significant increase in male pregnancies • Non-significant increase in female pregnancies	No significant impact • Non-significant decrease in male pregnancies • Non-significant decrease in female pregnancies	No significant impact • Non-significant decrease in male pregnancies • Non-significant decrease in female pregnancies
Fetal-Placental Growth	Correlated fetal and placental growth	Correlated fetal and placental growth	Correlated fetal and placental growth
Maternal Metabolism	• No significant effect	• No significant effect	• Hallmarks of cardiac hypertrophy
Placental Metabolism	**Altered tryptophan metabolism** • Upregulation of serotonin and acetyl-5-hydroxy-tryptamine **Altered fatty acid β-oxidation** • Downregulation of FFA 17, FFA 20 • Upregulation of long-chain and short chain acylcarnitines – AC18, AC18:1, AC16, AC16:1, AC6 • Sex-dependent effects demonstrated in the placental metabolome and lipidome	**Altered tryptophan metabolism** • Downregulation of serotonin, acetyl-5-hydroxy-tryptamine and 5-HIAA • Sex-dependent effects demonstrated in the placental metabolome and lipidome	**Altered lipid transfer to fetus** • Downregulation of FFA 14:0, 16:0, 22:2, 17:1, 22:3, 22:4, 22:1 and DAG 16:1-18:0, 18:1-18:1, 16:0-18:0, 18:1- 18:3. **Altered tryptophan metabolism** • Downregulation of serotonin, 5-HIAA and acetyl-5-hydroxy-tryptamine • Sex-dependent effects demonstrated in the placental metabolome and lipidome
Placental Zones	No significant effect	No significant effect	No significant effect
Summary	Maternal EVs play a key role in regulating fetal and placental growth by altering placental lipid and amino acid metabolism to ensure sufficient nutrient supply to the developing fetus. Through maternal EV activity, placental amino acid metabolism is altered in GDM compared to healthy pregnancy, suggesting a compensatory mechanism to reduce fetal overgrowth as a consequence of a diabetic environment. However, when GDM is complicated by fetal overgrowth, maternal EVs play a role in maternal cardiometabolic maladaptation and the dysregulation of placental lipid and amino acid metabolism, whereby the developing fetus may be subject to altered nutrient bioavailability.		

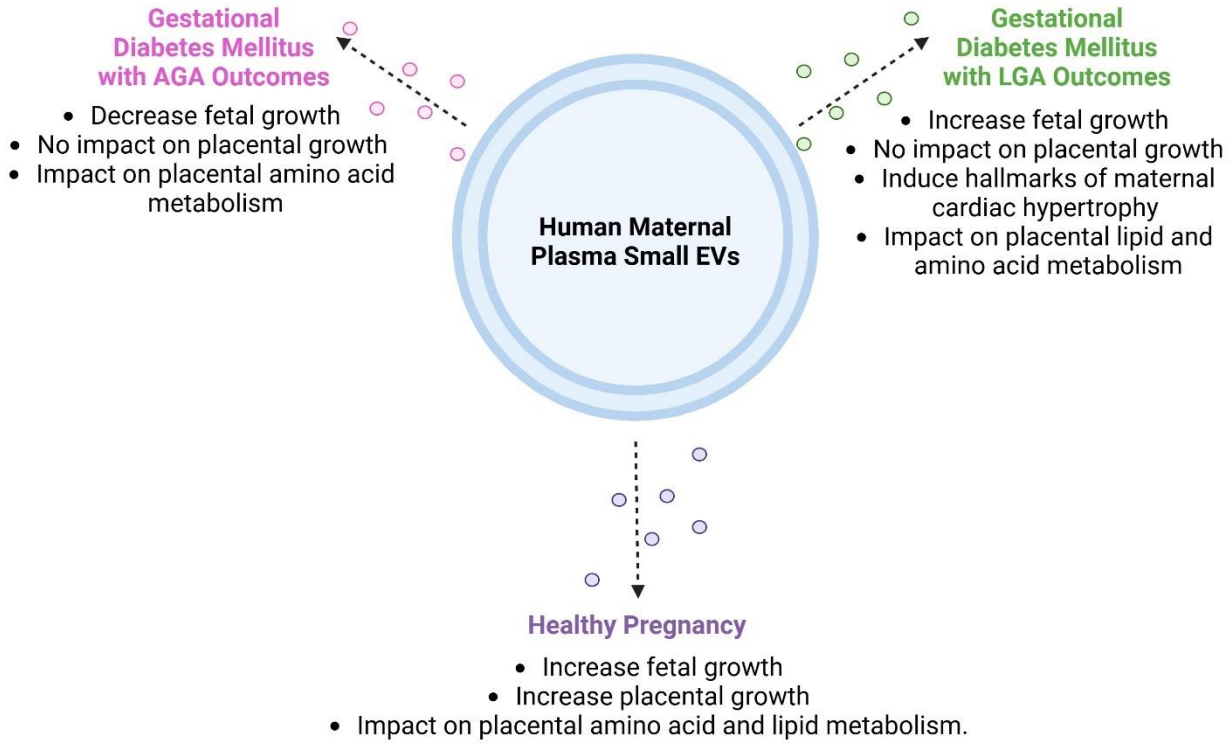

Figure 114 Graphical summary of the effect of human maternal plasma small EVs from various pregnancy outcomes on fetal and placental development in healthy pregnant mice.

Human maternal plasma small EVs from healthy pregnancy and GDM pregnancy with AGA and LGA outcomes all differentially impact mouse fetal and placental development. Created using Biorender.com.

6 General Discussion

6.1 Main Findings and Models of Pregnancy

Findings from this thesis demonstrate that factors in the maternal circulation in pregnancies complicated by GDM can both directly or indirectly influence events in the placenta, and that this may contribute towards altered fetal growth. As such, the choice of model to study the effects of specific factors in the maternal circulation is important, as the direct and indirect effects on the placenta are not captured in many models of pregnancy. Comparing the placental transcriptome of obese women with GDM treated with or without metformin in-vivo, with the direct impact of metformin on human placental explants ex-vivo, demonstrated that metformin may exert direct and indirect effects on placental development, growth and metabolism. It has previously been demonstrated that metformin impacts circulating EV and miRNA profile *(***Table 25***,* **Table 26***).* It is therefore possible that metformin acts on maternal organs to alter release and/or cargo of EVs into the circulation and that these EVs and their miRNA content traffic to the placenta to influence placental and fetal growth. As a result, in addition to utilising in-vitro or ex-vivo models to study the impact of specific factors on placental biology, models to study the in-vivo influence of maternal EVs and their cargo should be considered since they allow further insight into whole physiology of pregnancies complicated by GDM.

Due to the complex heterogeneity of circulating EVs (590), determining the origin of circulating maternal EVs and miRNAs is difficult. However, the Forbes group have previously demonstrated that miR-375-3p, a pancreas-specific miRNA, is upregulated in the circulation and placenta of human pregnancies complicated by GDM and LGA. By using an *in-vivo* model in Chapter 4, a causative mechanism could be established between maternal circulating miR-375-3p and altered fetal growth in GDM pregnancies. Although it was established that most placental targets of miR-375-3p are homologous in human and mouse, whereby placental growth, metabolism and vascular development are affected, some placenta targets were differently impacted in the *in-vivo* mouse model compared to the human *ex-vivo* placental model. Although these differences may be an interspecies effect, it is also possible that the impact of miR-375-3p on the

placenta may vary depending on whether an *in-vivo* or *ex-vivo* model is used. Moreover, these findings provide further evidence that maternal metabolic adaptations contribute towards the underlying pathophysiology of GDM pregnancies complicated by altered fetal growth.

This is further exemplified in Chapter 5, where maternal circulating EVs from various pregnancy outcomes, including healthy and GDM pregnancies with AGA/LGA births, exerted different effects on fetal and placental growth. This strongly demonstrates that EVs mediate maternal metabolic adaptations during pregnancy which in turn indirectly impact fetal outcomes by influencing placental development. Findings from this thesis therefore highlight the importance of considering *in-vivo* circulating factors when designing models of pregnancy.

6.2 Clinical Biomarkers and Therapeutic Applications for Managing Pregnancies Complicated by GDM

EVs and their miRNA cargo have a clear role in the progression of maternal and fetal complications in pregnancies affected by maternal diabetes. While further research is still needed to elucidate their pleiotropic effects, mechanisms and impact on long-term health, their biomarker potential to detect adverse maternal and fetal outcomes in pregnancies complicated by maternal diabetes is well recognised. Not only do EVs and miRNAs increase understanding of underlying *in-vivo* pathophysiology and altered target genes associated with diseases, but they may also provide an alternative means of non-invasive testing. GDM is usually diagnosed through an OGTT at weeks 24-28 gestation when pregnancy is at an advanced stage, meaning minimal interventions can be implemented to avoid or manage adverse maternal and fetal outcomes (591). However, recent studies are suggesting that earlier detection and treatment is associated with better maternal and neonatal outcomes (592). There is currently a lack of consensus on the gold standard diagnostic criteria that should be used for GDM, which has led to heterogenous guidelines and confusion about the prevalence of GDM worldwide (593). As such, many people with hyperglycaemia go undetected throughout pregnancy.

There are certain maternal circulating miRNAs that have been identified as potential diagnostic biomarkers for GDM, however intra-study reproducibility is an essential factor to consider when identifying miRNAs as biomarkers (591,594,595). There are currently only 6 miRNAs (miR-195, miR-330, miR-342, miR-520h, miR-657, miR-1323) that have been similarly differentially expressed in people with GDM across multiple studies, with these studies using a range of methodologies and involving individuals of different populations and age range (255). Most of these miRNAs have been identified to be altered in the placenta of people with GDM (Table 2, Chapter 1). Using miRNAs as biomarkers for GDM diagnosis would provide another layer of screening for improved consensus (255). This would allow for adverse maternal and fetal outcomes to be detected at an earlier stage of pregnancy and thus allow more time for intervention strategies to be implemented, such as exercise, diet and medication (591).

Medications such as metformin have also demonstrated to alter circulating EV cargo and miRNA profile *(**Table 25**, **Table 26**).* This may explain the discrepancy between the effect of direct metformin exposure and in-vivo metformin exposure on placental development. However, these results also suggest that minimising the effects of metformin on placenta may be a potential therapeutic avenue to improve fetal outcomes in GDM pregnancies while still maintaining its beneficial effects on maternal metabolism. Currently, there is still controversy on whether initiating metformin treatment earlier in pregnancy may lead to improved maternal outcomes and thus reduce the risk of adverse outcomes for the fetus (596–598). Moreover, recent evidence shows that the prevalence of circulating EVs may serve as biomarkers for the response to metformin therapy (369). In future, this finding could be expanded where associations could be made between response to metformin therapy and adverse fetal outcomes. As such, screening maternal EV profile during different stages of pregnancy may assist with improving management and monitoring of GDM pregnancies at risk of altered fetal growth.

It has also been shown that exercise during pregnancy can alter the plasma miRNA profile in individuals with GDM, giving rise to potential biomarkers that may be used to detect GDM risk (599). Indeed, reports show that maternal exercise during pregnancy may improve female offspring hepatic metabolism by

modulating miRNA activity and reverse the dysregulated fetal cardiac miRNA profile identified in GDM pregnancies (600,601).

Since maternal diabetes increases the risk of altered fetal growth and predisposes offspring to cardiometabolic complications throughout life (244), infants of pregnancies complicated by maternal diabetes would benefit from primary prevention strategies. Identifying pregnancies at risk of altered fetal growth would also allow suitable birth planning and improved clinical management of mother and offspring throughout pregnancy. Additionally, follow-up screening of the neonatal EV and miRNA profile may provide better identification of congenital abnormalities that are associated with pregnancies complicated by maternal diabetes and medications such as metformin, including cardiovascular and cerebrovascular complications (45,54,304) (**Table *1***). Maternal diabetes is also associated with an increased risk of postpartum maternal cardiometabolic disease and cancer. Thus, identifying the altered maternal EV and miRNA profiles associated with these complications would also improve clinical management of maternal health after pregnancy.

Currently, there is a lack of study reproducibility of miRNAs being used as biomarkers. Sample collection, storage, isolation and processing methodologies all influence miRNA quality and stability (602–604). Therefore, improving consensus on the appropriate methods to use for miRNA biomarker studies would increase reproducibility.

6.2.1 Potential Therapeutics

EV-based therapy has previously been explored in the literature, where EV cargo and receptors may be modified and delivered to targets cells in the context of many diseases (605,606). Cargo such as small drugs and RNA molecules can be loaded into EVs via exogenous or endogenous methods (605). It has previously been reported that platelet-released EVs may have therapeutic potential for a wide-range of conditions, including cancer, atherosclerosis and rheumatoid arthritis (605). Indeed, there are currently three clinical trials investigating the efficiency of platelet-released EVs therapy for ear infection, temporal bone cavity inflammation and lower back pain, where promising results

have been reported in the management of patient symptoms (605). However, at present, engineering and upscaling EVs to express certain cargo in-vitro is a time-consuming process (605). EV mimetics have recently been developed which may prove promising to address this issue of EV upscaling (607), however further research is needed to confirm the efficiency and safety of EV mimetics. Targeting the delivery of EV mimetics to the placenta may potentially overcome various safety factors in pregnancy (123,608–610). Moreover, particularly in pregnancies complicated by maternal diabetes and altered fetal growth, exploring how maternal EVs are internalised into the placenta is another therapeutic avenue that could be exploited to minimise their adverse effects on pregnancy outcomes.

miRNA-based therapy is currently being explored as an alternative therapeutic intervention for many disease areas. Indeed, various miRNA mimics and antagonists have been explored as cancer therapy *in-vivo* and are able to be delivered locally or systemically (611). miRNAs manifest low molecular weight and are very water-soluble therefore are suitable for subcutaneous and intravenous modes of administration (611). Levels of miRNA mimics and antagonists also remain high in target cells once internalised, thereby maximising therapeutic action. However, therapeutic efficacy may vary depending on how well the miRNA mimic/antagonist is retained by the target tissue and EV uptake into non-target cells may induce off-target effects (606,611). Method of administration should also be considered, as saliva enzymes or stomach acidity may degrade RNAs (606). Unencapsulated miRNAs are rapidly degraded in the circulation and those encapsulated in > 100nm nanoparticles have higher affinity of promoting off-target effects due to increased non-specific uptake (611). To improve the stability of miRNA mimics and antagonists, alternative approaches such as chemical modifications, viral delivery and non-viral delivery (inorganic nanoparticles, polymer- and lipid-based delivery) have been explored (611). Moreover, blocking the actions of miR-375-3p on the placenta may be a potential therapeutic approach to manage fetal overgrowth in GDM pregnancies; a concept which has previously been explored in the literature (123).

6.3 Overall Limitations and Future Research

While this study utilised several different models and methodologies to explore the contribution of the maternal environment to placental and fetal development in GDM, there were some limitations to the study design which should be considered. To study the direct effects of metformin, human placental explants were collected from healthy, uncomplicated pregnancies to minimise confounding factors during analysis and data interpretation. However, in hindsight, this model was not directly comparable with the *in-vivo* model, where placentae were collected from GDM pregnancies. This may also have contributed towards the discrepancies in results between both models. Future work should therefore consider investigating the direct effects of metformin in human placental explants from GDM pregnancies, and further data analysis could be conducted on non-GDM patients from the EMPOWaR study. Moreover, analysis demonstrated placental lipid metabolism was impacted by *in-vivo* exposure to metformin in obese women with GDM. As such, future research should perform lipidomics analysis on human placental explants to further understand the direct effect of metformin on lipid metabolism. Additionally, it would be interesting to perform analyses, such as RNA sequencing on maternal EVs from GDM pregnancies treated with or without metformin to determine if metformin treatment impacts EV miRNA profiles, thus improving our understanding of the effect of metformin on whole maternal physiology. In addition, applying such EVs to human placental explants would provide a more comprehensive model of *in-vivo* pregnancy so that the direct and indirect effects of metformin on placental development and fetal growth can be established.

Due to limited samples, the maternal demographics were not best matched between individual patients. Variance in maternal BMI, ethnicity and fetal sex was identified in the human placental explant samples treated with metformin. It has previously been reported that metformin may induce sex-specific effects on offspring long-term health (612,613), and therefore fetal sex should be considered in future experimental design. Sex-specific effects were also observed in mouse feto-placental development in response to *in-vivo* delivery of maternal EVs into pregnant mice. As such, future research should aim to profile maternal plasma EVs from male and female GDM pregnancies with various

growth outcomes in order to our further understanding of the aetiology of sex-specific effects in GDM pregnancies complicated by altered fetal growth. Although matched as best as possible, maternal plasma EV samples demonstrated variance in maternal ethnicity, BMI and age. As such, these discrepancies may have served as confounding factors in this study. Unfortunately, at the time of this PhD project, the effect of maternal EVs from healthy, uncomplicated pregnancies with LGA outcomes on mouse fetal and placental growth was not explored. Interestingly, when miRNAs from EVs of such pregnancies was previously profiled by the Forbes group, no significant differences were observed. Moreover, given the heterogenous cargo of EVs, future research should consider exploring the effect of non-GDM LGA EVs on mouse fetal and placental growth. Adding this group to our analysis would further our understanding of the contribution of EVs to LGA in non-diabetic pregnancies, as well as the additive impact of GDM in pregnancies with LGA outcomes.

Maternal EVs were collected at the time of GDM diagnosis (24-28 weeks' gestation). Although this is helpful to understand the whole physiology of GDM pregnancy outcomes at the time of diagnosis, future research would benefit from investigating if these changes are also observed earlier in pregnancy, where the fetus is less developed, and any adverse outcomes could be better treated or managed. This was not explored in this study as it is difficult to obtain maternal blood samples from GDM pregnancies prior to diagnosis at 24-28 weeks' gestation. However, the MAGiC study, which is designed to recruit women in early pregnancy who are at risk of developing GDM (614), may provide the opportunity to explore this in future.

Although performing a continuous infusion of EV and miRNA treatments would better mimic the diabetic circulation *in-vivo*, due to ethical regulations and sample availability, only three periodical injections were given to pregnant mice. As such, this may have minimised the true effects of the EV and miRNA treatments on mouse fetal and placental development in this study. Moreover, previous research delivering miRNA inhibitors via three periodical injections to healthy pregnant mice reported that predicted effects were observed with this injection schedule (123). Although it is assumed that maternal EVs traffic to the placenta, fluorescently labelling human maternal EVs from various pregnancy outcomes in

healthy pregnant mice may provide further insight into the biodistribution of circulating EVs during pregnancy and therefore the maternal metabolic tissues or organs which may be predominantly and differentially impacted. Indeed, further identifying the source of maternal EVs and circulating miRNAs may also provide insight into the underlying pathophysiology associated with various pregnancy outcomes.

By identifying miR-375-3p as pancreas-specific, this suggests that GDM pregnancies complicated by LGA manifest underlying pancreatic dysfunction. Moreover, it has previously been shown that microRNA sponges can induce tissue-specific silencing of miRNAs to investigate the impact of miRNAs in various tissues (615). As such, future research should consider blocking the effects of miR-375-3p on the placenta *in-vivo*, to further strengthen our findings of the causative association between miR-375-3p and LGA in human GDM pregnancies.

Although it was established that most placental miR-375-3p targets were homologous in human and mouse, it is possible that interspecies effects may have been observed, where various discrepancies in placental structure, function and genetic features have previously been reported between mouse and human (447). *In-vivo* miR-375-3p delivery into healthy pregnant mice also demonstrated different effects in fetal and placental development of male and female offspring. It is therefore possible that the effect of miR-375-3p overexpression on human placental explants may differ depending on fetal sex. As such, future research should aim to subcategorise human models of pregnancy according to fetal sex.

Observations within this thesis primarily focused on the role of maternal circulating *in-vivo* factors. However, sex-dependent effects observed in our findings may indicate that the fetus itself may contribute towards its own development. Indeed, evidence demonstrates that circulating factors impacting the placenta, such as miRNAs and EVs, may also originate from fetal tissues, where it has been shown that EV transfer is bidirectional between the placenta and the fetus (557). Interestingly, it has been demonstrated that miR-375 dysregulation is associated with fetal pancreatic dysfunction (550). It has also been reported that metformin alters fetal hepatocyte signalling and metabolism

(616). Future research should therefore aim to examine the effect of maternal circulating factors on fetal pancreas development, as well as consider fetal-derived circulating factors and their contribution towards impacting placental development during gestation.

Although not shown in this thesis, fetal cardiac tissue weights at E18.5 were impacted by both miR-375-3p and maternal pregnancy EVs. GDM is associated with cardiac congenital malformation and miR-375 has been identified as a key regulator of cardiovascular development and is associated with impaired cardiac function (459,554,617–621). Therefore, follow-up studies on the offspring may also provide further understanding of the long-term effects of pregnancy EVs and miR-375 on offspring development. However, maternal diabetes is also associated with adverse maternal outcomes postpartum, including increased risk of cardiovascular dysfunction and T2DM postpartum (19,20). Therefore, future research would also benefit from conducting long-term follow-up of pregnant dams treated with miR-375-3p and pregnancy EVs to determine their potential contribution to adverse maternal outcomes postpartum, including effects on cardiovascular energetics and maternal metabolism.

References

1. International Diabetes Federation. Brussels Belgium. IDF Diabetes Atlas, 10th edn. 2021. Available from: https://www.diabetesatlas.org [Internet]. [cited 2024 Sep 25]. Available from: https://www.diabetesatlas.org

2. Katsarou A, Gudbjörnsdottir S, Rawshani A, Dabelea D, Bonifacio E, Anderson BJ, et al. Type 1 diabetes mellitus. Nat Rev Dis Primers. 2017 Mar 30;3(1):17016.

3. DeFronzo RA, Ferrannini E, Groop L, Henry RR, Herman WH, Holst JJ, et al. Type 2 diabetes mellitus. Nat Rev Dis Primers. 2015 Jul 23;1(1):15019.

4. Fong A, Serra A, Herrero T, Pan D, Ogunyemi D. Pre-gestational versus gestational diabetes: A population based study on clinical and demographic differences. J Diabetes Complications. 2014 Jan;28(1):29–34.

5. Sugiyama T, Saito M, Nishigori H, Nagase S, Yaegashi N, Sagawa N, et al. Comparison of pregnancy outcomes between women with gestational diabetes and overt diabetes first diagnosed in pregnancy: A retrospective multi-institutional study in Japan. Diabetes Res Clin Pract. 2014 Jan;103(1):20–5.

6. Sonagra AD, Shivaleela M Biradar, Dattatreya K, Jayaprakash Murthy D S. Normal Pregnancy- A State of Insulin Resistance. JOURNAL OF CLINICAL AND DIAGNOSTIC RESEARCH. 2014;

7. Plows JF, Stanley JL, Baker PN, Reynolds CM, Vickers MH. The Pathophysiology of Gestational Diabetes Mellitus. Int J Mol Sci. 2018 Oct 26;19(11):3342.

8. Magliano DJ, Sacre JW, Harding JL, Gregg EW, Zimmet PZ, Shaw JE. Young-onset type 2 diabetes mellitus — implications for morbidity and mortality. Nat Rev Endocrinol. 2020 Jun 20;16(6):321–31.

9. Temple R, Murphy H. Type 2 diabetes in pregnancy – An increasing problem. Best Pract Res Clin Endocrinol Metab. 2010 Aug;24(4):591–603.

10. McIntyre HD, Catalano P, Zhang C, Desoye G, Mathiesen ER, Damm P. Gestational diabetes mellitus. Nat Rev Dis Primers. 2019 Jul 11;5(1):47.

11. Gauster M, Desoye G, Tötsch M, Hiden U. The Placenta and Gestational Diabetes Mellitus. Curr Diab Rep. 2012 Feb 19;12(1):16–23.

12. Diabetes in pregnancy: management from preconception to the postnatal period. NICE guideline [NG3]. 2015 Feb. Available from: www.nice.org.uk/guidance/ng3.

13. Weissgerber TL, Mudd LM. Preeclampsia and Diabetes. Curr Diab Rep. 2015 Mar 3;15(3):9.

14. Phipps E, Prasanna D, Brima W, Jim B. Preeclampsia: Updates in Pathogenesis, Definitions, and Guidelines. Clinical Journal of the American Society of Nephrology. 2016 Jun;11(6):1102–13.

15. Xiong X, Saunders LD, Wang FL, Demianczuk NN. Gestational diabetes mellitus: prevalence, risk factors, maternal and infant outcomes. International Journal of Gynecology & Obstetrics. 2001 Dec 26;75(3):221–8.

16. Rana S, Lemoine E, Granger JP, Karumanchi SA. Preeclampsia. Circ Res. 2019 Mar 29;124(7):1094–112.

17. Ornoy A, Reece EA, Pavlinkova G, Kappen C, Miller RK. Effect of maternal diabetes on the embryo, fetus, and children: Congenital anomalies, genetic and epigenetic changes

and developmental outcomes. Birth Defects Res C Embryo Today. 2015 Mar 16;105(1):53–72.

18. Memon S, Ahsan S, Riaz Q, Basit A, Sheikh SA, Fawwad A, et al. Frequency of retinopathy in patients with diabetes screened by fundus photographs: a study from primary health care. Pak J Med Sci. 1969 Dec 31;30(2).

19. Bellamy L, Casas JP, Hingorani AD, Williams D. Type 2 diabetes mellitus after gestational diabetes: a systematic review and meta-analysis. The Lancet. 2009 May;373(9677):1773–9.

20. Thirunavukarasu S, Ansari F, Cubbon R, Forbes K, Bucciarelli-Ducci C, Newby DE, et al. Maternal Cardiac Changes in Women With Obesity and Gestational Diabetes Mellitus. Diabetes Care. 2022 Dec 1;45(12):3007–15.

21. Stacey T, Tennant P. Authors' reply re: Gestational diabetes and the risk of late stillbirth: a case–control study from England, UK. BJOG. 2019 Aug 4;126(9):1184–1184.

22. Browne K, Park BY, Goetzinger KR, Caughey AB, Yao R. The joint effects of obesity and pregestational diabetes on the risk of stillbirth. The Journal of Maternal-Fetal & Neonatal Medicine. 2021 Feb 1;34(3):332–8.

23. Wu Y, Liu B, Sun Y, Du Y, Santillan MK, Santillan DA, et al. Association of Maternal Prepregnancy Diabetes and Gestational Diabetes Mellitus With Congenital Anomalies of the Newborn. Diabetes Care. 2020 Dec 1;43(12):2983–90.

24. Miao H, Wu H, Zhu Y, Kong L, Yu X, Zeng Q, et al. Congenital anomalies associated with ambient temperature variability during fetal organogenesis period of pregnancy: Evidence from 4.78 million births. Science of The Total Environment. 2021 Dec;798:149305.

25. Eriksson UJ. Congenital anomalies in diabetic pregnancy. Semin Fetal Neonatal Med. 2009 Apr;14(2):85–93.

26. Padmanabhan S, Zen M, Lee V, Cheung NW. Pre-existing diabetes in pregnancy. Minerva Endocrinol. 2016 Jan 14;

27. KC K, Shakya S, Zhang H. Gestational Diabetes Mellitus and Macrosomia: A Literature Review. Ann Nutr Metab. 2015;66(Suppl. 2):14–20.

28. Mikolajczyk RT, Zhang J, Betran AP, Souza JP, Mori R, Gülmezoglu AM, et al. A global reference for fetal-weight and birthweight percentiles. The Lancet. 2011 May;377(9780):1855–61.

29. Cyganek K, Skupien J, Katra B, Hebda-Szydlo A, Janas I, Trznadel-Morawska I, et al. Risk of macrosomia remains glucose-dependent in a cohort of women with pregestational type 1 diabetes and good glycemic control. Endocrine. 2017 Feb 11;55(2):447–55.

30. de Valk HW, van Nieuwaal NHG, Visser GHA. Pregnancy outcome in type 2 diabetes mellitus: a retrospective analysis from the Netherlands. Rev Diabet Stud. 2006;3(3):134–42.

31. Beta J, Khan N, Khalil A, Fiolna M, Ramadan G, Akolekar R. Maternal and neonatal complications of fetal macrosomia: systematic review and meta-analysis. Ultrasound in Obstetrics & Gynecology. 2019 Sep 2;54(3):308–18.

32. Yang J, Cummings EA, O'Connell C, Jangaard K. Fetal and Neonatal Outcomes of Diabetic Pregnancies. Obstetrics & Gynecology. 2006 Sep;108(3, Part 1):644–50.

33. Hong YH, Lee JE. Large for Gestational Age and Obesity-Related Comorbidities. J Obes Metab Syndr. 2021 Jun 30;30(2):124–31.

34. Catalano PM, Hauguel-De Mouzon S. Is it time to revisit the Pedersen hypothesis in the face of the obesity epidemic? Am J Obstet Gynecol. 2011 Jun;204(6):479–87.

35. Dunne F, Owens LA, Avalos G, Dennedy C, O'Sullivan EP, O'Reilly M. Gestational diabetes mellitus results in a higher prevalence of small for gestational babies. In43rd Annual Meeting of DPSG Cambridge 2011. Diabetic Study Pregnancy Group (DSPG).

36. Bamfo JEAK, Odibo AO. Diagnosis and Management of Fetal Growth Restriction. J Pregnancy. 2011;2011:1–15.

37. Pignotti M, Donzelli G. Preterm babies at a glance. J Clin Neonatol. 2015;4(2):75.

38. O'Connor C, Stuart B, Fitzpatrick C, Turner MJ, Kennelly MM. A review of contemporary modalities for identifying abnormal fetal growth. J Obstet Gynaecol (Lahore). 2013 Apr 3;33(3):239–45.

39. Crispi F, Miranda J, Gratacós E. Long-term cardiovascular consequences of fetal growth restriction: biology, clinical implications, and opportunities for prevention of adult disease. Am J Obstet Gynecol. 2018 Feb;218(2):S869–79.

40. Scifres CM. Short- and Long-Term Outcomes Associated with Large for Gestational Age Birth Weight. Obstet Gynecol Clin North Am. 2021 Jun;48(2):325–37.

41. Yu Y, Arah OA, Liew Z, Cnattingius S, Olsen J, Sørensen HT, et al. Maternal diabetes during pregnancy and early onset of cardiovascular disease in offspring: population based cohort study with 40 years of follow-up. BMJ. 2019 Dec 4;l6398.

42. West NA, Crume TL, Maligie MA, Dabelea D. Cardiovascular risk factors in children exposed to maternal diabetes in utero. Diabetologia. 2011 Mar 14;54(3):504–7.

43. Agarwal P, Morriseau TS, Kereliuk SM, Doucette CA, Wicklow BA, Dolinsky VW. Maternal obesity, diabetes during pregnancy and epigenetic mechanisms that influence the developmental origins of cardiometabolic disease in the offspring. Crit Rev Clin Lab Sci. 2018 Feb 17;55(2):71–101.

44. Lapehn S, Paquette AG. The Placental Epigenome as a Molecular Link Between Prenatal Exposures and Fetal Health Outcomes Through the DOHaD Hypothesis. Curr Environ Health Rep. 2022 Apr 29;9(3):490–501.

45. Owen MD, Baker BC, Scott EM, Forbes K. Interaction between Metformin, Folate and Vitamin B12 and the Potential Impact on Fetal Growth and Long-Term Metabolic Health in Diabetic Pregnancies. Int J Mol Sci. 2021 May 28;22(11).

46. Yu Q, Aris IM, Tan KH, Li LJ. Application and Utility of Continuous Glucose Monitoring in Pregnancy: A Systematic Review. Front Endocrinol (Lausanne). 2019 Oct 11;10.

47. Scott EM, Murphy HR, Kristensen KH, Feig DS, Kjölhede K, Englund-Ögge L, et al. Continuous Glucose Monitoring Metrics and Birth Weight: Informing Management of Type 1 Diabetes Throughout Pregnancy. Diabetes Care. 2022 Aug 1;45(8):1724–34.

48. Stewart ZA, Wilinska ME, Hartnell S, Temple RC, Rayman G, Stanley KP, et al. Closed-Loop Insulin Delivery during Pregnancy in Women with Type 1 Diabetes. New England Journal of Medicine. 2016 Aug 18;375(7):644–54.

49. Tarry-Adkins JL, Aiken CE, Ozanne SE. Neonatal, infant, and childhood growth following metformin versus insulin treatment for gestational diabetes: A systematic review and meta-analysis. PLoS Med. 2019 Aug 6;16(8):e1002848.

50. Li LJ, Huang L, Tobias DK, Zhang C. Gestational Diabetes Mellitus Among Asians – A Systematic Review From a Population Health Perspective. Front Endocrinol (Lausanne). 2022 Jun 16;13.

51. Balsells M, García-Patterson A, Gich I, Corcoy R. Maternal and Fetal Outcome in Women with Type 2 *Versus* Type 1 Diabetes Mellitus: A Systematic Review and Metaanalysis. J Clin Endocrinol Metab. 2009 Nov 1;94(11):4284–91.

52. National Health Service (NHS). National Pregnancy in Diabetes Audit Report 2020. 2021. Available from: https://digital.nhs.uk/data-and-information/publications/statistical/national-pregnancy-in-diabetes-audit/2019-and-2020 .

53. Sun T, Meng F, Zang S, Li Y, Zhang R, Yu Z, et al. The effects of insulin therapy on maternal blood pressure and weight in women with gestational diabetes mellitus. BMC Pregnancy Childbirth. 2021 Dec 27;21(1):657.

54. Wakeman M, Archer DT. Metformin and Micronutrient Status in Type 2 Diabetes: Does Polypharmacy Involving Acid-Suppressing Medications Affect Vitamin B12 Levels? Diabetes Metab Syndr Obes. 2020 Jun;Volume 13:2093–108.

55. Balani J, Hyer SL, Rodin DA, Shehata H. Pregnancy outcomes in women with gestational diabetes treated with metformin or insulin: a case–control study. Diabetic Medicine. 2009 Aug 30;26(8):798–802.

56. Feig DS, Donovan LE, Zinman B, Sanchez JJ, Asztalos E, Ryan EA, et al. Metformin in women with type 2 diabetes in pregnancy (MiTy): a multicentre, international, randomised, placebo-controlled trial. Lancet Diabetes Endocrinol. 2020 Oct;8(10):834–44.

57. Salomäki H, Vähätalo LH, Laurila K, Jäppinen NT, Penttinen AM, Ailanen L, et al. Prenatal Metformin Exposure in Mice Programs the Metabolic Phenotype of the Offspring during a High Fat Diet at Adulthood. PLoS One. 2013 Feb 15;8(2):e56594.

58. Francisca S, Gloria AF, Marco PB, Camila NC, Víctor C, Bredford K. Metformin exposure during pregnancy and lactation affects offspring's long-term body weight and adipose tissue mass independent of the maternal metabolic state. Biochimica et Biophysica Acta (BBA) - Molecular Basis of Disease. 2024 Aug;1870(6):167258.

59. Hanem LGE, Salvesen Ø, Juliusson PB, Carlsen SM, Nossum MCF, Vaage MØ, et al. Intrauterine metformin exposure and offspring cardiometabolic risk factors (PedMet study): a 5–10 year follow-up of the PregMet randomised controlled trial. Lancet Child Adolesc Health. 2019 Mar;3(3):166–74.

60. Ijäs H, Vääräsmäki M, Saarela T, Keravuo R, Raudaskoski T. A follow-up of a randomised study of metformin and insulin in gestational diabetes mellitus: growth and development of the children at the age of 18 months. BJOG. 2015 Jun 16;122(7):994–1000.

61. Rowan JA, Rush EC, Obolonkin V, Battin M, Wouldes T, Hague WM. Metformin in Gestational Diabetes: The Offspring Follow-Up (MiG TOFU): body composition at 2 years of age. Diabetes Care. 2011 Oct 1;34(10):2279–84.

62. Rowan JA, Rush EC, Plank LD, Lu J, Obolonkin V, Coat S, et al. Metformin in gestational diabetes: the offspring follow-up (MiG TOFU): body composition and metabolic outcomes at 7–9 years of age. BMJ Open Diabetes Res Care. 2018 Apr 13;6(1):e000456.

63. Feig DS, Sanchez JJ, Murphy KE, Asztalos E, Zinman B, Simmons D, et al. Outcomes in children of women with type 2 diabetes exposed to metformin versus placebo during pregnancy (MiTy Kids): a 24-month follow-up of the MiTy randomised controlled trial. Lancet Diabetes Endocrinol. 2023 Mar;11(3):191–202.

64. Desforges M, Sibley CP. Placental nutrient supply and fetal growth. Int J Dev Biol. 2010;54(2–3):377–90.

65. Tong M, Abrahams VM. Immunology of the Placenta. Obstet Gynecol Clin North Am. 2020 Mar;47(1):49–63.

66. Jansson T, Powell TL. Role of the placenta in fetal programming: underlying mechanisms and potential interventional approaches. Clin Sci. 2007 Jul 1;113(1):1–13.

67. Turco MY, Moffett A. Development of the human placenta. Development. 2019 Nov 15;146(22).

68. Cindrova-Davies T, Sferruzzi-Perri AN. Human placental development and function. Semin Cell Dev Biol. 2022 Nov;131:66–77.

69. Burton GJ, Charnock-Jones DS, Jauniaux E. Regulation of vascular growth and function in the human placenta. REPRODUCTION. 2009 Dec;138(6):895–902.

70. Reyes L, Golos TG. Hofbauer Cells: Their Role in Healthy and Complicated Pregnancy. Front Immunol. 2018 Nov 15;9.

71. Byford A, Baird-Rayner C, Forbes K. Don’t sugar coat it: the effects of gestational diabetes on the placental vasculature. Biochem (Lond). 2021 Apr 12;43(2):34–9.

72. Aplin JD, Lewis RM, Jones CJP. Development of the Human Placental Villus. In: Reference Module in Biomedical Sciences. Elsevier; 2018.

73. Yang M, Lei ZM, Rao Ch V. The Central Role of Human Chorionic Gonadotropin in the Formation of Human Placental Syncytium. Endocrinology. 2003 Mar;144(3):1108–20.

74. Cole LA. Biological functions of hCG and hCG-related molecules. Reproductive Biology and Endocrinology. 2010;8(1):102.

75. Fisher JJ, McKeating DR, Cuffe JS, Bianco-Miotto T, Holland OJ, Perkins A V. Proteomic Analysis of Placental Mitochondria Following Trophoblast Differentiation. Front Physiol. 2019;10:1536.

76. Bustamante J, Ramírez-Vélez R, Czerniczyniec A, Cicerchia D, Aguilar de Plata AC, Lores-Arnaiz S. Oxygen metabolism in human placenta mitochondria. J Bioenerg Biomembr. 2014 Dec 19;46(6):459–69.

77. Forbes K, Westwood M, Baker PN, Aplin JD. Insulin-like growth factor I and II regulate the life cycle of trophoblast in the developing human placenta. American Journal of Physiology-Cell Physiology. 2008 Jun;294(6):C1313–22.

78. Farrokhnia F, Aplin JD, Westwood M, Forbes K. MicroRNA Regulation of Mitogenic Signaling Networks in the Human Placenta. Journal of Biological Chemistry. 2014 Oct;289(44):30404–16.

79. Forbes K, Westwood M. Maternal growth factor regulation of human placental development and fetal growth. Journal of Endocrinology. 2010 Oct;207(1):1–16.

80. Costa MA. The endocrine function of human placenta: an overview. Reprod Biomed Online. 2016 Jan;32(1):14–43.

81. Lager S, Powell TL. Regulation of Nutrient Transport across the Placenta. J Pregnancy. 2012;2012:1–14.

82. Cleal JK, Lewis RM. The Mechanisms and Regulation of Placental Amino Acid Transport to the Human Foetus. J Neuroendocrinol. 2008 Apr 7;20(4):419–26.

83. Illsley NP, Baumann MU. Human placental glucose transport in fetoplacental growth and metabolism. Biochimica et Biophysica Acta (BBA) - Molecular Basis of Disease. 2020 Feb;1866(2):165359.

84. Baumann MU, Deborde S, Illsley NP. Placental Glucose Transfer and Fetal Growth. Endocrine. 2002;19(1):13–22.

85. Teasdale F, Jean-Jacques G. Intrauterine growth retardation: Morphometry of the microvillous membrane of the human placenta. Placenta. 1988 Jan;9(1):47–55.

86. Teasdale F. Histomorphometry of the human placenta in maternal preeclampsia. Am J Obstet Gynecol. 1985 May;152(1):25–31.

87. Lüscher BP, Albrecht C, Stieger B, Surbek D V., Baumann MU. Glucose Transporter 9 (GLUT9) Plays an Important Role in the Placental Uric Acid Transport System. Cells. 2022 Feb 11;11(4):633.

88. Gude NM, Stevenson JL, Rogers S, Best JD, Kalionis B, Huisman MA, et al. GLUT12 Expression in Human Placenta in First Trimester and Term. Placenta. 2003 May;24(5):566–70.

89. Larqué E, Demmelmair H, Gil-Sánchez A, Prieto-Sánchez MT, Blanco JE, Pagán A, et al. Placental transfer of fatty acids and fetal implications. Am J Clin Nutr. 2011 Dec;94:S1908–13.

90. DUTTAROY A. Transport of fatty acids across the human placenta: A review. Prog Lipid Res. 2009 Jan;48(1):52–61.

91. Jansson T. Amino Acid Transporters in the Human Placenta. Pediatr Res. 2001 Feb;49(2):141–7.

92. Grillo MA, Lanza A, Colombatto S. Transport of amino acids through the placenta and their role. Amino Acids. 2008 May 3;34(4):517–23.

93. Cai Y, Yu X, Hu S, Yu J. A Brief Review on the Mechanisms of miRNA Regulation. Genomics Proteomics Bioinformatics. 2009 Dec 1;7(4):147–54.

94. Vishnoi A, Rani S. MiRNA Biogenesis and Regulation of Diseases: An Overview. In 2017. p. 1–10.

95. Budak H, Bulut R, Kantar M, Alptekin B. MicroRNA nomenclature and the need for a revised naming prescription. Brief Funct Genomics. 2015 Jul 6;elv026.

96. O'Brien J, Hayder H, Zayed Y, Peng C. Overview of MicroRNA Biogenesis, Mechanisms of Actions, and Circulation. Front Endocrinol (Lausanne). 2018 Aug 3;9.

97. Fu G, Brkić J, Hayder H, Peng C. MicroRNAs in Human Placental Development and Pregnancy Complications. Int J Mol Sci. 2013 Mar 8;14(3):5519–44.

98. Mouillet J, Chu T, Sadovsky Y. Expression patterns of placental microRNAs. Birth Defects Res A Clin Mol Teratol. 2011 Aug 21;91(8):737–43.

99. Bortolin-Cavaille ML, Dance M, Weber M, Cavaille J. C19MC microRNAs are processed from introns of large Pol-II, non-protein-coding transcripts. Nucleic Acids Res. 2009 Jun 1;37(10):3464–73.

100. Taylor AS, Tinning H, Ovchinnikov V, Edge J, Smith W, Pullinger AL, et al. A burst of genomic innovation at the origin of placental mammals mediated embryo implantation. Commun Biol. 2023 Apr 26;6(1):459.

101. Hume L, Edge JC, Tinning H, Wang D, Taylor AS, Ovchinnikov V, et al. MicroRNAs emerging coordinate with placental mammals alter pathways in endometrial epithelia important for endometrial function. iScience. 2023 Apr;26(4):106339.

102. Malnou EC, Umlauf D, Mouysset M, Cavaillé J. Imprinted MicroRNA Gene Clusters in the Evolution, Development, and Functions of Mammalian Placenta. Front Genet. 2019 Jan 18;9.

103. Donker RB, Mouillet JF, Chu T, Hubel CA, Stolz DB, Morelli AE, et al. The expression profile of C19MC microRNAs in primary human trophoblast cells and exosomes. Mol Hum Reprod. 2012 Aug 1;18(8):417–24.

104. Gong S, Gaccioli F, Dopierala J, Sovio U, Cook E, Volders PJ, et al. The RNA landscape of the human placenta in health and disease. Nat Commun. 2021 May 11;12(1):2639.

105. Xie L, Mouillet JF, Chu T, Parks WT, Sadovsky E, Knöfler M, et al. C19MC MicroRNAs Regulate the Migration of Human Trophoblasts. Endocrinology. 2014 Dec 1;155(12):4975–85.

106. Kobayashi N, Okae H, Hiura H, Kubota N, Kobayashi EH, Shibata S, et al. The microRNA cluster C19MC confers differentiation potential into trophoblast lineages upon human pluripotent stem cells. Nat Commun. 2022 Jun 2;13(1):3071.

107. Mouillet JF, Ouyang Y, Coyne CB, Sadovsky Y. MicroRNAs in placental health and disease. Am J Obstet Gynecol. 2015 Oct;213(4):S163–72.

108. Poirier C, Desgagné V, Guérin R, Bouchard L. MicroRNAs in Pregnancy and Gestational Diabetes Mellitus: Emerging Role in Maternal Metabolic Regulation. Curr Diab Rep. 2017 May 4;17(5):35.

109. Morales-Prieto DM, Ospina-Prieto S, Chaiwangyen W, Schoenleben M, Markert UR. Pregnancy-associated miRNA-clusters. J Reprod Immunol. 2013 Mar;97(1):51–61.

110. Paquette AG, Chu T, Wu X, Wang K, Price ND, Sadovsky Y. Distinct communication patterns of trophoblastic miRNA among the maternal-placental-fetal compartments. Placenta. 2018 Dec;72–73:28–35.

111. Dini P, Daels P, Loux SC, Esteller-Vico A, Carossino M, Scoggin KE, et al. Kinetics of the chromosome 14 microRNA cluster ortholog and its potential role during placental development in the pregnant mare. BMC Genomics. 2018 Dec 20;19(1):954.

112. Inno R, Kikas T, Lillepea K, Laan M. Coordinated Expressional Landscape of the Human Placental miRNome and Transcriptome. Front Cell Dev Biol. 2021 Jul 21;9.

113. Smith MD, Pillman K, Jankovic-Karasoulos T, McAninch D, Wan Q, Bogias KJ, et al. Large-scale transcriptome-wide profiling of microRNAs in human placenta and maternal plasma at early to mid gestation. RNA Biol. 2021 Oct 15;18(sup1):507–20.

114. Addo KA, Palakodety N, Hartwell HJ, Tingare A, Fry RC. Placental microRNAs: Responders to environmental chemicals and mediators of pathophysiology of the human placenta. Toxicol Rep. 2020;7:1046–56.

115. Paquette AG, Chu T, Wu X, Wang K, Price ND, Sadovsky Y. Distinct communication patterns of trophoblastic miRNA among the maternal-placental-fetal compartments. Placenta. 2018 Dec;72–73:28–35.

116. Morales-Prieto DM, Chaiwangyen W, Ospina-Prieto S, Schneider U, Herrmann J, Gruhn B, et al. MicroRNA expression profiles of trophoblastic cells. Placenta. 2012 Sep;33(9):725–34.

117. Dini P, Daels P, Loux SC, Esteller-Vico A, Carossino M, Scoggin KE, et al. Kinetics of the chromosome 14 microRNA cluster ortholog and its potential role during placental development in the pregnant mare. BMC Genomics. 2018 Dec 20;19(1):954.

118. Maccani MA, Marsit CJ. REVIEW ARTICLE: Epigenetics in the Placenta. American Journal of Reproductive Immunology. 2009 Aug 9;62(2):78–89.

119. Tsamou M, Nawrot TS, Carollo RM, Trippas AJ, Lefebvre W, Vanpoucke C, et al. Prenatal particulate air pollution exposure and expression of the miR-17/92 cluster in cord blood: Findings from the ENVIRONAGE birth cohort. Environ Int. 2020 Sep;142:105860.

120. Chen D bao, Wang W. Human Placental MicroRNAs and Preeclampsia1. Biol Reprod. 2013 May 1;88(5).

121. Kumar P, Luo Y, Tudela C, Alexander JM, Mendelson CR. The c-Myc-Regulated MicroRNA-17~92 (miR-17~92) and miR-106a~363 Clusters Target hCYP19A1 and hGCM1 To Inhibit Human Trophoblast Differentiation. Mol Cell Biol. 2013 May 1;33(9):1782–96.

122. Quilang RC, Lui S, Forbes K. miR-514a-3p: a novel SHP-2 regulatory miRNA that modulates human cytotrophoblast proliferation. J Mol Endocrinol. 2022 Feb 1;68(2):99–110.

123. Beards F, Jones LE, Charnock J, Forbes K, Harris LK. Placental Homing Peptide-microRNA Inhibitor Conjugates for Targeted Enhancement of Intrinsic Placental Growth Signaling. Theranostics. 2017;7(11):2940–55.

124. Cao H, Hu X, Zhang Q, Wang J, Li J, Liu B, et al. Upregulation of let-7a inhibits vascular smooth muscle cell proliferation in vitro and in vein graft intimal hyperplasia in rats. Journal of Surgical Research. 2014 Nov;192(1):223–33.

125. Johnson CD, Esquela-Kerscher A, Stefani G, Byrom M, Kelnar K, Ovcharenko D, et al. The *let-7* MicroRNA Represses Cell Proliferation Pathways in Human Cells. Cancer Res. 2007 Aug 15;67(16):7713–22.

126. Sachdeva M, Mo YY. miR-145-mediated suppression of cell growth, invasion and metastasis. Am J Transl Res. 2010 Mar 25;2(2):170–80.

127. Zhang L, Li K, Tian S, Wang X qin, Li J hui, Dong Y chao, et al. Down-regulation of microRNA-30d-5p is associated with gestational diabetes mellitus by targeting RAB8A. J Diabetes Complications. 2021 Aug;35(8):107959.

128. Zhao Q, Yuan X, Zheng L, Xue M. miR-30d-5p: A Non-Coding RNA With Potential Diagnostic, Prognostic and Therapeutic Applications. Front Cell Dev Biol. 2022 Jan 27;10.

129. Wang K, Liufu S, Yu Z, Xu X, Ai N, Li X, et al. miR-100-5p Regulates Skeletal Muscle Myogenesis through the Trib2/mTOR/S6K Signaling Pathway. Int J Mol Sci. 2023 May 17;24(10):8906.

130. Cordes KR, Sheehy NT, White MP, Berry EC, Morton SU, Muth AN, et al. miR-145 and miR-143 regulate smooth muscle cell fate and plasticity. Nature. 2009 Aug 5;460(7256):705–10.

131. Yang H, Hu T, Hu P, Qi C, Qian L. miR-143-3p inhibits endometriotic stromal cell proliferation and invasion by inactivating autophagy in endometriosis. Mol Med Rep. 2021 Mar 12;23(5):356.

132. Jenike AE, Halushka MK. miR-21: a non-specific biomarker of all maladies. Biomark Res. 2021 Dec 12;9(1):18.

133. Zhou F, Sun Y, Gao Q, Wang H. microRNA-21 regulates the proliferation of placental cells via FOXM1 in preeclampsia. Exp Ther Med. 2020 Jun 24;

134. Yamada M, Kubo H, Ota C, Takahashi T, Tando Y, Suzuki T, et al. The increase of microRNA-21 during lung fibrosis and its contribution to epithelial-mesenchymal transition in pulmonary epithelial cells. Respir Res. 2013 Dec 24;14(1):95.

135. Chen D, Xu L, Wu J, Liang H, Liang Y, Liu G. Downregulating miR-96-5p promotes proliferation, migration, and invasion, and inhibits apoptosis in human trophoblast cells via targeting DDAH1. Reprod Biol. 2021 Mar;21(1):100474.

136. Tian L, Cai D, Zhuang D, Wang W, Wang X, Bian X, et al. miR-96-5p Regulates Proliferation, Migration, and Apoptosis of Vascular Smooth Muscle Cell Induced by Angiotensin II via Targeting NFAT5. J Vasc Res. 2020;57(2):86–96.

137. Gu Y, Bian Y, Xu X, Wang X, Zuo C, Meng J, et al. Downregulation of miR-29a/b/c in placenta accreta inhibits apoptosis of implantation site intermediate trophoblast cells by targeting MCL1. Placenta. 2016 Dec;48:13–9.

138. Alizadeh M, Safarzadeh A, Beyranvand F, Ahmadpour F, Hajiasgharzadeh K, Baghbanzadeh A, et al. The potential role of miR-29 in health and cancer diagnosis, prognosis, and therapy. J Cell Physiol. 2019 Nov 4;234(11):19280–97.

139. Sun F, Cai H, Tan L, Qin D, Zhang J, Hua J, et al. Placenta-Specific miR-125b Overexpression Leads to Increased Rates of Pregnancy Loss in Mice. Int J Mol Sci. 2022 Jan 15;23(2):943.

140. Giroud M, Pisani DF, Karbiener M, Barquissau V, Ghandour RA, Tews D, et al. miR-125b affects mitochondrial biogenesis and impairs brite adipocyte formation and function. Mol Metab. 2016 Aug;5(8):615–25.

141. Maccani MA, Padbury JF, Marsit CJ. miR-16 and miR-21 Expression in the Placenta Is Associated with Fetal Growth. PLoS One. 2011 Jun 15;6(6):e21210.

142. Meng M, Cheng YKY, Wu L, Chaemsaithong P, Leung MBW, Chim SSC, et al. Whole genome miRNA profiling revealed miR-199a as potential placental pathogenesis of selective fetal growth restriction in monochorionic twin pregnancies. Placenta. 2020 Mar;92:44–53.

143. Lim S, Deaver JW, Rosa-Caldwell ME, Lee DE, Morena da Silva F, Cabrera AR, et al. Muscle miR-16 deletion results in impaired insulin sensitivity and contractile function in a sex-dependent manner. American Journal of Physiology-Endocrinology and Metabolism. 2022 Mar 1;322(3):E278–92.

144. Wang Y, Yang LZ, Yang DG, Zhang QY, Deng ZN, Wang K, et al. MiR-21 antagomir improves insulin resistance and lipid metabolism disorder in streptozotocin-induced type 2 diabetes mellitus rats. Ann Palliat Med. 2020 Mar;9(2):394–404.

145. Ling H y., Hu B, Hu X b., Zhong J, Feng S d., Qin L, et al. MiRNA-21 Reverses High Glucose and High Insulin Induced Insulin Resistance in 3T3-L1 Adipocytes through Targeting Phosphatase and Tensin Homologue. Experimental and Clinical Endocrinology & Diabetes. 2012 Sep 6;120(09):553–9.

146. Yan ST, Li CL, Tian H, Li J, Pei Y, Liu Y, et al. MiR-199a is overexpressed in plasma of type 2 diabetes patients which contributes to type 2 diabetes by targeting GLUT4. Mol Cell Biochem. 2014 Dec 2;397(1–2):45–51.

147. LEACH L. Placental Vascular Dysfunction in Diabetic Pregnancies: Intimations of Fetal Cardiovascular Disease? Microcirculation. 2011 May 26;18(4):263–9.

148. Evers I, Nikkels P, Sikkema J, Visser G. Placental Pathology in Women with Type 1 Diabetes and in a Control Group with Normal and Large-for-Gestational-Age Infants. Placenta. 2003 Oct;24(8–9):819–25.

149. Huynh J, Dawson D, Roberts D, Bentley-Lewis R. A systematic review of placental pathology in maternal diabetes mellitus. Placenta. 2015 Feb;36(2):101–14.

150. Huynh J, Yamada J, Beauharnais C, Wenger JB, Thadhani RI, Wexler D, et al. Type 1, type 2 and gestational diabetes mellitus differentially impact placental pathologic characteristics of uteroplacental malperfusion. Placenta. 2015 Oct;36(10):1161–6.

151. Pietryga M, Brązert J, Wender-Oėgowska E, Biczysko R, Dubiel M, Gudmundsson S. Abnormal Uterine Doppler Is Related to Vasculopathy in Pregestational Diabetes Mellitus. Circulation. 2005 Oct 18;112(16):2496–500.

152. Vajnerova O, Kafka P, Kratzerova T, Chalupsky K, Hampl V. Pregestational diabetes increases fetoplacental vascular resistance in rats. Placenta. 2018 Mar;63:32–8.

153. Eriksson UJ, Jansson L. Diabetes in Pregnancy: Decreased Placental Blood Flow and Disturbed Fetal Development in the Rat. Pediatr Res. 1984 Aug;18(8):735–8.

154. Rizzo G, Mappa I, Bitsadze V, Słodki M, Khizroeva J, Makatsariya A, et al. Role of first-trimester umbilical vein blood flow in predicting large-for-gestational age at birth. Ultrasound in Obstetrics & Gynecology. 2020 Jul;56(1):67–72.

155. Ferrazzi E, Bulfamante G, Mezzopane R, Barbera A, Ghidini A, Pardi G. Uterine Doppler Velocimetry and Placental Hypoxic-ischemic Lesion in Pregnancies with Fetal Intrauterine Growth Restriction. Placenta. 1999 Jul;20(5–6):389–94.

156. Salavati N, Sovio U, Mayo RP, Charnock-Jones DS, Smith GCS. The relationship between human placental morphometry and ultrasonic measurements of utero-placental blood flow and fetal growth. Placenta. 2016 Feb;38:41–8.

157. Browne VA, Julian CG, Toledo-Jaldin L, Cioffi-Ragan D, Vargas E, Moore LG. Uterine artery blood flow, fetal hypoxia and fetal growth. Philosophical Transactions of the Royal Society B: Biological Sciences. 2015 Mar 5;370(1663):20140068.

158. Desoye G, Shafrir E. The human placenta in diabetic pregnancy. Diabetes reviews. 1996;4(1):70-89.

159. DASKALAKIS G, MARINOPOULOS S, KRIELESI V, PAPAPANAGIOTOU A, PAPANTONIOU N, MESOGITIS S, et al. Placental pathology in women with gestational diabetes. Acta Obstet Gynecol Scand. 2008 Apr 31;87(4):403–7.

160. Carrasco-Wong I, Moller A, Giachini FR, Lima V V., Toledo F, Stojanova J, et al. Placental structure in gestational diabetes mellitus. Biochimica et Biophysica Acta (BBA) - Molecular Basis of Disease. 2020 Feb;1866(2):165535.

161. Aldahmash WM, Alwasel SH, Aljerian K. Gestational diabetes mellitus induces placental vasculopathies. Environmental Science and Pollution Research. 2022 Mar 2;29(13):19860–8.

162. Rong C, Cui X, Chen J, Qian Y, Jia R, Hu Y. DNA Methylation Profiles in Placenta and Its Association with Gestational Diabetes Mellitus. Experimental and Clinical Endocrinology & Diabetes. 2015 Apr 21;123(05):282–8.

163. Enquobahrie DA, Williams MA, Qiu C, Meller M, Sorensen TK. Global placental gene expression in gestational diabetes mellitus. Am J Obstet Gynecol. 2009 Feb;200(2):206.e1-206.e13.

164. Reichetzeder C, Dwi Putra SE, Pfab T, Slowinski T, Neuber C, Kleuser B, et al. Increased global placental DNA methylation levels are associated with gestational diabetes. Clin Epigenetics. 2016 Dec 26;8(1):82.

165. Coughlan MT, Vervaart PP, Permezel M, Georgiou HM, Rice GE. Altered Placental Oxidative Stress Status in Gestational Diabetes Mellitus. Placenta. 2004 Jan;25(1):78–84.

166. Pan X, Jin X, Wang J, Hu Q, Dai B. Placenta inflammation is closely associated with gestational diabetes mellitus. Am J Transl Res. 2021;13(5):4068–79. .

167. Yu J, Zhou Y, Gui J, Li A zhen, Su X ling, Feng L. Assessment of the number and function of macrophages in the placenta of gestational diabetes mellitus patients. Journal of Huazhong University of Science and Technology [Medical Sciences]. 2013 Oct 20;33(5):725–9.

168. Magee TR, Ross MG, Wedekind L, Desai M, Kjos S, Belkacemi L. Gestational diabetes mellitus alters apoptotic and inflammatory gene expression of trophobasts from human term placenta. J Diabetes Complications. 2014 Jul;28(4):448–59.

169. Biri A, Onan A, Devrim E, Babacan F, Kavutcu M, Durak İ. Oxidant Status in Maternal and Cord Plasma and Placental Tissue in Gestational Diabetes. Placenta. 2006 Feb;27(2–3):327–32.

170. Li Y xiao, Long D lu, Liu J, Qiu D, Wang J, Cheng X, et al. Gestational diabetes mellitus in women increased the risk of neonatal infection via inflammation and autophagy in the placenta. Medicine. 2020 Oct 2;99(40):e22152.

171. Fisher JJ, Vanderpeet CL, Bartho LA, McKeating DR, Cuffe JSM, Holland OliviaJ, et al. Mitochondrial dysfunction in placental trophoblast cells experiencing gestational diabetes mellitus. J Physiol. 2021 Feb 15;599(4):1291–305.

172. Leach L, Taylor A, Sciota F. Vascular dysfunction in the diabetic placenta: causes and consequences. J Anat. 2009 Jul 22;215(1):69–76.

173. Jirkovská M, Kučera T, Kaláb J, Jadrníček M, Niedobová V, Janáček J, et al. The branching pattern of villous capillaries and structural changes of placental terminal villi in type 1 diabetes mellitus. Placenta. 2012 May;33(5):343–51.

174. Higgins M, Felle P, Mooney EE, Bannigan J, McAuliffe FM. Stereology of the placenta in type 1 and type 2 diabetes. Placenta. 2011 Aug;32(8):564–9.

175. Whittington JR, Cummings KF, Ounpraseuth ST, Aughenbaugh AL, Quick CM, Dajani NK. Placental changes in diabetic pregnancies and the contribution of hypertension. The Journal of Maternal-Fetal & Neonatal Medicine. 2022 Feb 1;35(3):486–94.

176. Stanirowski PJ, Szukiewicz D, Majewska A, Wątroba M, Pyzlak M, Bomba-Opoń D, et al. Placental expression of glucose transporters GLUT-1, GLUT-3, GLUT-8 and GLUT-12 in pregnancies complicated by gestational and type 1 diabetes mellitus. J Diabetes Investig. 2022 Mar 21;13(3):560–70.

177. Radaelli T, Lepercq J, Varastehpour A, Basu S, Catalano PM, Hauguel-De Mouzon S. Differential regulation of genes for fetoplacental lipid pathways in pregnancy with gestational and type 1 diabetes mellitus. Am J Obstet Gynecol. 2009 Aug;201(2):209.e1-209.e10.

178. Majali-Martinez A, Weiss-Fuchs U, Miedl H, Forstner D, Bandres-Meriz J, Hoch D, et al. Type 1 Diabetes Mellitus and the First Trimester Placenta: Hyperglycemia-Induced Effects on Trophoblast Proliferation, Cell Cycle Regulators, and Invasion. Int J Mol Sci. 2021 Oct 12;22(20):10989.

179. Xie L, Galettis A, Morris J, Jackson C, Twigg SM, Gallery EDM. Intercellular adhesion molecule-1 (ICAM-1) expression is necessary for monocyte adhesion to the placental bed endothelium and is increased in type 1 diabetic human pregnancy. Diabetes Metab Res Rev. 2008 May 7;24(4):294–300.

180. Sanches JC, Favaro RR, Barrence FC, Bevilacqua E, Fortes ZB, Zorn TMT. Distinct effects of short- and long-term type 1 diabetes to the placental extracellular matrix and fetal development in mice. Placenta. 2017 May;53:1–7.

181. Favaro RR, Salgado RM, Covarrubias AC, Bruni F, Lima C, Fortes ZB, et al. Long-term type 1 diabetes impairs decidualization and extracellular matrix remodeling during early embryonic development in mice. Placenta. 2013 Dec;34(12):1128–35.

182. Gauster M, Majali-Martinez A, Maninger S, Gutschi E, Greimel PH, Ivanisevic M, et al. Maternal Type 1 diabetes activates stress response in early placenta. Placenta. 2017 Feb;50:110–6.

183. Hastie R, Lappas M. The effect of pre-existing maternal obesity and diabetes on placental mitochondrial content and electron transport chain activity. Placenta. 2014 Sep;35(9):673–83.

184. Araújo JR, Ramalho C, Correia-Branco A, Faria A, Ferraz T, Keating E, et al. A parallel increase in placental oxidative stress and antioxidant defenses occurs in pre-gestational type 1 but not gestational diabetes. Placenta. 2013 Nov;34(11):1095–8.

185. Beauharnais CC, Roberts DJ, Wexler DJ. High Rate of Placental Infarcts in Type 2 Compared with Type 1 Diabetes. J Clin Endocrinol Metab. 2012 Jul;97(7):E1160–4.

186. Bisseling TM, Wouterse AC, Steegers EA, Elving L, Russel FG, Smits P. Nitric Oxide-mediated Vascular Tone in the Fetal Placental Circulation of Patients with Type 1 Diabetes Mellitus. Placenta. 2003 Nov;24(10):974–8.

187. Stanley JL, Cheung CC, Rueda-Clausen CF, Sankaralingam S, Baker PN, Davidge ST. Effect of Gestational Diabetes on Maternal Artery Function. Reproductive Sciences. 2011 Apr 30;18(4):342–52.

188. Morton JS, Care AS, Davidge ST. Mechanisms of Uterine Artery Dysfunction in Pregnancy Complications. J Cardiovasc Pharmacol. 2017 Jun;69(6):343–59.

189. Razak AA, Leach L, Ralevic V. Impaired vasocontractile responses to adenosine in chorionic vessels of human term placenta from pregnant women with pre-existing and gestational diabetes. Diab Vasc Dis Res. 2018 Nov 22;15(6):528–40.

190. Calles-Escandon J, Cipolla M. Diabetes and Endothelial Dysfunction: A Clinical Perspective. Endocr Rev. 2001 Feb 1;22(1):36–52.

191. Ramsay JE, Simms RJ, Ferrell WR, Crawford L, Greer IA, Lumsden MA, et al. Enhancement of Endothelial Function by Pregnancy. Diabetes Care. 2003 Feb 1;26(2):475–9.

192. Castillo-Castrejon M, Yamaguchi K, Rodel RL, Erickson K, Kramer A, Hirsch NM, et al. Effect of type 2 diabetes mellitus on placental expression and activity of nutrient transporters and their association with birth weight and neonatal adiposity. Mol Cell Endocrinol. 2021 Jul;532:111319.

193. Capobianco E, Martínez N, Fornes D, Higa R, Di Marco I, Basualdo MN, et al. PPAR activation as a regulator of lipid metabolism, nitric oxide production and lipid peroxidation in the placenta from type 2 diabetic patients. Mol Cell Endocrinol. 2013 Sep;377(1–2):7–15.

194. Kapustin R V., Kopteyeva E V., Tral TG, Tolibova GKh. Placental morphology in different types of diabetes mellitus. Journal of obstetrics and women's diseases. 2021 Jun 17;70(2):13–26.

195. Napso T, Lean SC, Lu M, Mort EJ, Desforges M, Moghimi A, et al. Diet-induced maternal obesity impacts feto-placental growth and induces sex-specific alterations in placental morphology, mitochondrial bioenergetics, dynamics, lipid metabolism and oxidative stress in mice. Acta Physiologica. 2022 Apr 15;234(4).

196. Chen KH, Chen LR, Lee YH. The Role of Preterm Placental Calcification in High-Risk Pregnancy as a Predictor of Poor Uteroplacental Blood Flow and Adverse Pregnancy Outcome. Ultrasound Med Biol. 2012 Jun;38(6):1011–8.

197. Myatt L, Maloyan A. Obesity and Placental Function. Semin Reprod Med. 2016 Jan 6;34(01):042–9.

198. Jaiman S, Romero R, Pacora P, Jung E, Bhatti G, Yeo L, et al. Disorders of placental villous maturation in fetal death. J Perinat Med. 2020 Apr 1;0(0).

199. ASMUSSEN I. ULTRASTRUCTURE OF THE VILLI AND FETAL CAPILLARIES OF THE PLACENTAS DELIVERED BY NONSMOKING DIABETIC WOMEN (WHITE GROUP D). Acta Pathologica Microbiologica Scandinavica Series A :Pathology. 1982 Jul 19;90A(1–6):95–101.

200. BOYD PA, SCOTT A, KEELING JW. Quantitative structural studies on placentas from pregnancies complicated by diabetes mellitus. BJOG. 1986 Jan 23;93(1):31–5.

201. Fox H. Pathology of the placenta in maternal diabetes mellitus. Obstet Gynecol. 1969 Dec;34(6):792-8.

202. Shah KB, Chernausek SD, Teague AM, Bard DE, Tryggestad JB. Maternal diabetes alters microRNA expression in fetal exosomes, human umbilical vein endothelial cells and placenta. Pediatr Res. 2021 Apr 14;89(5):1157–63.

203. Sun DG, Tian S, Zhang L, Hu Y, Guan CY, Ma X, et al. The miRNA-29b Is Downregulated in Placenta During Gestational Diabetes Mellitus and May Alter Placenta Development by Regulating Trophoblast Migration and Invasion Through a HIF3A-Dependent Mechanism. Front Endocrinol (Lausanne). 2020 Mar 31;11.

204. Muralimanoharan S, Maloyan A, Myatt L. Mitochondrial function and glucose metabolism in the placenta with gestational diabetes mellitus: role of *miR-143*. Clin Sci. 2016 Jun 1;130(11):931–41.

205. Guan CY, Tian S, Cao JL, Wang XQ, Ma X, Xia HF. Down-Regulated miR-21 in Gestational Diabetes Mellitus Placenta Induces PPAR-α to Inhibit Cell Proliferation and Infiltration. Diabetes Metab Syndr Obes. 2020 Aug;Volume 13:3009–34.

206. ZHAO C, ZHANG T, SHI Z, DING H, LING X. MicroRNA-518d regulates PPARα protein expression in the placentas of females with gestational diabetes mellitus. Mol Med Rep. 2014 Jun;9(6):2085–90.

207. Cao JL, Zhang L, Li J, Tian S, Lv XD, Wang XQ, et al. Up-regulation of miR-98 and unraveling regulatory mechanisms in gestational diabetes mellitus. Sci Rep. 2016 Aug 30;6(1):32268.

208. Ding R, Guo F, Zhang Y, Liu XM, Xiang YQ, Zhang C, et al. Integrated Transcriptome Sequencing Analysis Reveals Role of miR-138-5p/ TBL1X in Placenta from Gestational Diabetes Mellitus. Cellular Physiology and Biochemistry. 2018;51(2):630–46.

209. Zhao C, Zhao C, Zhao H. Defective insulin receptor signaling in patients with gestational diabetes is related to dysregulated miR-140 which can be improved by naringenin. Int J Biochem Cell Biol. 2020 Nov;128:105824.

210. Zhou X, Xiang C, Zheng X. miR-132 serves as a diagnostic biomarker in gestational diabetes mellitus and its regulatory effect on trophoblast cell viability. Diagn Pathol. 2019 Dec 25;14(1):119.

211. Du R, Wu N, Bai Y, Tang L, Li L. circMAP3K4 regulates insulin resistance in trophoblast cells during gestational diabetes mellitus by modulating the miR-6795-5p/PTPN1 axis. J Transl Med. 2022 Dec 21;20(1):180.

212. Zhang C, Wang L, Chen J, Song F, Guo Y. Differential Expression of miR-136 in Gestational Diabetes Mellitus Mediates the High-Glucose-Induced Trophoblast Cell Injury through Targeting E2F1. Int J Genomics. 2020 Oct 20;2020:1–10.

213. Li Y, Zhuang J. miR-345-3p serves a protective role during gestational diabetes mellitus by targeting BAK1. Exp Ther Med. 2020 Nov 2;20(6):1–1.

214. Tan L, Peng QJ, Chen LC. miR-95, -548am and -1246 expression in placenta tissue of gestational diabetes mellitus as well as their relationship with adipocytokines and glucose transporters. Journal of Hainan Medical University. 2016;22(23):5–8.

215. Li W, Yuan X, He X, Yang L, Wu Y, Deng X, et al. The downregulation of miR-22 and miR-372 may contribute to gestational diabetes mellitus through regulating glucose metabolism via the PI3K/ AKT/GLUT4 pathway. J Clin Lab Anal. 2022 Jul 17;36(7).

216. Liu L, Zhang J, Liu Y. MicroRNA-1323 serves as a biomarker in gestational diabetes mellitus and aggravates high glucose-induced inhibition of trophoblast cell viability by suppressing TP53INP1. Exp Ther Med. 2021 Jan 20;21(3):230.

217. Wang P, Wang Z, Liu G, Jin C, Zhang Q, Man S, et al. miR-657 Promotes Macrophage Polarization toward M1 by Targeting FAM46C in Gestational Diabetes Mellitus. Mediators Inflamm. 2019 Dec 13;2019:1–9.

218. Guan CY, Cao JL, Zhang L, Wang XQ, Ma X, Xia HF. miR-199a Is Upregulated in GDM Targeting the MeCP2-Trpc3 Pathway. Front Endocrinol (Lausanne). 2022 Jul 14;13.

219. Zheng H, Yu Z, Wang H, Liu H, Chen X. MicroRNA-195-5p facilitates endothelial dysfunction by inhibiting vascular endothelial growth factor A in gestational diabetes mellitus. Reprod Biol. 2022 Mar;22(1):100605.

220. Wang P, Ma Z, Wang Z, Wang X, Zhao G, Wang Z. MiR-6869-5p Induces M2 Polarization by Regulating PTPRO in Gestational Diabetes Mellitus. Mediators Inflamm. 2021 Apr 30;2021:1–8.

221. Floris I, Descamps B, Vardeu A, Mitić T, Posadino AM, Shantikumar S, et al. Gestational Diabetes Mellitus Impairs Fetal Endothelial Cell Functions Through a Mechanism Involving MicroRNA-101 and Histone Methyltransferase Enhancer of Zester Homolog-2. Arterioscler Thromb Vasc Biol. 2015 Mar;35(3):664–74.

222. Ke W, Chen Y, Zheng L, Zhang Y, Wu Y, Li L. miR-134-5p promotes inflammation and apoptosis of trophoblast cells via regulating FOXP2 transcription in gestational diabetes mellitus. Bioengineered. 2022 Jan 30;13(1):319–30.

223. Peng HY, Li HP, Li MQ. High glucose induces dysfunction of human umbilical vein endothelial cells by upregulating miR-137 in gestational diabetes mellitus. Microvasc Res. 2018 Jul;118:90–100.

224. Zhang Muling, Zhu Xiaohong. miR-9-5p plays an important role in gestational diabetes mellitus (GDM) progression by targeting HK-2. Int J Clin Exp Med . 2018;11(7):6694–701. .

225. Liao X, Zhou Z, Zhang X. Effects of miR-195-5p on cell proliferation and apoptosis in gestational diabetes mellitus via targeting EZH2. Mol Med Rep. 2020 May 12;22(2):803–9.

226. Yu X, Liu Z, Fang J, Qi H. miR-96-5p: A potential diagnostic marker for gestational diabetes mellitus. . Medicine. 2021 May 28;100(21):e25808.

227. Ji Y, Zhang W, Yang J, Li C. MiR-193b inhibits autophagy and apoptosis by targeting IGFBP5 in high glucose-induced trophoblasts. Placenta. 2020 Nov;101:185–93.

228. Song F, Cai A, Ye Q, Chen X, Lin L, Hao X. MiR-34b-3p Impaired HUVECs Viability and Migration via Targeting PDK1 in an In Vitro Model of Gestational Diabetes Mellitus. Biochem Genet. 2021 Dec 15;59(6):1381–95.

229. Wang S, Wei D, Sun X, Li Y, Li D, Chen B. MiR-190b impedes pancreatic β cell proliferation and insulin secretion by targeting NKX6-1 and may associate to gestational diabetes mellitus. Journal of Receptors and Signal Transduction. 2021 Jul 4;41(4):349–56.

230. Xu K, Bian D, Hao L, Huang F, Xu M, Qin J, et al. microRNA-503 contribute to pancreatic beta cell dysfunction by targeting the mTOR pathway in gestational diabetes mellitus. EXCLI J. 2017;16:1177–87.

231. Zhang L, Zhang T, Sun D, Cheng G, Ren H, Hong H, et al. Diagnostic value of dysregulated microribonucleic acids in the placenta and circulating exosomes in gestational diabetes mellitus. J Diabetes Investig. 2021 Aug 22;12(8):1490–500.

232. Li L, Wang S, Li H, Wan J, Zhou Q, Zhou Y, et al. microRNA-96 protects pancreatic β-cell function by targeting PAK1 in gestational diabetes mellitus. BioFactors. 2018 Nov 8;44(6):539–47.

233. Chen X, Yang F, Zhang T, Wang W, Xi W, Li Y, et al. MiR-9 promotes tumorigenesis and angiogenesis and is activated by MYC and OCT4 in human glioma. Journal of Experimental & Clinical Cancer Research. 2019 Dec 22;38(1):99.

234. Song TR, Su GD, Chi YL, Wu T, Xu Y, Chen CC. Dysregulated miRNAs contribute to altered placental glucose metabolism in patients with gestational diabetes via targeting GLUT1 and HK2. Placenta. 2021 Feb;105:14–22.

235. Shi Z, Zhao C, Guo X, Ding H, Cui Y, Shen R, et al. Differential Expression of MicroRNAs in Omental Adipose Tissue From Gestational Diabetes Mellitus Subjects Reveals miR-222 as a Regulator of ERα Expression in Estrogen-Induced Insulin Resistance. Endocrinology. 2014 May 1;155(5):1982–90.

236. Lee A, Papangeli I, Park Y, Jeong H neul, Choi J, Kang H, et al. A PPARγ-dependent miR-424/503-CD40 axis regulates inflammation mediated angiogenesis. Sci Rep. 2017 May 31;7(1):2528.

237. Caporali A, Meloni M, Völlenkle C, Bonci D, Sala-Newby GB, Addis R, et al. Deregulation of microRNA-503 Contributes to Diabetes Mellitus–Induced Impairment of Endothelial Function and Reparative Angiogenesis After Limb Ischemia. Circulation. 2011 Jan 25;123(3):282–91.

238. Hou LJ, Han JJ, Liu Y. Up-regulation of microRNA-503 by high glucose reduces the migration and proliferation but promotes the apoptosis of human umbilical vein endothelial cells by inhibiting the expression of insulin-like growth factor-1 receptor. Eur Rev Med Pharmacol Sci. 2018 Jun;22(11):3515–23. .

239. Joshi NP, Mane AR, Sahay AS, Sundrani DP, Joshi SR, Yajnik CS. Role of Placental Glucose Transporters in Determining Fetal Growth. Reproductive Sciences. 2022 Oct 2;29(10):2744–59.

240. Chassen S, Jansson T. Complex, coordinated and highly regulated changes in placental signaling and nutrient transport capacity in IUGR. Biochimica et Biophysica Acta (BBA) - Molecular Basis of Disease. 2020 Feb;1866(2):165373.

241. Sferruzzi-Perri AN, Lopez-Tello J, Salazar-Petres E. Placental adaptations supporting fetal growth during normal and adverse gestational environments. Exp Physiol. 2023 Mar 9;108(3):371–97.

242. Chappell J, Aughwane R, Clark AR, Ourselin S, David AL, Melbourne A. A review of feto-placental vasculature flow modelling. Placenta. 2023 Oct;142:56–63.

243. Goldstein JA, Gallagher K, Beck C, Kumar R, Gernand AD. Maternal-Fetal Inflammation in the Placenta and the Developmental Origins of Health and Disease. Front Immunol. 2020 Nov 13;11.

244. Owen MD, Kennedy MG, Quilang RC, Scott EM, Forbes K. The role of microRNAs in pregnancies complicated by maternal diabetes. Clin Sci. 2024 Sep 18;138(18):1179–207.

245. Forbes K, Farrokhnia F, Aplin JD, Westwood M. Dicer-dependent miRNAs provide an endogenous restraint on cytotrophoblast proliferation. Placenta. 2012 Jul;33(7):581–5.

246. Rahimi G, Jafari N, Khodabakhsh M, Shirzad Z, Dogaheh HP. Upregulation of microRNA Processing Enzymes Drosha and Dicer in Gestational Diabetes Mellitus. Gynecological Endocrinology. 2015 Feb 8;31(2):156–9.

247. Yang W, Lu Z, Zhi Z, Liu L, Deng L, Jiang X, et al. Increased miRNA-518b inhibits trophoblast migration and angiogenesis by targeting EGR1 in early embryonic arrest†. Biol Reprod. 2019 Oct 25;101(4):664–74.

248. Wu HM, Lo TC, Tsai CL, Chen LH, Huang HY, Wang HS, et al. Extracellular Vesicle-Associated MicroRNA-138-5p Regulates Embryo Implantation and Early Pregnancy by Adjusting GPR124. Pharmaceutics. 2022 May 30;14(6):1172.

249. Ni H, Wang X, Qu H, Gao X, Yu X. MiR-95-5p involves in the migration and invasion of trophoblast cells by targeting low density lipoprotein receptor-related protein 6. Journal of Obstetrics and Gynaecology Research. 2021 Jan 13;47(1):184–97.

250. Zhou D, Xu X, Liu Y, Liu H, Cheng X, Gu Y, et al. MiR-195-5p facilitates the proliferation, migration, and invasion of human trophoblast cells by targeting <scp>FGF2</scp>. Journal of Obstetrics and Gynaecology Research. 2022 Aug 18;48(8):2122–33.

251. LAURINI R, VISSER G, VANBALLEGOOIE E, SCHOOTS C. Morphological findings in placentae of insulin-dependent diabetic patients treated with continuous subcutaneous insulin infusion (CSII). Placenta. 1987 Mar;8(2):153–65.

252. Adaikalakoteswari A, Vatish M, Alam MT, Ott S, Kumar S, Saravanan P. Low Vitamin B12 in Pregnancy Is Associated With Adipose-Derived Circulating miRs Targeting PPARγ and Insulin Resistance. J Clin Endocrinol Metab. 2017 Nov 1;102(11):4200–9.

253. Baker BC, Mackie FL, Lean SC, Greenwood SL, Heazell AEP, Forbes K, et al. Placental dysfunction is associated with altered microRNA expression in pregnant women with low folate status. Mol Nutr Food Res. 2017 Aug 21;61(8).

254. Shah T, Mishra S, More A, Otiv S, Apte K, Joshi K. Combination of vitamin B12 active forms improved fetal growth in Wistar rats through up-regulation of placental miR-16 and miR-21 levels. Life Sci. 2017 Dec;191:97–103.

255. Masete M, Dias S, Malaza N, Adam S, Pheiffer C. A Big Role for microRNAs in Gestational Diabetes Mellitus. Front Endocrinol (Lausanne). 2022 Jul 25;13.

256. Crescitelli R, Lässer C, Szabó TG, Kittel A, Eldh M, Dianzani I, et al. Distinct RNA profiles in subpopulations of extracellular vesicles: apoptotic bodies, microvesicles and exosomes. J Extracell Vesicles. 2013 Jan 12;2(1).

257. Zealy RW, Wrenn SP, Davila S, Min K, Yoon J. microRNA-binding proteins: specificity and function. WIREs RNA. 2017 Sep 28;8(5).

258. Welsh JA, Goberdhan DCI, O'Driscoll L, Buzas EI, Blenkiron C, Bussolati B, et al. Minimal information for studies of extracellular vesicles (MISEV2023): From basic to advanced approaches. J Extracell Vesicles. 2024 Feb 7;13(2).

259. Jayabalan N, Lai A, Ormazabal V, Adam S, Guanzon D, Palma C, et al. Adipose Tissue Exosomal Proteomic Profile Reveals a Role on Placenta Glucose Metabolism in Gestational Diabetes Mellitus. J Clin Endocrinol Metab. 2019 May 1;104(5):1735–52.

260. Doyle L, Wang M. Overview of Extracellular Vesicles, Their Origin, Composition, Purpose, and Methods for Exosome Isolation and Analysis. Cells. 2019 Jul 15;8(7):727.

261. Mulcahy LA, Pink RC, Carter DRF. Routes and mechanisms of extracellular vesicle uptake. J Extracell Vesicles. 2014 Jan 4;3(1).

262. Tong M, Chen Q, James JL, Wise MR, Stone PR, Chamley LW. In vivo targets of human placental micro-vesicles vary with exposure time and pregnancy. Reproduction. 2017 Jun;153(6):835–45.

263. Adam S, Elfeky O, Kinhal V, Dutta S, Lai A, Jayabalan N, et al. Review: Fetal-maternal communication via extracellular vesicles – Implications for complications of pregnancies. Placenta. 2017 Jun;54:83–8.

264. Zierden HC, Marx-Rattner R, Rock KD, Montgomery KR, Anastasiadis P, Folts L, et al. Extracellular vesicles are dynamic regulators of maternal glucose homeostasis during pregnancy. Sci Rep. 2023 Mar 20;13(1):4568.

265. Chang G, Mouillet J, Mishima T, Chu T, Sadovsky E, Coyne CB, et al. Expression and trafficking of placental microRNAs at the feto-maternal interface. The FASEB Journal. 2017 Jul 13;31(7):2760–70.

266. Morales-Prieto DM, Favaro RR, Markert UR. Placental miRNAs in feto-maternal communication mediated by extracellular vesicles. Placenta. 2020 Dec;102:27–33.

267. Herrera-Van Oostdam A, Toro-Ortíz J, López J, Noyola D, García-López D, Durán-Figueroa N, et al. Placental exosomes isolated from urine of patients with gestational diabetes exhibit a differential profile expression of microRNAs across gestation. Int J Mol Med. 2020 Jun 3;46(2):546–60.

268. Gillet V, Ouellet A, Stepanov Y, Rodosthenous RS, Croft EK, Brennan K, et al. miRNA Profiles in Extracellular Vesicles From Serum Early in Pregnancies Complicated by Gestational Diabetes Mellitus. J Clin Endocrinol Metab. 2019 Nov 1;104(11):5157–69.

269. Delorme-Axford E, Donker RB, Mouillet JF, Chu T, Bayer A, Ouyang Y, et al. Human placental trophoblasts confer viral resistance to recipient cells. Proceedings of the National Academy of Sciences. 2013 Jul 16;110(29):12048–53.

270. Kovács ÁF, Fekete N, Turiák L, Ács A, Kőhidai L, Buzás EI, et al. Unravelling the Role of Trophoblastic-Derived Extracellular Vesicles in Regulatory T Cell Differentiation. Int J Mol Sci. 2019 Jul 14;20(14):3457.

271. Ospina-Prieto S, Chaiwangyen W, Herrmann J, Groten T, Schleussner E, Markert UR, et al. MicroRNA-141 is upregulated in preeclamptic placentae and regulates trophoblast invasion and intercellular communication. Translational Research. 2016 Jun;172:61–72.

272. Holder B, Jones T, Sancho Shimizu V, Rice TF, Donaldson B, Bouqueau M, et al. Macrophage Exosomes Induce Placental Inflammatory Cytokines: A Novel Mode of Maternal–Placental Messaging. Traffic. 2016 Feb 26;17(2):168–78.

273. Quilang R, Godinho E, Timms K, Scott EM, Forbes K. ODP434 Maternally-Derived Pancreatic Extracellular Vesicle Encompassed miRNAs Influence Placental Development in Pregnancies Complicated by Gestational Diabetes. J Endocr Soc. 2022 Nov 1;6(Supplement_1):A671–2.

274. Kennedy, Margeurite Gina. Circulating miRNAs as key regulators of placental vascular dysfunction and altered fetal growth in pregnancies complicated by diabetes. PhD thesis, University of Leeds. 2022.

275. Timms K, Holder B, Day A, Mclaughlin J, Forbes KA, Westwood M. Watermelon-Derived Extracellular Vesicles Influence Human Ex Vivo Placental Cell Behavior by Altering Intestinal Secretions. Mol Nutr Food Res. 2022 Oct 19;66(19).

276. Baker BC, Lui S, Lorne I, Heazell AEP, Forbes K, Jones RL. Sexually dimorphic patterns in maternal circulating microRNAs in pregnancies complicated by fetal growth restriction. Biol Sex Differ. 2021 Dec 17;12(1):61.

277. Nair S, Guanzon D, Jayabalan N, Lai A, Scholz-Romero K, Kalita de Croft P, et al. Extracellular vesicle-associated miRNAs are an adaptive response to gestational diabetes mellitus. J Transl Med. 2021 Dec 20;19(1):360.

278. Salomon C, Scholz-Romero K, Sarker S, Sweeney E, Kobayashi M, Correa P, et al. Gestational Diabetes Mellitus Is Associated With Changes in the Concentration and Bioactivity of Placenta-Derived Exosomes in Maternal Circulation Across Gestation. Diabetes. 2016 Mar 1;65(3):598–609.

279. Zhang Q, Ye X, Xu X, Yan J. Placenta-derived exosomal miR-135a-5p promotes gestational diabetes mellitus pathogenesis by activating PI3K/AKT signalling pathway via SIRT1. J Cell Mol Med. 2023 Dec 4;27(23):3729–43.

280. Gao Z, Wang N, Liu X. Human placenta mesenchymal stem cell-derived exosome shuttling microRNA-130b-3p from gestational diabetes mellitus patients targets ICAM-1 and perturbs human umbilical vein endothelial cell angiogenesis. Acta Diabetol. 2022 Aug 8;59(8):1091–107.

281. Zhang L, Wu Q, Zhu S, Tang Y, Chen Y, Chen D, et al. Chemerin-Induced Down-Regulation of Placenta-Derived Exosomal miR-140-3p and miR-574-3p Promotes Umbilical Vein Endothelial Cells Proliferation, Migration, and Tube Formation in Gestational Diabetes Mellitus. Cells. 2022 Nov 1;11(21):3457.

282. Nair S, Jayabalan N, Guanzon D, Palma C, Scholz-Romero K, Elfeky O, et al. Human placental exosomes in gestational diabetes mellitus carry a specific set of miRNAs associated with skeletal muscle insulin sensitivity. Clin Sci. 2018 Nov 30;132(22):2451–67.

283. Sun X, Lin J, Zhang Y, Kang S, Belkin N, Wara AK, et al. MicroRNA-181b Improves Glucose Homeostasis and Insulin Sensitivity by Regulating Endothelial Function in White Adipose Tissue. Circ Res. 2016 Mar 4;118(5):810–21.

284. Zhang Z, Xu Q, Chen Y, Sui L, Jiang L, Shen Q, et al. The possible role of visceral fat in early pregnancy as a predictor of gestational diabetes mellitus by regulating adipose-

derived exosomes miRNA-148 family: protocol for a nested case-control study in a cohort study. BMC Pregnancy Childbirth. 2021 Dec 30;21(1):262.

285. Jiang H, Wu W, Zhang M, Li J, Peng Y, Miao T t, et al. Aberrant upregulation of miR-21 in placental tissues of macrosomia. Journal of Perinatology. 2014 Sep 1;34(9):658–63.

286. ZHANG JT, CAI QY, JI SS, ZHANG HX, WANG YH, YAN HT, et al. Decreased miR-143 and increased miR-21 placental expression levels are associated with macrosomia. Mol Med Rep. 2016 Apr;13(4):3273–80.

287. Guo D, Jiang H, Chen Y, Yang J, Fu Z, Li J, et al. Elevated microRNA-141-3p in placenta of non-diabetic macrosomia regulate trophoblast proliferation. EBioMedicine. 2018 Dec;38:154–61.

288. Elfeky O, Longo S, Lai A, Rice GE, Salomon C. Influence of maternal BMI on the exosomal profile during gestation and their role on maternal systemic inflammation. Placenta. 2017 Feb;50:60–9.

289. Li J, Song L, Zhou L, Wu J, Sheng C, Chen H, et al. A MicroRNA Signature in Gestational Diabetes Mellitus Associated with Risk of Macrosomia. Cellular Physiology and Biochemistry. 2015;37(1):243–52.

290. Marei E, Gabr Youssef H. Evaluation of MicroRNA-16 and MicroRNA-221 in Serum and Placenta in Gestational Diabetes Mellitus: Correlation with Macrosomia. Egyptian Journal of Radiation Sciences and Applications. 2021 Jan 9;0(0):0–0.

291. Calimlioglu B, Karagoz K, Sevimoglu T, Kilic E, Gov E, Arga KY. Tissue-Specific Molecular Biomarker Signatures of Type 2 Diabetes: An Integrative Analysis of Transcriptomics and Protein–Protein Interaction Data. OMICS. 2015 Sep;19(9):563–73.

292. Marei E, Gabr Youssef H. Evaluation of MicroRNA-16 and MicroRNA-221 in Serum and Placenta in Gestational Diabetes Mellitus: Correlation with Macrosomia. Egyptian Journal of Radiation Sciences and Applications. 2021 Jan 9;0(0):0–0.

293. Calimlioglu B, Karagoz K, Sevimoglu T, Kilic E, Gov E, Arga KY. Tissue-Specific Molecular Biomarker Signatures of Type 2 Diabetes: An Integrative Analysis of Transcriptomics and Protein–Protein Interaction Data. OMICS. 2015 Sep;19(9):563–73.

294. Guiyu S, Quan N, Ruochen W, Dan W, Bingnan C, Yuanyua L, et al. LncRNA-SNX17 Promotes HTR-8/SVneo Proliferation and Invasion Through miR-517a/IGF-1 in the Placenta of Diabetic Macrosomia. Reproductive Sciences. 2022 Feb 16;29(2):596–605.

295. Lowe WL, Lowe LP, Kuang A, Catalano PM, Nodzenski M, Talbot O, et al. Maternal glucose levels during pregnancy and childhood adiposity in the Hyperglycemia and Adverse Pregnancy Outcome Follow-up Study. Diabetologia. 2019 Apr 15;62(4):598–610.

296. Lowe WL, Scholtens DM, Kuang A, Linder B, Lawrence JM, Lebenthal Y, et al. Hyperglycemia and Adverse Pregnancy Outcome Follow-up Study (HAPO FUS): Maternal Gestational Diabetes Mellitus and Childhood Glucose Metabolism. Diabetes Care. 2019 Mar 1;42(3):372–80.

297. Wroblewska-Seniuk K, Wender-Ozegowska E, Szczapa J. Long-term effects of diabetes during pregnancy on the offspring. Pediatr Diabetes. 2009 Nov;10(7):432–40.

298. Yuan L, Shi R, Zhao L, Cai W, Zhou X, Zhang Y, et al. Maternal Exosomes Contribute to the Fetal Cardiac Development Deficiency in Mother with Pre-Existing Diabetes: A Fetal Echocardiography Based Animal Study. Ultrasound Med Biol. 2017;43:S10.

299. Shi R, Zhao L, Cai W, Wei M, Zhou X, Yang G, et al. Maternal exosomes in diabetes contribute to the cardiac development deficiency. Biochem Biophys Res Commun. 2017 Jan;483(1):602–8.

300. Liu Y, Wang Y, Wang C, Shi R, Zhou X, Li Z, et al. Maternal obesity increases the risk of fetal cardiac dysfunction via visceral adipose tissue derived exosomes. Placenta. 2021 Feb;105:85–93.

301. Ormazabal V, Nair S, Carrión F, Mcintyre HD, Salomon C. The link between gestational diabetes and cardiovascular diseases: potential role of extracellular vesicles. Cardiovasc Diabetol. 2022 Sep 3;21(1):174.

302. Tryggestad JB, Vishwanath A, Jiang S, Mallappa A, Teague AM, Takahashi Y, et al. Influence of gestational diabetes mellitus on human umbilical vein endothelial cell miRNA. Clin Sci. 2016 Nov 1;130(21):1955–67.

303. Houshmand-Oeregaard A, Schrölkamp M, Kelstrup L, Hansen NS, Hjort L, Thuesen ACB, et al. Increased expression of microRNA-15a and microRNA-15b in skeletal muscle from adult offspring of women with diabetes in pregnancy. Hum Mol Genet. 2018 May 15;27(10):1763–71.

304. Hromadnikova I, Kotlabova K, Dvorakova L, Krofta L, Sirc J. Substantially Altered Expression Profile of Diabetes/Cardiovascular/Cerebrovascular Disease Associated microRNAs in Children Descending from Pregnancy Complicated by Gestational Diabetes Mellitus—One of Several Possible Reasons for an Increased Cardiovascular Risk. Cells. 2020 Jun 26;9(6):1557.

305. Maloyan A, Muralimanoharan S, Huffman S, Cox LA, Nathanielsz PW, Myatt L, et al. Identification and comparative analyses of myocardial miRNAs involved in the fetal response to maternal obesity. Physiol Genomics. 2013 Oct 1;45(19):889–900.

306. He L, Wang X, Jin Y, Xu W, Guan Y, Wu J, et al. Identification and validation of the miRNA–mRNA regulatory network in fetoplacental arterial endothelial cells of gestational diabetes mellitus. Bioengineered. 2021 Jan 7;12(1):3503–15.

307. Ferland-McCollough D, Fernandez-Twinn DS, Cannell IG, David H, Warner M, Vaag AA, et al. Programming of adipose tissue miR-483-3p and GDF-3 expression by maternal diet in type 2 diabetes. Cell Death Differ. 2012 Jun 6;19(6):1003–12.

308. Fornes D, White V, Higa R, Heinecke F, Capobianco E, Jawerbaum A. Sex-dependent changes in lipid metabolism, PPAR pathways and microRNAs that target PPARs in the fetal liver of rats with gestational diabetes. Mol Cell Endocrinol. 2018 Feb;461:12–21.

309. Joshi A, Azuma R, Akumuo R, Goetzl L, Pinney SE. Gestational diabetes and maternal obesity are associated with sex-specific changes in miRNA and target gene expression in the fetus. Int J Obes. 2020 Jul 18;44(7):1497–507.

310. Strutz J, Cvitic S, Hackl H, Kashofer K, Appel HM, Thüringer A, et al. Gestational diabetes alters microRNA signatures in human feto-placental endothelial cells depending on fetal sex. Clin Sci. 2018 Nov 30;132(22):2437–49.

311. Shyamasundar S, Ramya S, Kandilya D, Srinivasan DK, Bay BH, Ansari SA, et al. Maternal Diabetes Deregulates the Expression of Mecp2 via miR-26b-5p in Mouse Embryonic Neural Stem Cells. Cells. 2023 May 30;12(11):1516.

312. Wang F, Xu C, Reece EA, Li X, Wu Y, Harman C, et al. Protein kinase C-alpha suppresses autophagy and induces neural tube defects via miR-129-2 in diabetic pregnancy. Nat Commun. 2017 May 5;8(1):15182.

313. Frørup C, Mirza AH, Yarani R, Nielsen LB, Mathiesen ER, Damm P, et al. Plasma Exosome-Enriched Extracellular Vesicles From Lactating Mothers With Type 1 Diabetes

Contain Aberrant Levels of miRNAs During the Postpartum Period. Front Immunol. 2021 Oct 8;12.

314. Fu J, Retnakaran R. The life course perspective of gestational diabetes: An opportunity for the prevention of diabetes and heart disease in women. EClinicalMedicine. 2022 Mar;45:101294.

315. Zhang C, Li Q, Ren N, Li C, Wang X, Xie M, et al. Placental miR-106a~363 cluster is dysregulated in preeclamptic placenta. Placenta. 2015 Feb;36(2):250–2.

316. Hromadnikova I, Kotlabova K, Ondrackova M, Kestlerova A, Novotna V, Hympanova L, et al. Circulating C19MC MicroRNAs in Preeclampsia, Gestational Hypertension, and Fetal Growth Restriction. Mediators Inflamm. 2013;2013:1–12.

317. Laganà AS, Vitale SG, Sapia F, Valenti G, Corrado F, Padula F, et al. miRNA expression for early diagnosis of preeclampsia onset: hope or hype? The Journal of Maternal-Fetal & Neonatal Medicine. 2018 Mar 19;31(6):817–21.

318. Joglekar M V., Wong WKM, Ema FK, Georgiou HM, Shub A, Hardikar AA, et al. Postpartum circulating microRNA enhances prediction of future type 2 diabetes in women with previous gestational diabetes. Diabetologia. 2021 Jul 23;64(7):1516–26.

319. Lu W, Hu C. Molecular biomarkers for gestational diabetes mellitus and postpartum diabetes. Chin Med J (Engl). 2022 Aug 20;135(16):1940–51.

320. Ares Blanco J, Lambert C, Fernandez-Sanjurjo M, Morales-Sanchez P, Pujante P, Pinto-Hernández P, et al. miR-24-3p and Body Mass Index as Type 2 Diabetes Risk Factors in Spanish Women 15 Years after Gestational Diabetes Mellitus Diagnosis. Int J Mol Sci. 2023 Jan 6;24(2):1152.

321. Valerio J, Barabash A, Garcia de la Torre N, De Miguel P, Melero V, del Valle L, et al. The Relationship between Serum Adipokines, miR-222-3p, miR-103a-3p and Glucose Regulation in Pregnancy and Two to Three Years Post-Delivery in Women with Gestational Diabetes Mellitus Adhering to Mediterranean Diet Recommendations. Nutrients. 2022 Nov 8;14(22):4712.

322. Kameswaran V, Bramswig NC, McKenna LB, Penn M, Schug J, Hand NJ, et al. Epigenetic Regulation of the DLK1-MEG3 MicroRNA Cluster in Human Type 2 Diabetic Islets. Cell Metab. 2014 Jan;19(1):135–45.

323. Xiang Y. miR-24 in diabetes. Oncotarget. 2015 Jul 10;6(19):16816–7.

324. Bo S, Valpreda S, Menato G, Bardelli C, Botto C, Gambino R, et al. Should we consider gestational diabetes a vascular risk factor? Atherosclerosis. 2007 Oct;194(2):e72–9.

325. Hromadnikova I, Kotlabova K, Krofta L. Cardiovascular Disease-Associated MicroRNAs as Novel Biomarkers of First-Trimester Screening for Gestational Diabetes Mellitus in the Absence of Other Pregnancy-Related Complications. Int J Mol Sci. 2022 Sep 13;23(18):10635.

326. Aldhous, M., Norman, J. and Reynolds, R. E-MTAB-6418 - Investigation of placental gene expression in obese women exposed to Metformin during pregnancy. ArrayExpress. [Online]. 2019. Available from: https://www.ebi.ac.uk/arrayexpress/experiments/E-MTAB-6418.

327. Chiswick C, Reynolds RM, Denison F, Drake AJ, Forbes S, Newby DE, et al. Effect of metformin on maternal and fetal outcomes in obese pregnant women (EMPOWaR): a randomised, double-blind, placebo-controlled trial. Lancet Diabetes Endocrinol. 2015 Oct;3(10):778–86.

328. Athar A, Füllgrabe A, George N, Iqbal H, Huerta L, Ali A, et al. ArrayExpress update – from bulk to single-cell expression data. Nucleic Acids Res. 2019 Jan 8;47(D1):D711–5.

329. Zhao S, Jing W, Samuels DC, Sheng Q, Shyr Y, Guo Y. Strategies for processing and quality control of Illumina genotyping arrays. Brief Bioinform. 2018 Sep 28;19(5):765–75.

330. Benjamini Y, Hochberg Y. Controlling the False Discovery Rate: A Practical and Powerful Approach to Multiple Testing. J R Stat Soc Series B Stat Methodol. 1995 Jan 1;57(1):289–300.

331. Makhijani RK, Raut SA, Purohit HJ. Fold change based approach for identification of significant network markers in breast, lung and prostate cancer. IET Syst Biol. 2018 Oct;12(5):213–8.

332. O'Connell JD, Paulo JA, O'Brien JJ, Gygi SP. Proteome-Wide Evaluation of Two Common Protein Quantification Methods. J Proteome Res. 2018 May 4;17(5):1934–42.

333. Peltz ED, Moore EE, Zurawel AA, Jordan JR, Damle SS, Redzic JS, et al. Proteome and system ontology of hemorrhagic shock: Exploring early constitutive changes in postshock mesenteric lymph. Surgery. 2009 Aug;146(2):347–57.

334. Krämer A, Green J, Pollard J, Tugendreich S. Causal analysis approaches in Ingenuity Pathway Analysis. Bioinformatics. 2014 Feb 15;30(4):523–30.

335. Desforges M, Whittaker H, Farmer E, Sibley CP, Greenwood SL. Effects of Taurine Depletion on Human Placental Syncytiotrophoblast Renewal and Susceptibility to Oxidative Stress. In 2015. p. 63–73.

336. Kerby A, Graham N, Wallworth R, Batra G, Heazell A. Development of dynamic image analysis methods to measure vascularisation and syncytial nuclear aggregates in human placenta. Placenta. 2022 Mar;120:65–72.

337. Frank JW, Steinhauser CB, Wang X, Burghardt RC, Bazer FW, Johnson GA. Loss of ITGB3 in ovine conceptuses decreases conceptus expression of NOS3 and SPP1: implications for the developing placental vasculature†. Biol Reprod. 2021 Mar 11;104(3):657–68.

338. Yamamoto H, Zhang S, Mizushima N. Autophagy genes in biology and disease. Nat Rev Genet. 2023 Jun 12;24(6):382–400.

339. Heath-Engel HM, Chang NC, Shore GC. The endoplasmic reticulum in apoptosis and autophagy: role of the BCL-2 protein family. Oncogene. 2008 Oct 27;27(50):6419–33.

340. Guak H, Sheldon RD, Beddows I, Vander Ark A, Weiland MJ, Shen H, et al. PGC-1β maintains mitochondrial metabolism and restrains inflammatory gene expression. Sci Rep. 2022 Sep 26;12(1):16028.

341. Piccinin E, Peres C, Bellafante E, Ducheix S, Pinto C, Villani G, et al. Hepatic peroxisome proliferator-activated receptor γ coactivator 1β drives mitochondrial and anabolic signatures that contribute to hepatocellular carcinoma progression in mice. Hepatology. 2018 Mar 29;67(3):884–98.

342. Zougman A, Wilson JP, Roberts LD, Banks RE. Detergent-Free Simultaneous Sample Preparation Method for Proteomics and Metabolomics. J Proteome Res. 2020 Jul 2;19(7):2838–44.

343. Taylor GS, Smith K, Scragg J, McDonald TJ, Shaw JA, West DJ, et al. The metabolome as a diagnostic for maximal aerobic capacity during exercise in type 1 diabetes. Diabetologia. 2024 Jul 25;67(7):1413–28.

344. Wood N, Straw S, Cheng CW, Hirata Y, Pereira MG, Gallagher H, et al. Sodium–glucose cotransporter 2 inhibitors influence skeletal muscle pathology in patients with heart failure and reduced ejection fraction. Eur J Heart Fail. 2024 Apr 11;26(4):925–35.

345. Quillet A, Saad C, Ferry G, Anouar Y, Vergne N, Lecroq T, et al. Improving Bioinformatics Prediction of microRNA Targets by Ranks Aggregation. Front Genet. 2020 Jan 28;10.

346. Kunieda T, Xian M, Kobayashi E, Imamichi T, Moriwaki K, Toyoda Y. Sexing of Mouse Preimplantation Embryos by Detection of Y Chromosome-Specific Sequences Using Polymerase Chain Reaction1. Biol Reprod. 1992 Apr 1;46(4):692–7.

347. Ruiz-Villalba A, Mattiotti A, Gunst QD, Cano-Ballesteros S, van den Hoff MJB, Ruijter JM. Reference genes for gene expression studies in the mouse heart. Sci Rep. 2017 Feb 2;7(1):24.

348. Lopez-Tello J, Sferruzzi-Perri A. Histological Analysis of Trophoblast Cells in the Mouse Placental Labyrinth Zone. In 2024. p. 1–13.

349. De Clercq K, Lopez-Tello J, Vriens J, Sferruzzi-Perri AN. Double-label immunohistochemistry to assess labyrinth structure of the mouse placenta with stereology. Placenta. 2020 May;94:44–7.

350. Agius L, Ford BE, Chachra SS. The Metformin Mechanism on Gluconeogenesis and AMPK Activation: The Metabolite Perspective. Int J Mol Sci. 2020 May 3;21(9):3240.

351. Rena G, Hardie DG, Pearson ER. The mechanisms of action of metformin. Diabetologia. 2017 Sep 3;60(9):1577–85.

352. Eyal S, Easterling TR, Carr D, Umans JG, Miodovnik M, Hankins GD V., et al. Pharmacokinetics of Metformin during Pregnancy. Drug Metabolism and Disposition. 2010 May;38(5):833–40.

353. Charles B, Norris R, Xiao X, Hague W. Population Pharmacokinetics of Metformin in Late Pregnancy. Ther Drug Monit. 2006 Feb;28(1):67–72.

354. Vanky E, Zahlsen K, Spigset O, Carlsen SM. Placental passage of metformin in women with polycystic ovary syndrome. Fertil Steril. 2005 May;83(5):1575–8.

355. Liao MZ, Flood Nichols SK, Ahmed M, Clark S, Hankins GD, Caritis S, et al. Effects of Pregnancy on the Pharmacokinetics of Metformin. Drug Metabolism and Disposition. 2020 Apr;48(4):264–71.

356. Gormsen LC, Sundelin EI, Jensen JB, Vendelbo MH, Jakobsen S, Munk OL, et al. In Vivo Imaging of Human 11C-Metformin in Peripheral Organs: Dosimetry, Biodistribution, and Kinetic Analyses. Journal of Nuclear Medicine. 2016 Dec;57(12):1920–6.

357. Garbarino VR, Santos TA, Nelson AR, Zhang WQ, Smolik CM, Javors MA, et al. Prenatal metformin exposure or organic cation transporter 3 knock-out curbs social interaction preference in male mice. Pharmacol Res. 2019 Feb;140:21–32.

358. Han T (Kevin), Proctor WR, Costales CL, Cai H, Everett RS, Thakker DR. Four Cation-Selective Transporters Contribute to Apical Uptake and Accumulation of Metformin in Caco-2 Cell Monolayers. Journal of Pharmacology and Experimental Therapeutics. 2015 Mar;352(3):519–28.

359. Grube M, Schwabedissen HM zu, Draber K, Präger D, Möritz KU, Linnemann K, et al. EXPRESSION, LOCALIZATION, AND FUNCTION OF THE CARNITINE TRANSPORTER OCTN2 (SLC22A5) IN HUMAN PLACENTA. Drug Metabolism and Disposition. 2005 Jan;33(1):31–7.

360. Yang Q, Wang G, Fang D, Gao X, Liang Y, Wang L, et al. The role of MicroRNA networks in tissue-specific direct and indirect effects of metformin and its application. Biomedicine & Pharmacotherapy. 2022 Jul;151:113130.

361. Hsu WH, Hsiao PJ, Lin PC, Chen SC, Lee MY, Shin SJ. Effect of metformin on kidney function in patients with type 2 diabetes mellitus and moderate chronic kidney disease. Oncotarget. 2018 Jan 12;9(4):5416–23.

362. Musi N, Hirshman MF, Nygren J, Svanfeldt M, Bavenholm P, Rooyackers O, et al. Metformin Increases AMP-Activated Protein Kinase Activity in Skeletal Muscle of Subjects With Type 2 Diabetes. Diabetes. 2002 Jul 1;51(7):2074–81.

363. Demirsoy İH, Ertural DY, Balci Ş, Çınkır Ü, Sezer K, Tamer L, et al. Profiles of Circulating miRNAs Following Metformin Treatment in Patients with Type 2 Diabetes. J Med Biochem. 2018 Dec 1;37(4):499–506.

364. Ortega FJ, Mercader JM, Moreno-Navarrete JM, Rovira O, Guerra E, Esteve E, et al. Profiling of Circulating MicroRNAs Reveals Common MicroRNAs Linked to Type 2 Diabetes That Change With Insulin Sensitization. Diabetes Care. 2014 May 1;37(5):1375–83.

365. Ghai V, Kim TK, Etheridge A, Nielsen T, Hansen T, Pedersen O, et al. Extracellular Vesicle Encapsulated MicroRNAs in Patients with Type 2 Diabetes Are Affected by Metformin Treatment. J Clin Med. 2019 May 7;8(5):617.

366. Liao Z, Li S, Lu S, Liu H, Li G, Ma L, et al. Metformin facilitates mesenchymal stem cell-derived extracellular nanovesicles release and optimizes therapeutic efficacy in intervertebral disc degeneration. Biomaterials. 2021 Jul;274:120850.

367. Scindia YM, Gholam MF, Waleed A, Liu LP, Chacko KM, Desai D, et al. Metformin Alleviates Diabetes-Associated Hypertension by Attenuating the Renal Epithelial Sodium Channel. Biomedicines. 2023 Jan 21;11(2):305.

368. Soraya H, Sani NA, Jabbari N, Rezaie J. Metformin Increases Exosome Biogenesis and Secretion in U87 MG Human Glioblastoma Cells: A Possible Mechanism of Therapeutic Resistance. Arch Med Res. 2021 Feb;52(2):151–62.

369. Simeone PG, Liani R, Bologna G, Tripaldi R, Di Castelnuovo A, Simeone P, et al. Extracellular vesicles number and cell subtype may be influenced by diabetes mellitus and metformin in patients at high cardiovascular risk. Nutrition, Metabolism and Cardiovascular Diseases. 2023 Jan;33(1):124–32.

370. Nashif SK, Mahr RM, Jena S, Jo S, Nelson AB, Sadowski D, et al. Metformin impairs trophoblast metabolism and differentiation in a dose-dependent manner. Front Cell Dev Biol. 2023 May 12;11.

371. Brownfoot FC, Hastie R, Hannan NJ, Cannon P, Tuohey L, Parry LJ, et al. Metformin as a prevention and treatment for preeclampsia: effects on soluble fms-like tyrosine kinase 1 and soluble endoglin secretion and endothelial dysfunction. Am J Obstet Gynecol. 2016 Mar;214(3):356.e1-356.e15.

372. Brownfoot FC, Hastie R, Hannan NJ, Cannon P, Nguyen T V., Tuohey L, et al. Combining metformin and sulfasalazine additively reduces the secretion of antiangiogenic factors from the placenta: Implications for the treatment of preeclampsia. Placenta. 2020 Jun;95:78–83.

373. Kovo M, Kogman N, Ovadia O, Nakash I, Golan A, Hoffman A. Carrier-mediated transport of metformin across the human placenta determined by using the *ex vivo* perfusion of the placental cotyledon model. Prenat Diagn. 2008 Jun 28;28(6):544–8.

374. MIYOSHI H, KATO K, IWAMA H, MAEDA E, SAKAMOTO T, FUJITA K, et al. Effect of the anti-diabetic drug metformin in hepatocellular carcinoma in vitro and in vivo. Int J Oncol. 2014 Jul;45(1):322–32.

375. Hosni A, El-twab SA, Abdul-Hamid M, Prinsen E, AbdElgawad H, Abdel-Moneim A, et al. Cinnamaldehyde mitigates placental vascular dysfunction of gestational diabetes and protects from the associated fetal hypoxia by modulating placental angiogenesis, metabolic activity and oxidative stress. Pharmacol Res. 2021 Mar;165:105426.

376. Jiang S, Teague AM, Tryggestad JB, Jensen ME, Chernausek SD. Role of metformin in epigenetic regulation of placental mitochondrial biogenesis in maternal diabetes. Sci Rep. 2020 May 20;10(1):8314.

377. Cluver C, Walker SP, Mol BW, Hall D, Hiscock R, Brownfoot FC, et al. A double blind, randomised, placebo-controlled trial to evaluate the efficacy of metformin to treat preterm pre-eclampsia (PI2 Trial): study protocol. BMJ Open. 2019 Apr 24;9(4):e025809.

378. Kaitu'u-Lino TJ, Brownfoot FC, Beard S, Cannon P, Hastie R, Nguyen T V., et al. Combining metformin and esomeprazole is additive in reducing sFlt-1 secretion and decreasing endothelial dysfunction – implications for treating preeclampsia. PLoS One. 2018 Feb 21;13(2):e0188845.

379. Wang F, Cao G, Yi W, Li L, Cao X. Effect of Metformin on a Preeclampsia-Like Mouse Model Induced by High-Fat Diet. Biomed Res Int. 2019 Dec 7;2019:1–8.

380. Szukiewicz D, Szewczyk G, Pyzlak M, Stangret A, Bachanek M, Trojanowski S, et al. Anti-inflammatory Action of Metformin with Respect to CX3CL1/CX3CR1 Signaling in Human Placental Circulation in Normal-Glucose Versus High-Glucose Environments. Inflammation. 2018 Dec 10;41(6):2246–64.

381. Correia-Branco A, Keating E, Martel F. Involvement of mTOR, JNK and PI3K in the negative effect of ethanol and metformin on the human first-trimester extravillous trophoblast HTR-8/SVneo cell line. Eur J Pharmacol. 2018 Aug;833:16–24.

382. Arshad R, Kanpurwala MA, Karim N, Hassan JA. Effects of Diet and Metformin on placental morphology in Gestational Diabetes Mellitus. Pak J Med Sci. 2016 Nov 15;32(6).

383. Han CS, Herrin MA, Pitruzzello MC, Mulla MJ, Werner EF, Pettker CM, et al. Glucose and Metformin Modulate Human First Trimester Trophoblast Function: a Model and Potential Therapy for Diabetes-Associated Uteroplacental Insufficiency. American Journal of Reproductive Immunology. 2015 Apr 14;73(4):362–71.

384. Alzamendi A, Del Zotto H, Castrogiovanni D, Romero J, Giovambattista A, Spinedi E. Oral Metformin Treatment Prevents Enhanced Insulin Demand and Placental Dysfunction in the Pregnant Rat Fed a Fructose-Rich Diet. ISRN Endocrinol. 2012 Aug 16;2012:1–8.

385. Jamal A, Milani F, Al-Yasin A. Evaluation of the effect of metformin and aspirin on utero placental circulation of pregnant women with PCOS. Iran J Reprod Med. 2012 May;10(3):265–70.

386. Tarry-Adkins JL, Robinson IG, Reynolds RM, Aye ILMH, Charnock-Jones DS, Jenkins B, et al. Impact of Metformin Treatment on Human Placental Energy Production and Oxidative Stress. Front Cell Dev Biol. 2022 Jun 17;10.

387. Owen M, Hugh K, Quilang R, Scott E, Forbes K. Metformin Exposure *In-Utero* Influences Placental Pathways Associated with Mitochondrial Activity. Endocrine Abstracts. 2022 Oct 27;

388. Zheng Z, Li Y, Fan S, An J, Luo X, Liang M, et al. WW domain-binding protein 2 overexpression prevents diet-induced liver steatosis and insulin resistance through AMPKβ1. Cell Death Dis. 2021 Mar 3;12(3):228.

389. Sanders SS, Hou J, Sutton LM, Garside VC, Mui KKN, Singaraja RR, et al. Huntingtin interacting proteins 14 and 14-like are required for chorioallantoic fusion during early placental development. Dev Biol. 2015 Jan;397(2):257–66.

390. Jin J, Gu H, Anders NM, Ren T, Jiang M, Tao M, et al. Metformin Protects Cells from Mutant Huntingtin Toxicity Through Activation of AMPK and Modulation of Mitochondrial Dynamics. Neuromolecular Med. 2016 Dec 25;18(4):581–92.

391. Ji L, Chen Z, Xu Y, Xiong G, Liu R, Wu C, et al. Systematic Characterization of Autophagy in Gestational Diabetes Mellitus. Endocrinology. 2017 Aug 1;158(8):2522–32.

392. Huang W, Castelino RL, Peterson GM. Lactate Levels with Chronic Metformin Use: A Narrative Review. Clin Drug Investig. 2017 Nov 23;37(11):991–1007.

393. Cusi K, Consoli A, DeFronzo RA. Metabolic effects of metformin on glucose and lactate metabolism in noninsulin-dependent diabetes mellitus. J Clin Endocrinol Metab. 1996 Nov;81(11):4059–67.

394. Chan FKM, Moriwaki K, De Rosa MJ. Detection of Necrosis by Release of Lactate Dehydrogenase Activity. In 2013. p. 65–70.

395. Féry F, Plat L, Balasse EO. Effects of metformin on the pathways of glucose utilization after oral glucose in non—insulin-dependent diabetes mellitus patients. Metabolism. 1997 Feb;46(2):227–33.

396. Law GR, Alnaji A, Alrefaii L, Endersby D, Cartland SJ, Gilbey SG, et al. Suboptimal Nocturnal Glucose Control Is Associated With Large for Gestational Age in Treated Gestational Diabetes Mellitus. Diabetes Care. 2019 May 1;42(5):810–5.

397. VALAVANIDIS A, VLACHOGIANNI T, FIOTAKIS C. 8-hydroxy-2′ -deoxyguanosine (8-OHdG): A Critical Biomarker of Oxidative Stress and Carcinogenesis. Journal of Environmental Science and Health, Part C. 2009 May 7;27(2):120–39.

398. Hirsch A, Hahn D, Kempná P, Hofer G, Nuoffer JM, Mullis PE, et al. Metformin Inhibits Human Androgen Production by Regulating Steroidogenic Enzymes HSD3B2 and CYP17A1 and Complex I Activity of the Respiratory Chain. Endocrinology. 2012 Sep 1;153(9):4354–66.

399. Protti A, Lecchi A, Fortunato F, Artoni A, Greppi N, Vecchio S, et al. Metformin overdose causes platelet mitochondrial dysfunction in humans. Crit Care. 2012;16(5):R180.

400. Suwa M, Egashira T, Nakano H, Sasaki H, Kumagai S. Metformin increases the PGC-1α protein and oxidative enzyme activities possibly via AMPK phosphorylation in skeletal muscle in vivo. J Appl Physiol. 2006 Dec;101(6):1685–92.

401. Yubero D, Adin A, Montero R, Jou C, Jiménez-Mallebrera C, García-Cazorla A, et al. A statistical algorithm showing coenzyme Q10 and citrate synthase as biomarkers for mitochondrial respiratory chain enzyme activities. Sci Rep. 2016 Dec 5;6(1):15.

402. Batchuluun B, Al Rijjal D, Prentice KJ, Eversley JA, Burdett E, Mohan H, et al. Elevated Medium-Chain Acylcarnitines Are Associated With Gestational Diabetes Mellitus and Early Progression to Type 2 Diabetes and Induce Pancreatic β-Cell Dysfunction. Diabetes. 2018 May 1;67(5):885–97.

403. Weitzner O, Seraya-Bareket C, Biron-Shental T, Fishamn A, Yagur Y, Tzadikevitch-Geffen K, et al. Enhanced expression of αVβ3 integrin in villus and extravillous trophoblasts of placenta accreta. Arch Gynecol Obstet. 2021 May 28;303(5):1175–83.

404. Gumina DL, Ji S, Flockton A, McPeak K, Stich D, Moldovan R, et al. Dysregulation of integrin αvβ3 and α5β1 impedes migration of placental endothelial cells in fetal growth restriction. Development. 2022 Oct 1;149(19).

405. Aslonova MZ, GA I, NN M. Association of ITGB3 gene polymorphisms with the risk of developing fetal growth restriction syndrome. MOJ Women's Health. 2021 Aug 31;10(4):97–100.

406. Zhai J, Wang J, Chang Z, Ma L. Metformin regulates key micrornas to increase implantation marker gene expression in the uterus of PCOS patients. Fertil Steril. 2018 Sep;110(4):e112–3.

407. Malekpour-Dehkordi Z, Teimourian S, Nourbakhsh M, Naghiaee Y, Sharifi R, Mohiti-Ardakani J. Metformin reduces fibrosis factors in insulin resistant and hypertrophied adipocyte via integrin/ERK, collagen VI, apoptosis, and necrosis reduction. Life Sci. 2019 Sep;233:116682.

408. Sirico A, Rossi ED, Degennaro VA, Arena V, Rizzi A, Tartaglione L, et al. Placental diabesity: placental VEGF and CD31 expression according to pregestational BMI and gestational weight gain in women with gestational diabetes. Arch Gynecol Obstet. 2022 Jul 14;307(6):1823–31.

409. Anness AR, Baldo A, Webb DR, Khalil A, Robinson TG, Mousa HA. Effect of metformin on biomarkers of placental- mediated disease: A systematic review and meta-analysis. Placenta. 2021 Apr;107:51–8.

410. Triggle CR, Marei I, Ye K, Ding H, Anderson TJ, Hollenberg MD, et al. Repurposing Metformin for Vascular Disease. Curr Med Chem. 2023 Oct;30(35):3955–78.

411. Soobryan N, Murugesan S, Pandiyan A, Moodley J, Mackraj I. Angiogenic Dysregulation in Pregnancy-Related Hypertension—A Role for Metformin. Reproductive Sciences. 2018 Nov 30;25(11):1531–9.

412. Virtanen A, Huttala O, Tihtonen K, Toimela T, Heinonen T, Laivuori H, et al. Therapeutic doses of metformin do not have impact on angiogenesis in presence of sera from pre-eclamptic, IUGR and healthy pregnancies. Pregnancy Hypertens. 2020 Oct;22:7–13.

413. Tam Tam H, Dowling O, Xue X, Rochelson B, Metz C. 687: Metformin inhibits inflammatory cytokine production in placental cells. Am J Obstet Gynecol. 2008 Dec;199(6):S197.

414. Vega M, Mauro M, Williams Z. Direct toxicity of insulin on the human placenta and protection by metformin. Fertil Steril. 2019 Mar;111(3):489-496.e5.

415. Vanlalhruaii, Dasgupta R, Ramachandran R, Mathews JE, Regi A, Thomas N, et al. How safe is metformin when initiated in early pregnancy? A retrospective 5-year study of pregnant women with gestational diabetes mellitus from India. Diabetes Res Clin Pract. 2018 Mar;137:47–55.

416. Lautatzis ME, Goulis DG, Vrontakis M. Efficacy and safety of metformin during pregnancy in women with gestational diabetes mellitus or polycystic ovary syndrome: A systematic review. Metabolism. 2013 Nov;62(11):1522–34.

417. Barjaktarovic M, Korevaar TIM, Jaddoe VW V., de Rijke YB, Visser TJ, Peeters RP, et al. Human chorionic gonadotropin (hCG) concentrations during the late first trimester are associated with fetal growth in a fetal sex-specific manner. Eur J Epidemiol. 2017 Feb 5;32(2):135–44.

418. Deng, L., Liu, X., & He, L. Effect of metformin combined with insulin aspart on β-HCG and PAPP-A in gestational diabetes mellitus. 2020. .

419. Hardie DG, Ross FA, Hawley SA. AMPK: a nutrient and energy sensor that maintains energy homeostasis. Nat Rev Mol Cell Biol. 2012 Apr 22;13(4):251–62.

420. Elliott BD, Langer O, Schuessling F. Human placental glucose uptake and transport are not altered by the oral antihyperglycemic agent metformin. Am J Obstet Gynecol. 1997 Mar;176(3):527–30.

421. Sarabia V, Lam L, Burdett E, Leiter LA, Klip A. Glucose transport in human skeletal muscle cells in culture. Stimulation by insulin and metformin. Journal of Clinical Investigation. 1992 Oct 1;90(4):1386–95.

422. Huang CF, Tiao MM, Lin IC, Huang LT, Sheen JM, Tain YL, et al. Maternal Metformin Treatment Reprograms Maternal High-Fat Diet-Induced Hepatic Steatosis in Offspring Associated with Placental Glucose Transporter Modifications. Int J Mol Sci. 2022 Nov 17;23(22):14239.

423. Meng J, Han J, Wang X, Wu T, Zhang H, An H, et al. Twist1-YY1-p300 complex promotes the malignant progression of HCC through activation of miR-9 by forming phase-separated condensates at super-enhancers and relieved by metformin. Pharmacol Res. 2023 Feb;188:106661.

424. Kato K, Gong J, Iwama H, Kitanaka A, Tani J, Miyoshi H, et al. The Antidiabetic Drug Metformin Inhibits Gastric Cancer Cell Proliferation *In Vitro* and *In Vivo*. Mol Cancer Ther. 2012 Mar 1;11(3):549–60.

425. Wang L, O'Kane AM, Zhang Y, Ren J. Maternal obesity and offspring health: Adapting metabolic changes through autophagy and mitophagy. Obesity Reviews. 2023 Jul 13;24(7).

426. Yildirim RM, Ergun Y, Basar M. Mitochondrial Dysfunction, Mitophagy and Their Correlation with Perinatal Complications: Preeclampsia and Low Birth Weight. Biomedicines. 2022 Oct 12;10(10):2539.

427. Sobrevia L, Valero P, Grismaldo A, Villalobos-Labra R, Pardo F, Subiabre M, et al. Mitochondrial dysfunction in the fetoplacental unit in gestational diabetes mellitus. Biochimica et Biophysica Acta (BBA) - Molecular Basis of Disease. 2020 Dec;1866(12):165948.

428. Zhu HL, Shi XT, Xu XF, Xiong YW, Yi SJ, Zhou GX, et al. Environmental cadmium exposure induces fetal growth restriction via triggering PERK-regulated mitophagy in placental trophoblasts. Environ Int. 2021 Feb;147:106319.

429. Bhansali S, Bhansali A, Dutta P, Walia R, Dhawan V. Metformin upregulates mitophagy in patients with T2DM: A randomized placebo-controlled study. J Cell Mol Med. 2020 Mar 23;24(5):2832–46.

430. Huiniu HAO, Fang Wang, Ran Jia et al. The impact of metformin on the Bcl-2/Bax/Caspase3 signaling pathway in placental tissue of preeclampsia rats, 23 May 2024, PREPRINT (Version 1) available at Research Square.

431. Hebert JF, Myatt L. Metformin Impacts Human Syncytiotrophoblast Mitochondrial Function from Pregnancies Complicated by Obesity and Gestational Diabetes Mellitus in a Sexually Dimorphic Manner. Antioxidants. 2023 Mar 14;12(3):719.

432. Harris K, Desai N, Gupta M, Xue X, Chatterjee PK, Rochelson B, et al. The effects of prenatal metformin on obesogenic diet-induced alterations in maternal and fetal fatty acid metabolism. Nutr Metab (Lond). 2016 Dec 22;13(1):55.

433. Tarry-Adkins JL, Robinson IG, Pantaleão LC, Armstrong JL, Thackray BD, Holzner LMW, et al. The metabolic response of human trophoblasts derived from term placentas to metformin. Diabetologia. 2023 Dec 5;66(12):2320–31.

434. Villena JA. New insights into PGC-1 coactivators: redefining their role in the regulation of mitochondrial function and beyond. FEBS J. 2015 Feb 12;282(4):647–72.

435. Aye ILMH, Aiken CE, Charnock-Jones DS, Smith GCS. Placental energy metabolism in health and disease—significance of development and implications for preeclampsia. Am J Obstet Gynecol. 2022 Feb;226(2):S928–44.

436. Priya G, Kalra S. Metformin in the management of diabetes during pregnancy and lactation. Drugs Context. 2018 Jun 15;7:1–21.

437. Longo N, Frigeni M, Pasquali M. Carnitine transport and fatty acid oxidation. Biochimica et Biophysica Acta (BBA) - Molecular Cell Research. 2016 Oct;1863(10):2422–35.

438. Sidossis LS, Wolfe RR. Glucose and insulin-induced inhibition of fatty acid oxidation: the glucose-fatty acid cycle reversed. American Journal of Physiology-Endocrinology and Metabolism. 1996 Apr 1;270(4):E733–8.

439. Frayn KN. The glucose–fatty acid cycle: a physiological perspective. Biochem Soc Trans. 2003 Dec 1;31(6):1115–9.

440. Estrella J, Wiley V, Simmons D, Hng TM, McLean M. Effect of Maternal Metformin Treatment in Pregnancy on Neonatal Metabolism: Evidence From Newborn Metabolic Screening. Diabetes Care. 2021 Nov 1;44(11):2536–41.

441. Manta-Vogli PD, Schulpis KH, Loukas YL, Dotsikas Y. Quantitation and evaluation of perinatal medium-chain and long-chain acylcarnitine blood concentrations in 12,000 full-term breastfed newborns. Journal of Pediatric Endocrinology and Metabolism. 2021 Aug 26;34(8):1023–30.

442. Robitaille J, Grant AM. The genetics of gestational diabetes mellitus: evidence for relationship with type 2 diabetes mellitus. Genetics in Medicine. 2008 Apr;10(4):240–50.

443. Hemauer SJ, Patrikeeva SL, Nanovskaya TN, Hankins GDV, Ahmed MS. Role of human placental apical membrane transporters in the efflux of glyburide, rosiglitazone, and metformin. Am J Obstet Gynecol. 2010 Apr;202(4):383.e1-383.e7.

444. Fuentes P, Sesé M, Guijarro PJ, Emperador M, Sánchez-Redondo S, Peinado H, et al. ITGB3-mediated uptake of small extracellular vesicles facilitates intercellular communication in breast cancer cells. Nat Commun. 2020 Aug 26;11(1):4261.

445. Nguyen SL, Ahn SH, Greenberg JW, Collaer BW, Agnew DW, Arora R, et al. Integrins mediate placental extracellular vesicle trafficking to lung and liver in vivo. Sci Rep. 2021 Feb 18;11(1):4217.

446. Malassine A, Frendo JL, Evain-Brion D. A comparison of placental development and endocrine functions between the human and mouse model. Hum Reprod Update. 2003 Nov 1;9(6):531–9.

447. Schmidt A, Morales-Prieto DM, Pastuschek J, Fröhlich K, Markert UR. Only humans have human placentas: molecular differences between mice and humans. J Reprod Immunol. 2015 Apr;108:65–71.

448. Panja S, Paria BC. Development of the Mouse Placenta. In 2021. p. 205–21.

449. Clark DA. The use and misuse of animal analog models of human pregnancy disorders. J Reprod Immunol. 2014 Jun;103:1–8.

450. Damhuis SE, Ganzevoort W, Gordijn SJ. Abnormal Fetal Growth. Obstet Gynecol Clin North Am. 2021 Jun;48(2):267–79.

451. Yin FC, Spurgeon HA, Rakusan K, Weisfeldt ML, Lakatta EG. Use of tibial length to quantify cardiac hypertrophy: application in the aging rat. American Journal of Physiology-Heart and Circulatory Physiology. 1982 Dec 1;243(6):H941–7.

452. Szabo AndrewJ, Szabo O. PLACENTAL FREE-FATTY-ACID TRANSFER AND FETAL ADIPOSE-TISSUE DEVELOPMENT: AN EXPLANATION OF FETAL ADIPOSITY IN INFANTS OF DIABETIC MOTHERS. The Lancet. 1974 Aug;304(7879):498–9.

453. Hu B, Cheng JW, Hu JW, Li H, Ma XL, Tang WG, et al. KPNA3 Confers Sorafenib Resistance to Advanced Hepatocellular Carcinoma via TWIST Regulated Epithelial-Mesenchymal Transition. J Cancer. 2019;10(17):3914–25.

454. Kim JH, Ham S, Lee Y, Suh GY, Lee YS. TTC3 contributes to TGF-β1-induced epithelial−mesenchymal transition and myofibroblast differentiation, potentially through SMURF2 ubiquitylation and degradation. Cell Death Dis. 2019 Jan 29;10(2):92.

455. Sandovici I, Georgopoulou A, Pérez-García V, Hufnagel A, López-Tello J, Lam BYH, et al. The imprinted Igf2-Igf2r axis is critical for matching placental microvasculature expansion to fetal growth. Dev Cell. 2022 Jan;57(1):63-79.e8.

456. Sah N, Stenhouse C, Halloran KM, Moses RM, Seo H, Burghardt RC, et al. Creatine metabolism at the uterine–conceptus interface during early gestation in sheep. Biol Reprod. 2022 Dec 10;107(6):1528–39.

457. Shu C, Han S, Hu C, Chen C, Qu B, He J, et al. Integrin β1 regulates proliferation, apoptosis, and migration of trophoblasts through activation of phosphoinositide 3 kinase/protein kinase B signaling. Journal of Obstetrics and Gynaecology Research. 2021 Jul 11;47(7):2406–16.

458. Zou AX, Chen B, Li QX, Liang YC. MiR-134 inhibits infiltration of trophoblast cells in placenta of patients with preeclampsia by decreasing ITGB1 expression. Eur Rev Med Pharmacol Sci. 2018 Apr;22(8):2199–206.

459. Matveeva NA, Baulina NM, Kiselev IS, Titov B V., Favorova OO. MiRNA miR-375 as a Multifunctional Regulator of the Cardiovascular System. Mol Biol. 2022 Jun 3;56(3):363–71.

460. Yan JY, Wang XJ. [Expression and significance of adipocyte fatty acid-binding protein in placenta, serum and umbilical cord blood in preeclampsia]. Zhonghua Fu Chan Ke Za Zhi. 2010 Dec;45(12):885-90.

461. Paule SG, Airey LM, Li Y, Stephens AN, Nie G. Proteomic Approach Identifies Alterations in Cytoskeletal Remodelling Proteins during Decidualization of Human Endometrial Stromal Cells. J Proteome Res. 2010 Nov 5;9(11):5739–47.

462. Tang H, Pan L, Tang L, Liu J. Alpha-enolase 1 knockdown facilitates the proliferation and invasion of villous trophoblasts by upregulating <scp>COX</scp> -2. Mol Genet Genomic Med. 2023 Sep 8;11(9).

463. Zhou Y, Fisher SJ, Janatpour M, Genbacev O, Dejana E, Wheelock M, et al. Human cytotrophoblasts adopt a vascular phenotype as they differentiate. A strategy for successful endovascular invasion? Journal of Clinical Investigation. 1997 May 1;99(9):2139–51.

464. Delhaes F, Giza SA, Koreman T, Eastabrook G, McKenzie CA, Bedell S, et al. Altered maternal and placental lipid metabolism and fetal fat development in obesity: Current knowledge and advances in non-invasive assessment. Placenta. 2018 Sep;69:118–24.

465. Al Shoyaib A, Archie SR, Karamyan VT. Intraperitoneal Route of Drug Administration: Should it Be Used in Experimental Animal Studies? Pharm Res. 2020 Jan 23;37(1):12.

466. Sun CY, She XM, Qin Y, Chu ZB, Chen L, Ai LS, et al. miR-15a and miR-16 affect the angiogenesis of multiple myeloma by targeting VEGF. Carcinogenesis. 2013 Feb;34(2):426–35.

467. Amodio N, Leotta M, Bellizzi D, Di Martino MT, D'Aquila P, Lionetti M, et al. DNA-demethylating and anti-tumor activity of synthetic miR-29b mimics in multiple myeloma. Oncotarget. 2012 Oct 31;3(10):1246–58.

468. Kojima Y, Tam OH, Tam PPL. Timing of developmental events in the early mouse embryo. Semin Cell Dev Biol. 2014 Oct;34:65–75.

469. Qu F, Li W, Xu J, Zhang R, Ke J, Ren X, et al. Three-dimensional molecular architecture of mouse organogenesis. Nat Commun. 2023 Jul 31;14(1):4599.

470. Gilron S, Gabbay-Benziv R, Khoury R. Same disease - different effect: maternal diabetes impact on birth weight stratified by fetal sex. Arch Gynecol Obstet. 2023 Mar 1;

471. Ricart W, Lopez J, Mozas J, Pericot A, Sancho MA, Gonzalez N, et al. Maternal glucose tolerance status influences the risk of macrosomia in male but not in female fetuses. J Epidemiol Community Health (1978). 2009 Jan 1;63(1):64–8.

472. Dearden L, Bouret SG, Ozanne SE. Sex and gender differences in developmental programming of metabolism. Mol Metab. 2018 Sep;15:8–19.

473. Christians JK, Grynspan D, Greenwood SL, Dilworth MR. The problem with using the birthweight:placental weight ratio as a measure of placental efficiency. Placenta. 2018 Aug;68:52–8.

474. Du Q, Sompolinsky Y, Walfisch A, Zhong H, Liu Y, Feng W. The Sex Specific Association Between Maternal Gestational Diabetes and Offspring Metabolic Status at 1 Year of Age. Front Endocrinol (Lausanne). 2021 Feb 9;11.

475. Hayward CE, Lean S, Sibley CP, Jones RL, Wareing M, Greenwood SL, et al. Placental Adaptation: What Can We Learn from Birthweight:Placental Weight Ratio? Front Physiol. 2016 Feb 5;7.

476. Meakin AS, Cuffe JSM, Darby JRT, Morrison JL, Clifton VL. Let's Talk about Placental Sex, Baby: Understanding Mechanisms That Drive Female- and Male-Specific Fetal Growth and Developmental Outcomes. Int J Mol Sci. 2021 Jun 15;22(12):6386.

477. Angiolini E, Coan PM, Sandovici I, Iwajomo OH, Peck G, Burton GJ, et al. Developmental adaptations to increased fetal nutrient demand in mouse genetic models of Igf2-mediated overgrowth. The FASEB Journal. 2011 May 31;25(5):1737–45.

478. Constância M, Hemberger M, Hughes J, Dean W, Ferguson-Smith A, Fundele R, et al. Placental-specific IGF-II is a major modulator of placental and fetal growth. Nature. 2002 Jun;417(6892):945–8.

479. Murphy VE, Smith R, Giles WB, Clifton VL. Endocrine Regulation of Human Fetal Growth: The Role of the Mother, Placenta, and Fetus. Endocr Rev. 2006 Apr 1;27(2):141–69.

480. Gibson KS, Waters TP, Catalano PM. Maternal Weight Gain in Women Who Develop Gestational Diabetes Mellitus. Obstetrics & Gynecology. 2012 Mar;119(3):560–5.

481. MacLaughlin SM, Walker SK, Roberts CT, Kleemann DO, McMillen IC. Periconceptional nutrition and the relationship between maternal body weight changes in the periconceptional period and feto-placental growth in the sheep. J Physiol. 2005 May 11;565(1):111–24.

482. Li X. miR-375, a microRNA related to diabetes. Gene. 2014 Jan;533(1):1–4.

483. Poy MN, Eliasson L, Krutzfeldt J, Kuwajima S, Ma X, MacDonald PE, et al. A pancreatic islet-specific microRNA regulates insulin secretion. Nature. 2004 Nov;432(7014):226–30.

484. El Ouaamari A, Baroukh N, Martens GA, Lebrun P, Pipeleers D, van Obberghen E. miR-375 Targets 3′-Phosphoinositide–Dependent Protein Kinase-1 and Regulates Glucose-Induced Biological Responses in Pancreatic β-Cells. Diabetes. 2008 Oct 1;57(10):2708–17.

485. Barbour LA, McCurdy CE, Hernandez TL, Kirwan JP, Catalano PM, Friedman JE. Cellular Mechanisms for Insulin Resistance in Normal Pregnancy and Gestational Diabetes. Diabetes Care. 2007 Jul 1;30(Supplement_2):S112–9.

486. Myers MG, Cowley MA, Münzberg H. Mechanisms of Leptin Action and Leptin Resistance. Annu Rev Physiol. 2008 Mar 1;70(1):537–56.

487. Lei L, Zhou C, Yang X, Li L. Down-regulation of micro-RNA-375 regulates adipokines and inhibits inflammatory cytokines by targeting AdipoR2 in non-alcoholic fatty liver disease. Clin Exp Pharmacol Physiol. 2018 Aug 30;45(8):819–31.

488. Boden G. Free Fatty Acids, Insulin Resistance, and Type 2 Diabetes Mellitus. Proc Assoc Am Physicians. 1999 May 9;111(3):241–8.

489. Verma N, Srodulski S, Velmurugan S, Hoskins A, Pandey VK, Despa F, et al. Gestational diabetes triggers postpartum cardiac hypertrophy via activation of calcineurin/NFAT signaling. Sci Rep. 2021 Oct 22;11(1):20926.

490. Lyall F, Bulmer JN, Duffie E, Cousins F, Theriault A, Robson SC. Human Trophoblast Invasion and Spiral Artery Transformation. Am J Pathol. 2001 May;158(5):1713–21.

491. Mebane S, Zhou J, Choi S, Schust DJ. Immune Checkpoint Molecules and Maternal–Fetal Immunity. Curr Obstet Gynecol Rep. 2024 Feb 11;13(1):37–45.

492. E. Davies J, Pollheimer J, Yong HEJ, Kokkinos MI, Kalionis B, Knöfler M, et al. Epithelial-mesenchymal transition during extravillous trophoblast differentiation. Cell Adh Migr. 2016 May 3;10(3):310–21.

493. Kokkinos MI, Murthi P, Wafai R, Thompson EW, Newgreen DF. Cadherins in the human placenta – epithelial–mesenchymal transition (EMT) and placental development. Placenta. 2010 Sep;31(9):747–55.

494. Stenhouse C, Hogg CO, Ashworth CJ. Association of foetal size and sex with porcine foeto-maternal interface integrin expression. Reproduction. 2019 Apr;157(4):317–28.

495. Ellery SJ, Della Gatta PA, Bruce CR, Kowalski GM, Davies-Tuck M, Mockler JC, et al. Creatine biosynthesis and transport by the term human placenta. Placenta. 2017 Apr;52:86–93.

496. Ellery SJ, Murthi P, Davies-Tuck ML, Della Gatta PA, May AK, Kowalski GM, et al. Placental creatine metabolism in cases of placental insufficiency and reduced fetal growth. Mol Hum Reprod. 2019 Aug 1;25(8):495–505.

497. Harris LK, Pantham P, Yong HEJ, Pratt A, Borg AJ, Crocker I, et al. The role of insulin-like growth factor 2 receptor-mediated homeobox gene expression in human placental apoptosis, and its implications in idiopathic fetal growth restriction. Mol Hum Reprod. 2019 Sep 1;25(9):572–85.

498. Biesiada L, Sakowicz A, Grzesiak M, Borowiec M, Lisowska M, Pietrucha T, et al. Identification of placental genes linked to selective intrauterine growth restriction (IUGR) in dichorionic twin pregnancies: gene expression profiling study. Hum Genet. 2019 Jun 30;138(6):649–59.

499. M.N N, J K, S.R S, Raavi V. Alteration in the levels of IGF-axis components in small for gestational age neonates. Gene Rep. 2024 Jun;35:101891.

500. Tilley RE, McNeil CJ, Ashworth CJ, Page KR, McArdle HJ. Altered muscle development and expression of the insulin-like growth factor system in growth retarded fetal pigs. Domest Anim Endocrinol. 2007 Apr;32(3):167–77.

501. Alekseenkova EN, Selkov SA, Kapustin R V. Fetal growth regulation via insulin-like growth factor axis in normal and diabetic pregnancy. J Perinat Med. 2022 Sep 27;50(7):947–60.

502. Porter AC, Gumina DL, Armstrong M, Maclean KN, Reisdorph N, Galan HL, et al. Maternal Amino Acid Profiles to Distinguish Constitutionally Small versus Growth-Restricted Fetuses Defined by Doppler Ultrasound: A Pilot Study. Am J Perinatol. 2020 Sep 2;37(11):1084–93.

503. Tanianskii DA, Jarzebska N, Birkenfeld AL, O'Sullivan JF, Rodionov RN. Beta-Aminoisobutyric Acid as a Novel Regulator of Carbohydrate and Lipid Metabolism. Nutrients. 2019 Feb 28;11(3):524.

504. Audzeyenka I, Szrejder M, Rogacka D, Angielski S, Saleem MA, Piwkowska A. β-Aminoisobutyric acid (L-BAIBA) is a novel regulator of mitochondrial biogenesis and respiratory function in human podocytes. Sci Rep. 2023 Jan 14;13(1):766.

505. Katano S, Yano T, Kouzu H, Nagaoka R, Numazawa R, Yamano K, et al. Circulating level of β-aminoisobutyric acid (BAIBA), a novel myokine-like molecule, is inversely associated with fat mass in patients with heart failure. Heart Vessels. 2024 Jan 3;39(1):35–47.

506. Katano S, Yano T, Kouzu H, Nagaoka R, Numazawa R, Yamano K, et al. Elevated circulating level of β-aminoisobutyric acid (BAIBA) in heart failure patients with type 2 diabetes receiving sodium-glucose cotransporter 2 inhibitors. Cardiovasc Diabetol. 2022 Dec 20;21(1):285.

507. Minato T, Nakamura N, Saiki T, Miyabe M, Ito M, Matsubara T, et al. β-Aminoisobutyric acid, L-BAIBA, protects PC12 cells from hydrogen peroxide-induced oxidative stress and apoptosis via activation of the AMPK and PI3K/Akt pathway. IBRO Neurosci Rep. 2022 Jun;12:65–72.

508. Roberts LD, Boström P, O'Sullivan JF, Schinzel RT, Lewis GD, Dejam A, et al. β-Aminoisobutyric Acid Induces Browning of White Fat and Hepatic β-Oxidation and Is Inversely Correlated with Cardiometabolic Risk Factors. Cell Metab. 2014 Jan;19(1):96–108.

509. Friesen RW, Novak EM, Hasman D, Innis SM. Relationship of Dimethylglycine, Choline, and Betaine with Oxoproline in Plasma of Pregnant Women and Their Newborn Infants ,. J Nutr. 2007 Dec;137(12):2641–6.

510. Maitre L, Villanueva CM, Lewis MR, Ibarluzea J, Santa-Marina L, Vrijheid M, et al. Maternal urinary metabolic signatures of fetal growth and associated clinical and environmental factors in the INMA study. BMC Med. 2016 Dec 4;14(1):177.

511. Schupper A, Almashanu S, Coster D, Keidar R, Betser M, Sagiv N, et al. Metabolic biomarkers of small and large for gestational age newborns. Early Hum Dev. 2021 Sep;160:105422.

512. Jackson AA, Persaud C, Werkmeister G, McClelland ISM, Badaloo A, Forrester T. Comparison of urinary 5-L-oxoproline (L-pyroglutamate) during normal pregnancy in women in England and Jamaica. British Journal of Nutrition. 1997 Feb 9;77(2):183–96.

513. van der Pol A, Gil A, Silljé HHW, Tromp J, Ovchinnikova ES, Vreeswijk-Baudoin I, et al. Accumulation of 5-oxoproline in myocardial dysfunction and the protective effects of OPLAH. Sci Transl Med. 2017 Nov 8;9(415).

514. Fantasia I, Bussolaro S, Stampalija T, Rolnik DL. The role of melatonin in pregnancies complicated by placental insufficiency: A systematic review. European Journal of Obstetrics & Gynecology and Reproductive Biology. 2022 Nov;278:22–8.

515. Reiter RJ, Tan DX, Korkmaz A, Rosales-Corral SA. Melatonin and stable circadian rhythms optimize maternal, placental and fetal physiology. Hum Reprod Update. 2014 Mar 1;20(2):293–307.

516. de Almeida Chuffa LG, Lupi LA, Cucielo MS, Silveira HS, Reiter RJ, Seiva FRF. Melatonin Promotes Uterine and Placental Health: Potential Molecular Mechanisms. Int J Mol Sci. 2019 Dec 31;21(1):300.

517. Berbets AM, Davydenko IS, Barbe AM, Konkov DH, Albota OM, Yuzko OM. Melatonin 1A and 1B Receptors' Expression Decreases in the Placenta of Women with Fetal Growth Restriction. Reproductive Sciences. 2021 Jan 17;28(1):197–206.

518. Richter HG, Hansell JA, Raut S, Giussani DA. Melatonin improves placental efficiency and birth weight and increases the placental expression of antioxidant enzymes in undernourished pregnancy. J Pineal Res. 2009 May 9;46(4):357–64.

519. Nagai R, Watanabe K, Wakatsuki A, Hamada F, Shinohara K, Hayashi Y, et al. Melatonin preserves fetal growth in rats by protecting against ischemia/reperfusion-induced oxidative/nitrosative mitochondrial damage in the placenta. J Pineal Res. 2008 Oct 12;45(3):271–6.

520. Reiter RJ, Tan DX, Tamura H, Cruz MHC, Fuentes-Broto L. Clinical relevance of melatonin in ovarian and placental physiology: a review. Gynecological Endocrinology. 2014 Feb 9;30(2):83–9.

521. Iwasaki S, Nakazawa K, Sakai J, Kometani K, Iwashita M, Yoshimura Y, et al. Melatonin as a local regulator of human placental function. J Pineal Res. 2005 Oct 23;39(3):261–5.

522. Shukla P, Lemley CO, Dubey N, Meyer AM, O'Rourke ST, Vonnahme KA. Effect of maternal nutrient restriction and melatonin supplementation from mid to late gestation on vascular reactivity of maternal and fetal placental arteries. Placenta. 2014 Jul;35(7):461–6.

523. Pinto GDA, Murgia A, Lai C, Ferreira CS, Goes VA, Guimarães D de AB, et al. Sphingolipids and acylcarnitines are altered in placentas from women with gestational diabetes mellitus. British Journal of Nutrition. 2023 Sep 28;130(6):921–32.

524. Faulk WP, Jarret R, Keane M, Johnson PM, Boackle RJ. Immunological studies of human placentae: complement components in immature and mature chorionic villi. Clin Exp Immunol. 1980 May;40(2):299–305.

525. Bulla R, Bossi F, Agostinis C, Radillo O, Colombo F, De Seta F, et al. Complement production by trophoblast cells at the feto-maternal interface. J Reprod Immunol. 2009 Nov;82(2):119–25.

526. Saoi M, Kennedy KM, Gohir W, Sloboda DM, Britz-McKibbin P. Placental Metabolomics for Assessment of Sex-specific Differences in Fetal Development During Normal Gestation. Sci Rep. 2020 Jun 10;10(1):9399.

527. Sánchez-Pintos P, de Castro MJ, Roca I, Rite S, López M, Couce ML. Similarities between acylcarnitine profiles in large for gestational age newborns and obesity. Sci Rep. 2017 Nov 24;7(1):16267.

528. van Zundert SKM, van Egmond NCM, van Rossem L, Willemsen SP, Griffioen PH, van Schaik RHN, et al. First trimester maternal tryptophan metabolism and embryonic and fetal growth: the Rotterdam Periconceptional Cohort (Predict Study). Human Reproduction. 2024 May 2;39(5):912–22.

529. Magnusson AL, Waterman IJ, Wennergren M, Jansson T, Powell TL. Triglyceride Hydrolase Activities and Expression of Fatty Acid Binding Proteins in the Human Placenta in Pregnancies Complicated by Intrauterine Growth Restriction and Diabetes. J Clin Endocrinol Metab. 2004 Sep;89(9):4607–14.

530. Steinhauser CB, Askelson K, Lambo CA, Hobbs KC, Bazer FW, Satterfield MC. Lipid metabolism is altered in maternal, placental, and fetal tissues of ewes with small for gestational age fetuses†. Biol Reprod. 2021 Jan 4;104(1):170–80.

531. Visiedo F, Bugatto F, Sánchez V, Cózar-Castellano I, Bartha JL, Perdomo G. High glucose levels reduce fatty acid oxidation and increase triglyceride accumulation in human placenta. American Journal of Physiology-Endocrinology and Metabolism. 2013 Jul 15;305(2):E205–12.

532. Hulme CH, Nicolaou A, Murphy SA, Heazell AEP, Myers JE, Westwood M. The effect of high glucose on lipid metabolism in the human placenta. Sci Rep. 2019 Oct 1;9(1):14114.

533. Lindegaard MLS, Damm P, Mathiesen ER, Nielsen LB. Placental triglyceride accumulation in maternal type 1 diabetes is associated with increased lipase gene expression. J Lipid Res. 2006 Nov;47(11):2581–8.

534. Balachandiran M, Bobby Z, Dorairajan G, Jacob SE, Gladwin V, Vinayagam V, et al. Placental Accumulation of Triacylglycerols in Gestational Diabetes Mellitus and Its Association with Altered Fetal Growth are Related to the Differential Expressions of Proteins of Lipid Metabolism. Experimental and Clinical Endocrinology & Diabetes. 2021 Nov 22;129(11):803–12.

535. Segura MT, Demmelmair H, Krauss-Etschmann S, Nathan P, Dehmel S, Padilla MC, et al. Maternal BMI and gestational diabetes alter placental lipid transporters and fatty acid composition. Placenta. 2017 Sep;57:144–51.

536. Araújo JR, Correia-Branco A, Ramalho C, Keating E, Martel F. Gestational diabetes mellitus decreases placental uptake of long-chain polyunsaturated fatty acids: involvement of long-chain acyl-CoA synthetase. J Nutr Biochem. 2013 Oct;24(10):1741–50.

537. Duttaroy AK, Basak S. Maternal Fatty Acid Metabolism in Pregnancy and Its Consequences in the Feto-Placental Development. Front Physiol. 2022 Jan 20;12.

538. Ciborowski M, Zbucka-Kretowska M, Bomba-Opon D, Wielgos M, Brawura-Biskupski-Samaha R, Pierzynski P, et al. Potential first trimester metabolomic biomarkers of abnormal birth weight in healthy pregnancies. Prenat Diagn. 2014 Sep;34(9):870–7.

539. Hirschmugl B, Perazzolo S, Sengers BG, Lewis RM, Gruber M, Desoye G, et al. Placental mobilization of free fatty acids contributes to altered materno-fetal transfer in obesity. Int J Obes. 2021 May 26;45(5):1114–23.

540. Salbaum JM, Kruger C, Zhang X, Delahaye NA, Pavlinkova G, Burk DH, et al. Altered gene expression and spongiotrophoblast differentiation in placenta from a mouse model of diabetes in pregnancy. Diabetologia. 2011 Jul 14;54(7):1909–20.

541. Latreille M, Herrmanns K, Renwick N, Tuschl T, Malecki MT, McCarthy MI, et al. miR-375 gene dosage in pancreatic β-cells: implications for regulation of β-cell mass and biomarker development. J Mol Med. 2015 Oct 28;93(10):1159–69.

542. KALIVARATHAN J, SARAVANAN PB, LEVY MF, KANAK MA. 2102-P: Regulation of Alpha-Cell Function by Beta-Cell Extracellular Vesicles. Diabetes. 2020 Jun 1;69(Supplement_1).

543. Sun Y, Mao Q, Shen C, Wang C, Jia W. Exosomes from β-cells alleviated hyperglycemia and enhanced angiogenesis in islets of streptozotocin-induced diabetic mice . Diabetes Metab Syndr Obes. 2019 Oct;Volume 12:2053–64.

544. Reiher H, Fuhrmann K, Noack S, Woltanski KP, Jutzi E, Dorsche HH v, et al. Age-dependent Insulin Secretion of the Endocrine Pancreas In Vitro from Fetuses of Diabetic and Nondiabetic Patients. Diabetes Care. 1983 Sep 1;6(5):446–51.

545. Casu A, Nunez Lopez YO, Yu G, Clifford C, Bilal A, Petrilli AM, et al. The proteome and phosphoproteome of circulating extracellular vesicle-enriched preparations are associated with characteristic clinical features in type 1 diabetes. Front Endocrinol (Lausanne). 2023 Jul 28;14.

546. Pardo F, Villalobos-Labra R, Sobrevia B, Toledo F, Sobrevia L. Extracellular vesicles in obesity and diabetes mellitus. Mol Aspects Med. 2018 Apr;60:81–91.

547. Wei J, Wang Z, Han T, Chen J, Ou Y, Wei L, et al. Extracellular vesicle-mediated intercellular and interorgan crosstalk of pancreatic islet in health and diabetes. Front Endocrinol (Lausanne). 2023 May 25;14.

548. Nair S, Salomon C. Extracellular vesicles as critical mediators of maternal-fetal communication during pregnancy and their potential role in maternal metabolism. Placenta. 2020 Sep;98:60–8.

549. Shibata C, Otsuka M, Seimiya T, Ishigaki K, Miyakawa Y, Kishikawa T, et al. Smaller extracellular vesicles are released from pancreatic cancer cells by the alteration of the lipid composition under low glucose conditions. Biochem Biophys Res Commun. 2022 Dec;637:314–21.

550. Dumortier O, Hinault C, Gautier N, Patouraux S, Casamento V, Van Obberghen E. Maternal Protein Restriction Leads to Pancreatic Failure in Offspring: Role of Misexpressed MicroRNA-375. Diabetes. 2014 Oct 1;63(10):3416–27.

551. Joglekar M V., Joglekar VM, Hardikar AA. Expression of islet-specific microRNAs during human pancreatic development. Gene Expression Patterns. 2009 Feb;9(2):109–13.

552. WANG L, SONG G, LIU M, CHEN B, CHEN Y, SHEN Y, et al. MicroRNA-375 overexpression influences P19 cell proliferation, apoptosis and differentiation through the Notch signaling pathway. Int J Mol Med. 2016 Jan;37(1):47–55.

553. Zhuang S, Fu Y, Li J, Li M, Hu X, Zhu J, et al. MicroRNA-375 overexpression disrupts cardiac development of Zebrafish (Danio rerio) by targeting notch2. Protoplasma. 2020 Sep 28;257(5):1309–18.

554. Ornoy A, Becker M, Weinstein-Fudim L, Ergaz Z. Diabetes during Pregnancy: A Maternal Disease Complicating the Course of Pregnancy with Long-Term Deleterious Effects on the Offspring. A Clinical Review. Int J Mol Sci. 2021 Mar 15;22(6):2965.

555. Dumortier O, Fabris G, Pisani DF, Casamento V, Gautier N, Hinault C, et al. microRNA-375 regulates glucose metabolism-related signaling for insulin secretion. Journal of Endocrinology. 2020 Jan;244(1):189–200.

556. James-Allan LB, Rosario FJ, Barner K, Lai A, Guanzon D, McIntyre HD, et al. Regulation of glucose homeostasis by small extracellular vesicles in normal pregnancy and in gestational diabetes. The FASEB Journal. 2020 Apr 10;34(4):5724–39.

557. Kang M, Blenkiron C, Chamley LW. The biodistribution of placental and fetal extracellular vesicles during pregnancy following placentation. Clin Sci. 2023 Mar 15;137(5):385–99.

558. Salomon C, Torres MJ, Kobayashi M, Scholz-Romero K, Sobrevia L, Dobierzewska A, et al. A Gestational Profile of Placental Exosomes in Maternal Plasma and Their Effects on Endothelial Cell Migration. PLoS One. 2014 Jun 6;9(6):e98667.

559. Galjaard S, Ameye L, Lees CC, Pexsters A, Bourne T, Timmerman D, et al. Sex differences in fetal growth and immediate birth outcomes in a low-risk Caucasian population. Biol Sex Differ. 2019 Dec 9;10(1):48.

560. McCance DR. Diabetes in pregnancy. Best Pract Res Clin Obstet Gynaecol. 2015 Jul;29(5):685–99.

561. DiPietro JA, Voegtline KM. The gestational foundation of sex differences in development and vulnerability. Neuroscience. 2017 Feb;342:4–20.

562. Siemers KM, Baack ML. The importance of placental lipid metabolism across gestation in obese and non-obese pregnancies. Clin Sci. 2023 Jan 13;137(1):31–4.

563. Rosenfeld CS. Placental serotonin signaling, pregnancy outcomes, and regulation of fetal brain development†. Biol Reprod. 2020 Mar 13;102(3):532–8.

564. Tong M, Kleffmann T, Pradhan S, Johansson CL, DeSousa J, Stone PR, et al. Proteomic characterization of macro-, micro- and nano-extracellular vesicles derived from the same first trimester placenta: relevance for feto-maternal communication. Human Reproduction. 2016 Apr;31(4):687–99.

565. Klemetti MM, Pettersson AB V., Ahmad Khan A, Ermini L, Porter TR, Litvack ML, et al. Lipid profile of circulating placental extracellular vesicles during pregnancy identifies foetal growth restriction risk. J Extracell Vesicles. 2024 Feb 14;13(2).

566. Foley HB, Howe CG, Eckel SP, Chavez T, Gevorkian L, Reyes EG, et al. Extracellular vesicle-enriched miRNA profiles across pregnancy in the MADRES cohort. PLoS One. 2021 May 12;16(5):e0251259.

567. Retnakaran R, Ye C, Hanley AJ, Connelly PW, Sermer M, Zinman B, et al. Treating Gestational Diabetes Reduces Birth Weight but Does Not Affect Infant Adiposity Across the 1st Year of Life. Diabetes Care. 2022 May 1;45(5):1230–8.

568. Eriksson JG, Kajantie E, Osmond C, Thornburg K, Barker DJP. Boys live dangerously in the womb. American Journal of Human Biology. 2010 May 7;22(3):330–5.

569. Cui Y, Cruz M, Palatnik A, Olivier-Van Stichelen S. O-GlcNAc transferase contributes to sex-specific placental deregulation in gestational diabetes. Placenta. 2023 Jan;131:1–12.

570. Retnakaran R, Kramer CK, Ye C, Kew S, Hanley AJ, Connelly PW, et al. Fetal Sex and Maternal Risk of Gestational Diabetes Mellitus: The Impact of Having a Boy. Diabetes Care. 2015 May 1;38(5):844–51.

571. Noren Hooten N, Byappanahalli AM, Vannoy M, Omoniyi V, Evans MK. Influences of age, race, and sex on extracellular vesicle characteristics. Theranostics. 2022;12(9):4459–76.

572. Kwan HY, Chen M, Xu K, Chen B. The impact of obesity on adipocyte-derived extracellular vesicles. Cellular and Molecular Life Sciences. 2021 Dec 22;78(23):7275–88.

573. Barnes MVC, Pantazi P, Holder B. Circulating extracellular vesicles in healthy and pathological pregnancies: A scoping review of methodology, rigour and results. J Extracell Vesicles. 2023 Nov 16;12(11).

574. Thamotharan S, Ghosh S, James-Allan L, Lei MYY, Janzen C, Devaskar SU. Circulating extracellular vesicles exhibit a differential miRNA profile in gestational diabetes mellitus pregnancies. PLoS One. 2022 May 25;17(5):e0267564.

575. Kennedy M, Cartland S, Saravanan P, Simpson N, Scott E, Forbes K. miR-1-3p and miR-133-3p are altered in maternal serum EVs and placenta in pregnancies complicated by gestational diabetes with large-for-gestational age babies. Endocrine Abstracts. 2019 Nov 6;

576. Yang Y, Pan Z, Guo F, Wang H, Long W, Wang H, et al. Placental metabolic profiling in gestational diabetes mellitus: An important role of fatty acids. J Clin Lab Anal. 2021 Dec 9;35(12).

577. Makkar A, Mishima T, Chang G, Scifres C, Sadovsky Y. Fatty Acid Binding Protein-4 is expressed in the mouse placental labyrinth, yet is dispensable for placental triglyceride accumulation and fetal growth. Placenta. 2014 Oct;35(10):802–7.

578. Ranzil S, Walker DW, Borg AJ, Wallace EM, Ebeling PR, Murthi P. The relationship between the placental serotonin pathway and fetal growth restriction. Biochimie. 2019 Jun;161:80–7.

579. Fields AM, Welle K, Ho ES, Mesaros C, Susiarjo M. Vitamin B6 deficiency disrupts serotonin signaling in pancreatic islets and induces gestational diabetes in mice. Commun Biol. 2021 Mar 26;4(1):421.

580. Sinzato YK, Volpato GT, Iessi IL, Bueno A, Calderon I de MP, Rudge MVC, et al. Neonatally Induced Mild Diabetes in Rats and Its Effect on Maternal, Placental, and Fetal Parameters. Exp Diabetes Res. 2012;2012:1–7.

581. Padmanabhan R, Shafiullah M. Intrauterine Growth Retardation in Experimental Diabetes: Possible Role of the Placenta. Arch Physiol Biochem. 2001 Jan 3;109(3):260–71.

582. Olmos-Ortiz A, Flores-Espinosa P, Díaz L, Velázquez P, Ramírez-Isarraraz C, Zaga-Clavellina V. Immunoendocrine Dysregulation during Gestational Diabetes Mellitus: The Central Role of the Placenta. Int J Mol Sci. 2021 Jul 28;22(15):8087.

583. Napso T, Zhao X, Lligoña MI, Sandovici I, Kay RG, George AL, et al. Placental secretome characterization identifies candidates for pregnancy complications. Commun Biol. 2021 Jun 8;4(1):701.

584. Schaefer-Graf UM, Meitzner K, Ortega-Senovilla H, Graf K, Vetter K, Abou-Dakn M, et al. Differences in the implications of maternal lipids on fetal metabolism and growth between gestational diabetes mellitus and control pregnancies. Diabetic Medicine. 2011 Sep 15;28(9):1053–9.

585. Barbour LA, Hernandez TL. Maternal Lipids and Fetal Overgrowth: Making Fat from Fat. Clin Ther. 2018 Oct;40(10):1638–47.

586. Hu Y, Lin Y, Yang J, Wang S, Gao L, Bi Y, et al. Mitochondrial dysfunction and oxidative stress in selective fetal growth restriction. Placenta. 2024 Oct;156:46–54.

587. Shuoning Song, Yong Fu, Yingyue Dong et al. Fetal Sex, Glucose and Lipid Metabolism, and Perinatal Outcomes in Gestational Diabetes Mellitus: A Retrospective Cohort Study, 08 August 2024, PREPRINT (Version 1).

588. Yang B, Lin H, Xiao J, Lu Y, Luo X, Li B, et al. The muscle-specific microRNA miR-1 regulates cardiac arrhythmogenic potential by targeting GJA1 and KCNJ2. Nat Med. 2007 Apr 1;13(4):486–91.

589. Li M, Chen X, Chen L, Chen K, Zhou J, Song J. MiR-1-3p that correlates with left ventricular function of HCM can serve as a potential target and differentiate HCM from DCM. J Transl Med. 2018 Dec 9;16(1):161.

590. Li Y, He X, Li Q, Lai H, Zhang H, Hu Z, et al. EV-origin: Enumerating the tissue-cellular origin of circulating extracellular vesicles using exLR profile. Comput Struct Biotechnol J. 2020;18:2851–9.

591. Cao Y, Jia Y, Xing B, Shi D, Dong X. Plasma microRNA-16-5p, -17-5p and -20a-5p: Novel diagnostic biomarkers for gestational diabetes mellitus. Journal of Obstetrics and Gynaecology Research. 2017 Jun 16;43(6):974–81.

592. Simmons D, Immanuel J, Hague WM, Teede H, Nolan CJ, Peek MJ, et al. Treatment of Gestational Diabetes Mellitus Diagnosed Early in Pregnancy. New England Journal of Medicine. 2023 Jun 8;388(23):2132–44.

593. Behboudi-Gandevani S, Amiri M, Bidhendi Yarandi R, Ramezani Tehrani F. The impact of diagnostic criteria for gestational diabetes on its prevalence: a systematic review and meta-analysis. Diabetol Metab Syndr. 2019 Dec 1;11(1):11.

594. Guarino E, Delli Poggi C, Grieco GE, Cenci V, Ceccarelli E, Crisci I, et al. Circulating MicroRNAs as Biomarkers of Gestational Diabetes Mellitus: Updates and Perspectives. Int J Endocrinol. 2018;2018:1–11.

595. Zhu Y, Tian F, Li H, Zhou Y, Lu J, Ge Q. Profiling maternal plasma microRNA expression in early pregnancy to predict gestational diabetes mellitus. International Journal of Gynecology & Obstetrics. 2015 Jul 23;130(1):49–53.

596. Dunne F, Newman C, Alvarez-Iglesias A, Ferguson J, Smyth A, Browne M, et al. Early Metformin in Gestational Diabetes. JAMA. 2023 Oct 24;330(16):1547.

597. Bolte E, Dean T, Garcia B, Seferovic MD, Sauter K, Hummel G, et al. Initiation of metformin in early pregnancy results in fetal bioaccumulation, growth restriction, and renal dysmorphology in a primate model. Am J Obstet Gynecol. 2024 Sep;231(3):352.e1-352.e16.

598. Cantacorps L, Zhu J, Yagoub S, Coull BM, Falck J, Chesters RA, et al. Developmental metformin exposure does not rescue physiological impairments derived from early exposure to altered maternal metabolic state in offspring mice. Mol Metab. 2024 Jan;79:101860.

599. Pinto-Hernández P, Tomás-Zapico C, Iglesias-Gutiérrez E. Circulating microRNAs as modifiable diagnostic biomarkers of gestational and transgenerational metabolic risk: can exercise play a role? Noncoding RNA Investig. 2019 Aug;3:23–23.

600. Ye F, Lu X, van Neck R, Jones DL, Feng Q. Novel circRNA-miRNA-mRNA networks regulated by maternal exercise in fetal hearts of pregestational diabetes. Life Sci. 2023 Feb;314:121308.

601. Stevanović-Silva J, Beleza J, Coxito P, Rocha H, Gaspar TB, Gärtner F, et al. Exercise performed during pregnancy positively modulates liver metabolism and promotes mitochondrial biogenesis of female offspring in a rat model of diet-induced gestational diabetes. Biochimica et Biophysica Acta (BBA) - Molecular Basis of Disease. 2022 Nov;1868(11):166526.

602. Godoy PM, Barczak AJ, DeHoff P, Srinivasan S, Etheridge A, Galas D, et al. Comparison of Reproducibility, Accuracy, Sensitivity, and Specificity of miRNA Quantification Platforms. Cell Rep. 2019 Dec;29(12):4212-4222.e5.

603. Bertoia ML, Bertrand KA, Sawyer SJ, Rimm EB, Mukamal KJ. Reproducibility of Circulating MicroRNAs in Stored Plasma Samples. PLoS One. 2015 Aug 27;10(8):e0136665.

604. Mraz M, Malinova K, Mayer J, Pospisilova S. MicroRNA isolation and stability in stored RNA samples. Biochem Biophys Res Commun. 2009 Dec;390(1):1–4.

605. Ostermeier B, Soriano-Sarabia N, Maggirwar SB. Platelet-Released Factors: Their Role in Viral Disease and Applications for Extracellular Vesicle (EV) Therapy. Int J Mol Sci. 2022 Feb 19;23(4):2321.

606. Sherman CD, Lodha S, Sahoo S. EV Cargo Sorting in Therapeutic Development for Cardiovascular Disease. Cells. 2021 Jun 15;10(6):1500.

607. Zha Y, Lin T, Li Y, Zhang X, Wang Z, Li Z, et al. Exosome-mimetics as an engineered gene-activated matrix induces in-situ vascularized osteogenesis. Biomaterials. 2020 Jul;247:119985.

608. Deepak V, El-Balawi L, Harris LK. Placental Drug Delivery to Treat Pre-Eclampsia and Fetal Growth Restriction. Small. 2024 May 15;

609. King A, Ndifon C, Lui S, Widdows K, Kotamraju VR, Agemy L, et al. Tumor-homing peptides as tools for targeted delivery of payloads to the placenta. Sci Adv. 2016 May 6;2(5).

610. Schmidt JK, Wilson RL, Davenport BN, Hacker TA, Fitz C, Simmons HA, et al. Nanoparticle-mediated delivery of placental gene therapy via uterine artery catheterization in a pregnant rhesus macaque. bioRxiv. 2024 Apr 14;

611. Chen Y, Gao DY, Huang L. In vivo delivery of miRNAs for cancer therapy: Challenges and strategies. Adv Drug Deliv Rev. 2015 Jan;81:128–41.

612. Kusinski LC, Meek CL. Big babies, small babies: metformin exposure in pregnancy. Lancet Diabetes Endocrinol. 2023 Mar;11(3):145–6.

613. Paschou SA, Shalit A, Gerontiti E, Athanasiadou KI, Kalampokas T, Psaltopoulou T, et al. Efficacy and safety of metformin during pregnancy: an update. Endocrine. 2023 Oct 5;83(2):259–69.

614. Scott EM, Murphy HR, Myers J, Saravanan P, Poston L, Law GR. MAGIC (maternal glucose in pregnancy) understanding the glycemic profile of pregnancy, intensive CGM glucose profiling and its relationship to fetal growth: an observational study protocol. BMC Pregnancy Childbirth. 2023 Aug 3;23(1):563.

615. Loya CM, Lu CS, Van Vactor D, Fulga TA. Transgenic microRNA inhibition with spatiotemporal specificity in intact organisms. Nat Methods. 2009 Dec 15;6(12):897–903.

616. Swenson KS, Wang D, Jones AK, Nash MJ, O'Rourke R, Takahashi DL, et al. Metformin Disrupts Signaling and Metabolism in Fetal Hepatocytes. Diabetes. 2023 Sep 1;72(9):1214–27.

617. Bayoumy S, Habib M, Abdelmageed R. Impact of maternal diabetes and obesity on fetal cardiac functions. The Egyptian Heart Journal. 2020 Dec 31;72(1):46.

618. De Blasio MJ, Huynh N, Deo M, Dubrana LE, Walsh J, Willis A, et al. Defining the Progression of Diabetic Cardiomyopathy in a Mouse Model of Type 1 Diabetes. Front Physiol. 2020 Feb 20;11.

619. Cai L, Li W, Wang G, Guo L, Jiang Y, Kang YJ. Hyperglycemia-Induced Apoptosis in Mouse Myocardium. Diabetes. 2002 Jun 1;51(6):1938–48.

620. Gutierrez JC, Hrubec TC, Prater MR, Smith BJ, Freeman LE, Holladay SD. Aortic and ventricular dilation and myocardial reduction in gestation day 17 ICR mouse fetuses of diabetic mothers. Birth Defects Res A Clin Mol Teratol. 2007 Jun 2;79(6):459–64.

621. Kumar SD, Dheen ST, Tay SSW. Maternal diabetes induces congenital heart defects in mice by altering the expression of genes involved in cardiovascular development. Cardiovasc Diabetol. 2007 Dec 30;6(1):34.

Appendix

Appendix 1

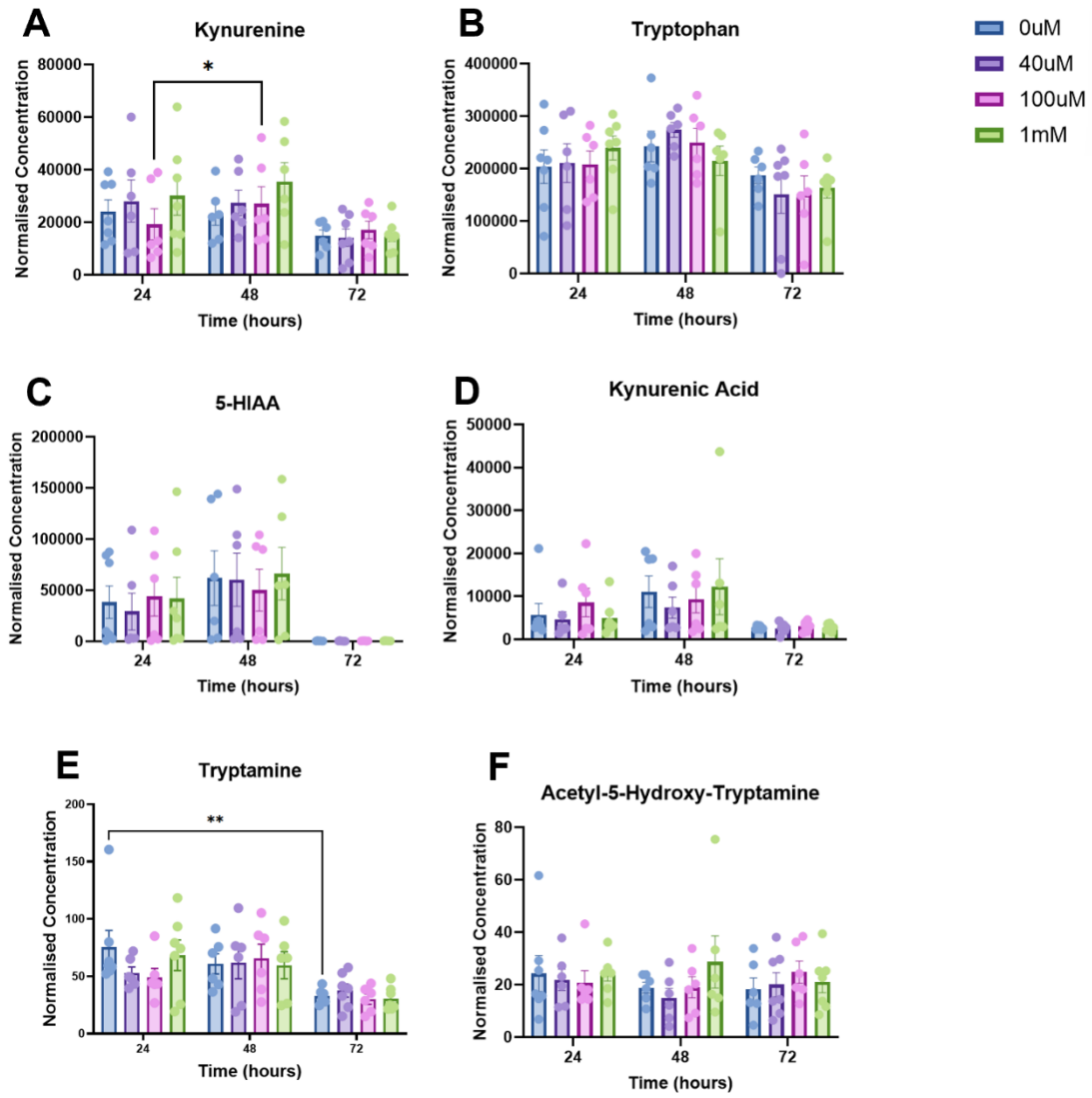

Tryptophan metabolites in placental villous explants treated with metformin (40μM-1mM), for 24-72 hours. Liquid chromatography-mass spectrometry was performed on aqueous placental explant fractions to detect tryptophan metabolites. Normally distributed data was analysed via a two-way mixed effects ANOVA, followed by a Geisser-Greenhouse correction and Tukey's multiple comparisons test and presented as mean ±SEM. Data that was not normally distributed was analysed via a Kruskall-Wallis test followed by a Dunn's post-hoc test and presented as median with 95% CI. (n=7); *=p ≤ 0.05, * *=p ≤ 0.01.

Appendix 2

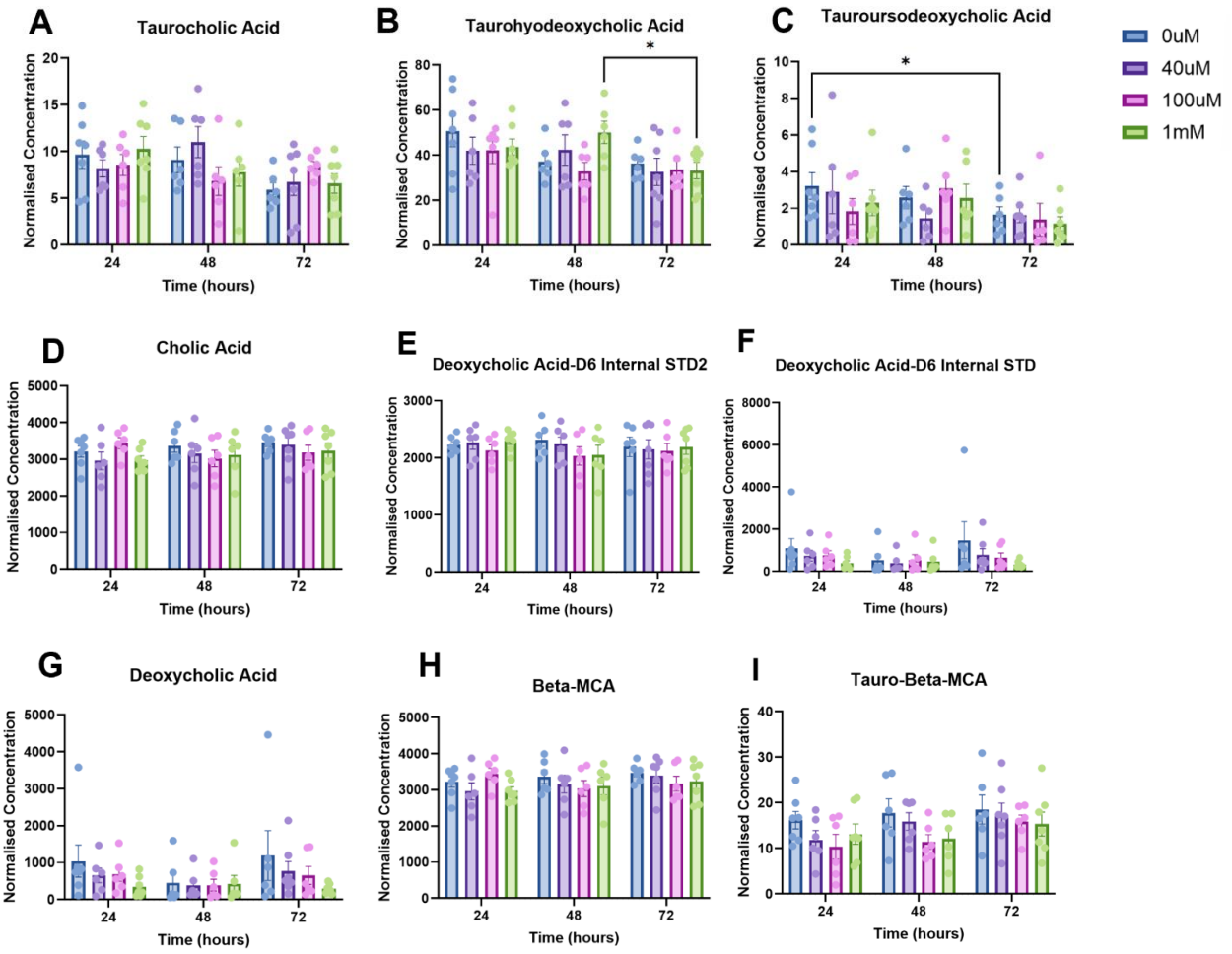

Bile acid metabolites in placental villous explants treated with metformin (40µM-1mM), for 24-72 hours. Liquid chromatography-mass spectrometry was performed on aqueous placental explant fractions to detect bile acid metabolites. Normally distributed data was analysed via a two-way mixed effects ANOVA, followed by a Geisser-Greenhouse correction and Tukey's multiple comparisons test and presented as mean ±SEM. Data that was not normally distributed was analysed via a Kruskall-Wallis test followed by a Dunn's post-hoc test and presented as median with 95% CI. (n=7); *=p ≤ 0.05, * *=p ≤ 0.01.

Appendix 3 - Mixed-effects linear regression model adjustments on E18.5 mouse fetal weight after being treated with PBS, NT miRNA and miR-375-3p during gestation.

Mouse Fetal Weight E18.5			
	(PBA vs NT miRNA)	**(PBS vs miR-375-3p)**	**(NT miRNA vs miR-375-3p)**
Clustered Litters			
Coefficient	0.0104	0.1054	0.0926
Std. Err.	0.0597	0.0589	0.0394
Z Score	0.17	1.79	2.35
P-Value	0.8614	0.0747	**0.0188**
95% Conf. Interval	-0.1066 0.1274	-0.0101 0.2210	0.0154 0.1699
Clustered Litters (Adjusted for Fetal Sex)			
Coefficient	-0.0001	0.1092	0.1067
Std. Err.	0.0599	0.0588	0.0466
Z Score	-0.00	1.86	2.29
P-Value	0.9980	0.0634	**0.0222**
95% Conf. Interval	0.1176 0.1173	0.0061 0.2244	0.0153 0.1981
Clustered Litters (Adjusted for Fetal Sex and Litter Size)			
Coefficient	0.0523	0.0733	0.0766
Std. Err.	0.0537	0.0481	0.0574
Z Score	0.97	1.53	1.33
P-Value	0.3296	0.1272	0.183
95% Conf. Interval	-0.0529 0.1576	-0.0209 0.1675	-0.0360 0.1891
Clustered Litters (Male Offspring Only)			
Coefficient	0.0083	0.1446	0.1402
Std. Err.	0.0592	0.0576	0.0502
Z Score	0.14	2.51	2.79
P-Value	0.8891	**0.0121**	**0.0052**
95% Conf. Interval	-0.1079 0.1244	0.0317 0.2575	0.0419 0.2385
Clustered Litters (Female Offspring Only)			
Coefficient	-0.0194	0.0435	0.0673
Std. Err.	0.0693	0.0698	0.0486
Z Score	-0.28	0.62	1.39
P-Value	0.7790	0.5331	0.1658
95% Conf. Interval	-0.1552 0.1163	-0.0933 0.1804	-0.0279 0.1625

Appendix 4 - Descriptive statistics of mouse fetal growth curves at E18.5 after being treated with PBS, NT miRNA or miR-375-3p mimics during gestation.

	PBS (g)	NT miRNA (g)	miR-375-3p (g)
Male and Female Offspring			
Minimum	0.919	0.9400	1.082
25% Percentile	1.1305	1.152	1.206
Median	1.197	1.198	1.302
75% Percentile	1.284	1.306	1.426
Maximum	1.4	1.445	1.581
Mean	1.1981	1.212	1.306
Std. Deviation	0.1113	0.1164	0.1286
Std. Error of Mean	0.0183	0.01614	0.02059
Lower 95% CI of mean	1.1610	1.179	1.264
Upper 95% CI of mean	1.2351	1.244	1.347
Male Offspring			
Minimum	1.068	1.023	1.178
25% Percentile	1.160	1.124	1.237
Median	1.202	1.192	1.370
75% Percentile	1.291	1.253	1.464
Maximum	1.400	1.445	1.581
Mean	1.214	1.206	1.361
Std. Deviation	0.09021	0.1166	0.1242
Std. Error of Mean	0.01923	0.02748	0.02927
Lower 95% CI of mean	1.174	1.148	1.299
Upper 95% CI of mean	1.254	1.264	1.422
Female Offspring			
Minimum	0.9190	0.9400	1.082
25% Percentile	1.093	1.119	1.175
Median	1.210	1.172	1.210
75% Percentile	1.303	1.249	1.354
Maximum	1.370	1.381	1.474
Mean	1.183	1.181	1.255
Std. Deviation	0.1351	0.1243	0.1171
Std. Error of Mean	0.03900	0.02649	0.02619
Lower 95% CI of mean	1.097	1.126	1.200
Upper 95% CI of mean	1.269	1.236	1.310

Appendix 5 – Mixed-effects linear regression model adjustments on E18.5 mouse placental weight after being treated with PBS, NT miRNA and miR-375-3p during gestation.

Mouse Placental Weight E18.5			
	(PBA vs NT miRNA)	**(PBS vs miR-375-3p)**	**(NT miRNA vs miR-375-3p)**
Clustered Litters			
Coefficient	0.0044	0.0249	0.0205
Std. Err.	0.0047	0.0047	0.0052
Z Score	0.94	5.33	3.98
P-Value	0.3467	**9.82560e-0.8**	**0.00007**
95% Conf. Interval	-0.0048 0.0135	0.0158 0.0341	0.0104 0.0307
Clustered Litters (Adjusted for Fetal Sex)			
Coefficient	0.0061	0.0260	0.0199
Std. Err.	0.0049	0.0048	0.0053
Z Score	1.25	5.38	3.75
P-Value	0.2124	**7.55362e-0.8**	**0.0002**
95% Conf. Interval	-0.0035 0.0156	0.0166 0.0355	0.0095 0.0304
Clustered Litters (Adjusted for Fetal Sex and Litter Size)			
Coefficient	0.0030	0.0281	0.0281
Std. Err.	0.0053	0.0046	0.0071
Z Score	0.57	6.06	3.97
P-Value	0.5687	**1.35730e-09**	**0.00007**
95% Conf. Interval	-0.0074 0.0134	0.0190 0.0372	0.0142 0.0419
Clustered Litters (Male Offspring Only)			
Coefficient	0.0015	0.0265	0.0251
Std. Err.	0.0053	0.0052	0.005
Z Score	0.28	5.09	5.05
P-Value	0.7830	**3.54713e-07**	**4.31E-07**
95% Conf. Interval	-0.0089 0.0119	0.0163 0.0367	0.0154 0.0348
Clustered Litters (Female Offspring Only)			
Coefficient	0.0090	0.0261	0.0173
Std. Err.	0.0058	0.0058	0.006
Z Score	1.56	4.48	2.86
P-Value	0.1192	**7.54937e-06**	**0.0042**
95% Conf. Interval	-0.0023 0.0202	0.0147 0.0376	0.0054 0.0291

Appendix 6 - Descriptive statistics of mouse placental growth curves at E18.5 after being treated with PBS, NT miRNA or miR-375-3p mimics during gestation.

	PBS (g)	NT miRNA (g)	miR-375-3p (g)
Male and Female Offspring			
Minimum	0.06100	0.07600	0.07800
25% Percentile	0.08000	0.08300	0.1000
Median	0.09150	0.09400	0.1160
75% Percentile	0.1020	0.1010	0.1280
Maximum	0.1180	0.1280	0.1560
Mean	0.09056	0.09409	0.1150
Std. Deviation	0.01483	0.01253	0.01836
Std. Error of Mean	0.002472	0.001911	0.002941
Lower 95% CI of mean	0.08554	0.09024	0.1090
Upper 95% CI of mean	0.09557	0.09795	0.1209
Male Offspring			
Minimum	0.06300	0.07800	0.08200
25% Percentile	0.07800	0.08200	0.1130
Median	0.09700	0.09400	0.1185
75% Percentile	0.1070	0.09700	0.1325
Maximum	0.1180	0.1010	0.1560
Mean	0.09333	0.09080	0.1196
Std. Deviation	0.01524	0.008108	0.01736
Std. Error of Mean	0.003326	0.002094	0.004092
Lower 95% CI of mean	0.08640	0.08631	0.1110
Upper 95% CI of mean	0.1003	0.09529	0.1282
Female Offspring			
Minimum	0.06100	0.07600	0.07800
25% Percentile	0.07025	0.08100	0.09575
Median	0.08550	0.09000	0.1090
75% Percentile	0.09400	0.09600	0.1268
Maximum	0.09700	0.1010	0.1500
Mean	0.08358	0.08800	0.1105
Std. Deviation	0.01284	0.007659	0.01901
Std. Error of Mean	0.003706	0.001757	0.004251
Lower 95% CI of mean	0.07543	0.08431	0.1016
Upper 95% CI of mean	0.09174	0.09169	0.1194

Appendix 7 - Mixed-effects linear regression model adjustments on E18.5 mouse fetal:placental weight after being treated with PBS, NT miRNA and miR-375-3p during gestation.

Mouse Fetal:Placental Weight E18.5			
	(PBA vs NT miRNA)	**(PBS vs miR-375-3p)**	**(NT miRNA vs miR-375-3p)**
Clustered Litters			
Coefficient	-1.0388	-2.3212	-1.2685
Std. Err.	1.0078	0.9931	0.6601
Z Score	-1.03	-2.34	-1.92
P-Value	0.3027	**0.0194**	0.0547
95% Conf. Interval	-3.0141 -0.3748	-4.2676 -0.3748	-2.5623 0.0253
Clustered Litters (Adjusted for Fetal Sex)			
Coefficient	-1.2056	-2.4064	-1.2499
Std. Err.	1.0200	1.0022	0.6791
Z Score	-1.18	-2.40	-1.84
P-Value	0.2372	**0.0163**	0.0657
95% Conf. Interval	-3.2047 0.7935	-4.3706 0.4421	-2.5808 0.0811
Clustered Litters (Adjusted for Fetal Sex and Litter Size)			
Coefficient	-0.4023	-3.1128	-2.2973
Std. Err.	1.0138	0.8811	0.7992
Z Score	-0.40	-3.53	-2.87
P-Value	0.6915	**0.0004**	**0.0040**
95% Conf. Interval	-2.3893 1.5846	-4.8397 -1.3858	-3.8636 -0.7309
Clustered Litters (Male Offspring Only)			
Coefficient	-0.4429	-2.0173	-1.4957
Std. Err.	1.0868	1.0568	0.7800
Z Score	-0.41	-1.91	-1.92
P-Value	0.6836	0.0563	0.0550
95% Conf. Interval	-2.5730 1.6872	-4.0887 0.0541	-3.0236 0.0322
Clustered Litters (Female Offspring Only)			
Coefficient	-1.7181	-2.9308	-1.2998
Std. Err.	1.0707	1.0816	0.7020
Z Score	-1.60	-2.71	-1.85
P-Value	0.1086	**0.0067**	0.0641
95% Conf. Interval	-3.8165 0.3804	-5.0506 -0.8109	-2.6759 0.0762

Appendix 8

A **Placental Metabolome**

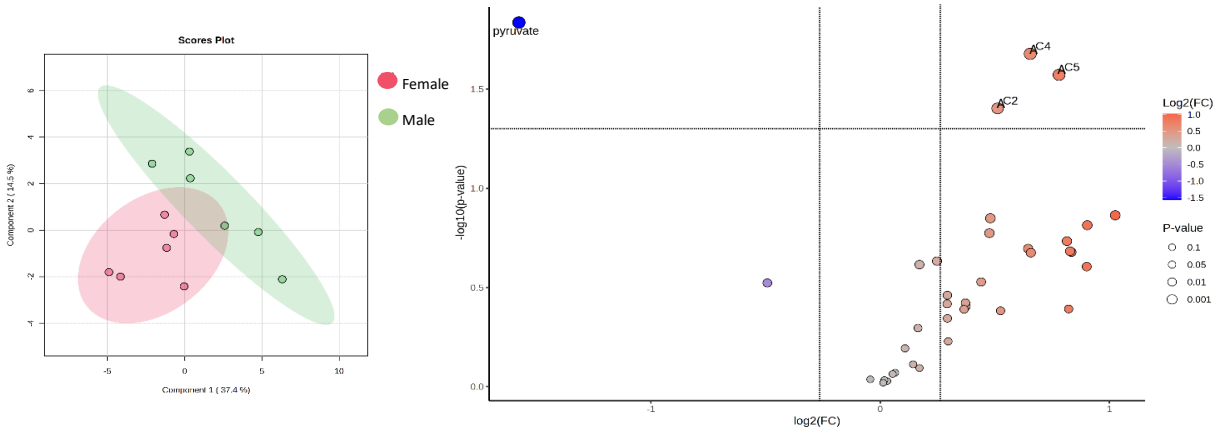

	FC	Log2(FC)	Raw P Value	Log10(p)
Pyruvate	0.3354	-1.576	0.014597	1.8357
AC4	1.5742	0.65461	0.020993	1.6779
AC5	1.7172	0.78005	0.026806	1.5718
AC2	1.4262	0.51214	0.03951	1.4033

B **Placental Lipidome**

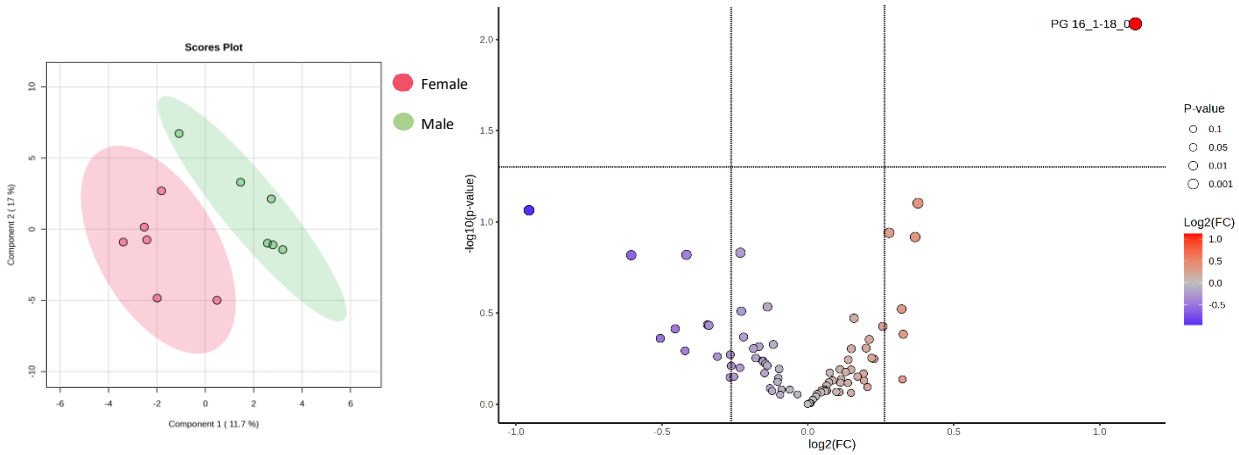

	FC	Log2(FC)	Raw P Value	Log10(p)
PG 16_1-18_0	2.177	1.1224	0.008209	2.0857

PCA, volcano plot and statistical scores of significantly altered placental metabolites in male and female mouse offspring exposed to NT miRNA mimic during gestation. Healthy pregnant C57BL6/J female mice were injected with NT miRNA (n=6) mimic at E11.5, E13.5 and E15.5 before being sacrificed at E18.5. Placental tissue from male (n=6) and female (n=6) pups was harvested and processed for metabolite extraction. LCMS was performed on aqueous and organic metabolite fractions, where peaks were normalised to placental tissue weight and analysed using MetaboAnalyst.ca. A one factor statistical analysis was performed, where data was auto scaled. PCA (2D score) plot was generated to measure placental metabolite and lipid profiles. Volcano plot; direction of comparison: male/female, FC threshold: 1.2, $p<0.05$: raw). Acylcarnitine (AC), phosphatidylglycerol (PG).

Appendix 9 - Mixed-effects linear regression model adjustments on E18.5 mouse fetal weight after being treated with PBS and human maternal plasma EVs from non-GDM AGA pregnancies.

Mouse Fetal Weight E18.5 (PBS vs Non-GDM AGA EVs)	
Clustered	
Coefficient	0.0928
Std. Err.	0.0601
Z Score	1.54
P-Value	0.1227
95% Conf. Interval	-0.0250 0.2106
Clustered (Adjusted for Fetal Sex)	
Coefficient	0.1123
Std. Err.	0.0604
Z Score	1.86
P-Value	0.0629
95% Conf. Interval	-0.0061 0.2244
Clustered (Adjusted for Fetal Sex and Litter Size)	
Coefficient	0.1121
Std. Err.	0.0532
Z Score	2.11
P-Value	**0.0353**
95% Conf. Interval	-0.0077 0.2164
Clustered (Male Offspring Only)	
Coefficient	0.1175
Std. Err.	0.0596
Z Score	1.97
P-Value	**0.0486**
95% Conf. Interval	-0.0007 0.2343
Clustered (Female Offspring Only)	
Coefficient	0.0814
Std. Err.	0.0704
Z Score	1.16
P-Value	0.2477
95% Conf. Interval	-0.0566 0.2193

Appendix 10 - Descriptive statistics of non-linear histogram on E18.5 mouse fetal weight after being treated with PBS and human maternal plasma EVs from non-GDM AGA pregnancies.

	PBS (g)	Non-GDM AGA (g)
Male and Female Offspring		
Minimum	0.919	0.977
25% Percentile	1.1305	1.17525
Median	1.197	1.242
75% Percentile	1.284	1.33575
Maximum	1.4	1.622
Mean	1.1981	1.2707
Std. Deviation	0.1113	0.1471
Std. Error of Mean	0.0183	0.0227
Lower 95% CI of mean	1.1610	1.2249
Upper 95% CI of mean	1.2351	1.3165
Male Offspring		
Minimum	1.068	1.108
25% Percentile	1.160	1.176
Median	1.202	1.285
75% Percentile	1.291	1.431
Maximum	1.400	1.622
Mean	1.214	1.317
Std. Deviation	0.09021	0.1562
Std. Error of Mean	0.01923	0.03583
Lower 95% CI of mean	1.174	1.241
Upper 95% CI of mean	1.254	1.392
Female Offspring		
Minimum	0.9190	0.9770
25% Percentile	1.093	1.193
Median	1.210	1.241
75% Percentile	1.303	1.317
Maximum	1.370	1.584
Mean	1.183	1.252
Std. Deviation	0.1351	0.1439
Std. Error of Mean	0.03900	0.03490
Lower 95% CI of mean	1.097	1.178
Upper 95% CI of mean	1.269	1.326

Appendix 11 - Mixed-effects linear regression model adjustments on E18.5 mouse placental weight after being treated with PBS and human maternal plasma EVs from non-GDM AGA pregnancies.

Mouse Placental Weight E18.5 (PBS vs Non-GDM AGA EVs)	
Clustered	
Coefficient	0.0105
Std. Err.	0.0048
Z Score	2.19
P-Value	**0.0286**
95% Conf. Interval	0.0011 0.0199
Clustered (Adjusted for Fetal Sex)	
Coefficient	0.0119
Std. Err.	0.0050
Z Score	2.41
P-Value	**0.0162**
95% Conf. Interval	0.0022 0.0216
Clustered (Adjusted for Fetal Sex and Litter Size)	
Coefficient	0.0130
Std. Err.	0.0052
Z Score	2.51
P-Value	**0.0120**
95% Conf. Interval	0.0029 0.0231
Clustered (Male Offspring Only)	
Coefficient	0.0104
Std. Err.	0.0053
Z Score	1.96
P-Value	**0.0499**
95% Conf. Interval	3.37e-06 0.0208
Clustered (Female Offspring Only)	
Coefficient	0.0130
Std. Err.	0.0060
Z Score	2.18
P-Value	0.2947
95% Conf. Interval	0.0013 0.0246

Appendix 12 - Descriptive statistics of non-linear histogram on E18.5 mouse placenta weight after being treated with PBS and human maternal plasma EVs from non-GDM AGA pregnancies.

	PBS (g)	Non-GDM AGA (g)
Male and Female Offspring		
Minimum	0.06100	0.07800
25% Percentile	0.08000	0.08950
Median	0.09150	0.1000
75% Percentile	0.1020	0.1090
Maximum	0.1180	0.1260
Mean	0.09056	0.1004
Std. Deviation	0.01483	0.01307
Std. Error of Mean	0.002472	0.002178
Lower 95% CI of mean	0.08554	0.09594
Upper 95% CI of mean	0.09557	0.1048
Male Offspring		
Minimum	0.06300	0.08700
25% Percentile	0.07800	0.09300
Median	0.09700	0.1020
75% Percentile	0.1070	0.1090
Maximum	0.1180	0.1260
Mean	0.09333	0.1033
Std. Deviation	0.01524	0.01073
Std. Error of Mean	0.003326	0.002462
Lower 95% CI of mean	0.08640	0.09809
Upper 95% CI of mean	0.1003	0.1084
Female Offspring		
Minimum	0.06100	0.07800
25% Percentile	0.07025	0.08500
Median	0.08550	0.09100
75% Percentile	0.09400	0.1090
Maximum	0.09700	0.1230
Mean	0.08358	0.09712
Std. Deviation	0.01284	0.01492
Std. Error of Mean	0.003706	0.003619
Lower 95% CI of mean	0.07543	0.08945
Upper 95% CI of mean	0.09174	0.1048

Appendix 13 - Mixed-effects linear regression model adjustments on E18.5 mouse fetal:placental weight after being treated with PBS and human maternal plasma EVs from non-GDM AGA pregnancies.

Mouse Fetal:Placental Weight E18.5 (PBS vs Non-GDM AGA)	
Clustered	
Coefficient	-0.6034
Std. Err.	1.0200
Z Score	-0.59
P-Value	0.5541
95% Conf. Interval	-2.6026 1.3957
Clustered (Adjusted for Fetal Sex)	
Coefficient	-0.7438
Std. Err.	1.0279
Z Score	-0.72
P-Value	0.4693
95% Conf. Interval	-2.7585 1.2709
Clustered (Adjusted for Fetal Sex and Litter Size)	
Coefficient	-0.7405
Std. Err.	0.9720
Z Score	-0.76
P-Value	0.4462
95% Conf. Interval	-2.6455 1.1646
Clustered (Male Offspring Only)	
Coefficient	-0.5962
Std. Err.	1.0927
Z Score	-0.55
P-Value	0.5854
95% Conf. Interval	-2.7379 1.5455
Clustered (Female Offspring Only)	
Coefficient	-1.0472
Std. Err.	1.0933
Z Score	-0.96
P-Value	0.3381
95% Conf. Interval	-3.1900 1.0956

Appendix 14 - Mixed-effects linear regression model adjustments on E18.5 mouse fetal weight after being treated with human maternal plasma EVs from non-GDM AGA or GDM AGA pregnancies.

Mouse Fetal Weight E18.5 (Non-GDM AGA vs GDM AGA EVs)	
Clustered	
Coefficient	-0.0457
Std. Err.	0.0629
Z Score	-0.73
P-Value	0.468
95% Conf. Interval	-0.1691 0.0776
Clustered (Adjusted for Fetal Sex)	
Coefficient	-0.0652
Std. Err.	0.0619
Z Score	-1.05
P-Value	0.292
95% Conf. Interval	-0.1865 0.0561
Clustered (Adjusted for Fetal Sex and Litter Size)	
Coefficient	-0.1147
Std. Err.	0.0442
Z Score	-2.60
P-Value	**0.0094**
95% Conf. Interval	-0.2012 0.0281
Clustered (Male Offspring Only)	
Coefficient	-0.0660
Std. Err.	0.0627
Z Score	-1.05
P-Value	0.292
95% Conf. Interval	-0.1888 0.0568
Clustered (Female Offspring Only)	
Coefficient	-0.0688
Std. Err.	0.0695
Z Score	-0.99
P-Value	0.322
95% Conf. Interval	-0.2050 0.0674

Appendix 15 - Descriptive statistics of non-linear histogram on E18.5 mouse fetal weight after being treated with human maternal plasma EVs from non-GDM AGA or GDM AGA pregnancies.

	Non-GDM AGA (g)	GDM AGA (g)
Male and Female Offspring		
Minimum	0.9770	1.011
25% Percentile	1.175	1.137
Median	1.242	1.241
75% Percentile	1.336	1.356
Maximum	1.622	1.526
Mean	1.271	1.242
Std. Deviation	0.1471	0.1286
Std. Error of Mean	0.02269	0.01856
Lower 95% CI of mean	1.225	1.204
Upper 95% CI of mean	1.317	1.279
Male Offspring		
Minimum	1.108	1.011
25% Percentile	1.176	1.203
Median	1.285	1.261
75% Percentile	1.431	1.363
Maximum	1.622	1.476
Mean	1.317	1.268
Std. Deviation	0.1562	0.1109
Std. Error of Mean	0.03583	0.02218
Lower 95% CI of mean	1.241	1.222
Upper 95% CI of mean	1.392	1.314
Female Offspring		
Minimum	0.9770	1.012
25% Percentile	1.193	1.096
Median	1.241	1.201
75% Percentile	1.317	1.270
Maximum	1.584	1.526
Mean	1.252	1.201
Std. Deviation	0.1439	0.1327
Std. Error of Mean	0.03490	0.02828
Lower 95% CI of mean	1.178	1.142
Upper 95% CI of mean	1.326	1.260

Appendix 16 - Mixed-effects linear regression model adjustments on E18.5 mouse placental weight after being treated with human maternal plasma EVs from non-GDM AGA or GDM AGA pregnancies.

Mouse Placental Weight E18.5 (Non-GDM AGA vs GDM AGA EVs)	
Clustered	
Coefficient	-0.0050
Std. Err.	0.0037
Z Score	-1.37
P-Value	0.172
95% Conf. Interval	-0.0122 0.0022
Clustered (Adjusted for Fetal Sex)	
Coefficient	-0.0051
Std. Err.	0.0039
Z Score	-1.31
P-Value	0.192
95% Conf. Interval	-0.0127 0.0026
Clustered (Adjusted for Fetal Sex and Litter Size)	
Coefficient	-0.0023
Std. Err.	0.0038
Z Score	-0.62
P-Value	0.536
95% Conf. Interval	-0.0098 0.0051
Clustered (Male Offspring Only)	
Coefficient	-0.0084
Std. Err.	0.0048
Z Score	-1.77
P-Value	0.077
95% Conf. Interval	-0.0177 0.0009
Clustered (Female Offspring Only)	
Coefficient	-0.0005
Std. Err.	0.0053
Z Score	-0.09
P-Value	0.926
95% Conf. Interval	-0.0109 0.0010

Appendix 17 - Descriptive statistics of non-linear histogram on E18.5 mouse placental weight after being treated with human maternal plasma EVs from non-GDM AGA or GDM AGA pregnancies.

	Non-GDM AGA (g)	GDM AGA (g)
Male and Female Offspring		
Minimum	0.07800	0.07100
25% Percentile	0.08950	0.08700
Median	0.1000	0.09600
75% Percentile	0.1090	0.1020
Maximum	0.1260	0.1270
Mean	0.1004	0.09536
Std. Deviation	0.01307	0.01106
Std. Error of Mean	0.002178	0.001771
Lower 95% CI of mean	0.09594	0.09177
Upper 95% CI of mean	0.1048	0.09894
Male Offspring		
Minimum	0.08700	0.07100
25% Percentile	0.09300	0.08375
Median	0.1020	0.09500
75% Percentile	0.1090	0.1070
Maximum	0.1260	0.1270
Mean	0.1033	0.09511
Std. Deviation	0.01073	0.01416
Std. Error of Mean	0.002462	0.003337
Lower 95% CI of mean	0.09809	0.08807
Upper 95% CI of mean	0.1084	0.1022
Female Offspring		
Minimum	0.07800	0.07500
25% Percentile	0.08500	0.09325
Median	0.09100	0.09550
75% Percentile	0.1090	0.1010
Maximum	0.1230	0.1060
Mean	0.09712	0.09550
Std. Deviation	0.01492	0.008065
Std. Error of Mean	0.003619	0.001803
Lower 95% CI of mean	0.08945	0.09173
Upper 95% CI of mean	0.1048	0.09927

Appendix 18 - Mixed-effects linear regression model adjustments on E18.5 mouse fetal:placental weight after being treated with human maternal plasma EVs from non-GDM AGA or GDM AGA pregnancies.

Mouse Fetal:Placental Weight E18.5 (Non-GDM AGA vs GDM AGA)	
Clustered	
Coefficient	-0.0471
Std. Err.	0.9971
Z Score	-0.05
P-Value	0.962
95% Conf. Interval	-2.0014 1.9072
Clustered (Adjusted for Fetal Sex)	
Coefficient	-0.0372
Std. Err.	1.0059
Z Score	-0.04
P-Value	0.970
95% Conf. Interval	-2.0088 1.9344
Clustered (Adjusted for Fetal Sex and Litter Size)	
Coefficient	-1.1274
Std. Err.	0.9672
Z Score	-1.17
P-Value	0.244
95% Conf. Interval	-3.0230 0.7682
Clustered (Male Offspring Only)	
Coefficient	0.6035
Std. Err.	1.0543
Z Score	0.57
P-Value	0.567
95% Conf. Interval	-1.4629 2.6698
Clustered (Female Offspring Only)	
Coefficient	-0.9354
Std. Err.	1.0769
Z Score	-0.87
P-Value	0.385
95% Conf. Interval	-3.0462 1.1753

Appendix 19 - Mixed-effects linear regression model adjustments on E18.5 mouse fetal weight after being treated with human maternal plasma EVs from GDM pregnancies with AGA or LGA pregnancies.

Mouse Fetal Weight E18.5 (GDM AGA EVs vs GDM LGA EVs)	
Clustered	
Coefficient	0.0963
Std. Err.	0.0526
Z Score	1.83
P-Value	0.0674
95% Conf. Interval	-0.0069 0.1995
Clustered (Adjusted for Fetal Sex)	
Coefficient	0.1049
Std. Err.	0.0526
Z Score	1.99
P-Value	**0.0460**
95% Conf. Interval	0.0018 0.2080
Clustered (Adjusted for Fetal Sex and Litter Size)	
Coefficient	0.1023
Std. Err.	0.0452
Z Score	2.26
P-Value	**0.0237**
95% Conf. Interval	0.0137 0.1909
Clustered (Male Offspring Only)	
Coefficient	0.1039
Std. Err.	0.0494
Z Score	2.10
P-Value	**0.0355**
95% Conf. Interval	0.0070 0.2009
Clustered (Female Offspring Only)	
Coefficient	0.1262
Std. Err.	0.0649
Z Score	1.94
P-Value	0.0519
95% Conf. Interval	-0.0010 0.2535

Appendix 20 - Descriptive statistics of non-linear histogram on E18.5 mouse fetal weight after being treated with human maternal plasma EVs from GDM pregnancies with AGA or LGA pregnancies.

	GDM AGA (g)	GDM LGA (g)
Male and Female Offspring		
Minimum	1.011	0.8830
25% Percentile	1.137	1.283
Median	1.241	1.364
75% Percentile	1.356	1.440
Maximum	1.526	1.590
Mean	1.242	1.355
Std. Deviation	0.1286	0.1450
Std. Error of Mean	0.01856	0.02030
Lower 95% CI of mean	1.204	1.315
Upper 95% CI of mean	1.279	1.396
Male Offspring		
Minimum	1.011	0.8830
25% Percentile	1.203	1.288
Median	1.261	1.391
75% Percentile	1.363	1.464
Maximum	1.476	1.565
Mean	1.268	1.367
Std. Deviation	0.1109	0.1465
Std. Error of Mean	0.02218	0.02929
Lower 95% CI of mean	1.222	1.306
Upper 95% CI of mean	1.314	1.427
Female Offspring		
Minimum	1.012	1.087
25% Percentile	1.096	1.193
Median	1.201	1.343
75% Percentile	1.270	1.432
Maximum	1.526	1.590
Mean	1.201	1.335
Std. Deviation	0.1327	0.1565
Std. Error of Mean	0.02828	0.03338
Lower 95% CI of mean	1.142	1.266
Upper 95% CI of mean	1.260	1.405

Appendix 21 - Mixed-effects linear regression model adjustments on E18.5 mouse placental weight after being treated with human maternal plasma EVs from GDM pregnancies with AGA or LGA pregnancies.

Mouse Placental Weight E18.5 (GDM AGA EVs vs GDM LGA EVs)	
Clustered	
Coefficient	0.0033
Std. Err.	0.0028
Z Score	1.17
P-Value	0.2436
95% Conf. Interval	-0.0022 0.0088
Clustered (Adjusted for Fetal Sex)	
Coefficient	0.0029
Std. Err.	0.0030
Z Score	0.96
P-Value	0.335
95% Conf. Interval	-0.0023 0.0087
Clustered (Adjusted for Fetal Sex and Litter Size)	
Coefficient	0.0011
Std. Err.	0.0049
Z Score	0.22
P-Value	0.829
95% Conf. Interval	-0.0086 0.0107
Clustered (Male Offspring Only)	
Coefficient	0.0073
Std. Err.	0.0050
Z Score	1.46
P-Value	0.144
95% Conf. Interval	-0.0025 0.0171
Clustered (Female Offspring Only)	
Coefficient	-0.0023
Std. Err.	0.0038
Z Score	-0.59
P-Value	0.554
95% Conf. Interval	-0.0098 0.0052

Appendix 22 - Descriptive statistics of non-linear histogram on E18.5 mouse placental weight after being treated with human maternal plasma EVs from GDM pregnancies with AGA or LGA pregnancies.

	GDM AGA (g)	GDM LGA (g)
Male and Female Offspring		
Minimum	0.07100	0.07100
25% Percentile	0.08700	0.08900
Median	0.09600	0.1005
75% Percentile	0.1020	0.1060
Maximum	0.1270	0.1250
Mean	0.09536	0.09861
Std. Deviation	0.01106	0.01237
Std. Error of Mean	0.001771	0.002062
Lower 95% CI of mean	0.09177	0.09443
Upper 95% CI of mean	0.09894	0.1028
Male Offspring		
Minimum	0.07100	0.07100
25% Percentile	0.08375	0.09300
Median	0.09500	0.1020
75% Percentile	0.1070	0.1105
Maximum	0.1270	0.1250
Mean	0.09511	0.1020
Std. Deviation	0.01416	0.01265
Std. Error of Mean	0.003337	0.002696
Lower 95% CI of mean	0.08807	0.09635
Upper 95% CI of mean	0.1022	0.1076
Female Offspring		
Minimum	0.07500	0.08200
25% Percentile	0.09325	0.08525
Median	0.09550	0.08950
75% Percentile	0.1010	0.1025
Maximum	0.1060	0.1140
Mean	0.09550	0.09336
Std. Deviation	0.008065	0.01025
Std. Error of Mean	0.001803	0.002739
Lower 95% CI of mean	0.09173	0.08744
Upper 95% CI of mean	0.09927	0.09927

Appendix 23 - Mixed-effects linear regression model adjustments on E18.5 mouse fetal:placental weight after being treated with human maternal plasma EVs from GDM pregnancies with AGA or LGA pregnancies.

Mouse Fetus:Placenta Weight E18.5 (GDM AGA EVs vs GDM LGA EVs)	
Clustered	
Coefficient	0.5376
Std. Err.	0.9212
Z Score	0.58
P-Value	0.560
95% Conf. Interval	-1.2680 2.3431
Clustered (Adjusted for Fetal Sex)	
Coefficient	0.5336
Std. Err.	0.9267
Z Score	0.58
P-Value	0.565
95% Conf. Interval	-1.2828 2.3499
Clustered (Adjusted for Fetal Sex and Litter Size)	
Coefficient	0.9543
Std. Err.	1.0931
Z Score	0.87
P-Value	0.383
95% Conf. Interval	-1.1882 3.0967
Clustered (Male Offspring Only)	
Coefficient	-0.0999
Std. Err.	1.0629
Z Score	-0.09
P-Value	0.925
95% Conf. Interval	-2.1832 1.9835
Clustered (Female Offspring Only)	
Coefficient	1.4946
Std. Err.	0.9562
Z Score	1.56
P-Value	0.118
95% Conf. Interval	-0.3794 3.3687

Appendix 24 Ethics Approval

Health Research Authority

West Midlands - South Birmingham Research Ethics Committee

The Old Chapel
Royal Standard Place
Nottingham
NG1 6FS

Please note: This is the favourable opinion of the REC only and does not allow the amendment to be implemented at NHS sites in England until the outcome of the HRA assessment has been confirmed.

04 September 2018

Dear

Study title:	**Micronutrients in Pregnancy as a Risk Factor for Diabetes and Effects on mother and baby: an MRC-funded study (PRiDE)**
REC reference:	**12/WM/0010**
Protocol number:	**N/A**
Amendment number:	**9**
Amendment date:	**18 June 2018**
IRAS project ID:	**90943**

The above amendment was reviewed on 22 August 2018 by the Sub-Committee in correspondence.

Ethical opinion

The members of the Committee taking part in the review gave a favourable ethical opinion of the amendment on the basis described in the notice of amendment form and supporting documentation.

Discussion: The committee requested clarification on what is meant by guardianship, whether samples were completely anonymised or link anonymised before stored and that only anonymised samples will be sent to other labs including those in the EEA. The committee was satisfied with the response they received and agreed there were no ethical concerns.

Approved documents

The documents reviewed and approved at the meeting were:

Document	*Version*	*Date*

Health Research Authority

Notice of Substantial Amendment (non-CTIMP)	9	18 June 2018
Research protocol or project proposal	6	02 July 2018

Membership of the Committee

The members of the Committee who took part in the review are listed on the attached sheet.

Working with NHS Care Organisations

Sponsors should ensure that they notify the R&D office for the relevant NHS care organisation of this amendment in line with the terms detailed in the categorisation email issued by the lead nation for the study.

Statement of compliance

The Committee is constituted in accordance with the Governance Arrangements for Research Ethics Committees and complies fully with the Standard Operating Procedures for Research Ethics Committees in the UK.

We are pleased to welcome researchers and R & D staff at our Research Ethics Committee members' training days – see details at http://www.hra.nhs.uk/hra-training/

12/WM/0010:	**Please quote this number on all correspondence**

Yours sincerely

PP

Professor Paula McGee
Chair

E-mail: NRESCommittee.WestMidlands-SouthBirmingham@nhs.net

Enclosures: *List of names and professions of members who took part in the review*

Copy to: *Ms Donna McLean, Chelsea and Westminster Hospital NHS Foundation Trust*
Dr Ponnusamy Saravanan, University of Warwick & George Eliot Hospital
Dr Peter Hedges, University of Warwick

NHS
Health Research Authority

West Midlands - South Birmingham Research Ethics Committee

Attendance at Sub-Committee of the REC meeting on 22 August 2018

Committee Members:

Name	*Profession*	*Present*	*Notes*
Ms Philippa Burgon	Retired Local Government Officer	Yes	
Professor Paula McGee	Professor of Nursing	Yes	

Health Research Authority

Yorkshire & The Humber - Leeds East Research Ethics Committee
NHSBT Newcastle Blood Donor Centre
Holland Drive
Newcastle upon Tyne
NE2 4NQ

Please note: This is the favourable opinion of the REC only and does not allow you to start your study at NHS sites in England until you receive HRA Approval

17 March 2020

Professor Eleanor M Scott
Professor of Medicine (Diabetes and Maternal Health)
University of Leeds and Leeds Teaching Hospitals NHS Trust
Leeds Institute of Cardiovascular and Metabolic Medicine, LIGHT Laboratories,
Clarendon Way, University of Leeds
Leeds
LS2 9JT

Dear Professor Scott

Study title:	**Understanding the glycemic profile of pregnancy: intensive CGM glucose profiling and its relationship to fetal growth.**
REC reference:	**20/YH/0011**
Protocol number:	**N/A**
IRAS project ID:	**271768**

Thank you for your letter of 28th February 2020, responding to the Committee's request for further information on the above research and submitting revised documentation.

The further information has been considered on behalf of the Committee by the Chair.

Confirmation of ethical opinion

On behalf of the Committee, I am pleased to confirm a favourable ethical opinion for the above research on the basis described in the application form, protocol and supporting documentation as revised, subject to the conditions specified below.

Health Research Authority

Conditions of the favourable opinion

The REC favourable opinion is subject to the following conditions being met prior to the start of the study.

You should notify the REC once all conditions have been met (except for site approvals from host organisations) and provide copies of any revised documentation with updated version numbers. Revised documents should be submitted to the REC electronically from IRAS. The REC will acknowledge receipt and provide a final list of the approved documentation for the study, which you can make available to host organisations to facilitate their permission for the study. Failure to provide the final versions to the REC may cause delay in obtaining permissions.

Confirmation of Capacity and Capability (in England, Northern Ireland and Wales) or NHS management permission (in Scotland) should be sought from all NHS organisations involved in the study in accordance with NHS research governance arrangements. Each NHS organisation must confirm through the signing of agreements and/or other documents that it has given permission for the research to proceed (except where explicitly specified otherwise).

Guidance on applying for HRA and HCRW Approval (England and Wales)/ NHS permission for research is available in the Integrated Research Application System.

For non-NHS sites, site management permission should be obtained in accordance with the procedures of the relevant host organisation.

Sponsors are not required to notify the Committee of management permissions from host organisations

Registration of Clinical Trials

It is a condition of the REC favourable opinion that **all clinical trials are registered** on a publicly accessible database. For this purpose, 'clinical trials' are defined as the first four project categories in IRAS project filter question 2. Registration is a legal requirement for clinical trials of investigational medicinal products (CTIMPs), except for phase I trials in healthy volunteers (these must still register as a condition of the REC favourable opinion).

Registration should take place as early as possible and within six weeks of recruiting the first research participant at the latest. Failure to register is a breach of these approval conditions, unless a deferral has been agreed by or on behalf of the Research Ethics Committee (see here for more information on requesting a deferral: https://www.hra.nhs.uk/planning-and-improving-research/research-planning/research-registration-research-project-identifiers/

As set out in the UK Policy Framework, research sponsors are responsible for making information about research publicly available before it starts e.g. by registering the research project on a publicly accessible register. Further guidance on registration is available at: https://www.hra.nhs.uk/planning-and-improving-research/research-planning/transparency-responsibilities/

Health Research Authority

You should notify the REC of the registration details. We will audit these as part of the annual progress reporting process.

It is the responsibility of the sponsor to ensure that all the conditions are complied with before the start of the study or its initiation at a particular site (as applicable).

After ethical review: Reporting requirements

The attached document "After ethical review – guidance for researchers" gives detailed guidance on reporting requirements for studies with a favourable opinion, including:

- Notifying substantial amendments
- Adding new sites and investigators
- Notification of serious breaches of the protocol
- Progress and safety reports
- Notifying the end of the study, including early termination of the study
- Final report

The latest guidance on these topics can be found at https://www.hra.nhs.uk/approvals-amendments/managing-your-approval/.

Ethical review of research sites

NHS/HSC sites

The favourable opinion applies to all NHS/HSC sites listed in the application subject to confirmation of Capacity and Capability (in England, Northern Ireland and Wales) or management permission (in Scotland) being obtained from the NHS/HSC R&D office prior to the start of the study (see "Conditions of the favourable opinion" below).

Non-NHS/HSC sites

I am pleased to confirm that the favourable opinion applies to any non-NHS/HSC sites listed in the application, subject to site management permission being obtained prior to the start of the study at the site.

Approved documents

The final list of documents reviewed and approved by the Committee is as follows:

Document	*Version*	*Date*
Copies of advertisement materials for research participants [POSTER]	1.0	24 October 2019
Copies of advertisement materials for research participants [INFOGRAPHIC]	1.0	24 October 2019
Evidence of Sponsor insurance or indemnity (non NHS Sponsors		26 September 2019

Health Research Authority

only) [SPONSOR INSURANCE]		
GP/consultant information sheets or letters [GP LETTER]	1.0	01 November 2019
IRAS Application Form [IRAS_Form_09122019]		09 December 2019
IRAS Checklist XML [Checklist_09122019]		09 December 2019
Letter from funder [AWARD LETTER]		27 September 2019
Letters of invitation to participant [INFOGRAPHIC]	1.0	24 October 2019
Other [Researchers email response to provisional opinion]		28 February 2020
Participant consent form	2.0	28 February 2020
Participant information sheet (PIS)	2.0	28 February 2020
Research protocol or project proposal [MAGIC PROTOCOL]	1.0	29 November 2019
Summary CV for Chief Investigator (CI) [CV]		01 November 2019
Summary of any applicable exclusions to sponsor insurance (non-NHS sponsors only) [SPONSOR LIABILITY]	1.0	25 September 2019

Statement of compliance

The Committee is constituted in accordance with the Governance Arrangements for Research Ethics Committees and complies fully with the Standard Operating Procedures for Research Ethics Committees in the UK.

User Feedback

The Health Research Authority is continually striving to provide a high quality service to all applicants and sponsors. You are invited to give your view of the service you have received and the application procedure. If you wish to make your views known please use the feedback form available on the HRA website:
http://www.hra.nhs.uk/about-the-hra/governance/quality-assurance/

HRA Learning

We are pleased to welcome researchers and research staff to our HRA Learning Events and online learning opportunities– see details at:
https://www.hra.nhs.uk/planning-and-improving-research/learning/

IRAS project ID: 271768 Please quote this number on all correspondence

With the Committee's best wishes for the success of this project.

Yours sincerely

Thomas Fairman
HRA Approvals Manager

Health Research Authority

On behalf of

Dr Nana Theodorou
Chair

Email: leedseast.rec@hra.nhs.uk

Enclosures: "After ethical review – guidance for researchers"

Copy to: Mrs Jean Uniacke

Health Research Authority
NRES Committee Yorkshire & The Humber - Bradford Leeds
North East REC Centre
Room 002
TEDCO Business Centre
Viking Industrial Park
Rolling Mill Road
Jarrow
NE32 3DT

Telephone: 0191 4283545

01 November 2013

Mohamed Elmoursi
University of Leeds
Clinical Sciences Building, Room 8.3,
St James' University Hospital
LS9 7TF

Dear Mohamed

Study title:	**Understanding the placental structure, function and pathophysiology underlying the development of adverse pregnancy outcomes such as pre-eclampsia, intrauterine growth restriction, gestational diabetes, and preterm birth**
REC reference:	**13/YH/0344**
IRAS project ID:	**130157**

Thank you for your letter of 30 October 2013, responding to the Committee's request for further information on the above research and submitting revised documentation.

The further information has been considered on behalf of the Committee by the Chair.

We plan to publish your research summary wording for the above study on the NRES website, together with your contact details, unless you expressly withhold permission to do so. Publication will be no earlier than three months from the date of this favourable opinion letter. Should you wish to provide a substitute contact point, require further information, or wish to withhold permission to publish, please contact the REC Manager Hayley Jeffries, nrescommittee.yorkandhumber-leedsbradford@nhs.net

Confirmation of ethical opinion
On behalf of the Committee, I am pleased to confirm a favourable ethical opinion for the above research on the basis described in the application form, protocol and supporting documentation as revised, subject to the conditions specified below.

Ethical review of research sites

NHS sites

The favourable opinion applies to all NHS sites taking part in the study, subject to management permission being obtained from the NHS/HSC R&D office prior to the start of the study (see "Conditions of the favourable opinion" below).

Non-NHS sites

Conditions of the favourable opinion

The favourable opinion is subject to the following conditions being met prior to the start of the study.

Management permission or approval must be obtained from each host organisation prior to the start of the study at the site concerned.

Management permission ("R&D approval") should be sought from all NHS organisations involved in the study in accordance with NHS research governance arrangements.

Guidance on applying for NHS permission for research is available in the Integrated Research Application System or at http://www.rdforum.nhs.uk.

Where a NHS organisation's role in the study is limited to identifying and referring potential participants to research sites ("participant identification centre"), guidance should be sought from the R&D office on the information it requires to give permission for this activity.

For non-NHS sites, site management permission should be obtained in accordance with the procedures of the relevant host organisation.

Sponsors are not required to notify the Committee of approvals from host organisations

Registration of Clinical Trials

All clinical trials (defined as the first four categories on the IRAS filter page) must be registered on a publically accessible database within 6 weeks of recruitment of the first participant (for medical device studies, within the timeline determined by the current registration and publication trees).

There is no requirement to separately notify the REC but you should do so at the earliest opportunity e.g when submitting an amendment. We will audit the registration details as part of the annual progress reporting process.

To ensure transparency in research, we strongly recommend that all research is registered but for non clinical trials this is not currently mandatory.

If a sponsor wishes to contest the need for registration they should contact Catherine Blewett (catherineblewett@nhs.net), the HRA does not, however, expect exceptions to be made. Guidance on where to register is provided within IRAS.

It is the responsibility of the sponsor to ensure that all the conditions are complied with before the start of the study or its initiation at a particular site (as applicable).

Approved documents

The final list of documents reviewed and approved by the Committee is as follows:

Document	*Version*	*Date*
Evidence of insurance or indemnity	Zurich Municipal	29 September 2012
Investigator CV	Mr Nigel Alastair Buist Simpson	17 June 2013
Other: CV- Darren Treanor- Supervisor 2		
Other: Student CV- Mohamed S.E Elmoursi		
Other: Critique Report		20 September 2013
Participant Consent Form	1	23 September 2013
Participant Information Sheet: Placental Origins of Adverse Pregnancy Outcome	2	30 October 2013
Protocol	1	23 September 2013
REC application	130157/504302/1/189	20 September 2013
Response to Request for Further Information		30 October 2013

Statement of compliance
The Committee is constituted in accordance with the Governance Arrangements for Research Ethics Committees and complies fully with the Standard Operating Procedures for Research Ethics Committees in the UK.

After ethical review

Reporting requirements

The attached document *"After ethical review – guidance for researchers"* gives detailed guidance on reporting requirements for studies with a favourable opinion, including:

- Notifying substantial amendments
- Adding new sites and investigators
- Notification of serious breaches of the protocol
- Progress and safety reports
- Notifying the end of the study

The NRES website also provides guidance on these topics, which is updated in the light of changes in reporting requirements or procedures.

Feedback

You are invited to give your view of the service that you have received from the National Research Ethics Service and the application procedure. If you wish to make your views known please use the feedback form available on the website.

Further information is available at National Research Ethics Service website > After Review

13/YH/0344	**Please quote this number on all correspondence**

We are pleased to welcome researchers and R & D staff at our NRES committee members' training days – see details at http://www.hra.nhs.uk/hra-training/

With the Committee's best wishes for the success of this project.

Yours sincerely

pp 

Dr Janet Holt
Chair

Email:nrescommittee.yorkandhumber-leedsbradford@nhs.net

Enclosures: "After ethical review – guidance for researchers" *[SL-AR2]*

Copy to: Claire Skinner, University of Leeds

Mr Mohammed Khan, R&D Co-ordinator, Research & Development, Leeds Teaching Hospitals NHS Trust.

Dr Simpson, Senior Lecturer and Honorary Consultant, University of Leeds